Naval Research Laboratory
Stennis Space Center, MS 39529-5004

NRL/MR/7431--94-7099

Coastal Benthic Boundary Layer Special Research Program: A Review of the First Year, Volume I

MICHAEL D. RICHARDSON

Seafloor Sciences Branch
Marine Geosciences Division

April 6, 1994

Approved for public release; distribution is unlimited.

REPORT DOCUMENTATION PAGE

Form Approved
OBM No. 0704-0188

1. Agency Use Only *(Leave blank).*

2. Report Date.
April 6, 1994

3. Report Type and Dates Covered.
Final

4. Title and Subtitle.
Coastal Benthic Boundary Layer Special Research Program: A Review of the First Year, Volume I

5. Funding Numbers.

Program Element No.	0601153N
Project No.	R3103
Task No.	000
Accession No.	DN252025
Work Unit No.	74525804

6. Author(s).
Michael D. Richardson

7. Performing Organization Name(s) and Address(es).
Naval Research Laboratory
Marine Geosciences Division
Stennis Space Center, MS 39529-5004

8. Performing Organization Report Number.
NRL/MR/7431--94-7099

9. Sponsoring/Monitoring Agency Name(s) and Address(es).
Naval Research Laboratory
Washington, DC 20375

10. Sponsoring/Monitoring Agency Report Number.

11. Supplementary Notes.

12a. Distribution/Availability Statement.
Approved for public release; distribution is unlimited.

12b. Distribution Code.

13. Abstract *(Maximum 200 words).*

The coastal benthic boundary layer special research program (CBBLSRP) is a 5-year Office of Naval Research program that addresses the physical characterization and modeling of benthic boundary layer processes and the impact of these processes on seafloor structure, properties, and behavior. In volume I of this report, we present preliminary results from the first years' experiments that were conducted on the gas-rich soft sediments of Eckemfoerde Bay (Baltic Sea) and on the sandy sediments of the northeastern Gulf of Mexico. Year-end reports for the 21 projects supported by the CBBLSRP are included along with a summary of the first years' accomplishments. Volume II will include four updated cruise reports along with sample descriptions, locations, and maps that will be provided for reference.

14. Subject Terms.
Acoustics, Sediments, Mines

15. Number of Pages.
323

16. Price Code.

17. Security Classification	18. Security Classification of Report.	19. Security Classification of This Page.	20. Limitation of Abstract. of Abstract.
Unclassified	Unclassified	Unclassified	SAR

NSN 7540-01-280-5500

Standard Form 298 (Rev. 2-89)
Prescribed by ANSI Std. Z39-18
298-102

CONTENTS

COASTAL BENTHIC BOUNDARY LAYER SPECIAL RESEARCH PROGRAM:

A REVIEW OF THE FIRST YEAR

VOLUME I

1.0 INTRODUCTION

Dr. Fred Saalfeld, Director, Office of Naval Research (ONR) requested that the Naval Research Laboratory (NRL) establish a Special Research Program (SRP) to increase the level of basic research that supports naval coastal warfare operations (Memorandum 10D/1097, dated 1 July 1991). During the SRP planning year (FY92), four workshops were convened. Recommendations from these workshops were used to establish scientific direction for the Coastal Benthic Boundary Layer Special Research Program (CBBLSRP) (Richardson 1992).

This report is a summary of the first year (FY93) of the Coastal Benthic Boundary Layer SRP. Volume I contains preliminary results of experiments conducted in the gas-rich sediments of Eckernfoerde Bay (Baltic Sea) and on sediments of the West Florida Sand Sheet. A summary report along with 24 final (FY93) reports by CBBLSRP scientists are also included in Volume I. Detailed cruise reports, station locations, acoustic measurements, and maps are presented in Volume II.

2.0 SUMMARY OF THE FIRST YEAR'S WORK

CBBLSRP is a 5-year ONR program that addresses physical characterization and modeling of benthic boundary layer processes and the impact these processes have on seafloor properties that affect shallow-water naval operations. In this summary we describe the development of the CBBLSRP and present preliminary results from experiments conducted on the gas-rich soft sediments of Eckernfoerde Bay (Baltic Sea) and on the sandy sediments of the northeastern Gulf of Mexico.

2.1 PROGRAM DEVELOPMENT

Recent world geopolitical changes have shifted the emphasis of United States naval operations from deep ocean to near-shore coastal regions. In response to these changes, ONR established an SRP to study the impact of the environment on mine countermeasure (MCM) systems. Four workshops, attended by approximately 100 university, government, and industrial scientists and engineers, were convened between November 1991 and February 1992 to establish program direction. Workshop topics included (a) seabed-structure interaction, (b) high-frequency acoustic scattering and propagation, (c) sediment classification, and (d) electromagnetic and electro-optic phenomena. Common threads among workshop recommendations were used to develop program objectives, and strategies (Richardson 1992).

Workshop recommendations led to a decision to focus program efforts on the physical characterization and modeling of benthic boundary layer processes and the effects these processes have on sediment structure, properties, and behavior (Figure 1). Dominant environmental processes at the benthic boundary layer were identified and include: bioturbation including sediment mixing, tube building, feeding, and pelletization; biogeochemical reactions that affect sediment properties and structure, principally gas bubble formation and other reactions controlled by organic matter oxidation and related pore water chemical changes; and wave-current induced hydrodynamic stresses at the sediment-water interface which control sediment erosion, deposition, and net accumulation rates. Considered equally important was an understanding of the effects of benthic boundary layer stresses, as well as consolidation history and pore pressure variations, on sediment properties. It was recommended that special emphasis be placed on the measurement and modeling of sediment three-dimensional structure. Sediment physical structure provides the common perspective to: (a) quantitatively model relationships among sediment physical, acoustic, electrical, and rheological (mechanical) properties; (b) quantify the effects of environmental processes on the spatial and temporal distribution of sediment properties; and (c) model sediment behavior (acoustic, electrical, and mechanical) under direct and remote stress.

Participants agreed that a basic understanding of the physical relationships among processes and properties would contribute to development of realistic models of: sediment strength, stability, and transport; sediment stress-strain relationships in cohesive and noncohesive sediments; dynamic seabed-structure interactions; animal-sediment interactions; high-frequency acoustic scattering and penetration phenomena; and propagation of high-frequency acoustic energy in a poro-elastic medium. Predictive models developed through this program should enhance MCM technological capabilities in several important areas, including: acoustic/magnetic detection, classification, and neutralization of proud and buried mines; prediction of mine burial; and sediment classification.

2.2 EXPERIMENTAL APPROACH

Quantitative physical models will be tested by a series of field experiments at coastal locations where differing environmental processes determine sediment structure. These experiments will integrate the methods, theories, and hypotheses of scientists from such diverse fields as ocean acoustics, physical oceanography, benthic ecology, marine geology, biogeochemistry, and sediment geoacoustics and geotechnics.

Experiments include investigators from 21 projects supported by the CBBLSRP and 8 related projects supported by the NRL, Forschungsanstalt der Bundeswehr für Wasserschall und Geophysik (FWG) and the University of Kiel (Table 1). Sediment structure from micron to hundreds of meter scales is being characterized using laboratory (TEM studies, CT-Scan, core logging and sediment analyses, x-radiography, electrical resistivity) and in situ measurement techniques (optical characterization of the sediment-water interface, geoacoustic, geotechnical and geophysical probing, echo sounding and side scan sonar). Sediment properties and behavior including rheological, geoacoustic, electrical, and acoustic are being measured and modeled with special emphasis on modeling relationships between sediment behavior and structure. Models

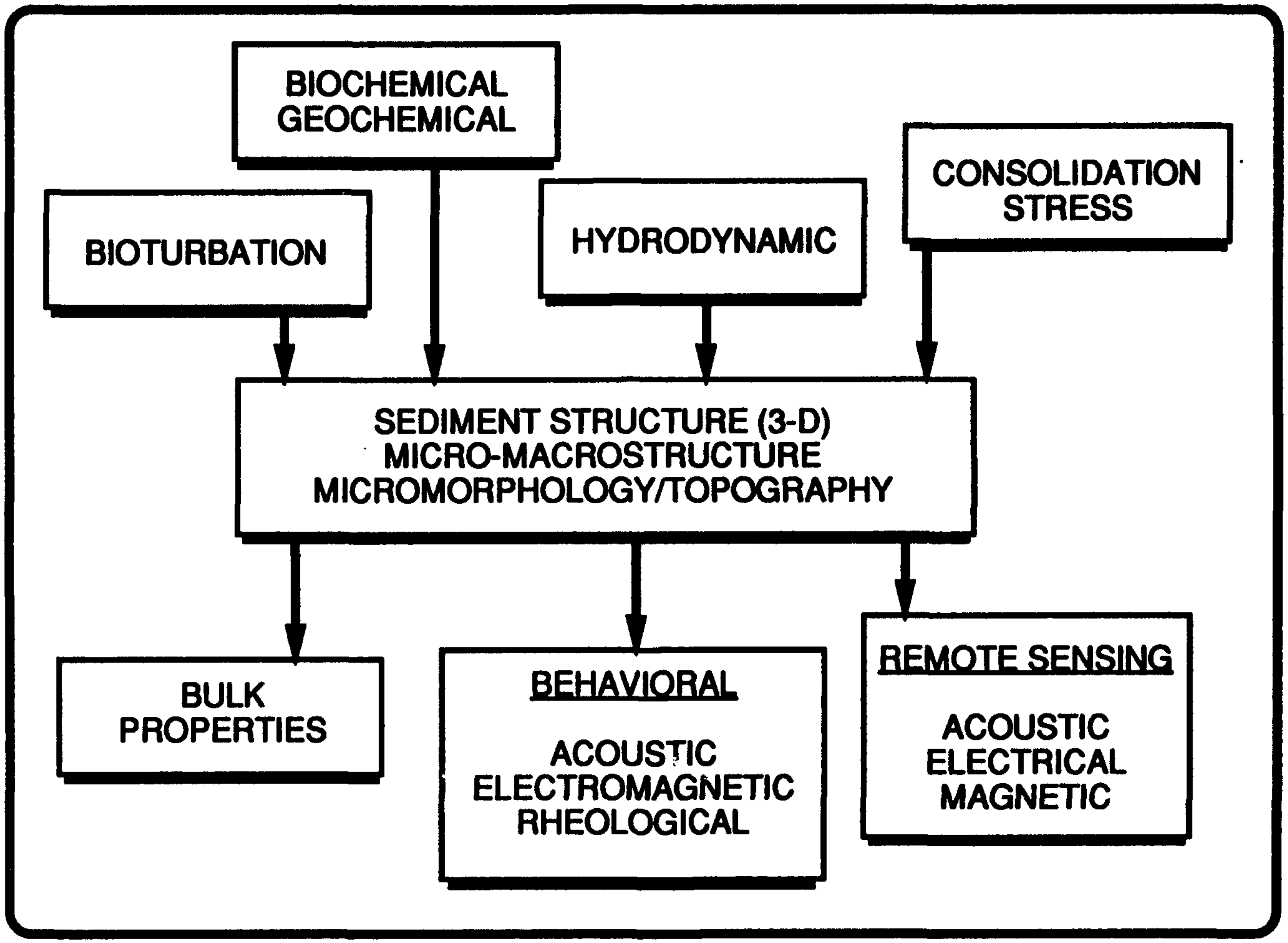

Figure 1. Schematic depiction of CBBLSRP program direction.

Table 1. Coastal Benthic Boundary Layer Research Projects Supported by the SRP with Contributing Projects Supported by NRL and FWG

Measurement and description of upper seafloor sub-decimeter heterogeneity for macrostructure geoacoustic modeling (Texas A&M) • *A.L. Anderson*

Sediment properties from grain and macrofabric measurement (NRL, University of New Orleans, and Resource Dynamics) • *R.H. Bennett, Dennis Lavoie, R.J. Baerwald, and M.H. Hulbert*

High-frequency acoustic scattering from sediment surface roughness and sediment volume inhomogeneities (NRL) • *K.B. Briggs and M.D. Richardson*

Processes of macro scale volume inhomogeneity in the benthic boundary layer (Texas A&M) • *W.A. Bryant and N.C. Slowey*

Analysis of data from in-situ acoustic scattering experiments (University of Texas) • *N.P. Chotiros*

Analysis of the rheological properties of nearbed (fluid mud) suspensions occurring in coastal environments (Lafayette College) • *R.W. Faas*

Statistical characterization of the benthic boundary layer for broadband acoustic scattering (Penn State) • *K.E. Gilbert, D.F. McCammon, and R.K. Young*

Measurement of high-frequency acoustic scattering from coastal sediments (University of Washington) • *D.R. Jackson and K.L. Williams*

Structural analysis of marine sediment microfabric (Quest Integrated Inc) • *J.J. Kollé*

Qualification of high frequency acoustic response to seafloor micromorphology in shallow water (NRL) • *D.N. Lambert and J.A. Hawkins*

Measurement of shear modulus in-situ and in the laboratory (NRL) • *Dawn Lavoie and H.A. Pittenger*

Quantification of gas bubble and dissolved gas sources and concentrations in organic-rich, muddy sediments (University of North Carolina at Chapel Hill) • *C.S. Martens and D. Albert*

Electrical conductivity in the benthic boundary layer (NRL) • *E.C. Mozley*

Physical and biological mechanisms influencing the development and evolution of sedimentary structure (State University of New York and Virginia Institute of Marine Science) • *C.A. Nittrouer, G.R. Lopez, L.D. Wright, and R. Gammish*

Characterization of surficial roughness and sub-bottom inhomogeneities from seismic data analysis (Woods Hole Oceanographic Institution) • *T.K. Stanton, D.J. Tang, and G.V. Frisk*

The detection of continuous impedance structures using full spectrum sonar (Florida Atlantic University) • *S.G. Schock and L.R. LeBlanc*

Variability of seabed sediment microstructure and stress-strain-time behavior in relation to acoustic characterization (University of Rhode Island) • *A.J. Silva, M.H. Sadd, G.E. Veyera, and H.G.Brandes*

High-resolution bottom backscattering measurements (NRL) • *S. Stanic*

Experimental and theoretical studies of near-bottom sediments to determine geoacoustic and geotechnical properties (Lamont-Doherty) • *R.D. Stoll*

Image analysis of sediment texture: A rapid predictor of physical and acoustic properties of unconsolidated marine sediments and processes affecting their relationships (NRL) • *D.K. Young and R.J. Holyer*

The relationship between high-frequency acoustic scattering and seafloor structure (University of Southern Mississippi) • *Li Zang*

NRL Projects Providing CBBLSRP Support

In-situ surficial sediment geoacoustic properties • *M.D. Richardson*
High-frequency acoustics and environmental physics for mine countermeasures • *S. Stanic*
Sediment geochemical processes • *K.M. Fischer*
MCM Tactical Environmental Data System: Acoustic seafloor classification technology • *D.N. Lambert and D.J. Walter*
Ambient and dynamic pore pressures • *R.H. Bennett*

FWG and University of Kiel Projects Providing Support

Measurement of bottom backscattering strength with digital side scan sonar (FWG) • *I.H. Stender, H. Fiedler, and G. Fencher*
Investigation of gas content in marine sediments (University of Kiel) • *F. Abegg, and R. Koester*
In-situ physical properties of marine sediments (University of Kiel) • *F. Theilen*

which relate high-frequency acoustic scattering and propagation to sediment structure are being developed and/or tested. Improved methods of sediment classification are being developed and tested. Hydrodynamic, biological, and biogeochemical controls of surficial sediment structure and properties will be quantified and modeled through in situ studies of sediment stability, sedimentology, radiochemistry, bioturbation, and microbial mediated chemical reactions. Models based on the observed relationships among various processes and properties (Figure 1) will be constructed for each experimental site.

The first experiment was a joint United States (NRL and CBBLSRP) and German (FWG and University of Kiel) study of the gas-rich muds of Eckernfoerde Bay in the Baltic Sea. At this site biogeochemical processes are responsible for the formation of subsurface layers of methane gas bubbles that significantly affect sediment structure, behavior, and properties. Episodic hydrodynamic and biological processes also alter near surface sediment structure. The second experiment was conducted on the West Florida Sand Sheet, southeast of Panama City, Florida. Sediments are a mixture of clastic sands and shells which are reworked by wave-current action. The third experiment (1995) will be conducted in a carbonate environment where biogeochemical diagenetic processes, such as mineralization and cementation, control sediment structure and properties. A fourth experiment (1996) is planned for a benthic environment where biological processes, such as bioturbation, exert the major environmental influence on near surface structure.

2.3 THE ECKERNFOERDE BAY EXPERIMENTS

Three of four planned joint U.S./German cruises investigating gassy sediments of Eckernfoerde Bay in the Baltic Sea have been completed. The first cruise, aboard the PLANET (1-20 February 1993), was a survey of potential study sites. Sediments were characterized by remote acoustic methods (side scan, narrow-beam normal incident and FM chirp sonars) and direct sediment sampling with gravity and box cores. A 1.0 x 2.3 km area with uniform sediments was chosen for further study. Sediments at the study site were soft muds, with high water contents and very low shear strengths. Remote acoustic measurements suggested methane bubbles were present as shallow as 0.5 to 0.7 m below the sediment-water interface (Figure 2). The existence of gas bubbles in sediments was confirmed by CT-scans of pressurized core samples (Figure 3). On the second cruise, also aboard the PLANET (29 March to 3 April), acoustic and environmental towers were deployed to monitor long-term changes in high-frequency bottom scattering, benthic boundary layer hydrodynamic processes (bed stress from bottom currents), and sediment transport processes (turbidity from photographs and optical backscatterance sensors). Box core samples were collected to characterize both initial biological and radiochemical conditions (benthic community structure and depths and rates of sediment reworking) and initial sediment structure and bulk properties.

The main experiment (20 April to 5 June) included 80 scientists, engineers and technicians from eighteen research organizations. Support from FWG, WTD-71, the German Navy, and the Institute of Geology and Paleontology University of Kiel consisted of seven ships, a Navy dive team, student assistance sampling equipment, navigation, a recompression chamber, laboratory space, customs, and numerous other shore-based logistic support activities. The NRL contingent

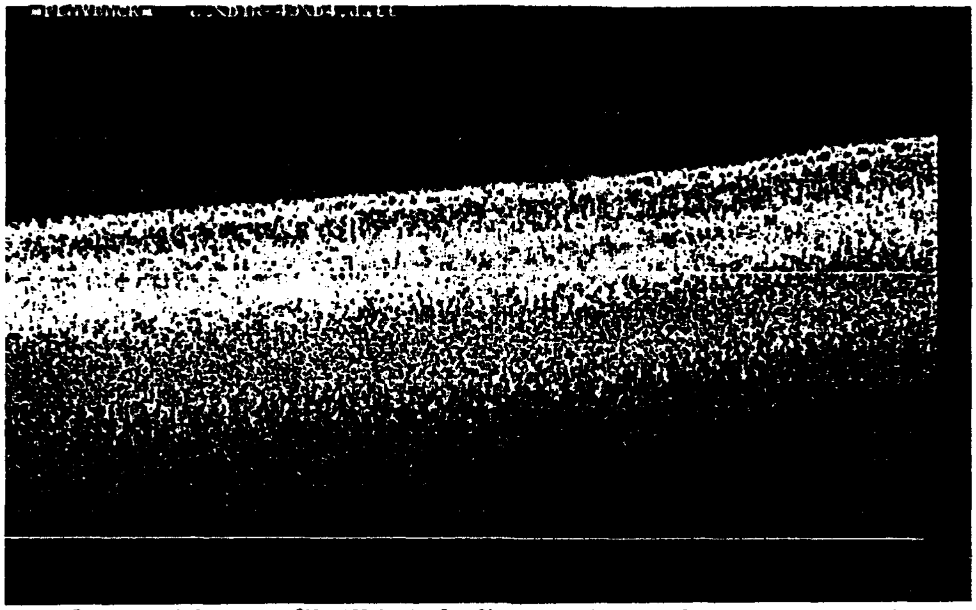

Figure 2. ASCS sub-bottom profile (30 kHz) of sediments at the Eckernfoerde Bay experimental site. A gas horizon was found 75 cm below the sediment-water interface.

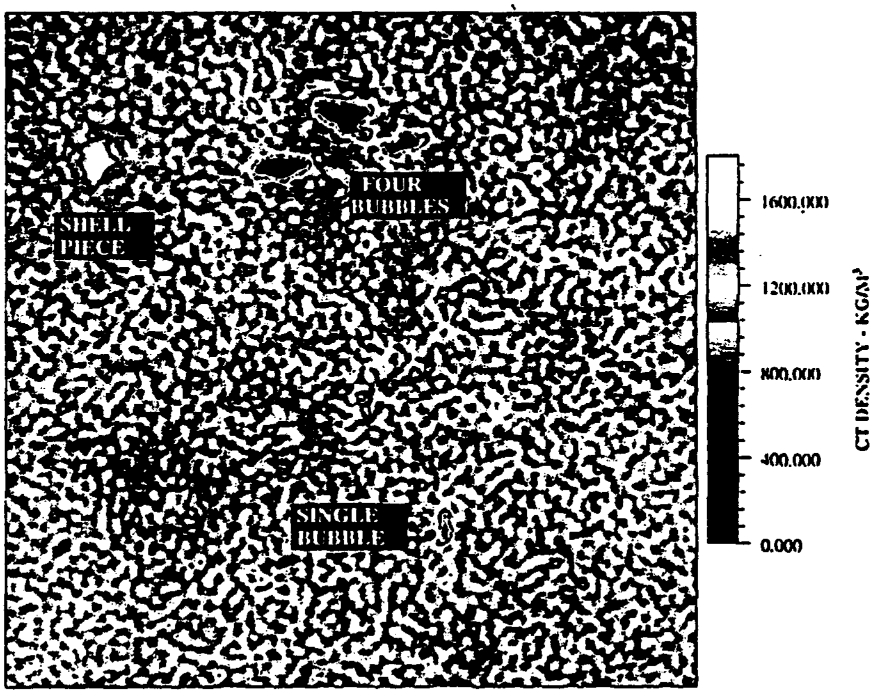

Figure 3. Portion of x-ray CT scan of Eckernfoerde bay sediments from 1.35m below the seafloor. This 5 cm x 5 cm portion of the image illustrates both high density (shell) and low density (bubble) heterogeneities.

(9 projects; 25 NRL scientists and engineers) concentrated on acoustic bottom scattering and propagation studies; sediment classification; and in situ geoacoustic, physical, optical, electrical, dynamic, and biogeochemical characterization of near surface sediments. University participants (10 projects; 36 scientists, students and technicians) conducted temporal studies of acoustic bottom scattering; sediment classification; biological processes (bioturbation rates, and benthic community structure); radiochemistry (reworking depths, mixing and accumulation rates); biogeochemical processes controlling methane distribution; and sediment dynamics (near bottom currents and suspended loads). Sediment structure from the micron to the kilometer scales was investigated and sediment properties including physical, geoacoustic, geophysical and geotechnical properties were quantified by NRL and university scientists. Methane gas distribution, bubble size, and generation were investigated by scientists from both Germany and the U.S.

A total of 382 bottom samples was collected during the three phases of the Eckernfoerde experiments. Samples consisted of 270 sediment cores (137 box cores, 76 gravity cores, 12 pressurized cores, 3 vibracores, and 42 diver-collected cores), 35 diver-assisted in situ probe deployments, 27 remote in situ sample deployments and approximately 50 bottom stereo photographs. NRL, university, and German military divers logged 134 dives during the experiment. Nearly 20 days of continuous acoustic (at 40 kHz) bottom scattering and near bottom current and turbidity measurements were made. Bistatic scattering measurements (@ 40 kHz) covering a wide range of angles were collected. Bottom and surface reverberation, reflection and scattering (20-250 kHz @ 5-30 degree grazing angles); bistatic bottom and surface reverberation (20-90 kHz @ 9, 26, and 30 degree angles); direct path (20-180 kHz); and sediment acoustic propagation measurements (10-180 kHz @ 12, 17, 30, and 90 degree grazing angles) were made using bottom-mounted acoustic towers. Normal incidence acoustic classification measurements were collected over nearly 700 km of track lines.

The following describes the experimental environment found at Eckernfoerde Bay in April-June 1993 and discusses a few of the potential scientific breakthroughs that are expected from these experiments. Eckernfoerde Bay sediments at the experimental site were soft silty-clays with considerable evidence of biological activity. The uppermost sediments consisted of a 2-3 cm layer of brown oxidized mud which overlay a soft, black sediment with a distinct hydrogen-sulfide odor. Radiochemical profiles of ^{234}Th and ^{210}Pb demonstrate that most biological mixing is restricted to the top 1-2 cm of the seabed. Sediment accumulation rates were approximately 2-5 mmy^{-1}. These surface sediments were heavily colonized by tube-dwelling spionid polychaetes. Other polychaetes, bivalves, and crustaceans were present in surficial sediments, some burrowing to 5-10 cm depth. Ventilation of surface sediment by the spionid polychaetes probably controls the depth of the brown oxidized layer and plays an important role in rates of near-surface biochemical processes. Low compressional wave (1425 ms^{-1}) and shear wave (4-7 ms^{-1}) velocities were typical for these high-porosity (88-93%), low-shear strength (0.4-1.6 kPa) surficial sediments (Figure 4). Shear wave velocity, sediment bulk density and shear strength increased with depth as porosity and water content decreased. Sufficient data were collected to characterize near surface sediments from the micron to the tens-of-meters scales.

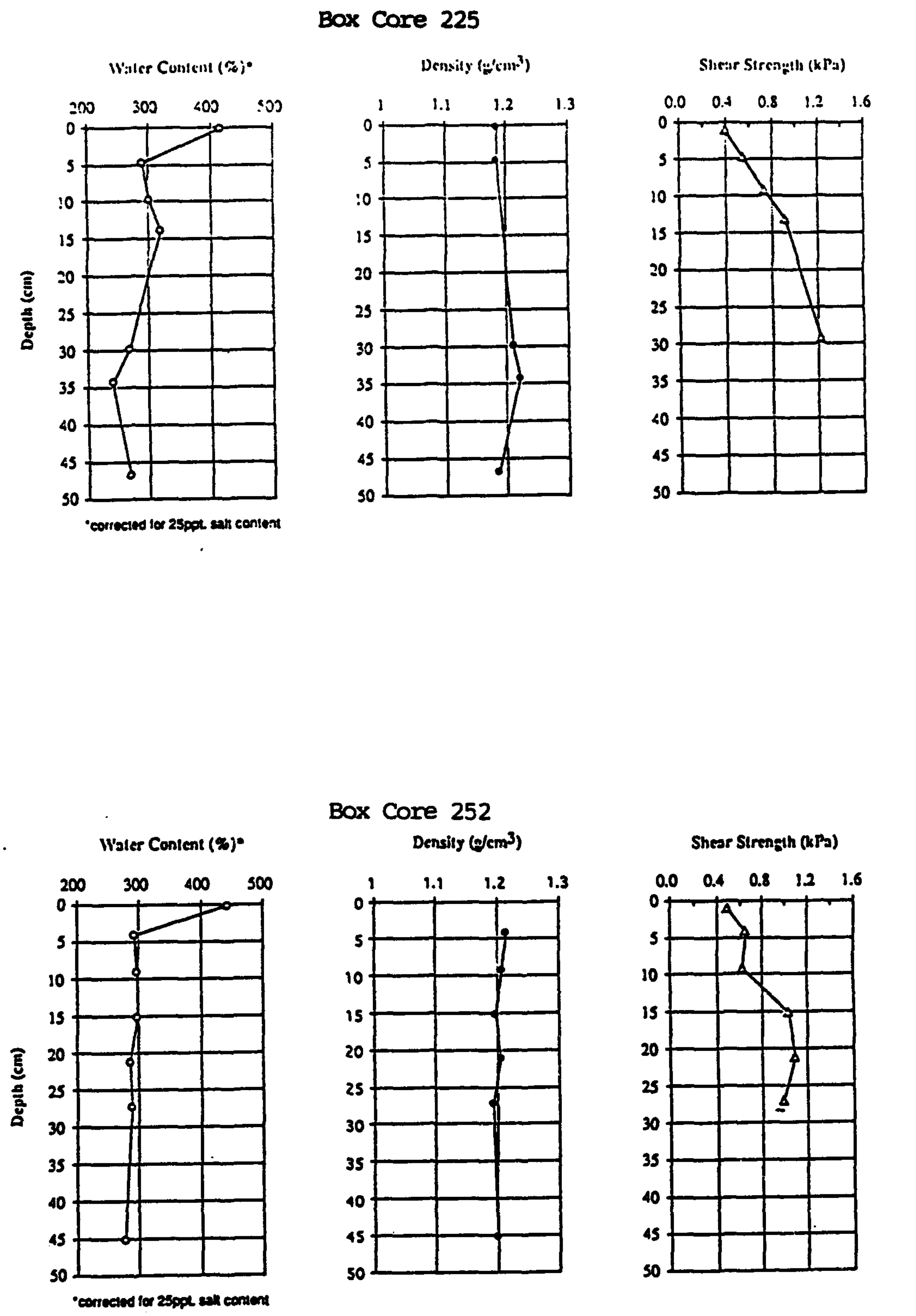

Figure 4. Water content, density, and shear strength profiles for sediments collected with box cores at sites 225 and 252 during the May 1993 experiment in Eckernfoerde Bay.

CT-scans of pressurized core samples revealed only occasional methane gas bubbles from 20 to 100 cm depth while below a meter, numerous clusters of small methane bubbles were found (Figure 3). Voids (probably gas bubbles) were also evident in TEM micrographs of pressurized sediment samples collected from 2 m below the sediment-water interface (Figure 5). Density variations in the uppermost sediments (0-20 cm) were a result of biological activity and erosional/depositional events, not gas bubbles. Sufficient data on both sediment structure (especially shear modulus) and methane bubble size and distribution are available to test models for the acoustic response of these gassy sediments. Data collected on the biogeochemical activity of methanogenic bacteria are more than sufficient to model the environmental processes responsible for the generation and distribution of methane gas bubbles. Study results also include stable isotopic characterization of methane and dissolved organic carbon and rates of microbial processes including sulfate reduction and anaerobic methane reduction, as a function of depth in the upper two meters of the sediment column. Therefore, predictive models relating biogeochemical processes, sediment structure and sediment behavior (acoustic, rheological, and electrical) are obtainable using this extensive data set.

A unique set of time-series data on bottom currents, turbidity and acoustic backscattering was collected during the experiments. Spectral analysis of current data indicate velocity fluctuations were primarily correlated with the local sieche period. During a period of strong winds bottom current speed intensified. Sediments were eroded, thus clouding bottom waters with suspended material. This erosional event changed the bottom characteristics and benthic animal communities and was clearly visible in acoustic scattering measurements. Physical modeling of the effects of bottom boundary layer energetics on sediment characteristics and bottom communities is underway.

Normal incidence high resolution seismic reflection (NRL Acoustic Seafloor Classification System @ 15 and 30 kHz; and the X-Star Full Spectrum sonar with a 20-msec FM pulse @ 2-15.5 kHz) and sidescan sonar (100 kHz Klein) profiling were conducted over a wide variety of sediment types (gassy and nongassy muds, muddy sands, sands and glacial tills) in Eckernfoerde and Kiel Bays. Combined with sediment physical property data, the sonar data (attenuation, impedance and scattering strengths) will be used to test and develop techniques for remote sediment classification. Fine-scale variations in sediment sound speed and density will be used to determine which spatial variations in impedance structure can be reconstructed from normal-incident reflection measurements and which pulse types and frequencies are required to completely reconstruct the impedance structure.

Sediment properties in Eckernfoerde Bay were measured in sufficient detail to characterize sediment structure on scales of microns to meters. Collected data will be used to develop and/or test models of sediment behavior under a wide variety of natural and laboratory stress-strain conditions. Sediment structure data will also be used to address fundamental acoustic issues, including the influence of sediment porosity and rigidity on propagation of acoustic energy and the effects of volume inhomogeneity on high-frequency acoustic scattering. The unique set of laboratory and in situ measured geoacoustic data not only will provide for comparisons of techniques but also, when combined with the physical property data, can be used to test frequency-dependent hypotheses of the velocity and attenuation of compressional and shear waves in a poro-elastic medium.

Figure 5. Survey view transmission electron micrograph of pressurized Eckenforder gassy sediment, May 1993. Sectioned vertical to the plane of sediment deposition. Note two large voids (V). X20,000.

2.4 THE WEST FLORIDA SAND SHEET EXPERIMENT

The experiment was conducted on the West Florida sand sheet 23 nmi southeast of Panama City, Florida (9-30 August 1993). The shelf of the northeastern Gulf of Mexico is currently sediment-starved with most material deposited by the Appalachicola River during lower sea stands. Recent large scale seafloor morphology is controlled by hydrodynamic process, especially major storms. Silt- and clay-sized particles are occasionally deposited over the sand sheet during severe storms. These finer sediments can be worked into the predominantly sandy surface sediments by biological activity creating a spatially and temporally variable sediment structure.

Acoustic surveys of a 20-km^2 area, using sidescan sonar, chirp sonar and 3.5-kHz echo sounding, allowed experimenters to delineate a 600 x 625 m primary experimental site which had uniformly high acoustic reflectivity (Figure 6). Preliminary observations of sediment collected with grabs, vibra cores and gravity cores combined with bottom video and diver observations suggest this high reflectivity was the result of microroughness from coarse-grained sediment rather than large scale bottom roughness features such as sand waves or ripples. Coarse-grained sandy sediments in this highly reflective area were mixed with shell hash, coralline algae fragments and numerous large mollusk shells. Sediments outside the experimental site were fine-grained sands of lower reflectivity, with little shell-hash and occasional muddy layers or inclusions. Microrelief in both types of sediments was dominated by biological features (mounds, pits and burrows) with little evidence of the type of wave-induced ripples or sand waves found in previous years (Stanic et al. 1988).

Mean values of surficial sediment geoacoustic properties between sediment types were similar with in situ near surface shear wave speeds of 80-150 m/s and compressional wave speeds of 1650-1740 m/s. Initial results show high variability in the values of compressional wave velocity and attenuation in the coarse sand (due to the heterogeneous mixture of shells and sand) but relatively low variability of those same properties in the fine sand. Spatial variability of sediment physical, geoacoustic and geotechnical properties will ultimately be determined from sediments collected using grab samplers (97 samples), gravity (14 samples) and vibra (8 samples) cores, and from 24 hand-collected diver cores. Surficial sediment properties provide ground truth to develop and test acoustic classification algorithms.

Acoustic boundary scattering experiments and time-lapse monitoring of environmental conditions were restricted to the highly reflective sediment. Preliminary results show high variability in acoustic scattering strengths over ping-to-ping, hour-to-hour, and day-to-day time scales. The near-bed hydrodynamic regime was dominated by reversing tidal currents with typical speeds of 10 cms^{-1} or less. Maximum bed shear stresses remained too low to resuspend or transport the sediments. The high temporal variability in acoustic scattering strengths must, therefore, be related to biologically induced changes in bottom roughness and bottom properties and/or to fluctuations in water column properties. CT-scans of sediment core samples will be used to determine sediment structure at scales of a millimeter to a few centimeters. Laboratory

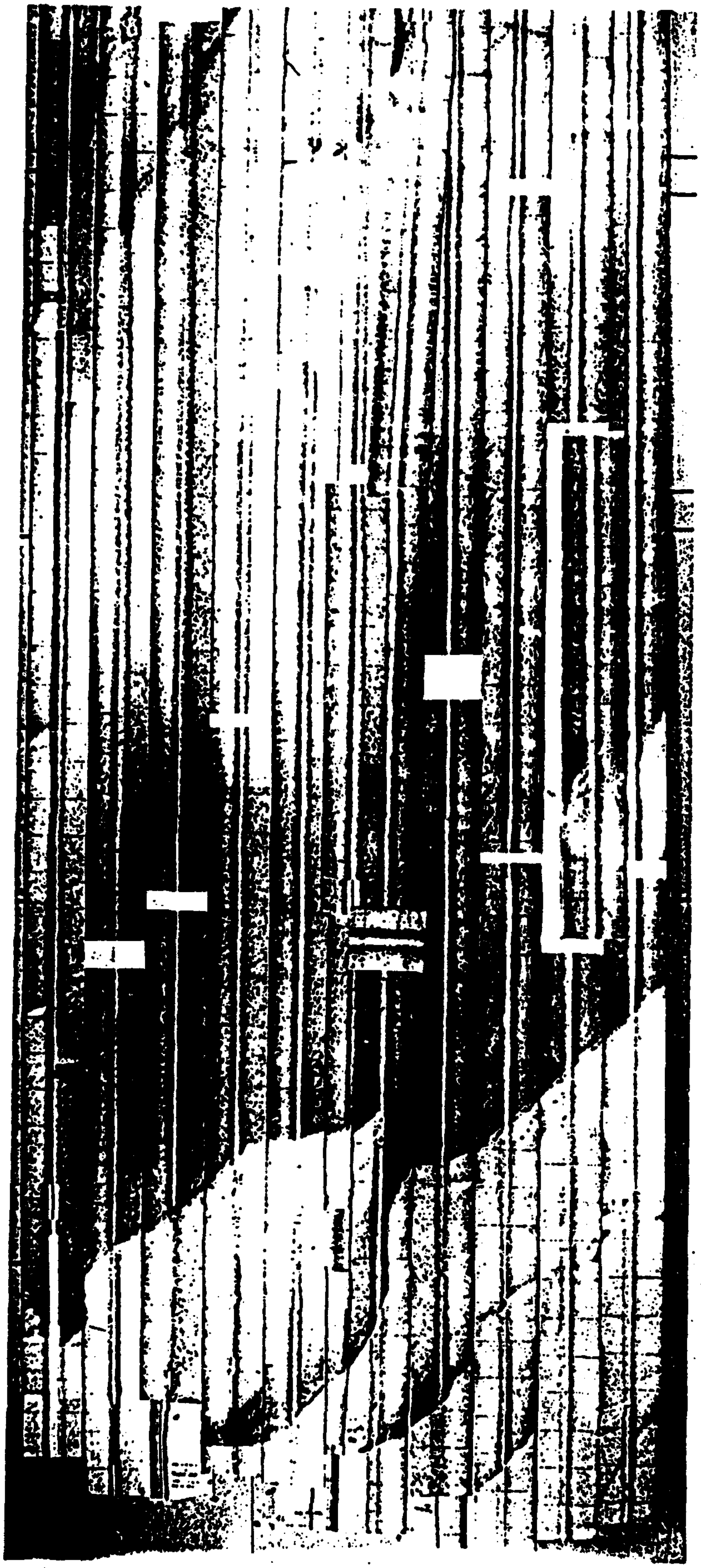

Figure 6. Sidescan sonar mosaic of surface sediments on the West Florida Sand Sheet. Darker colors represent the highly reflective sand shell-has mix while lighter colors depict the lower reflectivity of the fine sands.

analyses of sediment core samples and in situ geoacoustic measurements will provide data on sediment structure from the centimeter to meter scales. Bottom microtopography will be determined from approximately 65 stereo bottom photographs. Characterization of sediment structure (millimeter to meter scales) should enable us to predict frequency-dependent volume scattering. Measurements of bottom microroughness and sediment volume inhomogeneities from photographs and cores will be used to model the relative contribution of bottom interface roughness and volume scattering to high-frequency acoustic scattering and propagation. The contribution of spatial heterogeneity in sediment impedance-related properties, especially shells near the size of acoustic wavelengths, will be modeled and compared to experimental results.

2.5 FUTURE PLANS

The Eckernfoerde Bay and West-Florida Sand Sheet experiments provide data on important end-members of a spectrum of sediment types found in coastal littoral regions. Experiments are also planned for a carbonate environment where biogeochemical processes control sediment fabric and for an biologically rich environment were bioturbation by benthic fauna dominates sediment structure. The goal is to provide physical models that predict sediment structure and behavior from knowledge of environmental processes for each environment. A quantitative understanding of 3-D sediment structure is central to development of these models (Figure 1). Scientists interested in access to the extensive CBBLSRP data base should apply directly to the CBBLSRP chief scientist. Special sessions have been arranged at the 1994 AGU/ASLO Ocean Sciences Meeting (21-25 February, San Diego, CA) for the presentation of scientific results of the first two experiments. A symposium devoted to modeling experimental results of the Eckernfoerde experiments is planned for the summer of 1995 in Kiel Germany.

2.6 REFERENCES

Richardson, M.D. 1992. "The Coastal Benthic Boundary Layer Research Program: Workshop Recommendations and Program Direction," Naval Research Laboratory, Stennis Space Center, MS, SP 017: 361: 92.

Stanic, S., K.B. Briggs, P. Fleischer, R.I. Ray, and W.B. Sawyer. 1988. "Shallow-water high-frequency bottom scattering off Panama City, Florida," *J. Acoust. Soc. Am.* 85:2134-2144.

3.0 PROJECT REPORTS FOR FISCAL YEAR 1993

The following 24 reports summarize results for projects supported by the CBBLSRP

3.1 Measurement and Description of Upper Seafloor Sub-Decimeter Heterogeneity for Macrostructure Geoacoustic Modeling (Principal Investigator: A. L. Anderson)

CBBLSRP FY93 YEAR-END REPORT

Aubrey L. Anderson, Thomas H. Orsi and Anthony P. Lyons
Department of Oceanography
Mail Stop 3146
Texas A&M University
College Station, TX 77843-3146

BACKGROUND

The scientific problem of interaction of acoustic waves with the seafloor is of interest for at least two reasons. Energy reflected or scattered from the seafloor often determines the reverberant or interfering background against which one must discriminate to use sonar systems for location and identification of other targets of interest. One example might be the goal of detecting and classifying proud or buried sea mines. Thus it is necessary to understand the relationship between acoustic seafloor scattering and other parameters of the seafloor in order either to predict this interfering background or to have a basis for reasonable extrapolation of bottom interaction measurements.

Another reason for an interest in acoustic seafloor interaction is the goal to use acoustic systems as tools for the study, description or characterization of the seafloor. Although acoustic echo ranging bathymetry systems have progressed from simple single channel, vertical incidence profilers to the sophisticated swathmapping systems of today, of even more interest for many purposes are systems and techniques allowing, in some sense, the remote characterization of the seafloor. Although some degree of the scientific community's effort has been devoted to the problem of acoustic characterization of the seafloor for at least the last three decades, recent advances in system types, data processing and interpretation methods, modeling, and seafloor sample description have provided significant new capability both for such characterization and for testing the validity of the characterizations. The word characterization is used here purposely to indicate a broad scope of activity including the partitioning of the seafloor as indicated in a set of acoustic records (say profiler records) into different 'classes' on the basis of qualitative patterns which recur in such records, the identification of the probable nature of the seafloor material on the basis of any of an increasing variety of quantitative measurements (e.g. interval velocities, interval absorptions, interface reflectivities - both normal incidence and versus grazing angle, etc.), and the estimation of other characteristics of the seafloor material from the results of either the qualitative partitioning or the quantitative identification (estimation of seafloor undrained shear strength from estimated material type via reflectivity measurements or directly from empirical relationships between reflectivity and shear strength). As examples of end product practical goals for such seafloor acoustic remote sensing one might wish to have enough information to estimate probability of mine burial on impact or foundation requirements for a seafloor structure from remote acoustic profiling.

Advancement toward realization of such pragmatic goals requires increased scientific understanding of the interaction of high frequency acoustic waves with the usually complex structure of the near surface, shallow water seafloor. One of the goals of the CBBLSRP is to discover such an increase in knowledge and understanding by acoustic measurements, environmental sampling, application of forefront techniques for acoustic data and physical sample analysis, modeling and examination of the results of comparison of model predictions and measurements.

GOALS OF THIS PROJECT

In other studies, carried out at Texas A&M University prior to the initiation of the CBBLSRP, advances were made in the modeling of seafloor internal backscattering and in the description of internal heterogeneity of seafloor samples on scales relevant for such modeling of volume scattering. The first of these advances, scattering modeling, resulted from an addition to the widely used model of Jackson for seafloor scattering. The Jackson model separates the seafloor scattering estimation into surface interface and internal volume terms. The internal volume terms are included via a free parameter related to internal volume scattering cross section of the subseafloor heterogeneities. Our extension treats this volume scattering component in a manner allowing constraint of the volume scattering cross section by physical measurements on seafloor samples. In this formulation, the variance and correlation length for the depth profile of compressional wave velocity and of density are used to parameterize the internal heterogeneity. The volume backscattering cross section linearly increases with the variance while the relationship to correlation length is nonlinear. The volume scattering cross section peaks for a value of correlation length of about 4 cm at 5 kHz and between 1 and 2 cm at 30 kHz. In the one area that we have made comparison between the predictions of this model and seafloor scattering measurements (for the GLORIA side scan sonar system at a frequency of 6.5 kHz and for a distal lobe of a deep sea fan in water depths of about 4500 m), the seafloor density profile has been the primary parameter in constraining the volume scattering strength estimates.

The second advance has been the application of x-ray CT scanning to describe the internal heterogeneity of a seafloor core sample. The application of this technique was initiated to describe the gas content and distribution of gas bubbles (above a minimum size) within such a sample. CT scanning has proven useful for this application and has also provided estimates of the internal density structure of the sediment with a three dimensional resolution much finer than 1 cm.

The primary, specific goal of this project is the description of seafloor internal heterogeneity on a sub-decimeter scale (the decimeter being the size scale of most seafloor core samples). Although not constrained to only the x-ray CT scan method, this method will be a major part of our measurements. These heterogeneity measurements are directed toward a description of the internal distribution of density for the seafloor samples we measure. Although these measurements are not specifically directed toward a description of (only) gas bubbles within the samples, if bubbles are present above a diameter of about 1mm, they will be detected and described. A second important goal for our work is the estimation of acoustically relevant parameters from the heterogeneity measurements: specifically the internal volume scattering cross-section. While there will be components of the sediment internal geoacoustic model that will not be treated by our scale of measurements, our modeling work indicates that the scale of these measurements will likely provide one of the important components for evaluating the comparison between acoustic scattering measurements and model predictions. Relevant information on other scales, both smaller and larger than ours, will come from the measurements of other participants in the CBBLSRP.

METHODS

We have participated in two sampling field trips to Eckernfoerde Bay near Kiel, Germany and in one such field trip to the Gulf of Mexico continental shelf near Panama City, Florida. The general nature of these two regions is distinctly different. The seafloor at Eckernfoerde Bay is a very high water content mud with considerable evidence of gas within the seafloor. Thus, in this area, one goal of our studies is to quantify the seafloor gas bubble population in addition to an examination of the variation of density within the samples. On the other hand, the seafloor at the Panama City site is a very coarse grained sand and shell hash. Measurements by other investigators at Panama City (during the August 1993 field measurements) have been described to us as providing no indication of free gas in seafloor samples which were taken with the specific goal of seeking evidence for and samples of such seafloor free gas if it existed. Thus, our goal for measurement of samples from the Panama City site is to examine the fine scale variation of density within the samples. Because of the probable significant contrast in acoustic impedance between the seafloor and overlying seawater, and because of the probability of significant fine scale interface roughness on the seafloor (to be measured by other investigators), it is likely that interface scattering will dominate the interaction of acoustic signals with the seafloor at the Panama City site for the high acoustic frequencies of most of the CBBLSRP acoustic measurements. Our measurements are intended to contribute to constraining estimates of internal volume scattering strength as one step in testing this hypothesis.

Sampling

Samples for our studies have all been cylindrical cores contained within a thin sampling tube or core liner of material such as PVC plastic. Thicknesses of core tube walls have ranged from about 2 to 10 mm and inside diameters have ranged from 7 to 12.5 cm. Lengths of the core samples (primarily representing the depth interval below the surface of the seafloor) have ranged from about 15 cm to 5 m. At Eckernfoerde Bay, methods of obtaining the cores have included gravity corers operated entirely from the ship on the sea surface, gravity cores which have been cut into 1 m long sections and placed within pressure sealed metal chambers at the seafloor by divers, diver cores taken by inserting a plastic coring tube into the seafloor and sealing the sample into 1 m long metal pressure chambers at the seafloor and subsample cores taken at the surface from box cores obtained by a surface ship. At the Panama City site, all samples were diver collected cores which were not sealed in pressure tight chambers.

Gassy Regions

Results of measurements by other investigators using vertical incidence acoustic profilers implied that there was a topmost seafloor layer at the primary Eckernfoerde Bay acoustic measurement site with relatively low volume backscattering. Below this uppermost layer, with a thickness on the order of a meter or less, the profiler records imply that there is a much thicker layer of relatively high volume scattering. Previous investigators of Eckernfoerde Bay have suggested that the high volume scattering strength exhibited by some layers in some areas of the bay resulted from free gas bubbles within the seafloor. Thus one of our goals was to test the hypothesis that free gas bubbles exist within the seafloor (although many profiles of gas content for samples from Eckernfoerde Bay have provided ample evidence of significant quantities of methane within the seafloor, direct observation of gas bubbles, either *in situ* or with pressure tight samples, had not been made).

Much of the ensuing discussion of sampling with pressure tight metal chambers and measurement/analysis of samples taken within these chambers would not have been possible without the very productive collaboration we have had with Frederich (Fritz) Abegg of the University of Kiel. Fritz had already successfully sampled the Eckernfoerde Bay seafloor with a 5 m gravity corer and had described the methane gas concentration from small subsamples taken through the side of these cores at the surface (non-pressurized samples). He had also already built and used 5 steel pressure chambers which were used to obtain samples maintained at the pressure at the seafloor. This was done by raising a gravity corer from the seafloor until it was just above the seafloor, rotating the core to the horizontal, cutting the core (and liner) into 1 m sections and sealing each section into one of the pressure chambers. The work of cutting the core sample and sealing the segments into the chambers at the seafloor was accomplished by divers from the German Navy.

During our participation in Eckernfoerde Bay measurements in February 1993 (the preliminary field trip), in collaborative work with Fritz Abegg, we obtained a 5 m gravity core in exactly the same manner that Fritz had previously used. The unique aspect of this core (CBBL 55-BS-GC) is that it was taken from a location near the intended site of the acoustic tower measurements and it was examined by x-ray CT scanning. Both the core location (55) and the acoustic backscattering tower location (T) are indicated on Figure 1. Also shown on this figure is the location of another core (CBBL 16-BS-TC) which was examined by CT scanning during the February sampling. In fact, this was the first core we subjected to such scanning. It was one of three cores from a triple core sample obtained by Fritz Abegg. This sample was retrieved without any attempt to maintain it at *in situ* pressure. A major motivation of the CT scans of this core (16) was to test the condition of samples retrieved in the "normal" manner (without any efforts to pressure seal them). Each of these cores (the single 1 m section from CBBL 16-BS-TC on February 12 and the five 1 m sections from CBBL 55-BS-GC on February 18) was taken from the German research vessel

PLANET and was transported to Kiel for x-ray CT scanning. The sections were transported by automobile at ambient surface temperatures (air temperatures were about 1 to 4^{O} C).

In the time between the February and May 1993 field trips to Eckernfoerde, Fritz Abegg built five new aluminum pressure chambers for use in obtaining and CT scanning of pressure tight core samples. We used these during the May field measurements with two cores: CBBL 314-BS-DC and CBBL 315-BS-GC. Both of these cores were obtained from the German vessel HELMSAND on May 25. These were both taken at the same location which was near where the backscattering tower had been located as shown in Figure 1. Horizontal separation of the two cores was about 2 m. CBBL 314-BS-DC is a 1 meter diver core which was sealed in one of the aluminum pressure chambers at the seafloor. This core was taken to allow examination of a sample of the upper meter of the seafloor with the absolute minimum change of pressure conditions - the core was raised only one meter to retrieve the sample from the seafloor. CBBL 315-BS-GC is a two meter long gravity core which was cut into two 1 m long segments with each sealed in one of the pressure chambers at the seafloor. Unfortunately, the chamber containing the upper meter section of this core did not maintain pressure because of some tape which caught in the seal. Otherwise, all sections did retain pressure. A major goal of the 2 m core (CBBL 315-BS-GC) was the examination of a sample of the second meter of the seafloor with a minimum pressure change - the deeper 1 m section was only raised two meters in retrieving the sample from the seafloor. Fortunately, this goal was achieved because pressure was retained in the pressure chamber containing this deeper 1 m core section. All sections were placed into a refrigerator on deck and when the ship docked after taking these pressurized cores, the refrigerator was lifted from the ship to a truck and transported to Kiel with the core sections inside. The refrigerator and cores were offloaded at the Radiologische Gemeinschaftspraxis Prüner Gang in Kiel. The refrigerator was connected to electrical power and then each core section was maintained at a temperature of about 7^{O} C until it was removed from the refrigerator for scanning.

Gravity cores were taken by other participants using other schemes for maintaining the samples at seafloor pressures. In particular, expanding plugs were inserted into the PVC core barrel of the URI gravity corer by divers at the seafloor. Also, while at the seafloor, stabilizing bolts were inserted across the diameter of the core wall (outside the length of the core occupied by sample or expanding plug) in order to prevent excessive motion of the expanding plug along the length of the core. We CT scanned one core (CBBL 308-BS-GC), which was obtained in this manner by Drs. Bryant and Slowey, at the Radiologische Gemeinschaftspraxis Prüner Gang in Kiel.

Non-Gassy Regions

Although many portions of the Eckernfoerde Bay exhibit evidence of gas bubbles within the seafloor, some do not. In many cases, even in a region of the bay which seems to have seafloor gas bubbles, there are indications, both from vertical incidence acoustic profiling systems and from the CT scans of pressurized samples, that the upper 50 cm or more of the seafloor may have little or no free gas in bubbles *in situ*. Thus we have examined the microstructure of this upper seafloor with samples which were taken without maintaining pressure. During May 1993, subsample cores were obtained from box cores taken in Eckernfoerde Bay from the German research vessel KRONSORT. Two box cores were taken at each of three sites. The first site was located near the entrance to Eckernfoerde Harbor, the second within the central deeper part of the bay, and the third near Mittelgrund. Four cores (CBBL 227-BS-BC, CBBL 260-BS-BC, CBBL 263-BS-BC and CBBL 268-BS-BC) coincide with the SUNY benthic ecology/fine structure study, one with the NRL sediment geochemistry study (CBBL 250-BS-BC), and the other with the geotechnical study of URI (CBBL 264-BS-BC). Once onboard ship, the box cores were subsampled by carefully inserting a sharpened plastic liner into the sediments. Locations of the box cores, and thus the subsample cores we have measured, are shown in Figure 1. The retrieved subsamples were stored vertically as carry-on luggage during transport to the U.S. to avoid extreme pressure variations and minimize additional disturbances. Once in the laboratory, the subsamples were stored upright underwater at $4^{o}C$ until analyses.

During August 1993, three cores were collected by divers from the measurement site off Panama City, Florida. These are cores CBBL 413-2-PC-DC, CBBL 413-3-PC-DC and CBBL 490-PC-DC. The cores were stabilized by inserting an expandable plug into the top of the core until it touched the surface of the sediment sample, then expanding the plug. These cores were maintained in a vertical orientation in a refrigerator on the research vessel GYRE for five days after which they were transported in a vertical orientation, as cabin baggage, to College Station where they were stored upright at 4^{o} C.

Sample Characterization

X-ray CT

An ELSCINT Twin CT scanner, located in Kiel, Germany at the Radiologische Gemeinschaftspraxis Prüner Gang, was used to scan the gravity core and diver core samples from Eckernfoerde Bay (but not the box core subsamples). In-plane resolution (x- and y-dimensions) was .35 mm and slice thickness (z-dimension) was 1 mm. Two types of scanning sequence were used. A low-spatial-density sampling scheme (also referred to as low resolution) obtained 1 mm thick slices spaced at 1 cm intervals, thus providing a high resolution sampling (1 mm thick slices) at low spatial density (1 cm slice interval) which allowed scanning the entire length of long cores - even the 5 m core. A high-density (also called high resolution) scheme obtained 1 mm thick slice scans with the translate distance of the sample table incremented 1 mm between scans - thus producing continuous scan information but with no overlap. The lengths of core sections which were scanned at high resolution ranged from 4 to 11 cm. Core segments for high resolution scanning were selected by observing images taken with the low-density scheme as they were taken and identifying features for which continuous scan information would be informative. From one to three high resolution segments were typically selected for each core. The data (images) were stored in digital format by the ELSCINT system on Erasable Optical Disks (EODs). Duplicate EOD files were stored for each core with one set remaining in Fritz Abegg's custody in Germany and one returned to the United States for further analysis. Initial work with these scans was limited to qualitative assessment because of difficulties encountered in gaining access to the compressed data files as stored by the ELSCINT system. We have received good assistance from Dr. Shabtai Samilov of ELSCINT headquarters for the United States both in regard to access to the image data using the equipment at their headquarters facility and in guidance for developing an ability to access the data for our own quantitative analysis. We have recently completed the necessary software and are now able to decompress the files for further analysis. The decompression and translation is accomplished using a Mega 486 DOS computer with the EOD disks read on a Storage Dimensions Tahiti II EOD drive. Some of our analysis of the resulting data files is being carried out on the DOS computer with software we have written. Other of our analysis and processing is being done with a Macintosh II computer and Spyglass_ software.

A Technicare D-100 CT scanner, located at the Engineering Imaging Laboratory of Texas A&M University, was used to characterize the fine-scale structure of the box core subsamples. In-plane resolution (x- and y-dimensions) was 0.4 mm and slice thickness (z-dimension) was 2 mm. The subsamples were scanned using a 2-mm table translate distance with no overlap between images. Digital image processing and analyses were conducted using a Macintosh II computer and Spyglass_ Transform. Statistical parameters (e.g., mean CT density and standard deviation) were determined for each CT image using 10,000 voxels from a 100 x 100 voxel region-of-interest (ROI) selected from the geometric center of the scan.

Physical Measurements

After scanning at College Station, the box core subsamples from Eckernfoerde Bay were split longitudinally and slabbed into 1-cm thicknesses to make x-radiographs. A Picker-Andrex x-ray unit was used, operated for 20-30 secs at 40 kVp/4 mA. After x-raying, the slabs were subsampled at a 1-cm interval to determine the vertical distribution of water content, grain density, wet bulk density, and porosity. Each sample was first weighed wet and then reweighed after oven-drying for 24 hrs at 105^{o}C to determine water content. The oven-dry solids were subsequently powdered to determine grain density using a helium pycnometer. Wet bulk density (wet unit weight) and porosity were determined for each sample using water content and grain density [Bennett-Lambert method]. Corrections were made to account for residual salt left in the oven-dried solids by assuming a pore water salinity of 25^{o}/oo [as indicated by the preliminary results of Silva]. The remaining material not slabbed was sampled at a 1-cm interval to determine sand-silt-clay percentages. Due to the considerable organic content of Eckernfoerde sediments, the samples were treated with 10-30 ml of hydrogen peroxide before dispersing. The samples were disaggregated by soaking and shaking overnight in dispersant and then wet-sieved to separate the sand-size particles (< 4f) from the finer grained material. Silt and clay content was determined using the pipette technique (clay > 8f).

STATUS

All cores retrieved for scanning in Germany were scanned. Scans also were taken of other samples of known density to assist in relating the measured CT values from the ELSCINT scanner to bulk density values of the sediment volume elements in the core samples. All digital files were transported to College Station on Erasable Optical Disks (EODs) and a copy was left in Kiel as indicated previously. After considerable delay, it is now possible to retrieve the digital records for the scans from the EODs and to decompress the files. We are about 40% complete in the conversion of the files to workable format and are working with the data. Initially we are generating and examining images for indications of the locations and nature of heterogeneities including bubbles of free gas. We will also generate three dimensional files of sediment density distribution for use in determination of statistical parameters and estimation of acoustic internal volume scattering cross section.

The box core subsamples were transported to College Station and have been CT scanned and x-rayed, and all geotechnical measurements are complete. A malfunction of the D-100 CT scanner prevented us from scanning CBBL 263-BS-BC, but we were still able to obtain radiographs and physical property measurements to permit comparisons with the other box core subsamples. (The scanner malfunction was major and scanning of the Panama City cores is awaiting replacement of the system.) For the Eckernfoerde Bay box core subsamples, in order to convert CT numbers to equivalent bulk densities, an empirical relationship was developed for each core using a least-squares technique by matching sediment volumes used for physical property determinations (i.e., the x-ray slabs) with their corresponding CT volume. Correlation coefficients for the relationships were good, ranging from 0.76 to essentially 1.00 (mean: 0.90). Variations in the degree of correlation are attributed mainly to the difficulties and inaccuracies involved in fine-scale physical sampling and then matching the physical property volumes with the CT volumes.

EXAMPLES OF RESULTS

Sampling Issues

The x-ray CT scan results for some of the cores from Eckernfoerde Bay provide insight into sampling issues for these potentially gassy sediments.

The information from the cores taken in February indicates that, at least for some depths within the seafloor, it is imperative that cores be maintained at *in situ* pressures in order to describe the *in situ* density structure or fabric of the seafloor in this region. CT scans of the triple core (CBBL 16-BS-TC), which was obtained without retaining the sample under pressure, exhibited numerous long narrow gas filled voids from 0.5 to 2 cm in length and 0.1 to 0.2 cm in width. Image to image comparison of these features indicates that most of the gas filled fractures were also long in the vertical direction (original core orientation in the seafloor), extending up to 2 cm in this direction. Also, after completing the scans of the five 1 m sections of core CBBL 55-BS-GC while they remained under *in situ* pressure within the steel pressure chambers, the pressure was released from the deepest of these 1 m sections. Rescanning this section 1.5 hours after the pressure was released provided informative results as indicated in Fig. 2. Although the visual quality of the images in Fig. 2 is limited because the figure is made from hard copy photographic prints rather than computer files, nonetheless, the difference in the indicated condition of the sediment sample is obvious. In the images as shown here, lighter colors indicate lower x-ray absorption or bulk density, thus free gas would appear white. The highest density, darkest circle around the image represents the steel pressure chamber and serves to bound the gray scale limits. Before the pressure is released, although there is considerable "speckle" noise in the image (the very small scale black to white fluctuations) these do not represent free gas. In the original data set, the actual CT values clearly indicate densities appropriate for the mud matrix of the seafloor. Only two small linear white features to the right and below center of the top panel imply the presence of free gas in the pressurized section. However, after the pressure has been released, the bottom panel image of Fig. 2 clearly indicates a dramatic increase in the amount of free gas which is present within this sample. The implication is that, for depths in the Eckernfoerde Bay seafloor that are greater than the upper 'gas free' zone, pressurized samples will be required to determine the in situ characteristics of the sediment structure (at least any of the characteristics which might be affected by the presence of free gas bubbles which form upon sample pressure release).

A test for evidence of free gas within a core under various conditions was carried out also with the deeper segment of core CBBL 315-BS-GC. As a reminder, this core was taken from the central portion of Eckernfoerde Bay, recovered in a pressure tight aluminum chamber and refrigerated from the time of recovery until it was examined by CT scanning in Kiel. This entire sequence of activity was carried out on May 25, 1993. The afternoon of May 26, this core section was removed from refrigeration and allowed to warm for 4.5 hours at which time it was rescanned, still under pressure. Although the internal pressure in the chamber holding the core section had increased significantly, the CT scans indicated virtually identical conditions of the sediment as far as the presence or absence of free gas at any location along the length of the core section. Upon completion of this second scan, the pressure was released on this deeper section of core CBBL 315-BS-GC and the section was scanned a third time after 1.25 hours. As a result of the pressure release on this core section, numerous small fractures appeared throughout the core section. These fractures were similar in appearance to those which had been observed initially in core CBBL 16-BS-TC which was recovered in February with no attempt to maintain the sample at *in situ* pressure.

Fortunately, the CT scans of box core subsamples provided almost no indications of free gas in these nonpressurized samples. The limited indications of such gas in these samples are described in following sections of this report. These, 'no free gas features in the upper few centimeters' observations from the box core subsamples are consistent with observations from the pressurized cores which indicate that, under *in situ* pressure conditions, little or no evidence of free gas occurs for segments of samples of the upper 50 cm or so of the seafloor.

Unfortunately, the CT scan of core CBBL-308-BS-GC indicates that, at the time the core was scanned, it exhibited indications of a fairly large number of the free gas filled fractures which seem to be associated with pressure release of the samples. This may imply that at least some of the cores taken with the expanding plugs inserted may not have maintained their samples under *in situ* pressure conditions. At least this is a factor which will have to be taken into account in the interpretation of other measurements on the samples by other investigators.

Pressure Tight Samples

Both the Eckernfoerde Bay samples recovered under pressure tight conditions in February in the steel pressure chambers and those recovered in May in the aluminum pressure chambers are providing valuable information for use in constraining acoustic volume scattering models for this region. Although we have only recently developed the capability to access the image data files for these samples and thus much quantitative analysis remains to be done, indications are that the upper 50 to 100 cm of the samples contain no evidence of large free gas containing features when the samples are maintained under pressure tight conditions. These shallowest segments are to be examined in greater detail for indications of small free gas features and also to determine how the profile of density varies with depth (for estimating acoustic volume scattering cross section). Initial indications, based on data from the p-wave logger (supplied to us by Bill Bryant and Niall Slowey), are that the variance of sound speed and density is at least two to three orders of magnitude smaller than the values for these parameters in cores from a distal lobe of the Monterey Fan off the coast of California. Thus, in a semi-quantitative manner we can observe that the internal volume scattering from within this upper 50 cm or so of the Eckernfoerde Bay seafloor should be very small except when there are localized occurrences of scatterers such as shells or larger grain size sediment, etc. This is entirely consistent with the preliminary indications from the CBBLSRP profiling records for the area.

In contrast to the (almost) gas free indications for the upper 50 cm or so, the deeper samples which were recovered and CT scanned in pressure tight containers do indicate the presence of significant quantities of free gas bubbles within the seafloor under *in situ* conditions of temperature and pressure. The indications are not for a continuous 'cloud' of bubbles at all depths but rather for localized concentrations of a few bubbles separated by zones with no bubbles. The gassy and gas free zones are typically of a few cm extent in the vertical. Two examples of gassy images are shown in Fig. 3. This figure provides both an indication of the nature of some of the larger bubbles which have been noted in the scans and an illustration of the happy fact that we now are working with the decompressed files of data in College Station. For the images in Fig. 3, in contrast to those in Fig. 2, the more familiar convention of 'dark' indicating low density (e.g. bubbles) is used.

Box Core Subsamples

Environmental Characteristics of Sediment Structure
and Property Variability

Geotechnical property characteristics, the radiographs and CT results show clear geographic (environmental) differences in the nature of sediment structure and sediment physical properties (Fig. 4). The greatest physical variability (CT variability) occurs in sediments of the southwestern part of the bay near the harbor entrance (CBBL 260-BS-BC & CBBL 263-BS-BC). Radiographs reveal laminated sediments, presumably created by hydrodynamic processes. Of the environments examined, this region is generally the most vulnerable to storm wave activity, which is probably responsible for the creation and maintenance of these sedimentary structures. Evidence of biological activity is minimal, generally restricted to a few tubular structures within the oxidized layer (diameters: ~1 mm). Other inhomogeneities include consolidated clay balls (diameter: 2-5 mm), scattered pockets of low-density black organic detritus, twigs, and eel grass, all of which is indicative of a high energy environment. Shells and/or shell fragments are uncommon.

The lowest physical variability was found in sediments of the deep, muddy faces of central Eckernfoerde Bay (CBBL 227-BS-BC & CBBL 264-BS-BC). This is also the general vicinity of the acoustic scattering measurements taken with the towers and is near the location of other cores taken specifically to characterize the acoustic measurement sites (Fig. 4). Radiographs of cores CBBL 260-BS-BC and CBBL 263-BS-BC reveal laminae in the upper 7-8 cm of the sea floor, which overlie more homogenous material. Several small articulated shells (1-2 mm) and a few tubes (diameter: 1 mm) are the only other volume inhomogeneities observed on the radiographs. The silty quartz-rich laminae are interpreted as storm deposits. Suspended silts, eroded from Mittelgrund and from the beaches surrounding Eckernfoerde Bay, are deposited in the deeper, more quiescent environment of the central bay. CT images reveal that these deposits have been reworking somewhat by benthos, while other zones exhibit substantial evidence of horizontal burrowing.

Cores CBBL 250-BS-BC and CBBL 268-BS-BC, obtained along the southwestern flank of Mittelgrund, exhibit intermediate values of physical (CT) variability, but more closely resemble sediments of the SW bay in magnitude than those of the muddy central facies (Fig. 4). In contrast to the laminated structures of sediments of the harbor entrance, biological structures dominate the Mittelgrund sediments. The reduced muds are mottled and among the heterogeneities are numerous pockets of apparently coarser-grained sediment, i.e., feeding voids. In CBBL 268-BS-BC, one of the feeding voids consisted of well-defined zones of very clean, light gray sand; by contrast, a large feeding void in CBBL 250-BS-BC exhibited only a nominal change in grain size. Given the overall sandy nature of the sediments in CBBL 250-BS-BC, the higher density of the sediments within the feeding void may be due to a differential packing of particles. Other inhomogeneities are limited to a few scattered shells (~0.5 cm in diameter) throughout the cores.

Figure 5 shows an interesting relationship between CT bulk density and standard deviation. The peaks in standard deviation in the upper 2 cm of CBBL 227-BS-BC correspond to the oxidized zone, similar to the well-mixed layer of *Berger et al.* [*Mar. Geol.*, v. 32, 1979]. By contrast, density and standard deviation peaks from 2-11 cm depth are caused by silty storm laminae, and represent Berger's transition zone. At the base of the transition zone, CT bulk densities increase markedly while standard deviations decrease throughout the remainder of the core. This zone corresponds to the historical layer, which *Berger et al.* [1979] define as the zone of sediments that has subsided below the depth of active mixing by organisms. While this sequence is generally best developed within the central bay sediments, it is also observed in CBBL 250-BS-BC near Mittelgrund.

Common Horizontal Structures (Macroscale Fabric). Several common sediment fabric types were revealed by CT. In most instances, these CT fabrics were not readily apparent during visual inspection of the sediments or during examination of the radiographs of the subsamples.

(1) *Homogeneous Fabric* (Fig. 6). This fabric mainly corresponds to sediments of the oxidized layer. Commonly, no sedimentary structures are present but variability at very fine scale, as suggested by the standard deviation of CT bulk density (.006 to .010 Mg/m^3), can be moderately high (Fig. 5). Sediment bulk densities are low. Small-scale tubes and burrows, below the

resolution of the CT scanner, probably maintain the low density and induce variability through a fabric reminiscent of "speckle" noise.

(2) *Storm Deposits* (Fig. 7). Vertical CT density profiles of Eckernfoerde Bay sediments are commonly punctuated by density "peaks" corresponding to discrete silty storm deposits. The highest degree of variability observed in sediments of Eckernfoerde Bay is also associated with these sedimentary structures. CT images shows that the "higher density" sediments of the storm layers are patchily distributed, explaining the higher standard deviations associated with these layers. Differential sedimentation and/or burrowing, may be response for the observed patchiness.

(3) *Feeding Voids* (Fig. 8). Another type of high density and highly variable patchiness, similar to the fabric of the storm deposits, was observed in several CT sequences, but differs in that more-or-less linear structures are produced. This fabric probably represents feeding voids or pockets produced by benthic infauna.

(4) *Burrows* (Fig. 9). Burrows are common in Eckernfoerde Bay sediments and generally occur in zones. Individual burrows are large (typically 3-5 mm in diameter), generally well-developed, and are easily identified by a characteristic low density "trough" surrounded by "plateaus" of higher density sediments (Fig. 10). Burrows tend to migrate within a horizontal plane up to ~6 mm thick; and by doing so, they rarely cross-cut other burrows. The physical variability induced by the burrows appears to be nominal overall, although rapid fluctuations can occur over small vertical distances (e.g., from image to image). By contrast, tubes are not as common, but are of similar dimensions when present.

(5) *Gas Expansion Cavities* (Fig. 11). CT images of Core CCBL 250-BS-BC exhibit random structural patterns caused by low density features within the higher density matrix. The low density features are generally isolated and in many instances may be cavities within the sediments. Whether they are (or were) gas-filled, and more importantly, whether they were present *in situ* or are not known. In one instance, an accurate feature was observed that extended over a vertical distance greater than 1 cm. This "fracture" behavior is similar to fracture patterns that were observed in known gassy Eckernfoerde mud scanned at the Radiologische Gemeinschaftspraxis Prüner Gang. The vertical fracture patterns were caused by the expansion of gas resulting from the release of hydrostatic pressure; pressurized samples do not show these structures, or if so, they were much less abundant. Interestingly, the gas expansion features appear to have a nominal effect on the physical property variability.

Comparison with Other CBBL Investigations

Recently, Dr. Kathleen Fischer (NRL-SSC) provided us with her laboratory density measurements for another subsample from CBBL 250-BS-BC taken ~10 cm away from our subsample. The deviation of densities between the two data sets in the upper 11 cm is slight and probably a function of the natural variability of the sediments (Fig. 12). High density material associated with feeding voids in the sediments collected for this study is quite apparent, but the structure was not sampled by NRL-SSC. This attests to highly variable lateral characteristics of

Eckernfoerde Bay sediments. Interestingly, values for both data sets converge at about 11 cm (disregarding the mismatch between 11-15 cm caused by the feeding void). This depth corresponds to the depth of the historical layer where CT densities increase markedly while their standard deviations in fact decrease.

CONCLUSION

The information generated to date in this study indicates that we will be able to achieve the goals for the task. The internal heterogeneity on subdecimeter scales is clearly indicated, especially in the box core subsamples from Eckernfoerde Bay. The data files for samples scanned in Kiel are now available for further analysis which is proceeding. It is clear that information is available for describing the distribution of free gas in the samples we have taken.

The work to date has allowed interesting interpretation possibilities which should be compared with results from other investigators. Some of our comparisons so far have been very encouraging. The work has also provided considerable data for the sediment internal heterogeneity and has directly impacted the sampling methodology for studying the sediments.

There is much work yet to be done. The information in the scans for the gas tight samples must (and is to be) interpreted in terms of free gas concentration and distribution within the seafloor. These results together with the density distribution results will be incorporated into acoustic volume scattering cross section estimates.

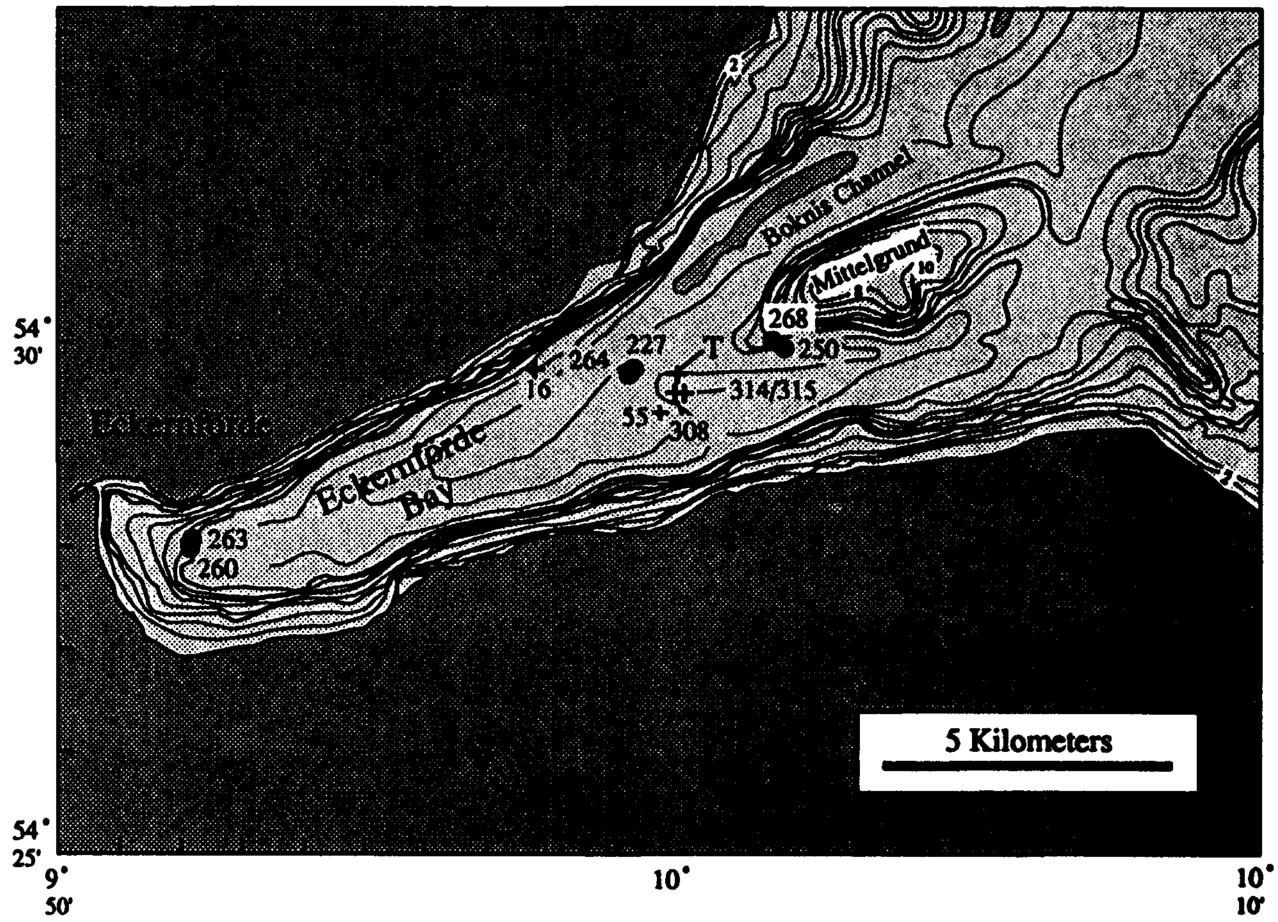

Fig. 1. Eckernförde Bay and location of sediment cores. Solid circles = box core subsamples scanned at Texas A&M University; pluses = samples scanned at Radiologische Gemeinschaftspraxis Prüner Gang in Kiel, Germany; and T = the backscattering tower.

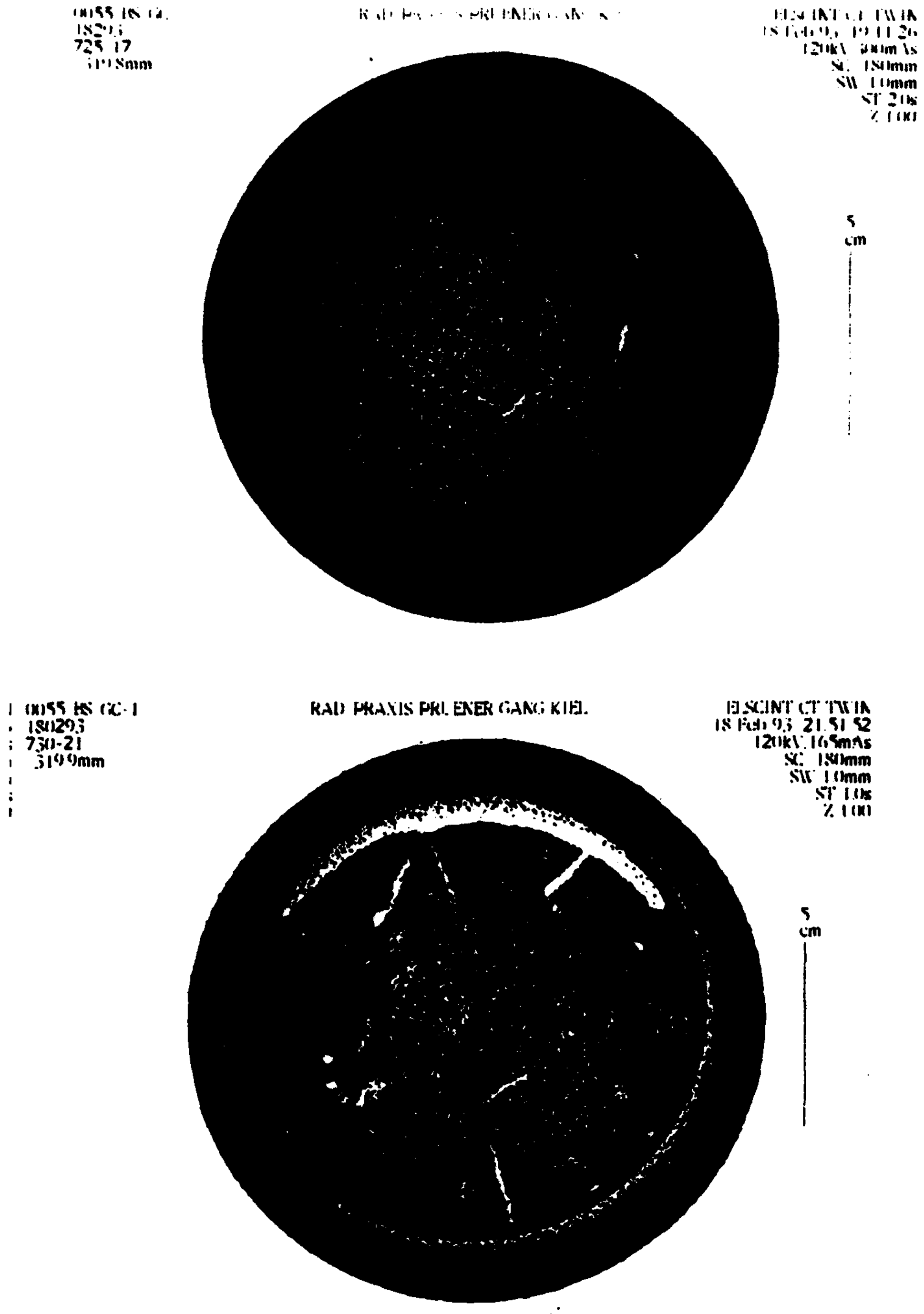

Fig. 2 CT scan images of single slices at equivalent locations in the deepest 1 m segment of core CBBL 55-BS-GC. The top image was made with the sample maintained at *in situ* pressure, the bottom image was made after the pressure chamber was opened and the section was allowed to equilibrate to atmospheric pressure.

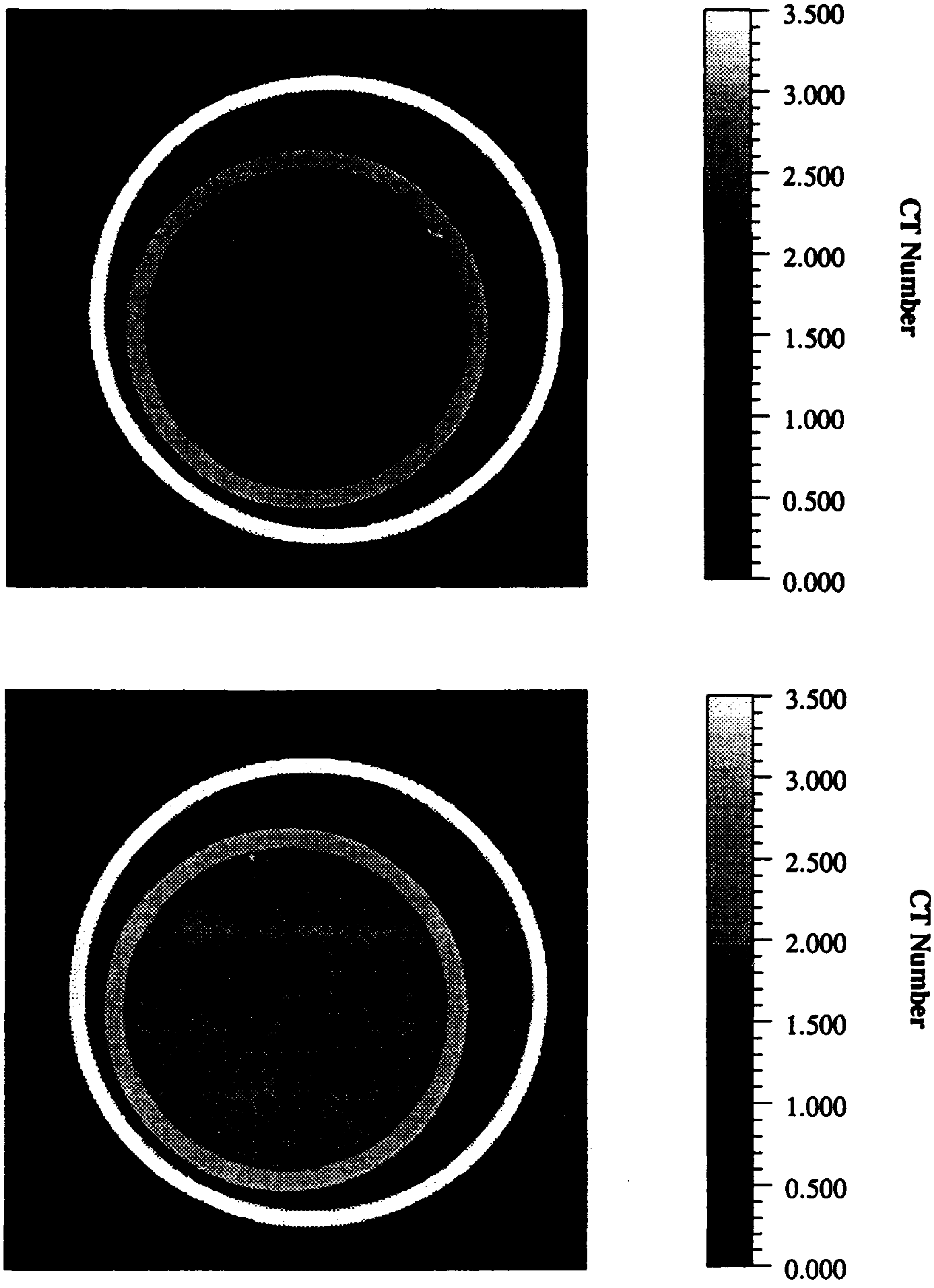

Fig. 3 Two images of different gassy sections of CBBL 315-BS-GC with free gas bubbles. Outer circle is the aluminum pressure chamber, inner circle is core liner. Gas bubbles are dark features with CT Number values below 1.0. Four or five bubbles are evident in the top image while only a single large bubble, together with several water filled features, are evident in the bottom image.

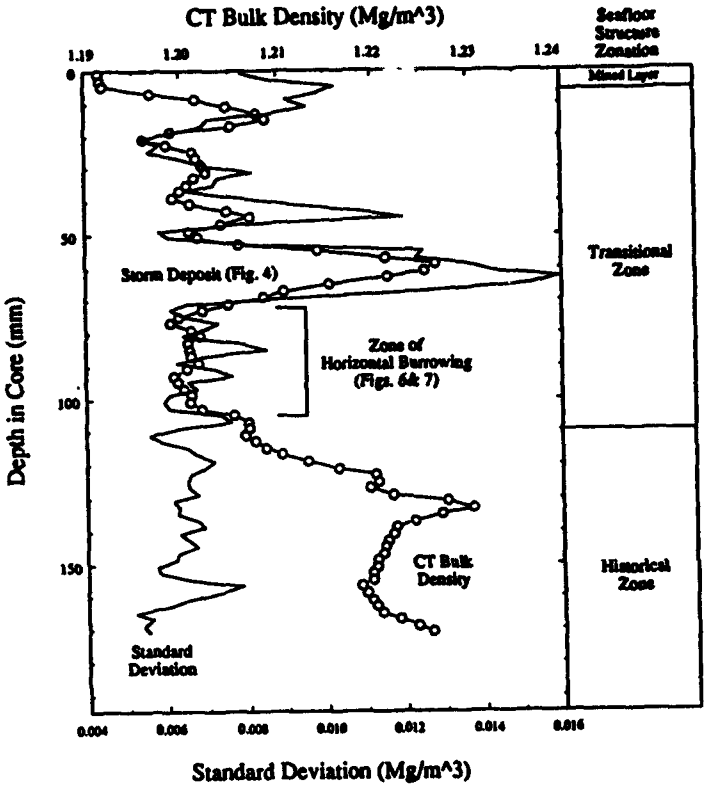

Fig. 5. Sediment depth profiles of CT bulk density and standard deviation for CBBL 227-BS-BC. Also shown is the seafloor structural zonation of Berger, developed using burrow stratigraphy in equatorial Pacific carbonate sediments. Interpreted zones imply a possible similar structural origin that may beuseful in developing a geoacoustic stratigraphy for Eckernförder Bay. The mixed layer is sediment zone of low density and moderate variability generated by small-scale bioturbation. The underlying transitional zone is a region of high density and variability created by large-scale mixing. The historical zone is characterized by a rapid increase in sediment bulk density and relatively low (or constant) variability, and represents sediments that have subsided below the zone of active mixing. Biological structures preserved in the historical zone were produced in the transitional zone and are typically large-scale.

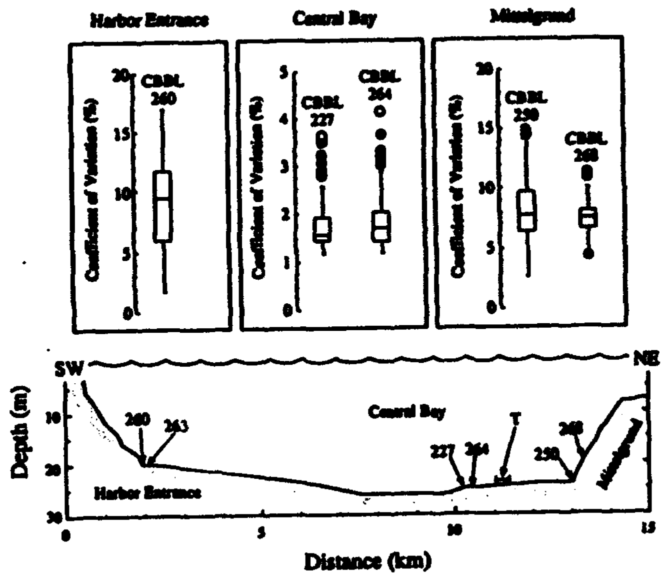

Fig. 4. Physical variability of Eckernförde Bay sediment based on CT results. Coefficient of variation (CV%) = 100(standard deviation/mean). Variability is highest among the laminated sediments in the southwestern portion of the bay near the harbor entrance and lowest in laminated-bioturbated sediments from the muddy central bay. Sediments along the southwestern flank of Mittelgrund exhibit large-scale biological structures and are characterized by intermediate, but still high, variability. T is site of backscattering tower and cores 308, 314 and 315.

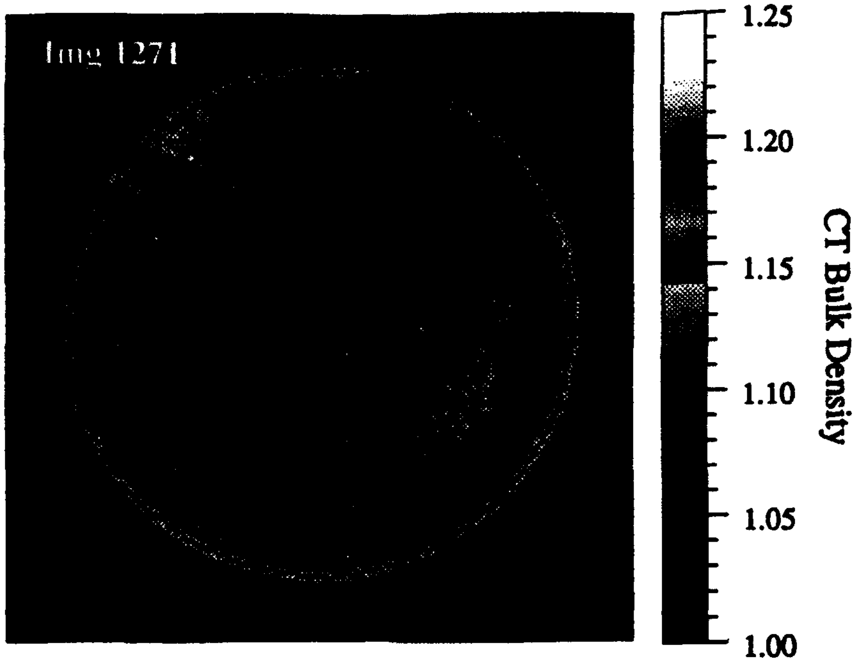

Fig. 6. Homogeneous fabric (Core CBBL 264-BS-BC, Central Bay, Eckernförde Bay). Depth in core: 23 mm; Mean CT bulk density: 1.188 Mg/m^3; CT density standard deviation: 0.006 Mg/m^3. The dimensions of this and all subsequent images are 85 mm x 85 mm x 2 mm unless specified otherwise.

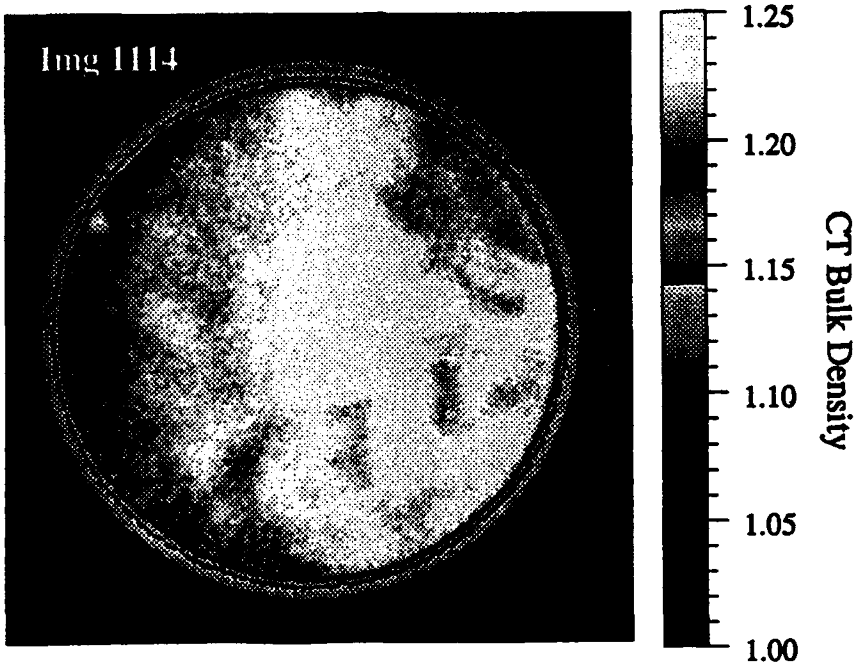

Fig. 7. Storm deposit (Core CBBL 227-BS-BC, Central Bay, Eckernförde Bay). Depth in core: 59 mm; Mean CT bulk density: 1.227 Mg/m^3; CT density standard deviation: 0.014 Mg/m^3.

Fig. 8. Feeding void (Core CBBL 250-BS-BC, Mittelgrund, Eckernförde Bay). Depth in core: 117 mm; Mean CT bulk density: 1.685 Mg/m^3; CT density standard deviation: 0.167 Mg/m^3.

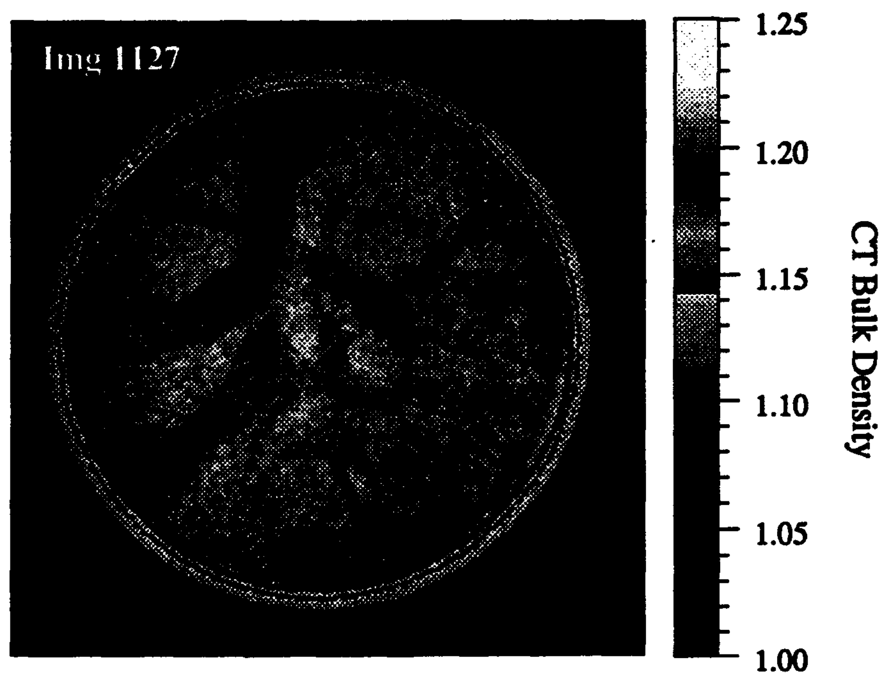

Fig. 9. Burrow fabric (Core CBBL 227-BS-BC, Central Bay, Eckernförde Bay). Depth in core: 85 mm; Mean CT bulk density: 1.201 Mg/m^3; CT density standard deviation: 0.009 Mg/m^3.

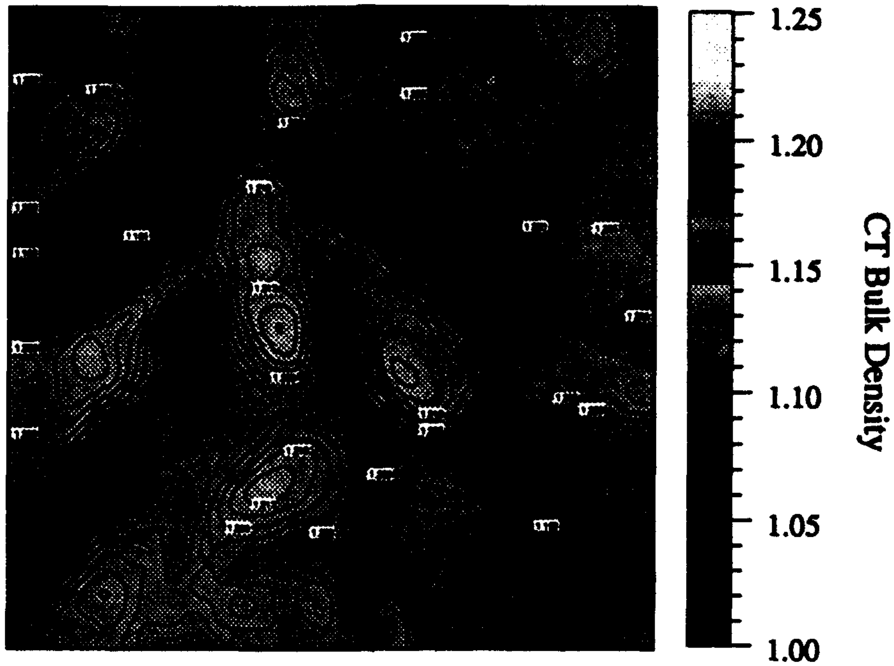

Fig. 10. Contoured region-of-interest from Image 1127 in Fig. 9. Original ROI (region-of-interest) at top and the contoured (smoothed) image at bottom have dimensions of 40 mm x 40 mm x 2 mm. C.I.: 0.0025 Mg/m^3. Note the "trough" of low density and surrounding "plateaus" of higher density.

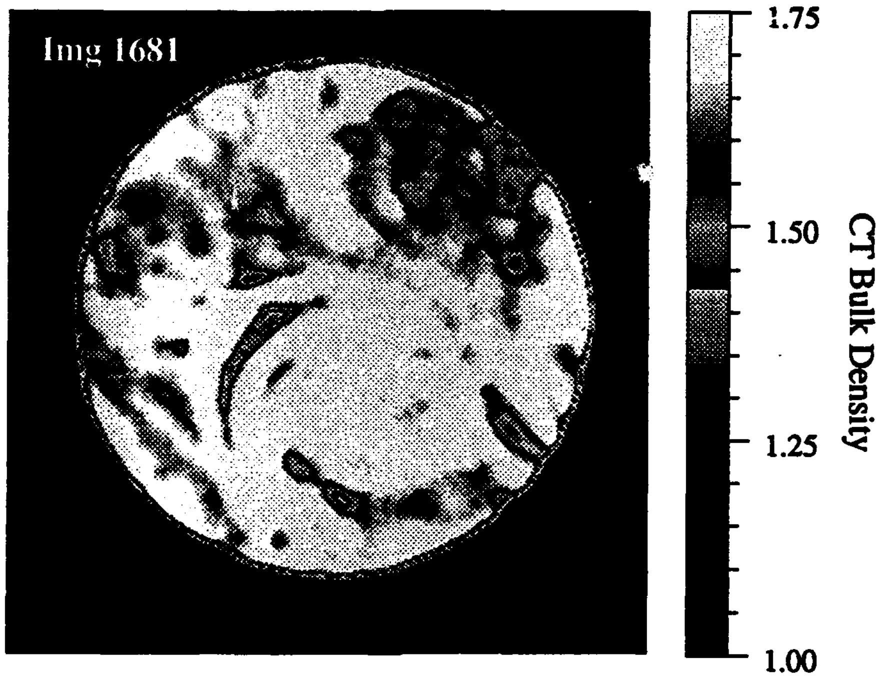

Fig. 11. Gas expansion cavities (Core CBBL 250-BS-BC, Mittelgrund, Eckernförde Bay). Depth in core: 157 mm; Mean CT bulk density: 1.709 Mg/m^3; CT density standard deviation: 0.098 Mg/m^3.

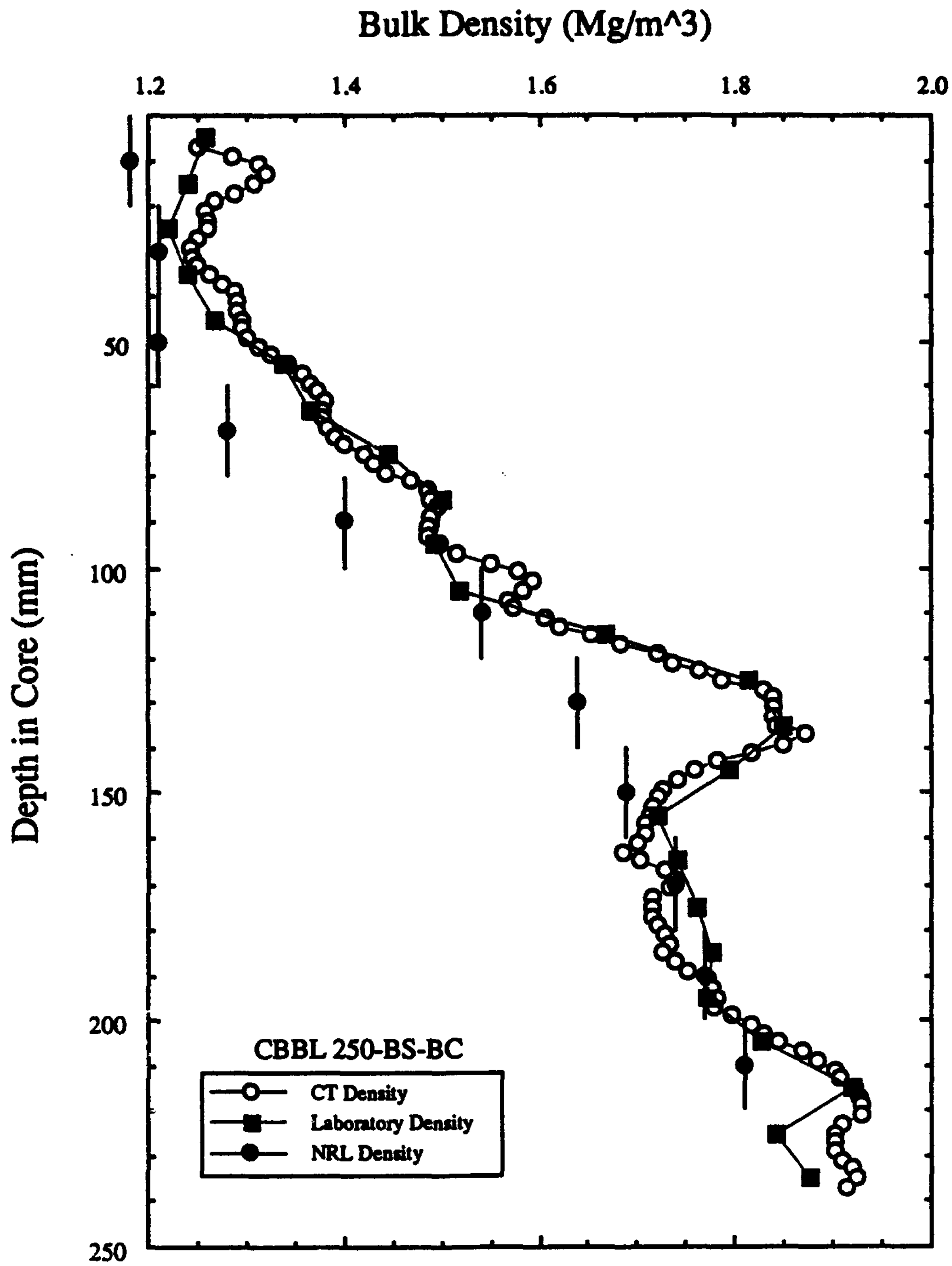

Fig. 12. CT and laboratory-derived bulk densities with depth for CBBL 250-BS-BC. Solid circles are measurements made by NRL-SSC [*Fischer*, unpublished data], where vertical bars denote extent of material sampled for each measurement.

APPENDIX

This appendix contains details of the CT scan and physical analysis results for the box core subsamples from Eckernförde Bay beyond those specifically referred to in the text. Information here includes:

Tables of values from the physical analysis for all six of the box core subsamples

Profiles of bulk density for the five box core subsamples which were CT scanned in College Station. On these five profiles, values are also plotted both for CT density estimates and for the actual densities determined from the physical sampling and analysis of the cores.

Profiles of water content versus depth for all six of the box core subsamples.

Geotechnical Properties of Core CBBL 227-BS-BC

Sample Interval (cm)	Water Content (%)	Grain Density (Mg/m^3)	Bulk Density (Mg/m^3)	Porosity (%)	Grain Size Distribution		
					% Sand	% Silt	% Clay
0-1	315	2.59	1.190	88.8	0.4	39.4	60.3
1-2	282	2.65	1.211	88.0	0.9	35.1	64.0
2-3	295	2.57	1.199	88.1	0.7	35.3	64.0
3-4	294	2.60	1.201	88.2	0.4	35.4	64.2
4-5	296	2.55	1.198	88.1	0.4	42.2	57.4
5-6	266	2.62	1.220	87.2	0.7	50.2	49.1
6-7	261	2.59	1.221	86.9	0.7	63.6	35.8
7-8	298	2.56	1.197	88.2	0.2	56.8	43.0
8-9	306	2.55	1.192	88.4	0.3	52.3	47.3
9-10	300	2.67	1.202	88.7	0.4	52.1	47.4
10-11	279	2.61	1.211	87.7	0.5	61.7	37.8
11-12	263	2.51	1.215	86.6	0.8	49.5	49.8
12-13	257	2.56	1.222	86.6	0.6	56.7	42.7
13-14	264	2.61	1.221	87.1	1.0	52.1	46.9
14-15	262	2.55	1.218	86.7	0.3	44.9	54.8
15-16	256	2.57	1.223	86.6	0.4	38.0	61.6
16-17	253	2.51	1.221	86.1	0.4	59.8	39.8
17-18	258	2.65	1.227	87.0	0.2	45.9	54.0
18-19.5	257	2.67	1.229	87.1	0.2	30.6	69.3

Note: Values have been corrected for a pore water salinity of 25 ppt.

Geotechnical Properties of Core CBBL 250-BS-BC

Sample Interval (cm)	Water Content (%)	Grain Density (Mg/m^3)	Bulk Density (Mg/m^3)	Porosity (%)	Grain Size Distribution % Sand	% Silt	% Clay
0-1	219	2.63	1.258	84.9	26.8	31.8	41.4
1-2	241	2.66	1.241	86.3	16.8	36.2	46.9
2-3	264	2.60	1.220	87.0	27.6	36.2	36.2
3-4	233	2.54	1.239	85.2	39.3	28.0	32.8
4-5	206	2.63	1.269	84.3	53.6	19.6	26.8
5-6	153	2.61	1.339	79.6	58.4	18.5	23.0
6-7	137	2.59	1.367	77.6	62.0	17.7	20.2
7-8	104	2.59	1.446	72.6	67.1	15.4	17.5
8-9	89	2.61	1.501	69.5	73.2	12.0	14.8
9-10	89	2.56	1.492	69.1	76.0	11.0	13.0
10-11	83	2.58	1.519	67.7	85.5	6.2	8.3
11-12	57	2.64	1.668	59.8	87.8	5.4	6.8
12-13	41	2.68	1.815	51.9	84.8	7.1	8.1
13-14	37	2.67	1.849	49.6	79.0	9.0	12.0
14-15	40	2.60	1.795	50.8	80.5	10.0	9.5
15-16	49	2.60	1.721	55.5	85.3	6.1	8.6
16-17	48	2.65	1.742	55.6	87.6	6.2	6.2
17-18	45	2.64	1.761	54.1	85.4	5.5	9.2
18-19	45	2.67	1.778	53.9	87.9	5.2	6.9
19-20	43	2.61	1.772	52.5	90.3	4.3	5.4
20-21	38	2.62	1.826	49.5	92.2	4.7	3.1
21-22	30	2.63	1.921	43.9	91.4	3.0	5.7
22-23	36	2.59	1.841	47.5	91.5	3.4	5.2
23-24	33	2.61	1.877	45.9	89.9	4.5	5.6

Note: Values have been corrected for a pore water salinity of 25 ppt.

Geotechnical Properties of Core CBBL 260-BS-BC

Sample Interval (cm)	Water Content (%)	Grain Density (Mg/m^3)	Bulk Density (Mg/m^3)	Porosity (%)	Grain Size Distribution		
					% Sand	% Silt	% Clay
0-1	201	2.59	1.273	83.6	4.1	51.1	44.8
1-2	178	2.74	1.314	82.7	3.2	34.4	62.3
2-3	137	2.68	1.376	78.4	7.1	61.5	31.4
3-4	103	2.67	1.462	73.1	9.3	61.4	29.3
4-5	162	2.69	1.333	81.0	5.2	60.3	34.5
5-6	122	2.70	1.412	76.4	10.1	64.4	25.5
6-7	172	2.54	1.303	81.1	33.2	39.2	27.6
7-8	69	2.64	1.596	64.2	83.8	9.4	6.8
8-9	41	2.72	1.827	52.3	78.9	14.1	7.0
9-10	43	2.71	1.802	53.6	69.6	21.7	8.7
10-11	65	2.62	1.613	62.7	58.9	25.7	15.4
11-12	103	2.57	1.446	72.2	53.6	30.3	16.1
12-13	93	2.68	1.497	71.1	65.2	22.5	12.3

Note: Values have been corrected for a pore water salinity of 25 ppt.

Geotechnical Properties of Core CBBL 263-BS-BC

Sample Interval (cm)	Water Content (%)	Grain Density (Mg/m^3)	Bulk Density (Mg/m^3)	Porosity (%)	Grain Size Distribution % Sand	% Silt	% Clay
0-1	201	2.61	1.274	83.7	4.9	57.1	38.0
1-2	247	2.62	1.233	86.4	2.2	57.2	40.6
2-3	182	2.63	1.298	82.5	3.1	58.2	38.7
3-4	182	2.71	1.305	82.9	12.7	67.1	20.3
4-5	120	2.72	1.420	76.3	4.9	56.4	38.7
5-6	90	2.71	1.516	70.5	15.2	63.1	21.7
6-7	193	2.71	1.291	83.7	10.6	55.7	33.7
7-8	128	2.70	1.398	77.3	11.0	63.3	25.7
8-9	118	2.66	1.417	75.6	11.1	53.4	35.5
9-10	192	2.67	1.289	83.4	15.5	49.3	35.2
10-11	159	2.61	1.329	80.3	36.0	35.3	28.7
11-12	91	2.56	1.485	69.5	82.4	8.7	8.9
12-13	43	2.64	1.786	52.6	79.2	13.0	7.8
13-14	76	2.64	1.564	66.2	31.6	41.3	27.1
14-15	112	2.66	1.434	74.5	5.4	54.3	40.3
15-16	86	2.67	1.484	71.6	4.2	63.1	32.7
16-17	61	2.65	1.646	61.4	11.9	64.3	23.7
17-18	96	2.63	1.479	71.3	11.5	57.6	31.0
18-19	137	2.63	1.370	78.0	8.9	66.0	25.1
19-20	162	2.55	1.319	80.2	6.0	57.4	36.6
20-21	166	2.64	1.322	81.1	4.7	54.9	40.4
21-22	161	2.63	1.328	80.6	10.1	61.1	28.8
22-23	118	2.55	1.403	74.7	7.8	61.1	31.1
23-24	114	2.68	1.431	75.0	6.7	56.9	36.4
24-25	100	2.62	1.465	72.0	4.6	56.0	39.5
25-26.5	108	2.61	1.437	73.5	12.2	55.3	32.4

Note: Values have been corrected for a pore water salinity of 25 ppt.

Geotechnical Properties of Core CBBL 264-BS-BC

Sample Interval (cm)	Water Content (%)	Grain Density (Mg/m^3)	Bulk Density (Mg/m^3)	Porosity (%)	Grain Size Distribution % Sand	% Silt	% Clay
0-1	333	2.51	1.177	89.1	1.1	39.5	59.4
1-2	310	2.54	1.189	88.5	1.2	51.7	47.1
2-3	332	2.49	1.177	88.9	0.7	45.5	53.8
3-4	289	2.54	1.200	87.7	0.9	56.3	42.9
4-5	268	2.53	1.212	86.9	1.2	59.4	39.3
5-6	293	2.63	1.204	88.3	1.2	55.5	43.2
6-7	290	2.51	1.199	87.7	0.7	52.9	46.4
7-8	290	2.53	1.199	87.8	0.8	58.7	40.5
8-9	269	2.59	1.216	87.2	1.0	57.9	41.1
9-10	269	2.55	1.213	87.0	1.0	49.1	49.9
10-11	259	2.54	1.220	86.5	0.9	57.1	42.1
11-12	246	2.51	1.227	85.8	1.9	59.7	38.5
12-13	244	2.59	1.234	86.0	2.5	50.5	47.0
13-14	255	2.57	1.225	86.5	1.6	56.4	42.0
14-15	269	2.47	1.208	86.6	1.4	50.7	47.9
15-16	265	2.50	1.213	86.6	1.1	52.3	46.6
16-17	259	2.59	1.223	86.8	1.0	58.2	40.8
17-18	265	2.58	1.218	87.0	0.9	55.7	43.4
18-19	261	2.52	1.217	86.6	0.9	57.8	41.3
19-20	272	2.48	1.207	86.8	0.5	57.9	41.6
20-21	280	2.61	1.210	87.7	0.4	50.2	49.4
21-22	280	2.67	1.213	88.0	0.4	59.5	40.1
22-23	263	2.54	1.216	86.7	0.4	50.9	48.7
23-24	264	2.56	1.217	86.9	0.6	44.1	43.5
24-25	275	2.51	1.207	87.1	0.8	59.5	39.7

Note: Values have been corrected for a pore water salinity of 25 ppt.

Geotechnical Properties of Core CBBL 268-BS-BC

Sample Interval (cm)	Water Content (%)	Grain Density (Mg/m^3)	Bulk Density (Mg/m^3)	Porosity (%)	Grain Size Distribution		
					% Sand	% Silt	% Clay
0-1	84	2.74	1.544	69.3	70.1	15.7	14.2
1-2	74	2.70	1.586	66.2	73.3	13.7	13.0
2-3	69	2.70	1.608	64.8	78.1	8.9	12.9
3-4	68	2.78	1.635	64.9	79.1	9.1	11.8
4-5	65	2.72	1.638	63.4	84.7	6.1	9.2
5-6	54	2.73	1.716	59.2	81.9	7.1	11.0
6-7	52	2.71	1.725	58.1	80.4	9.7	9.9
7-8	53	2.75	1.728	58.8	81.0	9.2	9.8
8-9	46	2.70	1.774	55.1	79.2	8.4	12.4
9-10	50	2.71	1.744	57.1	82.1	7.6	10.3
10-11	54	2.69	1.703	58.9	84.9	5.2	9.9
11-12	59	2.68	1.665	61.0	84.5	6.4	9.1
12-13	53	2.71	1.717	58.7	85.5	5.7	8.7
13-14	55	2.69	1.702	59.0	86.4	5.6	7.9
14-15	43	2.67	1.789	53.1	89.4	4.1	6.5
15-16	43	2.73	1.812	53.3	89.3	4.4	6.3

Note: Values have been corrected for a pore water salinity of 25 ppt.

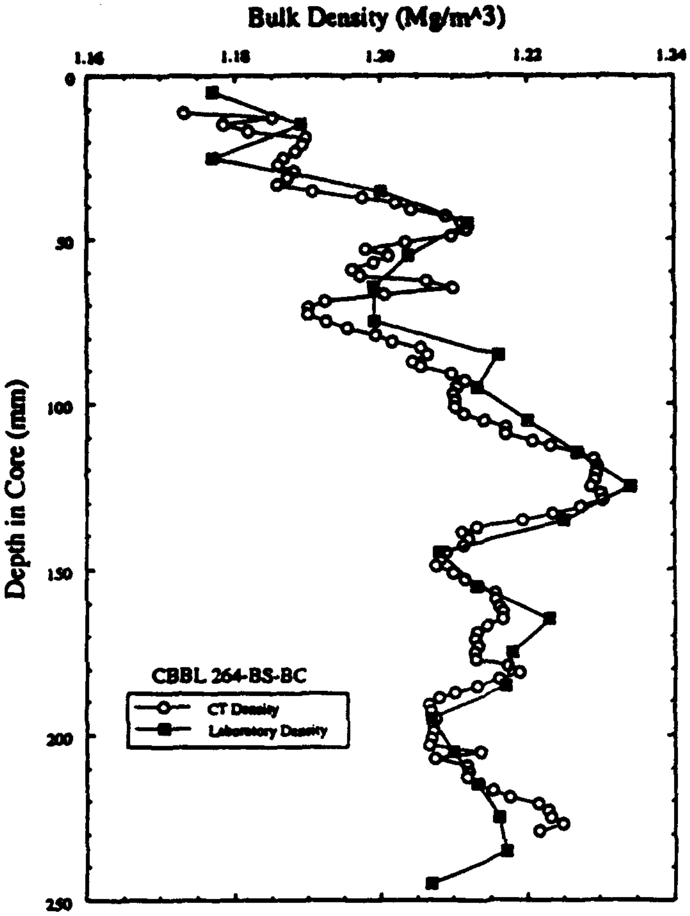
Bulk Density (Mg/m^3)
1.16
1.18
1.20
1.22
1.24
Depth in Core (mm)
0
50
100
150
200
250
CBBL 264-BS-BC
CT Density
Laboratory Density

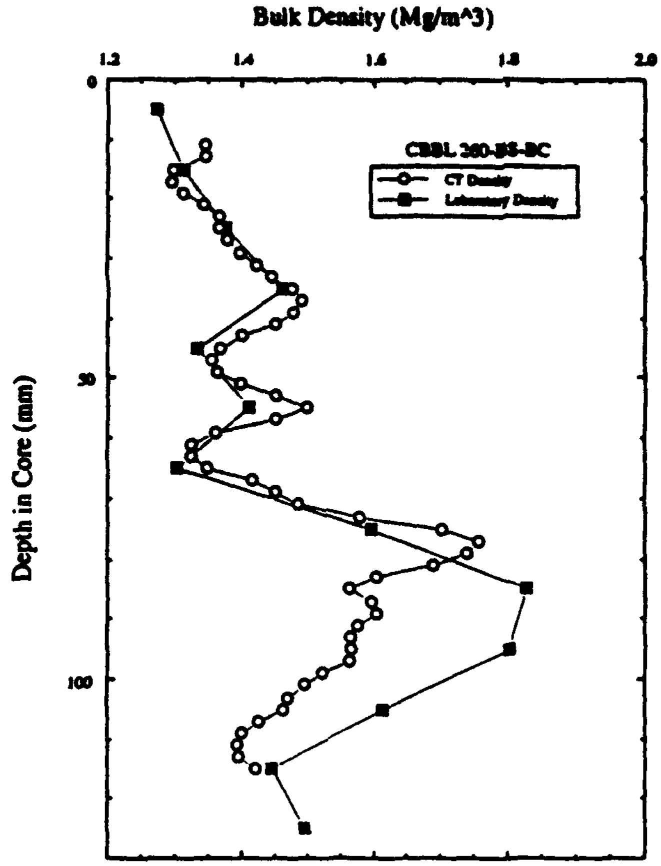
Bulk Density (Mg/m^3)
1.2
1.4
1.6
1.8
2.0
Depth in Core (mm)
0
50
100
CBBL 260-BS-BC
CT Density
Laboratory Density

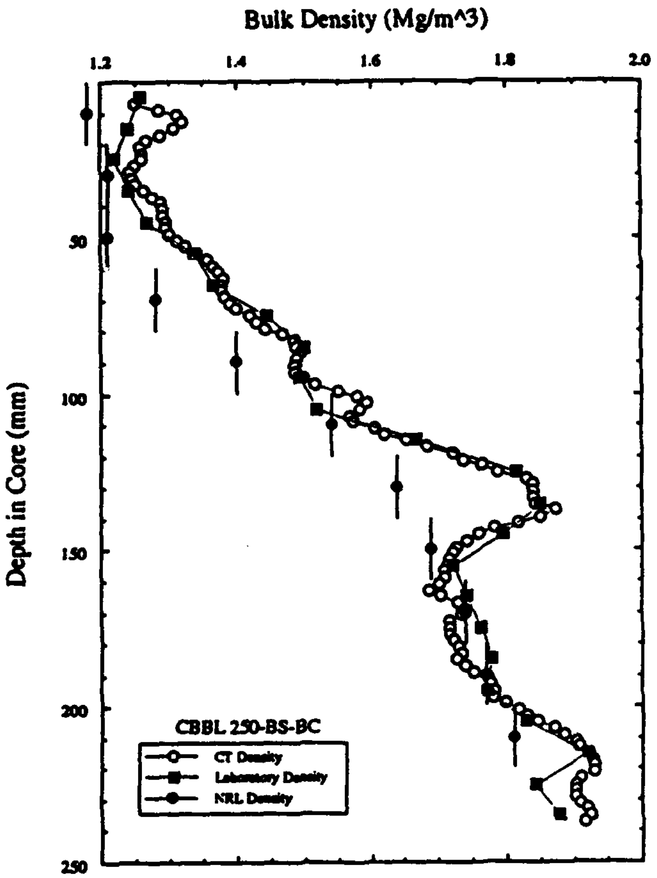
Bulk Density (Mg/m^3)
1.2
1.4
1.6
1.8
2.0
Depth in Core (mm)
50
100
150
200
250
CBBL 250-BS-BC
CT Density
Laboratory Density
NRL Density

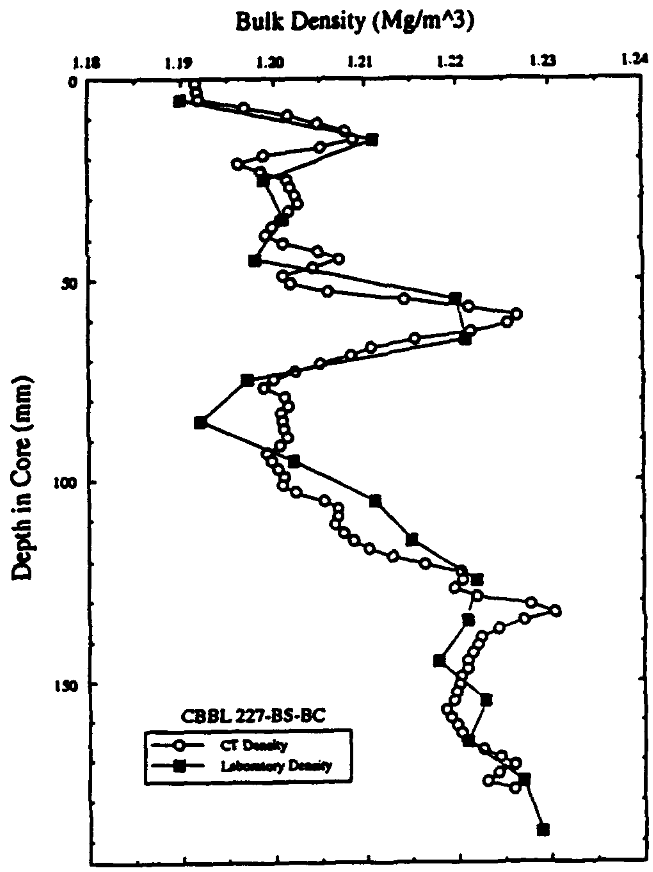
Bulk Density (Mg/m^3)
1.18
1.19
1.20
1.21
1.22
1.23
1.24
Depth in Core (mm)
0
50
100
150
CBBL 227-BS-BC
CT Density
Laboratory Density

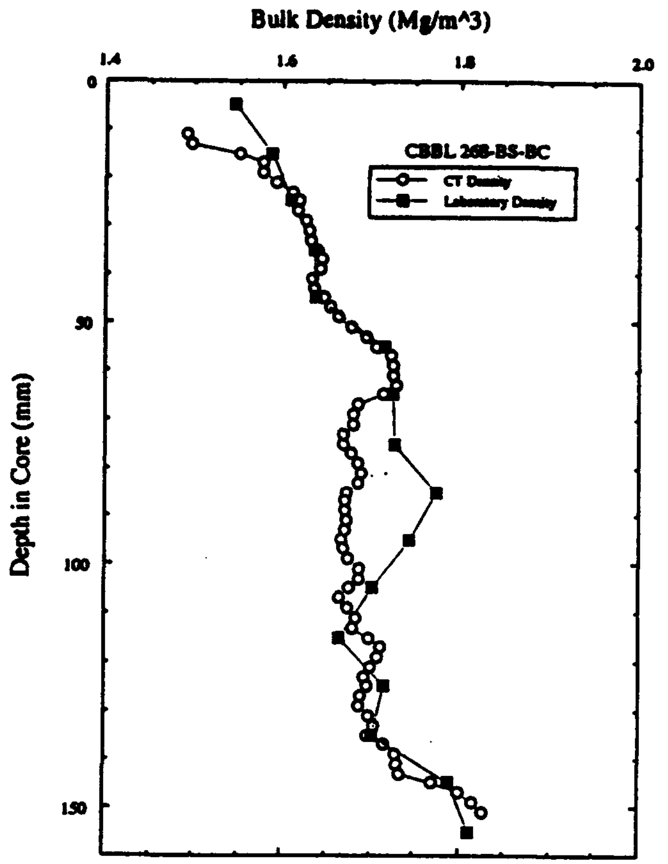

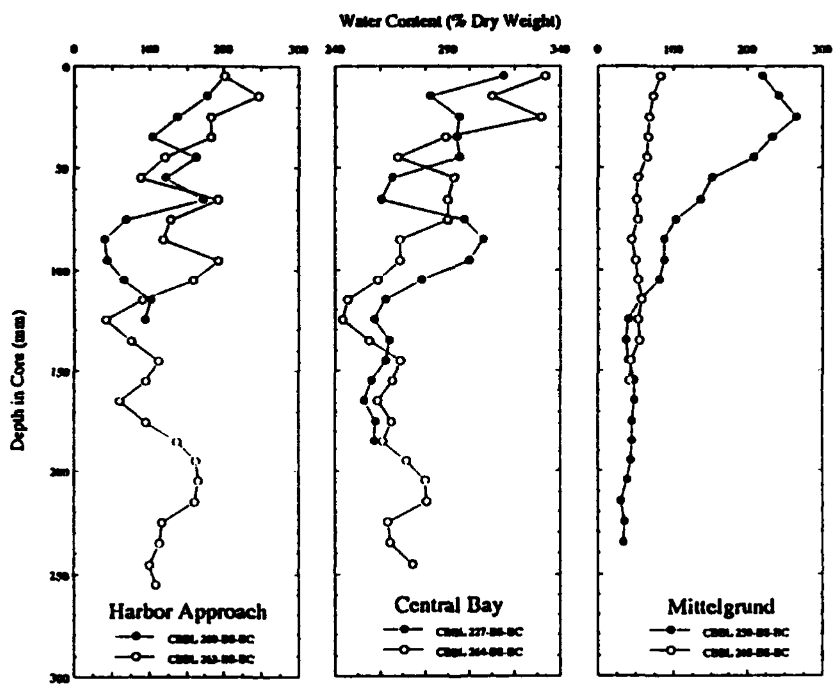

Sediment depth profiles of water content for cores of Eckernförder Bay.
Values have been corrected assuming a pore water salinity of 25 ppt.

3.2 Sediment Properties from Grain and Macrofabric Measurement (Principal Investigators: R. H. Bennett, R.J. Baerwald,, D. Lavoie, and M. H. Hulbert, University of New Orleans)

CBBLSRP FY93 YEAR-END REPORT

Roy J. Baerwald
Department of Biology
University of New Orleans
New Orleans, LA 70148

This report is a summary of research activities for the past 4.5 months, since the grant to UNO commenced as a new start in June, 1993. Technique development is one of the overall objectives of the grant.

I. First UNO efforts centered around coordinating activities with Dennis Lavoie and Dr. Richard Faas prior to the Eckernfoerde collecting trip, May, 1993. The objective was to supply them with an effective "in the field" working protocol for the collection of soda straw "minicore" sediment samples fixed with glutaraldehyde for the preservation of organics in the sediments. This was successful since both investigators were able to bring a number of properly fixed samples back to the states for future processing. Some field design changes were necessary for the successful collection of gassy sediments and are outlined in the Dennis Lavoie report. Details on the collection of minicores can be found in the Lavoie and Faas final reports.

II. Highest priority was assigned to pressurized microfabric samples that had been processed on site in Germany. Both horizontal and vertical oriented embedded sediment was supplied to the UNO lab for microfabric studies. The samples proved to be adequately dehydrated and embedded, so that high quality ultrasections were easily obtainable. These studies yielded several dozen photographs. Drs. Baerwald and Bennett collaborated on this phase at the UNO lab. Two representative horizontally (Fig. 1 and 2) and two vertically (Fig. 3 and 4) oriented sediment electron micrographs are presented in this report as preliminary data. An unusually high concentration of large voids (V) permeated the embedded sediment which greatly facilitated ultrasectioning. See Dr. Bennett for a discussions on the significance of the large pore spaces.

III. Technique development for serial sectioning for subsequent 3-D digital image processing is nearing completion. The technique employed Formvar coated narrow tabbed slot grids (12.5, 60, and 125 micron, and 0.4mm D). Critical technical considerations appear to be ideal slot width (0.4mm), study plastic support films, (Formvar), study grids (Cohen-Pelco Tabbed Grids #3HGC42S), and the use of a new and very sharp diamond knife. Preliminary microfabric studies indicate that the sediment, especially near the interface, are not highly consolidated. This greatly facilitated high quality ultrasections which is critical for serial section studies. Sediments that are not highly compressed have a higher ratio of embedding plastic to clay minerals which allowed for especially clean cut sections. We now have, in hand, serial sections of pressurized horizontal and vertical sediment material collected by Dennis Lavoie and are conducting electron microscope studies and EM photography of the material at UNO.

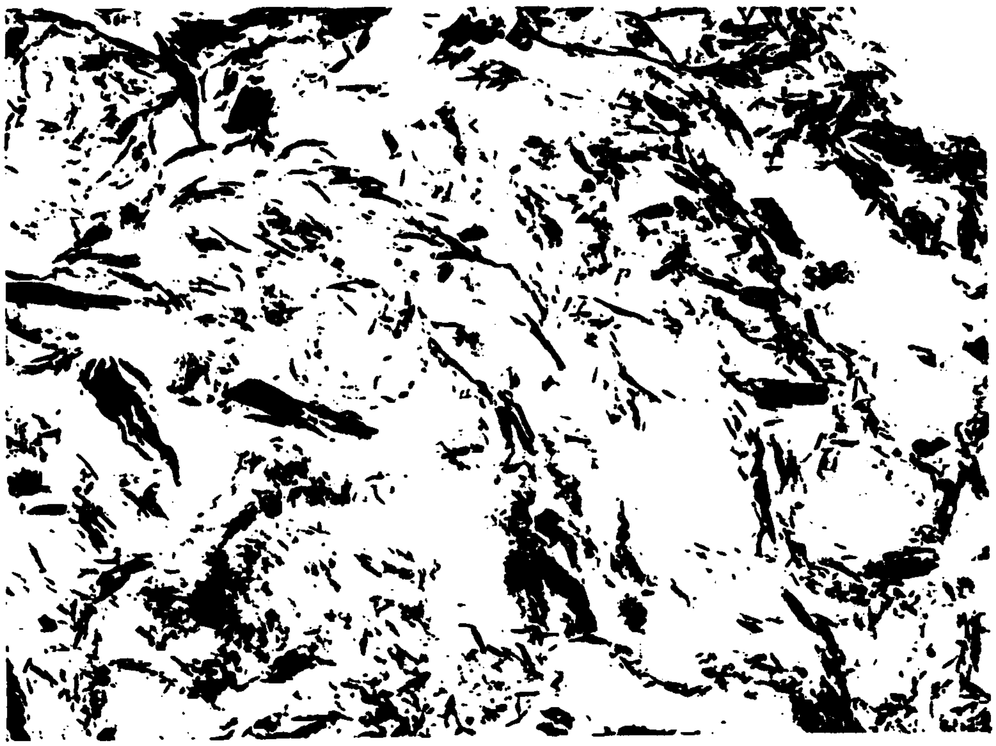

Fig. 1.Survey view transmission electron micrograph of pressurized Eckenforder gassy sediment, collected May, 1993. Sectioned parallel to the plane of sediment deposition (Horizontal) X 20,000.

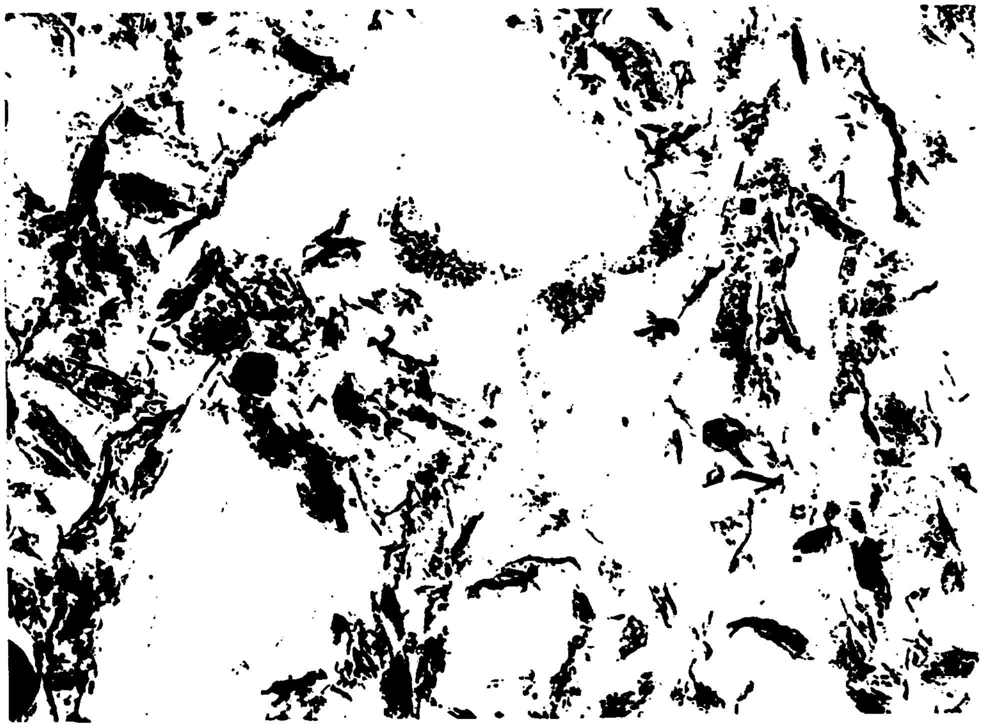

Fig. 2. Higher magnification view of horizontal section sediment showing 2 large voids. (V). Pressurized Eckenforder gassy sediment. X26,000.

Fig. 3. Survey view transmission electron micrograph of pressurized Eckenforder gassy sediment, May, 1993. Sectioned vertical to the plane of sediment deposition. Note two large voids (V). X20,000.

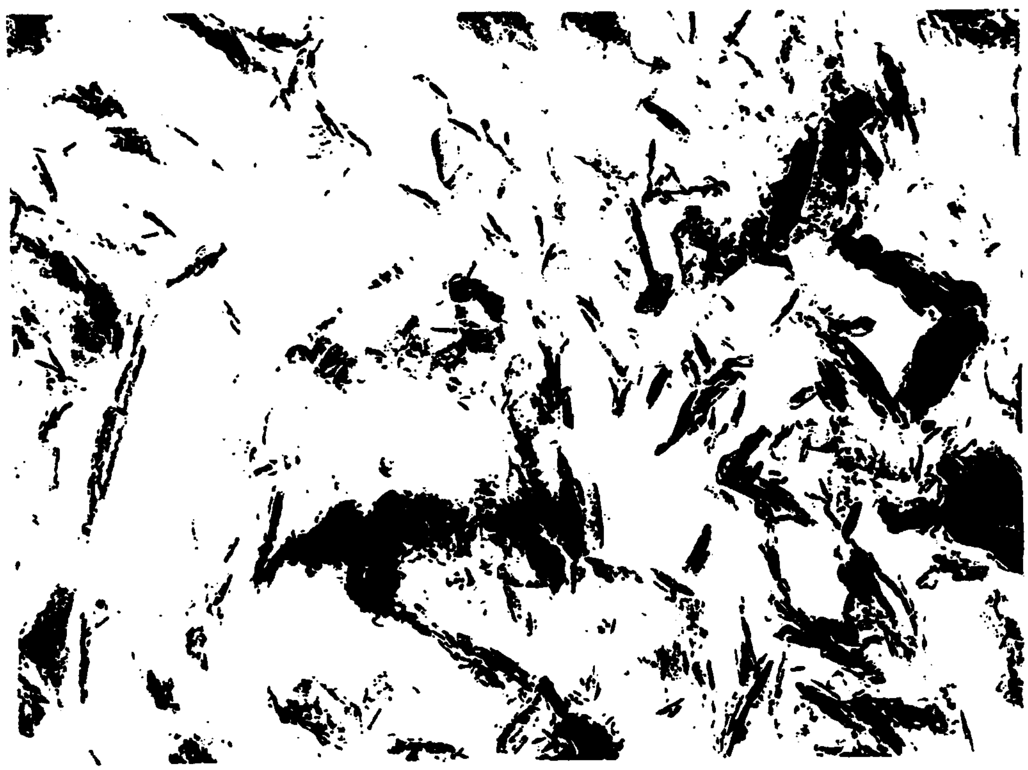

Fig. 4. Higher magnification of gassy sediment (vertical orientation) showing non-consolidated packing of clay particle clusters. X 32,000.

3.3 Sediment Properties from Grain and Macrofabric Measurement (Principal Investigators:

R. H. Bennett, R. J. Baerwald, D. Lavoie and M. H. Hulbert, NRL, University of New Orleans and Resource Dynamics)

CBBLSRP FY93 YEAR-END REPORT

Richard H. Bennett, Dennis M. Lavoie
Naval Research Laboratory
Stennis Space Center, MS 39529-5004
Matthew H. Hulbert
Resource Dynamics, Inc.
45 Heritage Drive
Terre Haute, IN 47803

LONG-TERM SCIENTIFIC OBJECTIVES

o To model the dynamic response of sediment bulk physical properties to environmental processes, applied stresses, and phenomena such as high frequency acoustic energy, based on fundamental micro-scale structure and properties.

Background: The seabed's interaction with such phenomena as high frequency acoustics is controlled by the physical properties of the sediment. Under given effective stress conditions, the important physical properties are: porosity, pore geometry, pore connectivity, permeability, electrical resistivity, bulk modulus, and shear modulus. These properties are determined by the fundamental properties of the sediment constituents, such as grain size, mineralogy, fabric and organic content. The multi-phase sedimentary system may be described as a three-dimensional microstructure consisting of various solid phase materials — primarily mineral particles and condensed organics — distributed within a water-filled pore network. The organic solids are in the form of adsorbed layers on the minerals or as polymeric gels between the minerals. The solid phases associate according to physico-chemical relationships governed by the attractive and repulsive forces between them and the chemical nature of the fluid. Our premise is that, if we can determine the nature of the solid constituents and their spatial relationships (microfabric), we can begin to estimate the physico-chemical forces involved in the association and ultimately model the sediment bulk properties. Once these parameters are understood, we can begin to model sediment's dynamic response to environmental processes and stresses. The hypothesis is that fundamental, micro-scale properties of sediment structure control the expression of macro-scale, bulk properties.

PROJECT OBJECTIVES

o To develop relevant parameters of sediment microstructure (microfabric and physico-chemistry, organic content, mineralogy, grain size, grain shape, and grains size distribution).
o To develop a sediment model using these parameters to predict crucial sediment bulk physical properties (porosity, pore geometry, pore connectivity, permeability, electrical resistivity, bulk modulus, shear strength, and shear modulus).
oTo extend the model to static and dynamic cases of applied stress and other energy inputs.

Approach: The general approach proposed was to integrate proven methodologies for studying sediment microstructure and physical properties. We proposed using these methodologies in a systematic cycle of analysis, model development, and verification for increasing levels of complexity in laboratory model sediments. These model sediments were to be increasingly complex synthetic systems, followed by model systems constructed with real-world sediments collected at the program's field sites (Kiel and Panama City). The results are to be validated for actual sediments by sampling at local sites and at selected program's field sites. The specific methodologies that will be used in this approach are as follows:

1) Microfabric analysis, including grain/pore parameters, and parameterization of two-dimensional TEM micrograph using image analysis techniques. Eventually, the image analysis will be extended to three-dimensions by 3-D volume reconstruction and visualization techniques in order to develop a physical model at the micro-scale. Time-gated laser probing will also be tested for its utility in non-destructive imaging of sediment structure and pore pathways.

2) Organic analysis. Organic compounds of possible importance to the early diagenesis of the sediment will be studied by a variety of means including GC-MS, TOC, Rock-Eval, and CHN to determine the bulk chemical character of the sediments. Specific and general stains for fluorescence and electron microscopy will be used to determine spatial relationships to the microfabric and morphology of key organics in the natural sediments.

3) Mineralogy. X-ray diffraction will be used to determine bulk mineralogy of the natural samples, and energy-dispersive X-ray spectroscopy (EDXS) will be used in the TEM to determine mineralogy on the microscopic scale in relation to the microfabric and organics.

4) Physical properties: Measurements by other CBBL participants will be used in our analyses and include physical properties determined on the same samples examined for microstructure. These measurements will include: grain size, porosity, permeability, bulk modulus, shear modulus, and electrical resistivity.

5) Modeling. The work will first be directed at developing the physical models of the sediment microfabric and finding appropriate parameters to represent the measurements provided by the laboratory and field work. These parameters will be used to develop numerical or stochastic models describing the sediment. At this point, there are no models that handle the dense, heterogeneous media represented by fine-grained marine sediments, so the results expected from this work are expected to be highly significant. The resulting models will then be used as a basis

this work are expected to be highly significant. The resulting models will then be used as a basis for the modeling of sediment bulk properties.

CURRENT STATUS AND PROGRESS

Programmatic changes have drastically altered the sequence of our proposed work. Although we had not intended to study a natural environment before gaining insights using the model (laboratory prepared) sediments, we used the opportunity to participate in the Eckernfoerder Bucht experiment in May, collecting microfabric samples and taking piezometer measurements, in order to take advantage of the ship time and the wealth of associated data that would be collected.

A total of 12 successful piezometer deployments were made, mostly during the four-point mooring period of the experiment. Poor weather limited attempts to get piezometer data at specific coring sites. This work was supported by the NRL Sediment Transport/Sediment Dynamics 6.1 Research Program.

Preliminary estimates of dissipation times for induced excess pore pressure were on the order of several hours based on the fine grain size of the sediment known to occur in the study site. To our surprise, dissipation times were on the order of 5 to 60 min (Figure 1). Early analysis of the microfabric reveals a possible explanation for this discrepancy (see below). Preliminary evaluation of the data also indicated that the behavior of the dissipation at a depth of about 1 m was somewhat anomalous compared to that of the shallower depths (9.2, 29.9, 50.6, and 71.3 cm), often exhibiting periodic fluctuations in pressure. The data are still being analyzed.

A variety of microfabric samples were collected using the newly developed mini-core subsampling technique. Approximately 48 samples were taken from diver-collected box cores and immediately treated with glutaraldehyde for preservation of the organics. These samples are in the process of being further treated by rapid dehydration techniques and examined for microbiota and condensed polymeric organics.

Approximately 120 samples were taken from 20 cm-long diver-collected cylindrical cores at intervals of 2 cm, i.e., high vertical resolution. These samples are being processed by the techniques developed by Bennett and co-workers for TEM examination of the microfabric. In addition to two-dimensional analyses of microfabric, serial sections of selected samples are being made with the goal of compiling a three-dimensional database suitable for visualizing the 3-D structure of the microfabric. Selected digitized TEM images have been given to Ron Holyer and Juanita Chase, who are co-participants in the program, for evaluation of image textural analyses . Preliminary efforts are very encouraging, indicating that parameters of anisotropy, characteristic structural scales, porosities, among others, can be developed for use as model inputs.

In addition, sub samples were collected from a pressurized core and processed under in situ pressure for examination of microfabric in the undisturbed gassey zone. The relevant samples cover from 165 to 245 cm below the seabed. Preliminary qualitative examination indicates that the clay grains are clumped into large aggregates with relatively large pores (passages) between them. Such a structure may account for the rapid dissipation of induced excess pore pressure that was seen in the piezometer data. If this observation stands up under further analysis, this would represent an example of the sediment micro-scale structure (fabric) provides important data for the explanation of a macro-scale physical property.

1993 PRODUCTS

Two papers describing the Eckernfoerder Bucht preliminary results have been submitted for presentation at the Winter Ocean Sciences Meeting, Special Session. In addition, a journal article describing the suite of methodologies being used to relate microstructure of the sediment to bulk physical properties is in preparation.

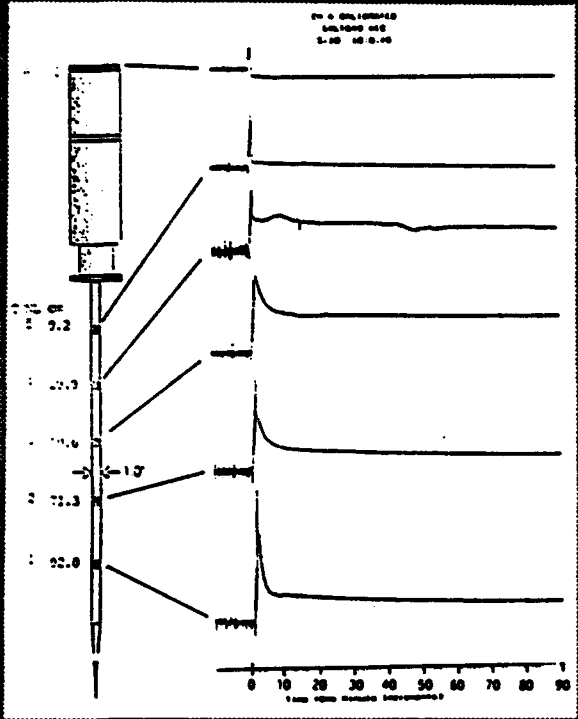

FIGURE 1: Piezometer data from Eckernförder Bucht, May 1993. Excess pore pressure dissipation (relative pressure) vs. time is shown at 5 depths next to a schematic of the piezometer probe (the sixth curve is the hydrostatic reference pressure). Note the extremely rapid dissipation in the upper layers of the column. Unprocessed data.

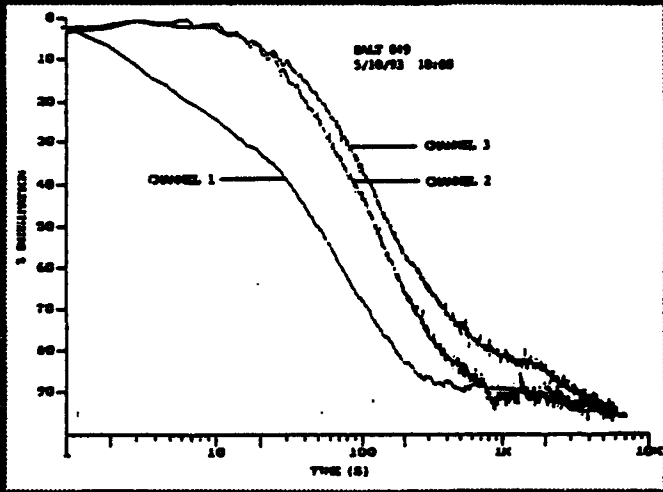

FIGURE 2: Normalized pore pressure dissipation curves plotted vs. log time for three depths. Dissipation rate at 92 cm (Channel 1) clearly differs from those at shallower depths.

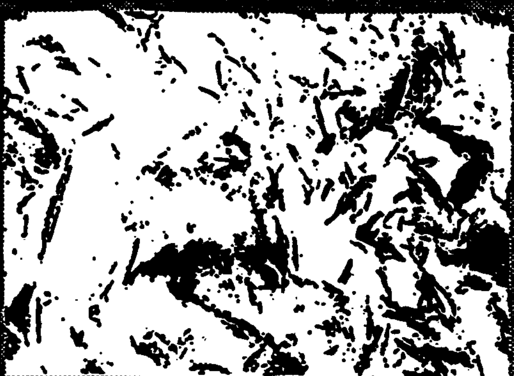

FIGURE 3: Eckernförder Bucht gassy sediment microfabric. TEM micrograph of section taken perpendicular to the bedding plane at 165 cm below surface and processed at in-situ pressure. Note the large number of edge-to-edge contacts among the electron-dense clay particles as well as the relatively large voids between aggregations of particles. Mag~20,000 x.

FIGURE 4: Eckernförder Bucht gassy sediment microfabric. TEM micrograph of section taken parallel to the bedding plane at 165 cm below surface and processed at in-situ pressure. The alignment of clay particles around the edges of these two voids indicates that they were formed in-situ and were not an artifact of the sectioning. It is not known whether the voids were filled with gas or liquid. Mag~ 20,000 x.

3.4 High-Frequency Acoustic Scattering from Sediment Surface Roughness and Sediment Volume Inhomogeneities (Principal Investigators: K. B. Briggs and M. D. Richardson, NRL)

CBBLSRP FY93 YEAR-END REPORT

Kevin Briggs and Michael Richardson
Naval Research Laboratory
Stennis Space Center, MS 39529-5004

Objectives

Investigators attempted to characterize inhomogeneities within the sediment volume and roughness features at the sediment-water interface in order to model acoustic backscattering at two experiment sites: Eckernfoerde and Panama City. Sediment properties that were measured in order to correspond to scattering model inputs were sediment compressional wave velocity and attenuation (at 400 kHz), sediment porosity, sediment density, and bottom roughness spectra from stereo photogrammetry. In addition, sediment shear strength, sediment density to x-rays, and electrical resistivity were measured at the Eckernfoerde site. Smith-McIntyre grabs were collected to ascertain the type and density of benthic fauna populating the Panama City site.

Of particular importance to this effort was the lateral and vertical variability of sediment velocity and porosity. This measure was to be obtained through standard "ear-muff" transducers through core liners for the velocity and water content assays. X-radiography and an electrical resistivity core scanner developed by Peter Jackson for porosity (or sediment density) were used in Eckernfoerde.

Results

Eckernfoerde

Twenty diver cores were collected from the HELMSAND for the purpose of measuring sediment compressional wave velocity and attenuation and porosity. Sixteen of the cores penetrated to an average depth of 22 cm into the surface sediment; four cores were collected with a piston plunger and penetrated to an average depth of 75 cm into the sediment. Pressure plugs were used on every core and velocity and attenuation measurements were made on pre- and post-pressure-released cores. Velocities varied from 1435 to 1422 m/s (see Fig. 1); attenuation varied from 40 to 100 dB/m; porosities varied from 89 % at the surface to 83 % at 2.5 m (see Figs. 2 & 3).

Fifteen diver vane shear tests were made to determine in situ shear strength. Six vane shear tests without a vane were attempted to account for the torque due to the frictional component only. One vane shear test was run at 1-16 cm sediment depth; six tests were run at 5-66 cm depth; three tests were run at 5-70 cm depth; five tests were run at 61-136 cm depth. Frictional components were calculated at 1-36 cm, 31-111 cm and 91-151 cm depths. Friction accounted for 33 to 50 % of the measured torque. Uncorrected shear strength values varied from 0.8 to 36.3 g/cm^2.

Seven x-radiograph cores were collected, x-rayed and measured with the electrical resistivity core scanner. Five cores were collected by divers and examined for resistivity 9-11 days later. Two cores were collected from a box core on the KRONSORT and examined the following morning. Relative resistivity measurements were made on the first two cores.

Two "sideways" cores for examining lateral variability of geoacoustic properties were collected from box cores from the KRONSORT. Compressional wave velocity and attenuation and sediment porosity were determined for these two cores.

Three photographic transects were made for determining bottom roughness. The first transect was taken between the backscatter and forward scatter towers and was of poor quality due to refractive differences within the water column. The second transect was taken between the towers and extended to beside the backscatter tower and was of marginal quality. The third transect was taken behind the backscatter tower and beyond the ship and is considered a good quality series of photographs.

Diver observations were made on every dive, including several swim-and-search dives in which a great area of the sea floor was observed.

Panama City

Twenty-six diver cores were collected from the R/V GYRE and M/V HOS CHIEF for the purpose of measuring sediment compressional wave velocity and attenuation, grain size and porosity. Four cores were located in the area where the APL acoustic tower was deployed. Six cores were located in the area of fine sand located south of the main experiment area and the remaining were located in the coarse sand in the main experiment area. Of the remaining cores collected in the coarse sand, seven were located between the NRL acoustic towers. Cores not collected in the immediate proximity of acoustic towers were collected in support of in situ measurements from ISSAMS, GISSAMS and DIAS. Four short cores (13 cm) were collected for the purpose of determining permeability in the coarse and fine sands.

Penetration of the diver cores was restricted to a maximum of 20 cm, with the majority of cores reaching only 14 to 15 cm depth in the sediment. A coarse shell layer was located at a depth of 9 to 15 cm, which hindered further penetration in the coarse sand. The sediment-water interface was relatively smooth and ripple-free with occasional biogenic mounds and pits and notable amounts of shell hash. A golden brown surface layer of diatoms covered the bottom except in areas where the interface had been disturbed by fish or mounds from burrowing infauna. In the area around the APL tower, a small (approximately 50 cm in diameter) mat of parenchymatous red algae was observed in the vicinity of the line leading to the target. This feature may have preserved undisturbed the interface on which it grew.

Sediment sound speeds varied from 1650 to 1750 m/s in coarse sand and 1700 to 1740 m/s in fine sand (see Figs. 4 & 5). Attenuation of the 400-kHz signal in coarse sand was very high due to the presence of carbonate shell hash and coralline algae fragments. Variability in values of sound speed was much higher in the coarse sand area than in the fine sand. This resulted from the inclusion of many shell and coralline algae fragments in the quartz sand matrix.

Sediment porosity varied from 37 to 46 % in the coarse sand; from 39 % to 41 % in the fine sand (see Fig. 6). Decreasing porosity values correlated with an increasing sound speed gradient into the coarse sediment. Wet bulk density values varied from 1.92 to 2.08 g/cm^3, and averaged 2.02 g/cm^3 in the coarse sand. An average grain density for coarse sand of 2.68 g/cm^3 was used from previous analyses of this area pending new determinations. Wet bulk density in the fine sand varied from 1.92 to 2.03 g/cm^3 (average: 2.00 g/cm^3). Average grain density in the fine sand varied from 2.64 to 2.73 g/cm^3.

Two photographic transects were made for determining bottom roughness between the backscatter and forward scatter towers. The first transect was taken along a line extending from 30 feet from the backscatter to 80 feet from the backscatter tower. The second transect was taken from the point where the first transect left off and extended to 35 feet from the forwardscatter tower. Unfortunately, many of the photographs from the end of the first transect and beginning of the second transect were damaged during the development process.

Three video camera drifts were made across the experiment site. One drift traversed the area between the VIMS tower and the southern boundary of coarse sand on a north-south trajectory. The other two drifts traversed the coarse sand area from west to east, including some of the area between the NRL towers.

Preliminary Conclusions

Eckernfoerde

Generally, not much vertical variability occurs in sediment compressional wave velocity and attenuation and porosity in the top 20 cm of sediment.

Porosity varies between 89% at the sediment water interface to 85% at 20 cm (see Fig. 2). Porosity decreases rapidly with increasing depth to 10 cm, and then fluctuates within a small range beyond this depth.

The dissolved methane saturation horizon at this time of the year exists at approximately 35 cm depth. An increase in temperature drives gas out of solution and creates gas voids. There is an increase in size and number of voids down to 75 cm. Release if pressure in cores allowed core to expand in the liners.

Rapid and timely measurement of diver cores resulted in good values for in situ velocity and attenuation measurements before gas disturbed the sediment fabric.

Vane shear strength values generally increased with depth.

Electrical resistivity measurements of x-ray cores show high lateral and vertical variability. Fresh cores have higher (and more credible) formation factors.

The sideways core taken without the piston plunger shows little variability in velocity and attenuation measurements. Core taken with plunger is disturbed in that it is filled with small voids and exhibits high variability.

The existence of cold, saline water near the bottom created occasional refraction problems for stereo photography. Some good quality photographs taken outside of the insonified area are considered reliable, but the photographs are not overlapping (no large-scale roughness measurements are possible).

Interface roughness is generally small in magnitude (< 1 cm) but some biogenic and anthropogenic features exist throughout the study sites. The features most frequently encountered were:

1. Spionid polychaete mats
2. Trawl scars
3. pits or gouges
4. mounds
5. burrow holes
6. ripples (3-4 cm height)

Panama City

The coarse sand region of the experiment area exhibits high variability in sediment sound speed due to the presence of carbonate fragments within the quartz matrix. The values for sound speed in the fine sand are more uniform, though a positive gradient in sound speed is present in both sediments in the upper 5 cm. Porosity fluctuates with increasing depth in the sediment, but exhibits an overall decreasing gradient in the coarse sand only.

Observations of the sea floor reveal the experiment site to be a very active bottom, with large gastropods and crustaceans moving across and consequently changing the shape of the interface. In addition, fishes interact with the bottom and change the roughness characteristics.

Fig. 1. Velocity Depth Profile at Eckernforde

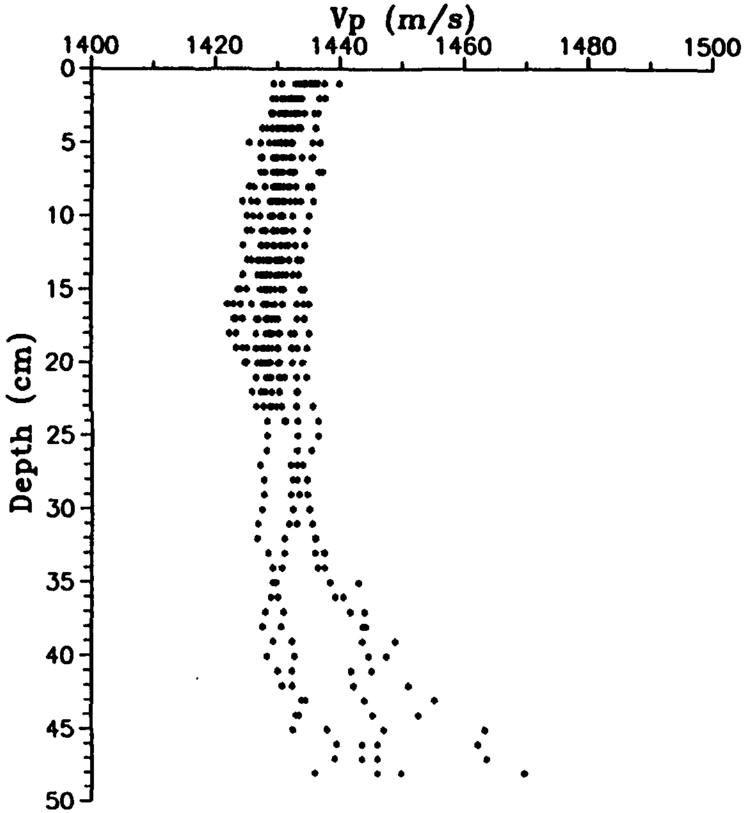

Fig. 2. Porosity Depth Profile at Eckernforde

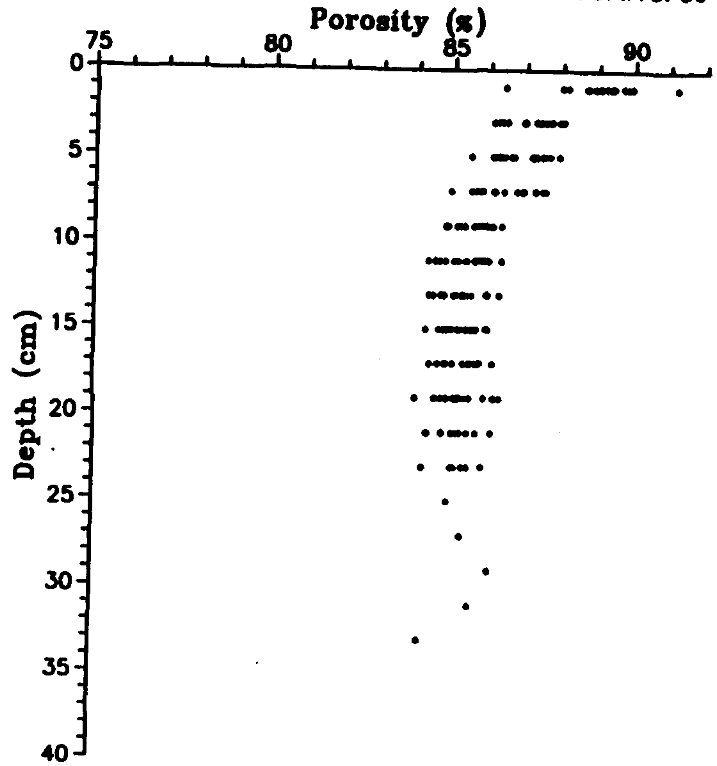

Fig. 3. Porosity Depth Profile at Eckernforde

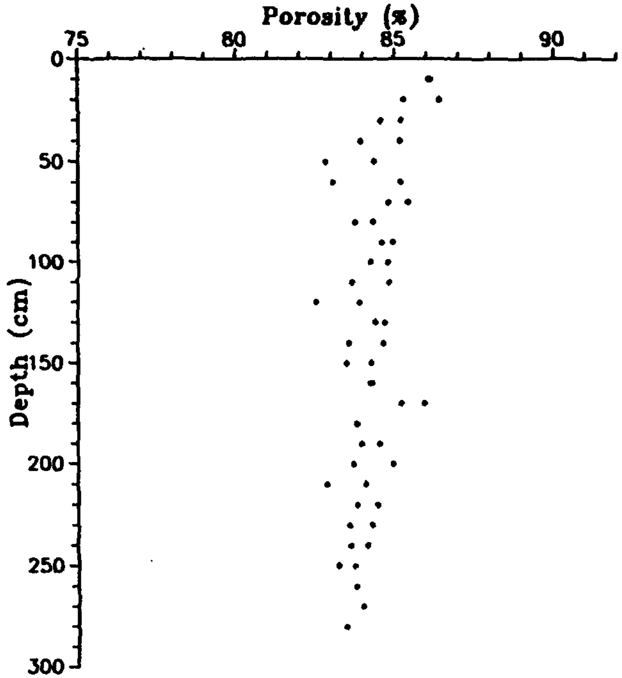

Fig. 4. Velocity Depth Profile at Panama City
(Coarse Sand, o = APL Tower)

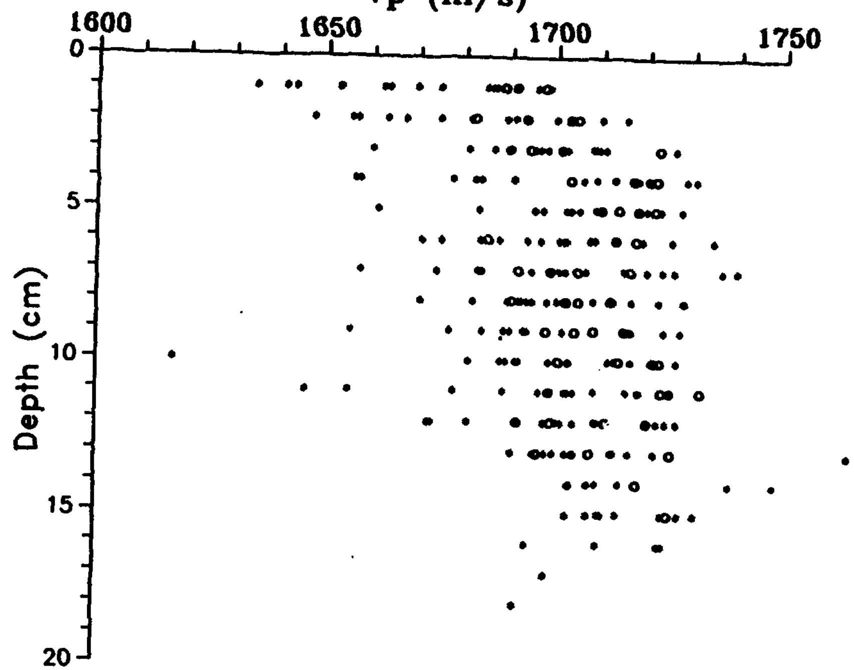

Fig. 5. Velocity Depth Profile at Panama City
(Fine Sand)

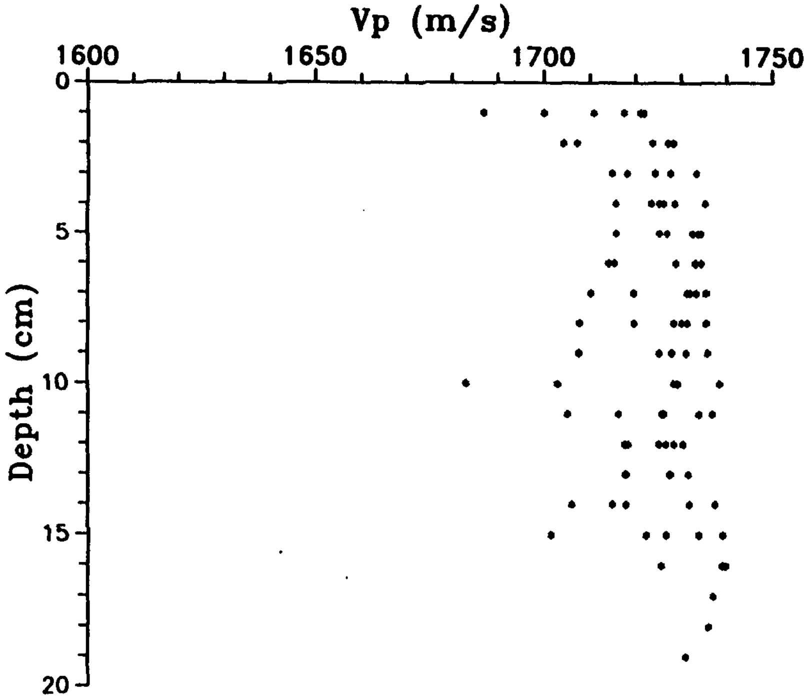

Fig. 6. Porosity Depth Profile at Panama City
(o = Fine Sand, Connected Pts = APL Tower)

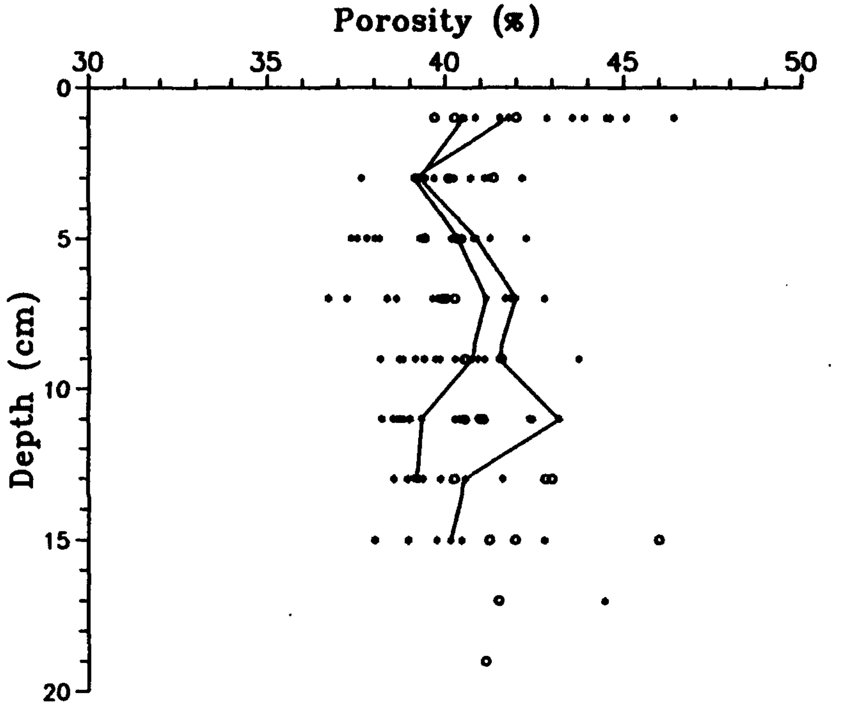

3.5 Processes of Macro Scale Volume Inhomogeneity in the Benthic Boundary Layer (Principal Investigators: W. R. Bryant and N. C. Slowey, Texas A&M University)

CBBLSRP FY93 YEAR-END REPORT

William R. Bryant and Niall C. Slowey
Department of Oceanography
Texas A & M University
College Station, TX 77843

Project Goal

It has been stated that "stratigraphy is the great unifying agency of geology and that stratigraphy makes possible the synthesis of a unified geological science from its component parts" (J. Marvin Weller, 1947). It is our contention that a knowledge of the lithostratigraphy and geotechnical stratigraphy are absolutely necessary in order to understand the significance of the interactions of sediment properties and their relationship to geoacoustical and engineering characteristics.

The goal of this project is to understand how and why the physical properties and the geology of the boundary layer vary in terms of time dependent physical, biological and chemical processes within various shallow water geological environments and relate these variations to the states of stress as a function of time and the penetration and stability of objects on the seafloor. Specifically, we will investigate the geotechnical stratigraphy, which includes the density, shear strength (cohesion), porosity, saturation (gas) and sediment and biological component distribution and their three dimensional structural arrangement, within the boundary layer in more detail than has previously been possible, leading to a description of boundary layer gradients of density, porosity and cohesion and their relation to time, sediment type and structural arrangement and states of stress as defined by in situ pore pressure measurements. In addition to sediments of a cohesive nature (clays and silts, clayey sands and sandy clays), fine-grained carbonate sediments will also be investigated. The measurements of the density, shear strength (cohesion) and compressibility will supply the parameters necessary for determining the bearing capacity and long-term stability of objects placed in or near the boundary layer. The knowledge gained will help generate the physical and numerical models that predict the penetration and stability of objects on the seafloor, supply data for models of the geoacoustic and magnetic nature of the boundary layer and arrive at realistic measures of sediment micro and macrostructural volume inhomogeneity that can be applied to geo and seismo-acoustic problems.

Introduction

The 1993 year of the project consisted mainly in the planning and execution of three field experiments, two in Eckernfoerde Bay on the Baltic and one off Panama City Florida. The majority of the 1993 effort consisted of obtaining samples from the use of a multitude of sampling devices and the measurement in the field of the bulk density, compressional wave velocity and in some cases magnetic susceptibility. This report in divided into three parts each part describing the events and some results of the analysis of cores from each field experiment.

Report Of Field Investigation Of Eckernfoerder Bay During February 1993.

From the 2nd to the 18th of February, Bryant and Slowey and graduate student A. Rutledge from the Department of Oceanography were involved in a multi-institutional investigation of the benthic boundary layer in Eckernfoerder Bay, Germany. Investigators Bryant and Slowey were mainly responsible for evaluating various available coring units (2 gravity cores, 2 box cores and 1 vibra core), for the up-coming May 1993 field investigation, and for the recovering gravity and box cores and testing them for geotechnical, sedimentary, geoacoustical and mineralogical properties. Evaluations of coring equipment were included in the initial cruise summary distributed to all CBBLSRP participants by the cruise chief scientists.

Thirty-four, 4 to 5 meter-long gravity cores were recovered aboard the R/V Planet. Most of these cores were of poor quality due to the lack of check valves in the coring units and the large amount of undercutting of the cored sediment. While undercutting allowed for the recovery of long cores, they could not be logged by Multi-Sensor Core Logger to determine compressional wave velocity, bulk density (by gamma ray attenuation) or magnetic susceptibility due to the lack of contact between the sediment and the core liner. The corer also over-penetrated into the sea floor. Aboard the ship, a check valve was built and fitted to the corer and modifications of the core catcher were experimented with, eliminating the over-penetration but not the undercutting. Of the 34 gravity cores recovered, the following 9 were logged: 8, 9, 10, 16, 29, 30, 33 and 34 - BS-GC. After evaluation of data obtained from these cores, efforts at logging the remaining gravity cores were suspended because cores were not judged to be of sufficient quality. Cores 29 and 34 BS-GC were split at the University of Kiel and the shear strength, water content, bulk density and degree of saturation was determined. The following gravity cores were returned to the U.S. and are undergoing additional testing: 8, 9, 10, 20, 21, 22, 23, 26, 28, 30, 33, 44 and 52 BS-GC.

In addition to the gravity cores, 9 box cores were obtained. From these box cores 19 sub-cores were obtained and logged at orthogonal orientations as part of our investigation of volume inhomogeneity. The box cores are as follows: 5 (1), 36 (4), 37 (4), 39 (4), 41 (2), 42 (2) and 48 (2) BS-BC where the number of subcores from each is indicated in parentheses. All sub-cores were returned to the U.S. for additional testing. The cores recovered in Eckernfoerde Bay using the gravity and box coring devices were split length wise and each half placed face down on a plastic plate. A slab of sediment 3.2 cm thick and 42 cm in length, with parallel sides , was sculptured from the core. The sediment slab was then X-rayed using a Picker Industrial X-ray and Kodak "AA" X-ray film. Each slab was X-rayed twice after being offset 8 cm left and right from the center of the X-ray beam. The resulting X-radiographs, when combined, in a stereo pair renders a three dimensional view of the internal structure of the sediment. After X-raying one of the slabs was tested for strength by the use of a Swedish Fall Cone. Strength was measured at 2 cm intervals along two and sometimes three lines that traverse the right and left side of the sediment slab. Forty to sixty strength measurements and other properties data are obtained from each 42 cm slab. After the Fall Cone measurements are completed the slab are again X-rayed and can make up one of the stereo pairs. The resulting stereo views allows us to determine the sediment structure and general macro-fabric at a resolution of approximately 30 micro-meters at each position where strength measurements were obtained (Figure 1). After the strength measurements constant volume samples are subtracted from the core at positions similar to where the strength measurements were obtained. Water content, wet bulk density, porosity and degree of saturation are computed from the constant volume samples. Figures 1 to 6, illustrates the method of displaying this data in conjunction with the stereo X-radiographs. In these figures only one half of the core is displayed in stereo view.

Examination of the X-radiographs by the use of a stereo-viewer or by the eye if one possesses stereo-vision results in the illustration of the internal micro-structure of the sediment. The stereo X-radiographs are arranged, after being photographed, next to graphs of the various physical properties. This procedure allows for a direct comparison of the properties of the sediment with the sediments structure. The internal nature of a whole core may be viewed by examination of two stereo pairs, each pair representing one side of the core. The process of using stereo X-radiographs in conjunction with the various measurements results in a new approach to the study of physical properties and supplies the litho and geotechnical stratigraphy that allows us to determine the basic lithology and the macro and semi-microstructure of the sediment relative to its velocity, porosity, density, water content and strength.

Figure 2 and 3 are the data for Box Core No. 41 subcore No. 1. Water content, cone penetration, bulk density and compressional wave velocity graphs are aligned to the stereo pair of the subcore. Velocity and density were measured in two direction each orthogonal to one another. The velocity data in Figure 4 shows that the sediment is acoustically anisotropic as the result of the gas fractures that appear below 27 cm and is observed in the subcore at the position one set of velocity determinations fall sharply as the gas fracture zone is interred. Figures 5 is a subcore from box No. 48 which was taken from the Pock Mark area. The veryt gassy nature of the core is shown in the stereo X-radiographs and the velocity determinations in Figure 6 indicate the presence of gas. Figure 7 illustrates the nature of subcore No. 2 of Box Core No. 41. The X-radiographs of this core illustrate the large worm tubes and the high degree of bioturbation below a subbottom depth of 20 cm.

In all cases, neither subcores from box cores nor gravity cores, showed any biotirbation or gas structures in the upper 15 to 20 cm.

Three schematic core logs are illustrated in Figures 8 and 9. These logs represent the three main types of sediment lithology and macro-fabric we have encountered in the examination of Box Cores No 35, 36, 39, 41, 42, 48, 52 and Gravity Cores 8, 9 and 10. As other cores are analyzed additional characterization logs will be developed.

Log "A", Figure 8, is the combined lithology of Box Cores Nos. 35, 36, 39, 41 and 42. Log "A" is the summary that results from the analysis of up to 4 subcores per Box Core. All the sediment in the Box Cores represented by this log were taken in or around the Test Site. The lithology of the log consists of 5 strata, the upper most consisting of 3 cm of very high water content muds followed by 4 to 9 cm of a higher silt content material underlain by a homogeneous and structureless mud. At Approximately 17 to 18 cm a shell hash horizon is present. This shell layer may be a lag deposit and the top of the Historic Layer. The section from 18 to 33 cm contains a uniform material (mud) which in some cores has thin convoluted tubes 3 to 5 mm in diameter. These tubes may be worn tubes or the feeding paths of other organisms. At 33 cm another shell layer is encountered and below that the sediment is bioturbated with convoluted tubes and contains gas structures in the form of linticular fractures whose orientation are parallel to the long axis of the core.

Log "B", Figure 9, is characteristic of the sediments found in the Pock Mark and is determined from Box Core 48. The sediments of this area have a multitude of gas fractures and appear to contain three distinct layers within the upper 42 cm. The upper 6 cm contains a sediment with an extremely high water content gradient that grades from 600 to 350 %. The next 19 cm of sediment contain an high water content gassy sediment and appears on the X-radiographs as being homogeneous to the eye but magnified 15 times shows a very complex micro-structure containing blocky micro-stratification's. Additional layers within the core below 28 cm are the results of slight variations in sediment density.

Log "C", Figure 9, represents the sediment section in the area north east of the Test Site and was developed using the data from Core 8, a 5.5 m gravity core. The lithology of the area appears to contain a repeated sediment sequence the most recent cycle being contained in the upper 180 cm. Each cycle consists of 25 cm of homogeneous material (mud) which may contain an occasional shell. This unit rests upon a very distinct silt layer 5 mm thick. The silt layer overlies 75 cm of stratified sediments containing numerous gas fractures. Sixty cm of horizontal thinly bedded non-gassy sediments are the base of the first or upper most sediment cycle. The next cycle is then repeated and is similar in thickness and lithology as the first. The second cycle however has a horizontal thinly bedded non-gassy section that continues to the total depth of the gravity core.

Report of Field Investigation of Eckernfoerder Bay During May ,1993.

From the 8th of May to the 1st of June five investigators from the Department of Oceanography were involved in a multi-institutional investigation of the benthic boundary layer in Eckernfoerder Bay, Germany. Investigators Bryant and Slowey with technician K. Davis and graduate students A. Lyons and J. Swanson were mainly responsible for the recovery and testing for the geotechnical, sedimentary, geoacoustical and mineralogical properties of high quality gravity cores requested by other investigators at a multitude of locations and to investigate the volume inhomogeneity. Thirty-nine gravity and diver collected cores, with an average length of 185 cm, were obtained during the period over 24 to 27 May. Of these, 22 cores were logged using Texas A & M's Multi-Sensor Core Logger. The logger determines the compressional wave velocity and bulk density (by gamma ray attenuation). Coring specifics are summarized in Table 1.

Cores taken with the URI gravity corer were generally of very good quality. However, if gaseous and dissolved methane were present in sufficient quantities within the sediment, gas expansion due to decreased hydrostatic pressure and increased ambient temperature upon core recovery created conditions where compressional wave velocity could not be measured with the Multi-

Sensor Core Logger. The upper 30 to 50 cm of sediment at all sample sites was generally non-gassy and preliminary analysis of the data do not suggest the occurrence of anomalous compressional wave velocities in these sediments. Cores taken along Lambert's line were also generally non-gassy their entire length as indicated by the relatively high amplitude of measured velocities.

Insight into the occurrence of gaseous methane in the sediments was provided by changes in the amplitude of transmitted compressional waves during velocity measurements on certain diver collected cores where the in situ pressure was maintained. Figure 10 is the velocity and density data for Core No. 338 and illustrates the nature of a non gassy sediment section, while Figure 11 is the velocity-density profiles of a gassy sediment section. The velocity and density in this core decrease below a subbottom depth of 30 cm.

The diver retrieved pressurized gravity core No. 314 show a constant velocity of 1500 m/s (Figure 12). The measurements on the depressurized core of No. 314 are shown in Figure 13. The decrease in velocity below 70 cm indicate the presence a gas coming out of solution with the release of pressure.

Acoustic relatively high amplitudes over the subbottom depth range of about 0 to 30 cm suggest the presence of little or no gaseous methane in these upper sediments. However. amplitudes decreased significantly over the depth range of about 30 to 150 cm, suggesting the presence of sound-attenuating gaseous methane in cores around and within the Test Site. Amplitudes increased again at depths greater than about 150 cm to the base of the sediment cores, implying that the deeper sediments were gas-free (i.e. methane is mainly in dissolved rather than gaseous form). Consistent with NRL's ASCS and Chirp sonar subbottom profiles, this observation suggests that gas in the Eckernfoerder sediments occurs in horizontally extensive intervals, **gas does not occur, as determined from structures within the cores, continuously with depth from near the sea floor to the underlying glacial-tills.**

Seventeen cores were returned to the U.S. for further testing. All of these cores were sealed with o-ring plugs and retaining pins in order to control sediment expansion due to temperature and methane gas generation. In addition a 7 gravity cores (numbers 206, 207, 208, 217, 218, 219, and 220) were collected at the NRL (Stanic) platform Test Site. These 7 cores were logged for velocity and gamma density, opened and tested for shear strength, bulk density and water content. The water content of these cores range from a high of 315% to an average of 250% over a length of 180 cm. The water contents were fairly constant with depth except at the upper 10 to 20 cm. Surprisingly, the shear strength (cohesion) increased down core at a rate that is not consistent with the water content. The shear strength increased from 10 psf at the surface to approximately 65 to 70 psf at the 180 cm level. This increase may reflect the influence of the biologic components of the sediments more than the property of the clays. The degree of saturation and the affects of surface tension may also be a governing factor.

Finally, we carried out a very brief in the water test of a set of compressional wave transducers designed for in situ measurements of velocities in sediments over a wide range of frequencies.

The workable frequency range was less than we anticipated so we will continue developing this tool.

Report For The CBBL-SRP Panama City Experiment

As part of the Coastal Benthic Boundary Layer Experiment, a cruise to the Panama City, Florida inner continental shelf was undertaken aboard the RV Gyre during August and early September of 1993 to further investigate the sedimentologic and acoustic characteristics of a predominantly clastic sand environment. The region selected for this study has been previously investigated and described (e.g., Stanic et al., 1988).

Texas A&M University-Oceanography personnel who participated in the Coastal Benthic Boundary Layer Panama City Experiment included Bryant , K. S. Davis, and A. Rutledge. This group contributed a total of 33 man days of effort during the actual experiment.

Sampling efforts at the Panama City test site included 20 SCUBA dives to deploy and recover instruments and to recover sediment samples; recovery of 90 surficial sediment samples by Shipeck Grab; multiple attempts at recovering piston cores, vibra cores and gravity cores; and recovery of 3.5 kHz seismic profiles. These activities were undertaken with the aim of understanding the distribution of sediment size, shape and compositional characteristics within the experiment site and their relationship environmental processes and acoustic back scatter observed by on side-scan sonar records.

Davis made a total of 20 dives in water depths of 92 to 97 feet. To help evaluate the effect of sediment texture at the sediment/water interface on acoustic back scatter, sediment peels (~8"x10") were collected at areas of high and low acoustic back scatter (as indicated by acoustic tower results). Davis participated with NRL divers during the deployment and operation of the Naval Research Laboratories ISSAMS and DIAS acoustic instrument packages. This effort involved driving the acoustic and shear modulus probes into the seafloor with a sledge hammer at specified intervals. While measurements were being taken, diver cores were taken a short distance from the instruments to provide ground truth data. Following completion of the acoustic measurements, divers made sure the electrical cables would not wrap around the instrument packages during retrieval. Other diving activities included assisting with stereo photographic transects, chain dragging to smooth local micro topography, buoy and anchor maintenance, sediment peels, and retrieval of APL and VIMS towers.

Sedimentologic samples were collected to characterize the physical and geological properties of the seafloor and to provide ground truth data for the acoustic studies. Four sampling devices were utilized during the cruise: piston core, Shipek grab sampler, electric vibra-core (all provided by TAMU), and a gravity corer (provided by URI). Station locations are contained in the trip report of Chief Scientist Dawn L. Lavoie.

To understand the vertical and temporal sequence of characteristics and the history of sediment deposition, 1 to 3 meter long cores are necessary. Given descriptions of sediments at the study site by prior studies, we declined to attempt using a gravity corer and anticipated only a fair chance of success using a piston corer. Bryant made ~6 attempts to recover piston cores at the experiment site and, indeed, it proved unsuitable for two reasons: the sediment was too hard to allow penetration of the core barrel, and the coarse-sized sediment was not cohesive enough to be retained in the core barrel by the core catcher. Davis and Rutledge attempted to recover cores using a Rossfelder electric vibra-corer fitted with a 10 foot pipe. Initial vibra-coring resulted in a severely bent pipe, most likely a result of the hardness of the seafloor (i.e., high sand content) and the inability of the ship to maintain station. Consequently, the pipe was shortened to 1.5 meters. Further coring resulted in minimal recovery of sediment and, unfortunately, all recovered sediments were so disturbed by the vibrations during the coring process that they were no longer representative of in situ material. In these cores, fine-grained material was suspended in the waterhead overlying the sand and pore waters appeared to have drained from the sand so that pore spaces contained air. Multiple attempts at recovering vibra-cores were made with little success and efforts were concluded following problems with electrical shorts in the vibrating head wire. After it was decided vibra-coring was not a viable means of recovering acceptable cores, Davis and Rutledge assisted University of Rhode Island personnel with their large diameter gravity coring operation.

Efforts at obtaining surficial sediment samples proved to be much more successful. Approximately 90 sediment samples were collected using a Shipek grab sampling device, which effectively sampled both coarse and fine-grained sediments. Sampling locations were selected to ensure a high density sample coverage of the study area. It is anticipated that these samples will yield grain size, shape, and compositional data that will contribute to our understanding of anomalous backscatter features found on the side-scan sonar records. Sediment samples will be analyzed for grain size distributions using the sieve and pipette method of Folk (1974), with the statistical parameters calculated using the method of moments. Percent $CaCO_3$ of the sand-sized fraction will be determined by weight loss after exposure to acid, and the textural maturity will be determined by analyzing the shapes of sand-sized grains with a coupled microscope-computer digital image processing system located at TAMU. The resulting data will be mapped and compared with side-scan sonar mosaics to gain insight into the relationships among the distributions of sediment characteristics, environmental processes at the seafloor, and changes in acoustic backscatter patterns.

The sands recovered by the grab samplers will be re-sedimentated to determine their minimum density and the associated compressional wave velocity. The re-sedimentated sands will be vibrated to achieve the densest packing arrangement and the maximum bulk density and velocity determined. Impregnated sands will be serially sectioned to determine the geometry of the pore spaces and the nature of the particle contacts as a function of particle shape, packing and degree of sorting.

A series of 3.5 kHz subbottom profile transects were collected to produce a bathymetric map of the study area, and to identify trends of large-scale bedforms that might be used to explain sediment distribution and backscatter patterns on the side-scan mosaics. Subbottom penetration was minimal due to the high reflectance of the seafloor. It is anticipated that two maps will be produced from this data set. The first is a bathymetry chart contoured in meters, and the second, a map of bedforms overlain by sediment statistical parameters to identify areas of active sediment transport.

Summary

1. In all cases neither subcores from box cores nor any gravity core showed any biotirbation or gas structures in the upper 15 to 20 cm except for the upper most 2 cm. This upper 15 to 20 cm is considered a storm deposite and may be a seasonal event.

2. Observation of the gravity cores and box cores suggests that while gas in the Eckernfoerder sediments occurs in horizontally extensive intervals, the gas does not occur, as determined from structures within the cores, continuously with depth from near the sea floor to the underlying glacial-tills. The gas that affect the cores is restrected along specific horizons.

3 Three schematic core logs were generated to describe the main types of sediment lithology and macro and micro-fabric that we have encountered in the examination of Box Cores No 35, 36, 39, 41, 42, 48, 52 and Gravity Cores 8, 9 and 10.

4. The diver retrieved pressurized gravity cores show a constant velocity of approximately 1500 m/s. The measurements on the depressurized cores showns a decrease in velocity below 70 cm indicating the presence a gas coming out of solution with the release of pressure.

5. The process of using stereo X-radiograph in conjunction with the various physical properties measurements results in a new approach to the study of physical properties as it now allows us to determine the basic lithostratigraphy and compare it to the geotechnical stratigraphy and the specific macro and semi-microstructure of the sediment relative to velocity, porosity, density, water content and strength.

6. The increase in shear strength observed in the cores where water content remains almost constant may reflect the influence of the biologic components of the sediments more than the state of stress or the property of the clays. The degree of saturation and the affects of surface tension may also be a governing factor.

7. The upper 30 to 50 cm of sediment at all sample sites was generally non-gassy and preliminary analysis of the data do not suggest the occurrence of anomalous compressional wave velocities in these sediments. Cores taken along Lambert's line were also generally non-gassy their entire length as indicated by the relatively high amplitude of measured velocities.

8. Acoustic relatively high amplitudes over the subbottom depth range of about 0 to 30 cm suggest the presence of little or no gaseous methane in these upper sediments. However, amplitudes decreased significantly over the depth range of about 30 to 150 cm, suggesting the presence of sound-attenuating gaseous methane in cores around and within the Test Site. Amplitudes increased again at depths greater than about 150 cm to the base of the sediment cores, implying that the deeper sediments were gas-free (i.e. methane is mainly in dissolved rather than gaseous form). Consistent with NRL's ASCS and Chirp sonar subbottom profiles,

this observation suggests that gas in the Eckernfoerder sediments occurs in horizontally extensive intervals.

THE BIG QUESTION: does gas exist under in situ conditions in the sediment in bubble form or the lenticular gas fractures we observe and associate with gas in the cores ? Are the lenticular gas fractures stress release features observed only in cores that have been physically altered. Are the gas bubbles in the sediment to small to resolve by the various X-ray techniques. Spherical objects have been observed in TEM photomicrographs and in X-radiographs but up to now they are a rare event.

References

Folk, R.L., 1974. Petrology of Sedimentary Rocks. Hemphill Publishing Company. 182 pp.

Stanic, S., K.B. Briggs, P. Fleischer, R.I. Ray, and W.B. Sawyer, 1988. Shallow-water high-frequency bottom scattering off Panama City, Florida. Journal of the Acoustical Society of America. v. 83(6), p. 2134-2144.

TABLE 1
CBBLSRP/JOBEX CORE SAMPLING
Eckernfoerder Bay

MAY 24 - 27, 1993

No.	Date	Location	Type	Investigator(s)	Result
300	24	Stanic Site N	GC-A	Abegg	OK, Chem Analysis only
301	24	Stanic Site N	GC-S	Martens/Albert	OK, Chem Analysis only
302	24	Stanic Site N	GC-A	Richardson/Lavoie	OK
303	24	Stanic Site N	GC-A	Richardson/Lavoie	OK
304	24	Stanic Site S	GC-S	Silva	OK, logged
305	24	Stanic Site S	GC-A	Richardson/Lavoie	OK
306	24	Stanic Site S	DS-GC	Bryant/Slowey	OK, logged
307	24	Stanic Site S	GC-S	Martens/Albert	OK, Chem Analysis only
308	24	Stanic Site S	DS-GC	Bryant/Slowey	OK, logged
309	25	APL, May	GC-S	Silva	NO RECOVERY, FAILURE
310	25	APL, May	DS-GC	Bryant/Slowey	OK, logged
311	25	APL, May	DS-GC	Bryant/Slowey	OK, logged
312	25	APL, May	GC-S	Silva	OK, logged
313	25	Stanic Site S	GC-S	Martens/Albert	OK, Chem Analysis only
314	25	Stanic Site S	DC-AC	Anderson	OK, CT scanned & logged
315	25	Stanic Site S	DS-GC-AC	Anderson	OK, CT scanned
316	26	Stoll-4	GC-S	Stoll	OK, logged
317	26	APL, Mar/ Apr	GC-S	Stoll (site 5)	OK, logged
318	26	APL, Mar/Apr	GC-S	Silva	OK, logged
319	26	APL, Mar/Apr	GC-S	Martens/Albert	OK, Chem Analysis Only
320	26	APL, Mar/Apr	DS-GC	Bryant/Slowey	OK, logged
321	26	Stoll-1	GC-S	Stoll	OK, logged
322	26	Abegg-1	GC-A	Abegg	OK,Chem Analysis Only
323	26	Stoll-2	GC-S	Stoll	NO RECOVERY, Glacial Till?
324	26	Abegg-2	GC-A	Abegg	OK, Chem Analysis Only
325	26	Schock-1	GC-S	Schock	NO RECOVERY, Sand?
326	26	Schock-1a	GC-S	Schock	OK, logged
327	26	Schock-2	GC-S	Schock	OK, logged
328	26	Abegg-3	GC-A	Abegg	OK, Chem Analysis Only
329	27	Schock-4	GC-S	Schock	NO RECOVERY, Sand?
330	27	Stanic	GC-S	Marte[illegible]Albert	OK, logged
331	27	Lambert Line	GC-S	Lam[illegible]	OK, logged
332	27	Lambert Line	GC-S	Lamb[illegible]	OK, logged

333	27	Lambert Line	GC-S	Silva	OK, logged
334	27	Lambert Line	GC-S	Lambert	OK, logged
335	27	Lambert Line	GC-S	Lambert	OK, logged
336	27	Lambert Line	GC-S	Lambert	OK, logged
337	27	Lambert Line	GC-S	Lambert	OK, logged
338	27	Lambert Line	GC-S	Lambert	OK, logged

GC-S	Gravity Core with Silva corer
GC-A	Gravity Core with Abegg corer
DS-GC	Gravity Core, Diver Sealed @ bottom
DS-GC-AC	Gravity Core, Diver Sealed @ bottom in Abegg Chamber
DC-AC	Diver Collected and Sealed @ bottom in Abegg Chamber

0036 BSBC Section 2

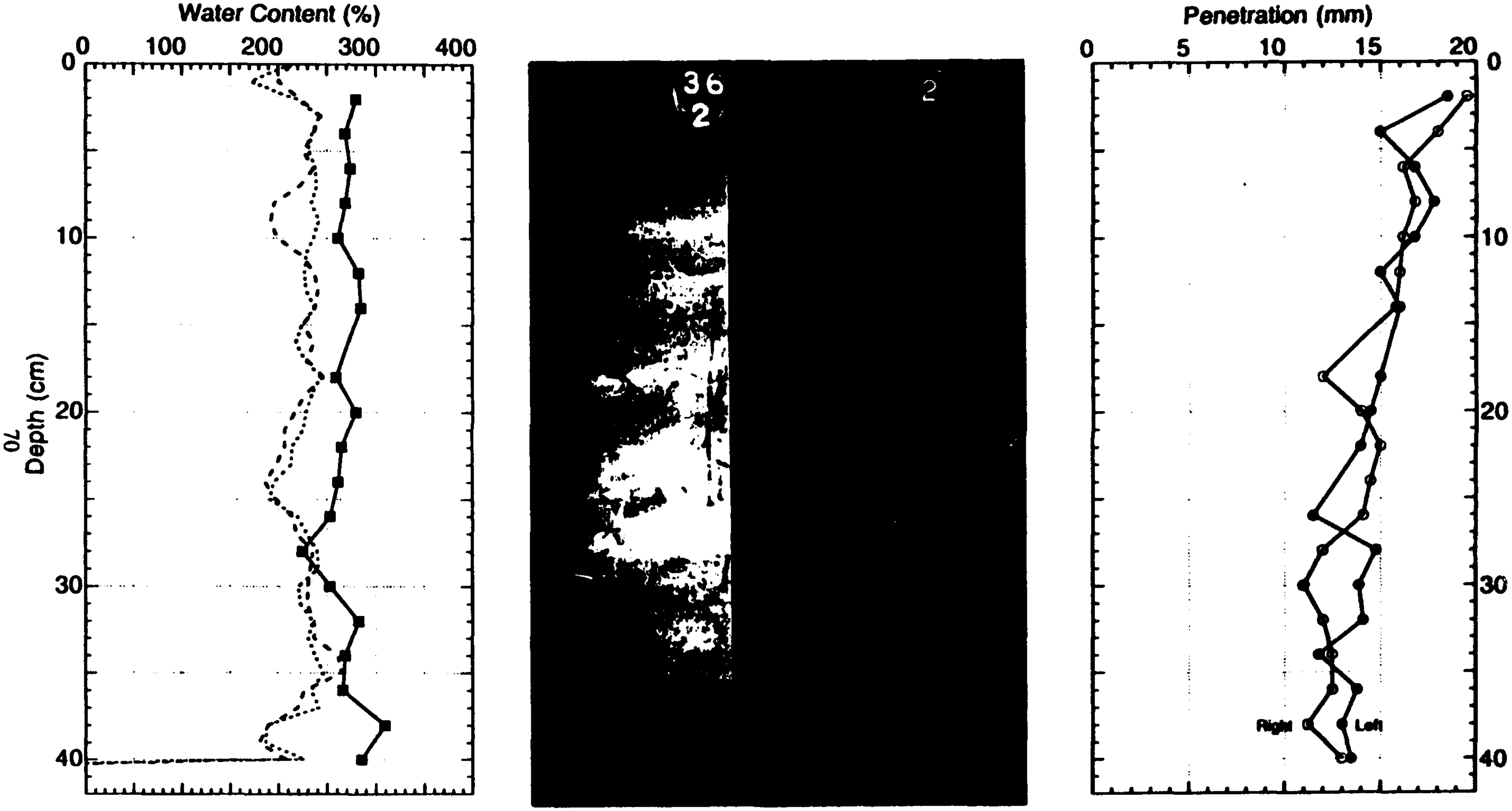

FIGURE 1

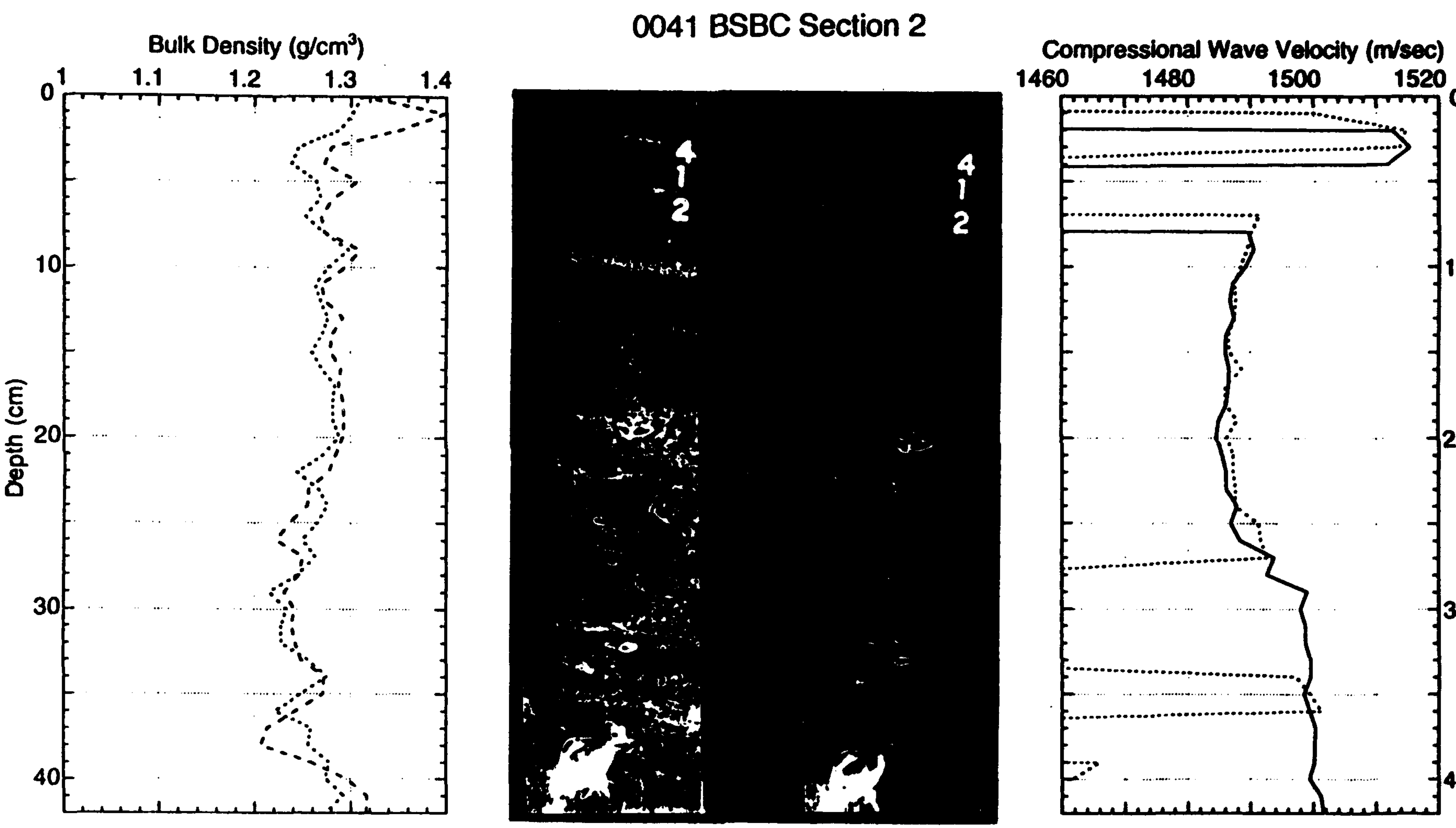

0041 BSBC Section 2
Bulk Density (g/cm³)
1
1.1
1.2
1.3
1.4
Depth (cm)
0
10
20
30
40
4
1
2
4
1
2
Compressional Wave Velocity (m/sec)
1460
1480
1500
1520

FIGURE 3

0041 BSBC Section 1

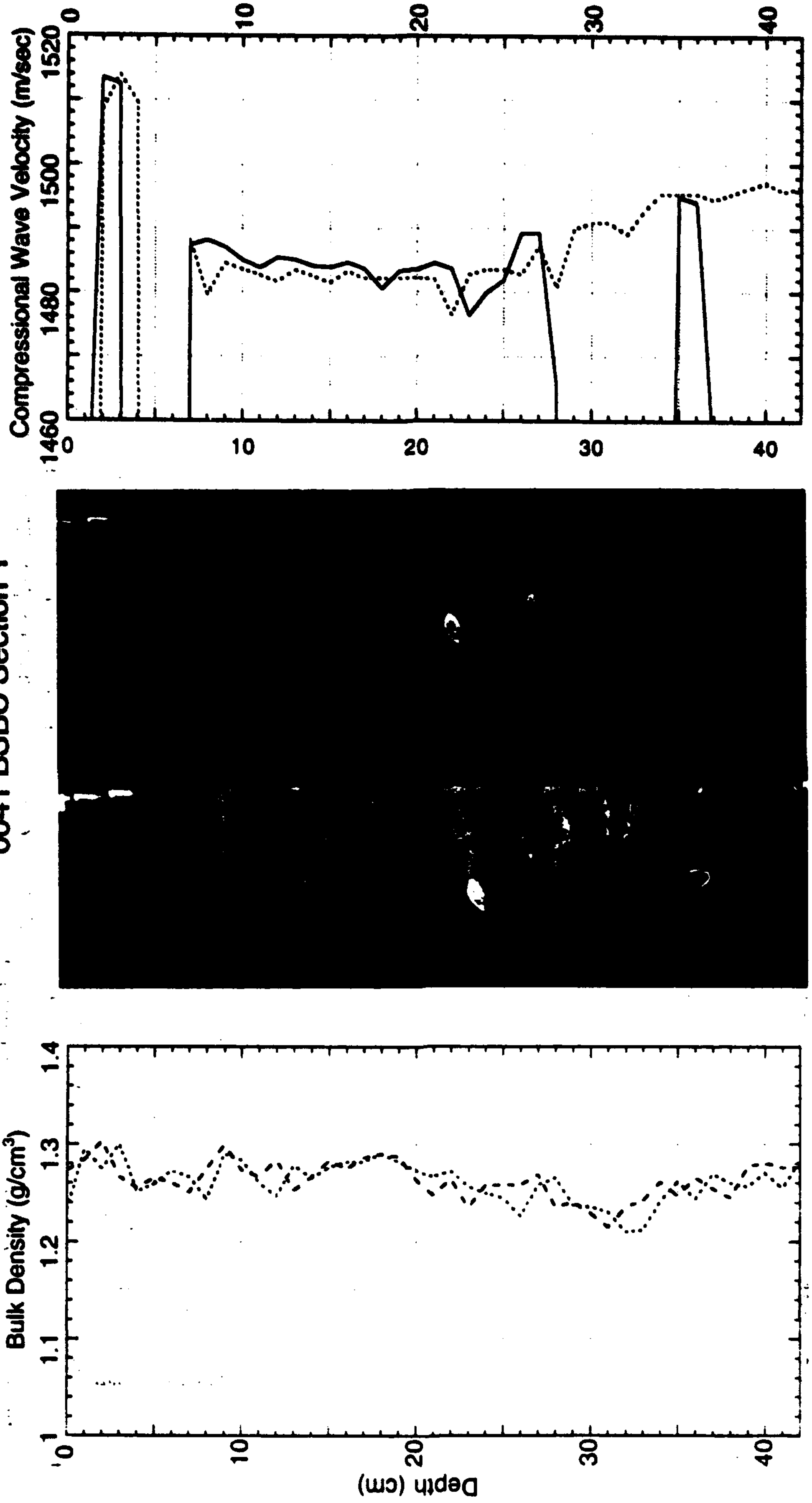

FIGURE 4

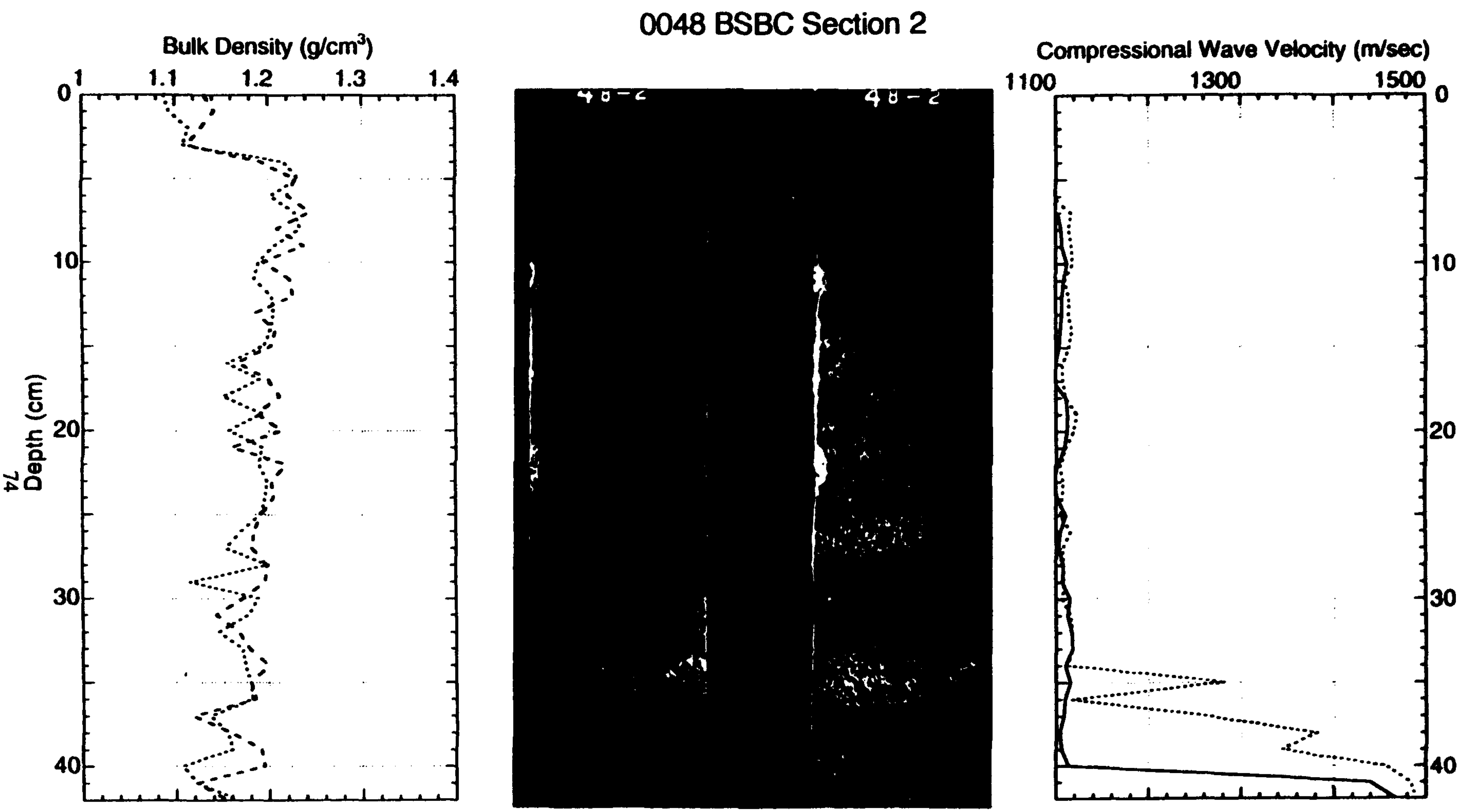
0048 BSBC Section 2
Bulk Density (g/cm³)
1
1.1
1.2
1.3
1.4
0
10
20
30
40
Depth (cm)
48-2
48-2
Compressional Wave Velocity (m/sec)
1100
1300
1500
0
10
20
30
40

FIGURE 5

0048 BSBC Section 2

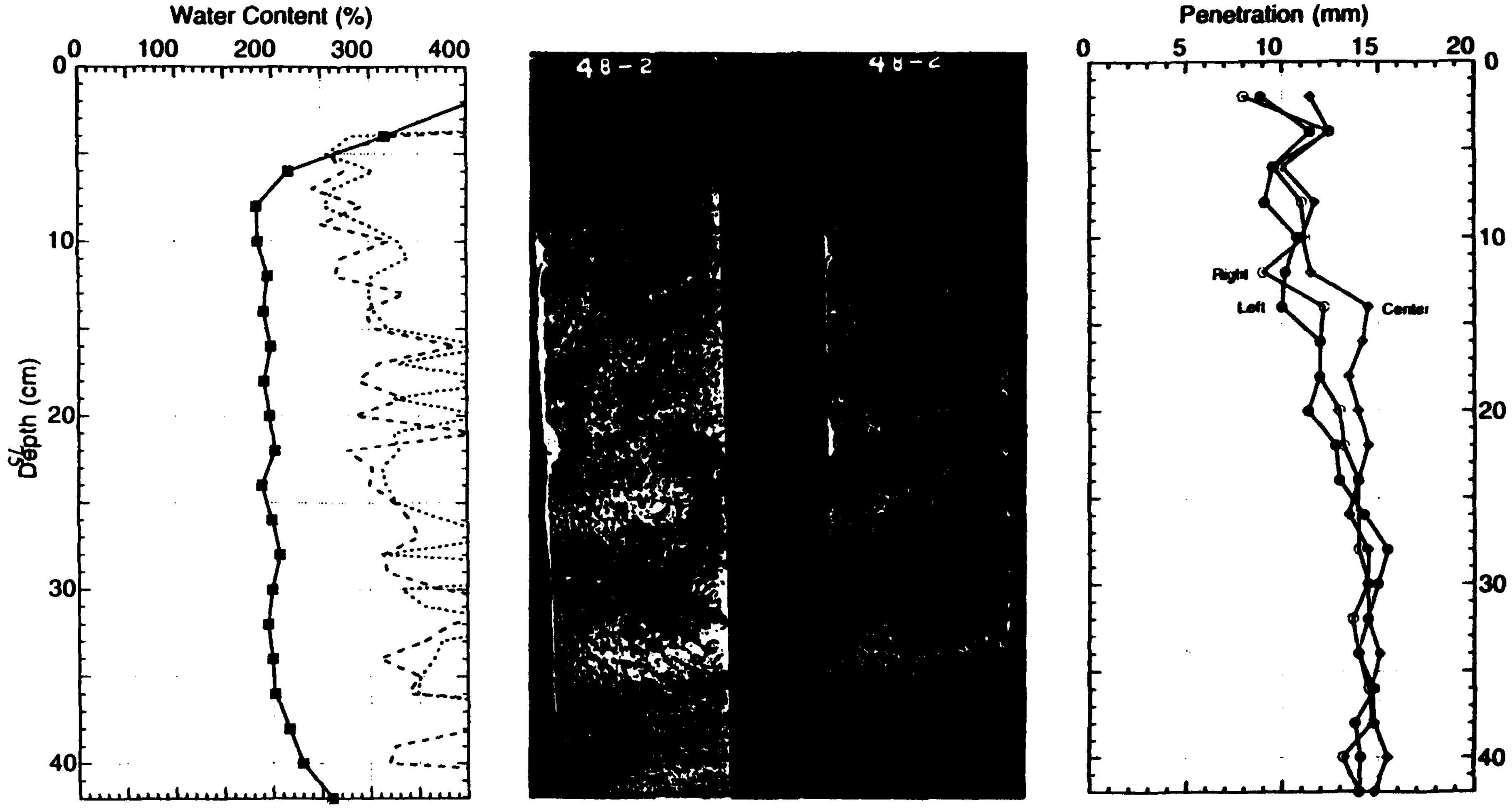

FIGURE 6

0042 BSBC Section 2

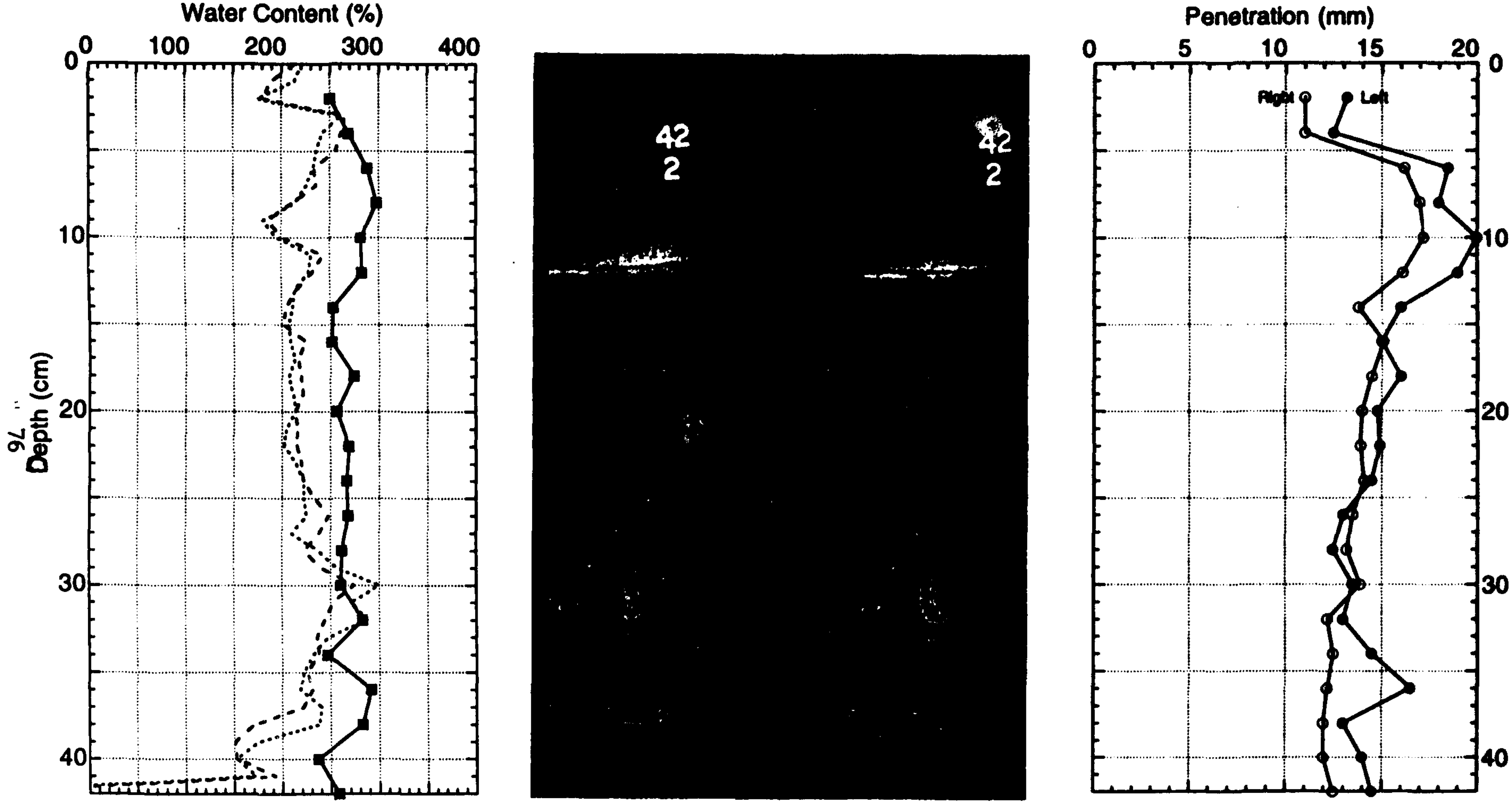

FIGURE 7

"A"

Date logged: November 25, 1993

Logged by:

Ground: 0.00 m KB: 0.00 m

Remarks:

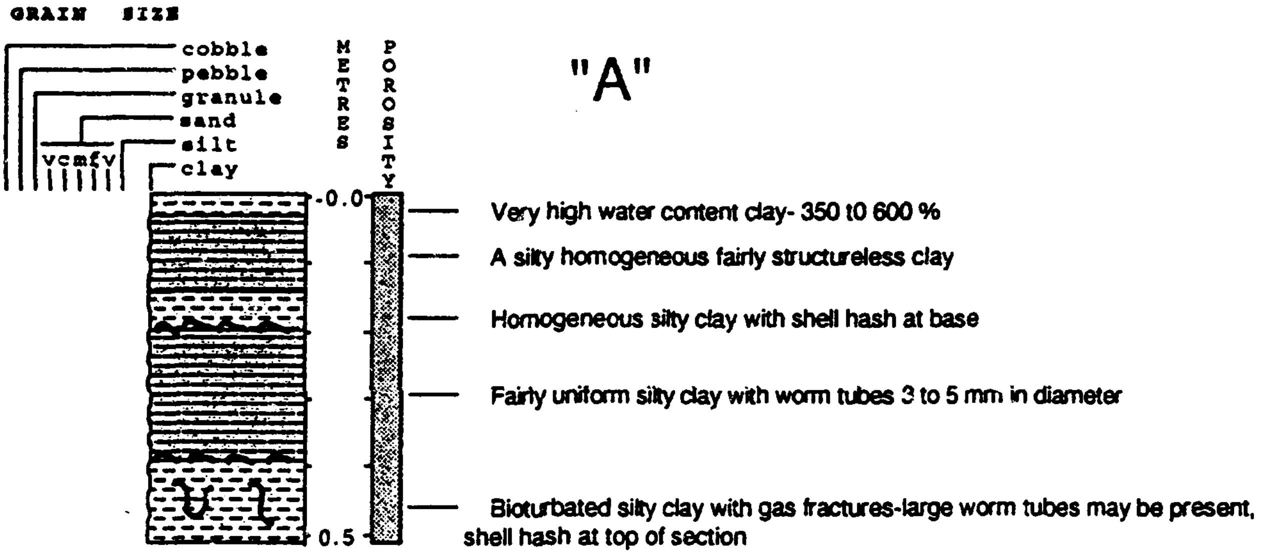

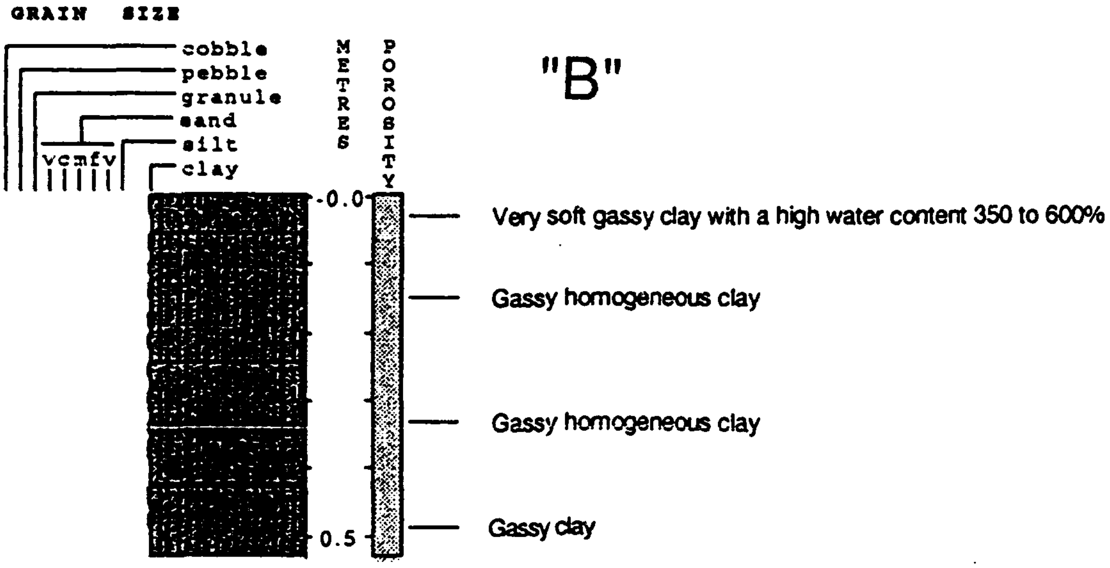

FIGURE 8

"C"

Date logged: November 25, 1993

Logged by:

Ground: 0.00 m KB: 0.00 m

Remarks:

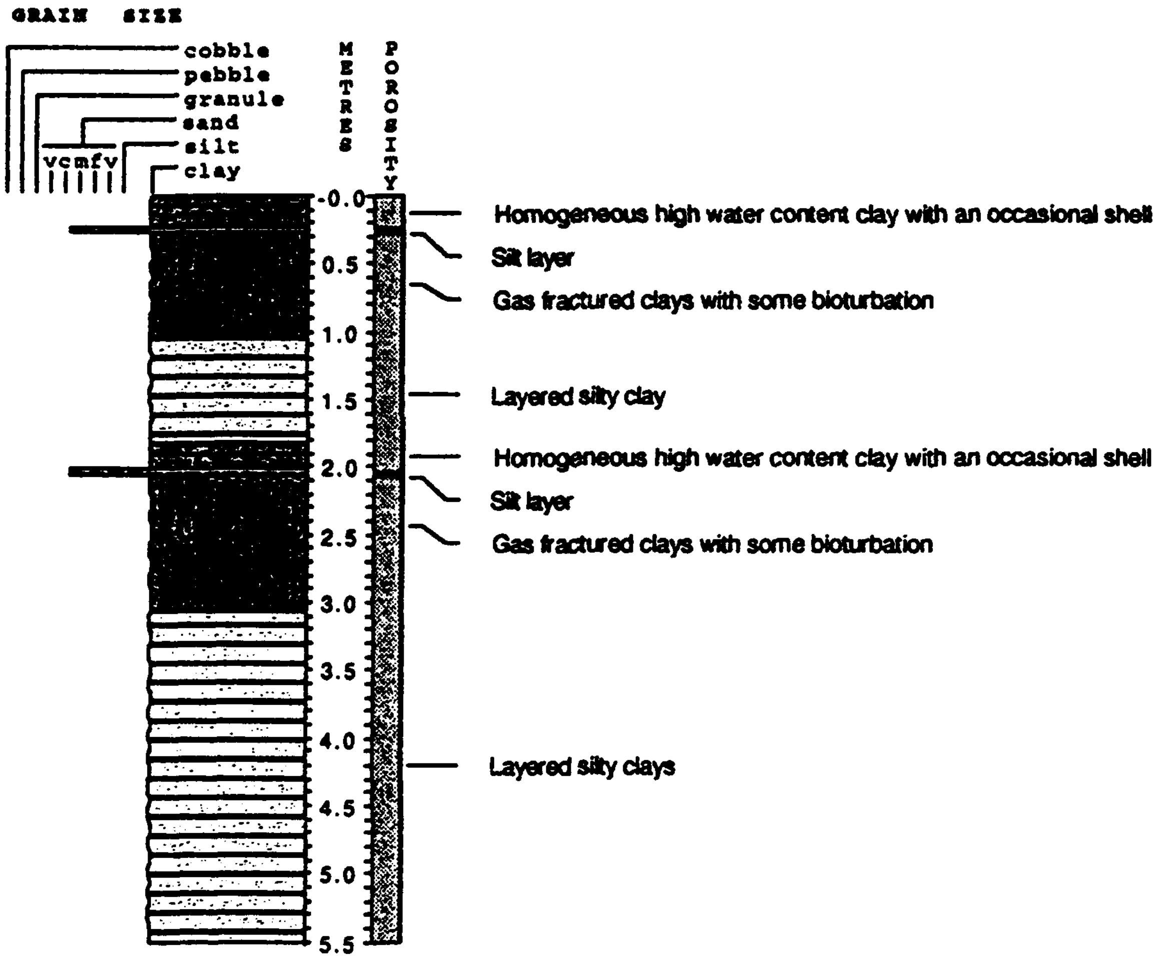

FIGURE 9

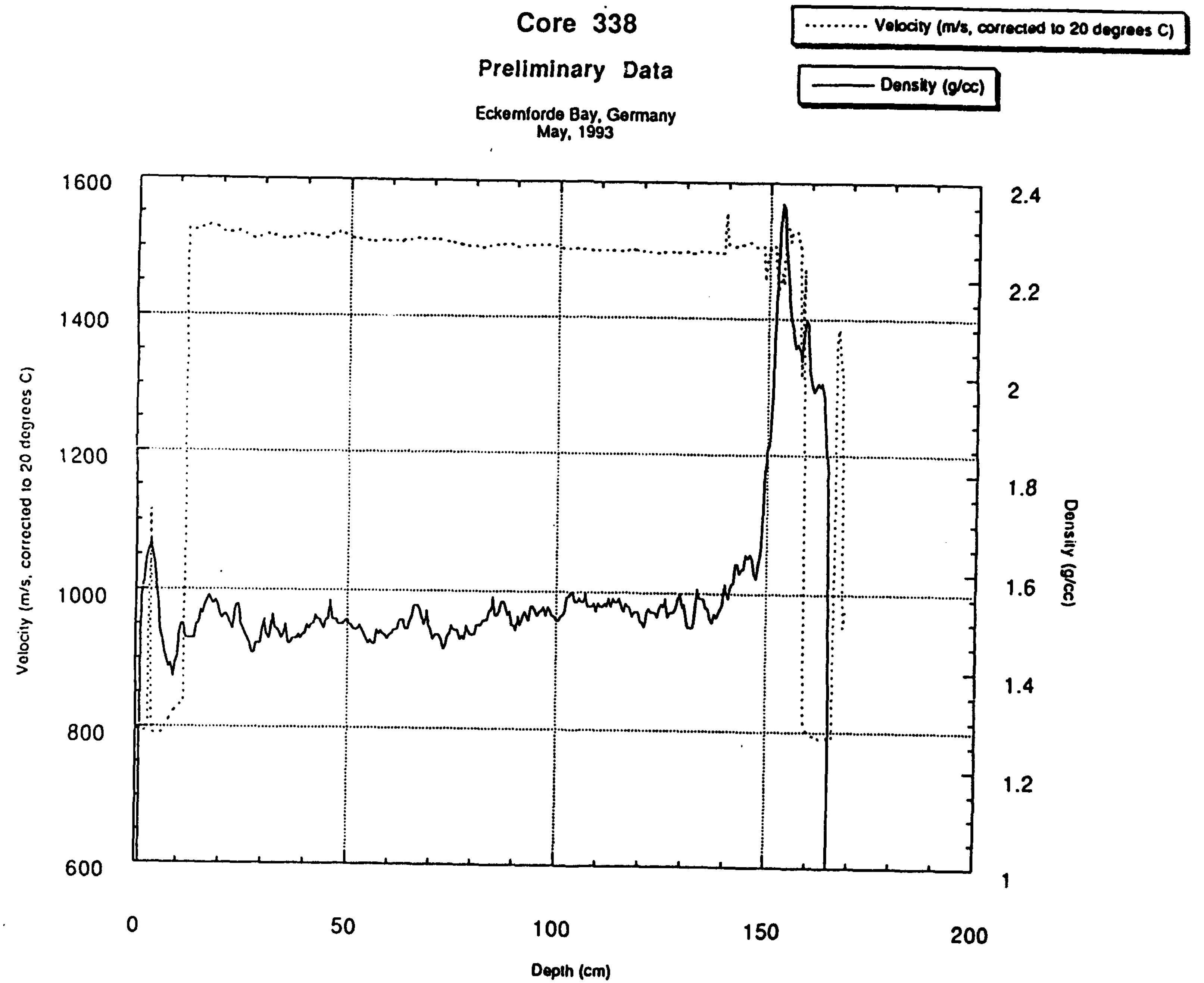

Core 338
Preliminary Data
Eckernforde Bay, Germany
May, 1993
Velocity (m/s, corrected to 20 degrees C)
Density (g/cc)
1600
1400
1200
1000
800
600
2.4
2.2
2
1.8
1.6
1.4
1.2
1
0
50
100
150
200
Depth (cm)

FIGURE 10

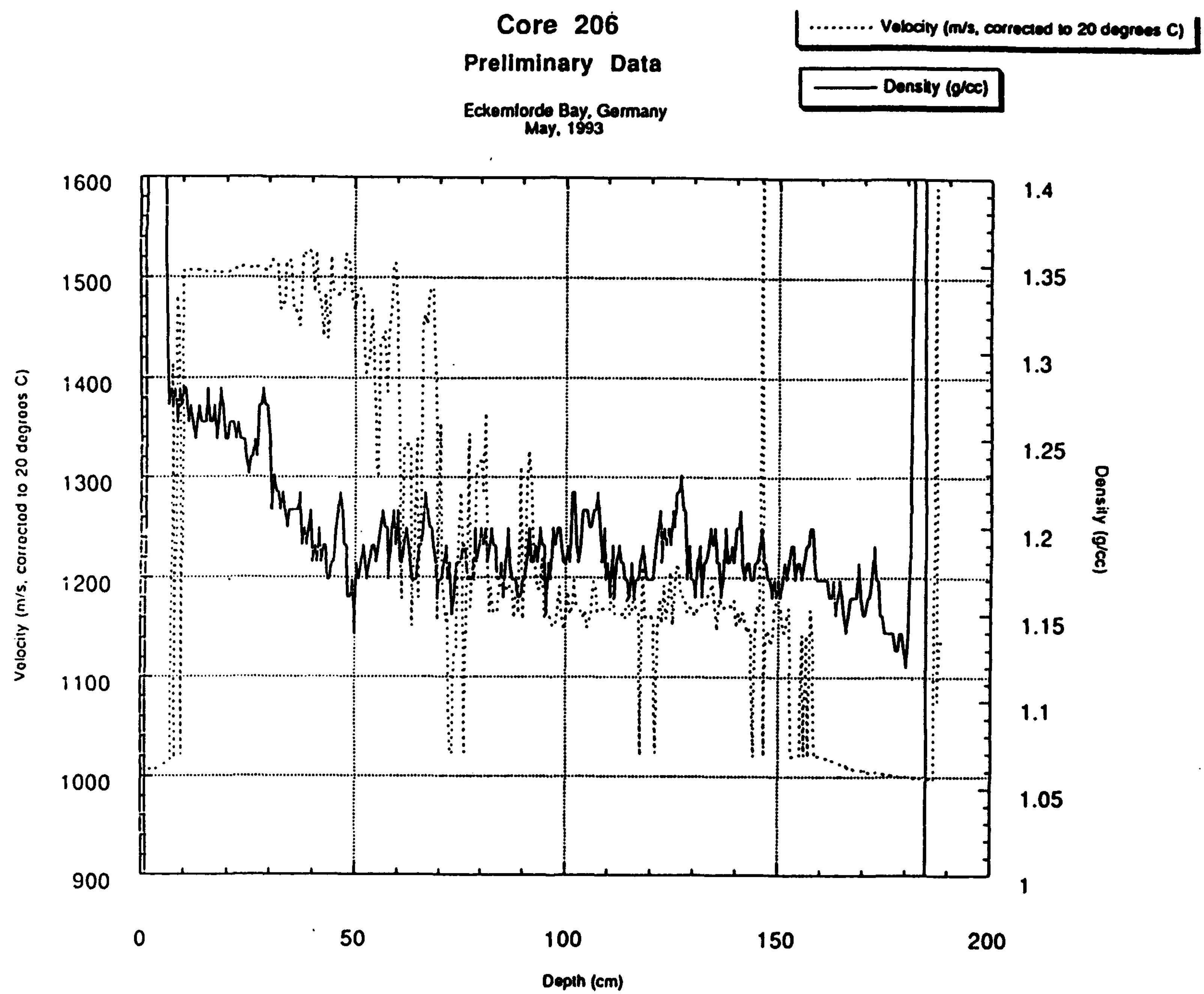
Core 206
Preliminary Data
Eckernforde Bay, Germany
May, 1993
Velocity (m/s, corrected to 20 degrees C)
Density (g/cc)
1600
1500
1400
1300
1200
1100
1000
900
1.4
1.35
1.3
1.25
1.2
1.15
1.1
1.05
1
0
50
100
150
200
Depth (cm)

FIGURE 11

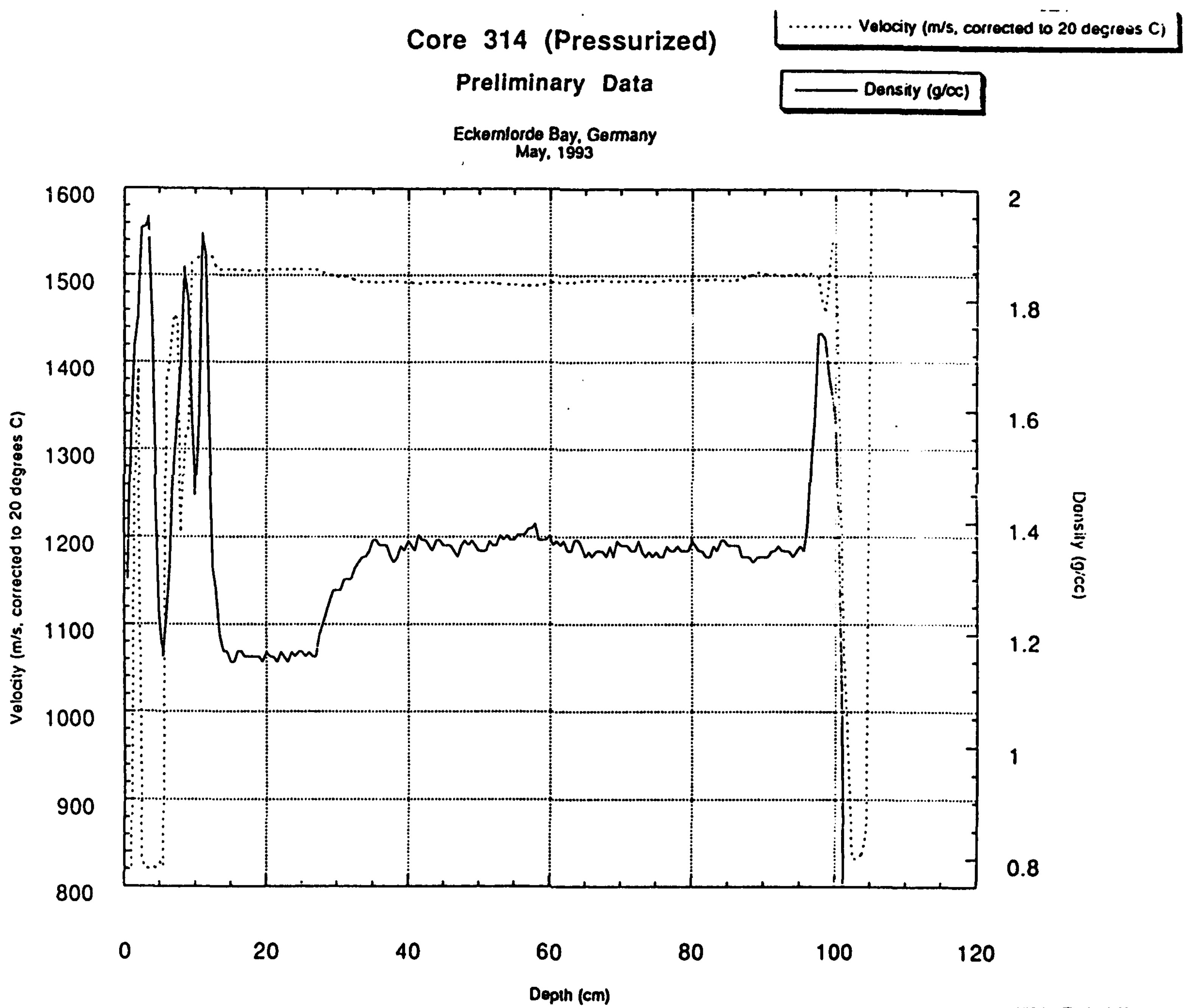

Core 314 (Pressurized)
Preliminary Data
Eckernforde Bay, Germany
May, 1993
Velocity (m/s, corrected to 20 degrees C)
Density (g/cc)
1600
1500
1400
1300
1200
1100
1000
900
800
2
1.8
1.6
1.4
1.2
1
0.8
0
20
40
60
80
100
120
Depth (cm)

FIGURE 12

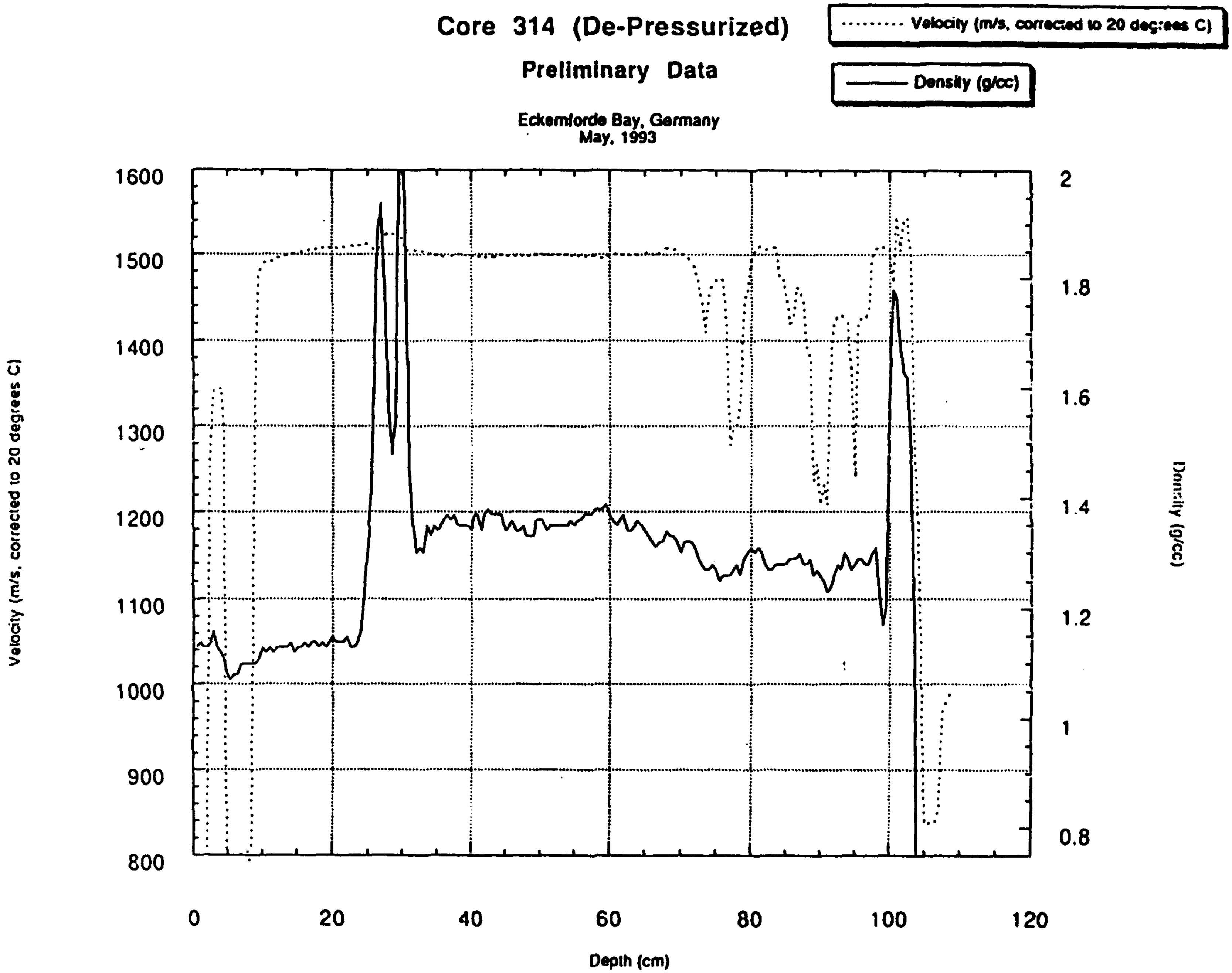

Core 314 (De-Pressurized)
Preliminary Data
Eckemforde Bay, Germany
May, 1993
Velocity (m/s, corrected to 20 degrees C)
Density (g/cc)
1600
1500
1400
1300
1200
1100
1000
900
800
2
1.8
1.6
1.4
1.2
1
0.8
0
20
40
60
80
100
120
Depth (cm)

FIGURE 13

3.6 Analysis of Data from In Situ Acoustic Scattering Experiments (Principal Investigator: N. P. Chotiros, University of Texas)

CBBLSRP FY93 YEAR-END REPORT

Nicholas P. Chotiros
Applied Research Laboratory
University of Texas at Austin
P.O. Box 8029
Austin, TX 77843-3146

Work started with participation in the January workshop to: (1) establish the scientific goals of the SRP and foster interaction among those investigators who have been selected to participate and (2) to develop detailed plans for the experiments to be conducted in the Baltic jointly with FWG, and then later off Panama City, FL. Contributions were made in the area of acoustic bottom interaction.

With regard to the topic of bottom backscatter by surface roughness, ARL/UT proposed that in situ measurements of bottom backscatter from rough and smooth sandy surfaces should be compared to establish the roughness contribution to scattering. This measurement has now been made by APL/UW, under Darrell Jackson.

With regard to acoustic bottom penetration, ARL/UT participated in the design of the bottom penetration experiment, by providing the design of the buried sensor configuration. The configuration was designed to allow measurement of both direction and speed of sediment acoustic waves. The penetration experiment was carried out by NRL under Steve Stanic. Preparation are being made to analyze the acoustic penetration data. Data analysis will commence as soon as the data is received.

A paper, Titled, "High Frequency Acoustic Bottom Backscatter Mechanisms at Shallow Grazing Angles," by N. P. Chotiros, was presented at the Ocean Reverberation Symposium at SACLANTCEN and subsequently published as a book of collected papers edited by Ellis, Preston and Urban.

3.7 Analysis of the Rheological Properties of Nearbed (Fluid Mud) Suspensions Occurring in Coastal Environments (Principal Investigator: R. W. Faas, Lafayette College)

CBBLSRP FY93 YEAR-END REPORT

Richard W. Faas
Department of Geology
Lafayette College
Easton, PA 18042

Field Phase

PI traveled to Eckernfoerde, Germany and participated in field sampling from May 24 to May 27, 1993. Sampling was confined to the upper 2-3 cm of various box cores. The purpose of this sampling was to provide sufficient material to study the rheological properties of the surficial muds in the Eckernfoerde Bight. Samples were taken from large and small box cores which were taken for specific (e.g., geotechnical, biological) purposes. In nearly all cases, the oxidized surficial layer comprised the sample - however, it was sometimes difficult to confine the sampling to the oxidized layer in some of the smaller box cores. Consequently, some missing of oxidized and reduced sediment may have occurred.

Laboratory Phase I

The samples were analyzed for TOC, carbonate carbon, particle size distribution and bulk properties. For the rheological work, the samples were converted into slurries of varying densities, and examined for their stress-rate of strain relationships using a Brookfield RVT 8-speed coaxial rotational viscometer. Testing for rheological behavior was performed in the laboratory of the Royal Belgian Institute for Natural Sciences, Brussels, Belgium, June 1-5, 1993. Fresh Eckernfoerde samples were diluted with 14 ppt water to various densities, remolded with a stirring apparatus, and analyzed in the Brookfield rotational viscometer. Each sample was analyzed through shear rates from 0.61 to 122.5 s_{-1}. Shear stresses varied, depending upon the mechanical strength of the slurry, but ranged from <2.0 dynes/cm^2 (0.2 Pa) to >430 dynes/cm2^2 (43 Pa). Slurry densities ranged from 1.038 to 1.250 Mg/m^3. Yield stresses were measured on all samples, using the shear stress at the moment of initiation of flow as the yield value (Faas, 1990). Bingham yield stresses were also determined, following computer analysis of the rheometric data.

Grain size was performed on all samples (see Table 1 for data) with the Micromeritics Sedigraph. Samples were initially freeze-dried (lyophylization), organic matter was removed by digestion with 30% H_2O_2 until effervescence ceased, calcium carbonate was determined using the Dietrich-Schiebler calcimeter, and the cleaned sample was then processed through the sedigraph. Subsamples were taken for TOC analysis, which involved heating in a muffle furnace at 550°C for one-hour. Weight loss of the sample after ignition was interpreted to represent oxidizable organic matter. Data are included in Table 1.

Laboratory Phase II

A second set of rheological analyses were performed on the Eckernfoerde samples during August 1993 at the Naval Research Laboratory, Stennis Space Center, MS. These analyses were performed on sediments which had been completely cleaned, through oxidation with 35% H_2O_2. The purpose of this work was to determine the effect of organic matter on the viscoelastic behavior of the sediments. The cleaned sediments provided a baseline from which the effects of biological additions could be assessed. As before, yield stress (determined from the shear stress at the initiation of flow). Bingham yield stress (determined from the rheogram) were correlated to the density of the sediment slurry. These data are included in Table 2.

Observations

During the investigations of the natural surficial sediment. Smear slides from BC 264 were examined with the petrographic microscope under magnifications ranging from 25x to 63x (unpolarized light). In addition to much undifferentiated organic matter, numerous elongate ellipsoidal and spindle-shaped bodies were observed to occupy a significant amount of the sediment (Plates 1 and 2). These particles appeared to be fecal pellets and accordingly, a size analysis of these bodies were made. The length (x) and width (y) axes of 200 pellets were measured, using a calibrated microscope ocular. Figures 1-3 show the length/width relationship (Figure 1), and histograms of pellet length (Figure 2) and pellet width (Figure 3). A correlation coefficient of 0.67 between pellet length and pellet width suggests the pellets are derived from a monospecific population of organisms. The histograms of pellet length and pellet width are decidedly unimodal (Figures 2 and 3), supporting the hypothesis of production by a single species of organisms. The nature of the organism producing the pellets is unclear.

The analysis of the stress-strain rate relationships between the treated and the natural (untreated) Eckernfoerde sediments is still being performed. There is a problem with selecting the appropriate statistical design to provide sufficiently constrained data for publication. However, this report can state some apparently secure observations concerning the behavior of the sediment slurries.

Rheological

1. The yield stress of the natural sediment is several orders of magnitude greater than the yield stress of the treated (cleaned) sediment at the same density. (Figures 4 and 5).

2. Flow behavior of natural and treated (cleaned) samples is almost exclusively shear-thinning (pseudoplastic), with greatest variation observed in the treated (cleaned samples (a few samples exhibited Newtonian and slight shear-thickening behavior). The mean values of the slope of the stress-strain rate curve (plotted on double log paper) are 0.6760 (natural) and 0.6438 (treated) respectively.

Interpretation

These interpretations are somewhat tentative inasmuch as the data still are being analyzed and digested. However it is suggested that the Eckernfoerde sediments have a tendency toward easy resuspension (due to shear-thinning flow behavior) and moderate yield stress development in the natural sediment. Once resuspended, the sediment will settle into a fluid mud quite rapidly. Hindered settling analysis (Figure 6) indicates that hindered settling of a 25 g/l suspension (14 ppt) will occur with 10-20 minutes, and a 50 g/l suspension will settle to a fluid mud (density of 1.05 Mg/m^3) in 35 minutes (without currents). Box cores indicate a complex sediment surface, one which is biologically bound by spionid worm activity and which is composed of highly organic sediment. This surface serves to resist normal expectable tidal shear stresses and exhibits a stable interface between the water and the sediment. However, in the event that the surface is disturbed (i.e., through dredging, trawling, anchoring, gas ebulition, or other means, the sediment would expect to behave in the manner suggested above. Stablilization of the substrate appears to result from biological activity.

Table 1

Sample #	Sand %	Silt %	Clay %	S/C	Mean dia. (μm)	OM %	$CaCo_3$ %
BC 223	3.63	40.73	55.84	0.74	0.71	18.32	0.3
BC 225	4.33	52.21	43.46	1.20	1.20	18.03	0.5
BC 237	3.82	44.37	51.31	0.86	2.24		
BC 238	2.75	41.55	55.70	0.75	0.68	20.03	1.1
BC 249	3.78	43.95	52.27	0.84	2.25		
BC 250	22.43	32.51	45.06	0.72	2.17	13.92	0.2
BC 251	1.42	45.47	53.11	0.86	0.68	10.72	0.2
BC 257	2.67	43.39	53.94	0.80	1.92	18.42	
BC 264	1.03	41.61	57.36	0.73	0.64	18.04	1.2
SITE H	11.41	48.71	39.88	1.22	2.12	15.01	7.5

Table 2

#	Ty	T_B	Density	Slope	#	Ty	T_B	Density	Slope
225	4.15	17.5	1.075	0.9622	225	1.17		1.0842	
-	36.5	92.0	1.315	0.7160	-	4.30	5.40	1.1213	0.3889
232	3.13	16.2	1.084	0.9700	232	3.13	16.20		0.9700
-	19.57	75.0	1.133	0.8239	-	19.57	75.0	1.130	0.8239
237	14.09	29.0	1.087	0.9208	237	0.39	1.25	1.098	1.0703
-	21.92	70.0	1.110	0.6726					
249	14.38	30.0	1.087	0.8888	249	4.79	6.4	1.1026	0.3010
-	114.71	95.0	1.196	0.1597	-	6.26	7.2	1.1095	0.4557
-	99.07	90.0	1.147	0.1934	-	14.08		1.1429	1.000
251	153.8		1.147	0.5099					
-	120.2	135.0	1.147	0.5863					
-	3.13	11.0	1.038	0.7959					
-	48.8	210.0	1.050	0.9208					
252		17.5		0.8451					
253	13.31	34.5	1.108	0.7368	253	4.60	6.2	1.1017	0.4664
-	59.54	140.0	1.137	0.5229	-	13.3	16.5	1.1287	0.4771
						21.1	36.5	.1491	0.3522
257	52.11	52.0	1.132	0.6837	257	8.62	8.0	1.1018	0.6601
					-	11.73	20.0	1.1357	0.7132
264	15.66	30.0	1.096	0.6532	264	0.39	0.75	1.1022	1.0414
-	145.91	310.0	1.162	0.5943	-	7.82	4.50	1.1442	0.6088
-	59.93	190.0	1.141	0.7501					
H	18.79	40.0		0.7270	H	43.81	57.0	1.2745	0.4674
-	88.59	205.0	1.212	0.5750	-	7.05	6.0	1.1620	0.5027
			Mean	0.6760				Mean	0.6438

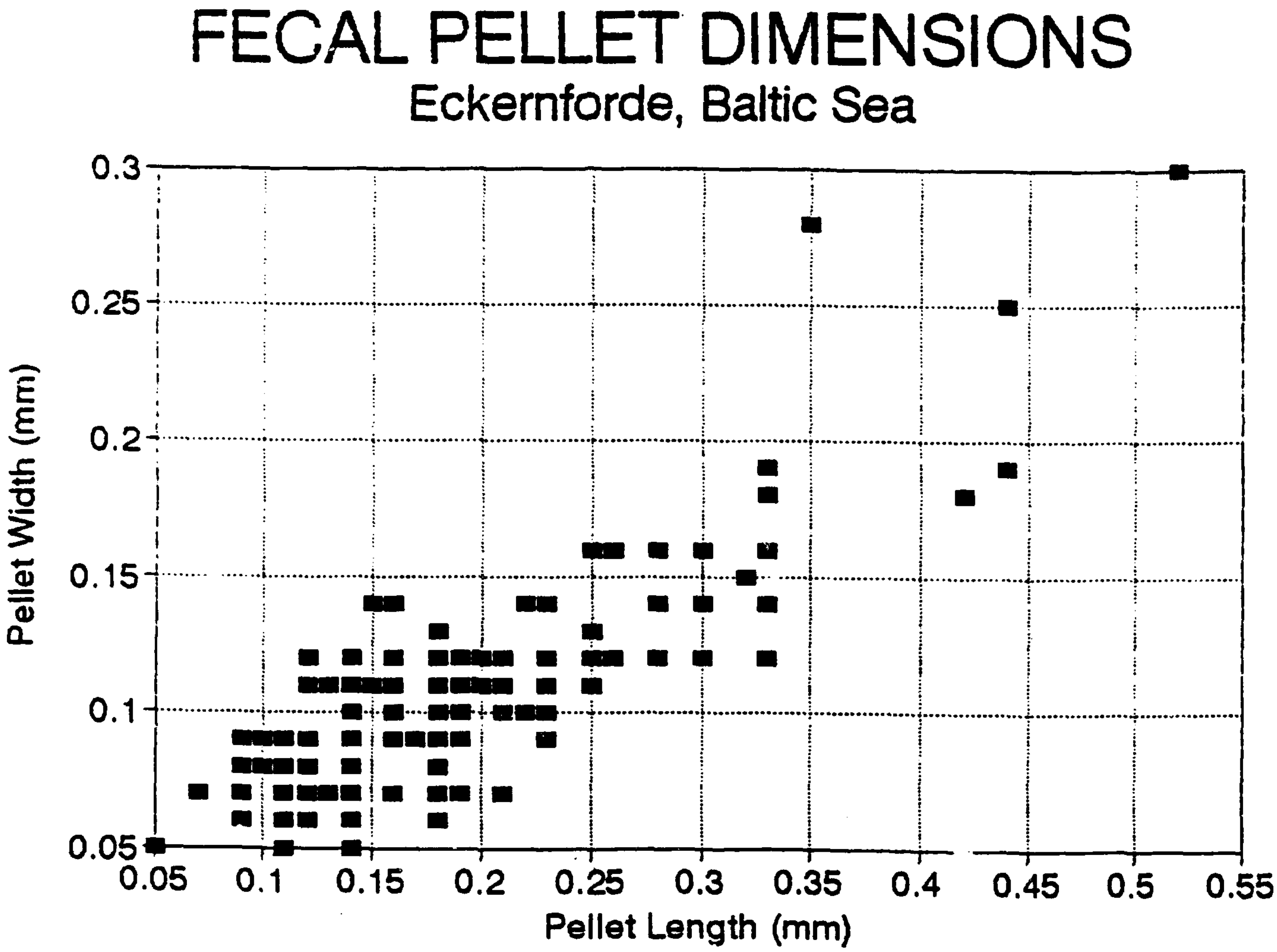

Figure 1. Measurements of fecal pellets in BC 264.

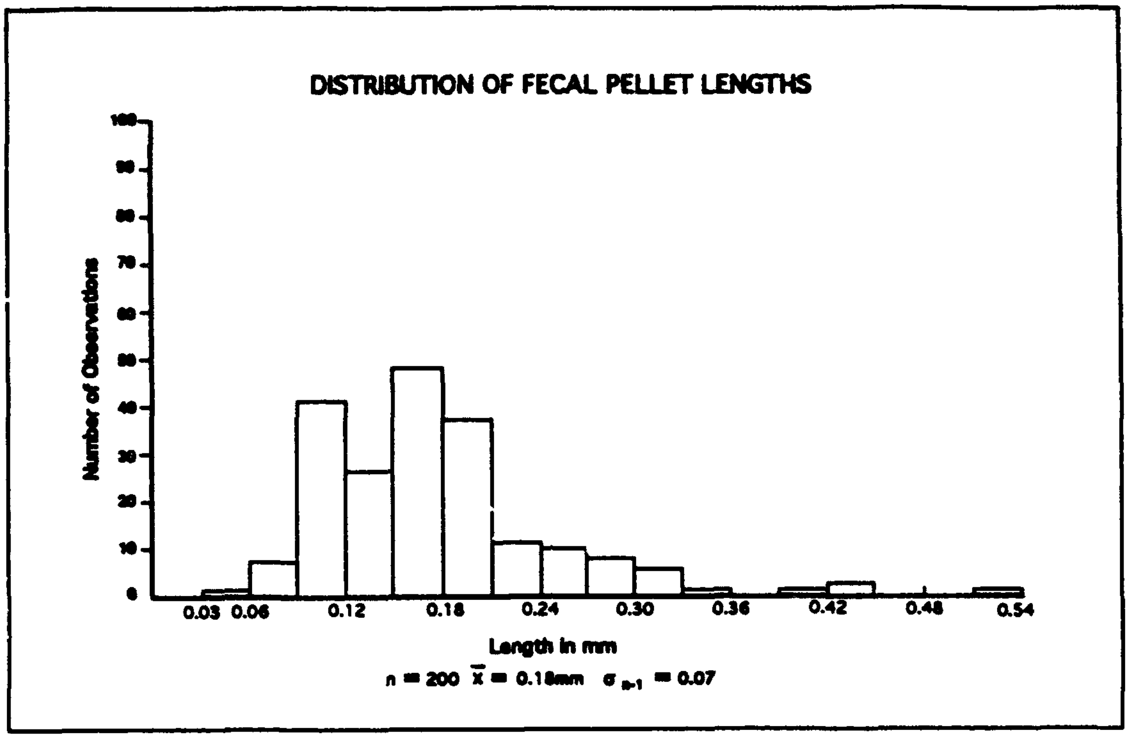

Figure 2. Histogram showing the distribution of fecal pellet lengths.

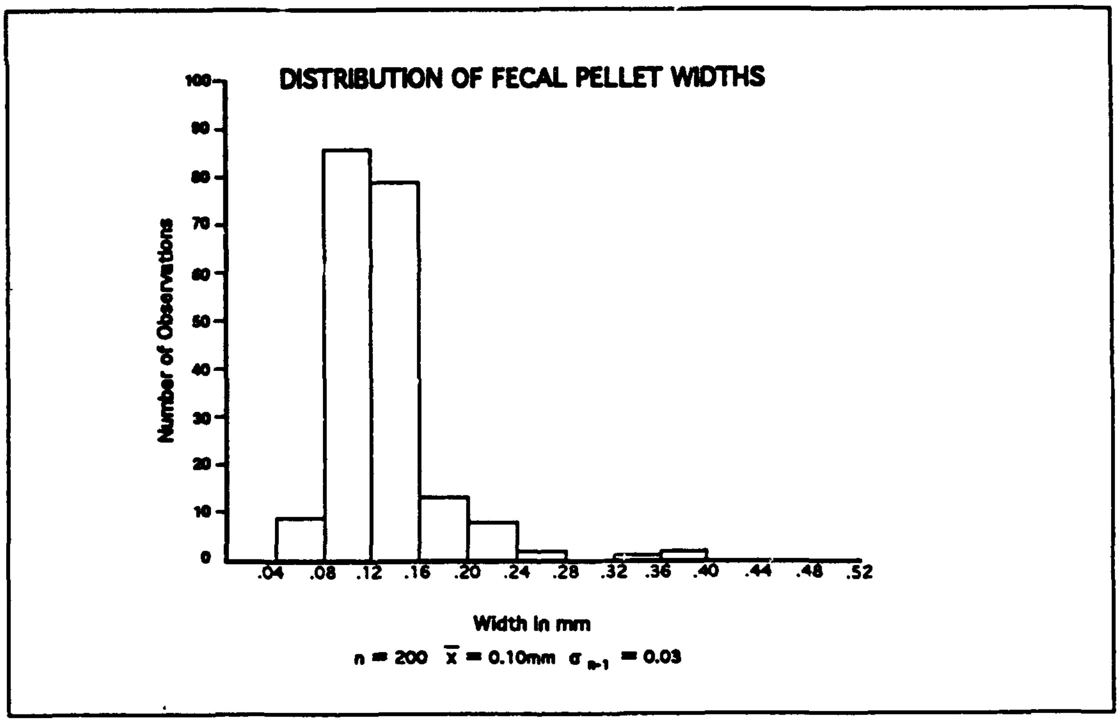

Figure 3. Histogram showing the distribution of fecal pellet widths.

Yield vs Slurry Density (clean)

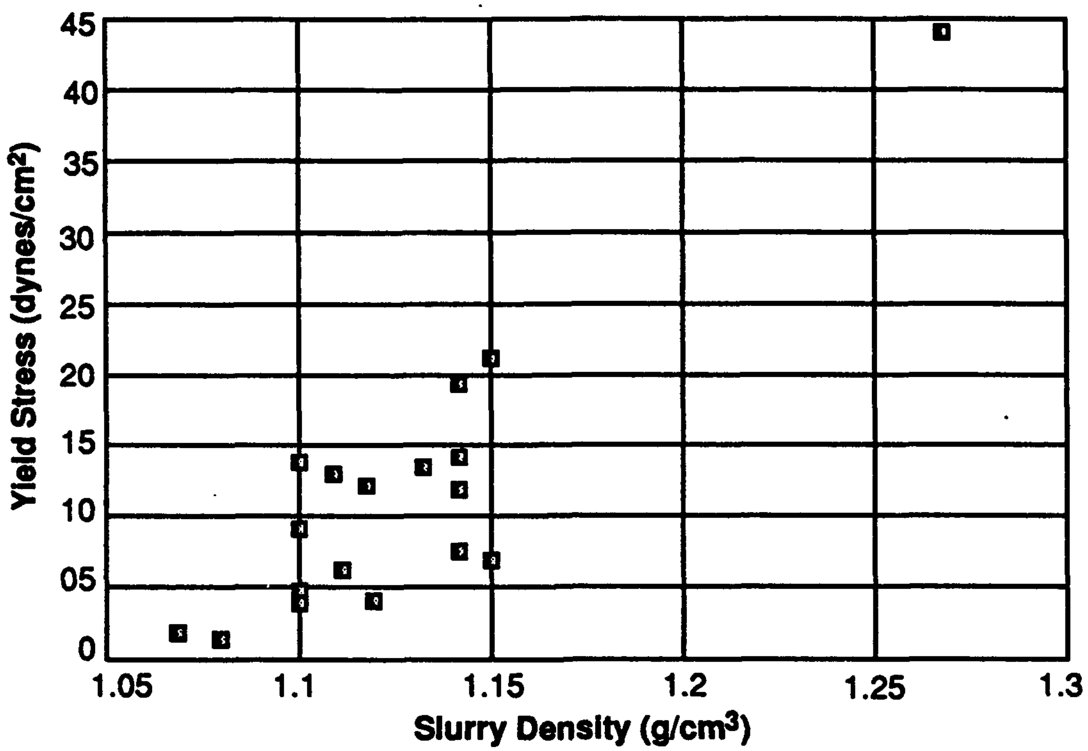

Figure 4. Yield stress versus slurry density (treated).

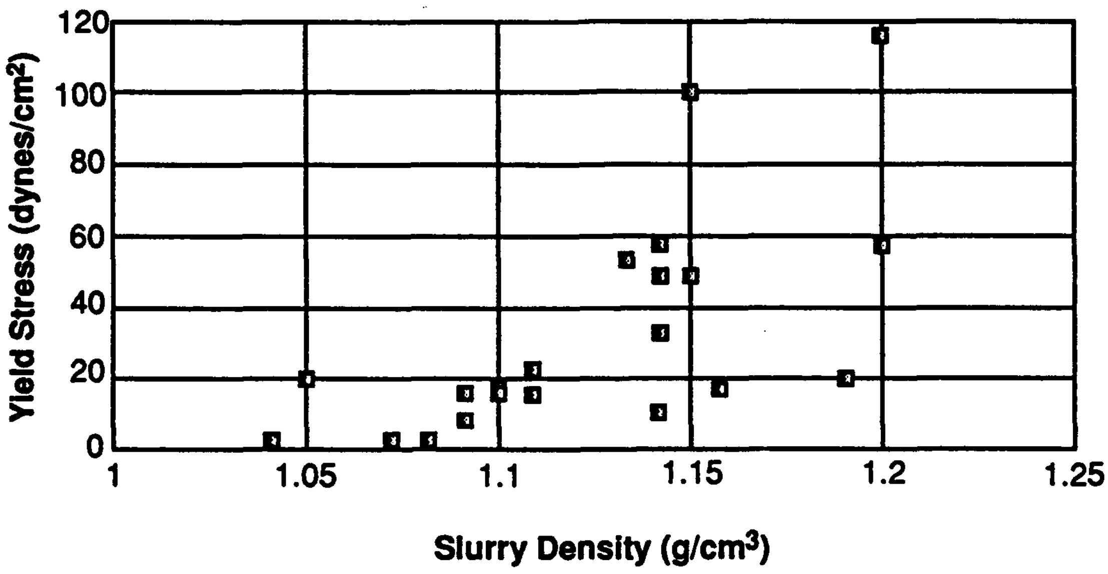

Figure 5. Yield stress versus slurry density (natural).

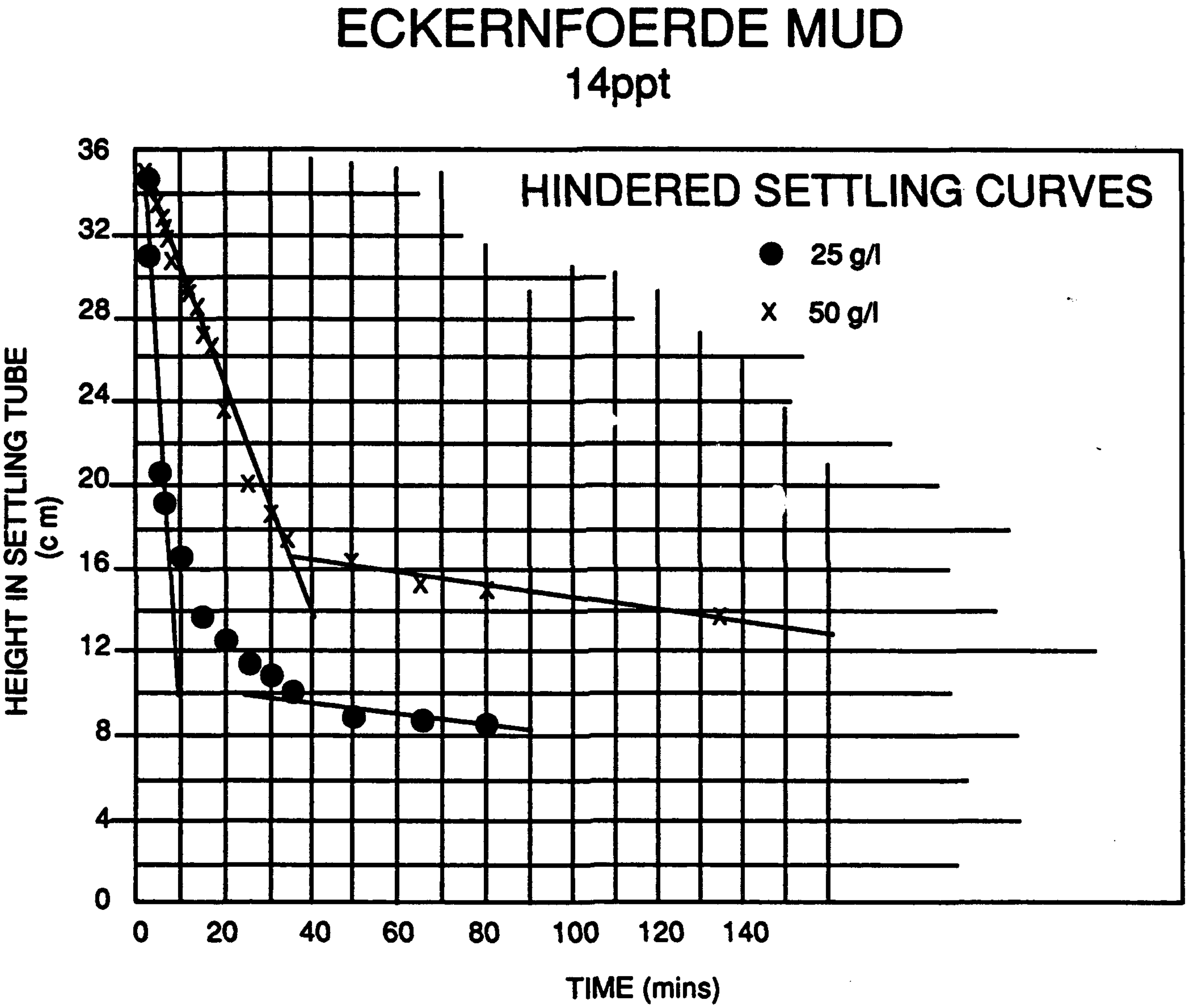

Figure 6. Hindered settling curves for 25 and 50 g/l muds.

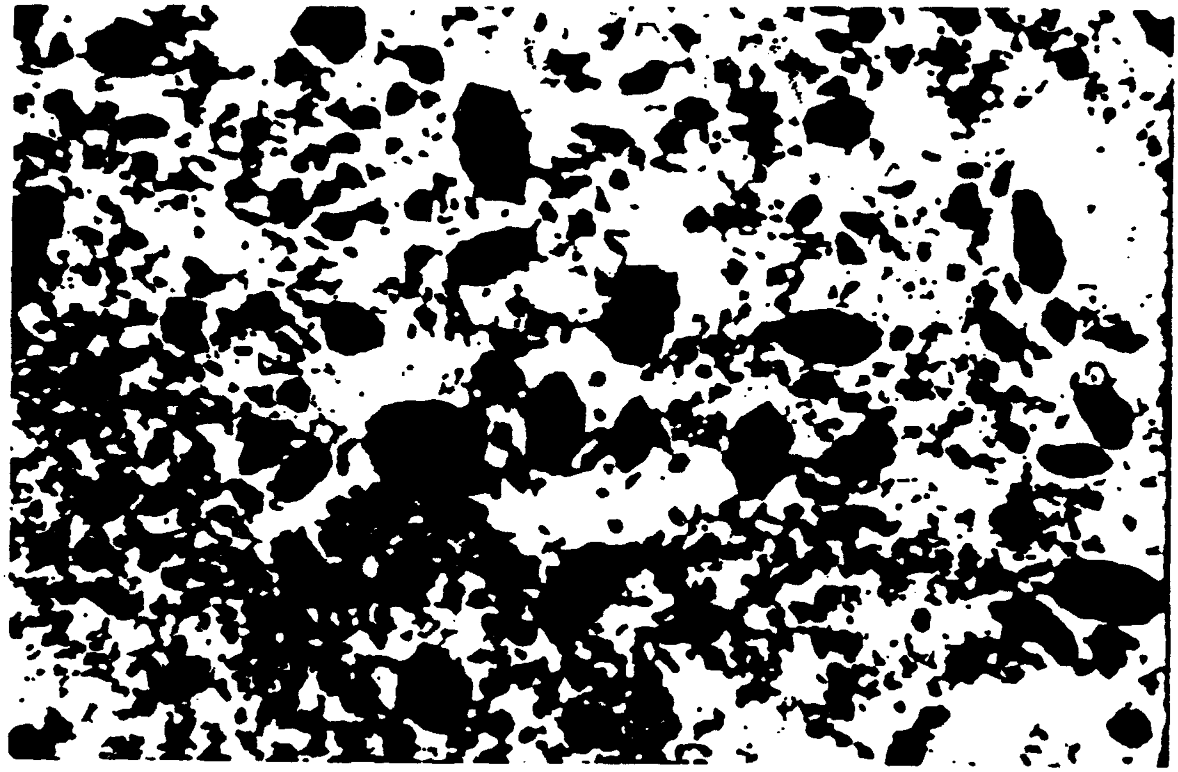

PLATE 1a. Sample BC264 25x unpolarized light - Eckernforde

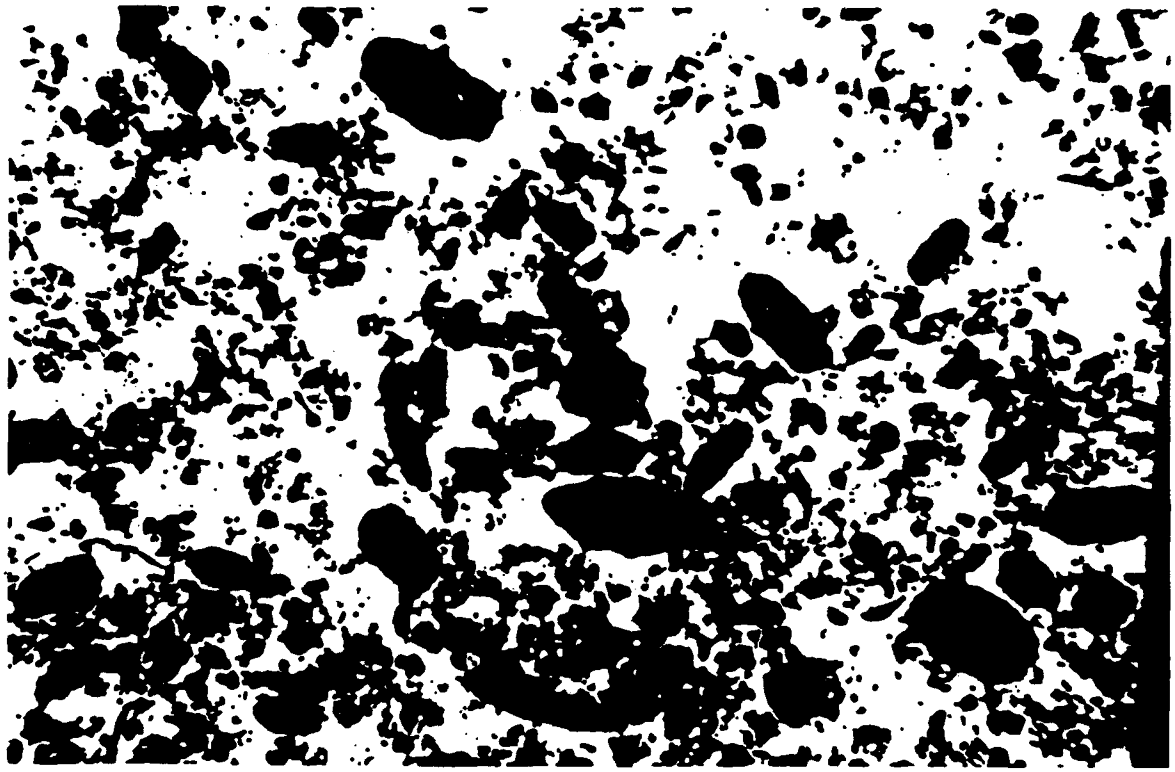

Plate !b - Sample BC 264 25x unpolarized light - Eckernforde

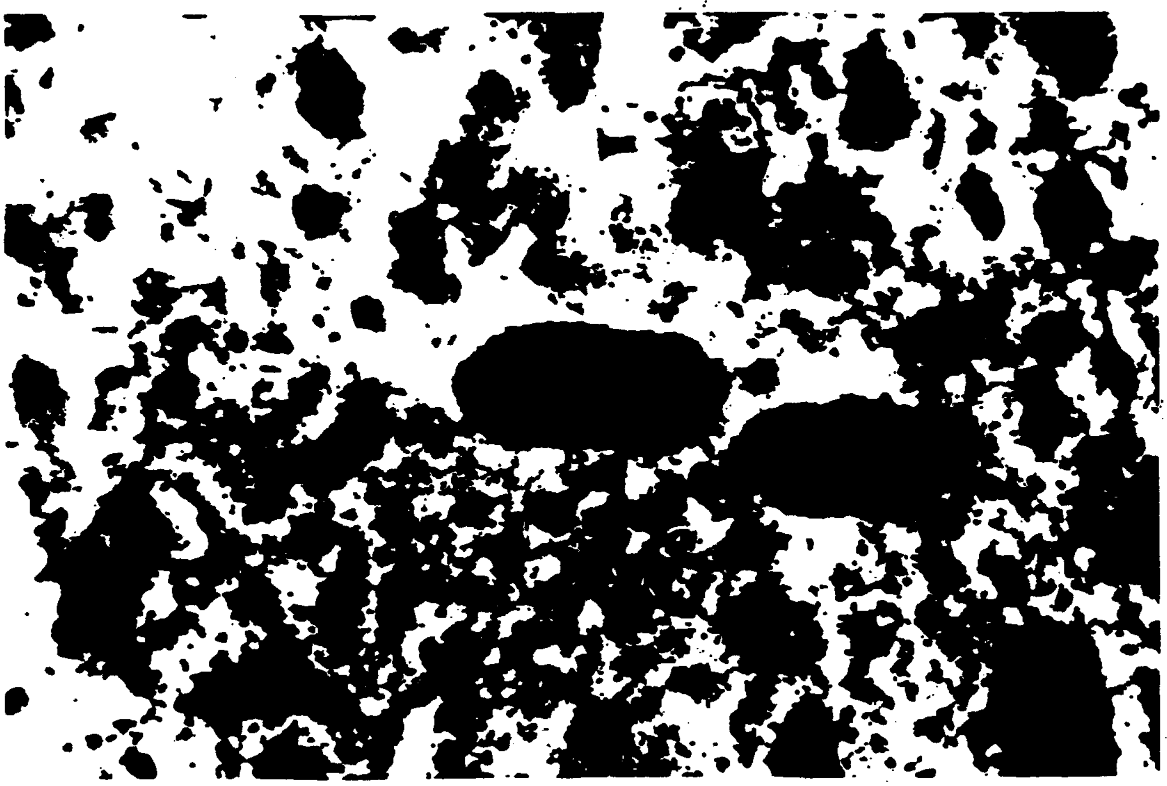

PLATE 2a. - Sample BC 264 63x unpolarized light - Eckernforde

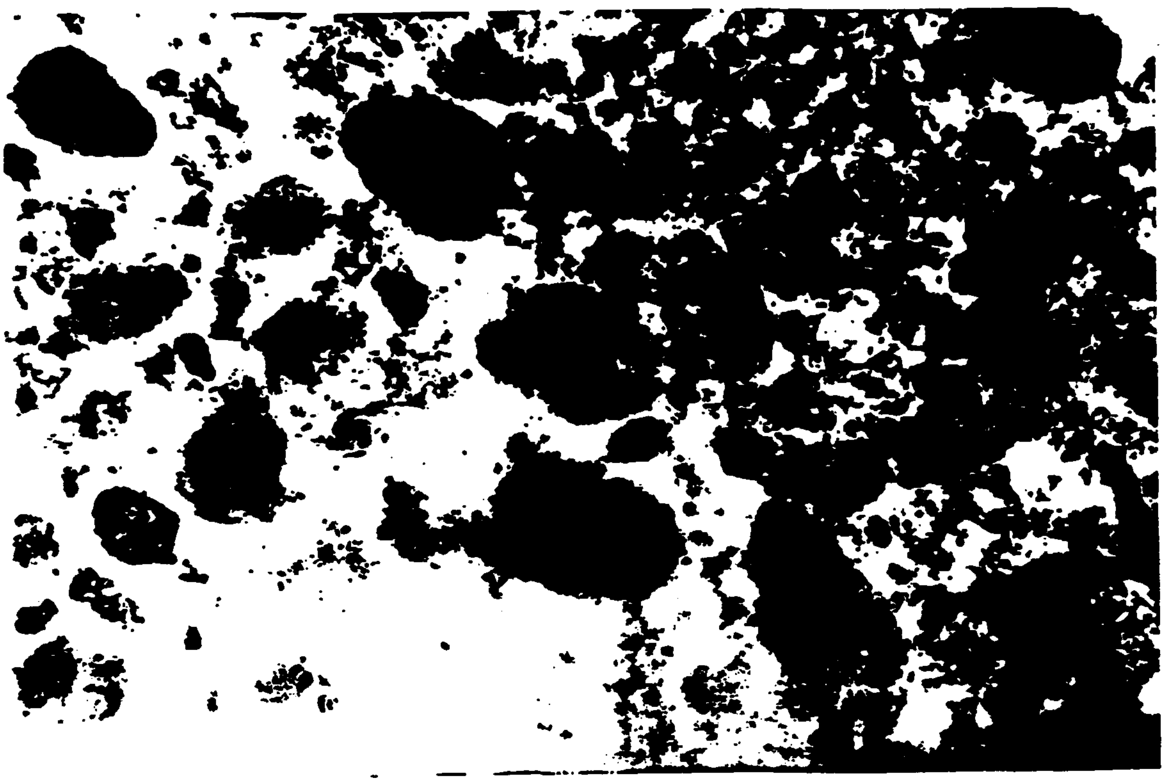

PLATE 2b. - Sample BC 264 63x unpolarized light - Eckernforde

3.8 Statistical Characterization of the Benthic Boundary Layer for Broadband Acoustic Scattering (Principal Investigators: K. E. Gilbert, D. F. McCammon and R. K. Young, Pennsylvania State University)

CBBLSRP FY93 YEAR-END REPORT

K. E. Gilbert, D. F. McCammon, R. K. Young
Applied Research Laboratory
Pennsylvania State University
P.O. Box 30
State College, PA 16804

OBJECTIVE:

The objective of the proposed work is to characterize the benthic boundary layer as a scatterer of high-frequency, broadband acoustic energy and to relate the broadband backscatter to sediment macrostructure and microstructure. It is hypothesized that high-resolution probe signals (large time-bandwidth product), together with wavelet analysis, will allow the extraction of important new bottom features, such as phase dispersion, and thereby significantly enhance the bottom characterization presently obtainable with standard approaches.

PROPOSED RESEARCH:

The proposed research has two parallel elements which will proceed together in two separate phases. The first element is numerical computation of the acoustics response of the sediment using realistic multi-scale, possibly fractal, sediment models. The second element is the analysis of backscattered signals (both computed and measured) using long-duration, wideband probe signals and novel signal analysis techniques, including wavelet transforms.

In the first phase of the research, we will numerically simulate the broadband acoustic response for finely layered, horizontally stratified (2-D) sediments. The simulated backscatter will be used as synthetic data to test and evaluate the utility of both conventional and wavelet analysis techniques. For the synthetic data the sediment structure is know in detail. hence the comparisons using synthetic data will serve as a benchmarks for comparisons using actual field data.

In the second phase, acoustic field data collected by other investigators will be analyzed to distinguish bottom-related features. Insights gained from the benchmark work will be used to design improved analysis schemes. At the same time, more advanced modeling efforts will be undertaken to model horizontally varying (3-D) sediments. The experimentally measured sediment structure information provided by other investigators in the program will be accepted as model/simulation inputs to verify the computational models. The aim in the second phase is to use a two-pronged signal analysis/acoustic modeling approach to characterize the sediment macrcstructure and microstructure in terms of extracted features (such as the phase dispersion extracted by wavelet analysis) and, at the same time, to verify the models and extracted features with actual sediment structure measurements.

RESEARCH PROGRESS TO DATE:

FY93 was a start-up year with initial funding to attend SRP workshops and reviews and to collaborate with other SRP participants to discuss databases and to identify important research issues. Funded SRP research at Penn State is scheduled to officially begin in FY94. However, to enable a student funded by a supplementary (AASERT)(grant to begin his research, we started work in the summer of FY93, a few months ahead of schedule. A particular problem pointed out to us by SRP researchers at NRL-Stennis (D. Lambert, D. Walter, and J. Hawkins) is the difficulty in acoustically distinguishing a soft gassy sediment with high reflectivity from a hard (non-gassy) reflective sediment. Beginning modeling efforts are presently focused on this general sediment characterization issue. A general, exact broadband reflectivity model has been developed and is being used to simulate the pressure-vs-time signals for gassy and non-gassy layered sediments. It is planned to compare the simulated acoustic response (broadband and narrowband) using conventional processing and wavelet processing with results obtained from existing SRP field data (e.g., data from D. Lambert, S. Schock) for both gassy and non-gassy sediments. A fundamental problem in the acoustic modeling is the intrinsic structure of gassy sediments, layers containing many small bubbles (continuum model) versus a relatively few larger bubbles (discrete scatterers). Issues concerning the basic structure of gassy sediments are being addressed with the advice of an SRP scientist, A. Anderson, who is analyzing gassy sediment structure in detail. The present layered continuum model is being extended to allow for scattering from individual bubbles in addition to scattering from gassy layers. Part of the current work will serve as the basis for a student's MS degree. Since the work has been underway for only a short time, results are still quite tentative. Preliminary results are to be presented at the San Diego AGU meeting in February 1994.

3.9 Measurement of High-Frequency Acoustic Scattering From Coastal Sediments (Principal Investigators: D. R. Jackson and K. L. Williams, University of Washington)

CBBLSRP FY93 YEAR-END REPORT

Darrell R. Jackson and Kevin L. Williams
Applied Physics Laboratory
College of Ocean and Fishery Sciences
University of Washington
Seattle, WA98195

General Summary of Work During This Period

The primary activities in FY93 were preparation for and execution of acoustic measurements at Eckernfoerde Bay near Kiel, Germany, and at a coastal site near Panama City, Florida. Measurements at both locations included long-term bottom backscattering observations using the APL-UW Benthic Acoustic Measurement System (BAMS, operating at 40 kHz) and shorter-term bottom bistatic scattering measurements using a mobile receiving array with BAMS serving as the acoustic source (Fig. 1). The BAMS backscatter data cover a 100-m diameter region, providing a large-scale, long-time view not obtainable by conventional sampling. Images formed by cross-correlating data separated in time provide an acoustic view of changes in bottom structure due to biological of hydrodynamic effects. These measurements were closely coordinated with the coring observations of Nittrouer and Lopez (SUNY Stony Brook) and the boundary-layer measurements of Wright (VIMS). The bistatic data are more extensive in angular coverage than previously published data and are expected to provide rigorous tests of scattering models. For example, gas bubbles tend to scatter sound omnidirectionally, while inhomogeneities due to bioturbation produce a more complex characteristic angular pattern.

Data Collection

The following table summarizes the backscatter and bistatic data sets acquired in FY93 in terms of numbers of 360\(de scans recorded, and the time interval between scans.

	Eckernfoerde Early Deployment	Eckernfoerde Main Experiment	Panama City
Deployment Date	3 April, 1993	3 May, 1993	13 August, 1993
Backscatter Data	350 Scans, 1/Hour	650 Scans, 2/Hour	1320 Scans, 3/Hour
Bistatic Data		20 Scans, 2/Hour	34 Scans, 3/Hour

Bistatic data are difficult to obtain in statistically significant quantity because there are three independent angular variables, specifying the directions of incident and scattered sound. These angular variables were controlled by varying the range between source and receiver and by varying the pointing direction of the bistatic receiving array (Fig. 1). Figure 2 shows the angular coverage obtained at Eckernfoerde Bay. While this coverage is believed sufficient for estimation of bistatic scattering strengths, somewhat greater coverage was attempted and achieved at Panama City.

Interpretation

The Bistatic data have not yet been analyzed, but preliminary analysis of the backscattering data from Eckernfoerde Bay and Panama City has revealed interesting phenomena. The backscatter correlation images from Eckernfoerde Bay (Fig. 3) show an overall decorrelation with a time scale on the order of a few days. We will fit a model to these data in order to extract quantitative estimates of the time- and space-scales of reworking. In determining the depth of reworking, the depth of acoustic penetration is an important model input that will be available from other CBBL investigators. In addition to the general decorrelation, there are "hot spots" seen in Fig. 3 which are areas of more intense activity. Collaborative study with VIMS and SUNY may reveal the mechanisms operating in these areas.

The VIMS boundary-layer apparatus detected a strong event during the early deployment at Eckernfoerde; this event was observed in both current and optical measurements. Figure 4 compares two correlation images, one formed from data taken during a quiet period and the other spanning the period of the event reported by VIMS. Strong decorrelation is seen in the latter image, indicative of a substantial change in the bottom.

Figure 5 shows that the Panama City backscatter data showed unusually rapid decorrelation. This may indicate an unusually high level of activity, or it may indicate very shallow acoustic penetration, leading to extreme sensitivity of the measurement to changes in surficial structure. The later scenario seems consistent with the fact that the sediment was a coarse sand, but must be considered in light of the acoustic penetration measurements made by Stanic (NRL Stennis). Interpretation of the Panama City correlation data may be aided by an experiment by Briggs (NRL Stennis) in which divers altered the bottom in the field of view of BAMS by dragging a heavy chain and by injecting air into the sediment. Careful study of the backscatter data obtained before, during, and after these alterations may aid our understanding of the acoustic scattering mechanisms.

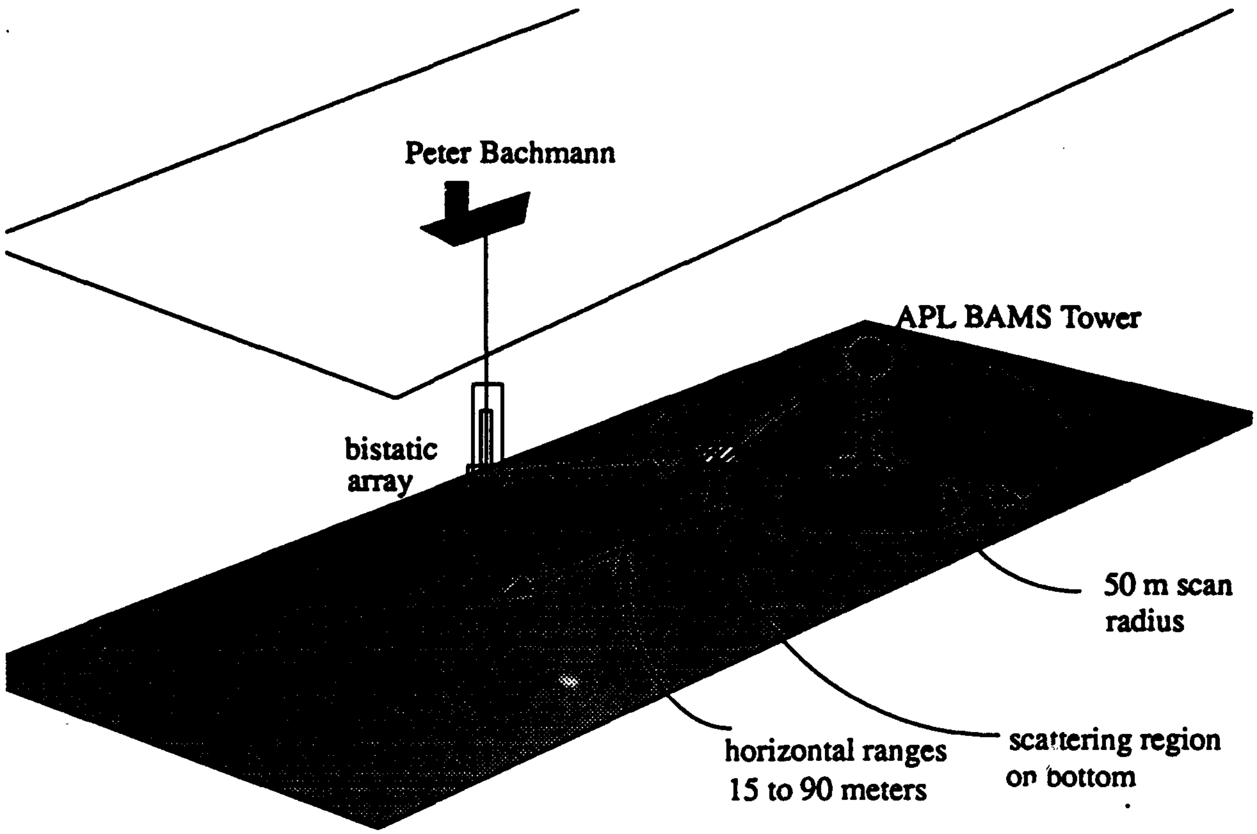

Figure 1. Simplified diagram of the elements involved in the APL bottom scattering measurements. The BAMS tower was used to autonomously collect acoustic backscattering scans of the bottom for several weeks and the correlation of these returns calculated over the scanned region as a function of time. The bistatic array was used in conjunction with the tower to collect data that will be processed to obtain bistatic scattering strength as a function of three bistatic angles.

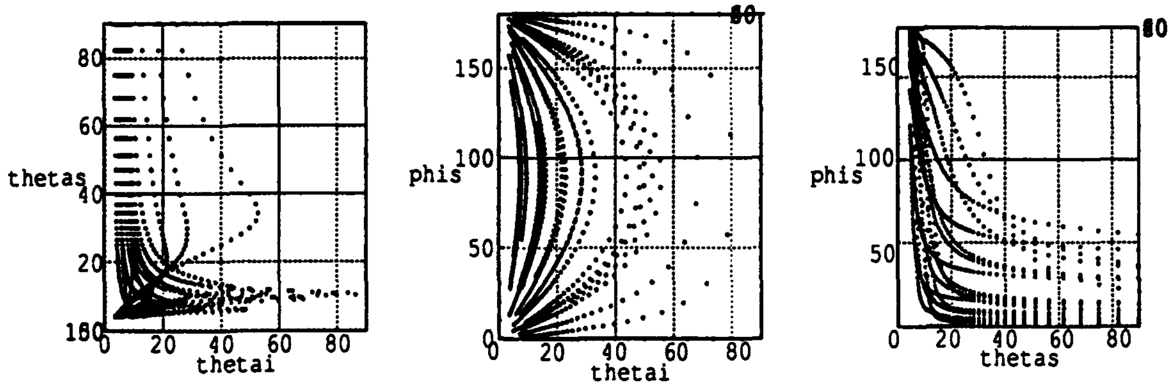

Figure 2. Bistatic scattering angles covered for the geometries obtained in the combined tower/array experiments. Tower/array horizontal ranges of 15 to 90 meters were obtained using a single point moor. The angle thetai is the angle of the incident sound energy relative to the horizontal, and thetas is similarly defined for the scattered sound. The angle phis is the change in azimuth between incident and scattered sound

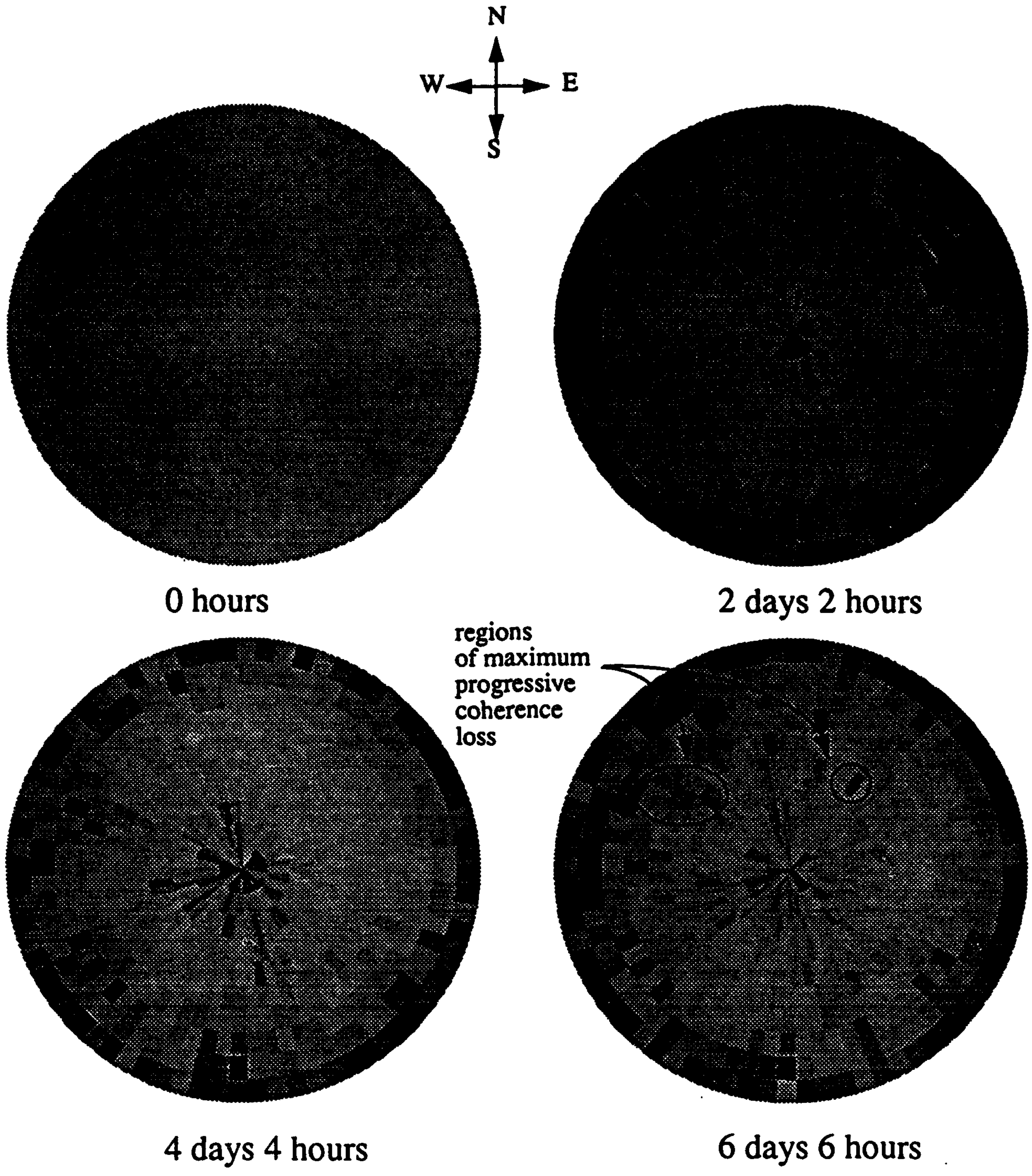

Figure 3. Acoustic correlation images, data taken April 1993 by APL-UW during CBBL SRP Joint High-Frequency Bottom Backscattering Experiment in Eckernfoerde Bay. Light gray indicates regions of little change (correlation near unity), black indicates regions of significant change (correlation 0.5 or less). Each pixel is 5 degrees wide in azimuth and 5 m long in range (maximum range is 50 m). The black pixel at range 40-45 m and due South is due to transient interference in the reference scan. Two "hot spots", localized regions of activity, are shown.

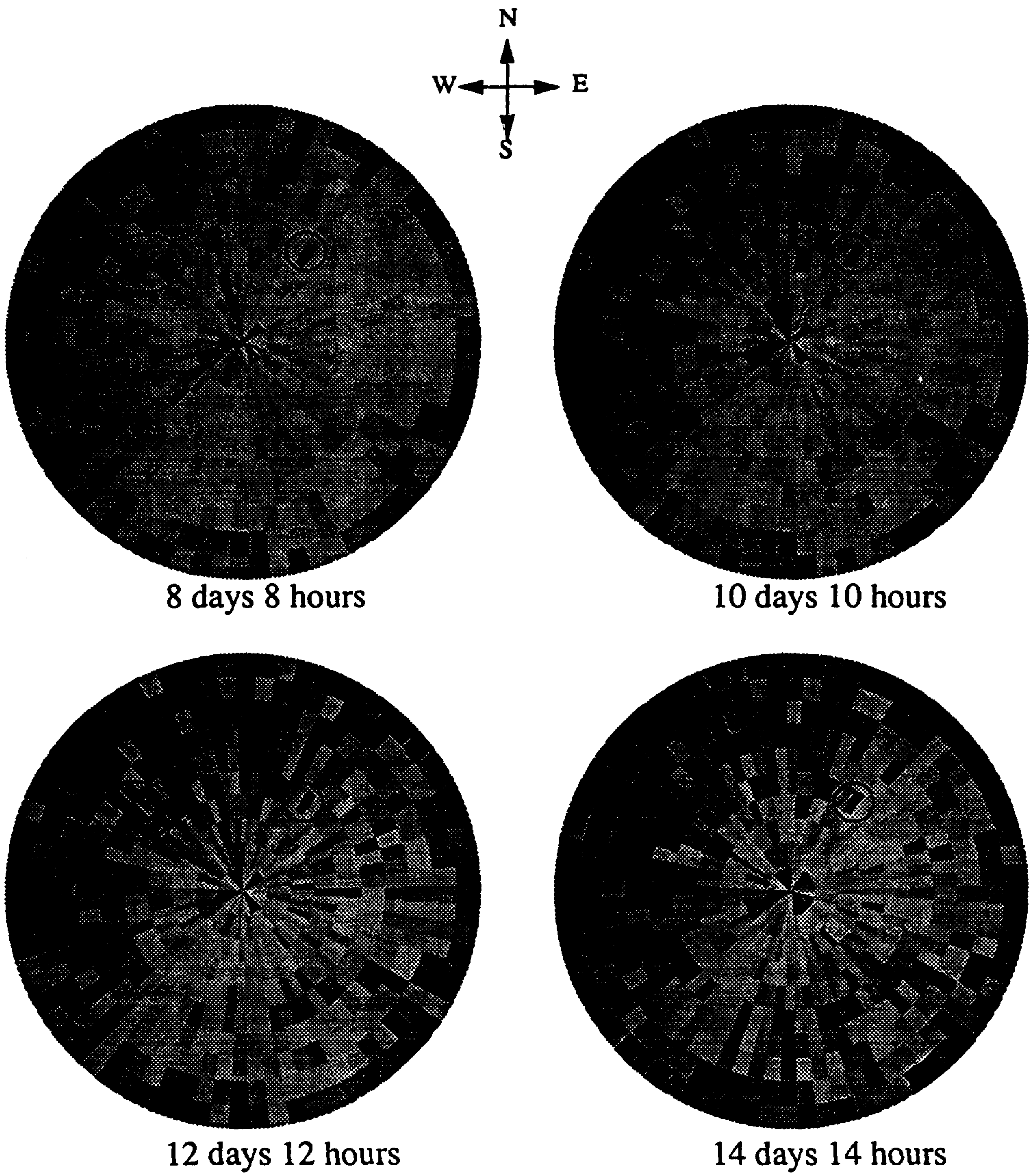

Figure3 (cont.). Acoustic correlation images, data taken April 1993 by APL-UW during CBBL SRP Joint High-Frequency Bottom Backscattering Experiment in Eckernfoerde Bay. Light gray indicates regions of little change (correlation near unity), black indicates regions of significant change (correlation 0.5 or less). Each pixel is 5 degrees wide in azimuth and 5 m long in range (maximum range is 50 m). The black pixel at range 40-45 m and due South is due to transient interference in the reference scan. Two "hot spots", localized regions of activity, are shown.

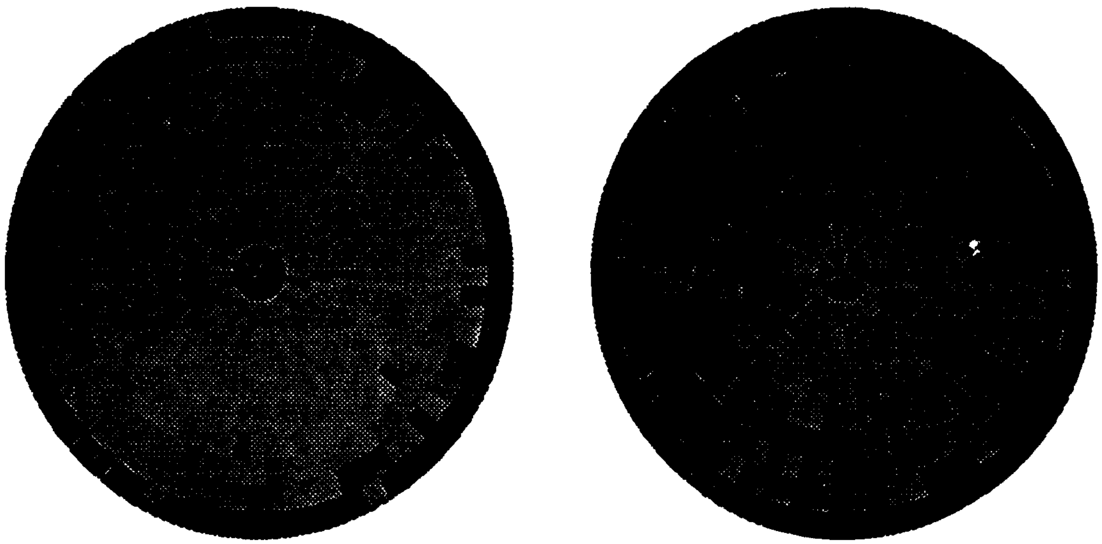

3 April, 1500 GMT
to
5 April, 0100 GMT

8 April, 0800 GMT
to
9 April, 1800 GMT

Figure 4. Each acoustic correlation image above was generated using scans separated by 34 hours. The image on the right spans a time when a significant current event was recorded on the VIMS tripod sensors. The image on the left is for a non-event time range. Light gray indicates regions of little change (correlation near unity), black indicates regions of significant change (correlation 0.75 or less). An enhanced decorrelation during the event time range is seen.

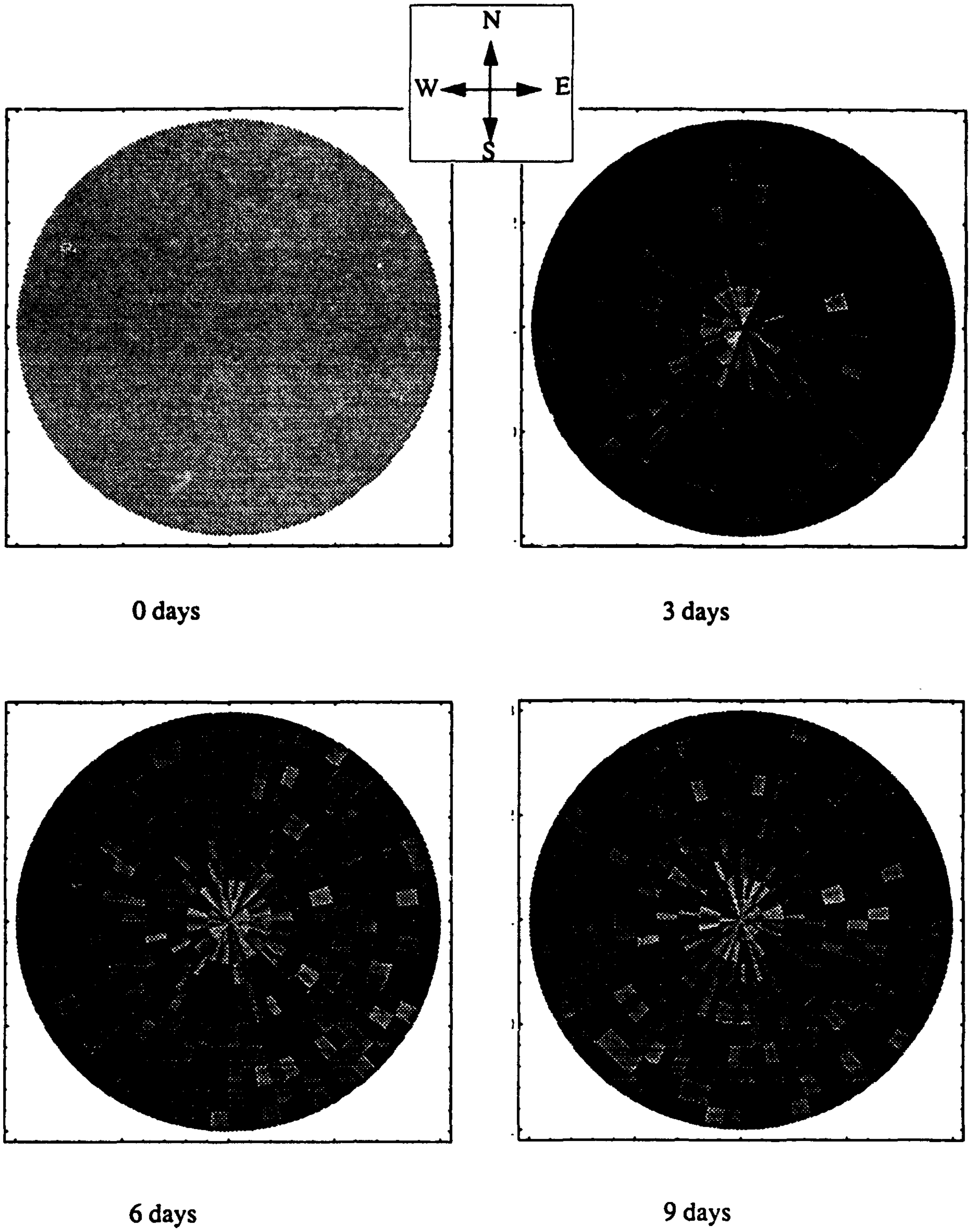

Figure 5. Acoustic correlation images, data taken August 1993 by APL-UW during CBBL SRP Bottom Backscattering Experiment off Panama City. The top, left image is for a scan 3 days after deployment. Light gray indicates regions of little change (correlation near unity), black indicates regions of significant change (correlation 0.125 or less). Each pixel is 5 degrees wide in azimuth and 5 m long in range (maximum range is 50 m). A "cold spot" (localized region of little activity) is shown.

3.10 Structural Analysis of Marine Sediment Microfabric (Principal Investigator: J. J. Kollé, Quest Integrated, Inc.)

CBBLSRP FY93 YEAR-END REPORT

J. J. Kollé

Quest Integrated, Inc.
21414 68th Avenue
Kent, A 98032

Overview

This project will test the idea that the geoacoustic and geotechnical properties of marine boundary layer sediments can be evaluated and linked through microstructural analysis. This problem will be approached initially through an integration of sediment microstructure analysis and geoacoustic property modeling. An existing microstructure analysis code will be used to generate saturated and unsaturated poroelastic constants from sediment microfabric images. These parameters can then be used to constrain Biot models used to derive attenuation and velocity dispersion constants for pressure and shear waves. The proposed work will be coordinated with the experimental component of the Coastal Benthic Boundary Layer Special Research Program (CBBL-SRP). Predicted geoacoustic properties will be compared with experimental data to evaluate the capabilities of the analysis scheme. Limitations of semiemperical Biot models can be addressed in the later stages of the proposed work through direct numerical simulation of poroelastic deformation and fluid flow in a three-dimensional microstructure.

Work Completed in FY93

The first year of the CBBL-SRP has focused on field experiments. Our sediment microstructure analysis work was therefore scheduled for FY94 and our effort in FY93 has been limited primarily to providing input to planning meetings and ensuring that the data required for analysis will be available. Dr. Kolle attended the first CBBL-SRP planning meeting in November 1991 and made a presentation of the microstructural analysis techniques proposed. The analysis work will require microstructure imagery from the field test sites as well as frequency dependent acoustic velocity and attenuation data. The planning meetings and subsequent discussions ensured that this data will be available for the field test sites.

There are two components to the planned sediment microstructure analysis. We will first use finite element analysis techniques to evaluate the static poroelastic stiffness constants of the sediment. Microfabric image analysis can also be used to constrain fudge factors in existing Biot models (squirt length in Biot-Squirt model; structure, pore size and complex modulus parameters in Biot-Stoll model). These factors must presently be inferred empirically from analysis of velocity and attenuation dispersion data. The second component of the analysis involves applying constrained Biot models to infer sediment permeability.

A number of preliminary numerical analyses were carried out to test the capabilities of our existing microstructure analysis code MISTRA for analysis of saturated sediments. MISTRA was developed for the analysis of the thermal, elastic and yield characteristics of two-phase composites based on two-dimensional cross sections of the composite microstructure. Analysis of composites consisting of a continuous matrix phase reinforced with particles of a second phase are carried out by assuming a generalized plane strain boundary condition which constrains the mean out-of-plane stiffness to equal the in-plane transverse stiffness of the material. This approach has proven effective in the analysis of particulate reinforcement in relatively low concentrations. We would like to model saturated sediments as two phase composites using this generalized plane strain approach, since this would allow measurement of the sediment framework stiffness based on a two-dimensional microfabric image.

We have assumed that sediments can be modeled as a two-phase water/mineral composite. MISTRA requires that the properties of water be simulated by an elastic material. We have used a pseudowater parameterization with elastic moduli chosen to match the compressibility of water and very low shear modulus in our initial calculations of sediment P-wave velocity. Figure 1 shows a unit cell of a random sand/pseudowater composite. A number of these microstructures with varying porosity were generated using a statistical procedure contained with MISTRA. Average values of elastic moduli and inferred acoustic velocities are listed in Table 1. The P-wave velocities predicted by MISTRA are consistent with observations of velocity versus porosity in clean sandstones with porosities of up to 31%. Random variations in structure cause significant changes in acoustic velocities.

Table 1. MISTRA Analysis of Random Sandstone Microstructures

f, (Porosity)	C_{11}, GPa	C_{44}, GPa	r, kg/m^3	Cp, km/s	Cs, km/s
.20	37.2	12.8	2326	4.0	2.4
.21	26.1	9.5	2303	3.4	2.0
.22	34.0	10.2	2292	3.9	2.1
.26	30.3	9.9	2230	3.7	2.1
.31	15.4	0.8	2143	2.7	0.6

The existing MISTRA model appears to give reasonable results for cemented sandstones and may prove useful for data obtained from the Panama City experiment. We will also apply the model to the analysis of Biot parameters for the high porosity clay structures observed in the Eckernfoerde Bay experiment. The model cannot, however, account for non-linear elastic behavior of sediments related to contact effects in loose granular materials and we expect non-linear effects in clay structures as well.

In related work in FY93, we have improved our image processing and finite element analysis capabilities. We can now generate two-dimensional periodic adaptive grids which include gaps and frictional contact elements as shown in Figure 2. These features allow direct numerical simulation of non-linear effects related to frictional contact. We have also developed image processing techniques for generating periodic structures from images of random microstructure. This involves generation of Fourier transforms of the image, high-pass filtering and inverse transforming to generate a periodic structure with the same high frequency spectral content as the original image. It may also be possible to extend this technique to generation of three dimensional structures from two dimensional microfabric images. A similar approach which used fractal image analysis is also be evaluated.

Plans for FY94

We plan to carry out the bulk of the proposed work in FY94. A paper describing preliminary results and analysis plans will be prepared for presentation at the ASLO/AGU Ocean Sciences meeting in San Diego. We plan to obtain microstructure images from both field areas and initially apply MISTRA to the analysis of poroelastic constants. It is apparent that grain contact effects in three dimensions are critical to evaluation of acoustic properties of unconsolidated sediments, so we plan to use the adaptive grid and contact elements developed last year to the analysis of microfabrics. We also plan to enhance our present code to include three-dimensional contact elements. Finally, we plan to use the poroelastic constraints generated by microstructure analysis as inputs to the Biot-squirt and Biot-Stoll models. This analysis will allow us to evaluate how well the microstructure analysis and acoustic properties obtained by other workers in the CBBL-SRP can constrain sediment permeability. The Biot modeling will be carried out in collaboration with Jack Dvorkin at Stanford University.

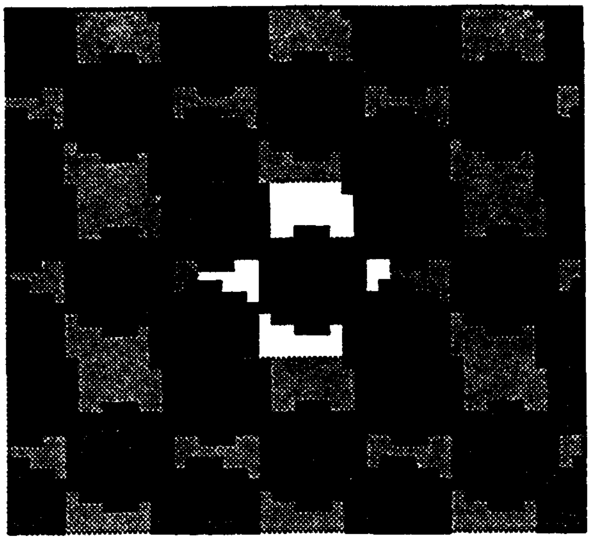

Figure 1. Random Sandstone Microstructure, $\phi = .26$

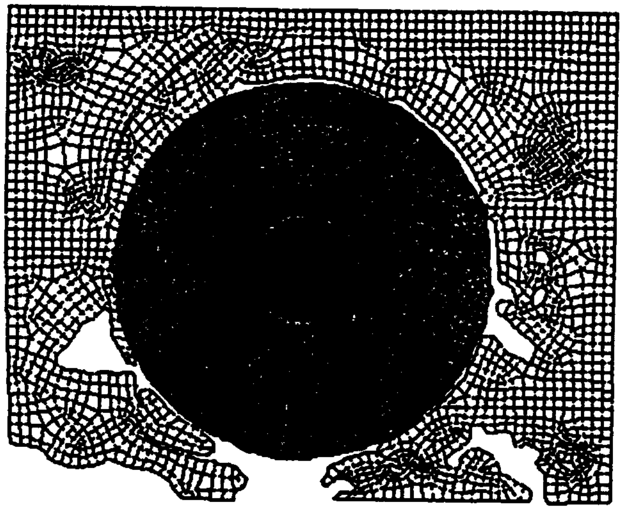

Figure 2. Adaptive Analysis Grid with Gaps and Contact Elements

3.11 Qualification of High Frequency Acoustic Response to Seafloor Micromorphology in Shallow Water (Principal Investigators: D. N. Lambert and J. A. Hawkins, NRL)

CBBLSRP FY93 YEAR-END REPORT

D.N. Lambert[1], D.J. Walter[1], J.C. Cranford[2], J.A. Hawkins[1], and R-D. Redell[3]

[1] Naval Research Laboratory, Code 7431, Stennis Space Center, MS 39529
[2] Neptune Sciences, Inc., 1118 Robert Blvd., Slidell, LA 70458
[3] Marineamt, SpezStAbt Geophysik, 26382 Wilhelmshaven, Germany

Project Objectives

The objectives of this project are (1) to investigate new methods of quantifying the effect of sediment micromorphologic structure on high frequency acoustic response in shallow water and its relationship to in situ acoustic and geotechnical properties and (2) to provide a 3-D digital high resolution micromorphologic characterization of the FY93 program experiment site in the Baltic Sea.

Current Status and Progress

The Naval Research Laboratory (NRL) is developing a high frequency, high resolution subseafloor characterization system that has the capability to digitize and display the return acoustic signal on a color monitor with a true dynamic range of greater than 90 dB. The system presently uses a narrow beamwidth transducer (6^{o} or 12^{o}) normally operated at either 30 kHz or 15 kHz using a short 0.1 to 0.3 ms pulse length. This system is designated the Acoustic Seafloor Classification System (ASCS) and consists of a 16 bit data acquisition, processing, and display controller integrated into a 486 microcomputer. A second integrated 486 microcomputer processes the raw acoustic data into near real time predictions of seafloor geotechnical properties, with depth into the bottom. This enhanced normal incidence acoustic system was first used in February 1993 (Baltic I) and later during April and May (Baltic II) in the Kiel and Eckernfoerde Bays of the Baltic Sea to characterize the complex sedimentary structures found in the area. It was also used to collect the raw acoustic data needed to quantify the effect of sediment micromorphologic structure on high frequency acoustic response and its relationship to in situ acoustic and geotechnical properties.

During the Baltic I Experiment 73 survey tracklines were run using an EDO 6991 broadband, narrow beam transducer mounted in the RV PLANET's transducer well. High resolution subbottom data was collected using the old ASCS hardware (Honeywell ELAC EMG2 and LAZ72) in conjunction with NRL's newly developed enhanced ASCS. Nearly all tracklines were run both at 15 kHz with a 0.3 ms pulse length and a 12^{o} beamwidth and at 30 kHz with a 0.3 or 0.1 ms pulse length and a 6^{o} beamwidth. The highest resolution data was collected using the new ASCS at 30 kHz with a 0.1 ms pulse length. All raw acoustic data was digitized at a rate greater than 78 kHz, stored on 90 MB Bernoulli disks and later transferred to backup tape for archiving. More than 3.05 gigabytes of raw data was collected during this experiment. All ASCS data collected is of extremely high quality and is available to other researchers involved in the CBBL-SRP.

Another unique data set was collected at each of the sites where cores were collected during the Baltic I Experiment. Because the transducer well was located less than 8 meters from the coring platform, NRL collected subbottom acoustic data at 15 kHz as the ship approached the core site and while the core was inserted into the seafloor. As the core was being extracted, the ASCS was switched to a higher resolution 30 kHz mode and operated while the core was recovered and as the ship began to move to the next core site. This data provides a unique opportunity to correlate this high resolution acoustic data to high quality ground truth core samples in an effort to quantify the effect of sediment micromorphologic structure on high frequency acoustic response.

Most of the ASCS tracklines were also traversed with a chirp sonar, 3.5 kHz subbottom profiler, and a 100 kHz side scan sonar. This data set provides the opportunity for intercomparison of these various remote sensors.

During the Baltic II Experiment an additional 700 MB of ASCS data was collected in the experiment site and on a few other selected tracklines. The majority of this data was acquired at 30 kHz with a pulse length of 0.1 ms with the EDO transducer mounted in the transducer well of the RV HELMSAND. In addition, a UQN-4 transducer was also mounted in the ship's well and operated with the digital ASCS. This transducer type is the Navy standard fathometer transducer on nearly all gray ships. It is normally operated at 12 kHz and has a nominal 30^{o} beamwidth which is not satisfactory for sediment classification. Therefore, the UQN-4 was operated at 25 kHz to reduce it's beamwidth to approximately 14^{o}. The data acquired with the UQN-4 appears satisfactory for remote sediment classification although it's resolution is not as good as the data collected with the EDO transducer.

Because the RV HELMSAND was in a four point moor for much of the Baltic II Experiment, this presented an opportunity to collect some additional unique acoustic data. A series of calibrated hydrophones was buried at varying depths in the sediment by divers directly underneath the EDO transducer. One transducer was allowed to rest directly on the surface of the seafloor. The ASCS was then operated in normal mode and data collected at a number of frequencies, beamwidths, and pulse lengths. The surface mounted transducer provided acoustic source levels at the sediment water interface for calibration. Signals received at each of the buried hydrophones was recorded and should yield some important information about the normal incidence high frequency response of the sediments in the test site. This data compliments the data collected by Steve Stanic over numerous frequencies and grazing angles in the test area.

The high resolution ASCS seismic records show that a late Pleistocene glacial till is present throughout most of the southwestern Baltic Sea and is either exposed at the seafloor surface or buried under a few to tens of meters of softer Holocene sediment. Much of the area is characterized by biogenic gas contained within the softer sediments, either as hydrogen sulfide gas in the upper 30 cm of the sediment column or as methane gas found in discontinuous layers normally 0.75 m or deeper in the sediment column. The operational characteristics of the ASCS provide for an excellent delineation of these gassy structures (Fig. 1). In general, sediment structure in the area is extremely complex with buried channels, pockmarks, highly variable sediment layering, and unusual appearing structures of gas origin being common. However, the sediment within the test area chosen for the high frequency tests is areally a homogeneous soft silty clay with vertical variability in acoustic reflectivity due to the presence of a biogenic gas layer beginning approximately 0.75 m below the sediment water interface (Fig. 2).

Publications

Lambert, D.N., J.C. Cranford, and D.J. Walter, 1993. Development of a Hogh Resolution Acoustic Seafloor Classification Survey System. Proc. Inst. Acoustics, Vol. 15, Part 2, pp. 149-156.

Lambert, D.N., J.C. Cranford, D.J. Walter, J.A. Hawkins and R-D. Redell, 1994. Geological Characterization of Kiel and Eckernfoerde Bay Sediments Using a High Resolution Remote Acoustic Seafloor Classification System. Abstract submitted to the American Geophysical Union, 1994 Ocean Sciences Meeting, Feb. 21-25, San Diego, CA.

Hawkins, J.A., D.N. Lambert, D.J. Walter and J.C. Cranford, 1994. Observations of Acoustic Reflectivity Associated with Near Surface (Shallow Subbottom) Gassy Sediments in Kiel and Eckernfoerde Bays. Abstract submitted to the American Geophysical Union, 1994 Ocean Sciences Meeting, Feb. 21-25, San Diego, CA.

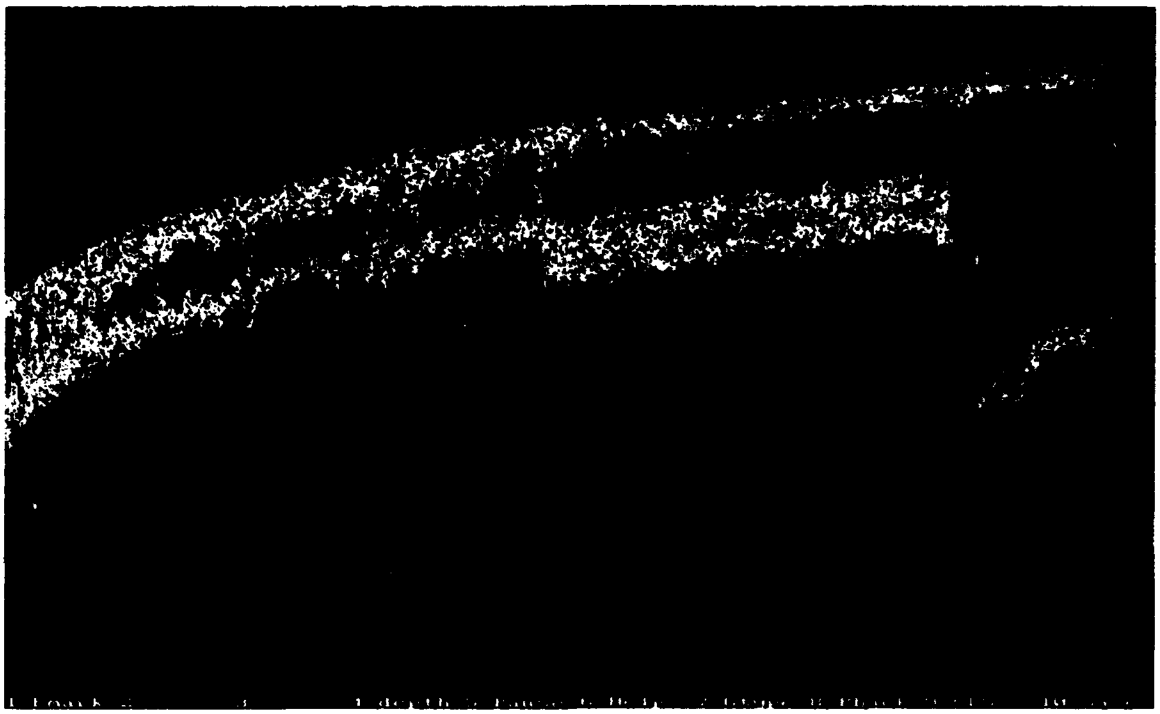

Figure 1. ASCS seismic record showing delineation of gas charged sediments.

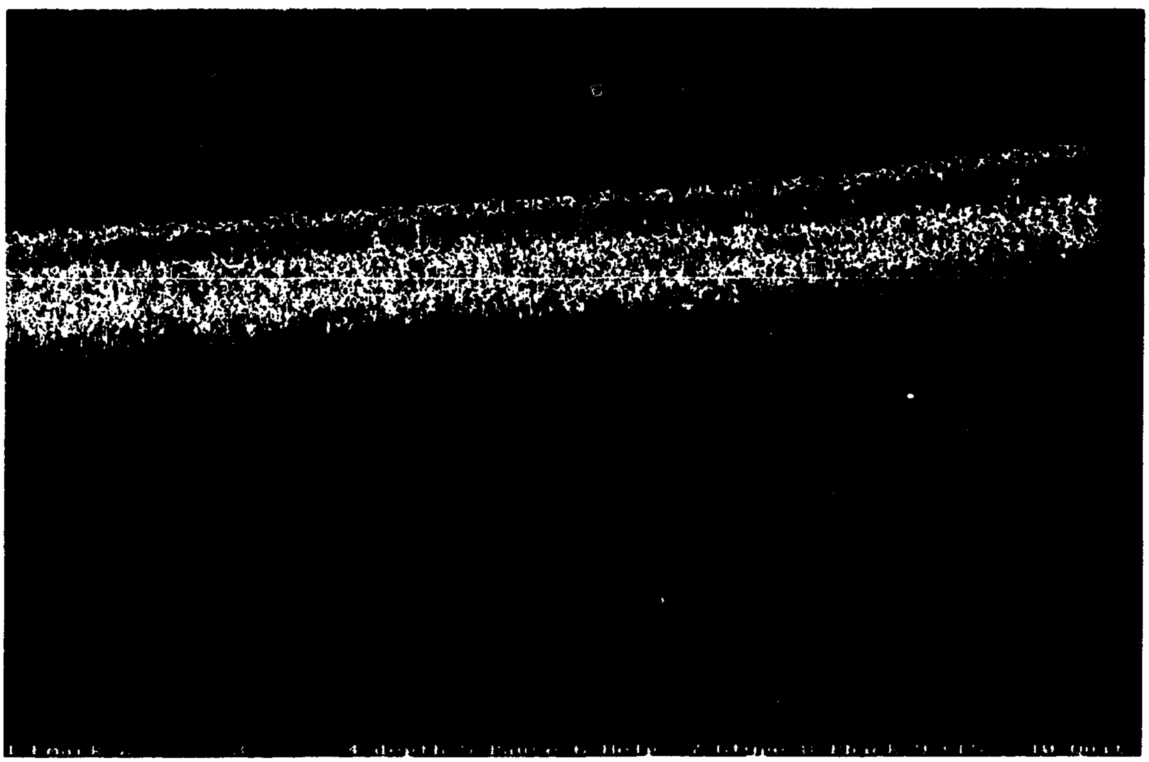

Figure 2. Typical ASCS seismic record across the test site.

3.12 Measurement of Shear Modulus In Situ and in the Laboratory (Principal Investigator: D.L. Lavoie and H.A. Pittenger, NRL)

CBBLSRP FY93 YEAR-END REPORT

Dawn Lavoie and H. Alan Pittenger
Naval Research Laboratory, Code 7431
Stennis Space Center, MS 39529-5004

Objectives

The long-term objectives of this effort over a three year period are to (1) investigate gradients of shear modulus in the field on the cm scale using a duomorph probe, (2) examine shear modulus as a function of direction (x and z planes) in the field, and in the laboratory in an instrumented triaxial cell where the shear wave velocity can be measured with the three principle stresses carefully controlled, and (3) relate in-situ shear modulus with geotechnical properties (particularly undrained shear strength) and other primitive sediment parameters (being investigated by other investigators under this SRP) as well as microfabric.

Our short term objectives for FY93 were to (1) repackage and adapt the duomorph from a laboratory to an in situ probe and (2) test the probe during the Baltic and Panama City CBBL cruises. Some of the preliminary data analyses and laboratory testing were to be initiated although the bulk of the laboratory testing was to be completed in FY94.

Progress

1. The duomorph technology, used successfully in the laboratory under low effective stresses (Lavoie, 1990; Breeding and Lavoie, 1988), has been repackaged as a probe for in-situ use that can be deployed from a wireline or by a diver. The duomorph is a bending plate device which consists of a stainless steel plate sandwiched between a pair of piezoceramic crystals (Figure 1). A metallic strain gage is fixed to the center of each crystal. The ratio between the unconstrained bending of the duomorph in air and in the sediment is a function of the sediment dynamic modulus. This differs from the standard pair of bender element transducers which generate and receive shear waves in that the duomorph measurement relies on strain gage technology and only one piezoceramic sandwich is required, thus eliminating any geometry problems.

Because strain gauges are used to measure the deflection of the piezoceramic crystals, a wheatstone bridge is required in the data collection hardware. Since cable length restrictions exist with the wheatstone bridge, a collection package in a canister was designed to go down with the probe. Within the canister is a 486 computer, a wheatstone bridge, and a signal conditioning board. This close proximity to the probe allows the bridge to be balanced automatically and data to be collected without diver manipulation, other than insertion of the probe. The underwater system is umbilically connected to another 486 on board ship from which the probe can be controlled,

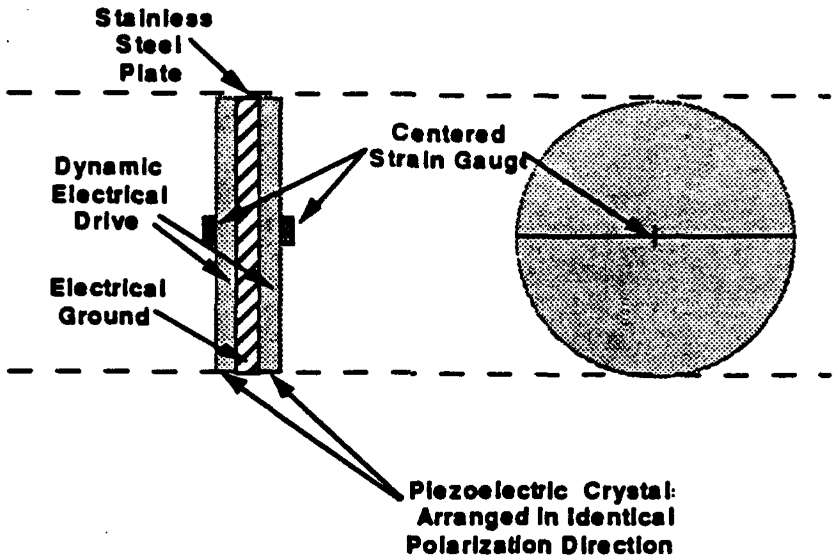

Figure 1. Schematic Diagram of the Duomorph sensor. A stainless steel plate is sandwiched between 2 piezoceramic crystals and excited with an alternating current. The resulting deflections are measured with strain gauge technology.

adjustments can be made as needed, and the signals displayed for continuous monitoring. Presently, the data processing is laboriously done by hand, but we are in the process of automating it so results can be displayed in near real time.

2. Baltic Cruise

Our goals for this field effort were (1) to field test the duomorph probes, and (2) investigate gradients of shear modulus in the shallow subbottom in the Baltic Sea using a duomorph probe. We spent several days testing the probes in diver-recovered box cores. Our goal was to get a general idea of the shear modulus of the Baltic mud, look at the effects of pore pressure decay after insertion of the probe, and measure the stability of the duomorph probes would be over time. A synopsis of results is given in Table 1.

Box core #164 was obviously layered about mid depth and the probe was inserted separately into each layer. Measurements were made immediately and showed no significant difference in values between the top and bottom layer. After remolding however; values of shear modulus were higher than initial values (Table 1). It became evident that time, in addition to remolding, is a consideration probably because the insertion of probes into the box cores causes an initial increase in pore pressure which dissipates with time. The shear modulus measured immediately after insertion of the probe can therefore, be expected to be lower than after the probe-mud system equilibrates.

Table 1: Eckernfoerde In Situ Results

Sample	Comments	G (N/m^2)	*Vs (m/s)
#164	Top	1.77×10^5	12
	Lower	$2{,}02 \times 10^5$	13
	Remolded	5.98×10^5	16
#168	Time 0	1.31×10^5	11
	93 Minutes	4.00×10^5	19
	200 Minutes (exptrapolated)	4.19×10^5	20
#175	0 Minutes	2.93×10^5	16
	220 Minutes	3.28×10^5	17
In Situ	25 cm	3.04×10^5	16
	60 cm	2.92×10^5	16
	110 cm	3.28×10^5	17
	160 cm	3.13×105	17
	200 cm	3.87×10^5	18

* A density of 1.15 gm/cm3 was used to convert G to Vs.

* A density of 1.15 g/cm^3 was assumed

Figure 2 illustrates with 8 separate signals the decrease in amplitude observed over time in Box core #168. The amplitude of the initial waves is significantly higher than subsequent waves which results in values of measured shear modulus which increase rapidly during the first 20 minutes, and then stabilize.

2A

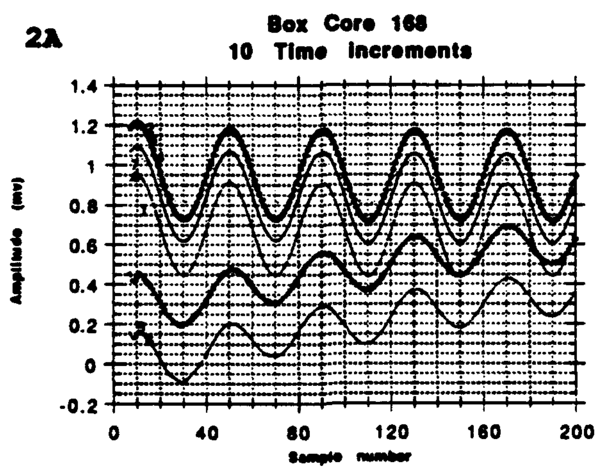

2B.

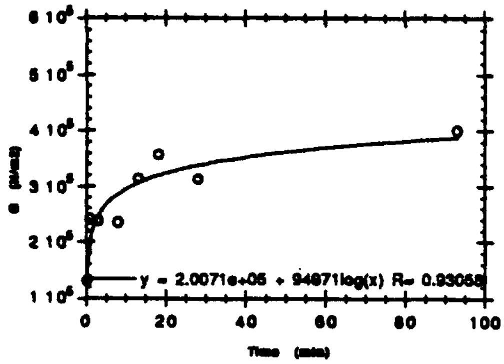

2C.

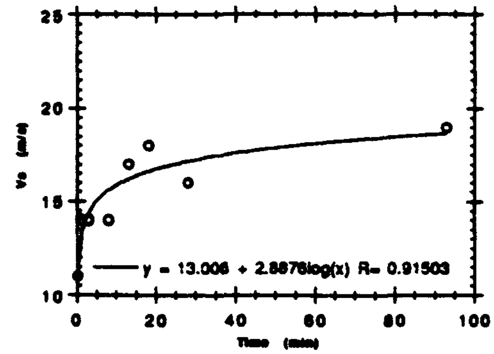

Figure 2. (a) The amplitude of received signal decreases with time. (b) shear Modulus increases sharply as pore pressures equilibrate after insertion. (c) Shear wave velocity is calculated from G and mirrors the same trend.

Figure 3 illustrates results of a similar test run in Box core #175 over 260 minutes. The initial increase in shear modulus is less than in box core #68, probably because the sediment was slightly different and possibly because the initial reading was taken a minute late. The measured values are stable after approximately 100 minutes.

3A.

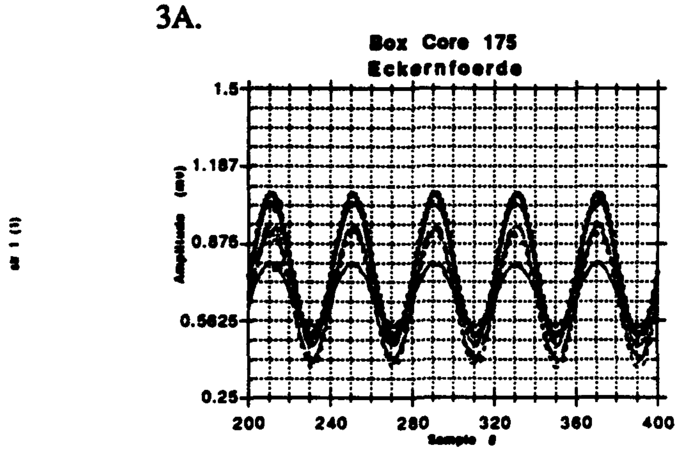

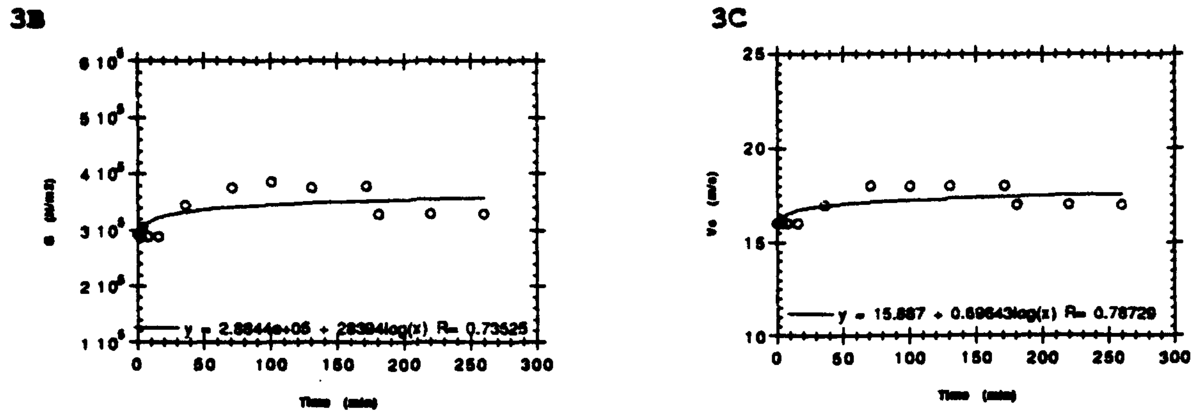

Figure 3.(a) Amplitude of the received waves decreases with time. (b) Shear modulus increases with timeand is stable around 100 minutes. (c) Shear wave velocity calculated from measured shear modulus mirrors the trend.

The probes were deployed around the Helmsand over several days. One or two measurements at different depths were achieved each day and the resulting five values were combined into one in situ profile of measured shear modulus, and estimated shear wave velocity using a density of 1.15 gm/cm^3 (Figure 4).

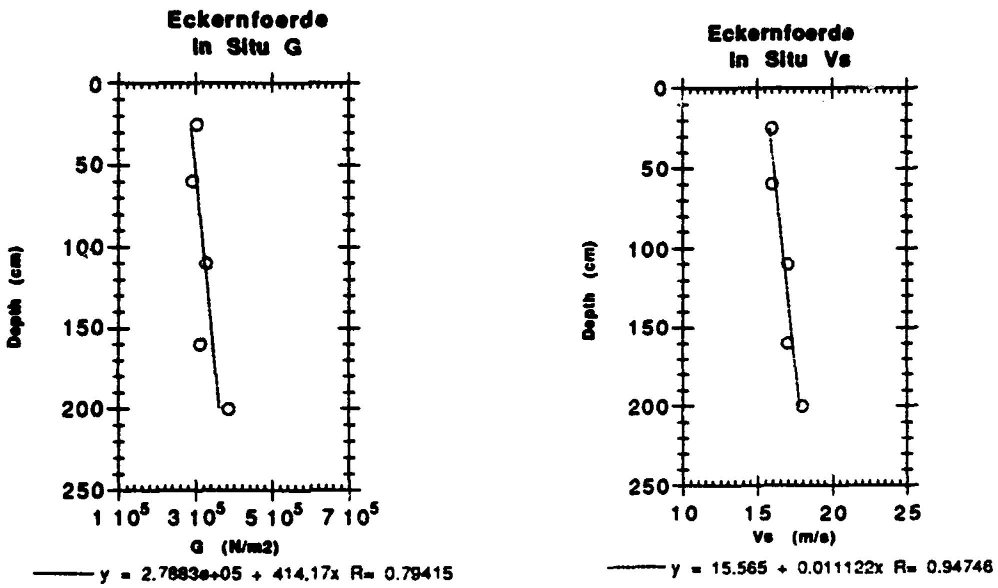

Figure 4. Results of in situ DIAS measurements over several days combined to make a composite in situ profile of shear modulus and shear wave velocity in Eckernfoerder Bay.

3. Panama City

It was known before the cruise that the Panama City site sediments would be sands and, therefore, coarser and presumably more competent than the Baltic Sea muds. It was decided, therefore, to use a stiffer probe during the Panama City Site than the initial probe used in the Baltic. The stainless steel plate was increased from 0.003" to 0.008" and a new probe built. The probes were deployed at six sites in coarse and fine sand. These data are currently being analyzed.

In addition to deploying the probes during the month of August, CTD data were taken at least twice daily and at all sampling and deployment sites. These data are being compiled and will be available to all CBBL participants by February. For locations and times of CTD data, see the complete sampling list for the August Panama City cruise.

4. Chesapeake Bay

The duomorph probes were deployed at three sites off the Patuxent River in Chesapeake Bay early this fall. In situ conductivity and CTD measurements were made at the same time and cores were recovered from the 3 test sites. The muddy sediments were similar to those found in Eckernfoerder Bay although perhaps less gassy and slightly more competent. These data, when analyzed will be compared with the Baltic Data.

5. Laboratory

The triaxial cells instrumented with both compressional and shear wave velocity probes are finally up and running. Testing on the Baltic samples has just begun and will continue during FY94.

Plans

Laboratory

During FY94, we would like to make a more detailed study of the probe transfer function so we do not have to rely so heavily on achieving an accurate zero reading. In addition, we would like to calibrate the probes against another instrument we feel gives accurate measurements, such as the in situ shear wave velocity probes, or in a material of known values (such as a Dow Corning rubber). We plan to test the probes in the laboratory to examine the effects of temperature, aging, pressure, and the potting compound used. We also plan to continue the triaxial testing using samples from the Baltic Sea, Panama city and Chesapeake Bay.

Field

We plan to take the DIAS system out on the Key West cruise in January/February in much shallower water and deploy it in conjunction with the shear wave velocity probes (M. Richardson), the piezometer probe (Bennett) and the conductivity probe (Lavoie). Cores will be collected for laboratory triaxial and consolidometer analyses in the laboratory.

REFERENCES

Breeding, Samantha, and Dawn Lavoie, 1988, Duomorph Sensing for Laboratory Measurement of Shear Modulus. Proceedings of the Oceans 88 Conference, Baltimore, Maryland, pp 391-396.

Lavoie, Dawn, 1990, Geotechnical Properties of Periplatform Car bonate Sediments. Naval Oceanographic and Atmospheric Research Laboratory, Report #9. Stennis Space Center, MS 39529.

3.13 Quantification of Gas Bubble and Dissolved Gas Bubble and Concentrations in Organic-Rich, Muddy Sediments (Principal Investigator: C. S. Martens, University of North Carolina at Chapel Hill)

CBBLSRP FY93 YEAR-END REPORT

Christopher S. Martens and Dan Albert
CB-3300, Marine Sciences Curriculum
University of North Carolina
Chapel Hill, NC 27599-3300

Quantification of Gas Sources and Concentrations in Sediments

Project Goals

The scientific priorities of the Coastal Benthic Boundary Layer Special Research Program (CBBLSRP) include determining and modeling the effects of environmental processes on sediment physical, geoacoustical, rheological and electrical properties. The potential influences of biogeochemical processes driven by microbial degradation of organic matter on sediment properties have been recognized (e.g., Jackson and Jumars, 1992 and references therein). Biogenic gas production, consumption, and transport processes combine to control the distributions of both dissolved and bubble gas phases which, in turn, control key sediment properties including structure and acoustic scattering. The primary goals of our project are to:

1) quantify sources and composition of gas bubbles and dissolved gases
2) quantitatively describe biogeochemical and physical processes controlling gas bubble and dissolved gas concentrations
3) development of a predictive model for the occurrence and characteristics of dissolved gases and gas bubbles in organic-rich sediments

The initial focus of our project was on the muddy, organic-rich sediments of the Eckernfoerde Bay near Kiel, Germany in the Baltic Sea. The CBBLSRP experiments underway at this site combined with those of German scientists provided opportunities to collect data essential to our primary goals. Our mission on the May, 1993 Baltic expedition, was to quantify concentrations of methane and sulfate in the sediments at the central Eckernfoerde Bay study site and the rates of microbiological processes involved in the degradation of organic carbon in these anoxic sediments. Specifically we were trying to measure the rates of sulfate reduction, methane production, and anaerobic methane oxidation in the upper (<2 m) of the sediment column.

Completed Research

The dominant processes controlling biogenic gas distributions in organic-rich sediments, such as those of the Eckernfoerde Bay, are sulfate reduction, methane production and methane oxidation. The distribution of dissolved and gas bubble methane expected to result from the combination of these processes is illustrated in Figure 1.

To date, we have completed measurements of methane concentrations in two cores from the central Eckernfoerde Bay study site. These profiles, which extend to 1.5 m depth, show pronounced upward concavity in the upper 25 cm of the sediment column (Fig. 2). Below 20 cm depth the methane concentration rises rapidly to a high value of about 3.2 mM at about 40 cm depth below which they drop slowly throughout the remainder of the core. Given the water column depth at this site, methane saturation should occur at about 4 mM. Our concentrations are not that high, but we know that these are methane saturated sediments. We interpret this to mean that we are seeing a degassing artifact in our data caused by degassing of the core on deck as we were sampling it. We were unable to recover our porewater equilibration samplers (peepers) deployed at the site and these are still in place. These samplers would have given us our best estimates of true *in situ* concentrations because they could have been sampled very quickly, minimizing the effects of degassing. We hope to recover them in 1994. The samples in them will be unaffected by the longer than intended deployment time.

The upward concavity in the methane profiles near the sediment-water interface are consistent with the upper sulfate-bearing sediments being a zone in which there is no active methane production and methane is actively consumed by an as-yet unidentified anaerobic organism. We measured rates of anaerobic methane oxidation by incubating sediments with radioactive methane and quantifying the amount of radioactive carbon dioxide produced. These rates were very low in the upper 10 cm of the sediments, but rose rapidly with depth below that to a sharp peak in activity at 22.5 cm. (Fig. 2). This peak occurs at the base of the sulfate-bearing sediments in a zone in which sulfate reducing bacteria are still active. These bacteria have been implicated as the active agents in other studies of anaerobic methane oxidation. We have not yet finished processing the sulfate reduction samples from the May cruise, so we do not know if we will see a subsurface peak in the sulfate reduction rates, corresponding to the peak in methane oxidation. It is this methane oxidation process which prevents the methane saturation zone from rising nearer the sediment-water interface via the diffusion of methane from below.

Independent evidence for the existence of a zone of methane oxidation in the upper 25-30 cm of the sediment column is seen in the isotopic data for carbon and hydrogen in the methane (Fig. 4). In the lower sediment column (below 20 cm) carbon isotopic (δ13C, ^{o}/oo) values for methane rise (become more positive) from -71 ^{o}/oo to -60 ^{o}/oo at 150 cm depth. This shift towards a greater abundance of the heavier isotope at depth is probably controlled by the isotopic composition of the carbon dioxide available to the methanogens for production of methane. We have not yet completed the isotopic analyses for the carbon dioxide to verify this. Above 20 cm depth the isotopic values become dramatically heavier, nearing the -60 ^{o}/oo seen at depth. An enrichment of 150 ^{o}/oo in deuterium, the heavier isotope of hydrogen in the methane, is also seen in the upper 20 cm of the sediment. These shifts for both carbon and hydrogen must be caused by fractionation during methane oxidation as isotopic fractionation associated with methane production effects should produce opposing isotopic shifts for carbon and hydrogen. The oxidizers utilize the isotopically lighter methane at a higher rate leaving the residual methane pool enriched in both of the heavier isotopes.

Work to be Completed on Eckernfoerde Bay Samples

We still have a substantial amount of work to do with our existing samples from the Baltic, including:

Sulfate Reduction Rates
Total CO_2 $\delta 13C$ isotopic values for porewaters
Carbon, nitrogen and sulfur elemental analysis of sediments
Carbon isotopic values for sedimentary carbon
Analysis of specific organic components of the sediments

We hope to return to Eckernfoerde Bay for the 1994 cruise on the PLANET. We want to measure rates of methane production, which we were unable to do this year due to logistical problems and further our work on anaerobic methane oxidation for which this site has proved ideal. We will also further our measurements of *in situ* gas concentrations. This should be more feasible in 1994 than it was this year given the longer lead time to solve the technical problems associated with handling samples prone to degassing. We would also like to investigate the potential for major methane fluxes through bubble ebullition at this site.

West Florida Sand Sheet Experiment

Data from acoustic backscatter studies of sandy sediments on the west Florida shelf off Panama City, Florida, appear to indicate the presence of small quantities of very small gas bubbles (N. Chotiros, personal communication, October 6, 1992). The participation of CBBLSRP scientists led by Dr. Michael Richardson in further studies of the course-grained sediments at this site provided an opportunity to determine whether or not gas bubbles were present. We hypothesized that gas bubbles might result from an unusual combination of biogeochemical and physical processes controlled by freshwater percolation from the Florida platform. Such percolation is known to produce springs of freshwater to the southeast of Appalachicola, Florida. The freshwater could contain high concentrations of biogenic gases such as methane or promote *in situ* methane production at the site by lowering concentrations of dissolved sulfate (Martens and Berner 1974). If percolation was active, chloride concentrations in sediment pore waters should also be lowered below normal seawater values.

We utilized shipboard ion chromatographic analyses to measure concentrations of dissolved sulfate and chloride in the pore waters of sand sheet sediments. Maximum depths for pore water measurements were approximately one meter in vibra-cores. Measurements were also obtained from short gravity core samples. No lowered sulfate or chloride concentrations were observed in any samples, hence, there is no chemical evidence for the sulfate depletion that would be required for biogenic methane production to be active in these sediments.

We also sought direct evidence for the presence of small quantities of gas bubbles utilizing a simple diver sampling method designed by Dennis Lavoie of the NRL-SSC. The method employs short, diver-inserted core tubes which are capped and sealed on the bottom after insertion into the coarse sediment. The top core cap is fitted with a sealed plastic tube into which any gas bubbles should migrate after the core is disaggregated by gentle rotation. Ten cores were successfully collected including four by the P.I. accompanied by Dr. Michael Richardson.

The sediment depths sampled by individual diver cores ranged from 5 to 23 cm. No gas bubbles were found in any cores. We conclude that there is no direct evidence for the presence of gas bubbles in the upper 5 to 20 cm of sediment at the sites.

Presentation at AGU/ASLO Meeting Session

Our research group will present a paper concerning the Eckernfoerde Bay results at the 1994 AGU/ASLO Ocean Sciences Meeting in the CBBLSRP Special Session. The presentation will emphasize our biogeochemical rate and stable isotope data.

References

Jackson, D. R. and P. A. Jumars (eds.), 1992. Interactions between environmental processes at the seabed and high-frequency acoustics: Workshop recommendations. In: M. D. Richardson (ed.) Coastal Benthic Boundary Layer Research Program: Program Direction and Workshop Recommendations. NOARL Special Project 017: 361:92. NOARL, Stennis Space Center.

Martens, C.S. and R.A. Berner, 1974. Methane production in the interstitial water of sulfate-depleted sediments. *Science*, 185: 1167-69.

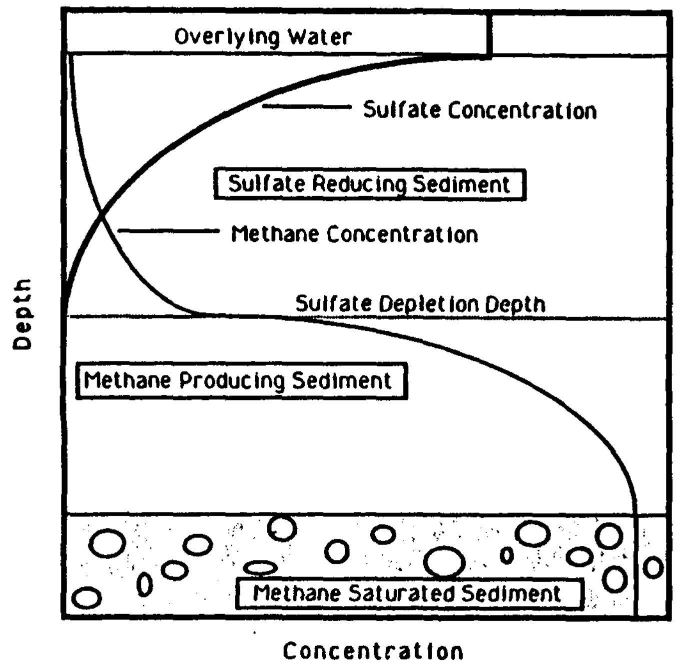

Figure 1. Hypothetical methane distribution in typical organic-rich coastal sediments.

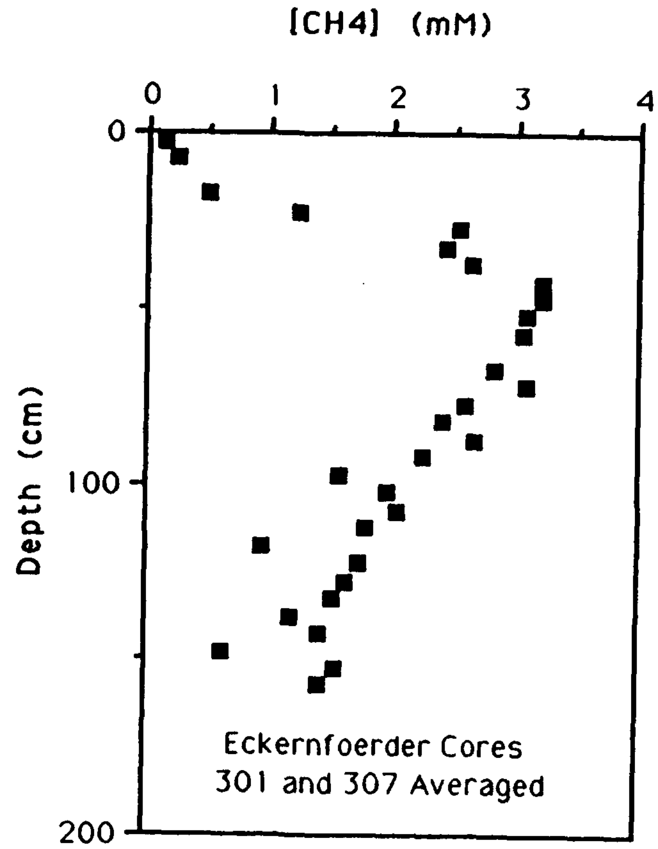

Figure 2. Methane concentration profile at the site of the geoacoustical studies in central Eckernfoerde Bay

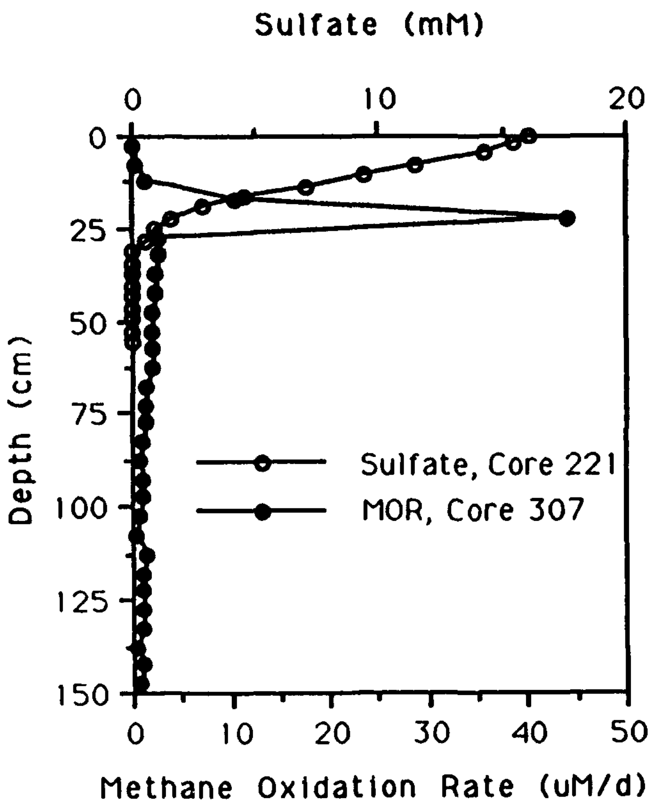

Figure 3. Porewater sulfate profile showing that the zone of sulfate reduction is confined to the upper 30 cm of the sediment column at the main Eckernfoerde study site. Methane oxidation rates are also plotted showing a major peak in the activity at the base of the sulfate-bearing sediments.

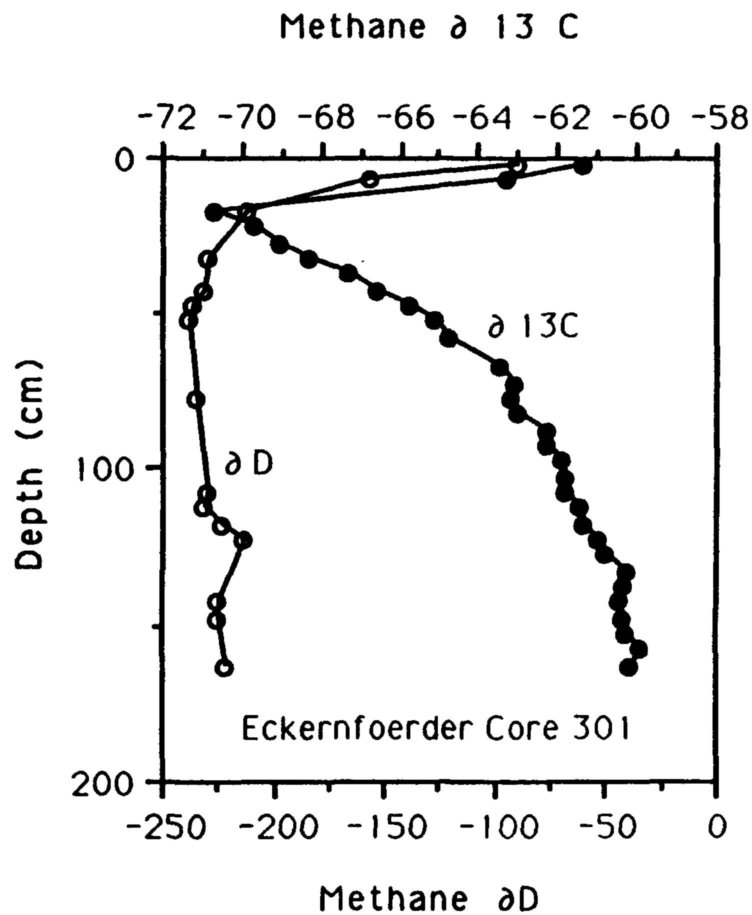

Figure 4. Carbon and hydrogen isotopic values for methane from the central Eckernfoerde study site showing independent evidence for methane oxidation in the upper sediment column.

3.14 Electrical Conductivity in the Benthic Boundary Layer (Principal Investigator: E. C. Mozley, NRL)

CBBLSRP FY93 YEAR-END REPORT

E. C. Mozley
Code 7442
Naval Research Laboratory
Stennis Space Center, MS 39529-5004\

No report available.

3.15 Physical and Biological Mechanisms Influencing the Development and Evolution of Sedimentary Structure (Principal Investigators: C. A. Nittrouer and G. R. Lopez, State University of New York)

CBBLSRP FY93 YEAR-END REPORT

Charles A. Nittrouer and Glenn R. Lopez
Marine Sciences Research Center
State University of New York
Stony Brook, NY 11794-5000

GENERAL SUMMARY OF WORK DURING THE FIRST YEAR

Research work completed during this year included the collection of samples in Eckernfoerde Bucht and the beginning of laboratory analyses for those samples. During March-May, we participated in three cruises. Replicate cores (4-7) were collected at 14 stations, and many of the stations were reoccupied on different cruises. Some of our work was completed in the field, but most awaited the return of samples to our laboratory. They were returned to the US in August, and since then we have completed preliminary analyses of sedimentological, radiochemical and biological properties.

The sample sites were concentrated at the deployment locations of acoustic and boundary-layer towers, as well as positions farther northeastward and southwestward within Eckernfoerde Bucht. Sedimentary structure is generally characterized by physical laminations, although biogenic mottling is present and becomes more common northeastward (toward the mouth). The benthos are an opportunistic community dominated by spionid polychaetes and tellinid bivalves, both surface deposit feeders. Profiles of ^{234}Th demonstrate that the community mixing depth is 1 cm or less. This observation combined with a relatively rapid accumulation rate (>5 mm y^{-1}) allows many physical laminae to be pass through the surface mixed layer intact, and to be preserved in the underlying portions of the seabed.

Our work has been coordinated with the dynamical boundary-layer measurements of our co-PI, Don Wright and his research group at VIMS, as well as the acoustical observations of Darrell Jackson and his research group at University of Washington. The combined efforts will provide an understanding of physical and biological reworking for the seabed in Eckernfoerde, and how this has affected sedimentological characteristics and the resultant acoustical properties.

SAMPLE COLLECTION

Description of Coring Stations

Most of the cores were collected at locations where the APL tower and the VIMS tetrapod were deployed, as shown below.

	Cruise Number		
	BS-1	BS-2	BS-3
APL/VIMS deployment site March-April	stations A,B,C,D,E,F	stations D,F	station D
APL/VIMS deployment site April-May	none	stations N,O,P	stations N,O

Two locations near Mittelgrund contained glacial sand and pebbles, and had a more diverse benthic community. The location at the west end of Eckernfoerde (near the Navy Base) had a large contribution of terrigeneous debris (sand, twigs, leaves, eel grass).

Sedimentological and Radiochemical Sampling

The radiochemical and sedimentological 6" subsample cores (RS/C samples in Tables 1-3) were extruded and dissected at 1 cm intervals to 15 cm depth in cores. Below 15 cm, sediment from alternate centimeters was saved. During cruises BS-2 and BS-3, entire box cores (20 cm x 30 cm) were extruded at 0.5-cm intervals to 15 cm depth in cores (identified as Th-234 samples in Tables 2 and 3).

The sediment will be divided and examined for both radiochemical and sedimentological properties. Some samples have been dried to calculate porosity, and Th-234 has been measured directly by γ-detection techniques. Pb-210 also was measured in these samples by γ-detection. Additional Pb-210 analyses are being done by α-detection techniques. Grain size will be examined by a combination of Sedigraph and automated settling-column techniques, for silt/clay and sand (respectively).

Sediment slabs were collected in Plexiglas trays (3 cm x 12 cm cross section) for radiographic examination of sedimentary structures. Vertical slabs were obtained with contrasting orientation, and horizontal slabs were obtained at several depths in core. Some of these same slabs will be dissected to examine microfabric.

Benthic Biological Sampling

The benthos subsample cores (BIO in Tables 1-3) were divided into 0-2 and 2-10 cm layers, and sieved through a 500 μm sieve. Animals collected on the sieve were then preserved in glass jars with 4% seawater formaldehyde and rose bengal. Animals will be counted and identified to the lowest taxonomic unit.

A bioturbation experiment was established to compare vertical and horizontal particle bioturbation rates in a variety of sediments and faunal communities. Six-inch cores (see Table 4) were brought to shore and placed in a running seawater system. Cores were drained and vertical plugs of fluorescent marker and mud were added to the center of each core to trace the horizontal component of bioturbation. Then cores were refilled with water and a 50 ml suspension of a second color of fluorescent particles (in seawater) was added to each core. These particles settled overnight onto the sediment surface.

Control cores were broken down during the following two days. There was one control core from each station. Nine to 12 subcores (small syringes) were taken from each control core. Each subcore was vertically sectioned at 7 depth intervals of 0-0.5, 0.5-1, 1-1.5, 1.5-2, 2-3, 3-4, and 4-5 cm. Cores for porosity also were taken and divided in the same manner. Small x-ray slabs were obtained from each core.

Salinity and temperature were monitored during the course of the experiment._ Experimental cores were incubated in the running seawater system for approximately 2 weeks, then were broken down in the same manner as the controls. After subcores were taken from the experimental cores, the remaining sediment (~70% of the total) was sieved through a 500-μm sieve, and the animals collected were preserved for later enumeration. Fluorescence from sediment subsamples will be extracted and measured by fluorometry.

Table 1. - List of samples collected in Eckernfoerde Bucht during Cruise BS-1 on R/V *PLANET*

STATION SUNY/FWG	DATE	TIME	LAT.	LONG.	DEPTH (M)	SAMPLES	NOTE
56/A-2	3/29/93	15:00	54 29.410	9 58.867	26.0	(1)R/SC, (3)BIO	TOWER SITE
57/A-3		15:19	54 29.416	9 58.860		(3)BIO, (1)ARC	
58/A-4		15:40	54 29.410	9 58.871		(3)BIO, (2)VX-R	
59/A-5		15:57	54 29.412	9 58.875		(1)R/SC, (1)VX-R, (3)HX-R	
60/B-1	3/29/93	16:24	54 29.396	9 59.145	25.5	(1)R/SC, (3)BIO	TOWER SITE
61/B-2		16:55	54 29.396	9 59.152		(3)BIO, (2)VX-R	
62/B-3		17:30	54 29.396	9 59.166		(3)BIO, (1)ARC	
63/B-4		17:40	54 29.388	9 59.138		(1)R/SC, (1)VX-R, (3)HX-R	
64/C-1	3/30/93	8:35	54 29.508	9 58.988	26.0	(1)R/SC, (3)BIO	TOWER SITE
65/C-2		9:00	54 29.489	9 58.995		(3)BIO, (2)VX-R	
66/C-3		9:21	54 29.485	9 58.992		(3)BIO, (1)ARC	
67/C-4		9:40	54 29.488	9 58.996		(1)R/SC, (1)VX-R, (3)HX-R	
DIVER/T	3/30/93	11:00	54 29.247	9 58.592	26.0	(1)R/SC, (2)BIO	S.W. OF TOWER SITE
69/G-1	3/30/93	18:16	54 30.038	10 01.905	22.0	(3)BIO, (1)VX-R	W. SIDE OF MITTELGRUND
70/G-2		18:37	54 30.056	10 01.919		(3)BIO, (1)VX-R, (2)HX-R	
71/G-3		18:44	54 30.051	10 01.912		(3)BIO, (1)ARC	
72/G-4		19:14	54 30.045	10 01.885		(1)R/SC, (1)VX-R,	
73/H-1	3/31/93	8:23	54 28.137	9 52.310	21.0	(1)R/SC, (3)BIO	ECKERNFOERDE NAVY BASE
74/H-2		8:44	54 28.163	9 52.276		(3)BIO, (2)VX-R	
75/H-3		8:55	54 28.136	9 52.289		(3)BIO, (1)ARC	
76/H-4		9:07	54 28.136	9 52.296		(1)R/SC, (1)VX-R, (3)HX-R	
77/D-1	3/31/93	9:56	54 29.518	9 58.943	26.0	(1)R/SC, (3)BIO	TOWER SITE
78/D-2		10:08	54 29.531	9 58.921		(3)BIO, (2)VX-R	
79/D-3		10:18	54 29.528	9 58.932		(3)BIO, (1)ARC	
80/D-4		10:28	54 29.530	9 58.908		(1)R/SC, (1)VX-R, (3)HX-R	

Table 1. - Continued

STATION SUNY/FWG	DATE	TIME	LAT.	LONG.	DEPTH (M)	SAMPLES	NOTE
81/E-1	3/31/93	10:42	54 29.451	9 59.122	26.0	(1)R/SC, (3)BIO	TOWER SITE
82/E-2		10:50	54 29.472	9 59.098		(3)BIO, (2)VX-R	
83/E-4		11:00	54 29.498	9 59.127		(3)BIO, (1)ARC	
84/E-5		11:10	54 29.498	9 59.128		(1)R/SC, (1)VX-R, (3)HX-R	
85/F-1	3/31/93	11:21	54 29.378	9 58.975	26.0	(1)R/SC, (3)BIO	TOWER SITE
86/F-2		11:34	54 29.414	9 59.028		(3)BIO, (2)VX-R	
87/F-3		11:44	54 29.427	9 59.043		(3)BIO, (1)ARC	
88/F-4		11:54	54 29.426	9 59.021		(1)R/SC, (1)VX-R, (3)HX-R	
89/I-1	4/1/93	8:24	54 30.010	10 01.893	24.0	(1)R/SC, (3)BIO	MITTELGRUND SAND/MUD BOUNDARY
90/I-2		8:32	54 30.001	10 01.935		(3)BIO, (2)VX-R	
91/I-3		8:48	54 30.016	10 01.936		(3)BIO, (1)ARC	
92/I-4		8:59	54 30.014	10 01.951		(1)R/SC, (1)VX-R, (3)HX-R	
93/K	4/1/93	9:26	54 29.298	9 58.991	26.0	(1)R/SC	BOX CORE/DIVER CORE COMPARISON
94/L	4/1/93	9:46	54 29.506	9 58.991	26.5	KC	
95/M	4/1/93	10:17	54 30.016	9 58.787	28.0	KC	POCK MARK

KEY: R/SC - 6" RADIOCHEMISTRY/SEDIMENTOLOGY CORE
BIO - 3" BIOLOGY CORE
ARC - 3" ARCHIVE CORE
VX-R - VERTICAL X-RAY TRAY (SAMPLED NORMAL TO SEABED)
HX-R - HORIZONTAL X-RAY TRAY (SAMPLED PARALLEL TO SEABED)
BE - 6" BIOTURBATION EXPERIMENT CORE
SC - 10cc SYRINGE CORE
Th-234 - 20x30cm BOX EXTRUDED FOR Th-234 CHEMISTRY
KC - KASTEN CORE

Table 2. - List of samples collected in Eckernfoerde Bucht during Cruise BS-2 on R/V *HELMSAND*

STATION SUNY/FWG	DATE	TIME	LAT.	LONG.	DEPTH (M)	SAMPLES	NOTE
101/I	4/27/93	13:15	54 30 00.8	10 01 59.4	24.0	(1)R/SC, (3)BIO	REOCCUPATION
102/I		13:30	54 30 00.8	10 01 59.4		(3)BIO, (1)ARC	
103/I		13:44	54 30 00.8	10 01 59.4		(3)BIO, (2)VX-R	
104/I		13:56	54 30 00.8	10 01 59.9		(1)R/SC, (1)VX-R, (3)HX-R	
105/I		14:10	54 30 00.7	10 01 59.4		Th-234	
106/I		14:20	54 30 00.6	10 02 00.0		(2)BE, (3)SC	
107/I		14:30	54 30 00.8	10 01 58.6		(2)BE, (3)SC	
110/H	4/28/93	8:45	54 28 00.2	9 52 11.2	24.0	(1)R/SC, (3)BIO	REOCCUPATION
111/H		9:00	54 28 00.1	9 52 10.8		(3)BIO, (1)ARC	
112/H		9:13	54 28 00.1	9 52 11.2		(1)R/SC, (1)VX-R, (2)HX-R	
113/H		9:22	54 28 00.1	9 52 11.0		Th-234	
114/H		9:45	54 28 01.2	9 52 10.5		(4)BE, (3)BIO, (2)VX-R,	50x50CM BOX
						(3)SC	
115/D	4/28/93	10:45	54 29 31.8	9 58 53.9	24.0	(1)R/SC, (3)BIO	REOCCUPATION
116/D		11:11	54 23 31.6	9 58 53.6		(3)BIO, (1)ARC	
117/D		11:20	54 23 31.2	9 58 53.5		(1)R/SC, (1)VX-R, (2)HX-R	
118/D		11:42	54 29 31.0	9 58 54.3		Th-234	
119/D		12:00	54 29 30.9	9 58 54.4		(4)BE, (3)BIO, (2)VX-R,	
						(3)SC	50x50CM BOX
124/N	4/29/93	16:00	54 29 44.3	9 59 29.6	24.0	(1)R/SC, (3)BIO	NEW TOWER
125/N		16:15	54 29 44.9	9 59 28.2		(3)BIO, (1)ARC	
126/N		16:30	54 29 45.0	9 59 28.6		(1)R/SC, (1)VX-R, (2)HX-R	
127/N		16:43	54 29 44.8	9 59 27.8		Th-234	
128/N		17:00	54 29 45.0	9 59 28.7		(4)BE, (3)BIO, (2)VX-R,	
						(3)SC	50x50CM BOX
139/O	4/29/93	9:58	54 29 36.4	9 59 19.4	?	(1)R/SC, (3)BIO	NEW TOWER
140/O		10:07	54 29 36.5	9 59 19.3		(3)BIO, (1)ARC	
141/O		10:19	54 29 36.5	9 59 18.9		(1)R/SC, (1)VX-R,	
142/O		10:45	54 29 36.7	9 59 19.7		Th-234	
143/O		11:01	54 29 36.7	9 59 19.2		(3)BE, (3)BIO, (1)VX-R,	

Table 2. - Continued

STATION SUNY/FWG	DATE	TIME	LAT.	LONG.	DEPTH (M)	SAMPLES	NOTE
145/G	4/29/93	12:41	54 30 03.9	10 01 54.2	20.0	(3)BIO, (1)VX-R	MITTELGRUND
146/G		13:32	54 30 04.4	10 01 54.0		(2)BE, (3)SC	
147/G		13:52	54 30 04.4	10 01 54.3		(1)BE, (1)R/SC	
148/F	4/29/93	14:47	54 29 28.9	9 58 49.4	?	(1)R/SC, (3)BIO	REOCCUPATION
149/F		14:58	54 29 28.9	9 58 49.8		(3)BIO, (1)ARC	
150/F		15:08	54 29 28.8	9 58 48.9		(1)R/SC, (1)VX-R,	
151/F		15:25	54 29 28.8	9 58 43.4		(4)BE, (3)BC, (1)VX-R, (3)SC	50x50CM BOX
152/P	4/30/93	9:20	54 29 37.4	9 59 37.5	?	(1)R/SC, (3)BIO	NEW TOWER
153/P		9:39	54 29 37.4	9 59 38.4		(3)BIO, (1)VX-R	
154/P		9:42	54 29 37.4	9 59 37.4		(3)BIO, (1)ARC	
155/P		10:02	54 29 37.3	9 59 37.4		(1)R/SC, (1)VX-R	

KEY: R/SC - 6" RADIOCHEMISTRY/SEDIMENTOLOGY CORE
BIO - 3" BIOLOGY CORE
ARC - 3" ARCHIVE CORE
VX-R - VERTICAL X-RAY TRAY (SAMPLED NORMAL TO SEABED)
HX-R - HORIZONTAL X-RAY TRAY (SAMPLED PARALLEL TO SEABED)
BE - 6" BIOTURBATION EXPERIMENT CORE
SC - 10cc SYRINGE CORE
Th-234 - 20x30cm BOX EXTRUDED FOR Th-234 CHEMISTRY
KC - KASTEN CORE

Table 3. - List of samples collected in Eckernfoerde Bucht during Cruise BS-3 on R/V *KRONSORT*

STATION SUNY/FWG	DATE	TIME	LAT.	LONG.	DEPTH (M)	SAMPLES	NOTE
225/N	5/24/93	11:30	54 29 43.2	9 59 26.8	?	(1)R/SC, (3)BIO (50x50CM)	REOCCUPATION
226/N		12:17	54 29 43.4	9 59 26.7		(3)BIO, (2)VX-R	
227/N		12:31	54 29 43.2	9 59 27.5		(3)BIO, (1)ARC	
228/N		12:44	54 29 44.9	9 59 27.7		Th-234	
229/N		13:05	54 29 43.9	9 59 26.8		(1)R/SC, (1)VX-R, (1) VX-R	
231/D	5/24/93	15:00	54 29 27.9	9 58 54.4	?	(1)R/SC, (3)BIO	REOCCUPATION
232/D		15:12	54 29 28.3	9 58 54.7		(3)BIO, (2)VX-R	
233/D		15:28	54 29 28.7	9 58 54.8		(3)BIO, (1)ARC	
234/D		15:38	54 29 28.5	9 58 54.5		(1)R/SC, (1)VX-R	
235/D		15:53	54 29 28.4	9 58 54.6		Th-234	
239/Q	5/25/93	10:20	54 29 34.7	10 00 11.7	?	(1)R/SC, (3)BIO	STANIC TOWER
240/Q		10:30	NO POS.			(3)BIO, (2)VX-R	
241/Q		10:43	54 29 35.7	10 00 12.3		(3)BIO, (1)ARC	
242/Q		11:06	54 29 34.8	10 00 11.7		(1)R/SC, (1)VX-R, (2)HX-R	
243/Q		11:28	54 29 35.8	10 00 11.5		Th-234	
244/Q		11:41	54 29 36.2	10 00 13.8			
245/I	5/25/93	14:16	54 29 59.5	10 01 54.3	?	(1)R/SC, (3)BIO	REOCCUPATION (MITTELGRUND)
246/I		14:29	54 29 57.3	10 01 56.8		(3)BIO, (2)VX-R	
247/I		14:40	54 29 59.3	10 01 55.8		(3)BIO, (1)ARC	
248/I		15:02	54 29 59.2	10 01 53.9		Th-234	
249/I		15:12	54 29 57.7	10 01 56.1		(1)R/SC, (1)VX-R, (2)HX-R	
250/I		15:23	54 29 57.7	10 01 56.1			
253/O	5/26/93	10:22	54 29 36.4	9 59 18.0	?	(1)RC, (3)BIO	REOCCUPATION
254/O		10:39	54 29 36.7	9 59 18.1		(3)BIO, (2)VX-R	
255/O		10:51	NO POS.			(3)BIO, (1)ARC	
256/O		11:11	NO POS.			(1)R/SC, (1)VX-R, (2)HX-R	
257/O		11:21	NO POS.			Th-234	

Table 3. - Continued

STATION SUNY/FWG	DATE	TIME	LAT.	LONG.	DEPTH (M)	SAMPLES	NOTE
259/H	5/26/93	15:35	54 27 58.2	9 52 06.7	?	(1)R/SC, (3)BIO	REOCCUPATION
261/H		15:59	54 27 57.6	9 52 13.6		(3)BIO, (2)VX-R	(NAVY BASE)
262/H		16:08	54 27 59.4	9 52 11.0		Th-234	
263/H		16:15	54 28 01.6	9 52 11.6		(1)R/SC, (1)VX-R, (2)HX-R	
268/G	5/27/93	14:02	54 30 2.25	10 01 42.1	?	(3)BIO, (2)VX-R	REOCCUPATION
269/G		14:14	54 30 3.10	10 01 40.9		(1)R/SC, (3)BIO	(MITTELGRUND)
270/G		14:21	54 30 2.61	10 01 40.6		(3)BIO, (1)ARC, (1)VX-R	
271/G		14:32	54 30 3.18	10 01 40.7		Th-234	

KEY: R/SC - 6" RADIOCHEMISTRY/SEDIMENTOLOGY CORE
BIO - 3" BIOLOGY CORE
ARC - 3" ARCHIVE CORE
VX-R - VERTICAL X-RAY TRAY (SAMPLED NORMAL TO SEABED)
HX-R - HORIZONTAL X-RAY TRAY (SAMPLED PARALLEL TO SEABED)
BE - 6" BIOTURBATION EXPERIMENT CORE
SC - 10cc SYRINGE CORE
Th-234 - 20x30cm BOX EXTRUDED FOR Th-234 CHEMISTRY
KC - KASTEN CORE

PRELIMINARY SEDIMENTOLOGICAL AND RADIOCHEMICAL RESULTS

Sedimentary Structure

The dominant character observed in x-radiographs is physical lamination. This is best developed at the site near the Eckernfoerde Navy Base (Fig. 1A) where a more diverse input of grain sizes accentuates the structure. Physical laminations also characterize the tower sites in the center of Eckernfoerde, but the laminations are less distinct (Fig. 1B). Presumably the reduced distinction is the result of a more uniform grain size distribution. We plan to examine the range of grain sizes present at both locations. Microfabric is another analytical approach, which is able to highlight particle segregations (i.e., laminations) through optical techniques. We have dissected the sediment slabs and are beginning the microfabric analysis. The two sites near Mittelgrund (one sandy site and a transition site with mixed sand and mud) show the greatest evidence of bioturbation destroying physical laminations and leading to mottled structure (Fig. 1C).

Mixing Depths

At the tower sites, excess ^{234}Th appears limited to the upper centimeter of the seabed (Fig. 2). ^{234}Th decay requires us to wait about 6 months before measuring supported levels and calculating excess ^{234}Th. We are just beginning those measurements now, but we can roughly estimate supported levels from profiles of total activity (e.g., Fig. 2). During the first cruise (BS-1), the subsampling interval was limited to 1-cm resolution, and excess activity appears present only in the uppermost sample. On the subsequent cruises, the subsampling was measured to 0.5-cm resolution. Excess activities are apparently limited to the upper two samples (i.e., upper cm). This is a very thin surface mixed layer, and reflects the local benthic community. It also precludes calculations of mixing coefficients.

Accumulation Rates

The absence of significant depths of bioturbation simplifies calculations of accumulation rates. The highest rates are observed at the tower site (Figs. 3 and 4; generally >0.5 cm y^{-1}), with lower rates toward the Navy Base and toward Mittelgrund (Figs. 5 and 6; <0.25 cm y^{-1}).

Perhaps the most interesting aspect of the study area is the potential for detailed chronology of environmental conditions. The high accumulation rates and absence of a significant surface mixed layer, allows fluctuations of sedimentological processes to be recorded in fine detail. For example, Figure 4 demonstrates changes in accumulation rate with depth in core, and should be tied to environmental conditions occurring within the past century. These historical changes in accumulation will be used to model their effects on the formation of sedimentary structures.

PRELIMINARY BIOLOGICAL OBSERVATIONS

Spatial Distributions

The muddy basin of Eckernfoerde Bay is dominated by the tube-building spionid polychaete *Polydora ciliata* and the tellinid bivalve *Abra alba*. Large ovoid fecal pellets are common in the >500µm fraction, and are produced by larger *A. alba* not found in the basin. It is likely that the pellets have been moved from shallower margins to the deeper basin. Most animals were very small; the largest *P. ciliata* was ~1 cm in length, and most *A. alba* were <4 mm in shell length. Several other species were found in lower densities (Table 5). They include *Pectinaria koreni*, *Sigambra* sp., orbiniid sp., *Mytilius edulis*, *Capitella capitata*, *Nepthys* sp., *Eteone* sp., a few amphipods, and pycnagonids. Abundances were high, samples to date ranging from 11,800 to 37,500 animals m^{-2}.

The sandy Mittlegrund site supported a distinctly different fauna. Density was lower (~4,700 animals m^{-2} but because there were more large animals, biomass appeared greater. The biomass dominants were *Nepthys* sp., *Pectinaria koreni*, *Mytilus edulis* and *Corbula gibba*. The numerical dominant was *Abra alba*; most were very small. Less abundant animals included *Harmathoe* sp., a corophiid amphipod, *Polydora ciliata*, an orbiniid worm, *Heteromastus filiformis* and a syllid.

The functional differences between the muddy and sandy fauna in Eckernfoerde Bay are more striking than the taxonomic and numerical differences described above. The mud fauna, dominated by a small tube-dwelling surface deposit feeder will have very limited potential to bioturbate the sediment. The small *Abra alba* do not add to this potential. Most of the vertical particle bioturbation appears to be limited to <1 cm depth.

In contrast, the sandy sediment is inhabited by several larger subsurface deposit feeders or burrowers. The dominant particle mixer is probably the head down deposit feeder *Pectinaria koreni*. It appears to plow slowly through the sediment (in the bioturbation experiment described below, the worms did not move appreciably over a three-week period), ingesting sediment ~1 to 2 cm below the surface, and defecating these particles at the sediment surface. Mixing depth approximated the length of *P. koreni* at this site. Their particle mixing pattern is therefore distinctly advective in character. The other major bioturbator in this sediment is Nepthys sp. Most nepthyds are described as burrowing predators, so they would be expected to mix sediments more or less randomly when burrowing. In general, these patterns of animal size and mixing patterns are consistent with other studies that have shown that bioturbation rates are commonly greater in sand than in muds, although bioturbation is relatively more important than physical mixing in muds than in sands.

Bioturbation Experiment

Samples returned to New York are being analyzed for fluorescence of tracer particles. Fluorescent particles were extracted from the sediment samples taken from the bioturbation experiment following established methods (Carey, 1989). Samples were dried overnight at 80°C and weighed. Sediment plugs were then added to 10 ml 90% acetone, vortexed for 1 minute and allowed to extract for 24 hours. Samples were kept refrigerated to minimize acetone evaporation. Samples were then vortexed again and centrifuged for 5 minutes at 2800 rpm. 3-ml aliquots of the supernate were analyzed with an Aminco spectrofluorometer. Intensity of the orange particles used to measure vertical bioturbation was measured at 420 nm excitation and 500 nm emission. Fluorescence of red particles was measured at 526 nm excitation and 550 nm emission. Maximum resolution of peak heights was obtained at these wavelengths (D. Carey, pers. comm.)(see Fig. 7). All values were corrected for background fluorescence.

Preliminary results indicate that vertical particle mixing is restricted to <1 cm in cores taken from the muddy central basin (Fig. 8). This is consistent with the interpretations from the faunal analysis. Duplicate subcores showed good agreement, suggesting that there is not much variability in vertical bioturbation on small (cm) spatial scales.

TABLE 4. - Preliminary faunal list for organisms observed to date

	Species	Functional Group
Polychaetes:		
	Polydora ciliata	tubicolous, surface selective deposit feeder
	Pectinaria koreni	head down deposit feeder
	Capitella capitata	burrowing, head down deposit feeder
	Heteromastus filiformis	head down deposit feeder
	orbiniid	head down deposit feeder
	syllid	mobile predator
	Harmathoe sp.	sit and wait? predator
	Nepthys. sp.	mobile predator
	Eteone sp.	mobile predator
	Sigambra sp.	
Molluscs:		
	Abra alba	burrowing, surface deposit feeder
	Mytilus edulis	suspension feeder
	Corbula gibba	suspension feeder
	unidentified bivalve	
Arthropods:		
	Corophiid amphipod	tubicolous, surface deposit feeder
	unidentified amphipod	

TABLE 5. - Description of samples for bioturbation experiment

Date sampled	Station	Box core #	Comments	
27 April 93	I	106, A, B 107, C, D	4 small box cores	Transition Site
28 April 93	D	119 A-C	Large box core	Old Tower Site
28 April 93	H	114 A-D	Large box core	Navy Base Site
28 April 93	N	128 A-D	Large box core	New Tower Site
29 April 93	O	143 A-C	Large box core	New Tower Site
29 April 93	G	146 A, B 147 C	Small box core	Mittelgrund Site
29 April 93	F	151 A-D	Large box core	Old Tower Site

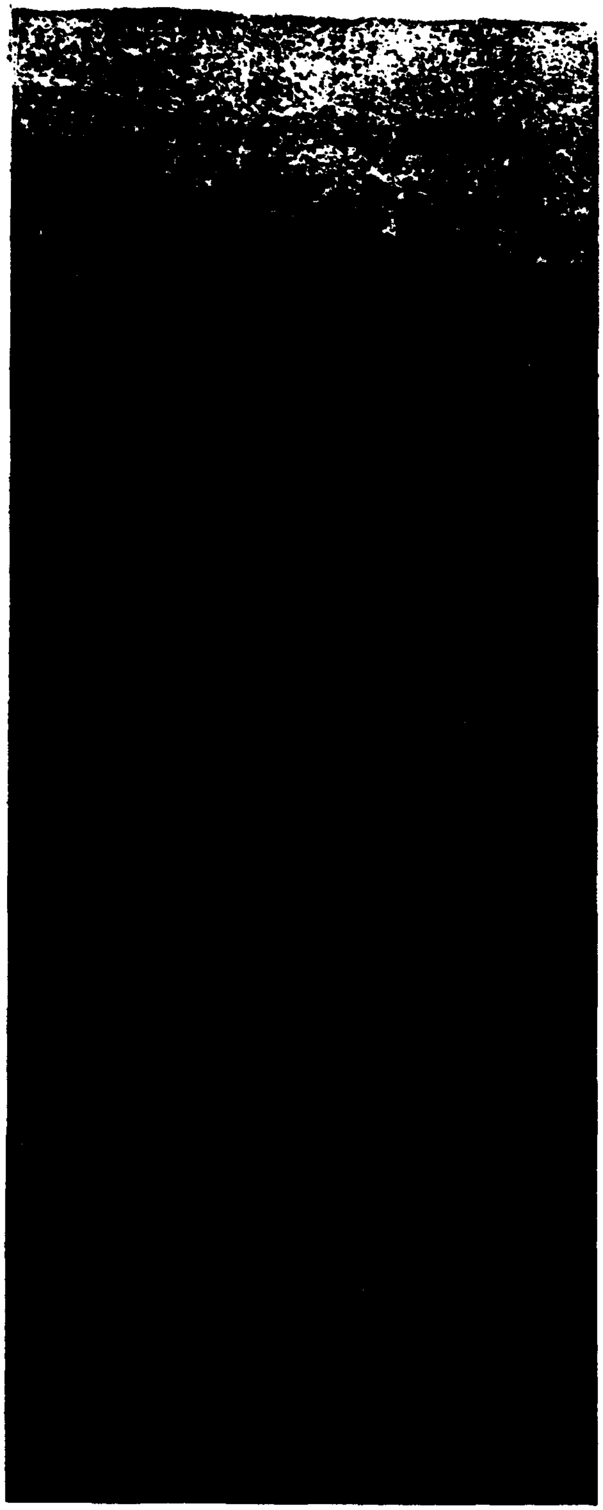

C

Figure 1.- X-radiograph positives (true scale) from: A) near Eckernfoerde Navy Base, B) Tower Site F (see Fig. 4), C) Mittelgrund transition site. Physical laminations are most distinct in 3A and least distinct in 3C.

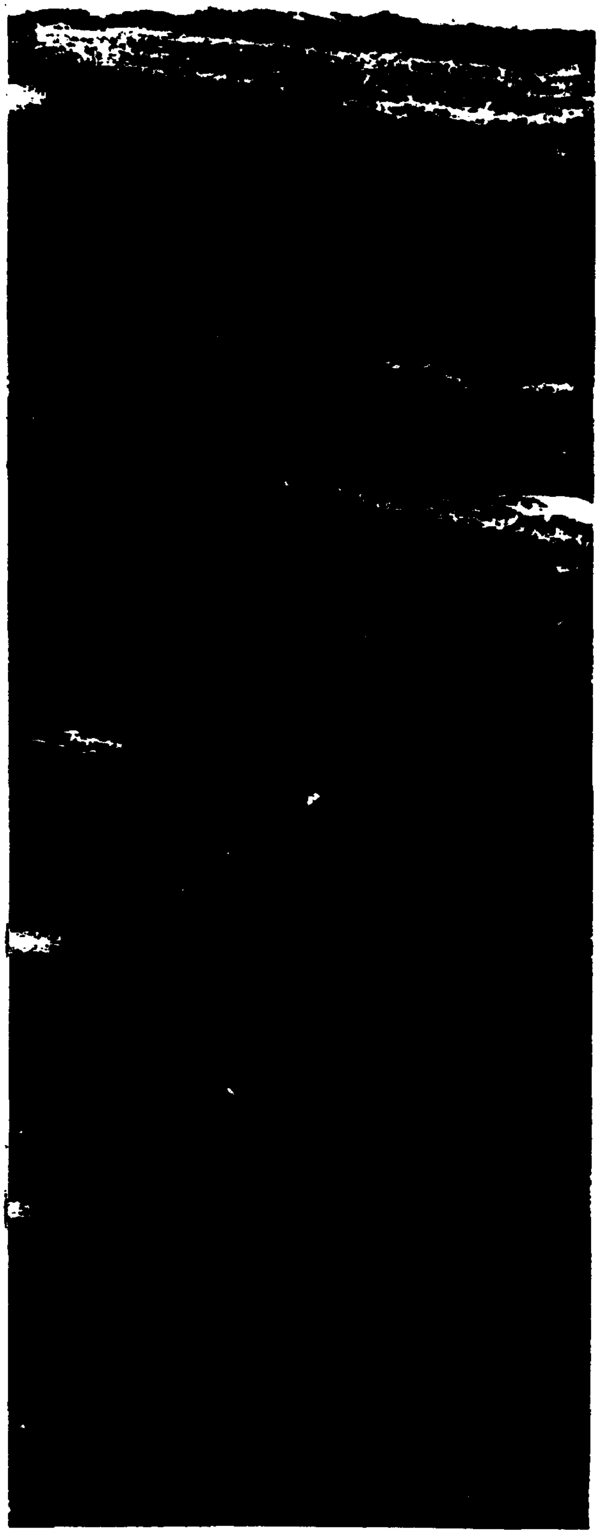

A

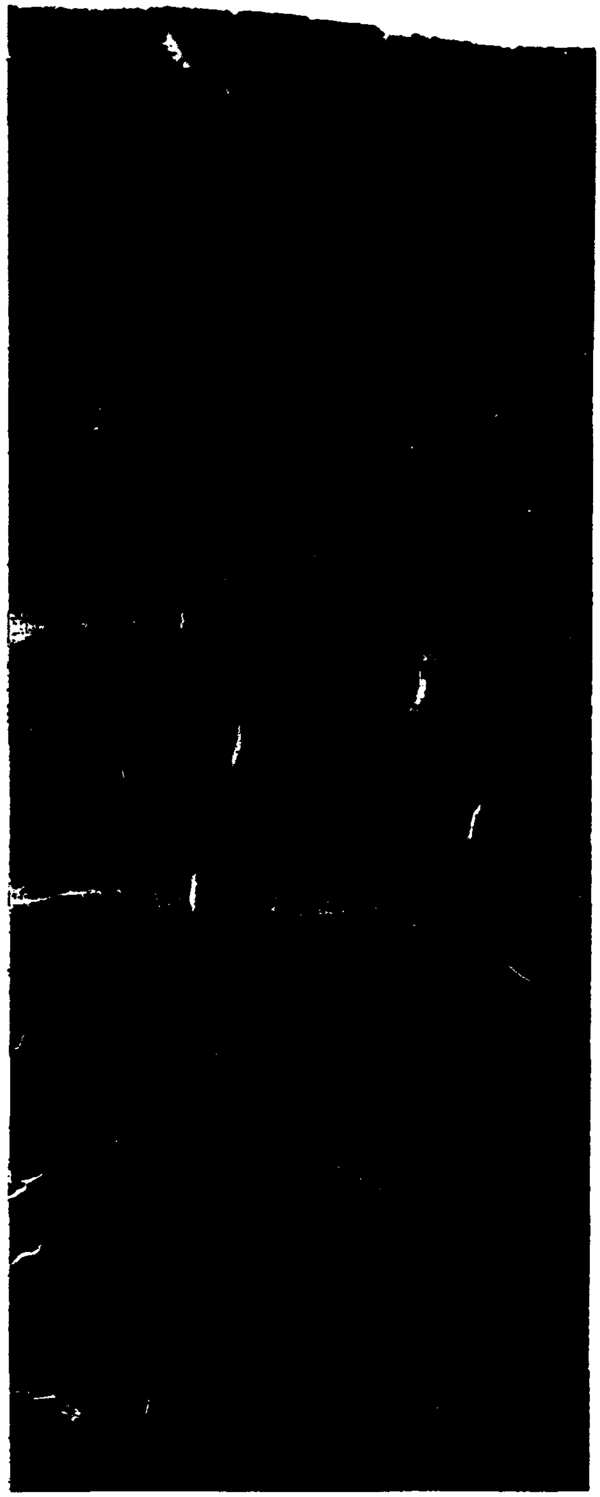

B

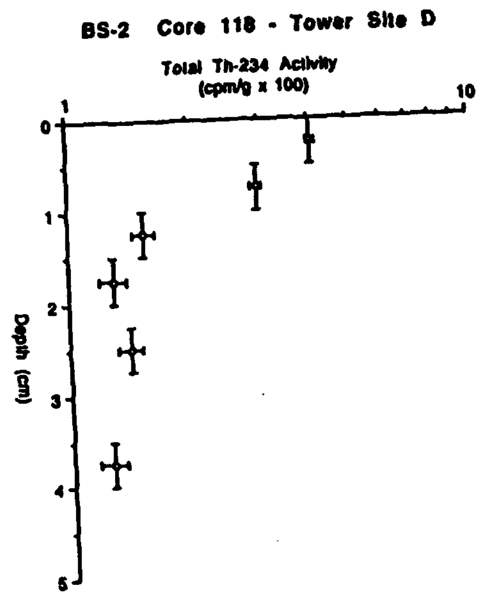

Figure 2.- Profile of total ^{234}Th activity. Supported levels have not yet been measured, but this profile appears to indicate that excess activities are limited to the upper centimeter. This is a very thin surface mixed layer relative to most coastal environments.

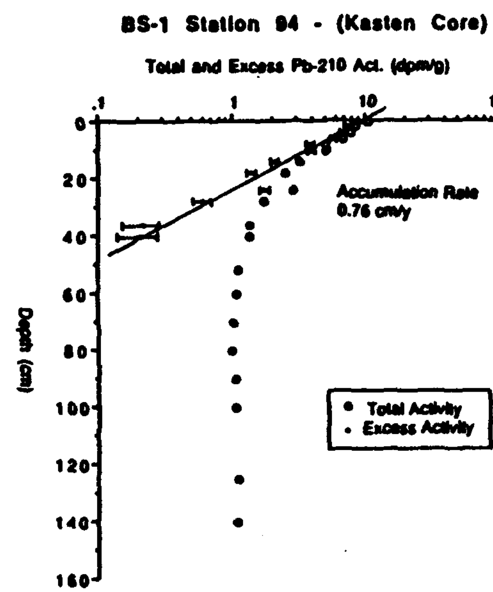

Figure 3.- Profile of total and excess ^{210}Pb from a kasten core. This profile indicates that the supported level is about 1 dpm g^{-1}, which can be used for other cores in this vicinity. The slope of the excess-activity profile allows calculation of the accumulation rate.

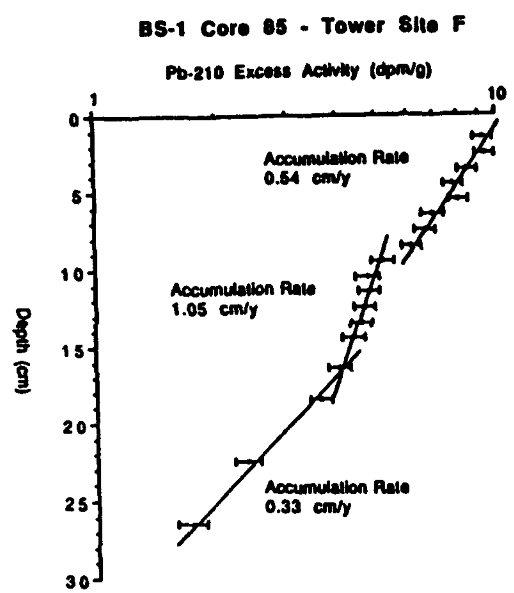

Figure 4.- Profile of excess ^{210}Pb, which indicates changes in accumulation rate during the past century.

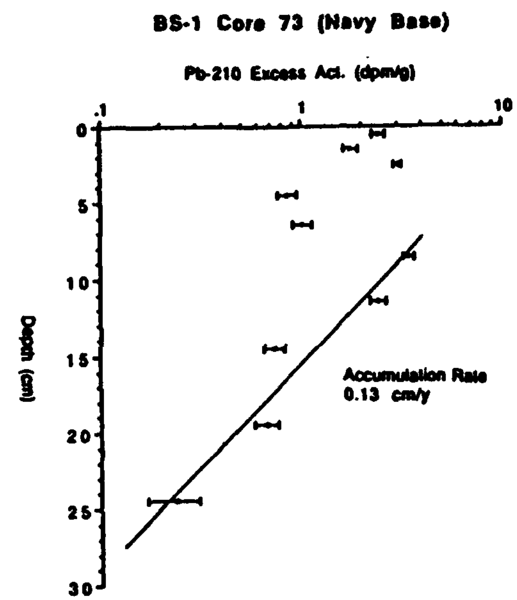

Figure 5.- Profile of excess ^{210}Pb obtained at site near Eckernfoerde Navy Base. Many of the activity variations in the core reflect distinct changes in grain size.

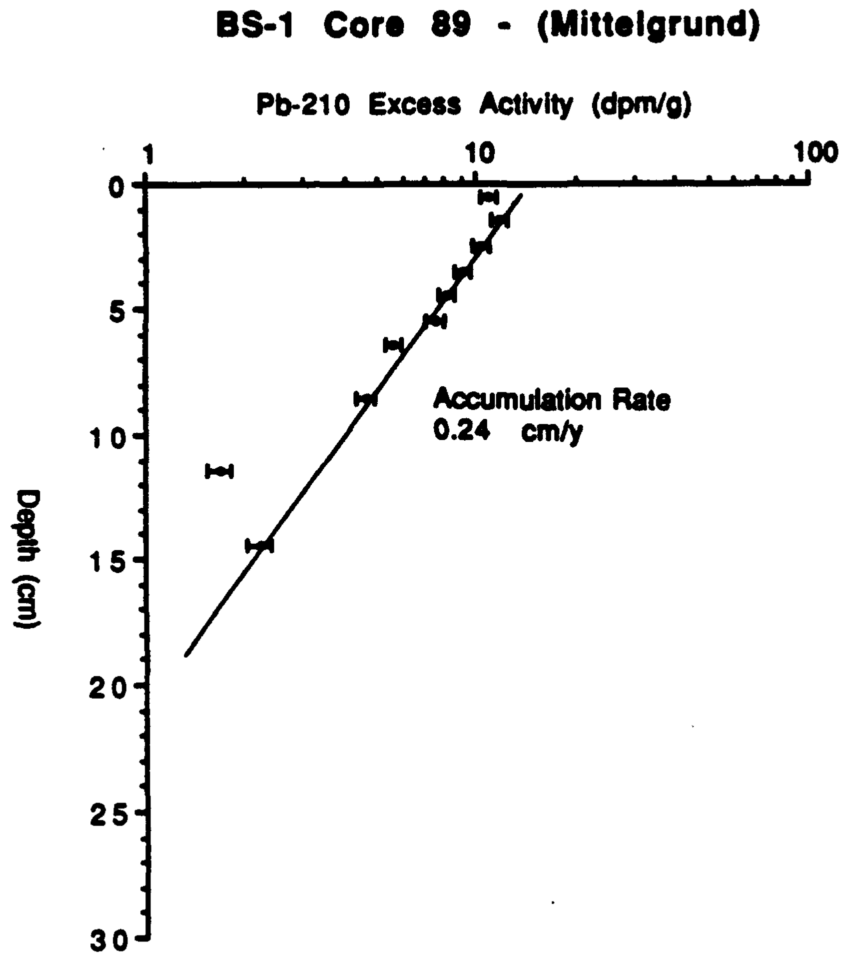

Figure 6.- Profile of excess ^{210}Pb obtained at the transition site near Mittelgrund.

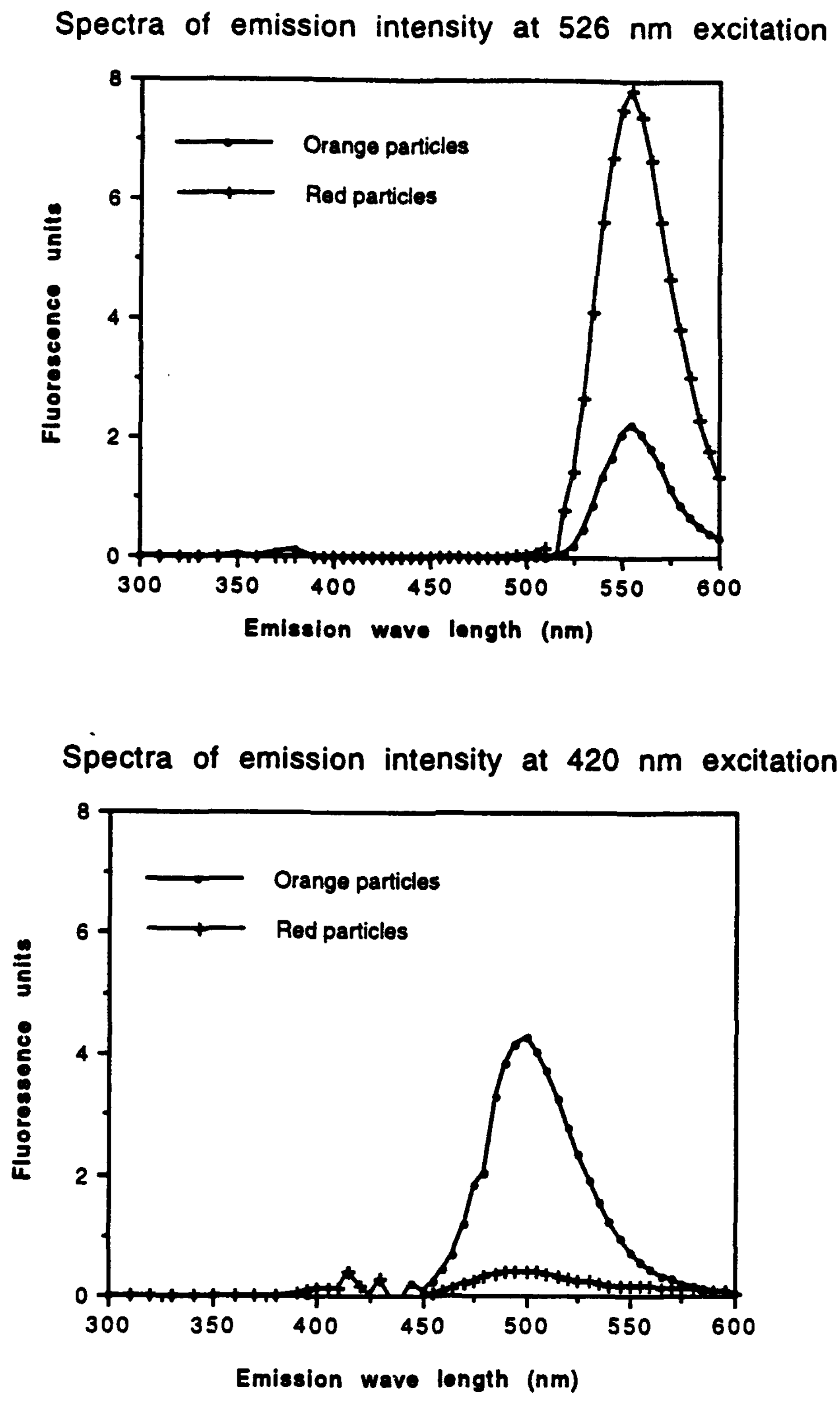

Figure 7.- Spectra of emission intensity for the fluorescent particles used in the bioturbation experiments.

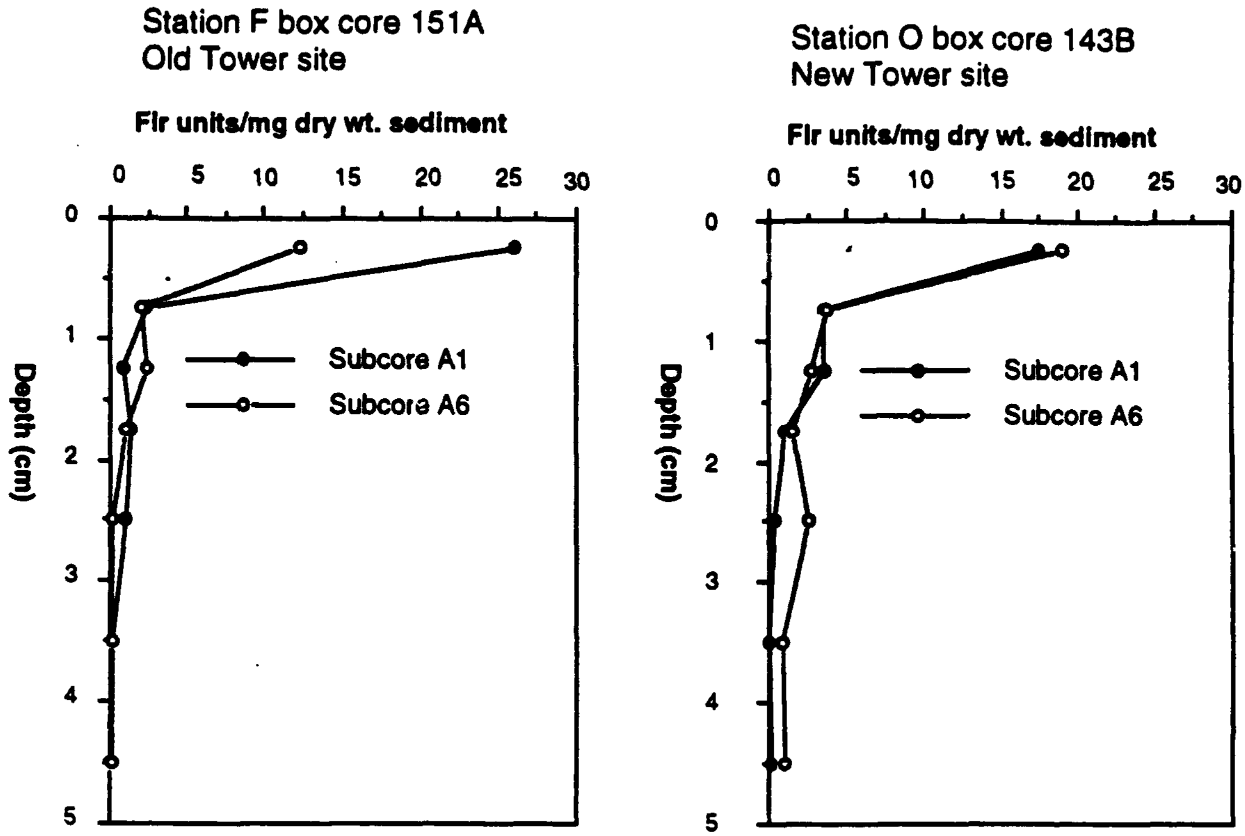

Figure 8.- Vertical profiles of fluorescence intensity from two subcores within a single 6" core from stations F and O. Values are corrected for background fluorescence.

3.16 In Situ Sediment Geoacoustic Properties (Principal Investigator: M. D. Richardson, NRL)

CBBLSRP FY93 YEAR-END REPORT

M.D. Richardson and S. R. Griffin
Naval Research Laboratory
Stennis Space Center, MS 39529-5004

Near surface sediment geoacoustic and physical properties were measured in gas-rich, muddy sediments of Eckernfoerde Bay, Baltic Sea and in hard-packed, sandy sediments of the northeastern Gulf of Mexico. The results of laboratory measurement of sediment geoacoustic (compressional wave speed and attenuation) and sediment physical (porosity, bulk density and shear strength) properties are reported in section 3.4 (Briggs & Richardson).

In situ compressional and shear wave speeds and compressional wave attenuation (@ 10-30 cm) were measured during 9 deployments of the In Situ Sediment Acoustic Measurement System (ISSAMS) in Eckernfoerde Bay and 7 deployments of ISSAMS on the sandy sediments of the West Florida Sand Sheet. Shear wave speed gradients (0-2 m) were also measured at Eckernfoerde Bay. Operational details for both systems have been reported by (Richardson et al, 1990 & 1991, Bennett et al., 1991 and Barbagelata et al., 1991).

In situ values of compressional wave speed (mean 1428 m s-1, standard deviation 2.47) and attenuation (4.11 dB m-1 @ 58 kHz, 1.74) in the soft, muddy sediments of Eckernfoerde Bay varied little compared to the values (1711 m s-1, 22.13; 30.4 dB m-1, 8.26) measured in northeastern Gulf of Mexico sediments. Near surface shear wave velocity (7-9 m s-1) in the soft, muddy sediments of Eckernfoerde Bay were much lower than in sandy Gulf of Mexico sediments (102-137 m s-1). Shear wave velocity measured in Eckernfoerde Bay sediments increased to 25 m s-1 at 2 m depth while gradients of compressional wave speed were difficult to measure because of scattering and attenuation from methane gas bubbles.

During FY94, values of sediment geoacoustic properties measured in this study will be placed in context of the larger data set previously collected with ISSAMS. Empirical relationships between values of in situ sediment geoacoustic properties and sediment physical properties will also be developed. Results and relationships developed from the in situ data set will be compared to a similar extensive laboratory geoacoustic and physical property set analyzed by Richardson (1986, 1993). Data and Results will be presented at the Spring AGU/ASLO "Ocean Sciences" meeting in San Diego and submitted from publication in the Journal of the Acoustical Society of America.

Field studies in FY94 will utilize the 3rd generation ISSAMS system to provide values of in situ sediment geoacoustic properties for the range of sediment types in Kiel Bay characterized by the sediment classification systems (see Lambert and Hawkins; Schock). Gradients of compressional and shear wave properties will be measured in the gas-rich sediments of Eckernfoerde Bay. Combined with data on sediment physical properties (Briggs & Richardson), sediment structure (Bennett & Lavoie; Anderson), normal incident echo sounding (Lambert & Hawkins) and acoustic propagation (Stanic) a model of acoustic bottom interaction in gassy sediment will be developed and validated.

Future analysis plans include:

1. Validation of the Biot model for geoacoustic properties in a three-phase medium (e.g. Baltic Sea gas-saturated sediments).

2. Use of spatial variability of sediment physical and geoacoustic data to provide the basis for statistical determination of sediment acoustic volume scattering, a key to understanding and modeling acoustic-bottom interaction at high-frequencies.

3. Comparison of values sediment physical and geoacoustic properties to sediment microstructure to provide the basis for understanding the propagation of acoustic energy through a poroelastic medium.

4. Evaluation of the effects of environmental processes on the spatial and temporal variability of sediment geoacoustic properties. This is a continuation of ongoing NRL studies which model the effects of environmental processes on sediment physical and geoacoustic properties(Richardson 1983, Richardson & Young, 1980; Richardson et al. 1983, 1985).

5. Comparison of values of geoacoustic properties measured by various techniques in the field (Lavoie & Pittenger; Stoll; this study) and under laboratory conditions (Bryant & Slowey; Silva et al.; Lavoie & Pittenger; this study).

REFERENCES

Barbagelata A., M.D. Richardson, B. Miaschi, E. Muzi, P. Guerrini, L. Troiano, and T. Akal, 1991. ISSAMS: An in situ sediment geoacoustic measurement system, pps. 305-312. In, Shear Waves in Marine Sediments (J.M. Hovem, M.D. Richardson and R.D. Stoll, Editors), Kluwer Academic Publishers, Dordrecht, The Netherlands.

Bennett, R.H., H. Li. M.D. Richardson, P. Fleischer, D.N. Lambert, D.J. Walter, K.B. Briggs, C.R. Rein, W.B. Sawyer, F.S. Carnaggio, D.C. Young and S.G. Tooma, 1991. Geoacoustic and geological characterization of surficial marine sediments by in situ probe and remote sensing techniques, pps. 295-350. In, CRC Handbook of Geophysical Exploration of the Sea, 2nd Editon, Hydrocarbons (R.A. Geyer, Editor), CRC Press, Boca Raton.

Richardson, M.D., 1986. Spatial variability of surficial shallow water sediment properties, pps 527-536. In T. Akal and J.M. Berkson (eds.) Ocean Seismo-Acoustics. Plenum press, London.

Richardson, M.D., 1983. The effects of bioturbation on sediment elastic properties. Bull. Soc. Geol. France, 25: 505-513.

Richardson, M.D. and K.B. Briggs. 1993. On the Use of Acoustic Impedance Values to Determine Sediment Properties, pps 15-25. In N.G. Pace & D.N. Langhorne (eds.) Acoustic Classification and Mapping of The Seabed. Institute of Acoustics, University of Bath.

Richardson, M.D., K.B. Briggs and D.K. Young, 1985. Effects of biological activity by benthic macroinvertebrates on sedimentary structure in the Venezuela Basin. Mar. Geol., 68: 243-267.

Richardson, M.D., E. Muzi, L. Troiano and B. Miaschi, 1990. Sediment Shear Waves: A comparison of in situ and laboratory measurements, Chapter 44, pps. 403-415. In R.H. Bennett, W.R. Bryant and M.H. Hurlbert (eds), Microstructure of Fine Grained Sediments. Springer-Verlaag, New York.

Richardson, M.D., E. Muzi, B. Miaschi and F. Turgutcan, 1991. Shear wave gradients in near-surface marine sediment, pps. 295-304. In, Shear Waves in Marine Sediments (J.M. Hovem, M.D. Richardson and R.D. Stoll Editors), Kluwer Academic Publishers, Dordrecht, The Netherlands.

Richardson, M.D. and D.K. Young, 1980. Geoacoustic models and bioturbation. Mar. Geol., 38: 205-218.

Richardson, M.D., D.K. Young and K.B. Briggs, 1983. Effects of hydrodynamic and biological processes on sediment geoacoustic properties in Long Island Sound, USA. Mar. Geol., 52: 201-226.

3.17 The Detection of Continuous Impedance Structures Using Full Spectrum Sonar (Principal Investigator: S. G. Schock, Florida Atlantic University)

CBBLSRP FY93 YEAR-END REPORT

Steven G. Schock
Center for Acoustics and Vibration
Dept. of Ocean Engineering
Florida Atlantic University
Boca Raton, FL 33431

Abstract

At Florida Atlantic University Dr. Schock and Dr. LeBlanc are developing remote acoustic methods of measuring sediment properties. During 1993 there were two main thrusts for the FAU investigators participating in the Coastal Benthic Boundary Layer Special Research Project. The first effort was the collection of normal incidence seabed reflection data using a broadband FM subbottom profiler at locations that would be later sampled for sound velocity and bulk density. The second program was the development of a bottom model for predicting the acoustic response of the seafloor given impedance data derived from compressional wave velocity and bulk density measurements on sediment cores and for evaluating the usefulness of acoustic pulses for estimating impedance over various frequency ranges. Additionally, some FM data was analyzed to obtain a remote measurement of sediment attenuation.

Normal incidence FM sonar data was collected in Eckernfoerde and Kiel Bays during the periods of 28 January to 10 February and 27 April to 7 May 1993, and off the coast of Panama City during the period of 9 to 13 August 1993. During the Baltic experiment, 20 msec FM pulses linearly swept over the bands of 2 to 10 kHz, 2.5 to 12.5 kHz and 2.5 to 15.5 kHz were used to measure the normal incidence response of the seabed. Because the Panama City site had a sandy floor, only a 20msec 2 to 10 kHz FM pulse was used to make acoustic measurements ensuring at least 5 meters of penetration.

A numerical model of a vertically continuous and horizontally homogeneous impedance structure was coded allowing prediction of the impulse response of the seabed and synthetic acoustic returns given impedance data derived from sediment cores. The model was used to study the acoustic response of synthetic impedance structures and structures derived from impedance data provided by NRL. The study showed that it is necessary to use frequencies below 1 kHz when measuring the surficial reflection coefficient or interlayer reflection coefficients. Transition zones, which commonly exist at the sediment-water interface and between subbottom layers, cause higher frequency acoustic pulses to smear and to sometimes destructively interfere preventing accurate measurement of impedance changes or imaging of the sediment structure.

Field experiments

Description of Equipment

Normal incidence reflection measurements of the seabed were performed using a X-Star Full Spectrum sonar. This sonar uses a Sparc workstation for display and sonar control. Figure 1 is a block diagram describing data flow through the X-Star. The user can select an FM pulse to transmit from a menu. For the CBBLSRP, 20 ms 2-10, 2.5-12.5 and 2.5-15.5 kHz FM pulses were used for subbottom profiling. These FM pulses are amplitude tapered, have quadratic phase and contain amplitude and phase corrections to prevent transducer ringing and to ensure that the correlated data has no significant correlation noise. The FM pulse is generated by a 20 bit D/A converter and is amplified by a 2 channel linear power amplifier operating push-pull. The output of the amplifier is matched to the array of projectors using a matching transformer. The transmitting array, mounted in the front of a towed vehicle (fish), consists of a 2 by 2 planar array of Tonpilz resonators forming a rectangular aperture of 30 by 30 cm. The fish was usually towed at a height of 2/3 of the water depth to prevent surface reflections from interfering with the subbottom data.

Subbottom reflections are measured with a line array which has an acoustic length of 50 cm and is mounted in the rear of the vehicle beneath a pressure release surface. A preamp in the array transmits the signal up a 50 meter cable to a programmable gain amplifier before being digitized by a 16 bit sigma-delta A/D converter. The gain of the preamp is automatically set by the Sparc workstation to ensure the full range of the A/D converter is utilized without clipping the received signal. In order to maintain the calibration of the sonar for measuring reflection coefficients, the programmed gain is recorded and is used to correct the amplitude of the digitized data.

The digitized acoustic return is compressed using a matched filter and is corrected for spherical spreading. The matched filtered return, corrected for spreading, is recorded on 8 mm tape in SEG-Y format in the analytic signal form. SEG-Y format records NMEA0183 navigation data with every acoustic return, along with programmable amplifier and other sonar settings. Figure 2 contains the SEG-Y format for the compressed FM data.

Field Experiments

The X-Star Full Spectrum Sonar was used to collect normal incidence reflection data over the following frequency ranges: 2 to 10, 2.5 to 12.5, and 2.5 to 15.5 kHz. The FM sonar tracklines for the Baltic and Panama City experiments are contained in Figures 3 through 25. A Trimble NavTrack GPS was used for positioning. The maximum positioning error was approximately 100 meters. Subbottom Images are provided in Figures 26 through 32 for FM data collected at the core sites in the Eckernfoerde/Kiel Bay that have been analyzed by Texas A&M to date.

Figures 33 and 34 show water column data displayed by either turning up the display gain or making the lower shades, corresponding to weak reflections, darker in the Image. Figure 33 shows that a strong acoustic reflection about 10 meters above the seafloor occurs at a discontinuity in the XBT salinity profile at the same distance above the seafloor. Figure 34 shows an interval wave generated by a change in seafloor height at the interface between brackish water over salt water.

Comparisons were made between the 3 acoustic pulses along the same tracklines. Figure 35 and 36 contain comparisons between images generated by 20 msec long pulses with the following bandwidths 2 to 10 kHz, 2.5 to 12.5 kHz and 2.5 to 15.5 kHz FM pulses. The images demonstrate that as the center frequency of the pulse decreases so does subbottom penetration and as the pulse bandwidth increases so does the image resolution, the ability to resolve two closely spaced reflectors.

Figures 37 and 38 contain images along the same trackline made by the X-Star and the ASCS. The X-Star Image was generated with 20 msec 2.5-15.5 kHz FM pulse while the ASCS images were produced with 15 kHz and 30 kHz CW pulses. One conclusion that can be made by examining the images is that higher frequency pulses (15 and 30 kHz) generate reflections from sediment layer boundaries that are commonly incoherent. This variation in the ping to ping reflection amplitude is due to the randomness of the interlayer interface and the relatively short wavelengths of the 15 and 30 kHz acoustic pulses. If the wavelength of the pulse is not significantly greater than the characteristic roughness length, constructive and destructive interference will cause the pulse amplitude and shape to vary randomly.

In Panama City, the floor at the survey site was primarily sand. Since sand has a high attenuation coefficient, the 20 msec, 2 to 10 kHz FM pulse, which has the lowest center frequency of the pulses available for transmission, was selected for the subbottom survey to ensure a subfloor penetration of at least 5 meters. An acoustic survey along lines in a 2 by 4 nm grid was performed over a 3 day period. Figure 39 shows the tracklines for the X-Star survey. Positioning data was generated with a Trimble NavTrack GPS which had a maximum positioning error of about 100 meters. The tracklines are shaded with grey levels showing 1 dB changes in the reflection coefficient. Tie lines made on day 3 of the survey show that the reflection coefficient measurement were within 1 dB of the reflection coefficient measurements of the previous 2 days at the same positions. The maximum range of the reflection coefficient measurements for the grided area is about 3 dB. When the trackline is a light shade of grey, the sediments are softer. Figure 40 shows that large changes in the standard deviation of the amplitude of the pressure reflection coefficient of the sediment-water interface. Near the right hand side of the figure, there was a large drop in the standard deviation of the reflection coefficient without any significant change in the mean reflection coefficient. The drop in the ping to ping variation of the reflection amplitude is probably due to a reduction in bottom roughness.

Figures 3 through 25 provide the tape IDs for the FM sonar data tapes, copies of which can be obtained upon request. SEG-Y data tapes of FM subbottom profiles can be displayed on any Sparc workstation that is running the Sunview windowing system and that has an Exabyte 8mm tape drive connected to the SCSI bus. If the Sparc workstation does not support Sunview, the tapes can be read using a C program and displayed using a locally written graphics program.

Figure 41 is map of surficial sediment types generated by previous coring surveys in Kiel Bay. This sediment map is provided to give the reader an overview of the local marine geology and to provide altitude/longitude information to be used with Figures 3 through 25.

Numerical Studies

A numerical model that estimates the interaction of normal incident sound with the seabed was coded using MATLAB to estimate how the seabed filters acoustic pulses. The input to the model is a vertically continuous impedance profile and the output is the impulse response of the seabed. The model assumes that the sediment structure is horizontally homogeneous. If pressure continuity and normal velocity continuity are applied at each infinitesimally small change in the vertical impedance profile, a ratio between the complex amplitudes of the upgoing and downgoing waves can be calculated for each incremental layer as shown in Figure 42. By iteration, ratios are calculated using impedance measurements made at 0.5 cm intervals from the lowest layer which is assumed to be a half space to the upper layer which is the water column. The last ratio calculated is the pressure reflection coefficient of the seafloor for one frequency. The calculation is performed for each frequency sample of the acoustic pulse's frequency spectrum. Modulating the frequency spectrum of the pulse with the reflection coefficient yields the frequency spectrum of the synthetic return. Inverse Fourier transformation of the return spectrum provides the synthetic return.

For example, Figure 43 contains shows how the impulse response changes with increasing thickness in the transition zone between to homogenous half spaces. As the thickness of the transition zone increases from 0 to 20 cm, the destructive interference of the higher frequency component of the pulse increases and the pulse broadens. Figures 44 through 46 show how pulses with a bandwidth of approximately two octaves behave as each interacts with a transition layer. The pulses with higher center frequencies are smeared over the transition causing extremely weak reflections. Only the pulse with energy between 125 and 625 Hz generates reflection amplitudes that accurately represent the change in impedance between the adjacent half spaces. The lower frequency pulse has a wavelength that is much greater than the thickness of the transition layer ensuring that reflected energy from each incremental part of the transition layer Is in phase with the energy from other parts of the transition. This analysis demonstrates the importance of using frequencies less than 1000 Hz for subbottom profiling.

Relaxation time, a measure of compressional wave attenuation, is estimated from Kiel Bay silts and Boca Raton sands to demonstrate the ability to measure attenuation remotely from a towed subbottom profiler. The upper graphs in figures 47 and 48 are plots of the center frequency of the compressed FM pulse as a function of depth beneath the seafloor. As the wavelet travels, the higher frequency components attenuate more rapidly than the lower frequency components causing a drop in the center frequency of the wavelet. As shown in the upper graphs, the wavelet's center frequency decreases at a higher rate in sand than in silts. The relaxation time can be estimated from the slope, the shift in the center frequency per unit time (Hz/msec). The lower graphs are plots of relaxation time vs subbottom depth. Figure 47 (Kiel Bay) shows that there is no significant drop in center frequency (relaxation time is less that 0.05 usec) until the pulse reaches gas causing a rapid drop in frequency and a relaxation time of 0.45 usec. The sands off of Boca Raton (Figure 48) have an estimated relaxation time of 0.15 usec.

Acknowledgments

I would like to thank Jian Long Zhang, a Master's candidate sponsored by this project, for his assistant in coding the impedance model and running the numerical simulations. Angela Reeder, a senior supported by ONR's AASERT program, contributed significantly to the preparation of this report by post processing the FM data sets and preparing the figures. I am also Indebted to Dr. LeBlanc for his supervision of the relaxation time numerical analyses, and Lachlan Munro, a graduate ONR AASERT student, for coding sediment classification procedures and running the relaxation time analyses.

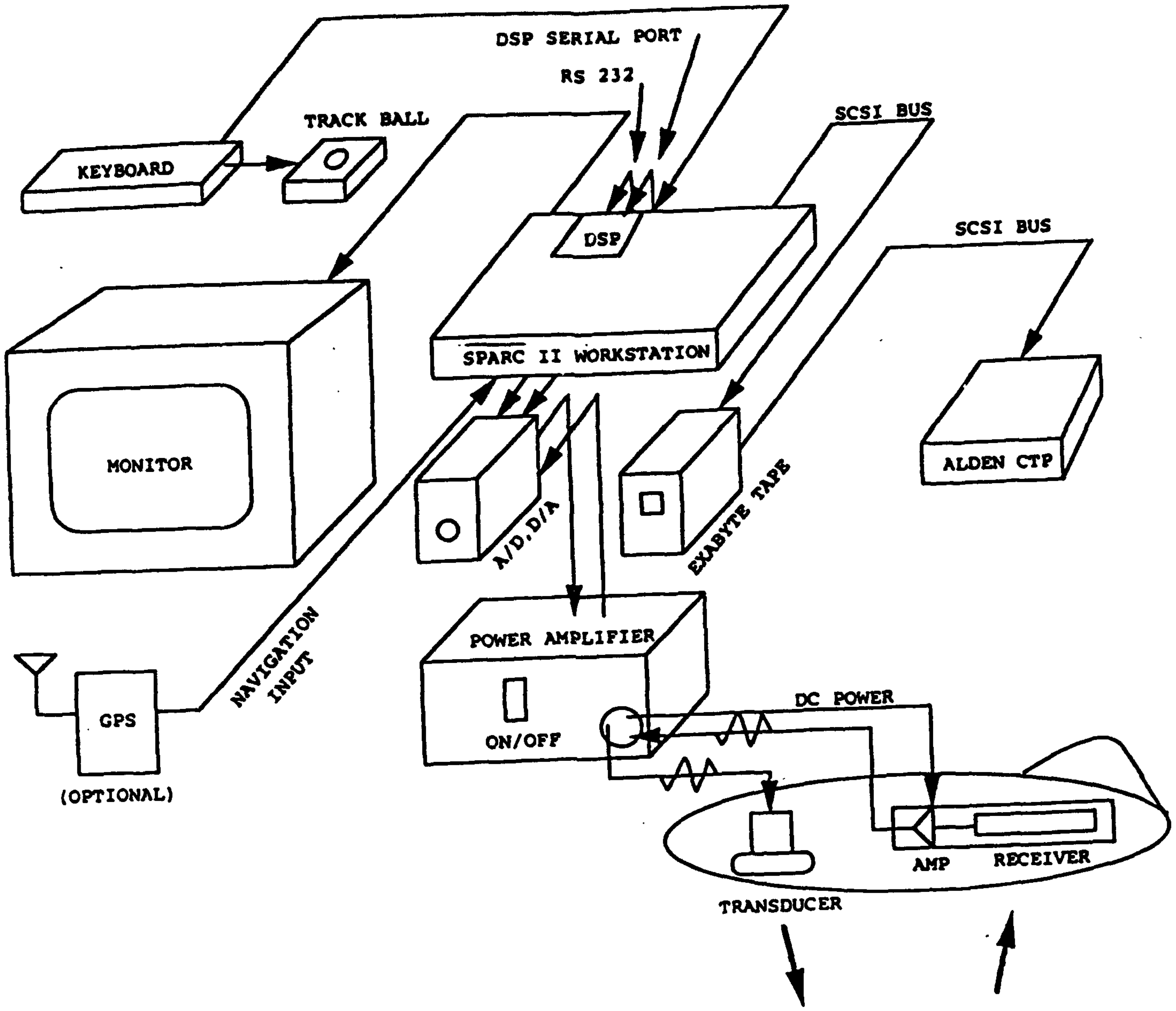

Figure 1 Functional block diagram of the X-Star Full Spectrum sonar

SEG-Y Format (rev4)

Tape Identification Header (3600 Bytes)(recorded at beginning of each file)

3200 Byte ASCII block(80 bytes per line)

C 1	COMPANY: (5E)
C 2	LINE(5E): AREA(21E)
C 3	TAPE NO: (5E) DAY: (23) YEAR: (45)
C 4	INSTRUMENT: X-Star Full Spectrum Profiler/Vehicle ID: (5)
C 6	SAMPLES/TRACE:3976(29) BYTES/SAMPLE: 2 (62)
C 8	SAMPLE CODE: FIXED POINT (5)
C 9	GAIN TYPE: FLOATING POINT(5)
C11	SOURCE: TYPE:FM (5)
C19	AMPLITUDE RECOVERY: SPHERICAL DIVERGENCE APPLIED(5)
C21	PROCESSING: DATA IN ANALYTIC FORM: REAL(0), IMAG(0),...,REAL(1987),IMAG(1987) (5)
C23	ENVELOPE AMPLITUDE = TRACE SCALE FACTOR* SQRT(REAL*REAL+IMAG*IMAG) (5)
C24	ENVELOPE SAMPLE INTERVAL = A/D SAMPLE INTERVAL*2 (5)
C26	SOURCE COORDINATES PROVIDE THE POSITION OF THE VEHICLE
C27	IN SECONDS OF ARC (Bytes 73-80)
C28	GROUP COORDINATES PROVIDE THE POSITION OF THE VEHICLE
C29	IN 1/10000 MINUTES (Bytes 81-88)

(A number within parentheses is the location of the first character within the 80 character string; E means keyboard entry at beginning of recording)

400 Byte binary block

Integer No.	Description
1600-1601	Not used
1602-1603	Line number
1604-1605	Not used
1606	Number of data traces per record =1
1607-1609	Not used
1610	Number of samples per trace =3976
1611	Not used
1612	Sample data format code: 3=fixed point (2 bytes)
1613-1799	Not used

Trace Data Block (8192 Bytes;4096 Short Integers)
(recorded every transmission)

240 Byte Trace Identification Header

6400 Bytes of Data (3200 samples)

1552 Bytes of Zeros (776 zeros)

Figure 2 SEG-Y format used for recording compressed FM data on 8 mm tape.

16 bit integer #	Description
0-1	Trace(record) number (integer-32 bit)
14	Trace identification code: 1=seismic data
36-37	NMEA Longitude (seconds of arc)
38-39	NMEA Latitude (seconds of arc)
40-41	NMEA Longitude (0.0001 minutes of arc)
42-43	NMEA Latitude (0.0001 minutes of arc)
44	Coordinate units: 2=seconds of arc
45-53	Not used
54	Delay between transmission and start of sampling (ms)
55-56	Not used
57	Number of samples(3976=3200+776 zeroes)
58	A/D sample interval (usec)
59	Not used
60	Gain of programmable amp:1, 2, 4, 8, 16, 32, 64, 128
61	Not used
62	Correlated: 2 = yes
63	Sweep start freq (Hz)
64	Sweep end freq (Hz)
65	Sweep length (ms)
66	Sweep type: 1= linear
67-68	Not used
69	Taper type: 3 = other
70	Alias filter freq: Sample freq/2 (Hz)
71-77	Not used
78	Computer year
79	Computer day of year
80	Computer hour
81	Computer minutes
82	Computer seconds
83	Time basis: 3=other
84-89	Not used
90	Number of zeros at end of unprocessed trace = 4096 (minus) number of samples acquired in a trace
91	Trigger (0=internal, 1=external)
92	Mark (0=no mark, 1=mark)
93	NMEA0183 hour
94	NMEA0183 minutes
95	NMEA0183 seconds
96	NMEA0183 course
97	NMEA0183 speed (tenths of knots)
98	NMEA0183 day
99	NMEA0183 year
100-101	Trace scale factor (floating point - 4 bytes)
102	Maximum value of unprocessed return
103	System constant in ?text.txt (tenths of a dB)
104	Vehicle ID (16bit integer, e.g., 21601,21604)
105-107	Software version(6 characters)
108-119	Annotation (24 characters)
120-3319	Correlated Return (3200 Short Integers)
3319-4095	Zeros

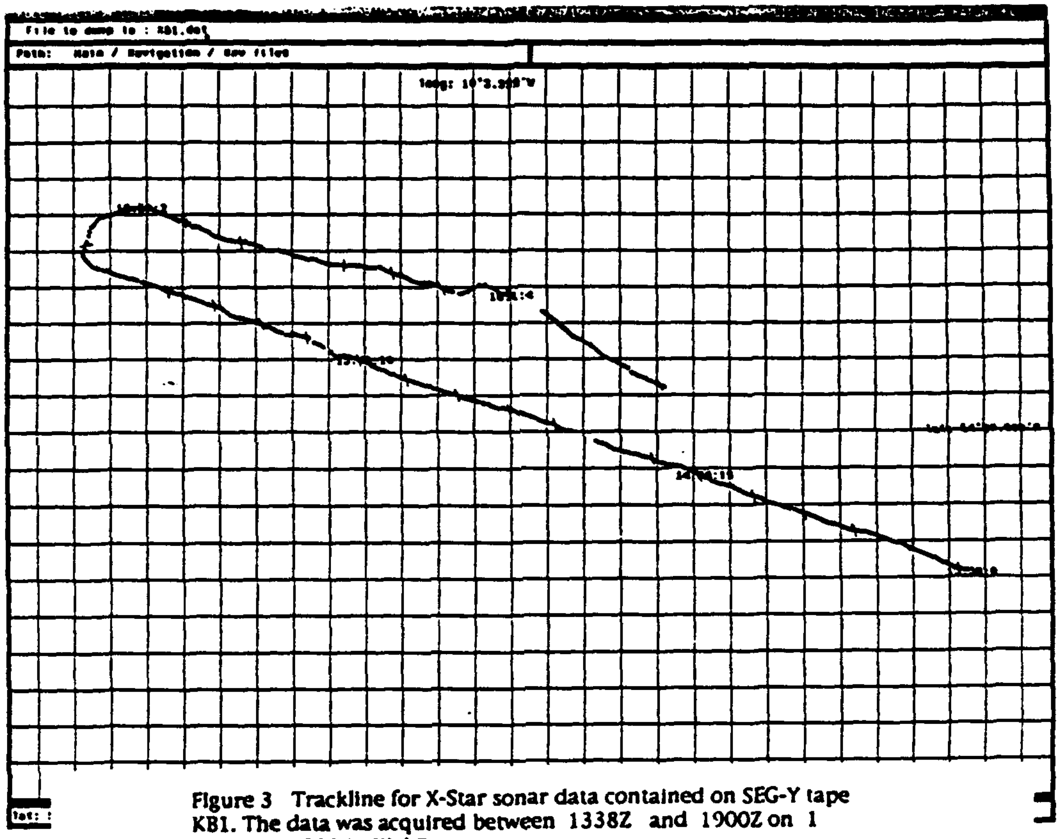

Figure 3 Trackline for X-Star sonar data contained on SEG-Y tape KB1. The data was acquired between 1338Z and 1900Z on 1 February 1993 in Kiel Bay.

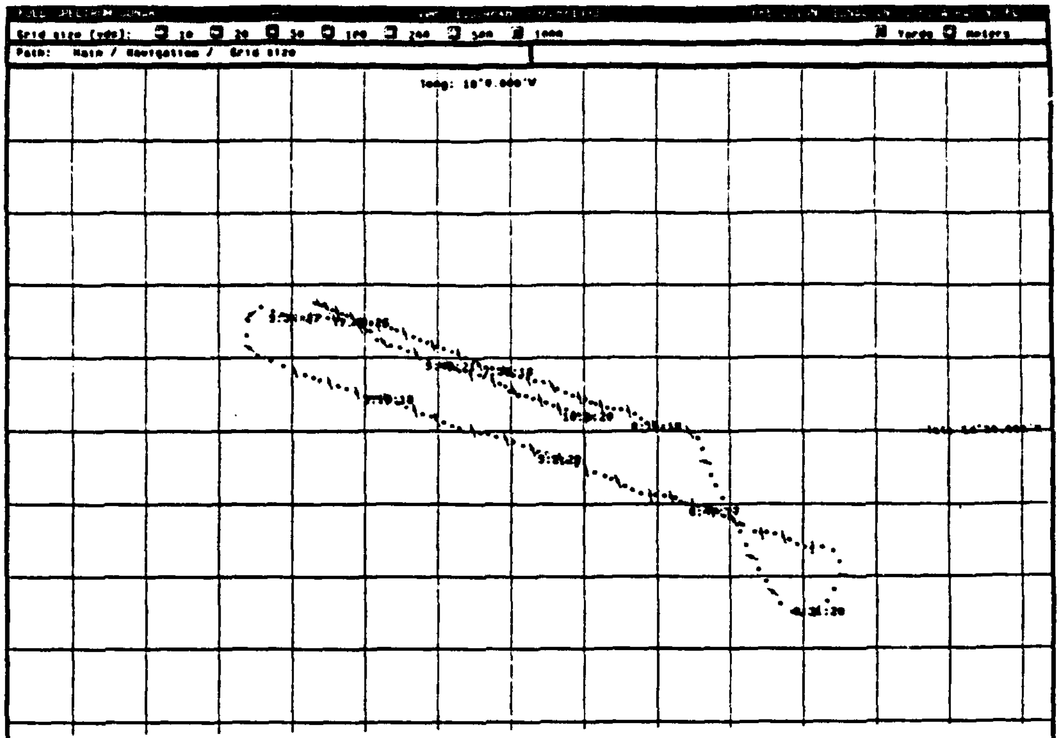

Figure 4 Trackline for X-Star sonar data contained on SEG-Y tape KB2. The data was acquired between 0719Z and 1005Z on 2 February1993 in Eckernforder Bay.

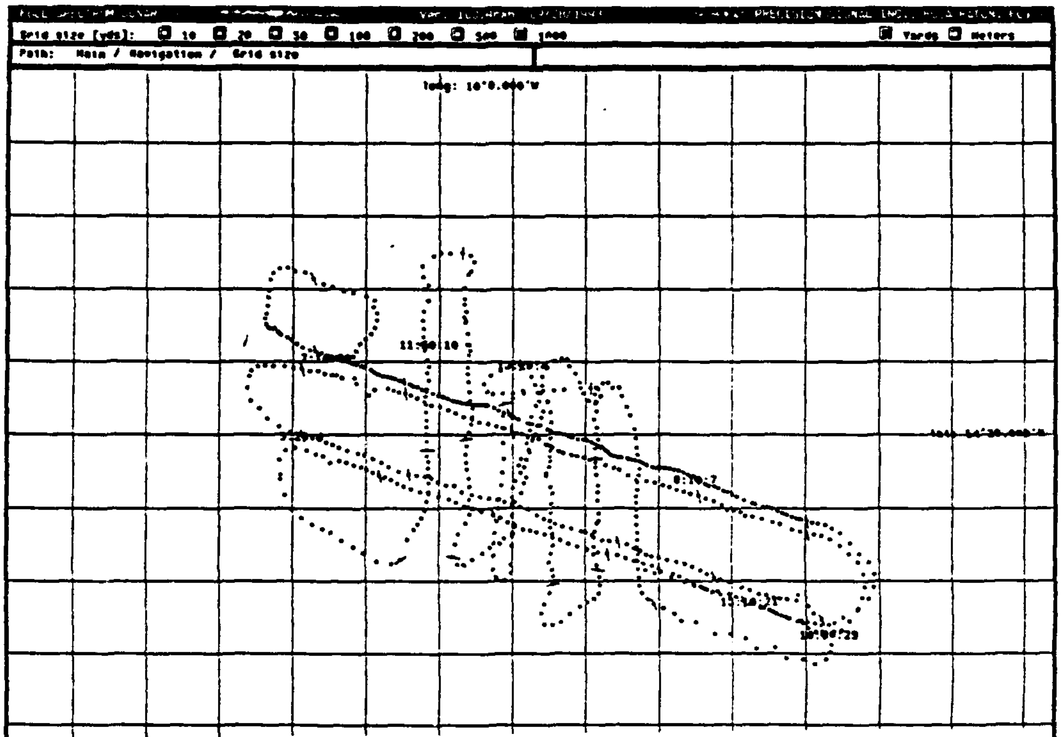

Figure 5 Trackline for X-Star sonar data contained on SEG-Y tape KB3. The data was acquired between 0710Z and 1510Z on 3 February 1993 in Eckernforder Bay.

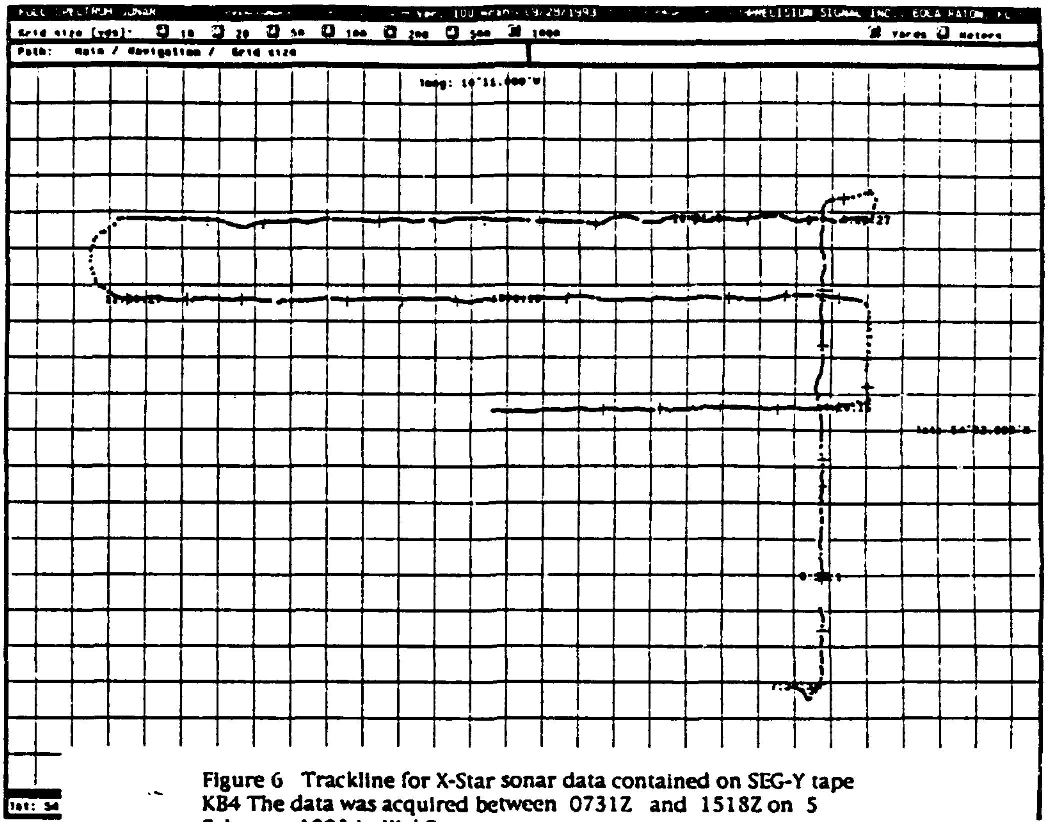

Figure 6 Trackline for X-Star sonar data contained on SEG-Y tape KB4 The data was acquired between 0731Z and 1518Z on 5 February 1993 in Kiel Bay.

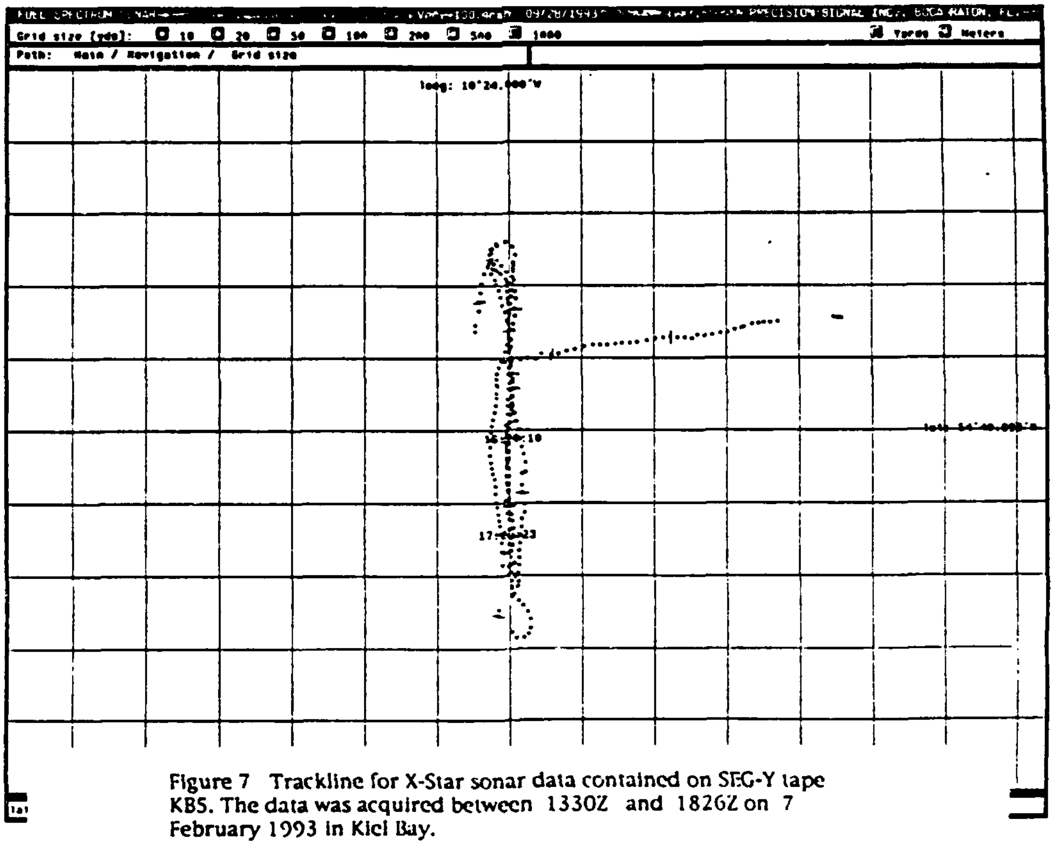

Figure 7 Trackline for X-Star sonar data contained on SEG-Y tape KB5. The data was acquired between 1330Z and 1826Z on 7 February 1993 in Kiel Bay.

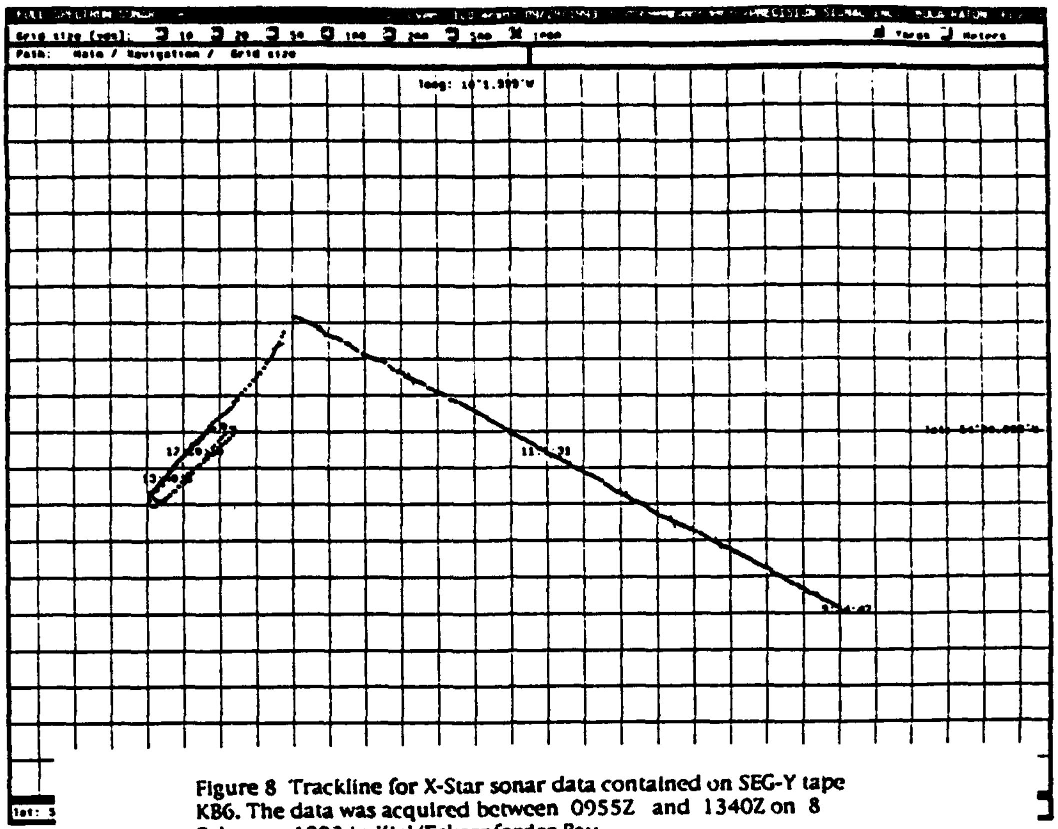

Figure 8 Trackline for X-Star sonar data contained on SEG-Y tape KB6. The data was acquired between 0955Z and 1340Z on 8 February 1993 in Kiel/Eckernforder Bay.

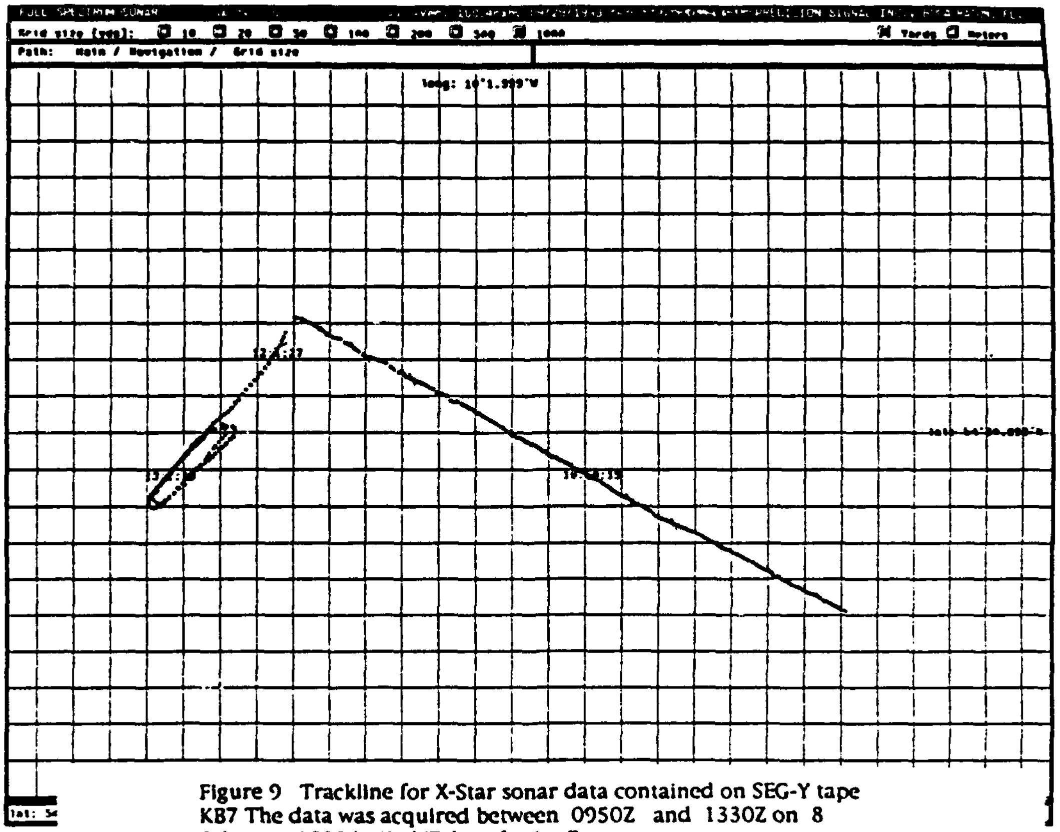

Figure 9 Trackline for X-Star sonar data contained on SEG-Y tape KB7 The data was acquired between 0950Z and 1330Z on 8 February 1993 in Kiel/Eckernforder Bay.

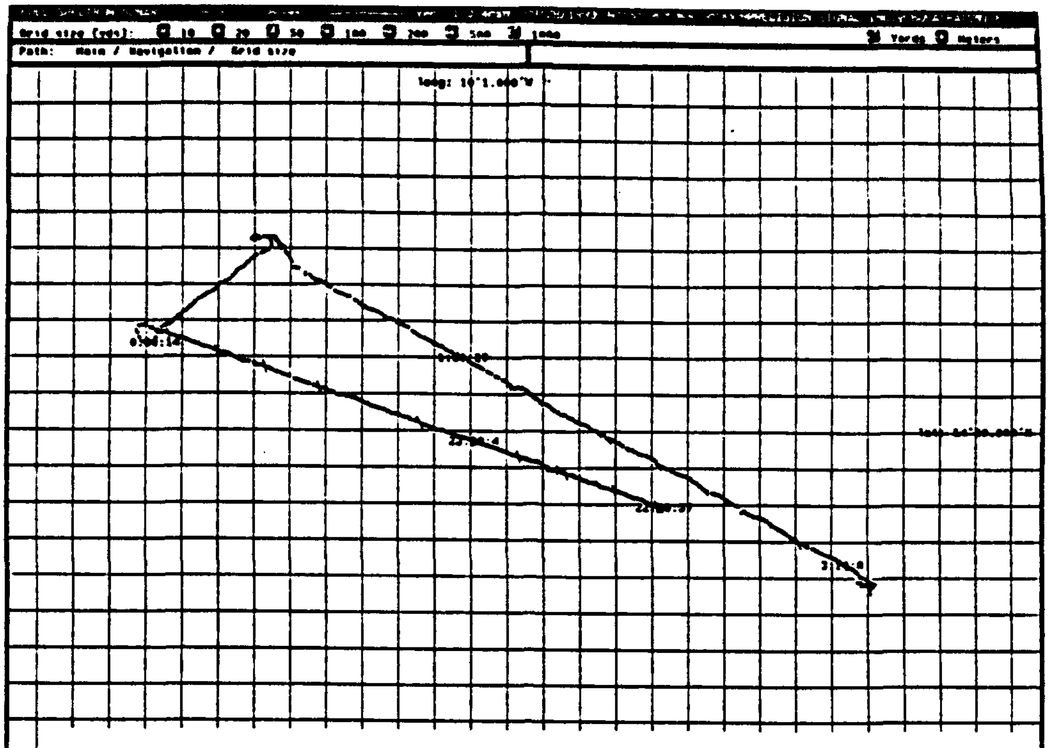

Figure 10 Trackline for X-Star sonar data contained on SEG-Y tape KB8. The data was acquired between 0040Z and 0517Z on 28 April 1993 in Eckernforder Bay.

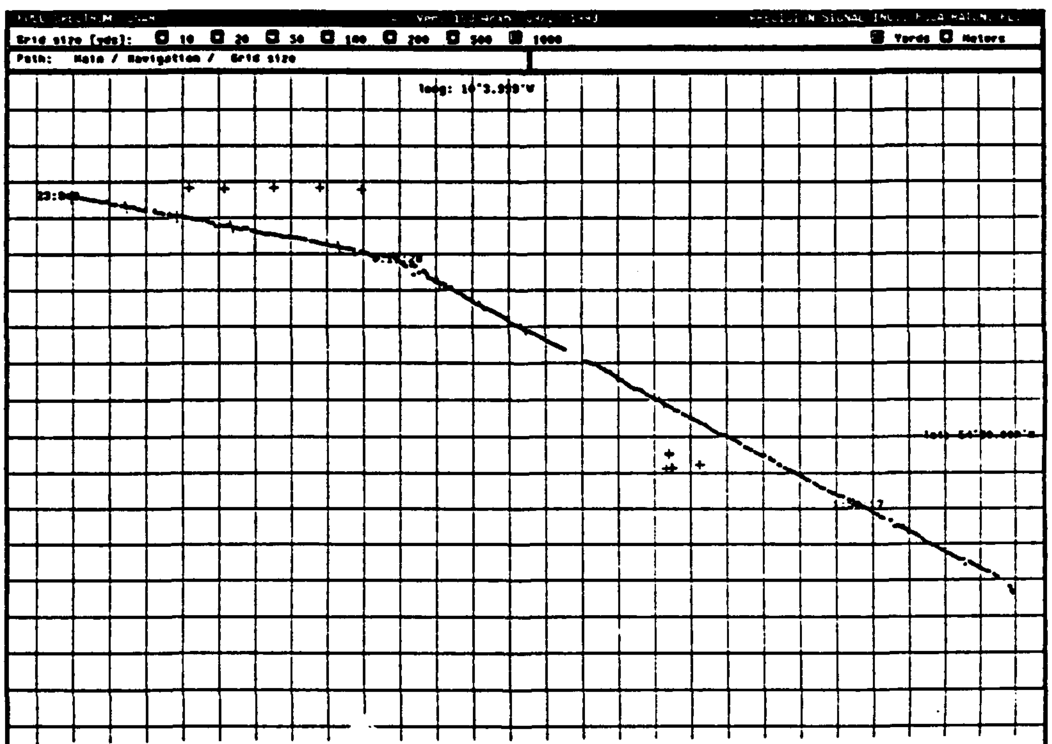

Figure 11 Trackline for X-Star sonar data contained on SEG-Y tape KB9. The data was acquired between 0100Z and 0420Z on 29 April 1993 in Eckernforder Bay.

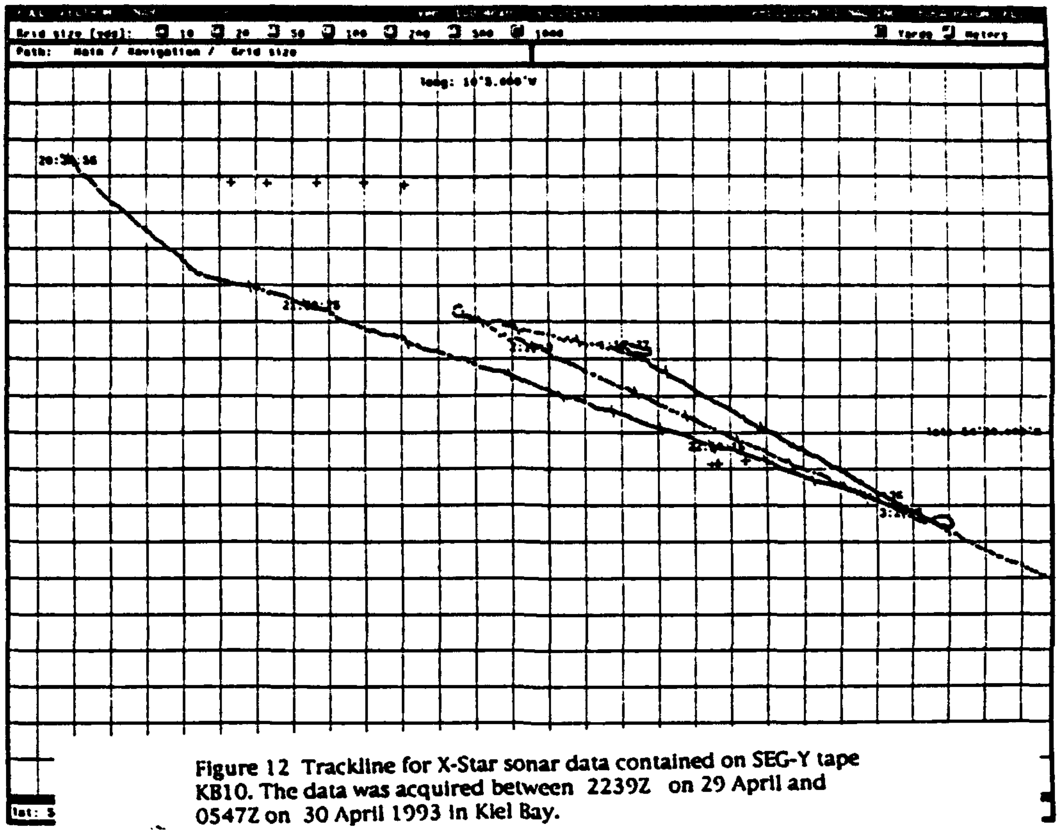

Figure 12 Trackline for X-Star sonar data contained on SEG-Y tape KB10. The data was acquired between 2239Z on 29 April and 0547Z on 30 April 1993 in Kiel Bay.

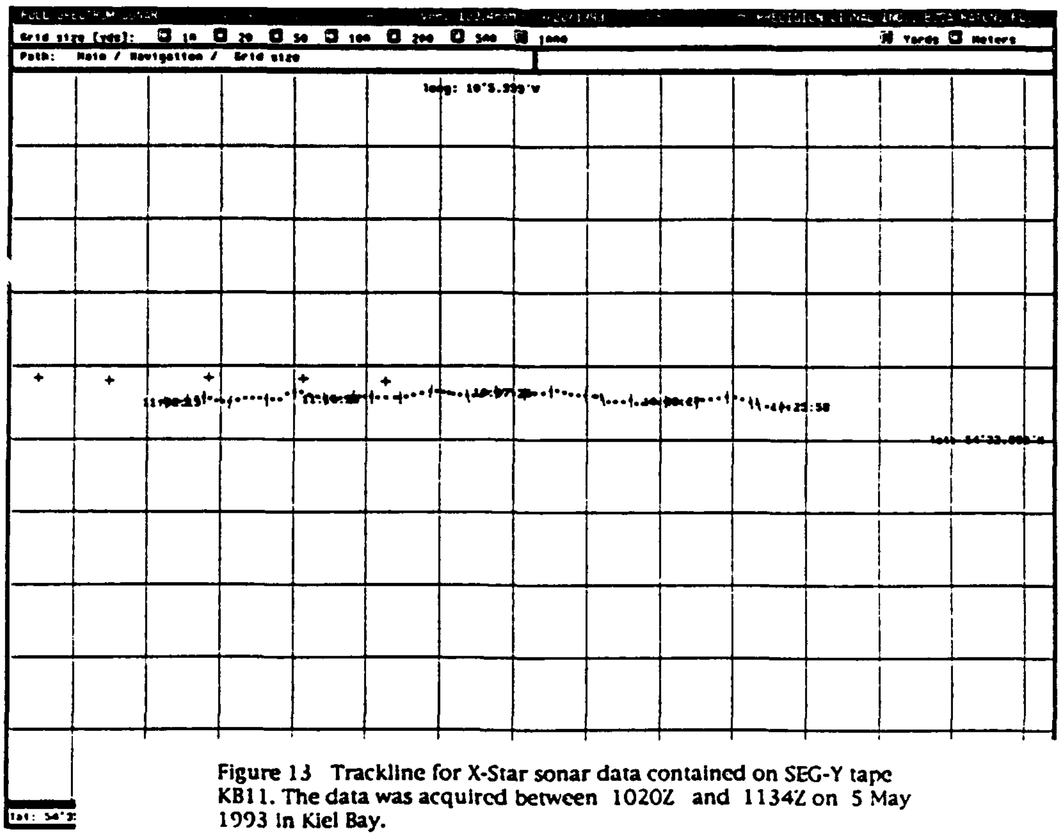

Figure 13 Trackline for X-Star sonar data contained on SEG-Y tape KB11. The data was acquired between 1020Z and 1134Z on 5 May 1993 in Kiel Bay.

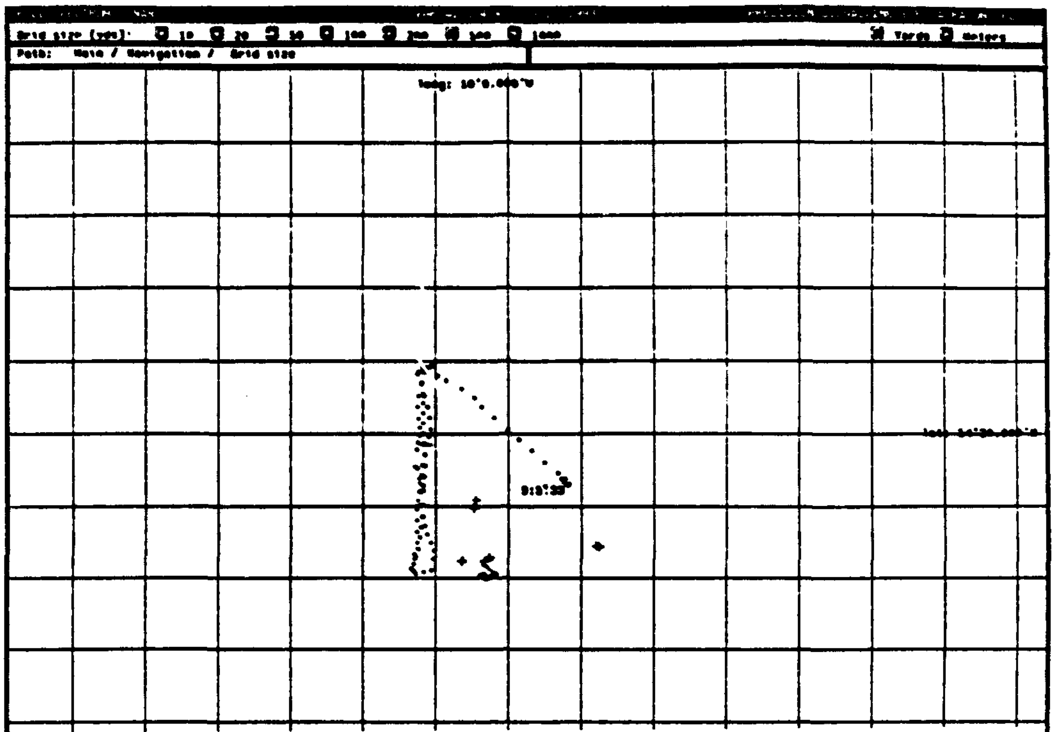

Figure 14 Trackline for X-Star sonar data contained on SEG-Y tape KB12. The data was acquired between 1120Z and 1220Z on 6 May 1993 in Kiel Bay.

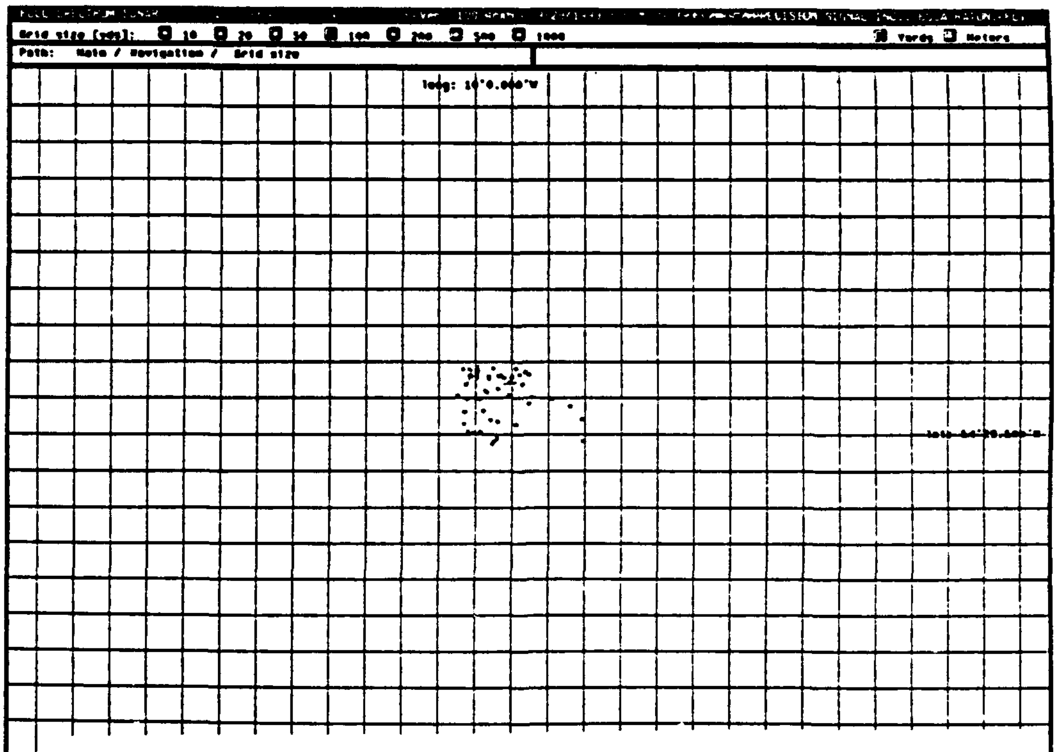

Figure 15 Trackline for X-Star sonar data contained on SEG-Y tape KB13. The data was acquired between 1316Z and 1348Z on 6 May 1993 in Eckernforder Bay.

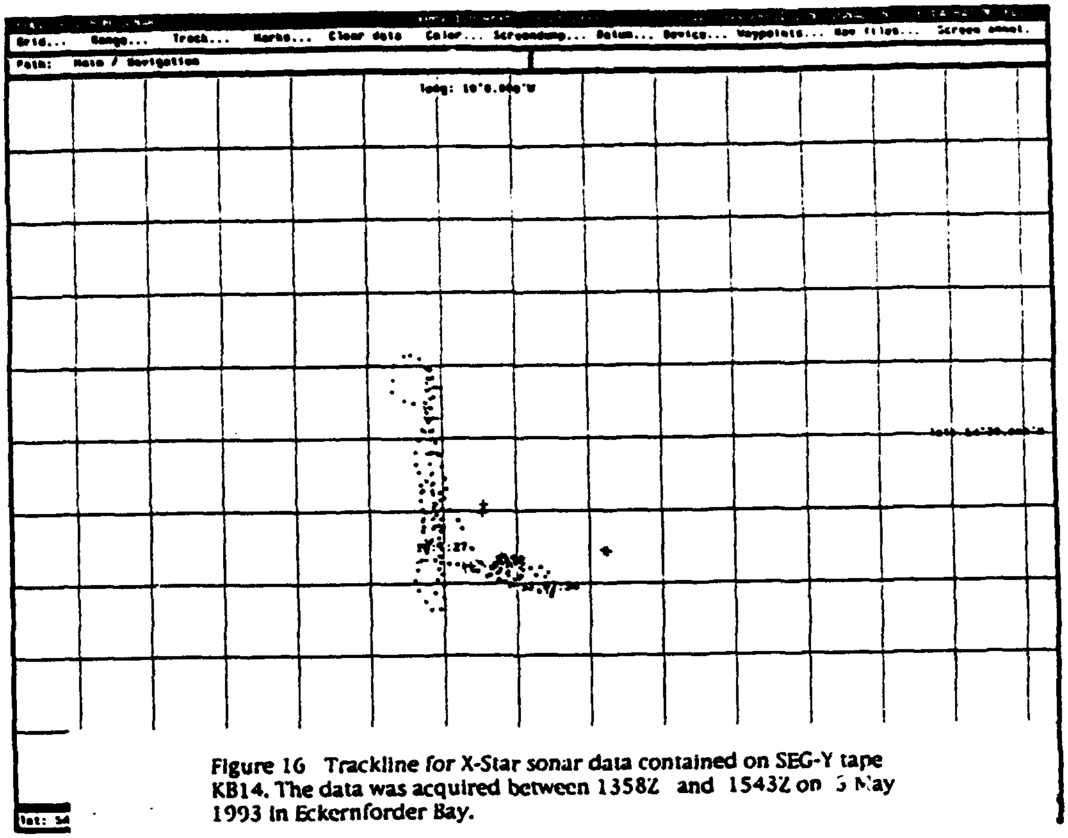

Figure 16 Trackline for X-Star sonar data contained on SEG-Y tape KB14. The data was acquired between 1358Z and 1543Z on 5 May 1993 in Eckernforder Bay.

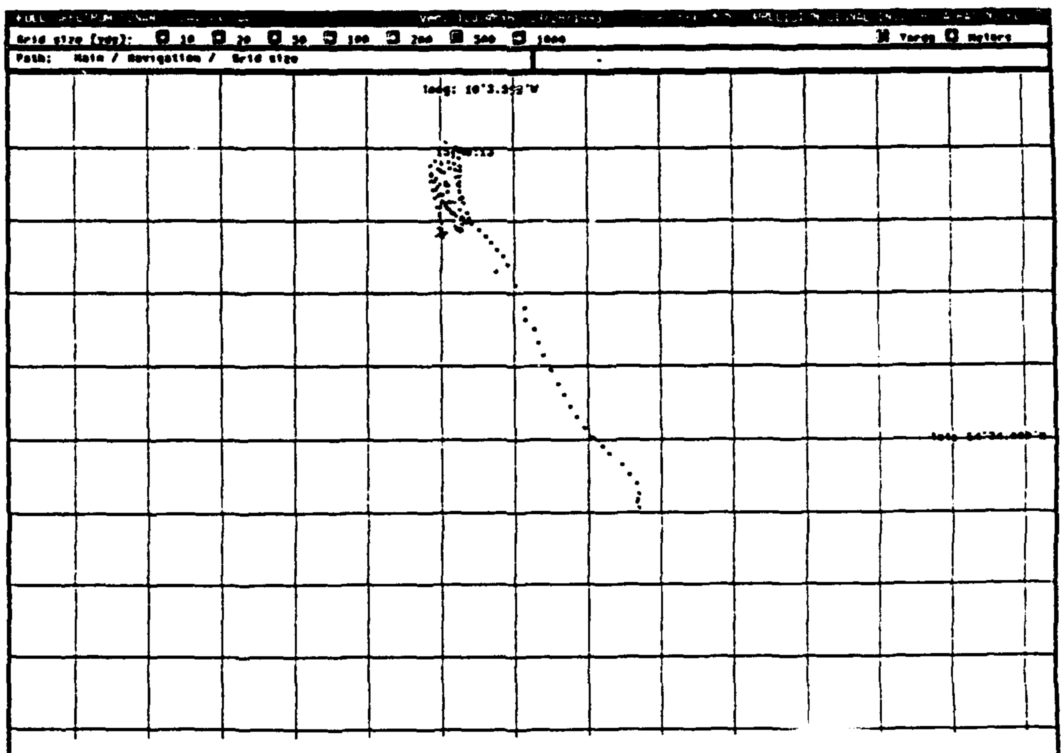

Figure 17 Trackline for X-Star sonar data contained on SE KB15. The data was acquired between 1640Z and 1731Z ay 1993 in Kiel Bay.

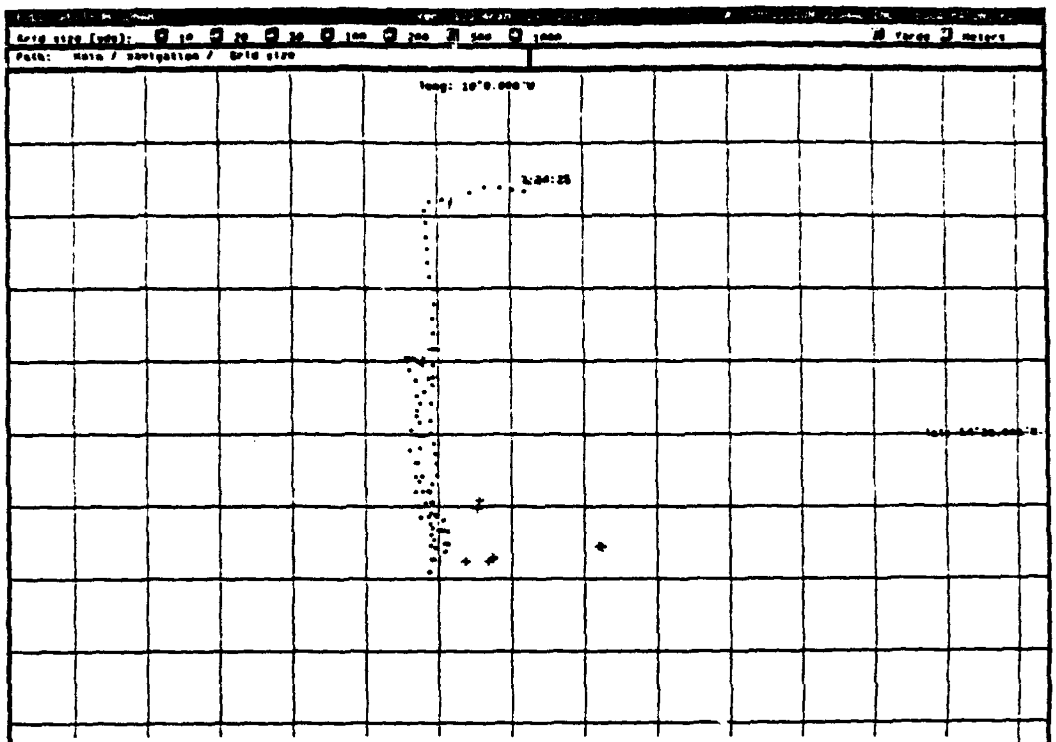

Figure 18 Trackline for X-Star sonar data contained on SEG-Y tape KB16. The data was acquired between 0930Z and 1028Z on 6 May 1993 in Eckernforder Bay.

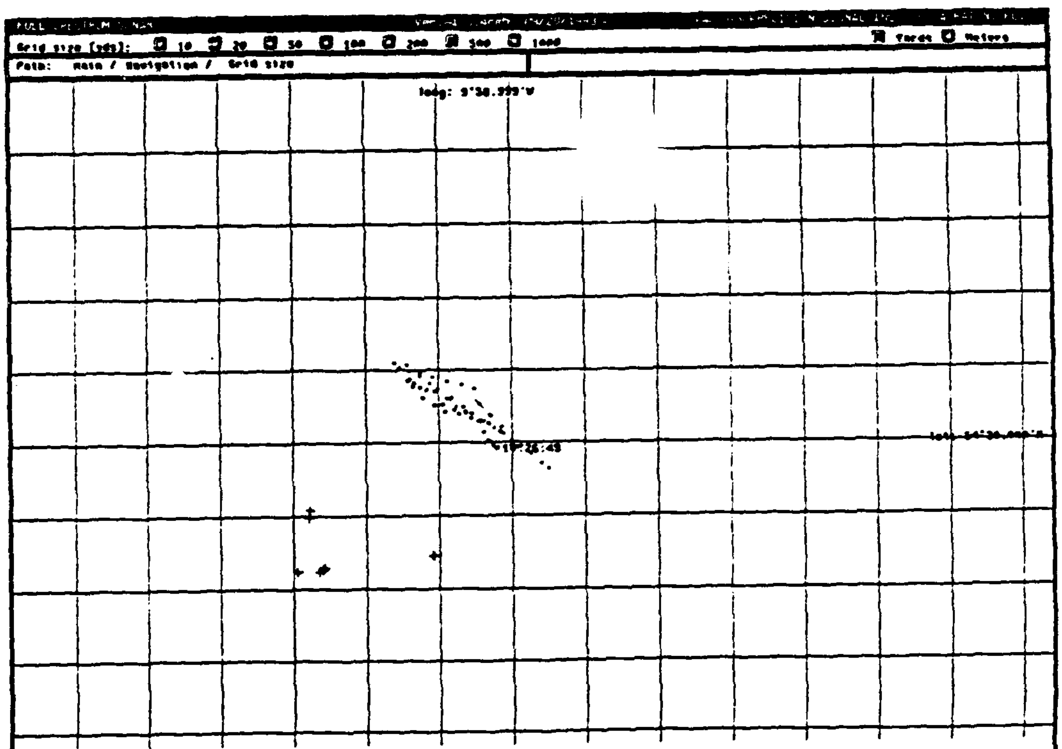

Figure 19 Trackline for X-Star sonar data contained on SEG-Y tape KB17. The data was acquired between 1226Z and 1306Z on 7 May 1993 in Eckernforder Bay.

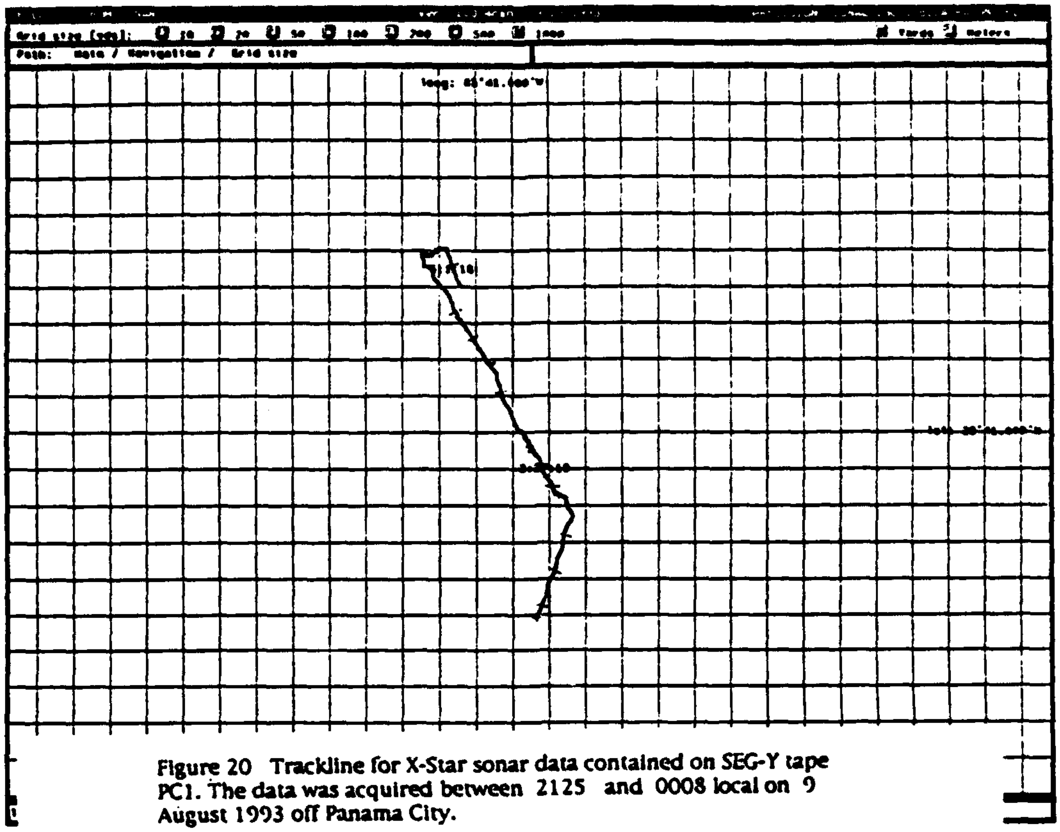

Figure 20 Trackline for X-Star sonar data contained on SEG-Y tape PC1. The data was acquired between 2125 and 0008 local on 9 August 1993 off Panama City.

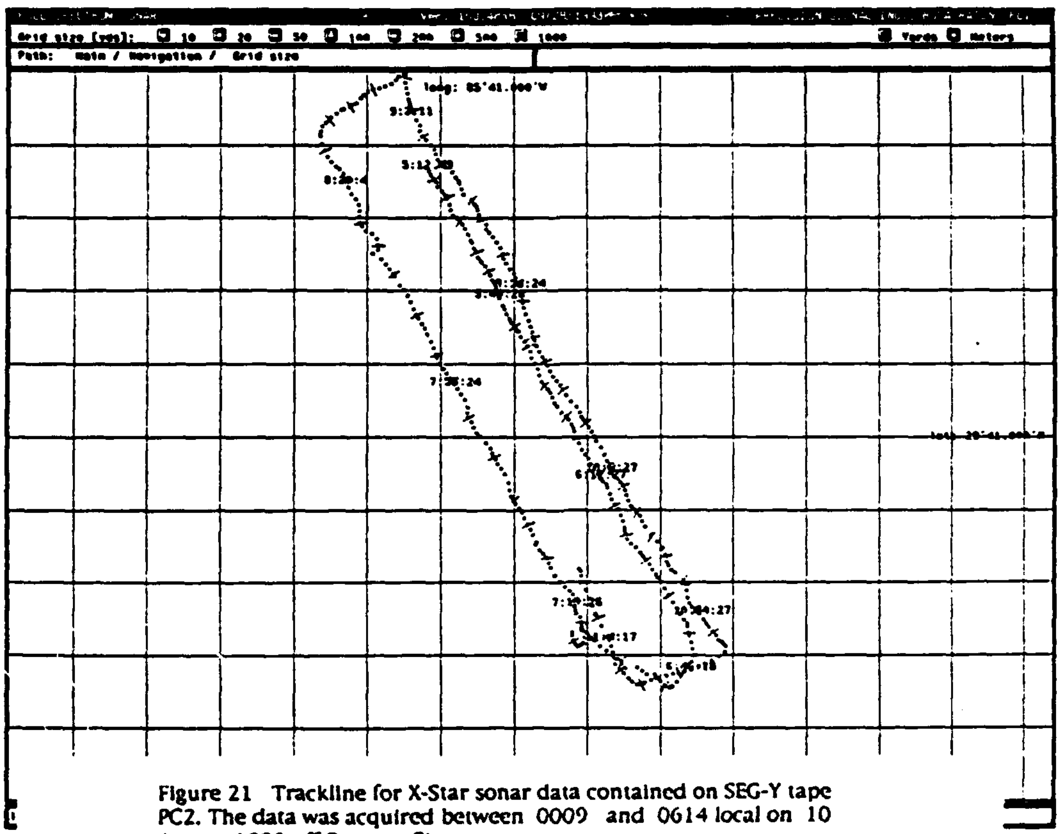

Figure 21 Trackline for X-Star sonar data contained on SEG-Y tape PC2. The data was acquired between 0009 and 0614 local on 10 August 1993 off Panama City.

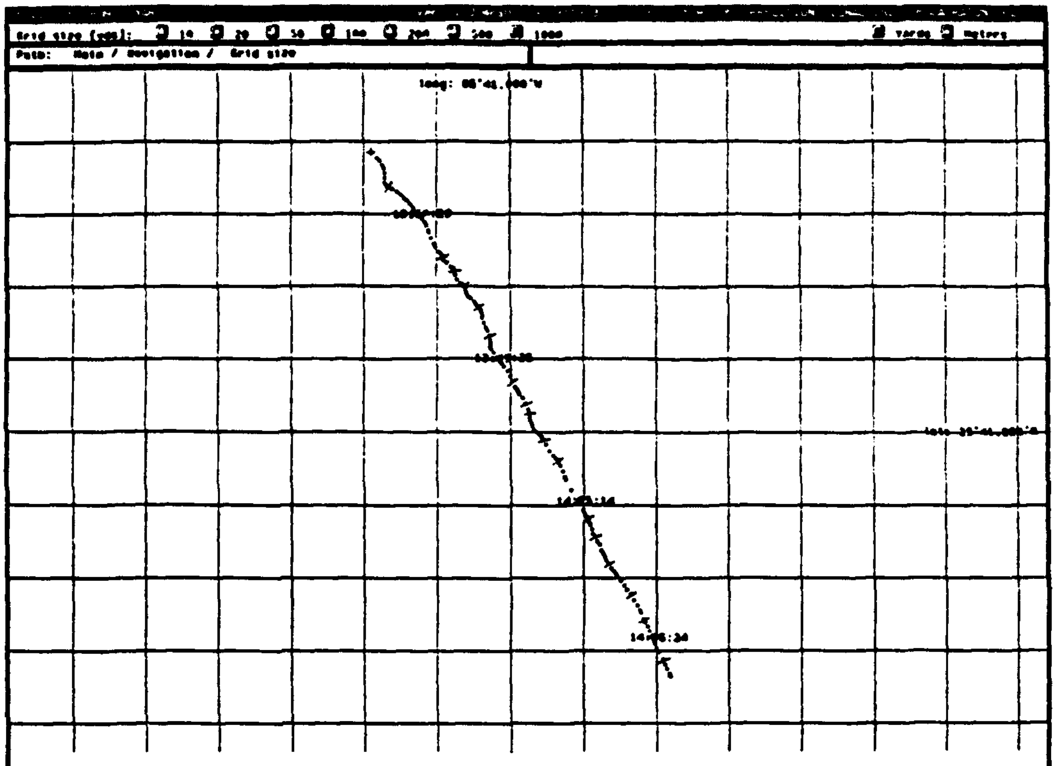

Figure 22 Trackline for X-Star sonar data contained on SEG-Y tape PC3. The data was acquired between 0800 and 1014 local on 10 August 1993 off Panama City.

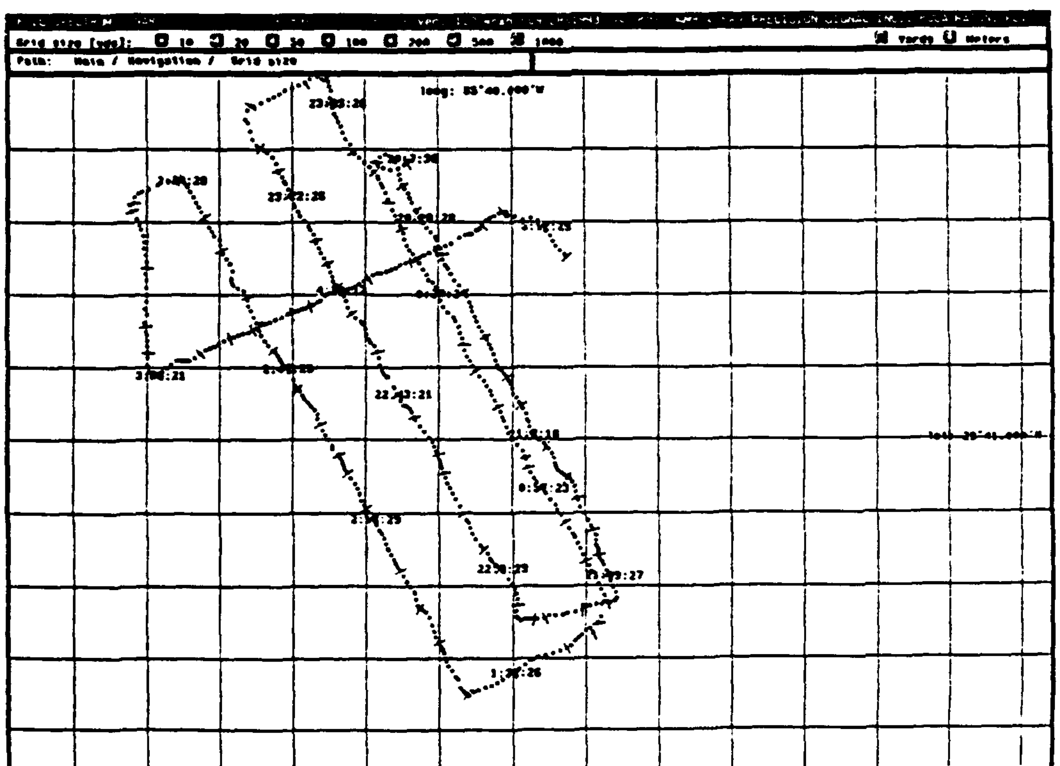

Figure 23 Trackline for X-Star sonar data contained on SEG-Y tape PC5. The data was acquired between 1505 and 0019 local on 11/12 August 1993 off Panama City.

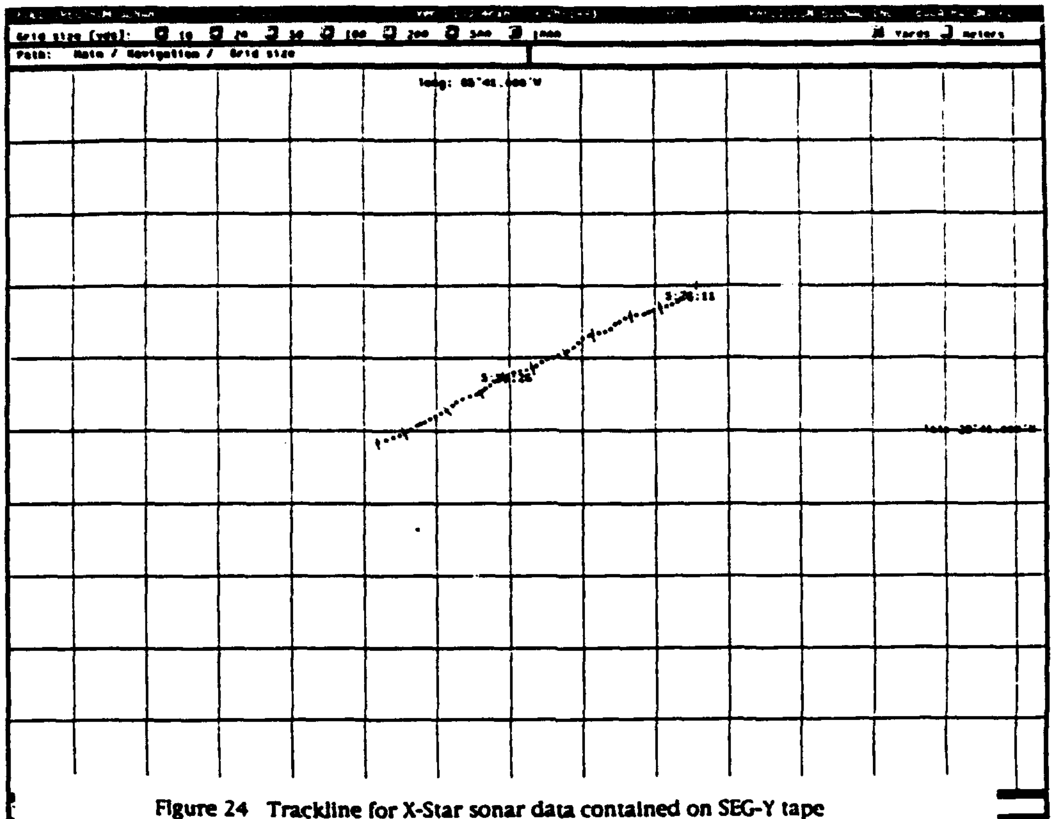

Figure 24 Trackline for X-Star sonar data contained on SEG-Y tape PC6. The data was acquired between 0019 and 0116 local on 12 August 1993 off Panama City.

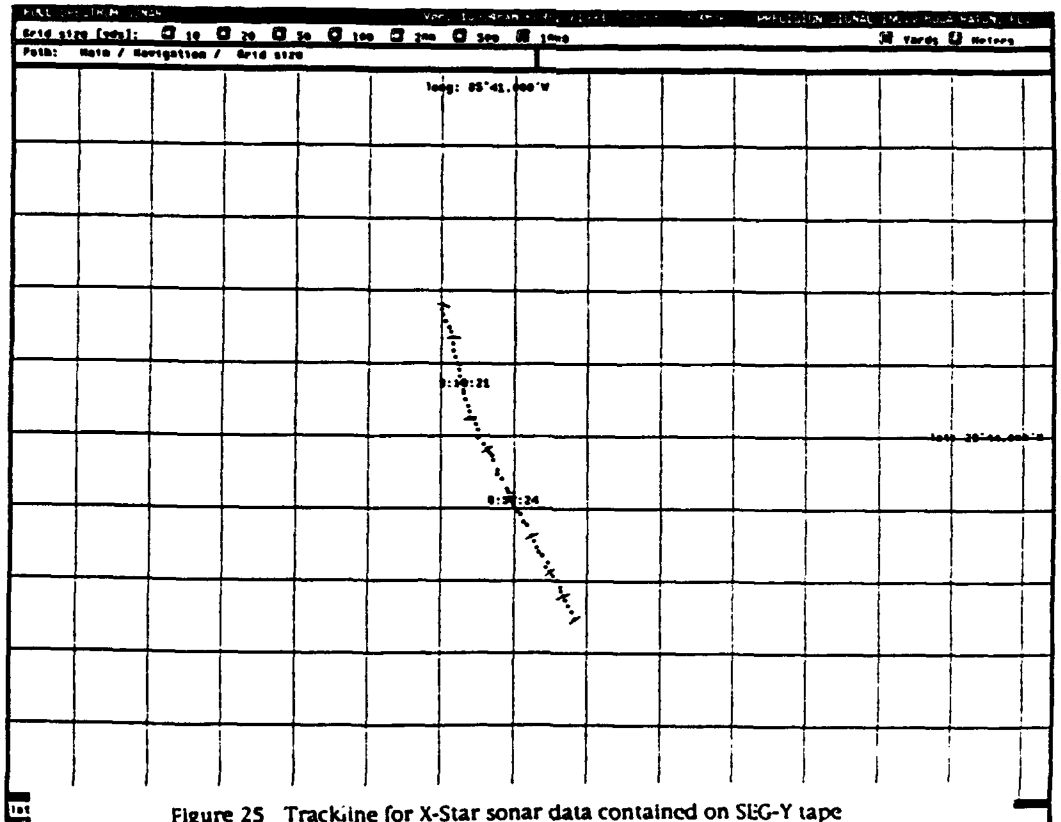

Figure 25 Trackline for X-Star sonar data contained on SEG-Y tape PC7. The data was acquired between 0338 and 0427 local on 13 August 1993 off Panama City.

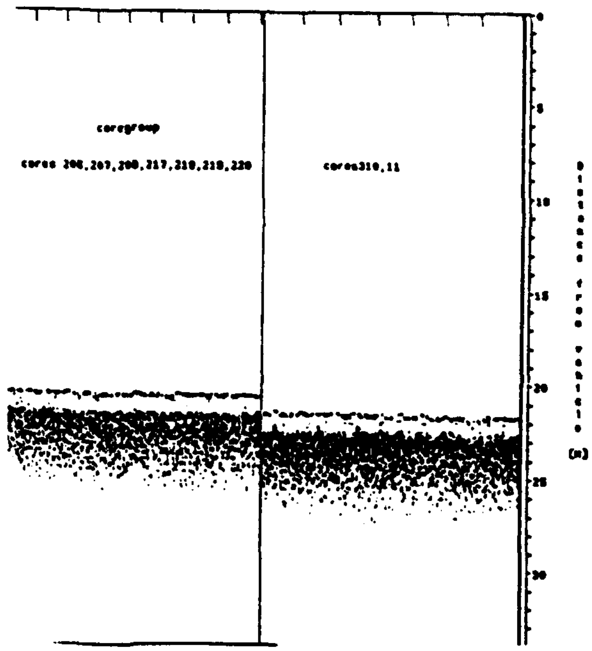

Figure 26 Images generated by X-Star at the sites for 1) cores 206, 207, 208, 217, 218, 219, 220 and 2) cores 310, 11 in Eckernforder Bay

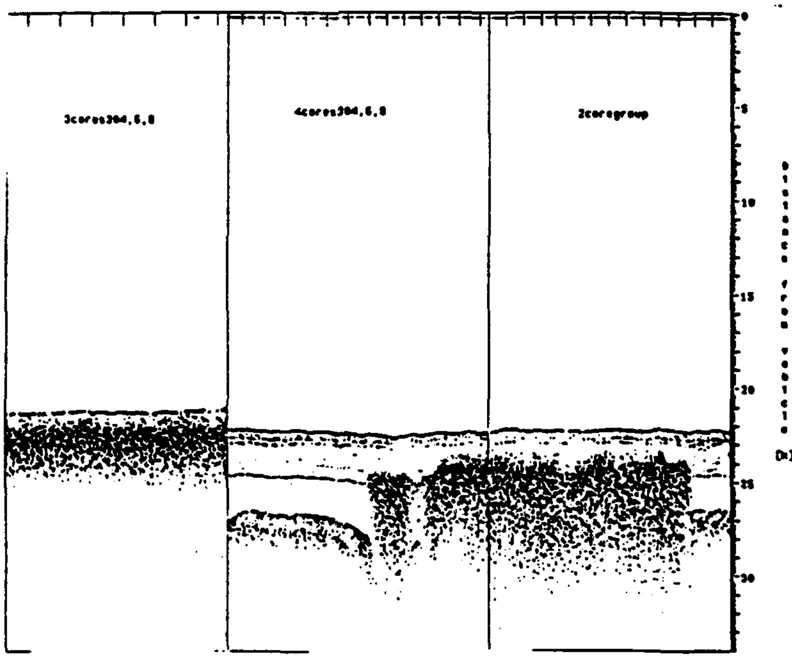

Figure 27 Images generated by X-Star near the site for cores 304, 306, 308 in Eckernforder Bay

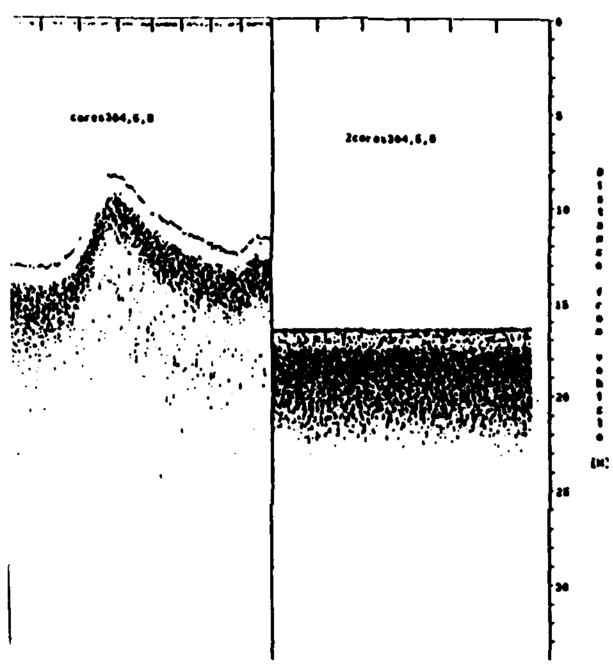

Figure 28 Images generated by X-Star near the site for cores 304, 306, 308 in Eckernforder Bay

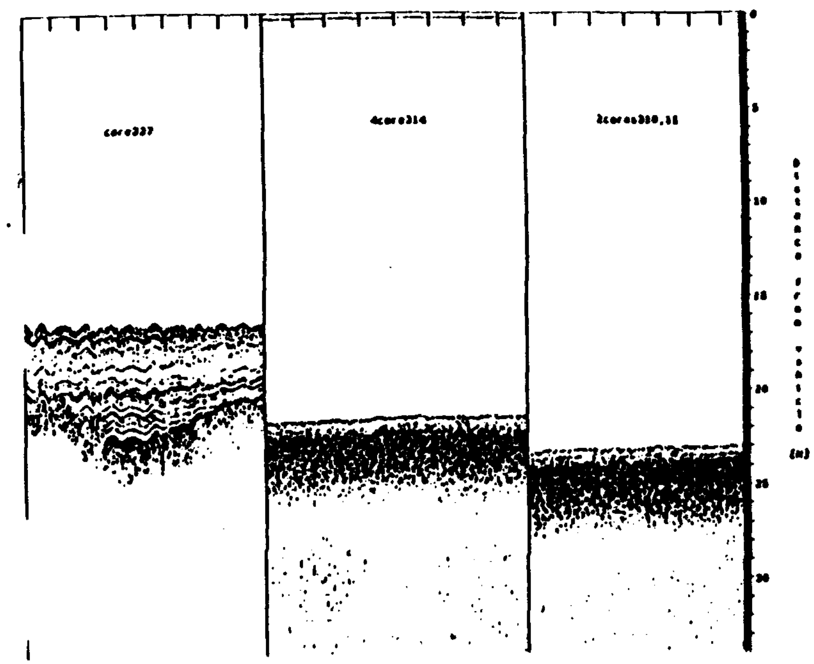

Figure 29 Images generated by X-Star at the sites for 1) core 337, cores 314, and cores 310, 311 in Eckernforder Bay

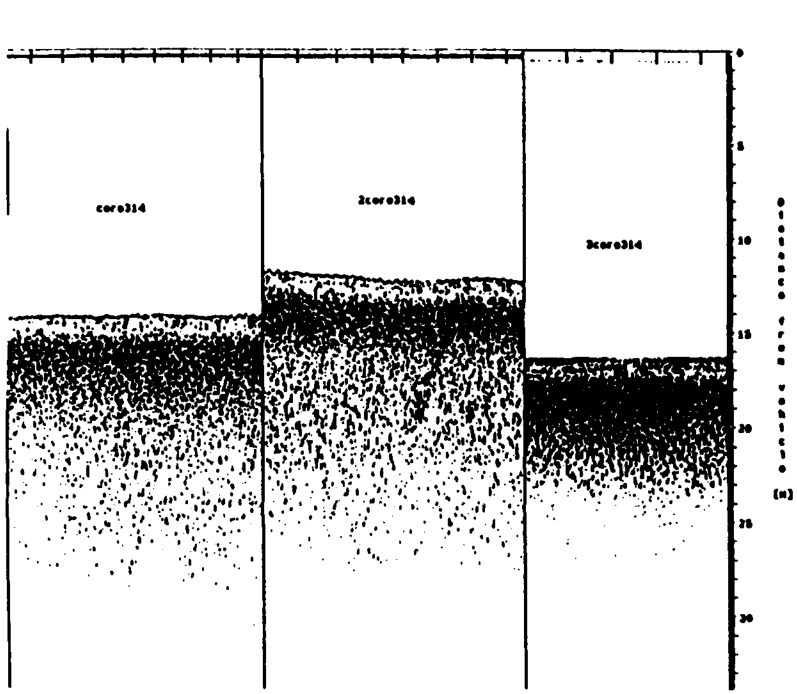

Figure 30 Images generated by X-Star at the sites for core 314 in Eckernforder Bay

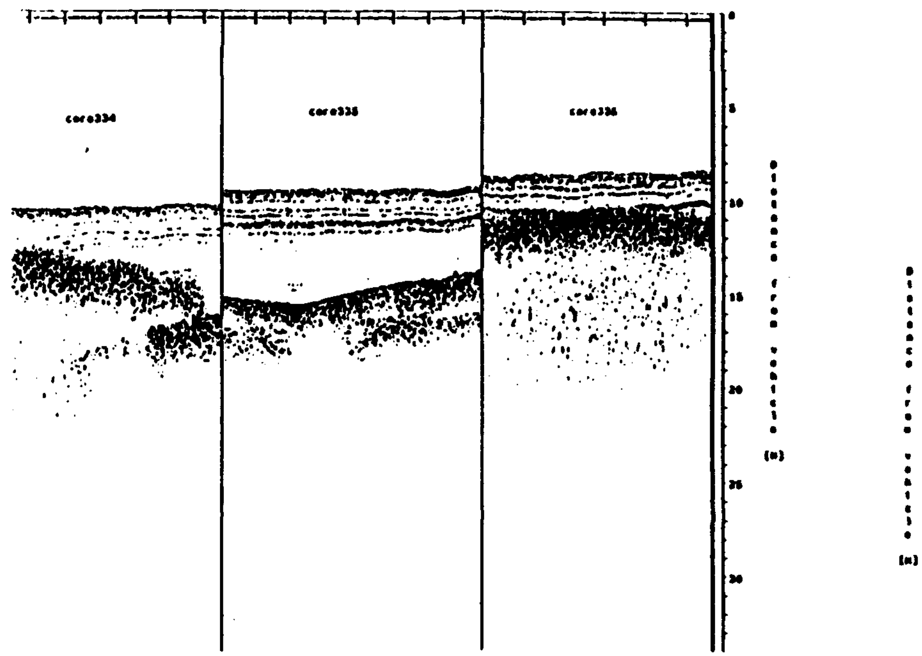

Figure 31 Images generated by X-Star at the sites for 1) core 334, 2) core 335 and 3) core 336 in Kiel Bay

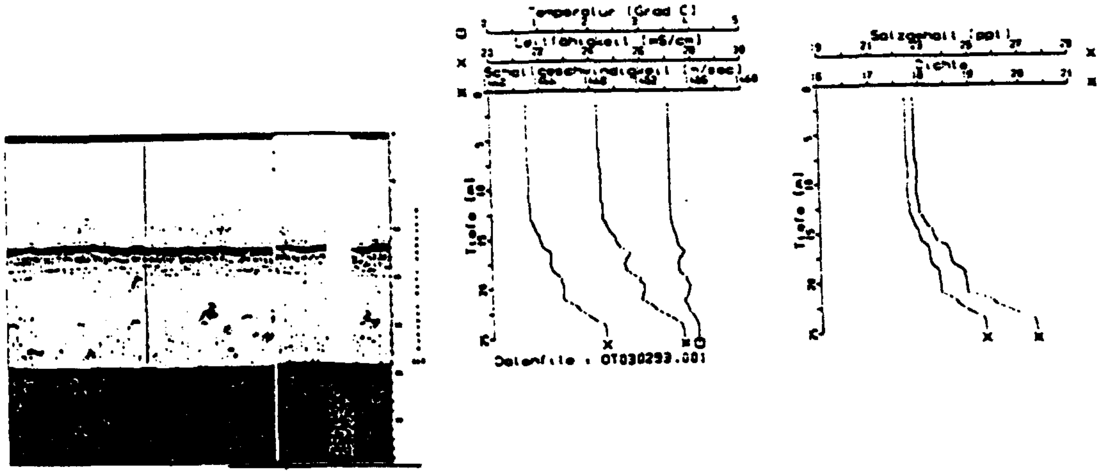

Figure 33 Comparison of water column profile generated by X-Star and an XBT measurement taken at 54 30.11 N and 10 00.05 W on 3 February 1993 in Eckernförder Bay

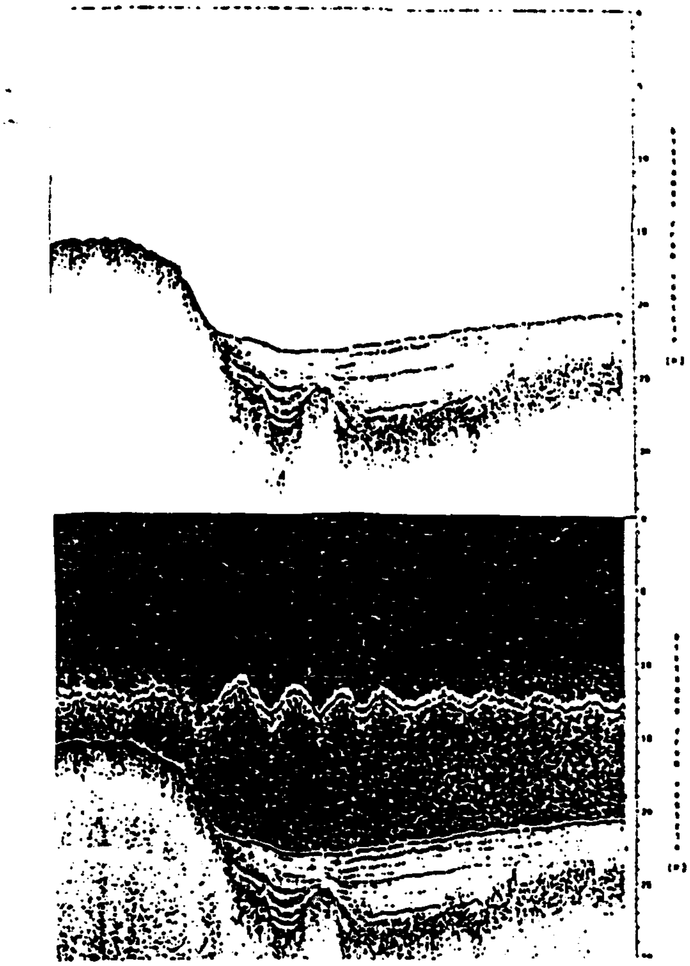

Figure 34 Comparison of a default subbottom display (top) and subbottom display modified so that the lowest reflection level is mapped to black. The black background allows weak reflectors such as an internal wave and other scatterers in the water column to be studied. The internal wave occurs at the interface between brackish water and salt water in Kiel Bay.

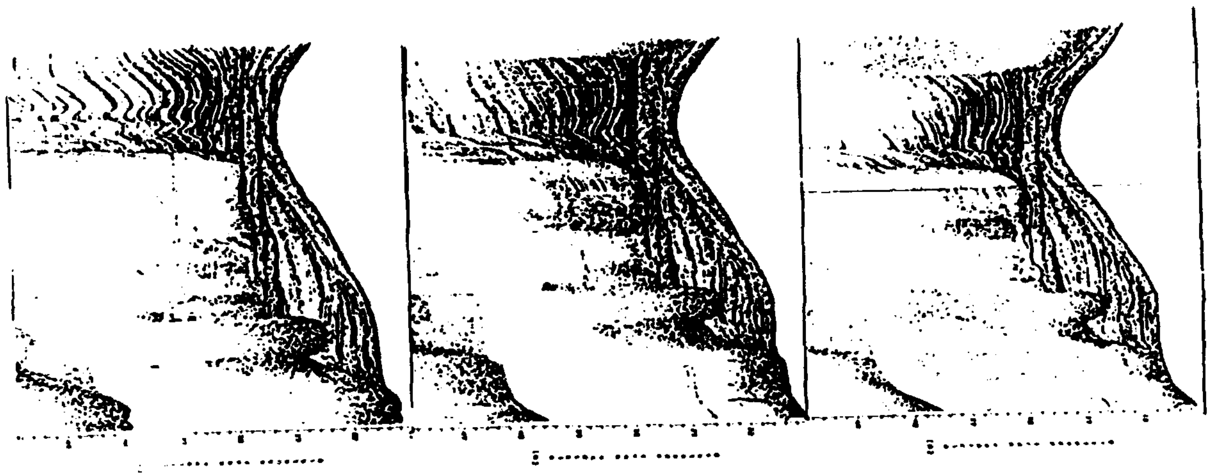

Figure 35 Comparison between images generated with 20 msec 2.5 to 15.5 kHz (top), 20 msec 2.5 to 12.5 kHz (middle), and 20 msec 2 to 10 kHz (bottom) FM pulses in northern Kiel Bay. The images demonstrate that 1) as bandwidth increases, vertical resolution increases, and 2) as the center frequency of the pulse decreases,

subfloor penetration improves (as the effective pulse attenuation decreases).

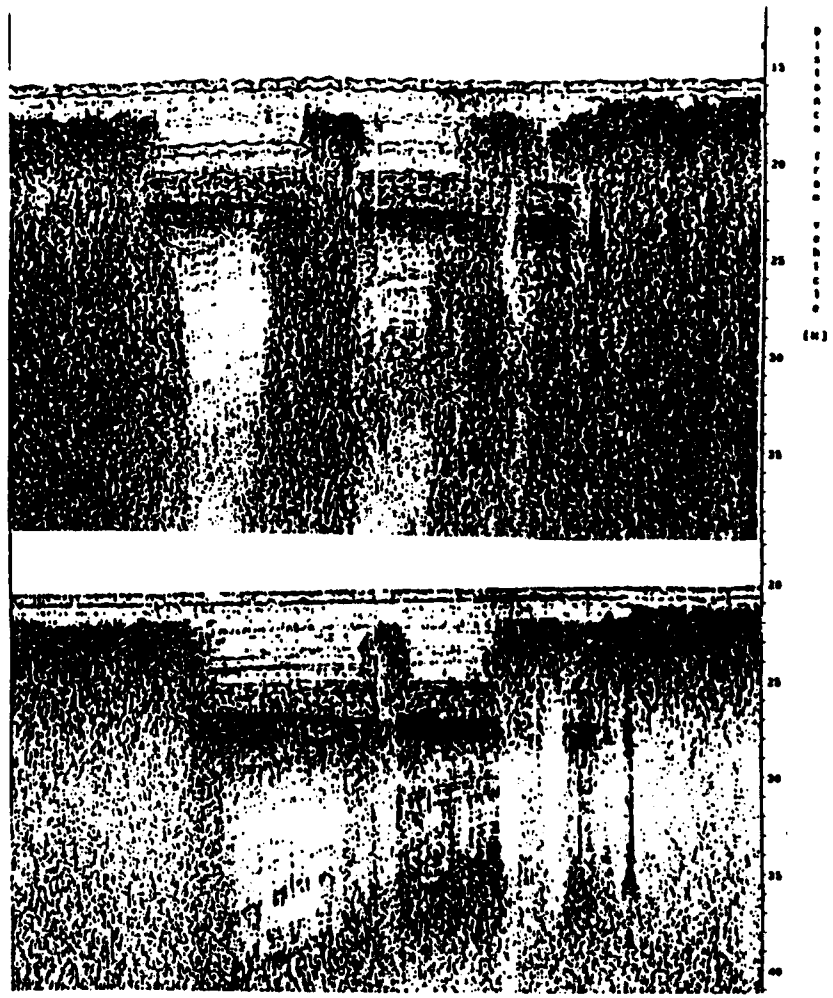

Figure 36 Comparison between images generated with 20 msec 2.5 to 15.5 kHz (upper) and 20 msec 2.5 to 12.5 kHz (lower) FM pulses along same line in Eckernforder Bay at an acoustic window in the gassy sediments.

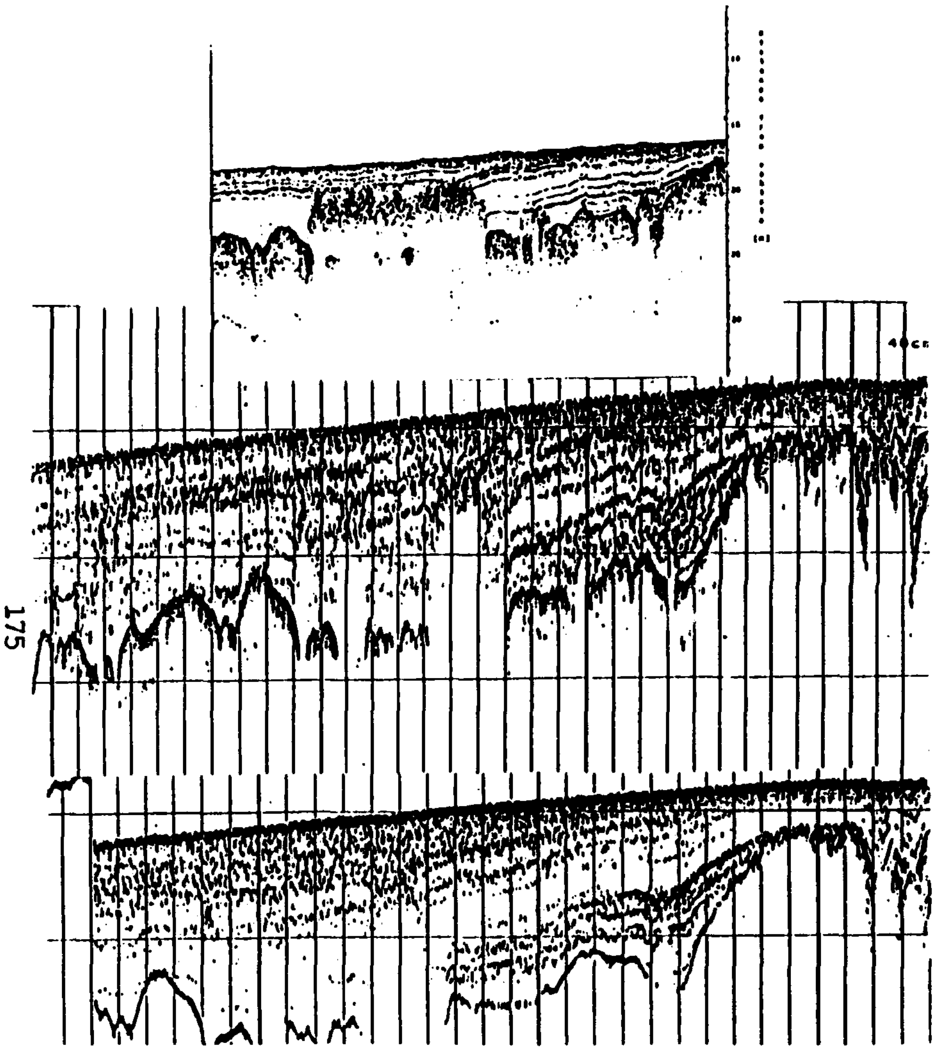

Figure 37 Comparison between images generated by an X-Star using a 20 msec 2.5 to 15.5 kHz FM pulse (upper) and the ASCS system using a 15 kHz CW pulse (center) and a 30 kHz CW pulse lower) in Kiel Bay.

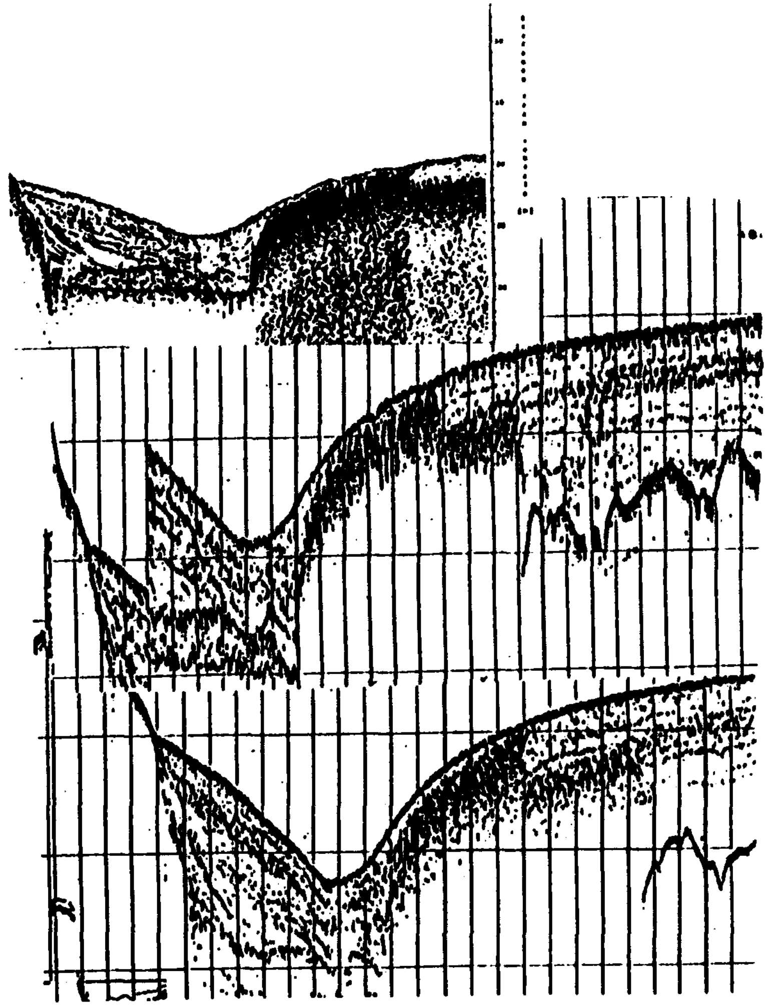

Figure 38 Comparison between images generated by an X-Star using a 20 msec 2.5 to 15.5 kHz FM pulse (upper) and the ACSC system using a 15 kHz CW pulse (center) and a 30 kHz CW pulse lower) in Kiel Bay.

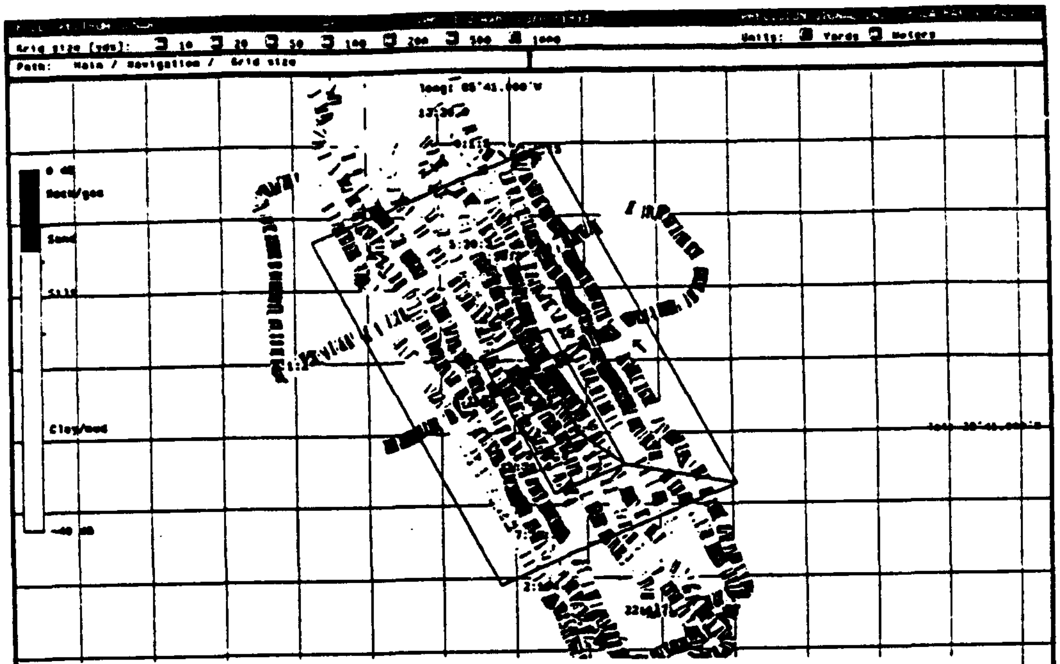

Figure 39 Pressure reflection coefficient map of the sediment-water interface off Panama City, FL generated with the X-Star Full Spectrum sonar transmitting a 20 msec 2 to 10 kHz FM pulse. The lines made on the 3rd day of the survey show that the maximum measurement error was less than 1 dB over the 3 day period. The bar along the left hand side shows how shades of grey are mapped to the pressure reflection coefficient (presented in dB). Note 0dB = 1 and -40dB = 0.01 . Sands fall within the range of -6 dB and -10 dB.

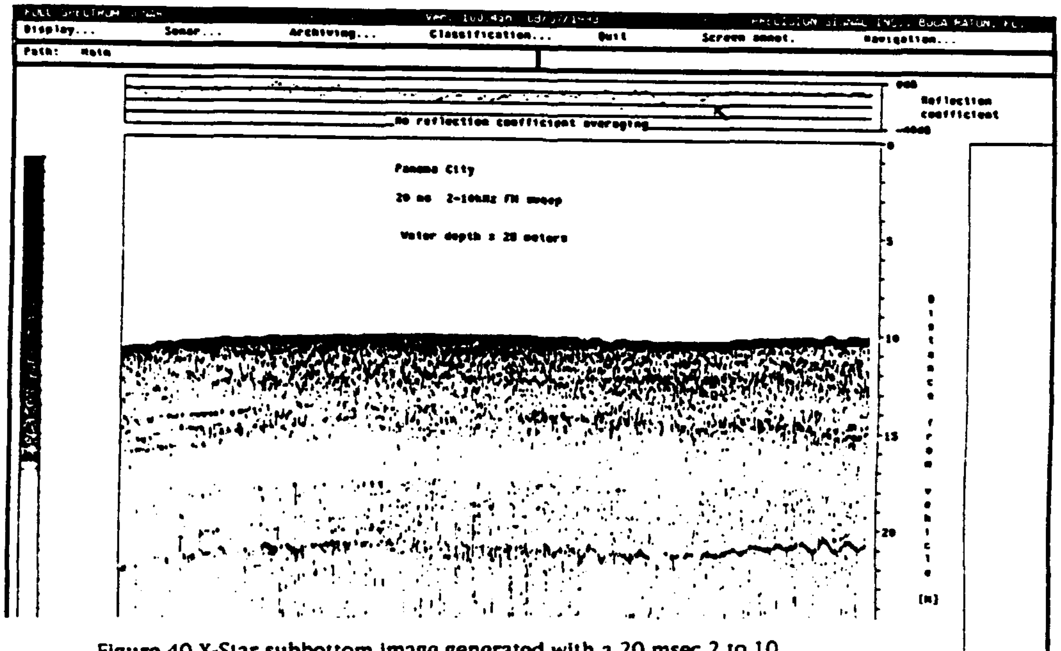

Figure 40 X-Star subbottom image generated with a 20 msec 2 to 10 kHz FM pulse off Panama City. The pressure reflection coefficient reported for each acoustic return is graphed along the top of the image. The standard deviation of the measurement drops sharply toward the right hand side of the graph indicating a reduction in the randomness of the sediment-water interface boundary. This drop in the standard deviation could be due to a reduction in bottom roughness.

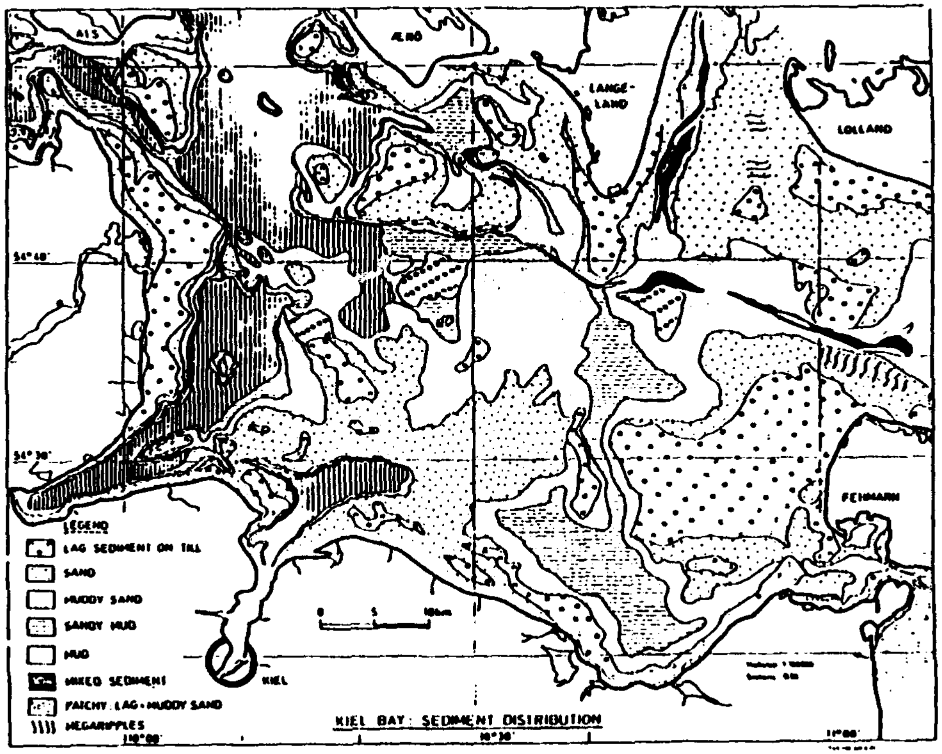

Figure 41 Surficial sediment map generated by other investigators in a previous study of Kiel Bay

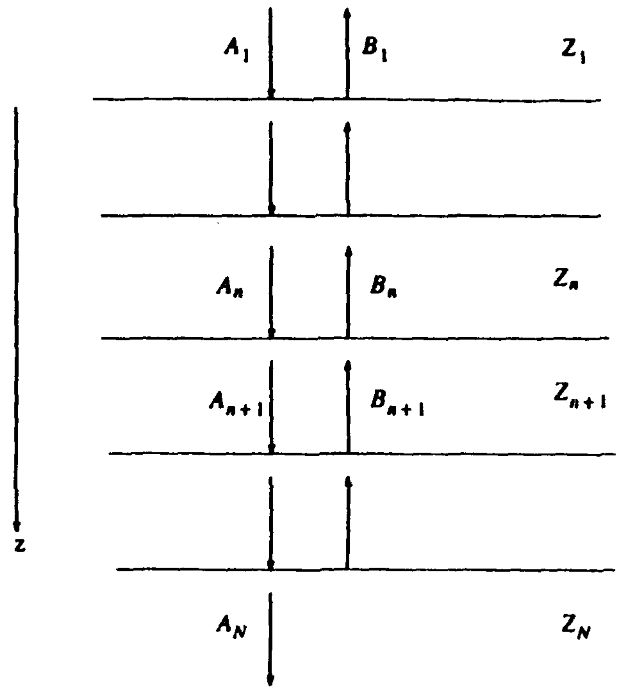

$$R_n = e^{-2ik_n z_n} \frac{(Z_{n+1} - Z_n) + (Z_{n+1} + Z_n) R_{n+1} e^{2ik_{n+1} z_n}}{(Z_{n+1} + Z_n) + (Z_{n+1} - Z_n) R_{n+1} e^{2ik_{n+1} z_n}}$$

Figure 42 Simple multilayer model of the seafloor showing the interlayer reflection coefficient, the ratio between the upward and downward traveling waves within a layer.

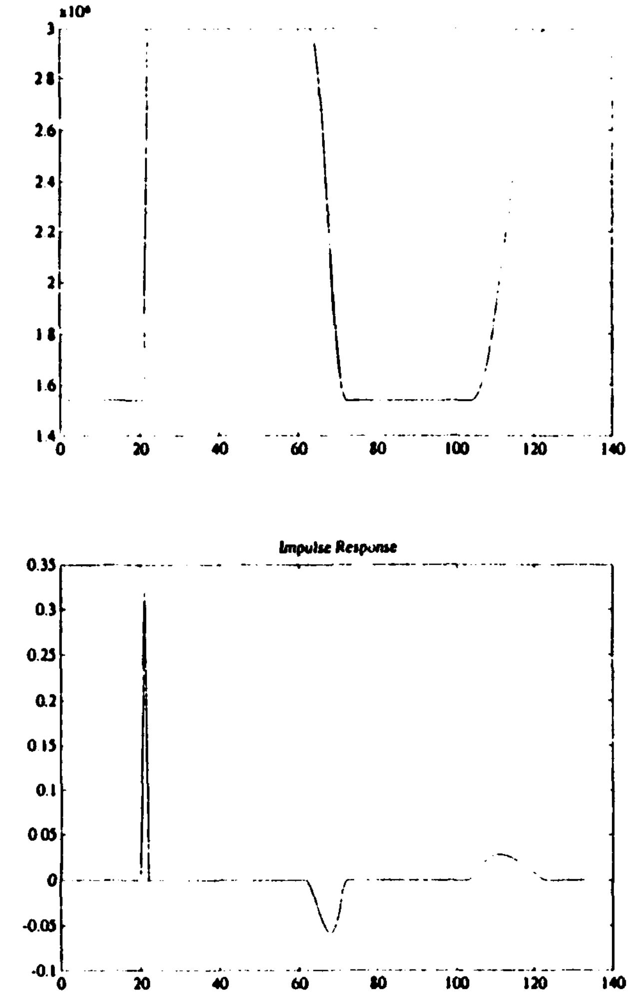

Figure 43 Comparison of the impulse response of a half space separated by a transition zone for 3 cases (not a seabed containing 3 transitions). The transition zone thicknesses for the 3 cases are 0 cm (left), 10 cm (center) and 20 cm (right). The thickness is the distance from one half space to another. The interlayer changes in impedance is a cosine function. The lower figure shows that the impulse response gets stretched as the transition zone gets wider due to the smearing of the higher frequencies.

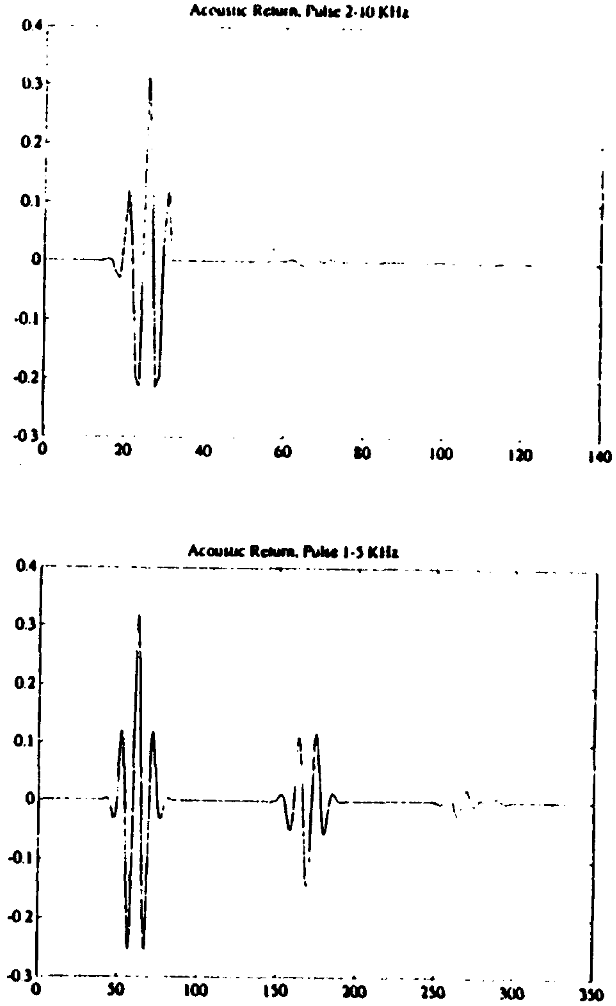

Figure 44 Synthetic acoustic returns generated by convolving a 2 to 10 kHz wavelet (top) and a 1 to 5 kHz wavelet (bottom) with the impulse response in Figure 43.

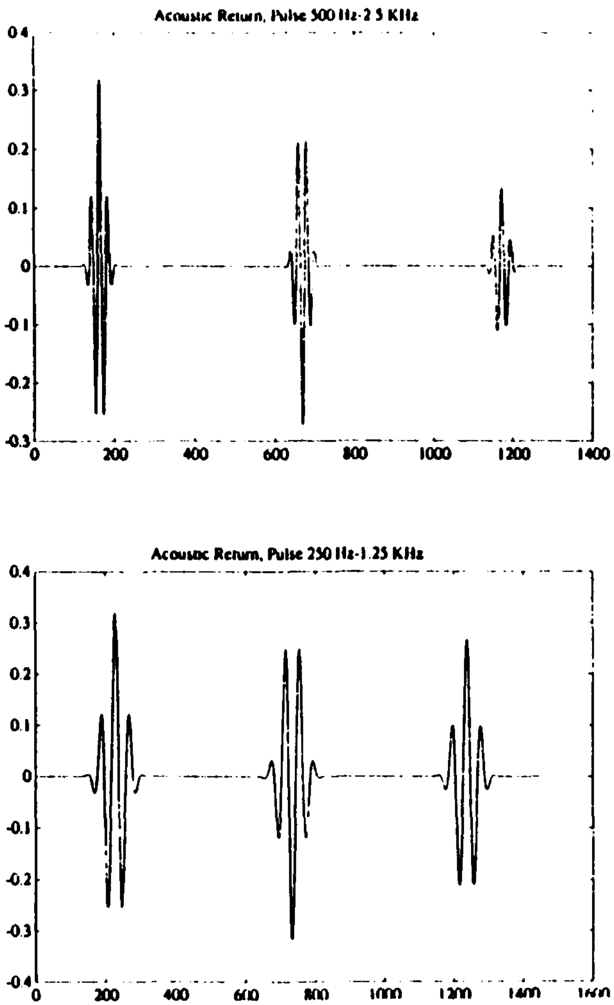

Figure 45 Synthetic acoustic returns generated by convolving a 0.5 to 2.5 kHz wavelet (top) and a 0.25 to 1.25 kHz wavelet (bottom) with the impulse response in Figure 43.

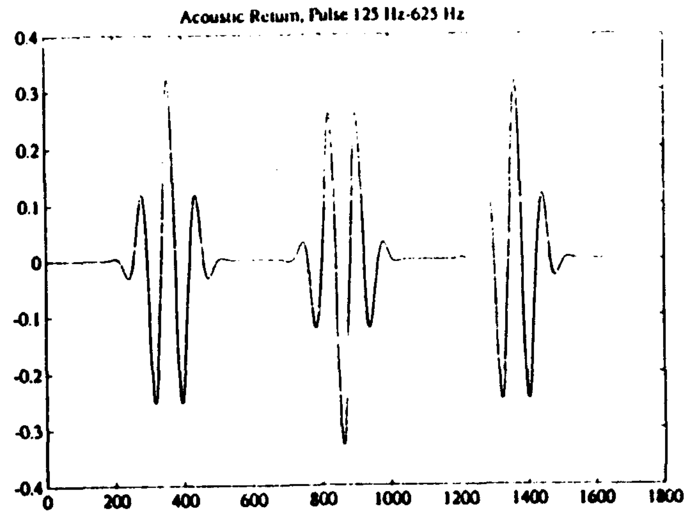

Figure 46 Synthetic acoustic returns generated by convolving a 125 to 625 Hz wavelet with the impulse response in Figure 43.

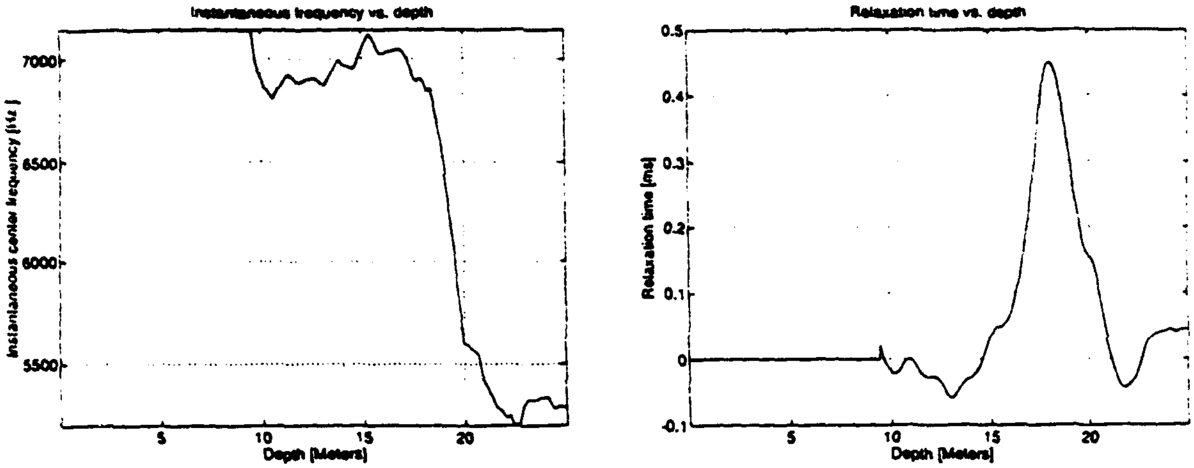

Figure 47 Plot of the center frequency of backscattered energy as a function of depth beneath the seabed (left) in Eckernforder Bay and the relaxation time of the attenuation process(right) which is related to the slope of the frequency vs depth plot.

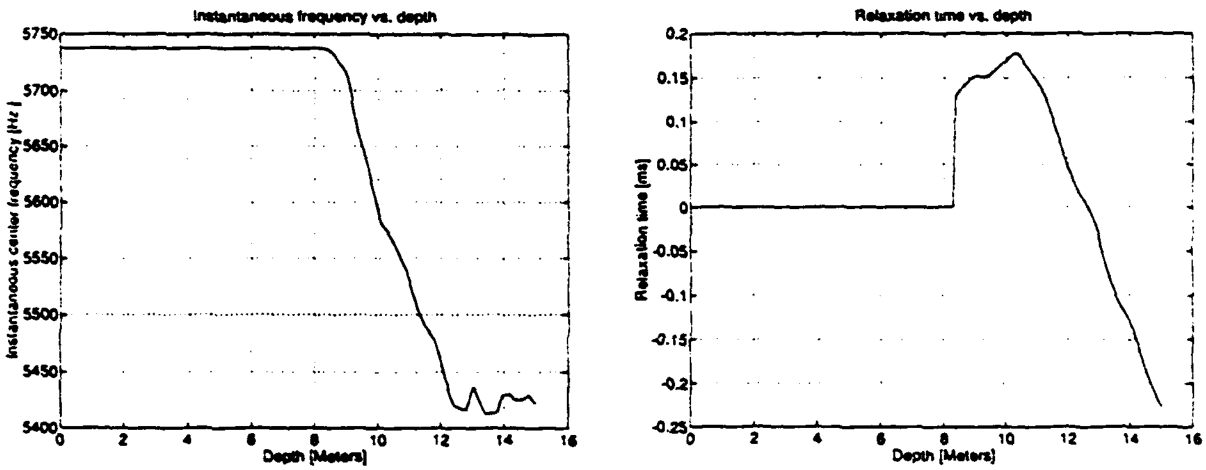

Figure 48 Plot of the center frequency of backscattered energy as a function of depth beneath the seabed (left) in sands off Boca Raton and the relaxation time of the attenuation process(right) which is related to the slope of the frequency vs depth plot.

3.18 Variability of Seabed Sediment Microstructure and Stress-Strain-Time Behavior in Relation to Acoustic Characterization (Principal Investigators: A. J. Silva, M. H. Sadd, G. E. Veyera and H. G. Brandes, University of Rhode Island)

CBBLSRP FY93 YEAR-END REPORT

Armand J. Silva
Martin H. Sadd
George E. Veyera
Horst G. Brandes

College of Engineering
Marine Geogeomechanics Laboratory
University of Rhode Island
Narragansett, RI 02882

1. Summary and Plans for FY94

This annual report describes the University of Rhode Island (URI) research progress for the Coastal Benthic Boundary Layer (CBBL), Special Research Project (SRP) sponsored by the Naval Research Laboratory (NRL). The impetus for this program comes from a need to better understand the benthic boundary processes that affect shallow-water naval operations, especially mine countermeasures. This summary document outlines the URI tasks, briefly describes some of the results to date (October, 1993) and outlines plans for the second year of this five year program.

1.1 Tasks, Facilities, and Personnel

The focus of the URI research program is on the variability of seabed sediment geotechnical properties and microstructure with particular attention to stress-strain behavior in relation to geoacoustic characteristics. Sediments being studied will include naturally deposited, undisturbed cohesive and cohesionless materials and completely remolded samples of the same materials. We are interested in investigating the contrasts of behavior, including the effects of intrusive objects such a mines on or in the seabed. The three main URI interrelated tasks include a) a comprehensive experimental laboratory program centered around triaxial compression, consolidation, permeability and geoacoustic testing systems, b) a discrete element microstructural modeling program, and c) a finite element modeling program for macroscopic prediction of geomechanical behavior.

The Marine Geomechanics Laboratory (MGL) at URI has several unique state-of-the-art experimental systems for analyzing marine sediments, including: a multi-sensor core logging system, a new triaxial compression system with flow pump instrumentation which will be outfitted with the NRL-type of acoustic devices, a new consolidation and permeability system with flow pump instrumentation, and various networked computational facilities.

MGL research personnel include: the Principal Investigator and Project Director, Armand J. Silva (Ocean Engineering) two Co-P.I.'s, Martin H. Sadd (Mechanical Engineering) and George E. Veyera (Civil Engineering); and a Post-Doctoral Research Associate, Horst G. Brandes. Other personnel include three graduate students, two undergraduate students and a part-time secretary. With the assistance of various other technical support personnel we have a very strong multi-disciplinary team for the project.

1.2 Research Cruises

Personnel from the URI/MGL participated in three program research cruises; February 1993 Baltic Sea cruise, May 1993 Baltic Sea cruise, and August/September 1993 Panama City, FL cruise. Samples from all three cruise efforts are in storage at URI/MGL and data analysis is now underway.

During the February cruise, two gravity cores and six box cores were processed, tested, and sampled. Water content profiles show a very steep gradient within the upper 5-10 cm with a maximum value at the surface of over 500% and a value of 250% at a depth of about 4 meters. All cores showed evidence of gas in the sediments.

During the May cruise, work concentrated on processing four 50 cm box cores, one smaller diver core and three gravity cores. The box cores did not contain as much gas as those from the February cruise, but the water content profiles are similar. A considerable amount of pressure was observed to build up in the gravity cores as the sediment was prevented from expanding by sealing plugs. Shear strength in the box cores is low at less than 0.4 kPa at one centimeter depth, increasing to 1.2 to 1.6 kPa at 25 cm depth. Rheological measurements were made at various depths in the box cores with a Brookfield instrument and a special 8 mm vane. Many subsamples were obtained for laboratory analysis.

The URI/MGL Large-diameter Gravity Corer (LGC) was used to obtain fourteen (14) cores of the sands at the Panama City, FL site. There cores were distributed among the URI, TAMU, and NRL research groups. No processing of cores was conducted on board ship. In addition, a number of grab samples were also obtained. A complete analysis of cores and samples will be conducted at the URI/MGL in the coming year.

1.3 Geotechnical Laboratory Experimental Program

The laboratory experimental program is oriented toward gaining insight into sediment stress-strain behavior, including geoacoustic characteristics, and providing information for the numerical modeling efforts. We are also looking at downcore and lateral variations in sediment characteristics including compressibility, stress history, permeability, and anisotropy. During this first year we have concentrated on consolidation and permeability testing of undisturbed subsamples from the Baltic site and on physical property variations.

The sediments at the Baltic site show very high compressibility characteristics with compression index, C_C, generally in the 4 to 6 range. The surficial sediments (upper 4 meters) show evidence of "apparent" overconsolidation, with OCR values ranging from about 4 to 10 in the upper 50 cm to about 2.0 at 4 m depth. The coefficient of permeability, k, is relatively low in these high porosity, fine grained materials with typical values of 3×10^{-7} to 2×10^{-5} cm/s. There is significant lateral variation within the experiment site.

1.4 Geoacoustic Microstructural Modeling

During this initial stage of the program, our efforts in modeling the acoustic response of marine sediments has been on the theoretical and numerical simulation of fluid-saturated granular materials using the discrete element method. We began with development of new contact laws governing particle interactions through a fluid. The derived contact laws were then used to investigate acoustic wave propagation in a one-dimensional single/straight chain of 2 mm diameter circular disks having properties of quartz, and water of given viscosity. For the assumed conditions and a 5 μs pulse of 2N, a wave speed of 840 m/s resulted. The effects of varying gap distance, viscosity and other parameters have also been studied.

We have also started to investigate wave propagation in two-dimensional granular materials using a random media generator to simulate more general particulate assemblies. We can now study interparticle loadings, attenuation, and dispersion characteristics with a variety of assemblies or microstructure. This gives us the ability to relate these idealized microstructures to geoacoustic wave propagational characteristics.

1.5 Finite Element Modeling

The objective of this portion of the program is to develop a numerical modeling capability to predict the macroscopic mechanical behavior of sediments that are of interest to the CBBL/SRP. The current efforts are centered on further development of the URI/MGL finite element code GEO-CP which is formulated based on critical state concepts and uses parameters that are defined accordingly.

The boundary value problem that has been solved involves a surface strip loading on a semi-infinite layer of sediment. The predicted deformations and stresses compare well with a closed-form solution. Improvements are possible by using a finer mesh and changing some of the boundary constraints. Future work includes modification of the formulation to incorporate time-dependent variation of certain parameters (such as permeability), interpretation of triaxial compression test results, application to other boundary value problems of interest to the program, and long-term vertical migration of objects, such as mines, into the soft seabed sediments.

1.6 Plans for FY 94

Following are the tentative plans for the URI/MGL research efforts during the second year of the CBBL/SRP. The actual activities may be altered as needs are identified within our own program and as a result of requests by other investigators in the overall program.

Research Cruises: We will participate in future research expeditions as needs arise. We are requesting participation in the Baltic Sea cruise scheduled for Summer, 1994 to obtain additional special samples and to perform in situ vane shear strength measurements. If there is a cruise to another site (Key West), we also intend to participate.

Experimental Laboratory Program: We will be intensifying and expanding this portion of our program. The new acoustic system for the triaxial compression equipment is being ordered and we hope to have it in operation by early 1994. We are short-handed for this important aspect of our research and have been exploring ways of bringing more personnel on board to assist in, and expand the testing program. Towards this end, we have submitted a proposal to the DoD AASERT program to obtain funding for two additional graduate students.

Microstructural Modeling: The plan is to bring the numerical modeling of granular materials to a significant milestone and compare the results with those from carefully controlled experiments in the triaxial cell. We also plan to begin the modeling effort for the much more complex structures typical of fine-grained cohesive sediments.

Finite Element Macroscopic Modeling: We will be devoting more time to further developm of our GEO-CP code to accommodate boundary value problems of interest to the CBBL/Sk This modeling capability will also be used to help direct the laboratory testing program.

Other Initiatives: We feel it is important to measure certain geotechnical properties in situ. This is especially true for measuring the very low strengths at the Baltic site (less than 0.5 kPa). We will be proposing to conduct in situ measurements during the next cruise to this site in Summer, 1994, either by modifying an existing system that was developed for deep sea research, or by designing and building a simpler system for this shallow water application.

We also will be continuing development of the experimental facilities at MGL. For example we would like to have the capability to perform dynamic stress-strain tests, either by adding this to the existing triaxial system or by purchasing a cyclic simple shear device. We are considering submittal of a proposal to the University Research Instrumentation program for assistance.

2. Introduction

This annual report describes our research covering the FY93 period of the University of Rhode Island, Marine Geomechanics Laboratory (URI/MGL) portion of the Coastal Benthic Boundary Layer (CBBL), Special Research Program (SRP) sponsored by the Naval Research Laboratory, Stennis Space Center (NRL/SSC). This is a five year multi-disciplinary program that seeks to better understand the physical properties of the seabed and model the benthic boundary processes that affect shallow-water naval operations. The URI/MGL activities focus on the variability of seabed sediment properties and microstructure with particular attention on stress-strain behavior in relation to geoacoustic characteristics.

During this first year, much of the URI efforts have, out of necessity, been devoted to field work with participation in two research cruises in Eckernfoerde Bay, Baltic Sea (February and May, 1993) and one research cruise in the West Florida sand sheet area southeast of Panama City, Florida (August, 1993). Significant progress has also been made on the laboratory experimental program and microstructural geoacoustic modeling. The results of all these efforts are summarized in the following report.

The three main tasks of our research, and the URI personnel involved are illustrated in Figure 2.1. The primary personnel include the project director, Armand J. Silva, Professor of Ocean and Civil Engineering and Director of the Marine Geomechanics Laboratory; two other faculty, Martin H. Sadd, Professor and Chairman of Mechanical Engineering and George E. Veyera, Associate Professor of Civil Engineering; and Horst G. Brandes, Post-Doctoral Research Associate in Ocean Engineering. Other personnel are identified in Section 6. The central and most active task will be the laboratory experimental program, which will be closely interrelated with the other two tasks. The microstructural modeling work is basically a theoretical effort, but the actual measured microstructural arrangements will provide a guide to this effort. Part of the laboratory work is driven by the macrostructural geomechanics modeling effort, which requires determination of material parameters. The various aspects of the three tasks are discussed further in Sections 8, 9, and 10.

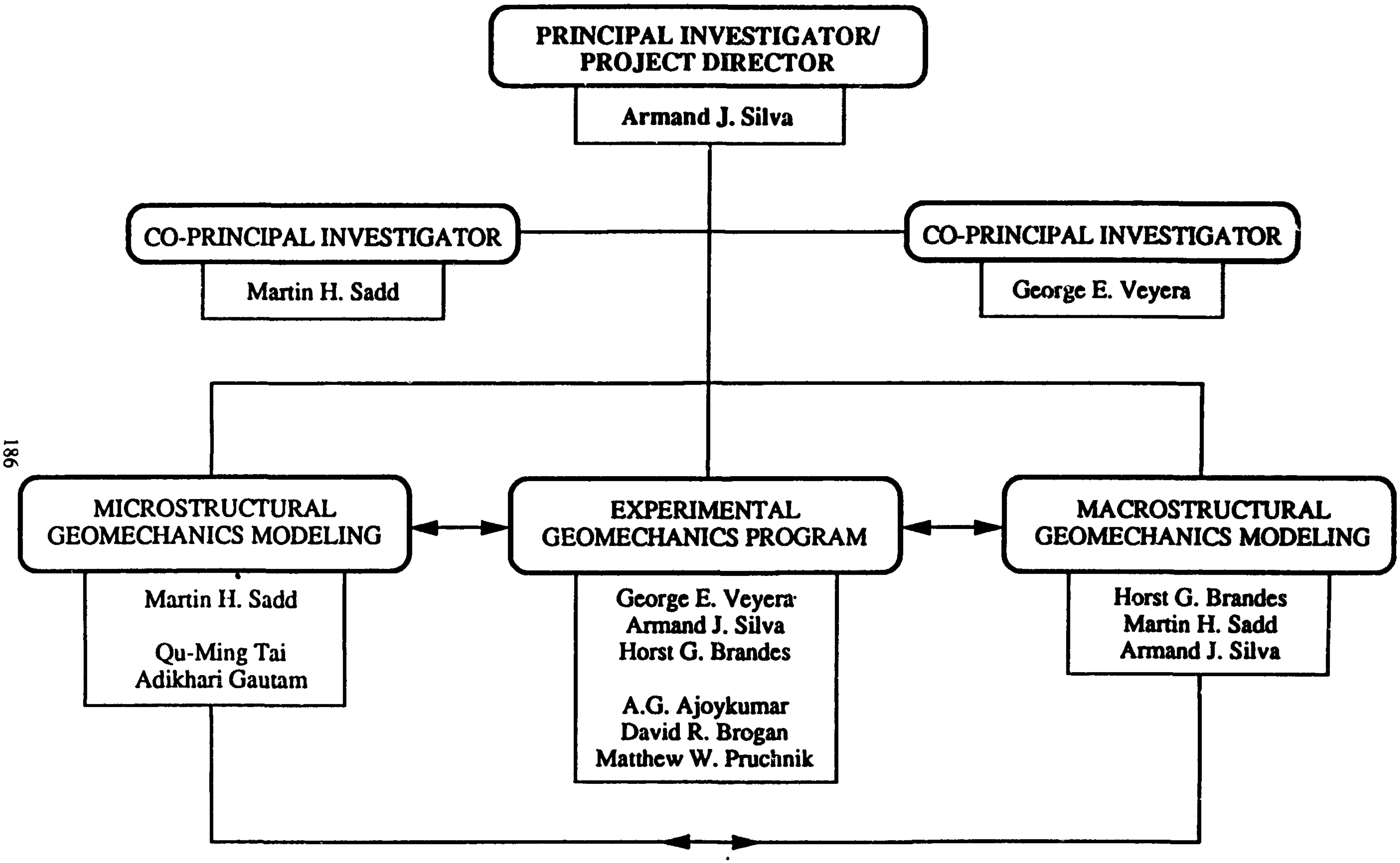

Figure 2.1 URI Marine Geomechanics Laboratory CBBL/SRP Organizational Chart.

3. Background and Objectives

The research program described in this report is an integrated part of the CBBL/SRP, initiated by the NRL. The major thrust of the overall program is to understand the role of sediment structure in controlling material properties in relation to high frequency acoustic characteristics, with eventual application to remote detection of objects resting on or buried in the seabed.

The behavior of a particular seabed sediment deposit is dependent on many interacting factors such as fluid properties, hydrodynamic forces, bioturbation, diagenetic alteration, and mechanical effects. The introduction of artificial disturbance caused by objects resting on or within the seabed can significantly influence behavioral properties of the sediment, mainly by changing the sediment structural configuration on scales ranging from microns to tens of centimeters.

In keeping with the hypothesis adopted by the overall project, the assumption controlling our efforts is that there is a fundamental linkage between the behavioral properties of fine-grained sediments; including the physical, chemical, electrical, and geoacoustic characteristics; and the microstructure of the sediment. We will be studying contrasts over a wide range of sediment microstructures that will include naturally deposited flocculated silt-clay mixtures, cohesionless sediments and completely remolded samples of these same materials. The assumption is that intrusive activities, such as objects that impact and/or penetrate the sediments will alter the properties and behavior of the parent materials. The particular focus of our work is on: a) triaxial compression and consolidation/permeability testing to determine stress-strain behavior and geoacoustic properties; b) *microstructural numerical modeling* of geoacoustic wave propagation; and c) macrostructural numerical modeling of stress-strain-time behavior.

The work is being conducted at the URI/MGL under the direction of three faculty: A. J.. Silva (Project Director/P.I.), M. H.. Sadd (Co-PI) and G. E.. Veyera (Co-PI), and a post-doctoral research associate, H. G.. Brandes. The research is comprised of three integrated tasks: 1) laboratory experiments of stress-strain-time behavior and acoustic properties, oriented toward determining the material constitutive relationships and acoustical characteristics of undisturbed and remolded seabed samples; 2) microstructural geoacoustic modeling for simulation of cohesive and cohesionless sediments to relate microstructure to acoustic wave propagation characteristics; and 3) numerical modeling of macroscopic mechanical behavior for predicting stress-strain properties in relation to microstructure and geoacoustic characteristics. An overview of the tasks and their relationship to the overall CBBL/SRP program is shown in Figure 3.1 and further described in Sections 8, 9, and 10.

University of Rhode Island

Research Program Overview

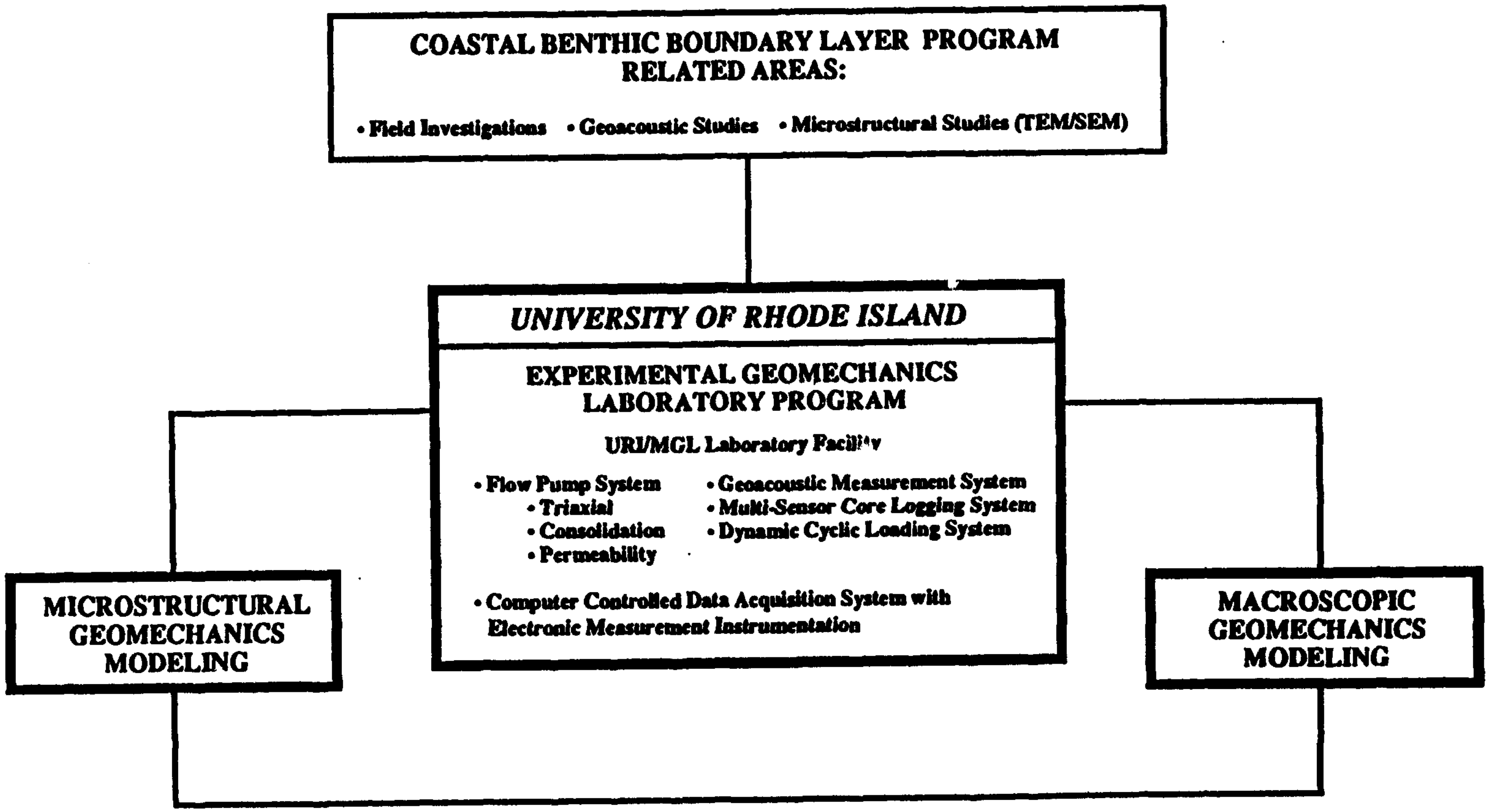

Figure 3.1 URI/MGL Research Program Overview and Relation to Overall CBBL/SRP.

4. Facilities

4.1 Marine Geomechanics Laboratory (MGL)

Testing of marine sediments requires special equipment since they are generally soft materials, with very low permeability and can exist in a variety of stress states. Applied load increments must be carefully controlled and pore pressure dissipation monitored. The URI/MGL facilities include several unique state-of-the-art equipment systems for studying ocean sediments under different loading and boundary conditions, equipped with integrated computer-controlled testing and data acquisition and fully instrumented for both nontraditional and standard geotechnical testing procedures. Capabilities include anisotropic consolidation, stress path loading, constant rate of deformation consolidation (CRD), very low gradient permeability testing, back-pressured consolidation, and long-term drained creep under triaxial and direct simple shear conditions. In addition, a new multi-sensor core logging system for whole core logging is now operational and acoustic devices are being added to the triaxial compression equipment.

Central to our triaxial and consolidation testing systems is a relatively new device in geotechnical engineering called a flow pump, which has been adapted from medical technology and is used for very accurate direct permeability and flow measurements in sediments (Olsen et al., 1989). The flow pump is a versatile device that can be used for constant rate of deformation consolidation testing, contaminant transport studies, and low gradient permeability measurements. It is well suited for testing of fine-grained marine sediments and is used to make very accurate permeability measurements during both triaxial and consolidation tests. This technique offers a distinct advantage over traditional testing methods in that permeability measurements can be made as the sediment microstructure changes during consolidation and during shear.

In the sections that follow, an overview of our laboratory facilities is given and the various aspects of each major component are briefly described.

4.1.1 Triaxial Compression Testing System

The URI/MGL laboratory facilities are equipped with a newly developed triaxial compression testing system instrumented with electronic measurement devices including pore pressure transducers, load cells, and DCDT's (displacement transducers). A computer is used for instrument control, data acquisition, data analysis and storage. The new system centers around flow pump technology (described in Section 4.1) and other significant improvements which allow precise measurements of compressibility, permeability and stress-strain behavior of ocean sediments (Figure 4.1). In addition, the system also has a set of three non-contacting radial deformation transducers to measure lateral deformations, which are used in conjunction with a servo-controller in a feedback control loop for anisotropic consolidation and stress path testing. We are currently in the process of further enhancing our existing triaxial testing station by incorporating an acoustic velocity measurement system to provide detailed geoacoustic data under various loading conditions. The new system will allow us to make both P-wave and S-wave measurements in undisturbed and remolded samples of marine sediments (see Section 4.1.3).

4.1.2 Back Pressure Consolidation and Permeability Measurement System

The URI/MGL laboratory facilities are equipped with a fully instrumented (pore pressure and displacement transducers), computer-controlled back pressured consolidation testing system that incorporates flow pump measurement technology (Figure 4.2). With this state-of-the-art system, samples can be tested under a back pressure and very accurate permeability measurements can be made throughout the test without disturbing the sample.

Since some coastal sediments may contain minute gas bubbles entrapped within the sediment skeleton matrix, back pressuring of the pore fluid is necessary to re-dissolve the gas and bring the sample to a saturated condition. In addition, the flow pump allows permeability data to be obtained at precisely controlled, very low gradients, which is a distinct advantage since gradients in natural sediment deposits are usually quite small (less than unity). Also, the time to complete an entire back pressured consolidation test with permeability measurements is reduced by as much as 90% when compared to standard test methods (Silva et al., 1981). This is a highly desirable feature when working with low permeability marine sediments. The consolidation and permeability data are especially important and useful in evaluating sediment behavior and determining the stress state of the seabed.

4.1.3 Geoacoustic Measurement System

Our laboratory facility is equipped with a newly acquired multi-sensor core logger system measurement equipment that enables us to obtain whole-core measurements of sections including compressional wave velocity, density, and magnetics. Data can be collected at spatial resolutions of up to 1 to 2 centimeters to provide fine scale information that might be needed for microstructural studies.

In addition, the NRL (Dawn Lavoie) is modifying our existing triaxial cell to incorporate newly developed acoustic equipment. This will provide a non-invasive, non-destructive measurement system that will significantly improve our triaxial testing facility. The system is unique in that the transducers (acoustic wave excitation elements and bender elements for shear wave generation), receivers and preamplifiers are mounted in the triaxial end caps. Detailed studies of sediment geoacoustic characteristics can be made in carefully controlled laboratory stress-strain tests. This system will provide data for developing correlations between microstructural characteristics and material, geoacoustic and microstructural properties.

4.2 Computational Facilities

The MGL is equipped with both Macintosh and IBM personal computers, which are linked to the Engineering Computer Lab (ECL) and Academic Computer Center (ACC) mainframe computers. The PC's are used for numerical computation, control of laboratory experiments and data acquisition from electronic instrumentation.

The URI/ECL operates a dedicated central VAX 4000/200 computer available to the engineering faculty and students. The computer is networked throughout URI and has access to remote computer facilities in the United States, including several supercomputers available to us, Network systems include Internet and BITNET. The ACC at URI provides computational resources for the research and instructional community with an IBM ES/9000 Model 210VF mainframe computer. Several hundred terminals are located in public terminal clusters and individual faculty and staff offices. The ECL and ACC also have several laboratories equipped with IBM and Macintosh personal computers, file servers, and DEC and SUN workstations which are available for research use.

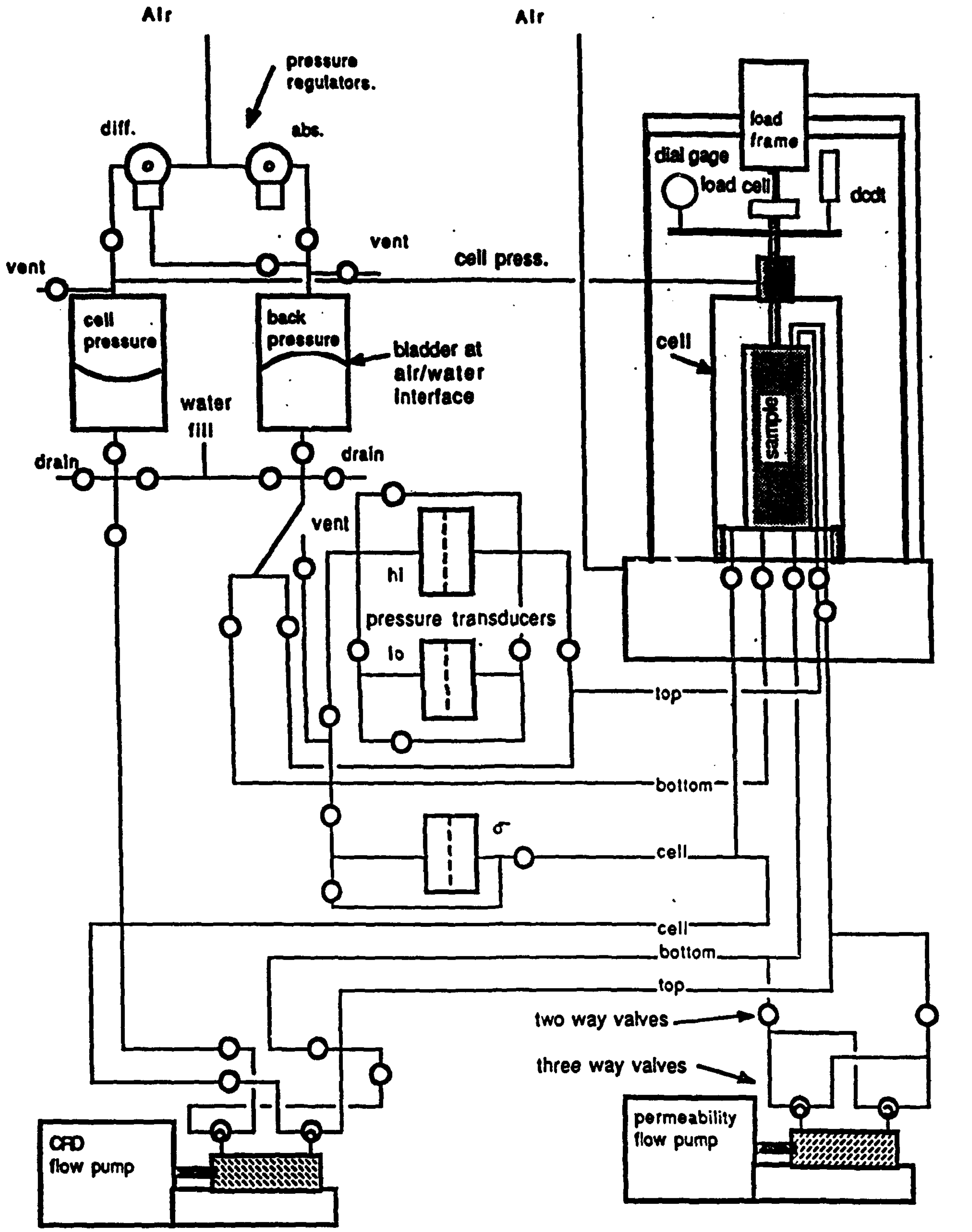

Figure 4.1 Triaxial Flow Pump Testing System

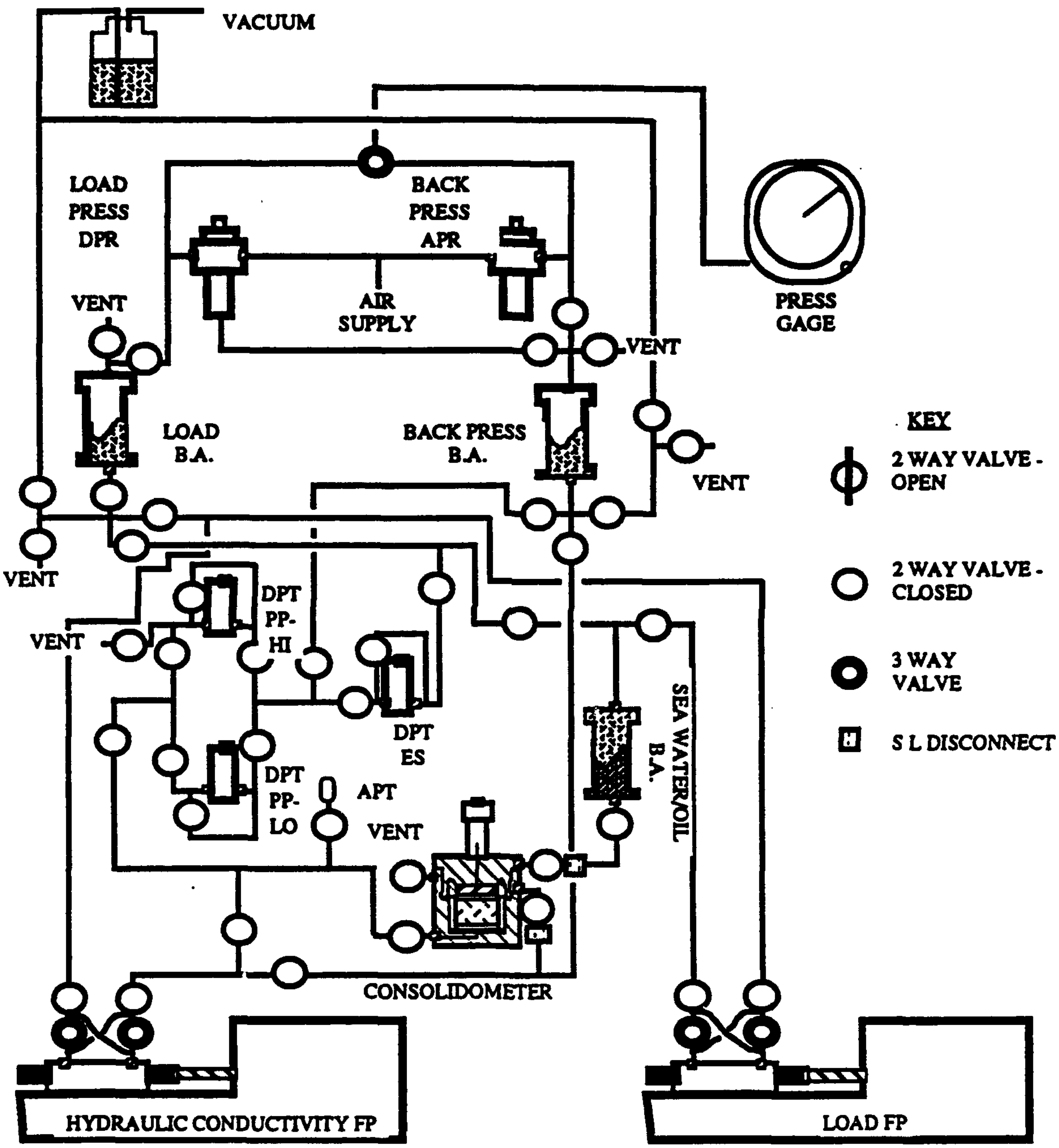

Figure 4.2 Back Pressured Consolidation Flow Pump System

Our research program is described here in terms of three separate but closely interrelated and integrated tasks (Figure 3.1) which are summarized in the following sections. The laboratory experimental program is being carefully tailored to provide information for use with the two modeling efforts. The results will be of direct benefit to other aspects of the overall program as well, such as interpretation of field conditions and geoacoustical modeling. The microstructural and macrostructural modeling will also be closely coordinated with a view toward studying correlations between the two.

5.1 Task 1: Laboratory Experiments of Stress-Strain-Time Behavior and Acoustic Properties.

A controlled set of laboratory experiments will be conducted to determine geotechnical parameters and acoustic characteristics of seabed sediments. Experimentally derived laboratory data will provide important information for the numerical modeling efforts. These results can also be helpful in the interpretation and analysis of in situ measurements.

Data obtained from this phase of the research program will provide information about the influence of individual parameters on soil microstructure, geoacoustic parameters and sediment behavior. The results can be used to study the interaction between the behavioral properties of fine-grained sediments; including the physical, chemical, electrical, and geoacoustic characteristics; and the microstructure of the sediment. In addition, the results will also provide necessary data for developing and calibrating appropriate quantitative microstructural models and constitutive models such as those described in Sections 9 and 10.

Recently developed state-of-the-art triaxial (CIU and CAU) compression, and back pressured consolidation/permeability systems are being used to conduct carefully controlled stress-strain-time tests on at least two distinctly different sediment types (clay and sand) from sites of interest to the program. The parameters to be measured include: stress-strain properties such as elastic modules, pore pressure parameters, compressibility parameters, rebound modules, and strength parameters; acoustic characteristics including compressional wave speed, shear wave speed and attenuation; and hydraulic conductivity (Figure 5.1). During FY93 the new triaxial compressional system was brought to an operational level but tests have not yet begun on the CBBL/SRP samples. The focus of this portion of the program during FY93 has been on determining compressibility and permeability characteristics of selected samples from the Baltic Sea site (Section 8).

In order to tie these laboratory studies to microstructure and chemical studies, we are obtaining and preserving samples from representative test specimens for shipment to other investigators in the CBBL/SRP program. Microstructure samples are oriented so that SEM and TEM results can be related to the experimental results and to the quantitative modeling analyses. This integrated approach has promise for yielding significant advances toward a basic understanding of sediment behavior.

Microstructural studies are being conducted to understand the variation of geoacoustic wave propagational characteristics in seafloor sediments. The main objective is to investigate candidate materials in order to determine the effect of fabric and elemental inter-particle interactions on the overall dynamic acoustic/mechanical behavior. Reasonable models of sediment fabric are being established in order to determine basic mechanisms involved in wave propagation processes (Figure 5.2). The geomaterials being studied contain very complex granular and clay microstructures, and therefore detailed modeling of these fabric mechanisms requires that several models be developed in order to simulate the varied mechanics which occur. We are currently constructing material models that will simulate granular (cohesionless) materials, which are being subjected to acoustic wave propagation in order to characterize their propagational behavior. Information from available SEM and TEM studies from other investigators will be used to guide the construction of our structural models.

With respect to granular sediments, we are constructing model granular materials as aggregate assemblies of circular and spherical particles with varying degrees of packing arrangements. These assembly model systems are being dynamically analyzed using the discrete/distinct element method, which has proven to be a fruitful computational scheme for modeling of particulate materials. For later efforts on clay sediments, assemblies of elastic rod and plate elements will be constructed to simulate the various microstructures observed in fine-grained marine sediments. These structural models will be analyzed using finite element techniques with nonlinear and time-stepping solution strategies.

Our microstructural modeling work incorporates the discretel/distinct element method, which was originally developed by Cundall (1971) and Cundall and Strack (1979). The distinct element method has been successfully used to simulate the behavior of discrete materials modeled as assemblies of spheres, disks, and blocks. Our existing distinct element computer code, *WAPRIPM* (Wave Propagation in Particulate Media), is being modified and extended to simulate the dynamic behavior of model particulate sediment materials. The code incorporates Ordered and Random Particulate Media Generators for preparing various assemblies of cohesionless circular particles to study various packing arrangements. Numerical results from our computer code have compared favorably with experimental data from photoelastic and strain gage tests of simulated granular media and have shown that granular fabric has a strong influence on wave propagation. The code will be further modified to address the complex behavior of clay-like structures, extending our past studies to cases involving particulate systems with cohesion and pore fluid. We intend to conduct studies of microstructural modeling of some typical fabrics that have been observed in both undisturbed and remolded clay sediments.

The important segments of our work in this task are: the generation of representative two- and three-dimensional microstructural models; dynamic acoustic studies of these models; and the development of relationships between fabric and geoacoustic behavior. The program has been initiated using two-dimensional modeling to be followed by three-dimensional studies. New particle interaction characteristics will be established for use in the computer code, and numerous simulations will be conducted on a variety of granular sediments in order to explore geoacoustic-microstructure relationships. We feel that important basic understandings will be found in the dynamic behavior of marine sediments through the microstructural modeling studies.

5.3 Task 3: Numerical Modeling of Macroscopic Mechanical Behavior

This task is directed at developing a numerical capability for the macroscopic mechanical analysis of seabed sediments that incorporates the findings from the previous two tasks and those of other investigators, to both guide our experimental program and to solve particular boundary value problems of interest to the SRP (Figure 5.3). Our efforts are centered on continuing the development of our general-purpose finite element code *GEO-CP*, which was developed specifically for the analysis of quasi-static stress-strain-time problems associated with marine sediments (Brandes, 1992). The *GEO-CP* program has shown excellent agreement between predictions and theoretical results for elastic problems where exact solutions are available.

We intend to use *GEO-CP* to guide the experimental program and track the mechanical behavior of laboratory specimens so that particular constitutive formulations can be evaluated. Modifications to the present formulation are being incorporated to allow for changes in key material properties that affect the transmission of shear and compressional waves, which are currently assumed to be constant throughout the analysis. A numerical sensitivity study will be conducted to determine the relationships between stress-strain behavior and material properties. We will also expand the capabilities for predicting seepage flow by including the effects of boundary hydrodynamic stress variations.

Task 1: EXPERIMENTAL GEOMECHANICS LABORATORY RESEARCH

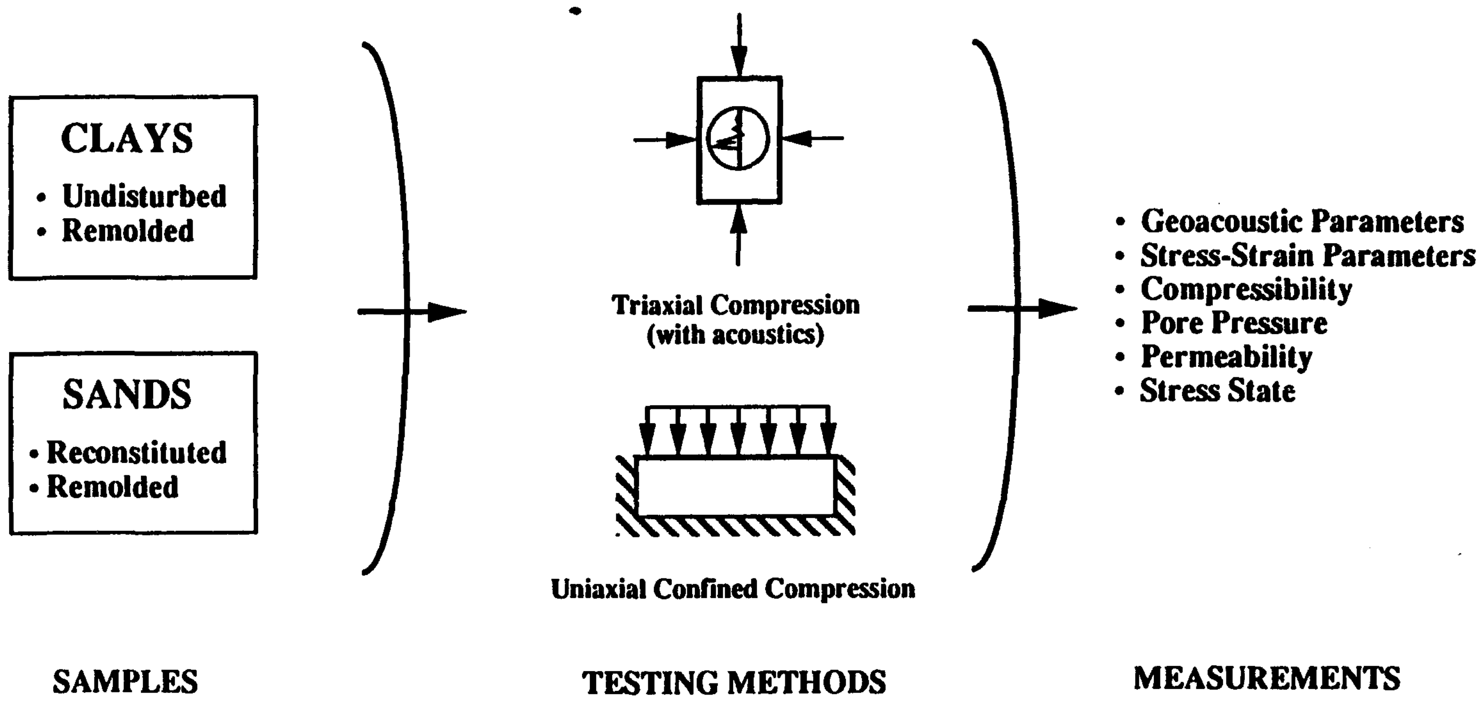

Objectives:

- Develop Constitutive Relationships for Macrosructural Geomechanics Modeling and Relate to Microstructural Effects
- Determine Geoacoustical and Mechanical Material Parameters

Figure 5.1 Overview of URI/MGL Experimental Geomechanics Laboratory Research for the CBBL/SRP.

Task 2: MICROSTRUCTURAL GEOMECHANICS MODELING OF WAVE PROPAGATION

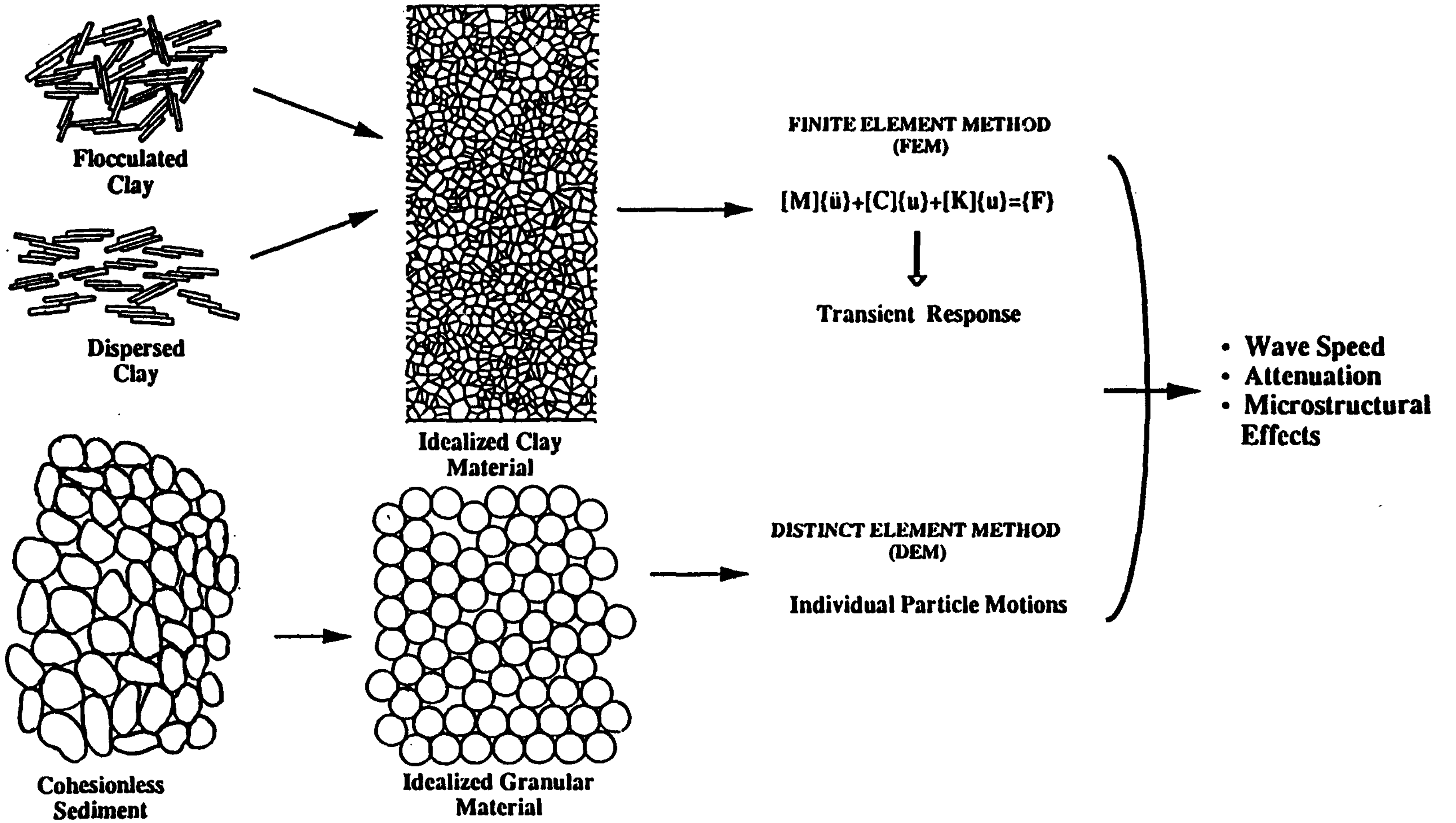

Objective: • Relate Microstructure/Fabric to Geoacoustic Behavior

URI/MGL

Figure 5.2 Overview of URI/MGL Microstructural Geomechanics Modeling for the CBBL/SRP.

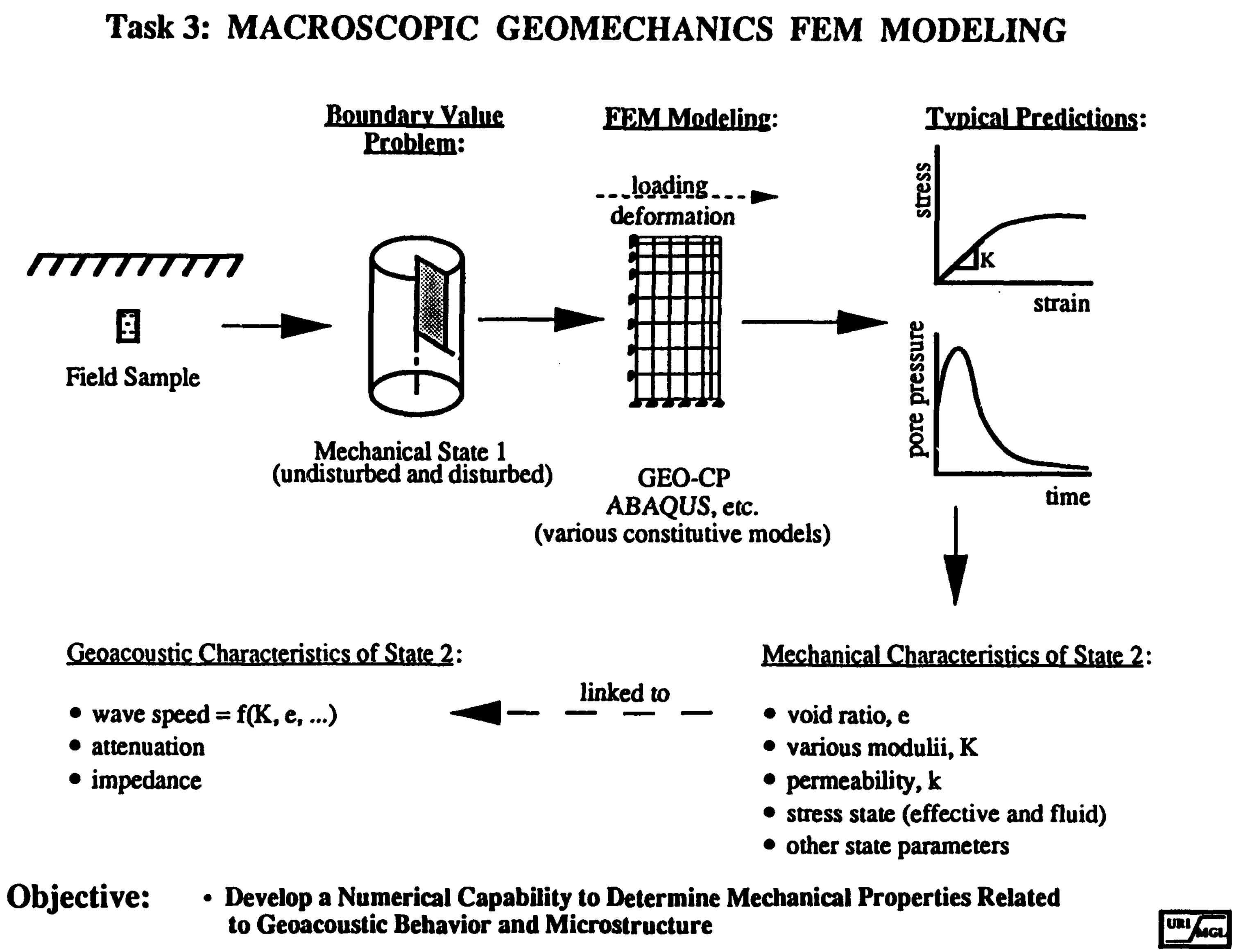

Figure 5.3 Overview of URI/MGL Macroscopic Geomechanics FEM Modeling for the CBBL/SRP.

6. Personnel and Summary of Activities

In this section, the URI/MGL personnel and their roles in the various aspects of our research program are identified (see Figure 2.1 also). Also, the participation of the MGL personnel in CBBL/SRP meetings and research cruises are summarized. Our participation in the three 1993 research cruises, as well as some preliminary results, are discussed in Section 7.

6.1. University of Rhode Island Personnel

- Dr. Armand J. Silva, **Project Director/PI**, Professor of Ocean and Civil Engineering
- Dr. Martin H. Sadd, **Co-PI**, Professor and Chairman of Mechanical Engineering and Applied Mechanics
- Dr. George E. Veyera, **Co-PI**, Associate Professor of Civil and Environmental Engineering
- Dr. Horst G. Brandes, **Post-Doctoral Research Associate**, Department of Ocean Engineering

6.1.2 Graduate Research Assistants:

- A. G. Ajoykumar - M.S. candidate in Ocean Engineering
  Tasks: Consolidation/permeability, core logging, physical properties.
- David R. Brogan - M.S. Candidate in Ocean Engineering
  Tasks: Stress-strain testing, core logging, physical properties.
- Qu-Ming Tai - Ph.D. Candidate in Mechanical Engineering (part time)
  Tasks: Discrete element microstructural modeling of geoacoustic stress wave propagation in sediments.
- Adhikari Gautam - M.S. Candidate in Mechanical Engineering (part time)
  Tasks: Discrete element microstructural modeling of geoacoustic stress wave propagation in sediments.

6.1.3 Undergraduate Research Assistants:

- Matthew W. Pruchnik - B.S. Candidate in Civil and Environmental Engineering
  Tasks: Assist graduate students in various aspects of the field and laboratory experimental investigations.

6.1.4 Clerical/Secretarial

- Kristine Walwood, (part time)

6.2 Meetings Attended

MGL personnel participated in the following meetings during 1992-1993:

- o November 18-19, 1993, at URI/MGL, RI (A.J. Silva, M.H. Sadd, G.E. Veyera and H.G. Brandes). Meeting of the SRP geotechnical/geological group.

- o August 8-9, 1993, at NRL/SSC, MS (A.J. Silva). CBBL/SRP planning meeting for Panama City, FL experiment.

- o January 7-8, 1993, at NRL/SSC, MS (A.J. Silva). CBBL/SRP planning meeting for Baltic Sea experiment.

- o October 29-30, 1992, at NRL/SSC, MS (A.J. Silva and H.G. Brandes). First CBBL/SRP planning meeting.

6.3 Research Cruise Participation

MGL personnel participated in the research cruises during 1992-1993:

- o February 11-18, 1993, Baltic Sea, Eckernfoerde Bay, Germany (A.J. Silva).

- o May 11-31, 1993, Baltic Sea, Eckernfoerde Bay, Germany (A.J. Silva and Horst G. Brandes).

- o August 28-September 3, 1993, Panama City, FL (A.J. Silva, G.E. Veyera and H.G. Brandes).

7. Research Cruises

7.1 Introduction

URI/MGL personnel participated in the three 1993 research cruises organized by NRL/SSC to the Baltic Sea and south of Panama City, FL. Our goal was to obtain gravity and box cores, make onboard geotechnical measurements and observations on some of these cores, and obtain undisturbed and bulk subsamples for our laboratory program (Tables 7.1 and 7.2). An array of specialized equipment was made available and shipped to both locations including, the URI/MGL Large-diameter Gravity Corer (LGC) and associated coring equipment, instruments to measure the shear strength and rheological characteristics of the sediments, and a number of tools and rigs for subsampling of the box and gravity cores. Specific activities, procedures, and equipment for each of the three cruises are described in the individual cruise reports included in the Addendum. Many of the onboard tasks and decisions were conducted in close cooperation with the TAMU group, especially coring operations and some of the on-site processing.

7.2 February, 1993 Baltic Cruise

One person from the URI/MGL, Armand J. Silva, participated in the first Baltic Sea cruise in Eckernfoerde, Germany (February 11-18, 1993). The types of cores recovered included LGC gravity cores, box cores, and special pressurized cores collected by divers (cruise report in Addendum). Two of the gravity cores, 029-BS-GC and 034-BS-GC, were extruded on-site. Water content and density profiles for these two cores are shown in Figure 7.1. In addition, six box cores were subsampled and tested (Figures 7.2 through 7.5 and Table 7.3). A number of undisturbed and bulk samples from the box cores and gravity cores were returned to URI/MGL (Table 7.2). Pore water from some of the bulk samples was analyzed with a hand-held refractometer to determine salinity. Figure 7.6 combines the results from samples taken across the study site. Most of the values in the upper 50 cm range between 15 ppt and 27 ppt. Below 50 cm the salinity appears to be relatively constant at 27 ppt. We have selected an average value of 25 ppt to correct the water contents reported here.

As indicated in the attached profiles, these surficial sediments have very high water contents, with values ranging from over 500% at the surface to 250% at a depth of about 4 meters. There is a very high water content gradient within the upper 5-10 cm. All cores showed evidence of degassing upon retrieval.

7.3 May, 1993 Baltic Cruise

Two URI/MGL personnel, Armand J. Silva and Horst G. Brandes, traveled to Eckernfoerde, Germany to participate in the second Baltic Sea experiment (May 11-31, 1993). Work at the site concentrated on processing of four large box cores, one diver box core, and three gravity cores (Table 7.1 and Cruise Report in Addendum). Water content and density data are presented in Figures 7.7 through 7.10 and in Table 7.3. Various types of undisturbed and bulk subsamples were taken from the box cores and are currently in storage at the URI/MGL (Table 7.2). Shear strength values were determined primarily with a Brookfield viscometer outfitted with a special 8 mm ¥ 8 mm miniature vane, operating at 0.5 rpm (Table 7.4 and Figures 7.7 through 7.10). Measurements were also made at higher rates of rotation ranging up to 100 rpm. We will be analyzing these data to investigate the rheological behavior of the undisturbed sediments. A few measurements of shear resistance of the surface sediment (approximately upper 2 mm) were also obtained with a special small torvane-type disk attached to the Brookfield viscometer. A motorized, instrumented miniature vane system (modified Wykeham-Farrance device with torque transducer) with a 1.27 cm¥ 1.27 cm vane was used to measure shear strength in the diver box core (Table 7.4). However, problems with the electronics prevented measurements in the large box cores. The standard springs could not be used since they were not sensitive enough. As shown in Table 7.4, there was excellent agreement between the miniature vane ([illegible] cm) measurements and those made with the Brookfield vane (8 mm). Therefore, we feel co[illegible]t in using the Brookfield measurements at 0.5 rpm as an indication of the shear strength. Shear stress versus rotation curves were obtained, mostly with the Brookfield instrument, at 21 levels throughout four box cores. The data are being processed and will be available in the coming year.

7.4 August/September, 1993 Panama City, FL Cruise

The URI group that participated in the Panama City, FL cruise (August 28 through September 3, 1993) consisted of Armand J. Silva, George E. Veyera, and Horst G. Brandes. Work during the six day period aboard the R/V GYRE centered on obtaining good quality gravity cores for future shore-based analysis. Although some difficulties were encountered due to the sandy nature of the sediments and other technical problems, a total of fourteen (14) successful cores were obtained (see Table 7.1 and Cruise Report in Addendum). These cores were distributed among URI, TAMU and NRL.

Table 7.1 Summary of Cores Obtained by URI/MGL.

Cruise	Core*	Location	Comments
February 1993 Baltic Sea	029-BS-GC	54° 30' 00.0N 09° 59' 59.0E	Split and processed at U. of Kiel
	034-BS-GC	54° 28' 19.8N 09° 59' 10.9E	Split and processed at U. of Kiel
	035-BS-BC	54° 30.21'N 10° 00.58'E	On board processing
	038-BS-BC	54° 29.74'N 09° 58.58'E	Detailed processing on board
	040-BS-BC	54° 29.20'N 09° 58.54'E	Detailed processing on board
	041-BS-BC	54° 29.37'N 09°59.64'E	Detailed processing on board
	048-BS-BC	54° 30' 01.2N 09° 52' 52.4E	Detailed processing on board
May 1993 Baltic Sea	210-BS-DC	N.A. (diver core)	Detailed processing on board
	225-BS-BC	54° 29' 43.2N 09° 59' 26.8E	Detailed processing on board
	238-BS-BC	54° 29' 35.7N 10° 00' 10.3E	Detailed processing on board
	252-BS-BC	54° 29' 36.3N 10° 00' 03.5E	Detailed processing on board
	264-BS-BC	54° 29' 37.18N 09° 59' 19.02E	Subsampled horizontally
	272-BS-BC	54° 30' 02.69N 10° 01' 40.63E	Minimum processing onboard

*GC: Gravity core BC: Box Core DC: Diver core (small box)

Table 7.1 (cont.).

Cruise	Core*	Location	Comments**
May 1993 Baltic Sea	304-BS-GC	54° 29' 33.5N 10° 00' 08.6E	Subsampled for undisturbed testing
	312-BS-GC	54° 29' 36.6N 09° 59' 28.6E	Subsampled for undisturbed testing
	318-BS-GC	54° 29' 32.4N 09° 58' 56.8E	Subsampled for undisturbed testing
	333-BS-GC	54° 33' 26.3N 10° 06' 06.4E	Subsampled for undisturbed testing
Aug./Sept. 1993 Panama City, FL	575-PC-GC	29° 41.52'N 85° 41.72'W	@URI
	576-PC-GC	29° 40.71'N 85° 40.84'W	@TAMU
	577-PC-GC	29° 40.95'N 85° 40.29'W	@URI
	581-PC-GC	29° 41.12'N 85° 40.43'W	@NRL
	584-PC-GC	29° 41.57'N 85° 40.94'W	@TAMU
	587-PC-GC	29° 41.09'N 85° 40.88'W	@URI
	590-PC-GC	29° 41.06'N 85° 40.81'W	@NRL
	592-PC-GC	29° 41.03'N 85° 40.49'W	@TAMU

*GC: Gravity core BC: Box Core DC: Diver core (small box)

**URI: University of Rhode Island TAMU: Texas A&M University

NRL: Naval Research Laboratory (at SSC).

Table 7.1 (cont.).

Cruise	Core*	Location	Comments**
Aug./Sep. 1993 Panama City, FL	596-PC-GC	29° 41.03'N 85° 40.50'W	@URI
	597-PC-GC	29° 42.11'N 85° 40.50'W	@URI
	622-PC-GC	29° 40.88'N 85° 40.91'W	@URI
	623-PC-GC	29° 41.02'N 85° 40.53'W	@URI
	628-PC-GC	29° 41.25'N 85° 40.20'W	@URI
	630-PC-GC	29° 40.83'N 85° 40.59'W	@TAMU

*GC: Gravity core BC: Box Core DC: Diver core (small box)

**URI: University of Rhode Island TAMU: Texas A&M University

NRL: Naval Research Laboratory (at SSC).

Table 7.2 Samples In Storage at URI/MGL, Taken During 1993 Cruises*.

Subsample Type	Cruise: Baltic Sea February 1993	Baltic Sea May 1993	Panama City, FL August 1993
1.5" Triaxial	10	11	0
2.0" Triaxial	9	41	0
2.0" Consol/Perm.	10	19	0
Shelby Tube	3	4	0
Bulk (in bag)	41	19	17
Gravity core	0	0	8
Vibracore	0	0	1
Diver Core	0	0	1

*Some of the these samples have already been tested and/or processed.

Table 7.3 Miscellaneous Water Contents and Densities (not in Figures) Baltic Sea, February and May 1993 Cruises.

Core	Cruise	Depth (cm)	Water Content* (%)	Bulk Density (g/cm^3)
035-BS-BC	Feb 93	2	382	1.12
264-BS-BC	May 93	27	278	1.23
272-BS-BC	May 93	1	267	-
		13	90	-

*corrected for 25ppt. salt content

Table 7.4 Peak Shear Strengths
Miniature Brookfield Vane*
Baltic Sea, May 1993 Cruise.

Core	Depth (cm)	Peak Strength (kPa)
210-BS-DC	1.2	0.32
	4.2	0.49
	4.9+	0.41
225-BS-BC	1.2	0.40
	4.7	0.55
	9.2	0.74
	13.2	0.92
	29.2	1.22
238-BS-BC	1.2	0.35
	4.2	0.57
	9.2	1.02
	14.7	1.22
	20.2	1.44
	26.2	1.60
252-BS-BC	1.2	0.50
	4.2	0.65
	9.2	0.63
	15.2	1.03
	21.2	1.09
	27.2	0.99

*Vane dimensions: 8mm × 8mm   Rotation speed: 0.5rpm

+ Taken with Wykeham-Farrance motorized vane device with torque transducer and 1.27cm×1.27cm vane.

Figure 7.1 Water Content and Density Profiles
Gravity Cores 029-BS-GC and 034-BS-GC
Baltic Sea, February 93 Cruise.

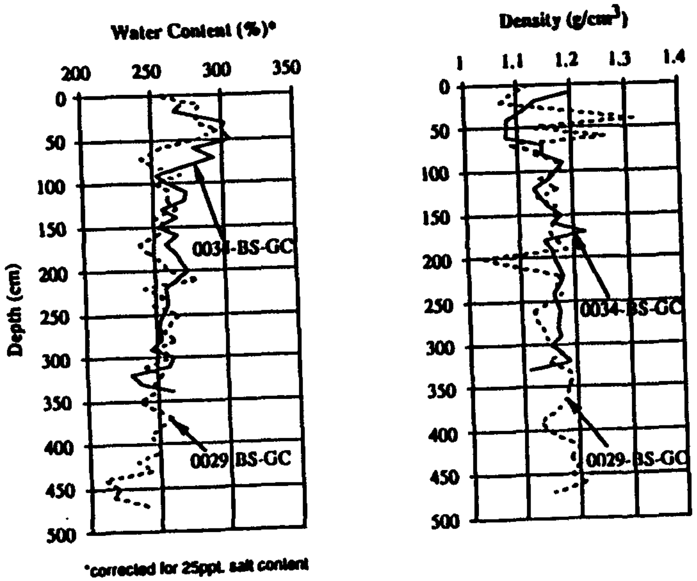

Figure 7.2 Water Content and Density Profiles
Box Core 038-BS-BC
Baltic Sea, February 93 Cruise.

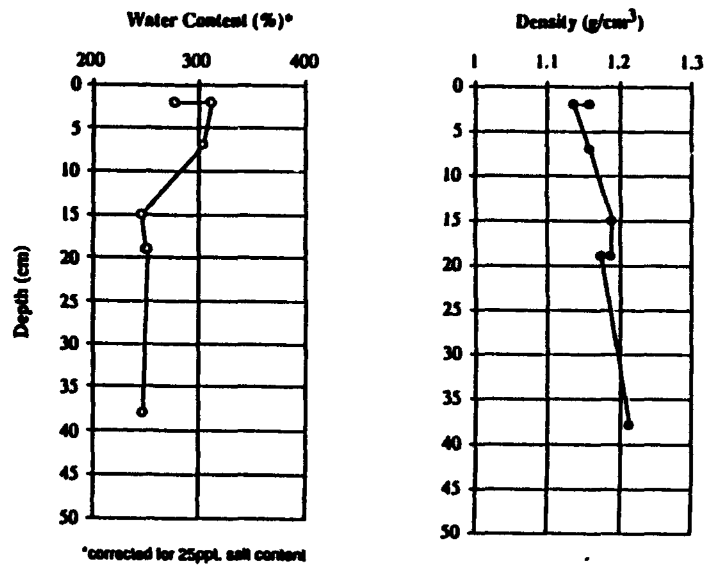

Figure 7.3 Water Content and Density Profiles
Box Core 040-BS-BC
Baltic Sea, February 93 Cruise.

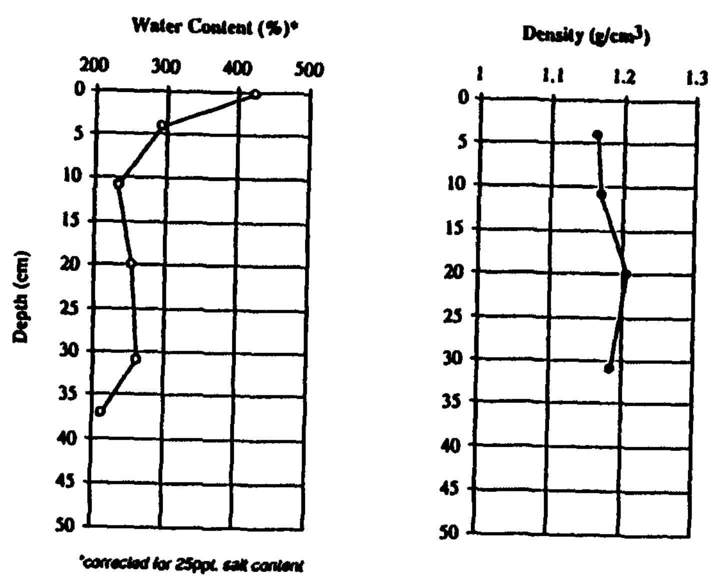

Figure 7.4 Water Content and Density Profiles
Box Core 041-BS-BC
Baltic Sea, February 93 Cruise.

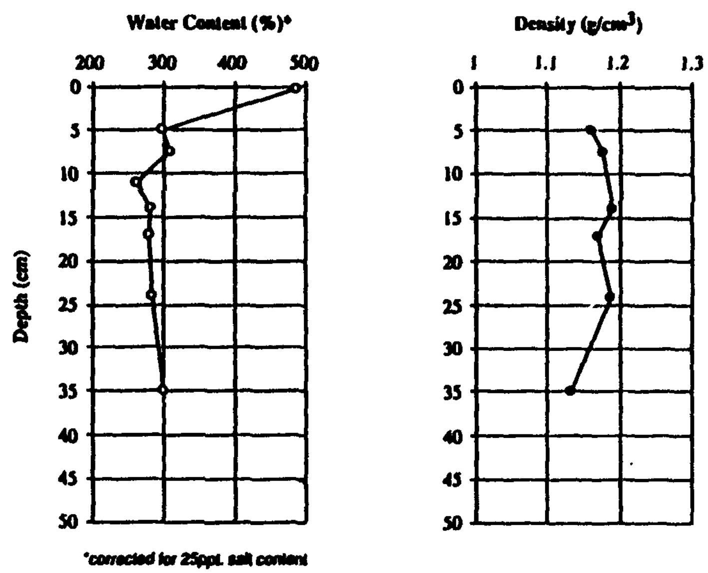

Figure 7.5 Water Content and Density Profiles
Box Core 048-BS-BC
Baltic Sea, February 93 Cruise.

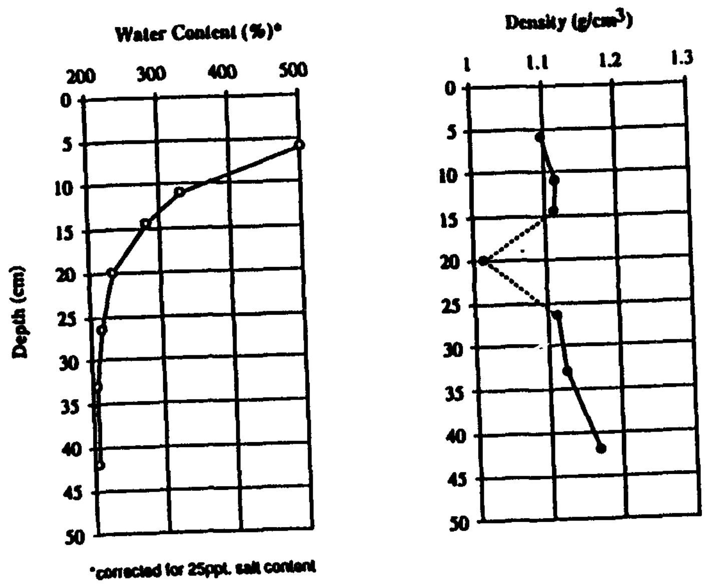

Figure 7.6
Salinity Profile
Box Cores and Gravity Cores
Baltic Sea, February 93 Cruise.

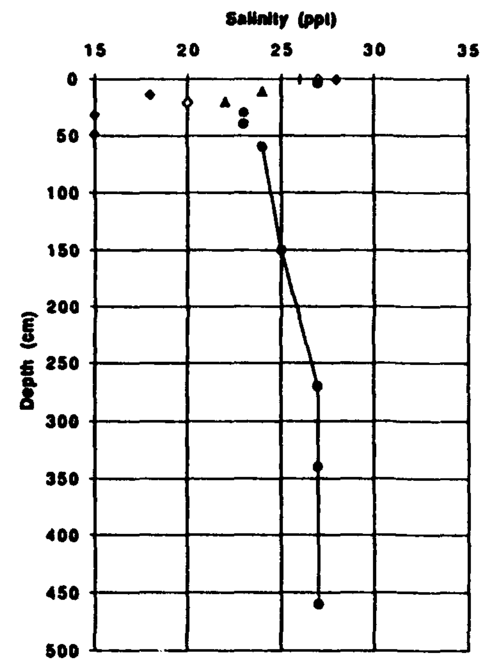

Figure 7.7 Water Content, Density and Shear Strength Profiles
Diver Box Core 210-BS-DC
Baltic Sea, May 93 Cruise.

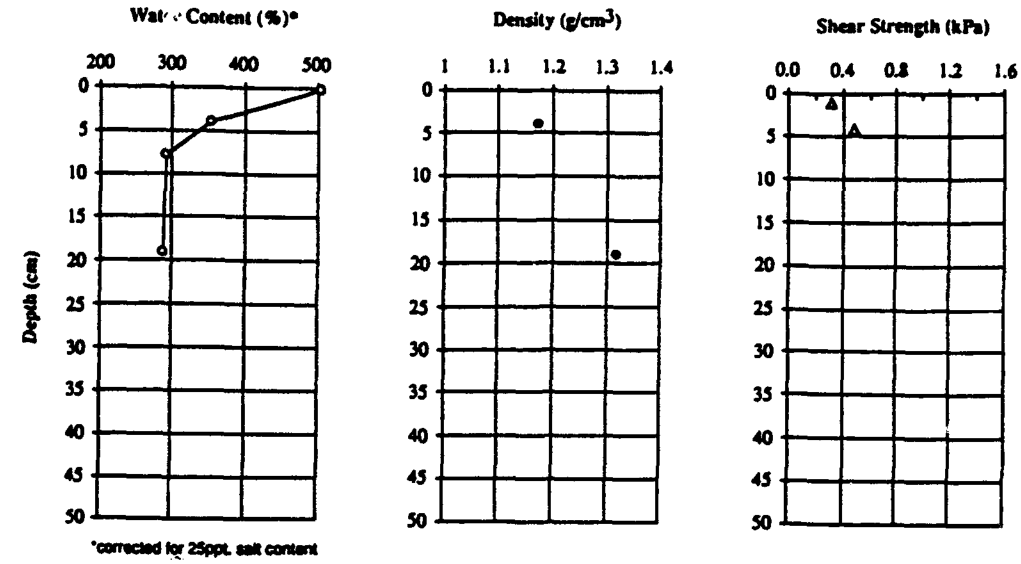

Figure 7.8 Water Content, Density and Shear Strength Profiles
Box Core 225-BS-BC
Baltic Sea, May 93 Cruise.

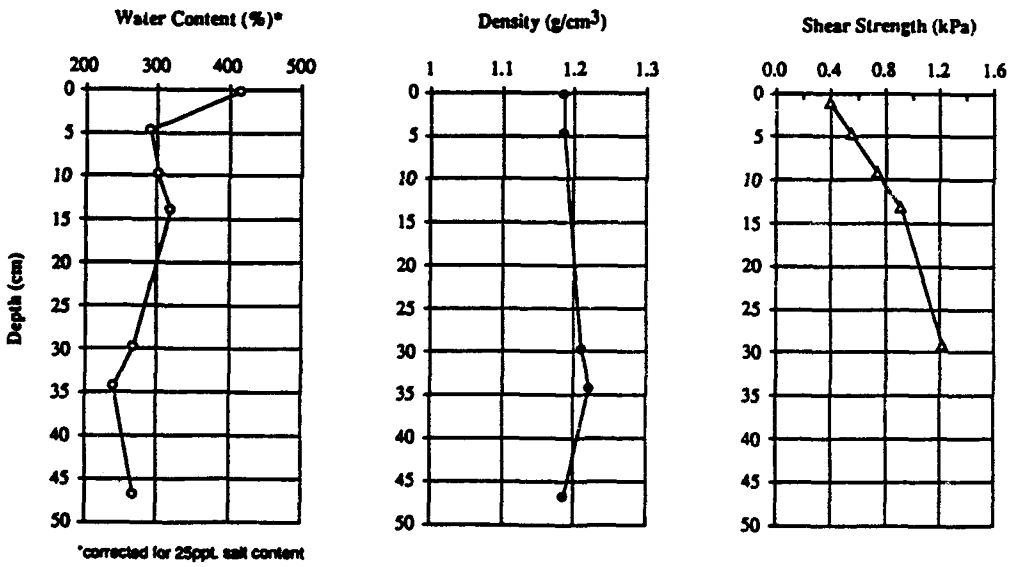

Figure 7.9 Water Content, Density and Shear Strength Profiles
Box Core 238-BS-BC
Baltic Sea, May 93 Cruise.

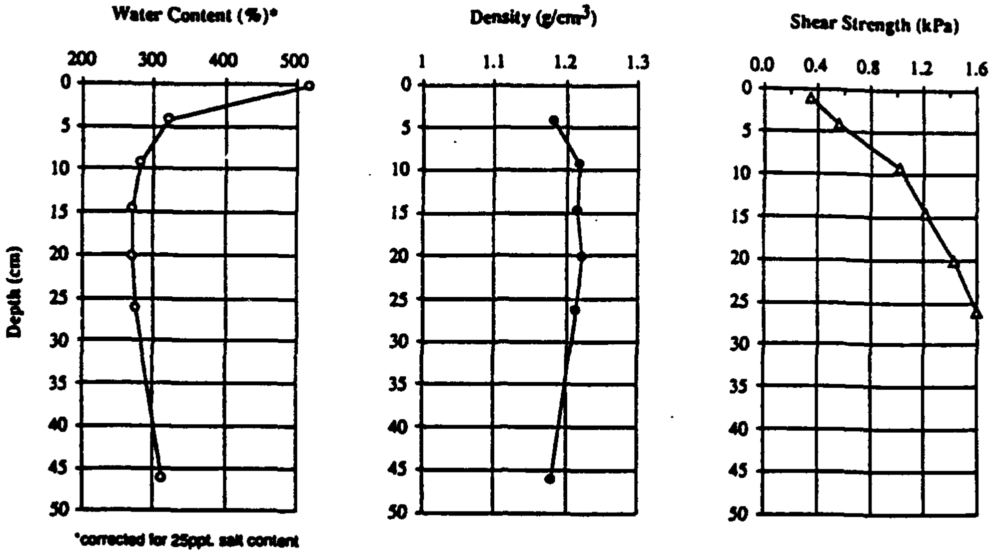

Figure 7.10 Water Content, Density and Shear Strength Profiles
Box Core 252-BS-BC
Baltic Sea, May 93 Cruise.

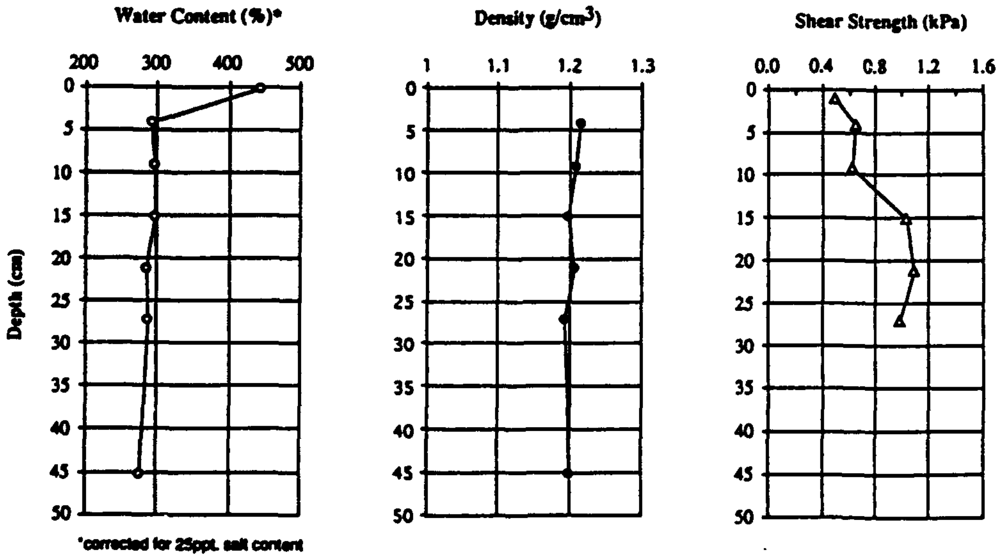

8. Geotechnical Laboratory Experimental Program

8.1 Introduction

A comprehensive geotechnical testing program has been initiated to analyze sediments obtained during the CBBL/SRP field experiments. The testing program involves an investigation of geotechnical properties, geoacoustic characteristics, and the relationships between them. Sediment samples have been obtained from the Baltic Sea and the Panama City, FL sites (Figure 8.1, Tables 7.1 and 7.2). To date, only sediments from the Baltic Sea site have been tested and this work is currently still in progress. Sediments recently obtained during the Panama City, FL experiment will be worked into the testing schedule and be evaluated in the coming year.

The primary geotechnical laboratory investigations performed to date include constant rate of deformation (CRD) consolidation, permeability and physical properties tests performed on the Baltic Sea site samples obtained during the February 93 and May 93 cruises. The consolidation and permeability data obtained to date correspond closely to permeability and consolidation data for similar ocean sediments reported by Nickerson (1978). In coming months, the testing program will also include triaxial compression stress-strain/strength and geoacoustic characterization with an emphasis on examining the effects of variability in microstructure and sediment type.

8.2 Experimental Test Plan

The focus of the overall testing plan is on investigating the effects of sediment variability and microstructure on geotechnical properties and geoacoustic characteristics. For the Baltic Sea sediments, we are using subsamples from gravity cores and box cores. In particular, we are looking at downcore and lateral variations in sediment characteristics with emphasis on variations in stress history, compressibility, consolidation, permeability, anisotropy, microstructure and geoacoustic response. We also intend to conduct tests on remolded sediment samples prepared under controlled conditions to study the same parameters for a completely disturbed condition. This will provide data for comparing the effects of microstructure at the in situ and remolded states. In addition, with our new triaxial acoustic measurement system, we will be studying the geoacoustic characteristics under the same types of conditions.

A comprehensive plan for the consolidation and permeability testing has been developed which considers the variations observed in sediment samples both laterally and vertically at the Baltic site. The test plan for triaxial compression and geoacoustic measurements is still being developed. Additionally, a detailed test plan for the Panama City, FL sediments will also be developed.

8.3 Consolidation and Permeability Testing

Consolidation and permeability tests are being performed using a constant rate of deformation (CRD), back-pressured consolidometer which uses state-of-the-art flow pump technology (Figure 8.2). The system employs two flow pumps, one of which is used to apply a constant rate of deformation during consolidation by infusing fluid at a constant rate into the load chamber of the consolidometer. Permeability measurement are made by using the second flow pump to induce a permanent flow across the sample and measuring the resulting pressure gradient. The deformation of the sample is measured by a Linear Variable Displacement Transducer (LVDT) located inside the consolidometer. The total stress on the sample as well as the pore pressure induced at the base of the sample are measured with reference to the back pressure by electronic differential pressure transducers. Special sensitive pressure transducers allow measurement of low pressures needed to test the very soft Baltic Sea sediments.

CRD tests have been conducted on a number of undisturbed Baltic Sea site samples obtained from the gravity and box cores. It should be noted that many samples showed evidence of gas expansion on-site and are probably somewhat disturbed. However, in the laboratory we resaturated and restressed the samples to near their in situ stress state, which probably restored some of the microstructure.

All CRD samples are 5.08 cm in diameter and 2.54 cm thick, and were backpressured to 414 kPa to ensure full saturation. In addition, a small seating load of 1.4 to 2.1 kPa was maintained during saturation. The back pressure was increased in steps of 34.5 kPa increments every thirty minutes up to 414 kPa. The 414 kPa pressure was maintained for 12 hours, after which a B-parameter test was performed to determine the degree of saturation. Back pressuring is especially effective for the Baltic Sea sediment samples, many of which showed evidence of gas bubbles. Measured B-parameters ranged from 0.95 to 0.99, thus indicating a high degree of saturation.

For CRD consolidation testing, constant rates of deformation were selected such that pore pressures developed were less than about 10% of total applied stress (Crawford, 1988). Continuous records of total stress, deformation and base pore pressure were recorded with the electronic data acquisition system and stored on disk. The progress of consolidation was monitored in real time during testing by the effective stress response of the sample, which was out-put to a strip chart recorder. Unloading was initiated after consolidation had progressed well beyond the preconsolidation pressure. In some of the tests the sample was also reloaded, thus completing a hysteresis loop from which the recompression index was obtained.

Permeability measurements were made three to eight times during each consolidation test using the flow pumps, which allowed low-gradient measurements that did not disturb the sample during consolidation. The approach used allowed sufficient time for establishing steady pore pressure levels between permeability tests. The permeant used in the system was sea water of salinity equivalent to that at the Baltic Sea site (25 ppt). Permeability was evaluated from the steady-state component of pore pressure difference across the sample as the permeant is forced through with the flow pump. The steady-state pressure drop across the sample, current sample thickness obtained from the deformation data, and the flow rate (known from the flow pump) are used to calculate permeability from Darcy's law.

8.4 Results and Discussion

8.4.1 CRD Consolidation Results

The results from CRD consolidation tests are given at Figures 8.3 to 8.15 and are summarized in Table 8.1. The effective preconsolidation stress, , was determined from these plots using Casagrande's procedure (Holtz and Kovacs, 1981). The compression index, C_c (slope of the straight-line portion of the *e-log* curve), and the overconsolidation ratio *OCR* (ratio of preconsolidation stress to existing in situ effective overburden stress), were also been determined from the CRD results. The preconsolidation stresses for all of the tested samples are plotted as a function of depth in Figure 8.16. Also included in that figure are the overburden stresses, , which were calculated using the unit weight versus depth relationships presented in Section 7 (Figures 7.1 through 7.5 and 7.7 through 7.10).

Figure 8.16 and Table 8.1 indicate that the sediments at the Baltic Sea site are in an *apparently* overconsolidated state. The *OCR* varies with depth, ranging between 4.0 and 9.3 in the upper 50 cm to 2.0 at 4 m depth (Figure 8.17). This type of OCR depth dependency has been observed at many other seabed locations around the world (Silva and Jordan, 1984). Since at the Baltic Sea site, as at many of these other locations, there is no evidence of overburden removal, it has been postulated that the observed overconsolidation is instead due to the formation of interparticle bonds in the presence of high concentrations of electrolytes, typical of sea water environments (Silva and Jordan, 1984). These high concentrations of interparticle bonds give rise to an *apparent overconsolidation* condition (preconsolidation stresses larger than existing in situ effective overburden stresses; Figure 8.16).

The compression index also varies with depth, ranging from slightly under 3.0 to nearly 6.0 in the upper 50 cm to 4.2 at 375 cm depth (Figure 8.18). Note however that the depth dependency of C_c is not well established since not many deep samples are available for testing. Nevertheless, the compression and recompression, C_r, values are quite large (Table 8.1 and Figure 8.18). This indicates that the Baltic Sea sediments are highly compressible, which is not surprising, given the large in situ void ratios (Section 7). It is possible that the large C_c and water content values may be due to the presence of smectites and high organics in the sediments.

Permeability, *k*, was measured at various void ratios, *e*, during each CRD test. The results are presented in Figures 8.3 through 8.15 along with the individual compression curves. As expected, the relationship between *e-log*, k is linear. The measured permeability ranged between 3 x 10^{-7} and 2 x 10^{-5} cm/s for void ratios from 3.8 to 7.2. This combination of large void ratios and relatively low permeabilities is typical of fine-grained marine sediments. The in situ permeability for each sample can be determined by extrapolating the linear *e-log k* relationship to the in situ void ratios.

Figure 8.19 shows the combined data from all tests conducted to date. The results appear to fall into two distinct categories, depending on whether the samples are from the Eastern or Western portions of the study site. A linear *e-log k* relationship is apparent for each category, regardless of whether the subsamples are from gravity cores or box cores. The only exceptions are the results from the two CRD tests conducted on samples 029-BS-GC (at 377 cm) and 333-BS-GC (at 59 cm). Since sample 029-BS-GC is much deeper and has a lower initial void ratio (e=6.2) than most of the other samples, the *e-log k* relationship is not expected to plot with either of the other two main categories. The reasons for the apparently inconsistent results for sample 333-BS-GC are not evident at this time.

8.5 Triaxial Compression and Geoacoustic Testing

In our previous research on deep sea clays, a significant difference in the stress-strain behavior of triaxial samples has been observed depending on whether the samples are consolidated isotropically (CIU) or anisotropically (CAU) prior to shear strength testing. Silva et al. (1983) conducted a comprehensive experimental laboratory study to investigate the strength and, isotropic and anisotropic quasi-static stress-strain behavior of fine-grained deep sea sediments. Triaxial compression tests were performed on undisturbed, reconstituted (remixed and reconsolidated) and remolded samples of deep sea clays from the North Central Pacific. Additionally, drained triaxial creep tests were also conducted. The test results indicated that microstructural rearrangements can significantly affect the stress-strain/strength characteristics and drained creep behavior of some sediments. In addition, Zizza and Silva (1988) conducted triaxial tests on Atlantic clays to study consolidation and stress history effects. It was observed that the CAU test specimens exhibited brittle failure, achieved failure at markedly smaller strains and generally had higher magnitude Mohr-Coulomb strength parameters than did the CIU samples. From both of these investigations it was concluded that laboratory studies to simulate in situ stress conditions should include CAU testing.

The URI/MGL triaxial testing program planned for the next phase of the CBBL/SRP will incorporate the experience from our previous research and some new approaches. This includes use of a new non-contacting radial deformation strain gage system for CAU testing, and a new acoustic system for compressional and shear wave measurements, the latter patterned after the existing system at NRL. The focus of this work will be on determining the relationships between sediment properties and geoacoustic behavior for variations in sediment microstructure, sediment type and state of stress.

Table 8.1 Summary of CRD Consolidation Test Results
Baltic Sea, February and May 1993 Cruises

Sample Designation	Mean Sample Depth (cm)	Water* Content (%)	Bulk Density (g/cm3)	Init. Void Ratio	σ'_c (kPa)	σ'_o (kPa)	OCR	C_c
029-BS-GC	73	252	1.17	6.6	3.8	1.0	3.6	3.0
029-BS-GC	377	238	1.17	6.2	11.0	5.4	2.0	4.2
034-BS-GC	142	250	1.18	6.5	6.0	2.1	2.9	3.7
035-BS-BC	16	285	1.17	7.4	1.9	0.3	7.4	3.2
035-BS-BC	26	254	1.17	6.6	1.9	0.3	5.7	3.0
035-BS-BC	33	274	1.17	7.1	2.8	0.5	6.0	4.5
038-BS-BC	19	249	1.18	6.6	2.6	0.3	9.3	5.8
040-BS-BC	32	238	1.18	6.2	2.4	0.5	4.4	4.8
238-BS-BC	31	284	1.20	7.4	2.3	0.5	4.4	4.0
252-BS-BC(1)	29	284	1.20	7.4	2.0	0.5	4.0	2.8
252-BS-BC(2)	29	276	1.20	7.2	2.3	0.5	4.6	3.4
304-BS-GC	141	280	1.20	7.3	4.3	2.4	1.8	2.9
333-BS-GC	60	266	1.20	6.9	3.5	0.9	4.1	2.9

* Corrected for 25 ppt salinity

Note σ'_c: Effective preconsolidation stress

σ'_o: Effective overburden stress (Calculated from Figures 7.1 through 7.10)

OCR: Overconsolidation ratio

C_c: Compression index

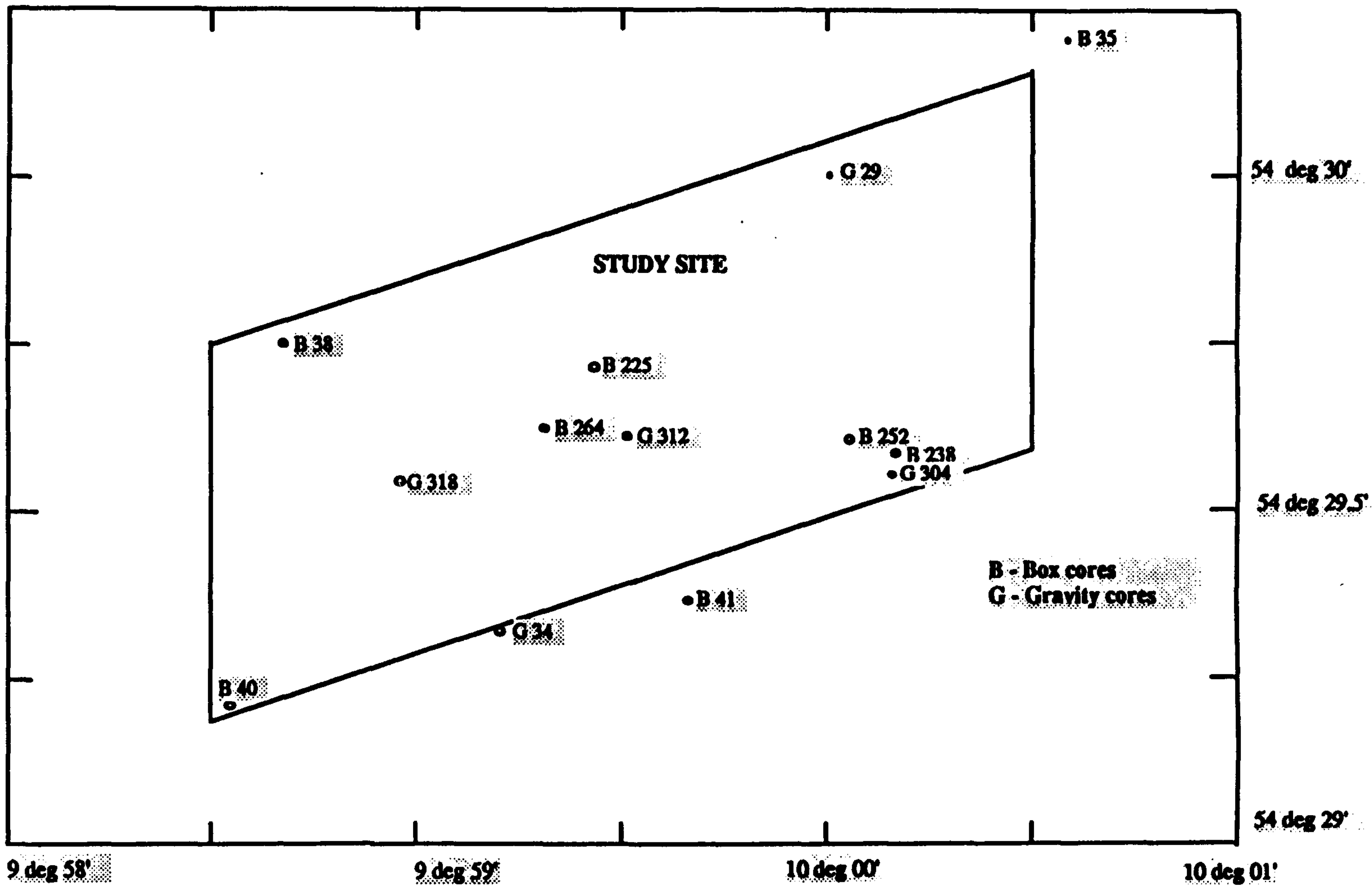

Figure 8.1 Location of principal URI/MGL Gravity and Box Cores at Baltic Site, February and May 1993 Cruises

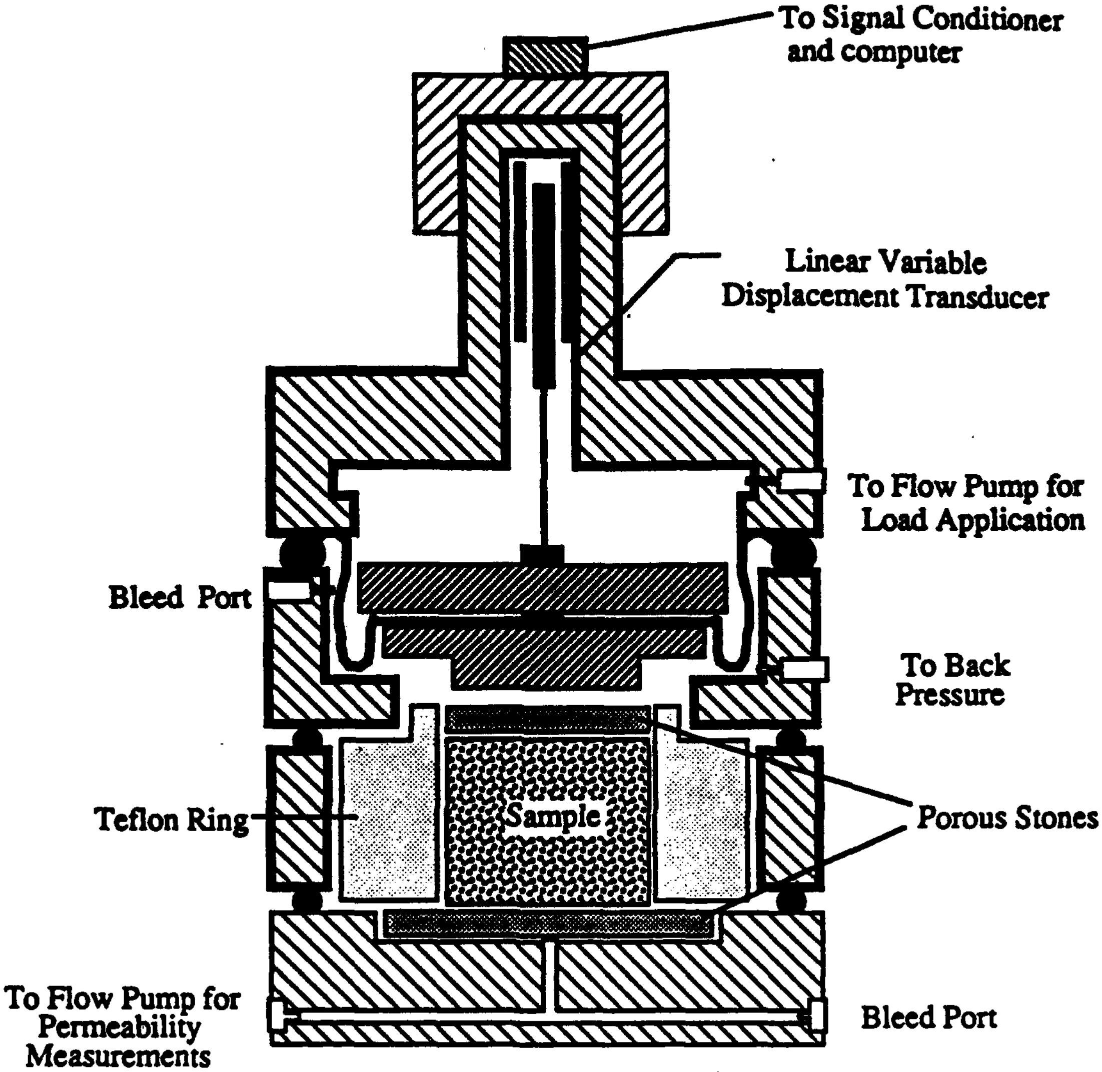

Figure 8.2 Schematic of Constant Rate of Deformation Consolidometer.

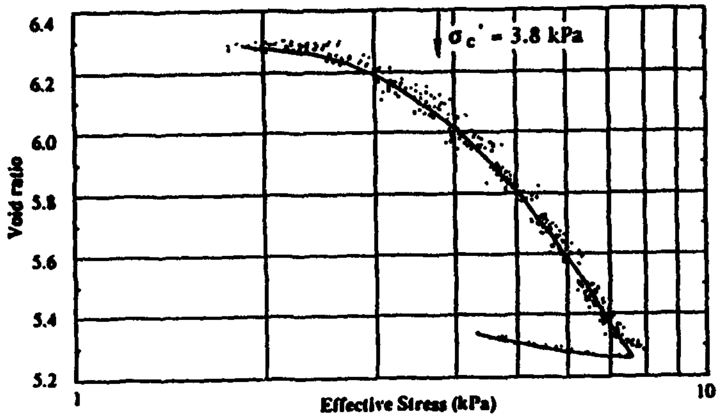

(a) Compression Curve

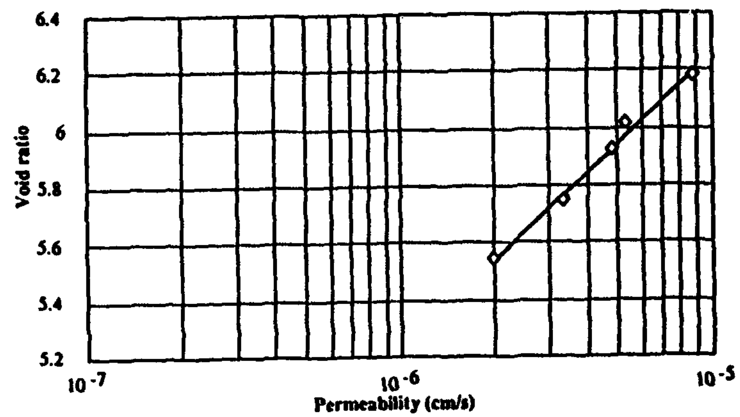

(b) Permeability Measurements

Figure 8.3 Sample 029-BS-BC, 73 cm Depth.

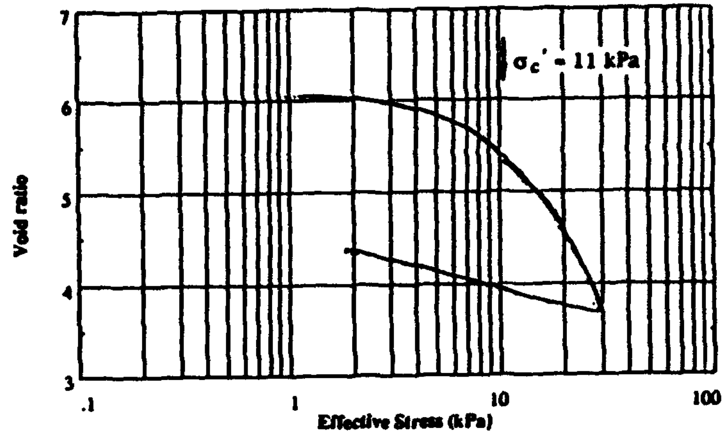

(a) Compression Curve

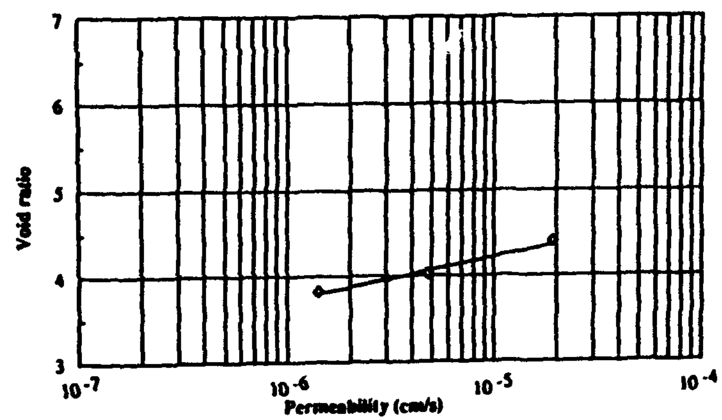

(b) Permeability Measurements

Figure 8.4 Sample 029-BS-BC, 377 cm Depth.

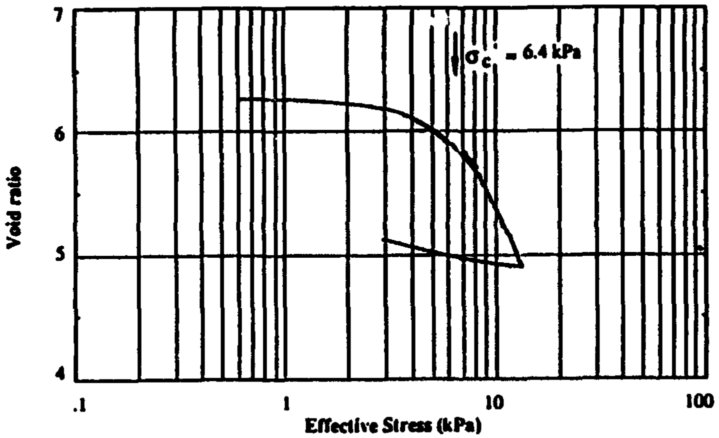

(a) Compression Curve

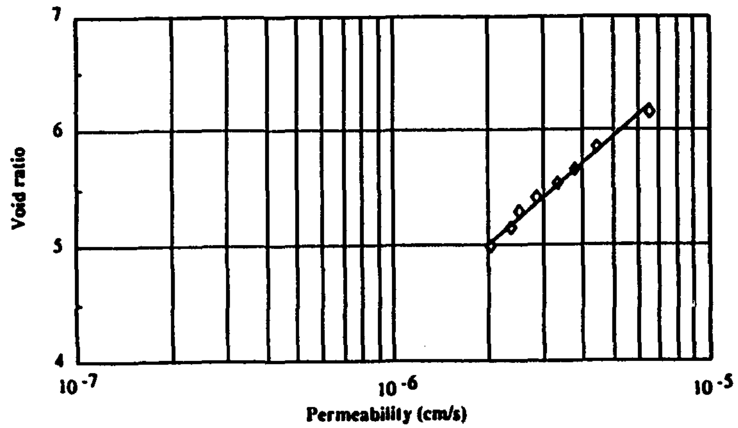

(b) Permeability Measurements

Figure 8.5 Sample 034-BS-BC, 142 cm Depth.

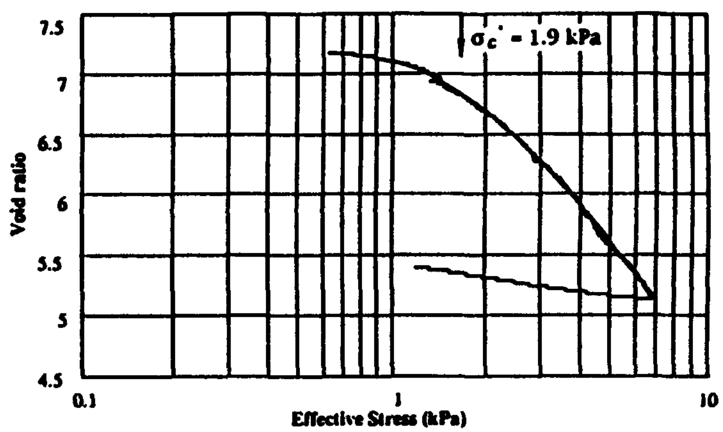

(a) Compression Curve

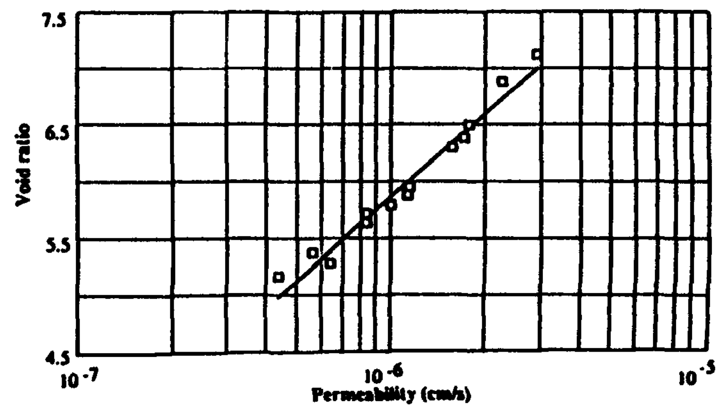

(b) Permeability Measurements

Figure 8.6 Sample 035-BS-BC, 16 cm Depth.

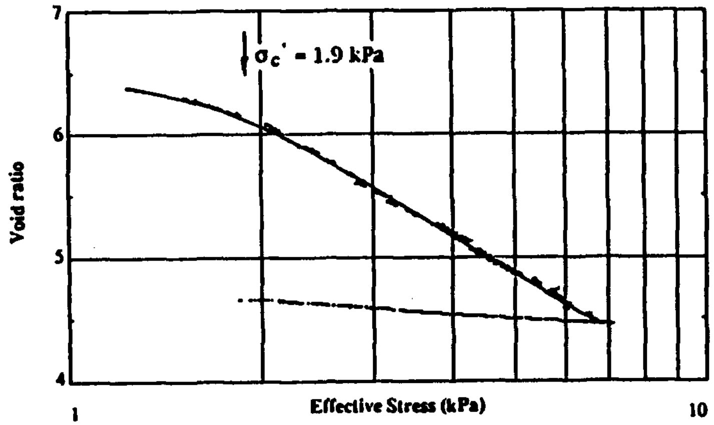

(a) Compression curve

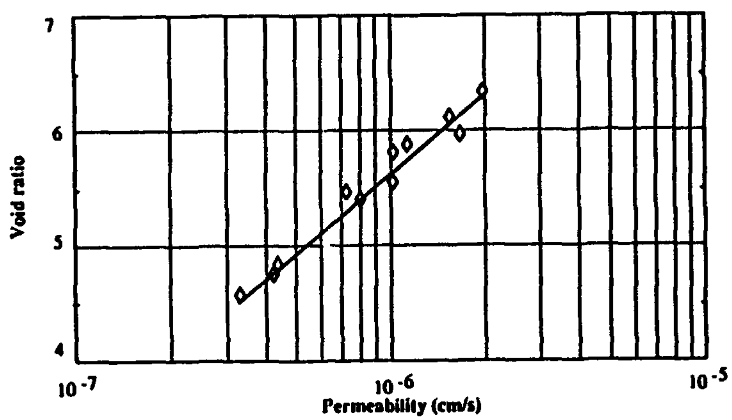

(b) Permeability Measurements

Figure 8.7 Sample 035-BS-BC, 26 cm Depth.

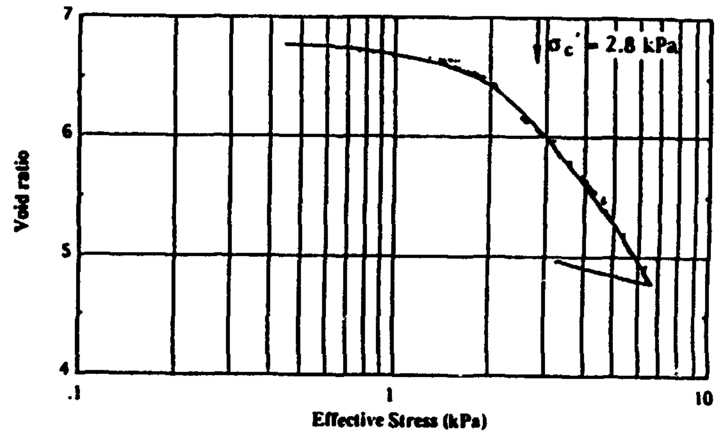

(a) Compression Curve

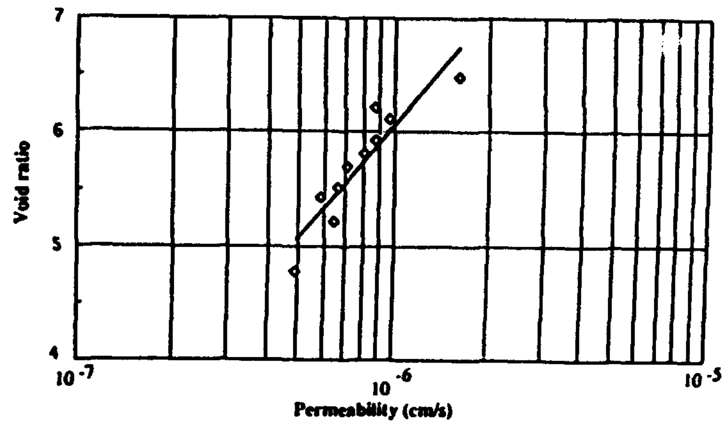

(b) Permeability Measurements

Figure 8.8 Sample 035-BS-BC, 33 cm Depth

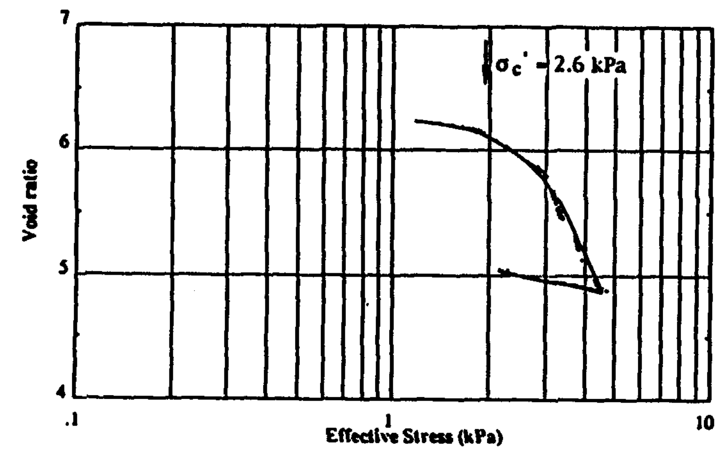

(a) Compression Curve

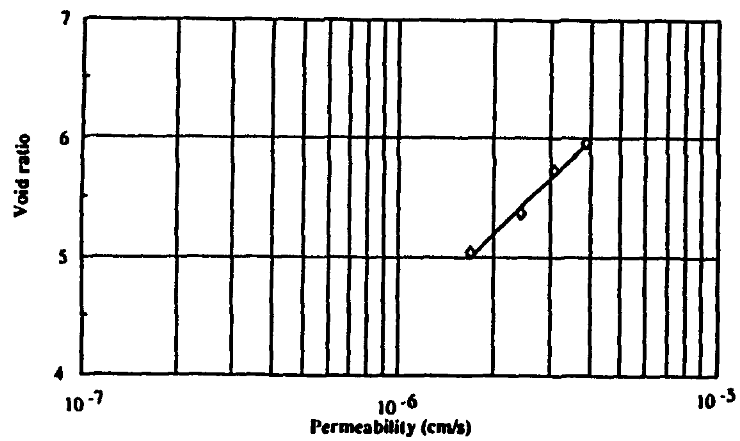

(b) Permeability Measurements

Figure 8.9 Sample 038-BS-BC. 19 cm Depth.

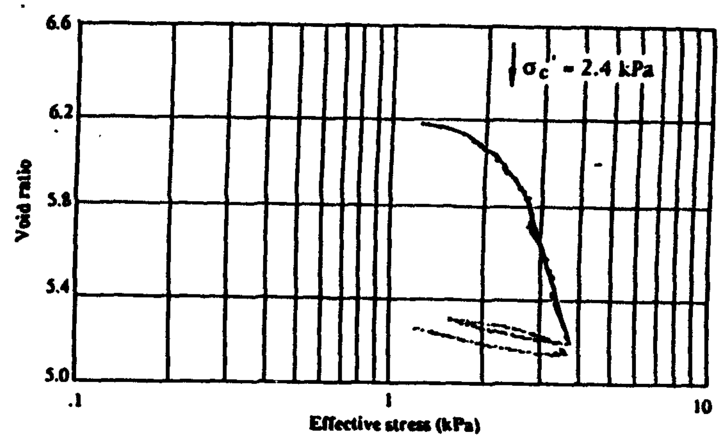

(a) Compression Curve

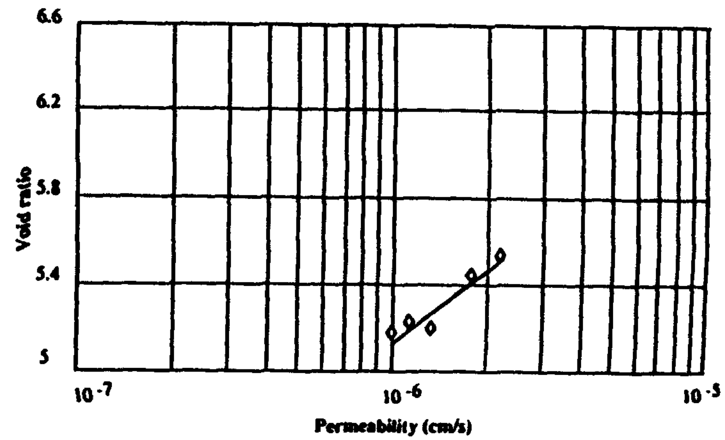

(b) Permeability Measurements

Figure 8.10 Sample 040-BS-BC, 32 cm Depth.

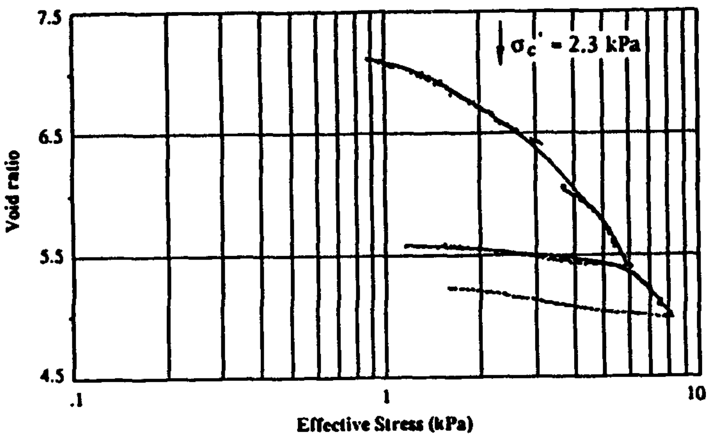

(a) Compression Curve

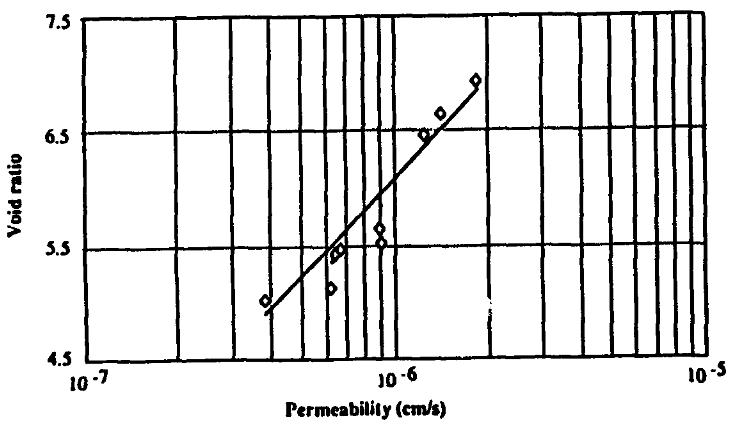

(b) Permeability Measurements

Figure 8.11 Sample 238-BS-BC, 31 cm Depth.

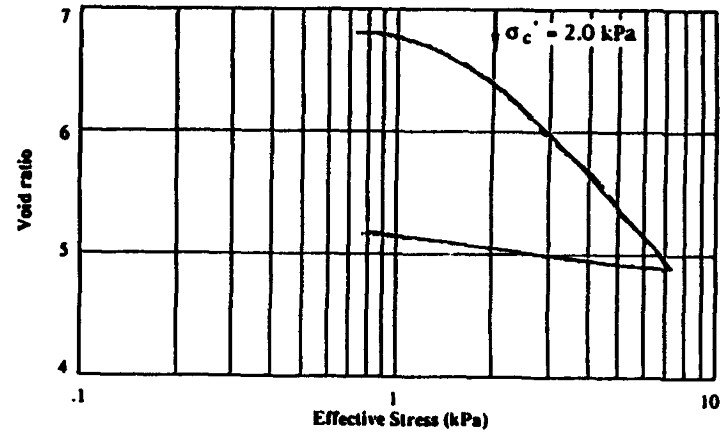

(a) Compression Curve

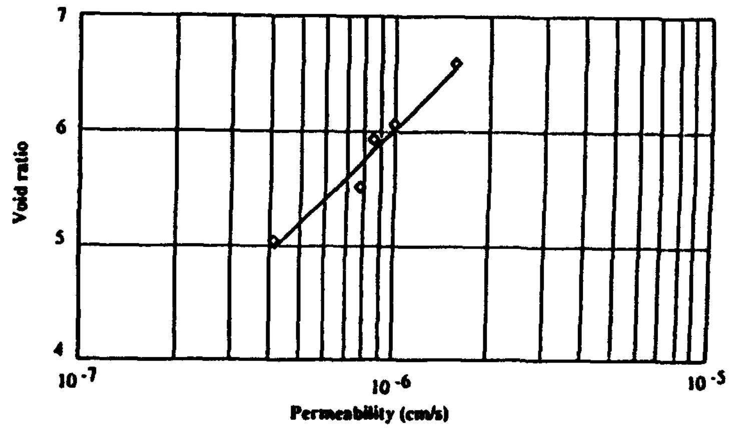

(b) PermeabilityMeasurements

Figure 8.12 Sample 252-BS-BC(1), 29 cm Depth.

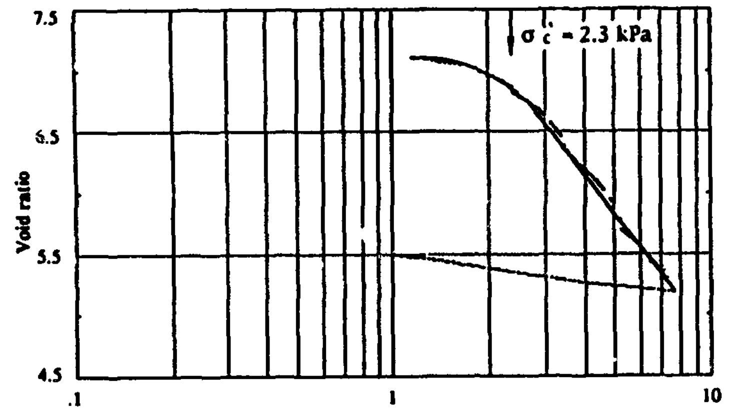

Effective Stress (kPa)

(a) *Compression* Curve

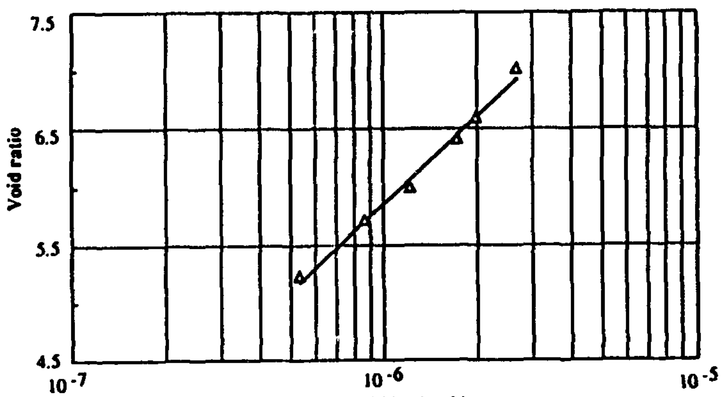

Permeability (cm/s)

(b) Permeability Measurements

Figure 8.13 Sample 252-BS-BC (2), 29 cm Depth.

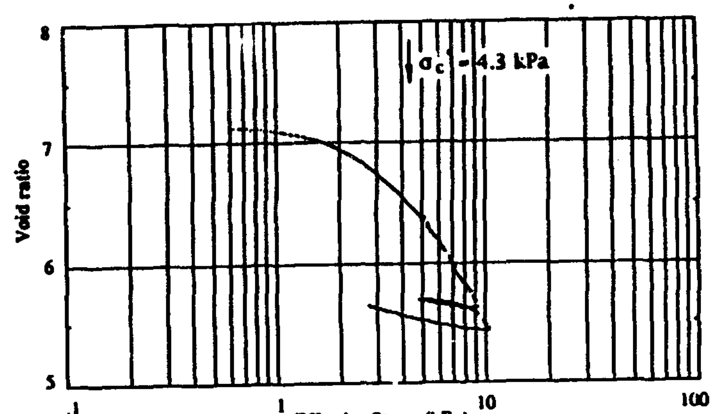

Effective Stress (kPa)

(a) Compression Curve

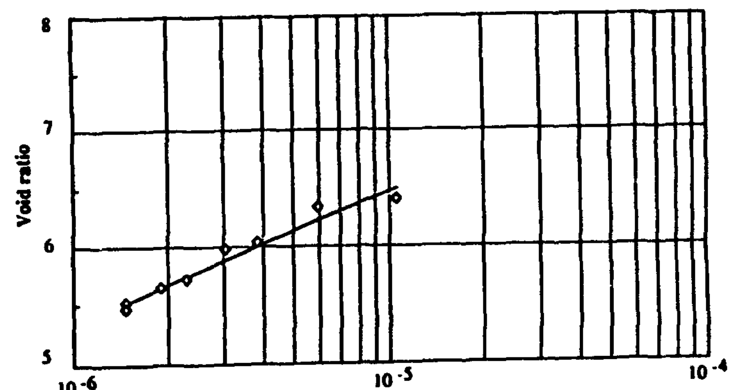

Permeability (cm/s)

(b) Permeability Measurements

Figure 8.14 Sample 304-BS-GC, 141 cm Depth.

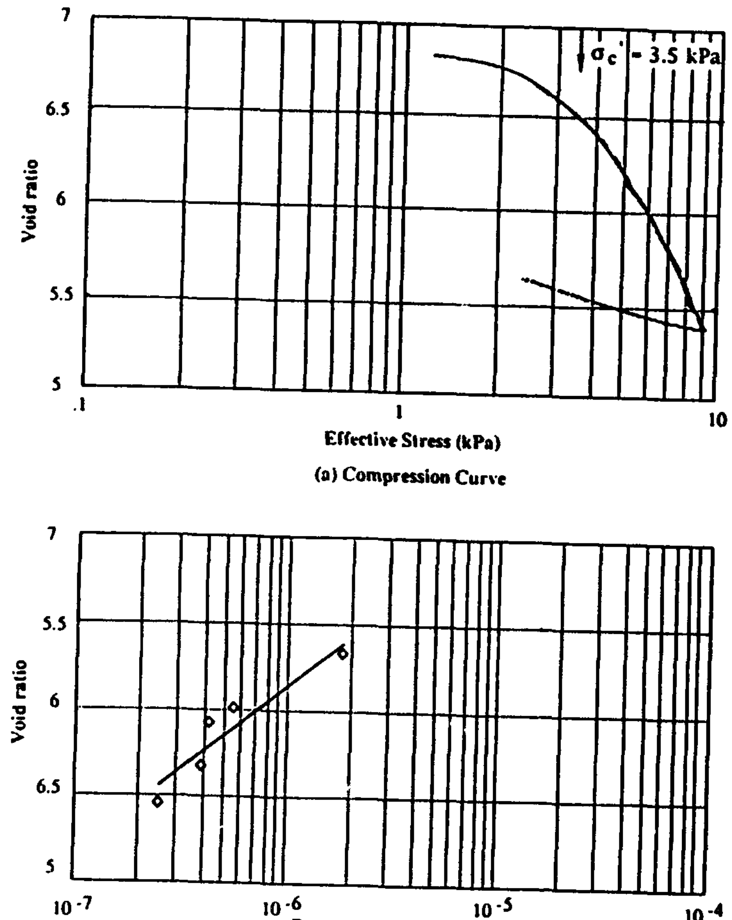

Effective Stress (kPa)

(a) Compression Curve

Permeability (cm/s)

(b) Permeability Measurements

Figure 8.15 Sample 333-BS-BC, 60 cm Depth.

Figure 8.16
In Situ Stress Profiles from Consolidation Tests; Baltic Sea, February and May 1993 Cruises

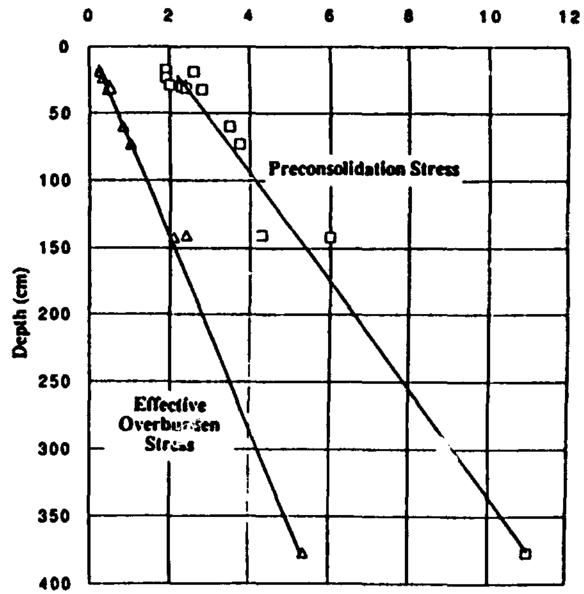

Figure 8.17
OCR Profile; Baltic Sea, February and May 1993 Cruises

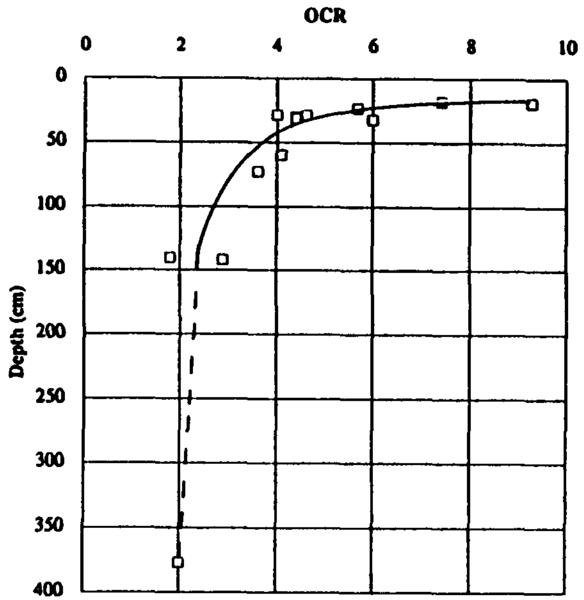

Figure 8.18
Compression Index Profile; Baltic Sea, February and May 1993 Cruises.

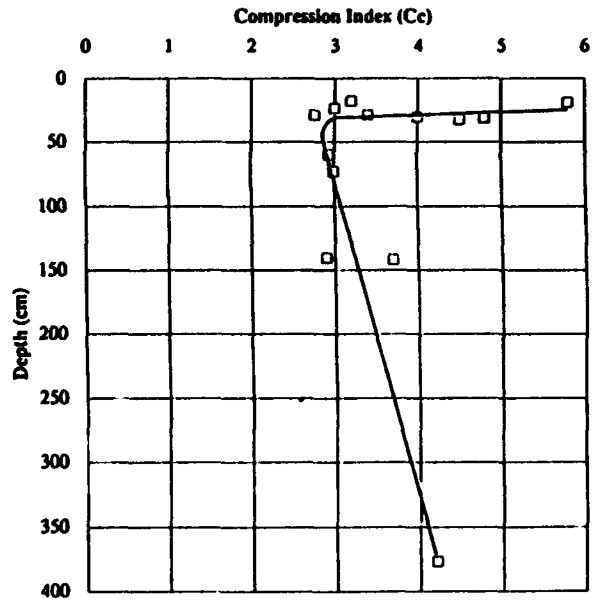

Figure 8.19 Variation of Permeability with Void Ratio for Box Core and Gravity Core Samples; Baltic Sea, February and May 1993 Cruises.

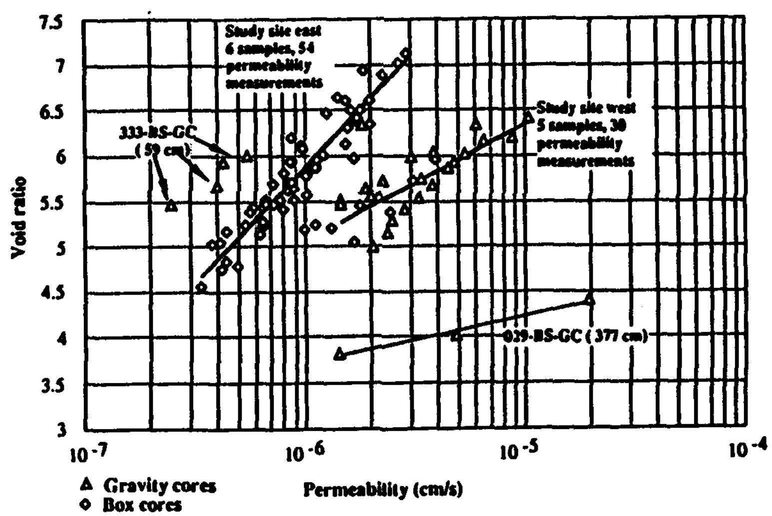

9. Geoacoustic Microstructural Modeling

9.1 Introduction

Our microstructural modeling efforts are being conducted in order to understand and theoretically simulate the variation of geoacoustic wave propagation characteristics that are related to the material fabric in seafloor sediments. The emphasis in this segment of our program is to establish reasonable models of sediment fabric, and to analyze geoacoustic propagational characteristics through such model media. To date our studies have been involved with granular type sediments, and thus our modeling has been associated with the creation and dynamic simulation of assemblies of particulate materials. Later research will address geoacoustic behavior of clay sediments, and new modeling strategies will be developed.

Our initial efforts in modeling the acoustic response of marine sediments has begun with the theoretical and numerical simulation of fluid-saturated granular materials using the *discrete element method.* This computational method was originally developed by Cundall (1971) and Cundall and Strack (1979) to model the response of discontinuous materials by studying the behavior of individual idealized particles in assembly systems. For applications to wave propagation, this scheme employs large assemblies of idealized particles to model the dynamic behavior of granular geomaterials. Numerous studies by Sadd, et. al. (1989, 1991 and 1993) have shown that such modeling techniques can simulate granular materials and predict results which compare with experimental data. The numerical strategy uses Newtonian rigid-body dynamics to calculate the translational and rotational motion of each particle in these model assemblies. Through assumed particle overlap or local elastic deformation, interparticle contact forces develop between adjacent grains. In this fashion, the dynamic/acoustic response of the model system may be determined, and parameters such as wave speed and amplitude attenuation can be calculated for specific model assemblies. Furthermore, these wave propagational characteristics can be related to the model material's microstructure or fabric.

Contact forces between adjacent particles in the assembly are developed through prescribed contact laws, and these laws play a key role in determining the constitutive response at the micro-level. Much of our beginning work focused on developing new contact models for particles interacting with each other through a fluid. The presence of pore fluid can have significant effects on the dynamic response of granular materials by adding viscous drag forces on particles and by changing the contact response between adjacent particles through *squeeze-film elastohydrodynamic action.*

9.2 The Discrete Element Method

As mentioned, the discrete or distinct element method is a modeling strategy which uses Newtonian rigid-body mechanics to model the translational and rotational motion of particles in model material assemblies (Figure 9.1). Contact laws between adjacent particles are constructed which serve to determine the contact force as a function of the relative displacement or relative velocity between the particles. Applying Newton's law to the *i-th* particle would yield

$$\sum_{j=1}^{n} \mathrm{F}^{(ij)} + \mathrm{F}^{(i)} = m_i \ddot{x}_i \tag{9.1}$$

where $F^{(ij)}$ are the j-contact forces on the *i-th* particle and $F^{(i)}$ represents any non-contacting forces (e.g. viscous drag). Equation (9.1) would then yield the particle acceleration with given contact and non-contact forces. The technique establishes a discretized time stepping numerical routine, in which granule velocities and positions are obtained from numerical integration of the computed accelerations. It is assumed that during each time step, disturbances cannot propagate from any particle further than its immediate neighbors. Under these assumptions, the method becomes explicit, and therefore at any time increment the resultant forces (and thus the accelerations) on any particle are determined solely by its immediate neighbor interactions. In wave propagation applications, the movements of the individual particles are a result of the propagation through the medium of disturbances originating at particular input loading points. Consequently, wave speed and amplitude attenuation (intergranular contact force) will be functions of the physical properties of the discrete medium, i.e. the microstructure. Figure 9.2 illustrates a typical flowchart of the discrete element method. In order to model actual geomaterials, the method is typically applied to granular systems containing large numbers of idealized particles (e.g. circular disks or spheres) in regular or random packing geometries. Such model materials can be computationally generated with varying degrees of microstructural fabric.

9.3 Contact Laws for Particles in Saturated Media

Our modeling efforts began with the development of new contact laws governing particle interactions through a fluid. As mentioned, the presence of pore-fluid will create several new forces at the particulate level. For the nearly fully saturated conditions that we would expect in marine sediments, the capillary forces would be negligible; whereas the phenomena of viscous drag and squeeze-film contact lubrication would produce sizeable particulate forces. Viscous drag effects would be predominant for large particle spacings where neighboring interaction forces are vanishingly small. On the other hand, squeeze-film contact forces would be the most significant for dense packings of particulate systems, and this would seem to be the predominant case for most consolidated marine sediments.

In order to model this squeeze-film effect, consider the case of two particles (approximated as two circular disks) embedded in a viscous fluid, and approaching each other with a relative normal velocity $V(t)$ (see Figure 9.3). The fluid film in the contact zone will be squeezed, and a sizeable pressure is thus built up in this contact region. The fluid pressure distribution in the gap will exert a loading on each particle surface, and this loading is sufficient in certain cases to produce significant particle deformation. In this fashion, the contact law governing particle interactions for saturated granular materials changes considerably from the contact mechanics for dry materials. The saturated case is more complicated since it involves a coupling of both fluid and solid behavior.

The contact force for such a problem can be modeled using the theory of *elastohydrodynamics*. The schematic of the two-disk squeeze-film problem shown in Figure 9.3 describes the problem geometry. The distance between particle surfaces is denoted by $h(x,t)$, a function of coordinate x and time t, and δ (x,t) is the granule deformation. Under certain assumptions the fluid pressure $p(x,t)$ can be related to $h(x,t)$ by the *Reynolds equation of lubrication theory*

$$\frac{\partial}{\partial x}\left(h^3 \frac{\partial p}{\partial x}\right) = 12\eta \frac{\partial h}{\partial t} \tag{9.2}$$

where η is the viscosity of the fluid.

Since $h(x,t)$ can include particle deformation δ (x,t), which is determined by elasticity theory, equation (9.2) is a *coupled relation*, and typically an iterative numerical method would be required to solve this equation for the pressure distribution $p(x,t)$. Incorporating such a numerical scheme into the discrete element method would result in a very computationally intensive procedure, and would therefore result in unreasonable amounts of CPU time to run the simulations. Therefore a simplified alternative procedure was developed in order to avoid the numerical complexities. This simplified approach first assumes that the particle is rigid, and this allows a closed-form solution for $p(x,t)$ from equation (9.2). Once this pressure distribution is found, the particle deformation may be calculated from elastic contact stress theory, and this new particle shape may be then used to calculate a new pressure distribution. Thus initially let δ (x,t) = 0, and the undeformed particle surface can be approximated by the relation

$$h(x,t) \approx h(0,t) + \frac{x^2}{2R} \tag{9.3}$$

where R is the particle radius. The solution to the Reynolds equation (9.2) for this case is

$$p(x,t) = -6R\eta \frac{V(t)}{h^2(x,t)} \tag{9.4}$$

With the pressure distribution known, the total contact load between the particles is given by integrating the pressure, i.e. $F = H \int pdx$, where H is the disk thickness. Carrying out the integration over the disk surface yields

$$F(t) = 3\sqrt{2}\pi\eta H\left(\frac{R}{h(0,t)}\right)^{3/2} V(t) \tag{9.5}$$

In order to include the effects of particle deformation, a combined model with two series-connected stiffness (spring) elements may be used. One spring element represents the fluid stiffness while the other element includes the solid (particle) stiffness resulting from the elastic deformation within the particle. The pressure loading will produce deformations such that the distance between particle surfaces will change from h to $h(x,t) + \delta\ (x,t)$, where $\delta\ (x,t)$ is the contact deformation for the dry case. If the disk shape is assumed to be unchanged, then the new load $F(t)$ is still given by equation (9.5) using the modified value of $h(x,t)$, i.e.

$$F(t) = 3\sqrt{2}\pi\eta H\left(\frac{R}{h(0,t)+\delta}\right)^{3/2} V(t) \tag{9.6}$$

In dry granular materials, our previous research has indicated that the normal contact force F can be related to contact deformation by the relation $F = K\delta^{1.4}$, where K is a material constant. Obviously the forces in the fluid and solid springs should be equal, and this leads to the result

$$F(t) = 3\sqrt{2}\pi\eta H\left(\frac{R}{h(0,t)+\delta}\right)^{3/2} V(t) = K\delta^{1.5} \tag{9.7}$$

where on the right-hand side, the exponent on δ has been modified for convenience to the value of 1.5. Solving equation (9.7) for δ and substituting the result into equation (9.6) yields

$$F(t) = \frac{C_1 V(t)}{\left(0.5\left(h(0t) + \sqrt{h^2(0,t) + 4(\frac{C_1}{K})^{2/3}}\right)\right)} \tag{9.8}$$

where $C_1 = 3\sqrt{2}\pi\eta R^{3/2} H$. Equation (9.8) then gives the normal contact force when two disks approach each other. For the case when the two particles move apart, contact law (9.8) is not suitable since a negative velocity V may lead to a negative value within the square root. For this case the solid contact law will be used.

The above results address only the normal contact response between particles. For the tangential contact behavior, a simple modeling scheme is created based upon the simple shearing of a Newtonian fluid within the small inter-particle gap as shown in Figure 9.4. If the gap is small then the fluid motion may be approximated by a linearly varying distribution, and the resulting shear stress between the particles will then be given by

$$\tau = \eta\frac{\partial U}{\partial z} = \eta\frac{\Delta U}{\Delta z} = \frac{V_1 - V_2}{h} \tag{9.9}$$

where U is the relative tangential velocity between particles. Thus the force between any two generic particles can be estimated by the product of this shear stress times an effective area within the gap zone. We are currently experimenting with various schemes to determine appropriate effective areas for the calculation of the tangential force.

9.4 Results

In order to investigate the merit of the proposed modeling scheme, several one- and two-dimensional material models were created, and the discrete element computer code was applied to each of these models under specific dynamic loading conditions designed to simulate geoacoustic wave propagation.

9.4.1 One-Dimensional, Single Chain Simulation

The previously described contact law has now been incorporated in our basic discrete element computer code. Preliminary computer runs have been conducted in order to simulate the acoustic wave propagation in a one-dimensional granular material simulated by a single straight chain of circular disks as shown in Figure 9.5. Considering the modeling of a coarse sand, the circular particles had a diameter of 2mm, thickness of 1mm, and were assumed to be of quartz with a density of 2650 kg/m^3. The simulations incorporated a 0.0001 mm gap between each neighboring particles, and the model system was assumed to be completely saturated with water of viscosity of 0.0008 N-s/m^2. The input loading applied to one end of the chain was taken to be a triangular time dependent pulse of duration of 5 μs with a peak value of 2 N to simulate a wave front acoustic pressure of 10^6 N/m^2 (i.e. 10 bar).

Using these parameters, a computer simulation was run and the wave attenuation results are shown in Figure 9.6. It was found that the attenuation is quite large during the passage through the first several particles, but then the attenuation rate decreases with the propagational distance. These preliminary simulations indicated that the wave speed was approximately 840 m/s. The effects of the gap distance and viscosity on the wave speed was also investigated, and these results are shown in Figure 9.7. As expected, the wave speed decreases with the gap distance, and when the gap is small, these effects are rather pronounced. An increase of fluid viscosity also leads to a decrease of the wave speed, and again this variation was most severe for the case of small gap distances.

9.4.2 Two-Dimensional Simulations

In order to investigate the use of the model for a multi-dimensional simulation, a two-dimensional granular model assembly was generated. The assembly shown in Figure 9.8 was created using one of our computational random media generators. These generating codes can create large random particulate assemblies with varying degrees of microstructural fabric such as porosity, coordination number, particle contact normal distributions, void vectors, etc. Dynamic input for wave propagation was created through simultaneous loading of particles along the left side of the assembly of the same magnitude and time history as used in the one-dimensional simulations. The transmitted wave output (measured by the inter-particle contact forces) was collected among the particles along the right side of the assembly. An example of this left-to-right transmission computer simulation is shown in Figure 9.9 which illustrates the normalized average wave transfer through the assembly. The vertical scale represents the average of all of the interparticle load transfers at the output (right) side of the assembly normalized with respect to the input. Specific attenuation and dispersion characteristics can thus be determined from the peak and spread of the transmitted profile. Several computer simulations of this type will be conducted on a variety of assemblies with different microstructures in an effort to relate microstructure to the geoacoustic wave propagational characteristics.

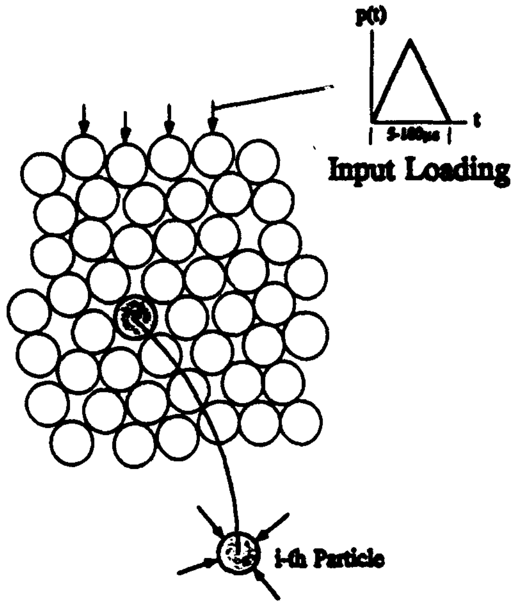

Figure 9.1 Discrete/Distinct Element Schematic

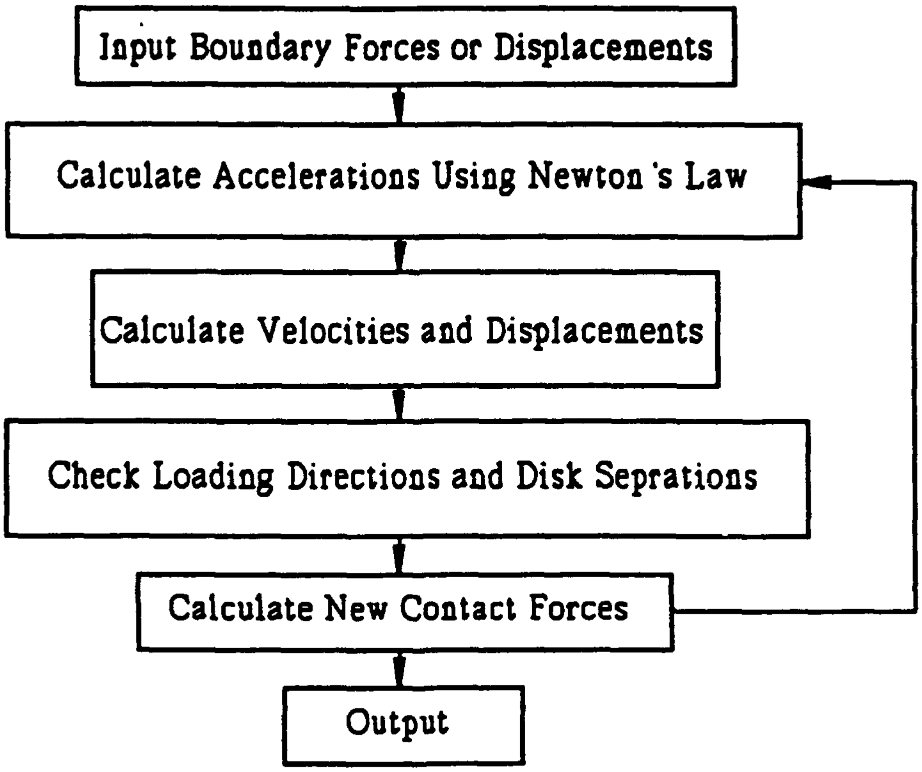

Figure 9.2 Discrete Element Method Flowchart

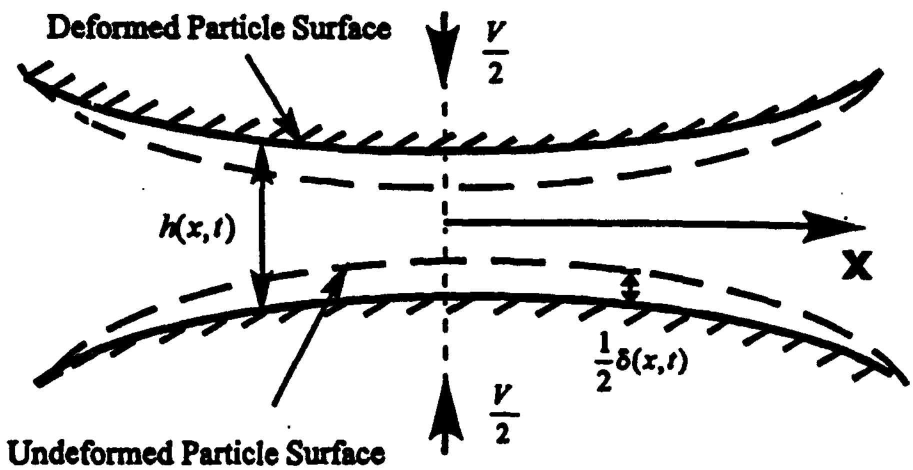

Figure 9.3 Elastohydrodynamic Action Between Particles

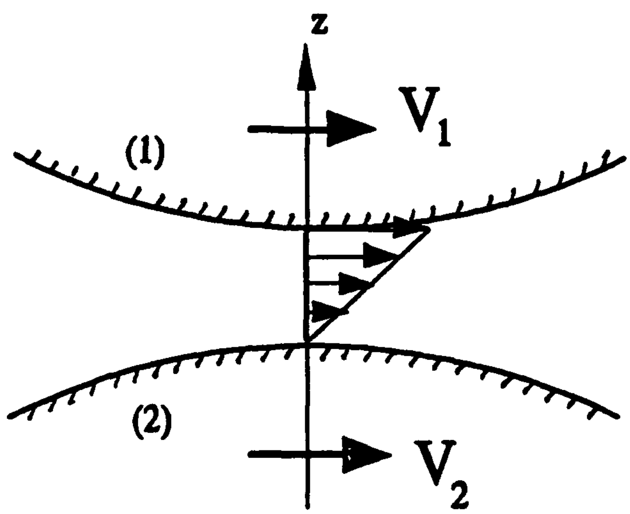

Figure 9.4 Tangential Velocity Distribution

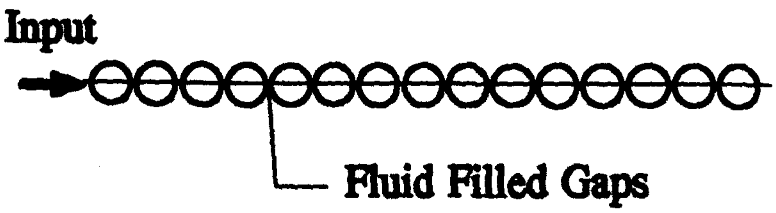

Figure 9.5 One-Dimensional Single Chain Model

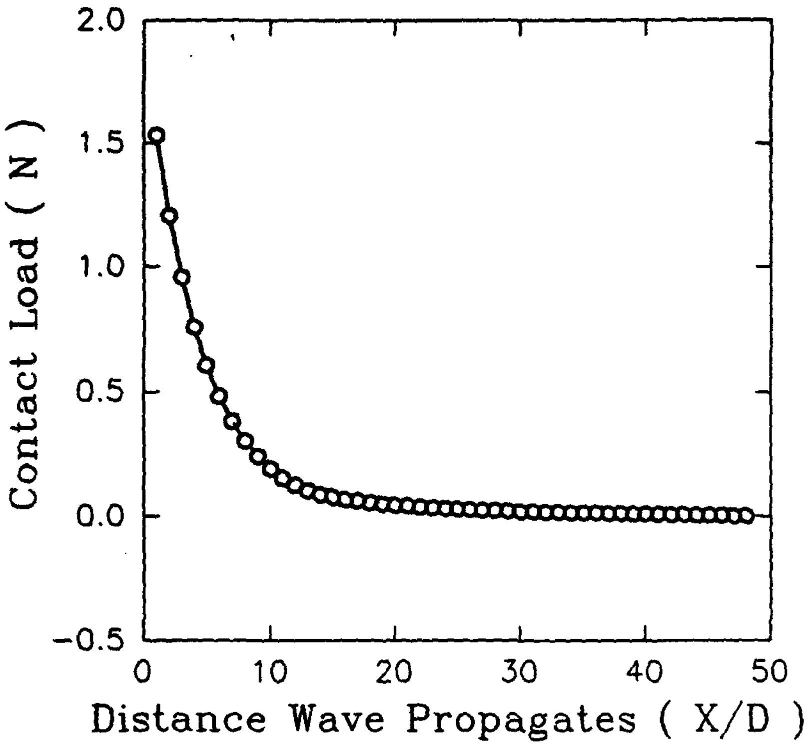

Figure 9.6 Wave Attenuation for Single Chain Model

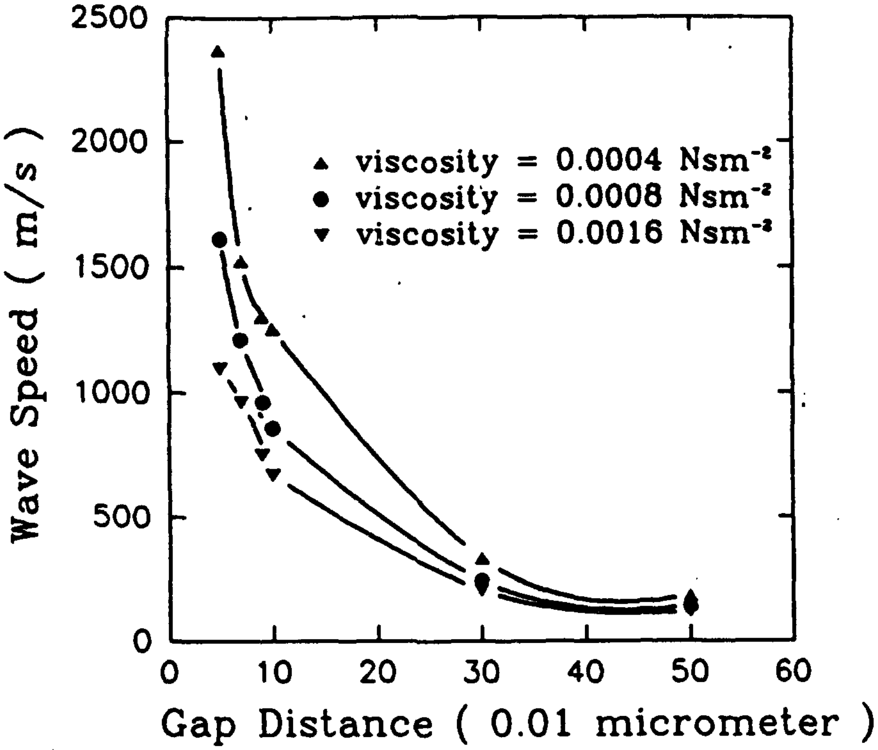

Figure 9.7 Wave Speed as a Function of Gap Spacing and Viscosity for Single Chain Model

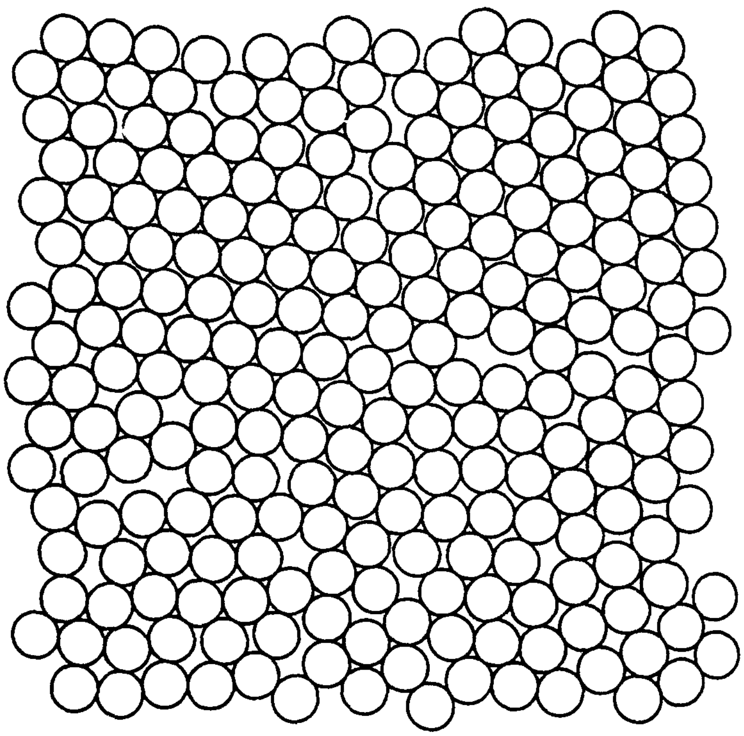

Figure 9.8 Two-Dimensional Random Granular Sediment Model

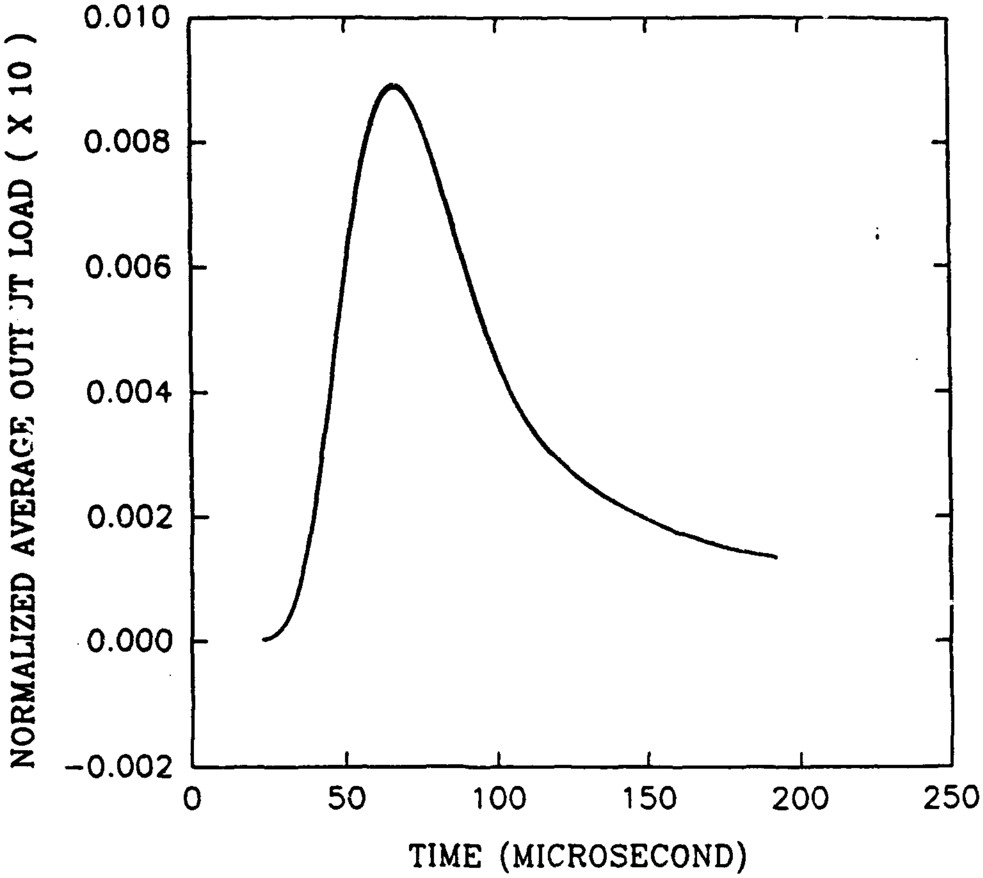

Figure 9.9 Normalized Average Transmitted Signal Through Random Granular Model

10. Finite Element Modeling

10.1 Introduction

The purpose of this portion of the program is to provide and exercise a numerical capability that describes the mechanical behavior of sediments in the CBBL/SRP as a result of a number of processes that are of interest to the program. These might include surface loading due to sedimentation, placement of objects on or in the seabed, and hydrodynamic effects from waves and currents. In turn, some of these processes might affect the acoustic character of the CBBL. Current macroscopic modeling efforts are centered on further development of the URI/MGL finite element code *GEO-CP* (Brandes, 1992) and on material characterization of the Baltic Sea and Panama City, FL sediments. A number of particular boundary value problems are to be investigated. Because the first year of the CBBL/SRP was focused on field work, where we were involved in these research cruises, it was not possible to devote a significant effort to the finite element modeling work. This aspect will receive more concentrated effort during the next 1-2 years or our research program.

10.2 Material Characterization

The plastic constitutive behavior in *GEO-CP* combines critical state soil plasticity (Schofield and Wroth, 1968) with the creep-inclusive approach of Borja and Kavazanjian (1984). The specific material parameters that are needed as input for the elastic and plastic models are listed in Table 10.1. Also listed are the types of tests needed to determine each of the parameters, as well as average preliminary values obtained from the consolidation testing program conducted on the Baltic Sea samples thus far. Note that although the current formulation in the code assumes that the permeability remains constant throughout the analysis, in Table 10.1 we have indicated permeability as a function of void ratio since we intend to modify the code to allow for such a dependence. Given the relatively large value of the average compression index for the Baltic site (Section 8), we can expect that even for moderate loading the sediment would undergo significant changes in void ratio, and thus permeability.

10.3 Formulation Development

The formulation in *GEO-CP* has been expanded to require balance of mass in addition to balance of momentum over the domain of interest at any time. This was done to improve convergence of the predicted to the actual solution for highly non-linear materials, such as the Baltic Sea sediments. Solution of incremental problems is now accomplished by applying Newton's iteration method (Borja, 1989) to a linearized set of residual equations including total momentum balance at time t_{n+1}:

$$\int_s N^T \tau_{n+1} dS + \int_\Omega N^T w_{n+1} d\Omega + \int_\Omega B^T \sigma'_{n+1} d\Omega - \int_\Omega B^T (\sigma + p)_{n+1}^{k+1} d\Omega + \Psi_{1n+1}^{k+1} = 0 \tag{10.1}$$

and incremental mass balance at time t_{n+1}:

$$\Delta H_n - G^T\left(d_{n+1}^{k+1} - d_n\right) + \Delta t\Phi\left[(1-\alpha)p_n + \alpha p_{n+1}^{k+1}\right] + \Psi_{2n+1}^{k+1} = 0 \qquad (10.2)$$

where τ are the boundary tractions acting along the boundary S, w the weight stresses effective in the domain Ω, σ' the relaxation stresses due to creep, **p** the nodal pore pressures, **d** the nodal displacements, **N** the element trial functions, **B** the strain-displacement matrix, **ΔH** the boundary seepage matrix, **Φ** the pore pressure stiffness matrix, **G** the coupling matrix, and Ψ_1 and Ψ_2 the unbalanced terms that should approach zero at the end of each time increment. Subscript *n* refers to increment number and superscript *k* refers to iteration number. This approach has resulted in a fast convergence rate for the elasto-plastic problems solved thus far.

10.4 An Example Problem

As mentioned above, the material can be characterized either as linear elastic or non-linear elasto-plastic with hardening. The linear elastic model is useful in applications where drainage is restricted (i.e. no consolidation) and in fully drained cases involving cohesionless materials such as the sandy sediments at the Panama City, FL site. As a first problem we have selected an elastic plane strain deposit with a uniform strip load, as shown in Figure 10.1. This might represent, for example, loading of the seabed by a pipeline. The predicted settlements and stresses should approach the theoretically available solution for an elastic half space (Poulos and Davis, 1974) if the bottom and far-end vertical boundaries are sufficiently removed from the area of load application. Indeed, Table 10.2 shows that the computed displacements directly under the load approach the theoretical ones. A better agreement would result if we had used a finer mesh and removed the boundaries further away. A comparison of stresses at an arbitrary internal location (Figure 10.2) reveals a relatively good agreement between predicted and theoretical stresses in the vertical direction (average predicted stress of 998 psi versus theoretical stress of 1000 psi), but not so good in the horizontal direction (average predicted stress of 380 psi versus theoretical stress of 254 psi). The poorer comparison in the x-direction can be attributed to the horizontal displacement restraint imposed by the vertical boundary at the far end. A better choice might be to specify a load boundary condition at that end.

Other field problems we intend to model include seabed loading due to sedimentation, mines or other objects, and due to waves. In each case we will be focusing not only on the resulting deformation and stress patterns, but also on significant volume changes, which are likely to have the greatest effect on the propagation of acoustic waves. Another case that merits attention is the possible long-term vertical migration of objects on or in the soft seabed sediments. This would involve a detailed analysis of creep deformations. We also intend to use *GEO-CP* in our laboratory program to track the mechanical evolution of triaxial specimens on which we will be measuring acoustic properties.

Table 10.1 Input Material Parameters for GEO-CP.

	Parameter	Symbol	Average value for Baltic Sea site	Test type
Elasto-plastic model	Young's modulus	E*	-	Triaxial compression
	Poisson's ratio	ν	-	Triaxial compression
	Compression index	λ	1.61	Consolidation
	Recompression index	κ	0.196	Consolidation
	Critical state intercept	Γ	-	Consolidation
	Critical state slope	M	-	Triaxial compression
	Bulk unit weight	γ_b	1.2 gm/cm^3	Bulk sampler, core logger
	Permeability**	$\Delta e / \Delta \log k$	1.998	Consolidation
	Hyperbolic constants	A, R_f	-	Triaxial compression
Creep parameters+	Secondary compression	Ψ	-	Consolidation, triaxial
	Singh-Mitchell constants	A, α, m	-	Triaxial creep

*Used only for linear elastic model **e is void ratio and k is permeability

+For problems with time-dependent behavior

Table 10.2 Comparison Between Theoretical and GEO-CP Predicted Values of Displacement for Strip Loading on Elastic Finite Layer.

Location	Theoretical* Displacement $\times 10^{-3}$ in	Predicted Displacement $\times 10^{-3}$ in
node 9 (under center of load)	Δy=-0.707	Δy=-0.714
node 45 (under edge of load)	Δy=-0.467	Δy=-0.510
	Δx=0.127	Δx=0.112

*Poulos and Davis (1974)

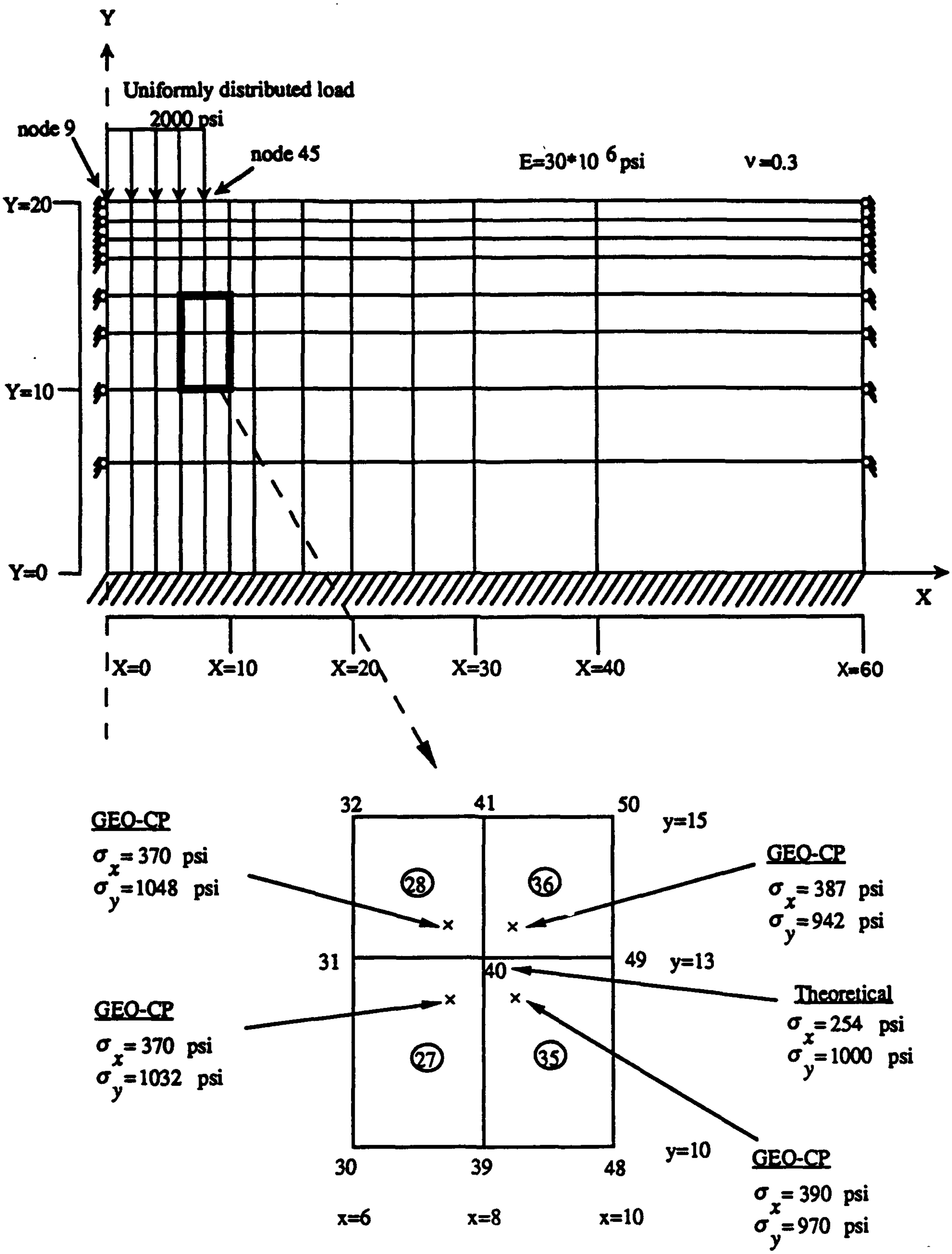

Figure 10.1 Strip Loading on Plane Strain Elastic Foundation

References

Borja, R.I. (1989). Linearization of elasto-plastic consolidation equations. Engineering Computations, 6, pp. 163-168.

Borja, R.I. and Kavazanjian, E. (1984). Finite element analysis of time-dependent behavior of soft clays. Geotechnical Engineering Research Report No. GTI, Stanford, CA: Stanford University, Department of Civil Engineering, 224p.

Brandes, H.G. (1992). Finite element modeling of time-dependent deformations in marine clays. Dissertation submitted in partial fulfillment of the requirements for the Doctor of Philosophy degree, Dept. Univ. of Rhode Island, Kingston, February, 136 p.

Crawford, C.B. (1988). On the importance of rate of strain in the consolidation test. Geotechnical Testing Journal, ASTM, Vol. 11, No. 1, Philadelphia, PA, pp. 60-62.

Cundall, P.A. (1971). A computer model for simulating progressive, large-scale movement in blocky rock systems. Proceedings of the Symposium of the International Society for Rock Mechanics, Vol. 2, No. 8.

Cundall, P.A. and Strack, O.L. (1979). A discrete numerical model for granular assemblies. Geotechnique, Vol. 29, No.1, pp. 47-65.

Holtz, R.D. and Kovacs, W.D. (1981). Introduction to Geotechnical Engineering, Prentice-Hall.

Nickerson, C.R. (1978). Consolidation and permeability characteristics of deep sea sediments: North Central Pacific ocean. Thesis submitted in partial fulfillment of the requirements for the Master of Science degree. Dept. of Civil Engineering, Worcester Polytechnic Institute, Worcester, MA, 212 p.

Olsen, H.W., Nelson, K.R. and Gill, J.D. (1989). Flow-pump applications in geotechnical measurements. Proceedings of the 2nd International, Symposium on Environmental Geotechnology, Tongji University, Shanghai, China, Vol. 2.

Poulos, H.G. and Davis, E.H. (1974). Elastic solutions for soil and rock mechanics. John Wiley and Sons.

Sadd, M.H., Shukla, A. and Mei. H. (1989). Computational and experimental modeling of wave propagation in granular materials. Proceedings of the 4th International Conference on Computational Methods and Experimental Measurements, Capri, Italy, pp. 325-334.

Sadd, M.H., Shukla, A., Tai, Q.M. and Xu, Y. (1991). Micromechanical constitutive behavior in granular media under dynamic loading conditions. Proceedings of the 3rd International. Conference Constitutive Laws for Engineering Materials., Univ. of Arizona, Tucson, AZ.

Sadd, M.S., Tai, Q.M. and Shukla, A. (1993). Contact law effects on wave propagation in particulate materials using distinct element modeling. International Journal of Non-Linear Mechanics, Vol. 28, No. 2, pp. 251-265.

Schofield, A. and Wroth, P. (1968). Critical state soil mechanics, McGraw-Hill.

Silva, A.J., Hetherman, J.R. and Calnan, D.I. (1981). Low-gradient permeability testing of fine-grained marine sediments. In: Permeability and groundwater contaminant transport, ASTM STP 746, American Society for Testing and Materials, Philadelphia, PA, pp. 121-136.

Silva, A.J. and Jordan, S.A. (1984). Consolidation properties and stress history of some deep sea sediments, In: Seabed Mechanics, Proceedings of IUTAM and IUGG Conference at Univ. of Newcastle Upon Tyne, UK, pp. 25-39.

Zizza, M.M. and Silva, A.J. (1988). Strength and stress-strain behavior of clays from the Nares Abyssal Plain. Marine Geotechnology, Vol. 7, pp. 221-244.

ADDENDUM

CRUISE REPORT
February 1993 Baltic Sea Cruise
Eckenfoerde, Germany

by

Armand J. Silva
February, 1993

Geotechnical Summary

The main objectives were to a) observe and assess the seabed sampling gear, b) process some typical core samples to assess general conditions of sediments and provide information to help plan and optimize operations for the May cruise, c) obtain representative sediment samples in order to begin the laboratory testing program, and d) make as many geotechnical measurements as possible on collected sediment samples. The geotechnical and geological measurements and observations were under the direction on A.Silva, W.Bryant and N.Slowey. Many of the samples will be shared by the URI and TAMU researchers with results made available to other interested groups.

Types of cores obtained were:

* Large-diameter gravity cores
* Box cores (50x50x55 cm)
* Special pressure cores: collected by divers, with pressure plugs inserted by divers

Gravity Cores

The gravity cores are being logged with the multi-sensor core logger at GEOMAR. Evidently there is an annular gap remaining inside most of the tubes, such that it is not possible to obtain velocity data. Some refinements made to the coring system (valves, lighter core catcher) may improve the situation. It seems obvious that we either need to correct this situation or arrange for a different type of coring system. Some of the better cores will be split and sampled at Kiel University upon completion of the cruise .

Special Pressure Core: The special pressure core will be put through the core logger and split to see if this system of obtaining a pressured core is feasible.

Box Cores

Most of the geotechnical work was concentrated on box cores samples. Six (6) box cores were subsampled and tested. Four of these were sampled and tested in greater detail. Following is a summary of methods, procedures, and results.

* Sub cores: short sections of the gravity core liner were pushed into the sediment, using a piston arrangement. These sections will be processed post-cruise at both GEOMAR and the University of Kiel.
* Thin-wall-subcores: Three stainless steel tubes were pushed into the sediment with a special piston arrangement. These cores will be hand-carried to URI.
* Density/Water Content samples: Approximately 30 calibrated density/water samples were collected. These will be taken to URI for completion of tests.
* Triaxial samples: Approximately 25 "undisturbed" sub-samples were taken with thin-walled tubes and a piston arrangement. These sealed samples will be hand-carried to URI.
* Consolidation/Permeability samples: Six undisturbed" subsamples will be hand-carried to URI.
* Bag samples: Some 50-60 samples were placed in sealed plastic bags. These will be shipped to URI.
* Shear Tests: Both a Torvane and a miniature vane (1x0.5in) with torque-watch were to make several measurements of shear strength in the four box cores samples.

Summary of Results and Observations

a) We need to improve the quality of recovered deeper cores (to about 3m).
b) The box core system is quite good.
c) The sediments of the upper 0.5 meters consist of a very soft black fine-grained material with a strong hydrogen sulfide odor. A thin (2-8mm) oxidized layer is present at the surface. The upper 10-20cm behaves like a viscous fluid with essentially zero shear strength. It is extremely difficult (impossible?) to take and preserve an undisturbed section of this zone. Special techniques will be required to transfer a sample into a laboratory apparatus.
d) Shear strength is essentially zero in the upper several centimeters and gradually increases to measurable values at 40-50cm depth. Actual shear strength values are not available yet.
e) Some organisms are present (polycheates and nudibranchs) near the surface of some cores. Twigs and grasses are present at depth.
f) A shelly zone exists at a depth of 25-30cm and larger clam shells (5cm) are found at the bottom of the box core sample (50cm).
g) Gas tubes and/or voids were found in most cores.
h) Samples are available from A.Silva (URI) or W.Bryant/N.Slowey (TAMU)

Appendix B

CRUISE REPORT
May, 1993 Baltic Sea Cruise
JOBEX Eckernfoerde Experiment

by

Armand J. Silva
Horst Brandes

Department of Ocean Engineering
Marine Geomechanics Laboratory
University of Rhode Island

July 9, 1993

Introduction:

This is a trip report covering the activities of Armand J. Silva (Principal Investigator) and Horst Brandes for the period of May 11 through June 1, 1993; which supplements the general report prepared by Michael Richardson (Chief Scientist, Naval Research Laboratory, SSC). The main objectives of the URI/MGL involvement were to:

- oMake geotechnical measurements and observations of selected core samples obtained in and around the main experiment site in Eckernfoerde Fiord, Baltic Sea.
- oObtain "undisturbed" subsamples of sediments for subsequent laboratory analysis at the URI/MGL facilities.
- oConduct detailed sampling of cores for testing to characterize the sediments.

It was decided that the URI, Large-diameter Gravity Corer (LGC) system would be needed to obtain high quality cores of the upper two meters of sediment. Therefore, this corer was prepared and shipped to the site along with other equipment. A new design nose cone/core catcher system was fabricated to eliminate the disturbance problems caused by conventional core catchers. This system is described elsewhere.

Because of the extremely soft nature of the sediments, special subsampling systems and racks for supporting vane shear equipment in the box corer were designed and fabricated. These new systems proved to be very successful.

Schedule of Activities:

Following is a summary of the schedule for MGL personnel.

11, 12, May (Tuesday, Wednesday)
A. Silva and Horst Brandes depart Rhode Island and arrive in Eckernfoerde.

13, May (Thursday)
A. Silva and Horst Brandes at Base, unpack gear.

14, May (Friday)
Load URI Gravity Corer (LGC) on Helmsand. Training of Bryant/Slowey group on LGC system. New nose cone/catcher system working well. Recover 5 LGC's. Recovery approximately 1.9m each core.

15, May (Saturday)
A. Silva and H. Brandes process diver box core (20cm x 28cm) on Helmsand. Miniature vane tests, viscometry/vane tests, subsamples (triaxial and consolidation/permeability), water content/density.

16, May (Sunday)
Coring on Helmsand (Bryant/Slowey group)

17, May (Monday)
At base, process cores, meet with Stoll's group, others. Plan sampling program.

18, May (Tuesday)
Load Konsort. Process cores. Prepare equipment and processing gear.

19, May (Wednesday)
Load Konsort, prepare work area, test equipment.

20-23, May (Thursday-Sunday)
German holidays.

24, May (Monday)
Box coring on Konsort. Bring up cores gradually in attempt to minimize disruption due to degassing. Continue processing at dockside until 2000.

25, May (Tuesday)
Box coring on Konsort. Continue processing at dockside until 1930.

26, May (Wednesday)
Box coring on Konsort. Continuing processing at dockside until 1930.

27, May (Thursday)
Box coring on Konsort.

28, May (Friday)
Pack and unload from Konsort. Process cores at Base. Degassing of gravity cores causes severe sediment disruption.

29, May (Saturday)
Process cores. Pack gear. Work on subsamples. Drill holes in gravity cores to more gradually degas. Seems to help somewhat. Subsample cores.

30, May (Sunday)
Process cores. Finish packing.

31, May (Monday)
A. Silva and Horst Brandes depart.

Equipment:

The geotechnical equipment supplied by URI/MGL included a Large-diameter Gravity Corer (LGC) that was made available for general coring operations, two instruments to measure the on-board shear strength of the sediments, and a number of specialized tools and rigs for subsampling of the box cores and gravity cores.

The configuration of the URI/MGL gravity corer used during the cruise consisted of a weight stand with adjustable weight, Schedule 40 PVC core pipe (4" I.D., 1/4" wall, and up to 10ft long), and a steel nose cone cutter with a core catcher. A modified version of the standard nose cone/catcher assembly, designed to minimize disturbance to the soft sediments, was also used. This new design incorporates a removable sleeve that keeps the fingers of the catcher completely open during penetration. This sleeve is designed to slide out during retrieval to allow the fingers to close and prevent the loss of the captured sediment. In order not to lose the sleeve each time a core was taken, this assembly was further modified by attaching a flexible steel wire to both the sleeve and the nose cone.

A Wyckehm Farrance vane shear device and a Brookfield viscometer were used to measure the shear strength and investigate the rheological characteristics of the sediments in the box cores at several depth intervals within the box cores. These measurements were obtained along with numerous subsamples for determining water content, bulk density and classification properties.

An adjustable rig and piston assembly designed to minimize disturbance was used to take 1.5" and 2.0" diameter thin stainless steel subsamples up to 5" long for laboratory testing to determine stress-strain/strength properties, consolidation characteristics and permeability of the sediments. Shelby tube samples (3.0" O.D., 2ft long) were taken in the box core uisng a piston with a relief valve and a stationary frame. Ancillary equipment included signal conditioners, transformers, and a strip-chart recorder.

Results and Observations

Gravity Coring

Gravity coring operations were conducted in two phases. The equipment was transported to the R/V Helmsand and tested on May 14. A total of five cores were taken during this trial operation. Coring was resumed on May 24 and lasted until May 27. The cores were sealed with specially designed single and double o-ring plugs. However, the sediments in many of the cores were very gassy, resulting in some of the plugs sliding of the ends of the barrels. In some of the cores the o-ring plugs were further secured in by bolts placed in previously drilled holes through the PVC immediately above the plugs.

Box Coring

One diver (20cm x 28cm) and four large box cores (50cm x 50cm) were subsampled and analyzed in detail for geotechnical purposes. The sediment in the box cores was very soft but relatively undisturbed. The upper one centimeter consisted of an oxidized layer that appeared to be of high organic content and often covered with worm-like burrows. There was no evidence of gas coming out of solution in any of the box cores. Below the surface layer the sediment consisted of a uniform fine black mud with strong organic smell that increased slightly in strength with depth. A layer of broken shells was observed in some of the box cores at about 10 to 20cm depth.

Sampling and Measurements

Four of the gravity cores were dedicated for geotechnical processing. These cores were brought onshore and subsampled. Expansion of the gas upon removal of the end plugs made it difficult to obtain good quality undisturbed subsamples from the gravity cores. Holes (1/8") were drilled along the axis of two cores in an attempt to allow gradual degassing that might reduce the amount of disruption to the sediments. This seemed to be somewhat effective. Each of the cores was cut into round sections of approximately equal length. Triaxial and consolidation 2.0" stainless steel tubes were inserted in the ends, and then the sediment in the cores was extruded to expose the subsamples. These were in turn carved out, cleaned, capped, and sealed with wax (Table 1).

On-board processing of the box cores included shear strength determination at various depths and different speeds of rotation, using a motorized vane device and a variable speed Brookfield viscometer; and subsampling for water content, bulk density, index properties, and laboratory triaxial and consolidation testing. Also, a two foot long, 3.0" O.D. Stainless steel Shelby tube was inserted into each of the four large box cores, using a piston arrangement, before any of the other processing. The purpose of the subsampling program was to obtain a detailed profile of sediment geotechnical characteristics in the upper 50cm. Triaxial and consolidation subsamples were taken by pushing thin stainless steel tubes (2.0" and 1.5" O.D.) into the sediment from a stationary piston positioned at the sediment surface. Two o-rings near the end of the piston created a tight seal and a suction effect on the sediment that greatly reduces drawdown and compression of the sediment upon insertion of the tubes. The Shelby tubes were excavated from the box core after completion of all other processing and sealed with o-ring plugs, caps and wax. They will provide additional undisturbed material for laboratory testing (Table 2).

The last of the box cores (0264-BS-BC) was subsampled horizontally by tilting the box and removing one of the side panels. Six 2.0" triaxial and three 2.0" consolidation tubes were inserted horizontally. They should provide a good set of samples to determine whether the sediment exhibits any anisotropic material characteristics.

Box coring attempts in sand areas near Middlegrund were not successful. Some bag samples were obtained for textural analysis.

Observations and Comments

A summary of the geotechnical shipboard measurements and subsampling accomplished during the cruise are listed in Tables 1, 2, and 3. All the triaxial and consolidation subsamples were capped, sealed with wax and hand carried back to URI/MGL, where they are being stored at 6°C and immersed in sea water. The Shelby tubes and the bulk samples in plastic bags were packed with the rest of the equipment and are being shipped with other cruise gear. The water content and bulk density samples were weighed, dried, and reweighed at the Navy Base facility in Germany. The dried out samples are also being shipped back to URI/MGL and will be available for future use. Detailed water content and bulk density profiles for each of the box cores have been prepared and are available upon request.

A preliminary review of viscometry data indicated that the strength initially increases somewhat as rate of rotation increases but then tends to decrease at higher rates of rotation (up to 100 rpm). The shear strength of the upper 1-2cm is very low at less than 1 kPa. As noted earlier in this report, there was no evidence of gas release in the box cores. This is in marked contrast to most of the cores recovered during the February, 1993 cruise where significant amounts of gas bubbled up through the sediment.

Table 1
Gravity Core Subsamples Taken for Geotechnical Laboratory Analysis
University of Rhode Island, Marine Geomechanics Laboratory
May 1993 Baltic Sea Cruise, CBBL/SRP/NRL Project

Core	Location	Undisturbed Samples 2.0" Triaxial	2.0" Cons/Perm
0304-BS-GC	54^{o} 29' 33.5" N 10^{o} 00' 08.6" E	74-84cm (1)* 90-100cm (1) 103-113cm (1) 120-135cm (1)	138-143cm (1) 147-152cm (1)
0312-BS-GC	54^{o} 29' 36.6" N 09^{o} 59' 28.6" E	72-86cm (1) 89-103cm (1) 105-119cm (1) 121-135cm (1) 139-153cm (1)	-
0318-BS-GC	54^{o} 29' 32.4" N 09^{o} 58' 56.8" E	72-87cm (1) 91-106cm (1) 107-122cm (1) 124-139cm (1)	141-146cm (1) 154-159cm (1)
0333-BS-GC	54^{o} 33' 26.3" N 10^{o} 06' 06.4" E	63-77cm(1) 81-95cm (1) 96-107cm (1) 115-126cm (1)	58-61cm (1)

*Number of subsamples in parenthesis

Table 2
Box Core Subsamples Taken for Geotechnical Laboratory Analysis
University of Rhode Island, Marine Geomechanics Laboratory
May 1993 Baltic Sea Cruise, CBBL/SRP/NRL Project

Core	Location	Undisturbed Samples 1.5" Triaxial	Undisturbed Samples 2.0" Triaxial	Undisturbed Samples 2.0" Cons/Perm	Undisturbed Samples Shelby Tubes	Bulk Samples Sealed Plastic Bags
0210-BS-DC	(diver core)	8-18cm (5)*	-	8-13cm (2)	-	0-0.5cm 17-19cm
0225-BS-BC	54° 29' 43.2" N 09° 59' 26.8" E	33-44cm (6)	13-27cm (6)	13-18cm (2) 28-33cm (2) 33-38cm (2)	One tube	3.5-5.5cm 8-10cm 15-18cm 28-30cm 34-36cm
0238-BS-BC	54° 29' 35.7" N 10° 00' 10.3" E	-	25-40cm (6)	28-33cm (2)	One tube	0-0.5cm 9-12cm 14-16cm 20-23cm 26-28cm
0252-BS-BC	54° 29' 36.3" N 10° 00' 03.5" E	-	27-42cm (6)	27-31cm (3)	One tube	0-0.5cm 4-6cm 9-12cm 15-18cm 21-24cm 27-29cm 46-48cm
0264-BS-BC	54° 29' 37.18" N 09° 59' 19.02" E	-	33cm (6) horiz. samples	33cm (3) horiz. samples	One tube	-

*Number of subsamples in parenthesis

Table 3
Summary of Shipboard Measurements and Subsampling
University of Rhode Island, Marine Geomechanics Laboratory
May 1993 Baltic Sea Cruise, CBBL/SRP/NRL Project

Diver Core (Box - 20cm×28cm)

1.5" Triaxial:	5 samples
Bulk:	2 samples
Water cont./density:	12 samples
Vane/viscometer:	@ 4 levels

Box Cores (50cm × 50cm)

1.5" Triaxial:	6 samples
2.0" Triaxial:	24 samples
2.0" Consol./perm.:	14 samples
Shelby Tube:	4 tubes
Bulk:	17 samples
Water cont./density:	72 samples
Vane/viscometer:	@ 5 levels in 0225-BS-BC
	@ 6 levels in 0238-BS-BC
	@ 6 levels in 0252-BS-BC

Gravity Cores (10.16cm I.D.)

2.0" Triaxial:	17 samples
2.0" Consol./perm.:	5 samples
Water cont./density:	4 samples

Note: Also obtained many water content/density samples from larger gravity cores for Mike Richardson and Kevin Briggs.

Summary

1.5" Triaxial:	11 samples
2.0" Triaxial:	41 samples
2.0" Consol./perm.:	19 samples
Shelby Tube:	4 tubes
Bulk:	19 samples
Water cont./density:	88 samples + M.R. and K.B. samples
Vane/viscometer:	@ 21 levels

Appendix C

CRUISE REPORT

COASTAL BENTHIC BOUNDARY LAYER PROJECT

Panama City, FL Cruise
August/September 1993

by

Armand J. Silva
George E. Veyera
Horst G. Brandes

MARINE GEOMECHANICS LABORATORY
University of Rhode Island

for

COASTAL BENTHIC BOUNDARY LAYER
SPECIAL RESEARCH PROGRAM
NAVAL RESEARCH LABORATORY
STENNIS SPACE CENTER

October, 1993

Introduction

Personnel from the University of Rhode Island, Marine Geomechanics Laboratory (URI/MGL) participated in the research cruise south of Panama City, Florida for the Coastal Benthic Boundary Layer (CBBL) project sponsored by the Naval Research Laboratory, Stennis Space Center (NRL/SSC). The overall work plan was focused on conducting geoacoustic experiments and physical characterization of the benthic boundary layer. The URI/MGL portion of the program was conducted from the R/V Gyre during the period of August 28 through September 4, 1993. The URI efforts were focused on obtaining undisturbed samples of the upper 0.5 to 1.0 meter of sediments for subsequent analysis.

The URI personnel participating in the Panama City experiment consisted of:

- o Armand J. Silva, P.I./Director of URI programs
- o George Veyera, Co-P.I.
- o Horst Brandes, Post-Doctoral Research Associate

Objective

The primary objective of this effort was to obtain physical core samples and grab samples for characterization of the sediments in the benthic boundary layer at the Panama City site. The URI/MGL Large-diameter Gravity Corer (LGC) was used to obtain undisturbed samples. The TAMU team obtained the grab samples and vibracores.

Schedule of Activities

The following is a general summary of activities for the URI/MGL personnel:

25, 26, 27 August (Wednesday, Thursday, Friday)
G.E. Veyera and H.G. Brandes depart from the University of Rhode Island in a rental truck, with equipment, and arrive in Panama City, FL.

27 August (Friday)
A.J. Silva departs from the University of Rhode Island, via Washington, D.C., and arrives in Panama City, FL.

28 August (Saturday)
A.J. Silva, G.E. Veyera and H.G. Brandes unpack gear and transfer to R/V Gyre. Coring using LGC (Large diameter Gravity Corer) on R/V Gyre.

29 August (Sunday)
Coring using LGC (Large diameter Gravity Corer) on R/V Gyre.

30 August (Monday)
Coring using LGC (Large diameter Gravity Corer) on R/V Gyre.

31 August (Tuesday)
Coring using LGC (Large diameter Gravity Corer) on R/V Gyre.

1 September (Wednesday)
Acoustic towers retrieved and off loaded at Naval Coastal Systems Station (NCSS). Coring operations suspended.

2 September (Thursday)
Coring using LGC (Large diameter Gravity Corer) on R/V Gyre.

3 September (Friday)
Coring using LGC (Large diameter Gravity Corer) on R/V Gyre. Return to Naval Coastal Systems Center (NCSS) late afternoon. A.J. Silva, G.E. Veyera and H.G. Brandes unload gear and samples from R/V Gyre and pack up truck for return to the University of Rhode Island. Cores and bag samples were packed in ice in coolers. Most of the cores were laid horizontally. Several long cores were placed vertically in ice due to their length.

4 September (Saturday)
A.J. Silva departs Panama City, FL and returns to the University of Rhode Island.

4, 5, 6 September (Saturday, Sunday, Monday)
G.E. Veyera and H.G. Brandes depart Panama City, FL and return to the University of Rhode Island.

Equipment and Procedures

The URI/MGL Large-diameter Gravity Corer (LGC) was used for most of the coring. The core barrel assembly used for this cruise consisted of a thin-walled 0.32cm (0.125in) steel barrel and a 0.32cm (0.125in) clear acrylic liner with an inside diameter of 10.2cm (4.0in). The steel barrel was 1.1m (3.61 ft) long and connected to the corer body through a set of eight bolts that were removed each time a sample was obtained. A nose cone and core catcher are attached to the penetrating end of the barrel (see Figure 1). A photograph of the prepared coring system in a vertical position on the stern of the R/V Gyre is shown in Figure 2. This photograph shows the trigger mechanism, swivel, bail with ball valve, shroud, and core barrel extending outboard.

Two attempts were made using the core body without the hydrodynamic shroud, but it was determined that the corer was falling over upon impact and samples were not recovered. However, a finned circular shroud was available to overcome this problem. The shroud was welded by ship personnel to the top of the corer body to give it necessary hydrodynamic stability during free fall and penetration. The corer body and shroud weighed approxima[illegible] kg (200lbs). This weight can be increased by attaching individual 22.7kg (50lbs) pound lead w[illegible]s. Most of the coring during this cruise was done using 8 of these weights (see Appendix). In order to increase penetration, a trigger mechanism was used that allows for an adjustable amount of free fall. Typical free fall lengths are 4.57 to 9.15m (15 to 30 feet) (see Appendix).

The LGC deployment procedures are outlined below:

a) Corer preparation: The core barrel, with nose cone and core catcher, were bolted to the corer. A predetermined amount of lead weight was attached to the corer weight stand.

b) Triggering mechanism: A length of winch cable slightly longer than the amount of desired free fall and anticipated penetration depth was passed through the trigger mechanism and coiled to hang to the side of the corer. The trigger was then attached to the pear link at the top of the corer along with the end of the winch cable. A safety pin was inserted in the trigger mechanism to prevent accidental triggering while positioning the corer overboard prior to deployment. The free fall weight of 114.5kg (32lbs) was attached to the trigger arm to hang a predetermined length below it to give the desired amount of free fall when the weight reached the seabed (Figure 1).

c) Deployment: The corer and triggering mechanism, along with the free fall weight, were deployed over the stern of the ship with the A-frame and winch cable. Tag lines were used to control handling of the LGC assembly as needed.

d) Recovery: The corer was retrieved following seabed penetration and brought on board in a vertical position. When a sample was recovered, the barrel was removed while keeping it vertical to avoid disturbing the sediment. The corer was then brought to a horizontal position and prepared for re-deployment.

e) Core processing: After the liner was extruded from the steel barrel, it was cut off a few inches above the sediment surface and capped at both the top and bottom using specially designed o-ring plugs that are highly effective in sealing and containing the sample. The plugs are flush with the sediment surface at both ends of the recovered core so that the sediment is retained in its natural sequence. The ends of the liner were then capped, taped and sealed by immersion in hot wax. Each core liner was labeled with complete identification information.

f) Core storage and transportation: The cores were stored vertically in the air-conditioned laboratory aboard the R/V GYRE for the duration of the cruise. The cores were packed in ice and transported back by truck to URI/MGL. They are being stored vertically at 6°C in a constant humidity refrigerator.

Results and Observations

Gravity coring operations were conducted on August 28-31 and September 2-3. The acoustic towers were retrieved on September 1 and no coring was done on that day. During the cruise, forty-two (42) attempts were made to obtain cores with the URI/MGL LGC. A total of fourteen (14) whole cores were recovered, ranging in length from 10cm to 51.5cm (Table 3). From the cores obtained, four (4) were given to TAMU researchers, two (2) to NRL researchers, and the remaining eight (8) were shipped to the URI/MGL. In addition, 10 bulk samples were collected from material recovered in the cone/core catcher section of some of the cores.

Most of the sediments at the site consisted of dense sand containing varying amounts/sizes of shells and shell fragments. In general, the upper 10cm (approximately) consisted of brown or gray well-graded medium or coarse sand. Below this depth, the material was typically gray, medium to coarse sand changing to well-graded fine gray sand. In many areas the surface sediment consisted of very dense well-graded medium to fine sand that was virtually impossible to penetrate with the gravity corer. In some locations where a coarse sand layer was present at the surface, it appeared that the corer penetrated a small distance (several centimeters) into the denser, finer material.

As is often the case with granular materials, the sand was difficult to sample, and it was not possible to obtain gravity cores longer than 52cm. In addition, sometimes the sediment fell through the core catcher, the fingers of which were held open by shell fragments or coarse sand particles wedged in between. A plastic bag was installed over the core catcher inside of the core barrel in an attempt to keep the sediment from falling through the fingers. Overall, this proved to be very successful. The only problem encountered with the bags was that on two occasions they were dragged into the core with the sediment.

No processing of cores was conducted on board ship. A complete analysis of cores and samples will be conducted at URI/MGL in the coming year, including whole core logging (density and acoustic velocity) and physical properties measurements (grain size, shear strength, geoacoustic characteristics, etc.).

Photographs of four recovered gravity cores are shown in Figures 3, 4, and 5. At the upper end of each core, note the specially deisigned gray PVC plugs with o-rings used to seal the sediment cores. Brief comments are presented below (also see Table 1).

Core 0575-PC-LGC (Figure 3, left): Medium to coarse sand with many shell fragments. Finer gray sand near bottom (probably some "smearing" upward near wall).

Core 576-PC-LGC (Figure 3, right): Coarse to medium sand with shell fragments at top, increasing fines toward bottom.

Core 577-PC-LGC (Figure 4): Coarse sand with shell fragments, grades to fine sand toward bottom (note plastic bag fragments along wall in lower section).

Core 623-PC-LGC (Figure 5): This was the longest gravity core (51.5cm). Medium to coarse sand with shell fragments, finer toward bottom.

Additional descriptions and comments are included in Tables 1 and 2 and the Coring and Sampling Log in the Appendix.

Table 1. URI/MGL Coring Summary, NRL/CBBL Project Panama City Cruise, August/September 1993

Core No.*	Location	Recovery	Sediment Description	Disposition**
575-PC-LGC	29º 41.52'N 85º 41.72'W	29cm	medium to coarse brown-gray sand with many small shell fragments	URI
576-PC-LGC	29º 40.71'N 85º 40.84'W	36cm	medium to coarse sand with small shell fragments, increasing fines toward bottom	TAMU
577-PC-LGC	29º 40.95'N 85º 40.29'W	47cm	brown coarse sand with shell fragments, grades to fine sand with fines toward bottom	URI
581-PC-LGC	29º 41.12'N 85º 40.43'W	24cm	coarse to medium sand with shell fragments	NRL
584-PC-LGC	29º 41.57'N 85º 40.94'W	19cm	coarse-medium sand, some shell fragments, fine sand at top, coarse sand above actcher	TAMU
587-PC-LGC	29º 41.09'N 85º 40.88'W	32cm	coarse-medium sand with many shell fragments, medium to fine sand toward bot.	URI
590-PC-LGC	29º 41.06'N 85º 40.81'W	25cm	coarse sand with lots of shell fragments, some half shells toward bottom	NRL
592-PC-LGC	29º 41.03'N 85º 40.49'W	10cm	coarse sand with shell fragments	TAMU
596-PC-LGC	29º 41.03'N 85º 40.50'W	20cm	coarse sand with shell fragments	URI
597-PC-LGC	29º 42.11'N 85º 40.50'W	38cm	coarse shelly sand, finer material near bottom	URI
599-PC-DC(C-4)	29º 40.71'N 85º 40.42'W	>24cm	brown-gray silty fine to medium sand with some clay	URI

*LGC: Large-diameter Gravity Corer (URI/MGL) VC: Vibracorer (TAMU) DC: Diver core (NRL)

**URI: University of Rhode Island TAMU: Texas A&M University NRL: Naval Research Laboratory

Table 1 (cont.): URI/MGL Coring Summary

Core No.*	Location	Recovery	Sediment Description	Disposition**
602-PC-VC	29° 40.75'N 85° 40.43'W	32cm	brown medium sand with small shell fragments, appears disturbed	URI
622-PC-LGC	29° 40.88'N 85° 40.91'W	20cm	gray coarse to medium sand with shell fragments	URI
623-PC-LGC	29° 41.02'N 85° 40.53'W	52cm	medium-coarse sand with many shell fragments, some fines toward bottom	URI
628-PC-LGC	29° 41.25'N 85° 40.20'W	24cm	gray coarse to medium sand	URI
630-PC-LGC	29° 40.83'N 85° 40.59'W	39cm	gray coarse sand with shell fragments	TAMU

*LGC: Large-diameter Gravity Corer (URI/MGL) VC: Vibracorer (TAMU) DC: Diver core (NRL)

**URI: University of Rhode Island TAMU: Texas A&M University NRL: Naval Research Laboratory

Table 2. Bulk Bag Samples at URI/MGL, NRL/CBBL Project Panama City Cruise, August/September 1993

Core No.*	Location	Sample	Sediment Description
425-PC-SG	29^o 40.94'N 85^o 40.78'W	bulk sample from Smith-MacIntire sampler	coarse sand with many small shell fragments
451-PC-SG	29^o 42.18'N 84^o 40.55'W	sample split from Smith-MacIntire sampler	coarse sand with many small shell fragments
464-PC-SG	29^o 41.36'N 85^o 41.63'W	sample split from Smith-MacIntire sampler	medium to coarse sand with small shell fragments
523-PC-SG	29^o 40.50'N 85^o 40.65'W	sample split from Smith-MacIntire sampler	fine to medium sand with a few shell fragments
526-PC-SG	29^o 60.63'N 85^o 40.73'W	sample split from Smith-MacIntire sampler	coarse sand with many small shell fragments
573-PC-LGC	29^o 42.66'N 85^o 41.34'W	*washed-out sample in* core catcher	brown-gray fine to medium sand
574-PC-LGC	29^o 41.71'N 85^o 41.28'W	washed-out sample in core catcher	brown-gray medium sand with many small shell fragments
583-PC-LGC	29^o 40.41'N 85^o 40.23'W	catcher sample	gray well-graded medium to fine sand, no shells
588-PC-LGC	29^o 40.74'N 85^o 40.41'W	catcher sample	gray well-graded medium sand, no shells
589-PC-LGC	29^o 40.77'N 85^o 40.48'W	catcher sample	gray well-graded medium sand, no shells
590-PC-LGC	29^o 41.06'N 85^o 40.81'W	catcher and a few cms from bottom of liner	coarse sand and shell fragments
599-PC-DC(C-1)	29^o 40.71'N 85^o 40.42'W	extruded from diver core	. brown-gray fine to medium sand with silty fine sand and some clay

*LGC: Large-diameter Gravity Corer (URI/MGL) SG: Smith-MacIntire grap sampler (TAMU) DC: Diver core (NRL)

Table 2 (cont.): Bulk Bag Samples at URI/MGL

Core No.*	Location	Sample	Sediment Description
607-PC-LGC	29° 41.43'N 85° 40.90'W	catcher sample	very coarse sand with many shells
608-PC-LGC	29° 41.47'N 85° 40.92'W	catcher sample	coarse sand with shell fragments
627-PC-LGC	29° 41.57'N 85° 41.03'W	catcher sample	coarse to medium shelly sand
629-PC-LGC	29° 40.78'N 85° 40.44'W	catcher sample	gray medium to fine well graded sand
639-PC-LGC	29° 41.23'N 85° 40.51'W	sample from bottom of liner, near catcher	gray coarse to medium sand with shell fragments

*LGC: Large-diameter Gravity Corer (URI/MGL) SG: Smith-MacIntire grap sampler (TAMU) DC: Diver core (NRL)

Table 3. Summary of URI/MGL LGC Cores Recovered During 1993 CBBL/SRP Panama City, FL Experiment (PC).

Core No.	Recovered Length (cm)	Condition/Comments	Disposition
0575-PC-LGC	29	Partially drained	URI
0576-PC-LGC	36	Excellent core (baggie in core)	TAMU
0577-PC-LGC	47	Excellent core (baggie in core)	URI
0581-PC-LGC	24	Good/Log[a]	NRL
0584-PC-LGC	19	Good/Log[a]	TAMU
0587-PC-LGC	31.5	Good/Log[a]	NRL
0590-PC-LGC	25	Partially drained	URI
0592-PC-LGC	10	Good	TAMU
0596-PC-LGC	20	Good/Log[a]	URI
0597-PC-LGC	37.5	Good/Log[a]	URI
0622-PC-LGC	20	Compacted	URI
0623-PC-LGC	51.5	Excellent/Log[a]	URI
0628-PC-LGC	24	Good/Log[a]	URI
0630-PC-LGC	39	Little drainage	TAMU
0639-PC-LGC[b]	20	Bagged	URI
			URI - 8
			TAMU - 4
			NRL - 2

Note: a Whole core will be analyzed using multi-sensor core logger at URI/MGL.
b Core liner split during recovery and entire sample was bagged.
URI/MGL - University of Rhode Island/Marine Geomechanics Laboratory
LGC - Large-diameter Gravity Corer
TAMU - Texas A&M University
NRL - Naval Research Laboratories

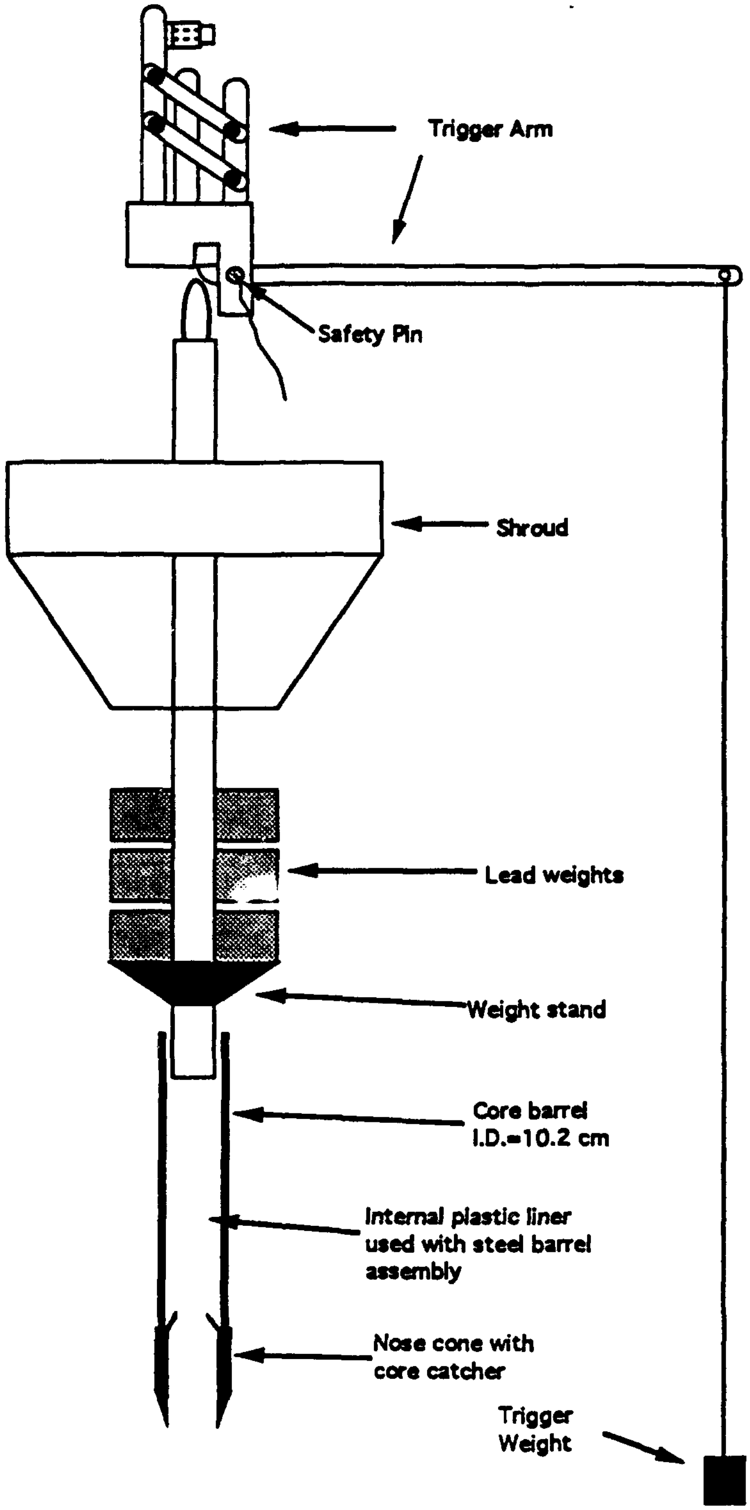

Figure 1. URI/MGL Large-diameter Gravity Corer

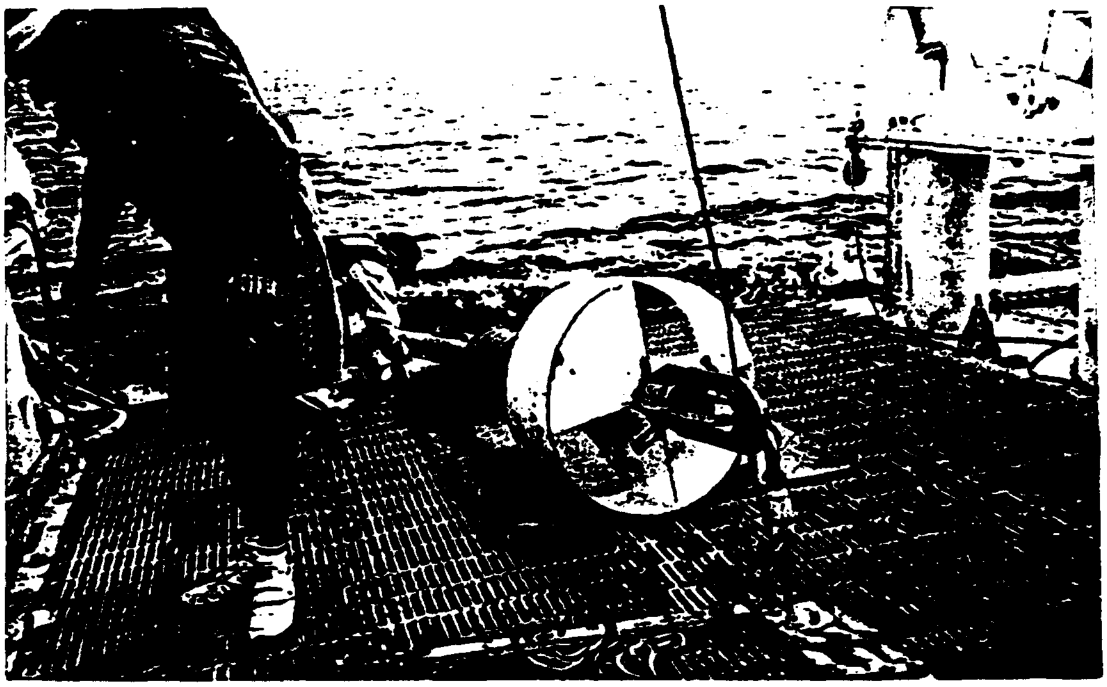

Figure 2. URI/MGL Large-diameter Gravity Corer

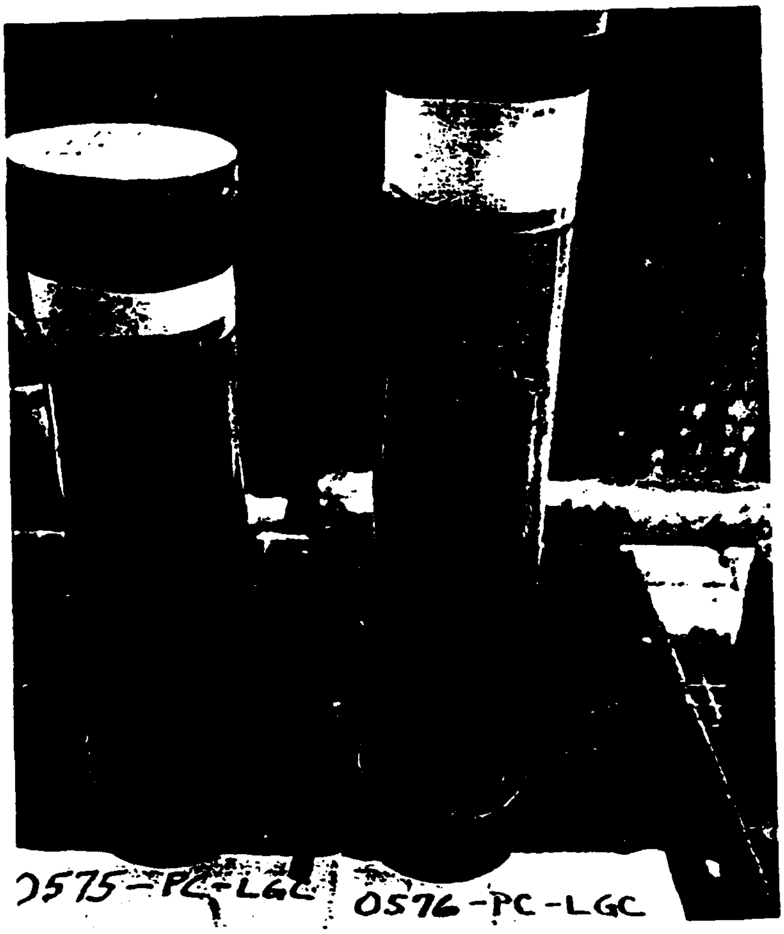

Figure 3. Core 575-PC-LGC (left), Core 576-PC-LGC (right)

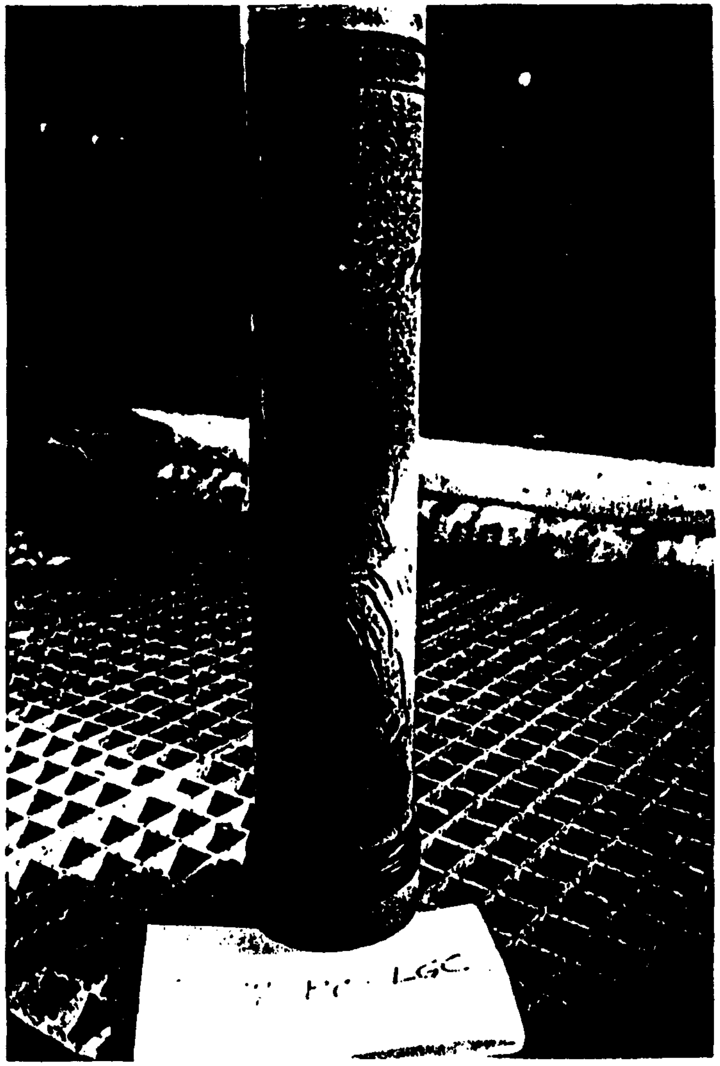

Figure 4. Core 577-PC-LGC

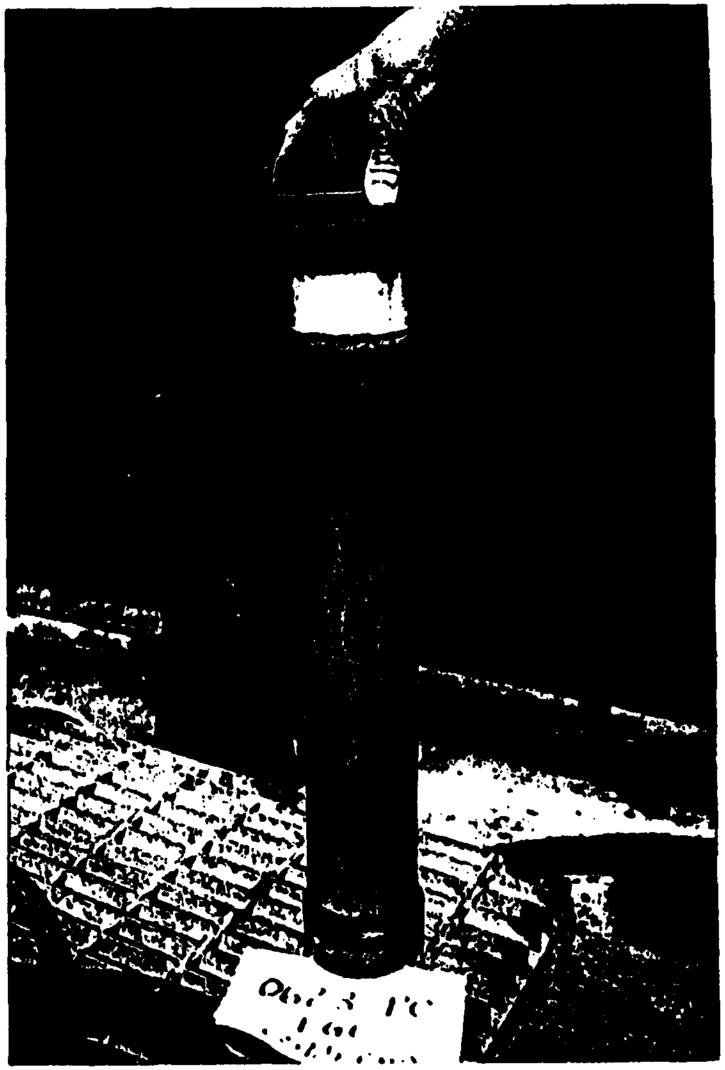

Figure 5. Core 623-PC-LGC

3.19 High-Frequency Acoustic Boundary Scattering Measurements in Eckernfoerde Bucht, Germany and Off Panama City, Florida (Principal Investigator: S. Stanic, NRL)

CBBLSRP FY93 YEAR-END REPORT

S. Stanic, E. Kennedy, B. Brown, R. Smith and E. Besancon
Code 7174
Naval Research Laboratory
Stennis Space Center, MS 39529-5004

INTRODUCTION: This brief report outlines the acoustic reverberation, scattering, and penetration data taken during two shallow-water high-frequency boundary scattering field experiments. These measurements were part of NRL's Coastal Benthic Boundary Layer (CBBL) and High-Frequency programs. The first took place in Eckernfoerde Bucht, Germany in May 1993 and the second took place in August 1993 in an area 26 miles south of Panama City, Florida. These experiments were designed to identify the mechanisms that control the interaction of high-frequency acoustic energy with the ocean bottom. These experiments will also provide the Coastal Systems Station with data and models needed for the development of various MCM systems. During both experiments, reverberation and reflection measurements were also taken from the rough ocean surface.

MEASUREMENTS SYSTEMS: The acoustic data were taken using NRL's high-frequency measurement systems. These systems use a series of high-frequency (20 kHz to 600 kHz) transmitting and spatial receiving arrays mounted on top of two stable towers and buried hydrophone arrays in the ocean bottom sediment. Figure 1 shows the experimental configuration used during the Eckernfoerde and Panama City series of measurements. The distance between the towers and positions of the buried hydrophone arrays were determined using CTD data and the Generic Sonar model.

ENVIRONMENTAL DATA: The high-frequency acoustic measurements were supported by data provided by CTD's and current meters. During the surface scattering measurements data on wind speed and direction was also recorded. These data will be documented in a separate report now in preparation. Additional environmental measurements detailing the character of the ocean bottom and water column were taken by the CBBL-SRP.

REAL TIME DATA RECORDING: The acoustic data were recorded using NRL's high-frequency digital data acquisition system. The digitizing system used to capture the high-frequency experimental data is centered around the Tachion Data Acquisition System supplied by Kinetics Systems.

System architecture is based on CAMAC technology and utilizes two CAMAC crates each with their own crate controller and FIFO buffer module. Each plug-in Analog/Digital module is capable of simultaneous sampling eight channels at a sample rate of 20 Khz.

Each crate is currently configured with 5 A/D modules for a maximum capacity of 80 channels. The system uses a high speed parallel transfer disk subsystem supplied by Storage Concepts to provide real-time data storage. The system is currently configured with 3 gigabytes of on-line storage, and can be expanded with plug-in modules to a maximum of 12 gigabytes.

The Tachion Data Acquisition System is hosted by a VAX 3500 Workstation. This system is utilized to provide interactive command and control of the real-time data acquisition and display utilizing crate FIFO buffer modules.

ACOUSTIC BOUNDARY SCATTERING AND PENETRATION DATA: Table I is an list of the data taken during the Eckernfoerde Bucht, Germany and Panama City, Florida experiments. A total of 150 pulses were taken for each experimental configuration.

TABLE I

ACOUSTIC MEASUREMENT	MEASUREMENT PARAMETERS
Bottom reverberation	Frequency: 20 - 600 kHz Grazing angles: 5° - 30° Pulse types: CW/LFM, 2-10 ms
Bottom reflection / scattering	Frequency: 20 - 180 kHz Grazing angles: 5° - 30° Pulse types: CW/LFM, 2-10 ms
Bottom bistatic scattering	Frequency: 20 - 90 kHz Grazing angles: 30° 90° Azimuthal angles: 5°, 14°, 25° Pulse types: CW, 1 - 5 ms
Direct path propagation	Frequency : 20 - 180 kHz Pulse types: CW, 1 - 5 ms
Bottom penetration	Frequency: 10 - 180 kHz Grazing angle: 90°, 30°, 20°, 17°, 10° Pulse types: CW/LFM, .35 - 5 ms
Surface reverberation	Frequency: 20 - 600 kHz Grazing angles: 10° - 30° Pulse types: CW/LFM, 1 - 3 ms
Surface reflection / scattering	Frequency: 20 - 180 kHz Grazing angle: 10° - 30° Pulse types: CW/LFM, 1 - 3 ms
Surface bistatic	Frequency: 20 - 90 kHz Grazing angles: 26 Azimuthal angles: 6°, 15°, 25° Pulse types: CW, 1 - 3 ms

DATA ANALYSIS: The acoustic reverberation, scattering, and penetration data will be analyzed to provide estimates of bottom scattering strengths, reflection loss, scattering statistics, direct path propagation loss and statistics, spatial and temporal coherence, and bottom penetration loss. These data will be combined with portions of the analyzed environmental data and used to develop, and validate models being developed by NRL's 6.1 CBBL-SRP and NRL's 6.1 and 6.2 High-frequency programs.

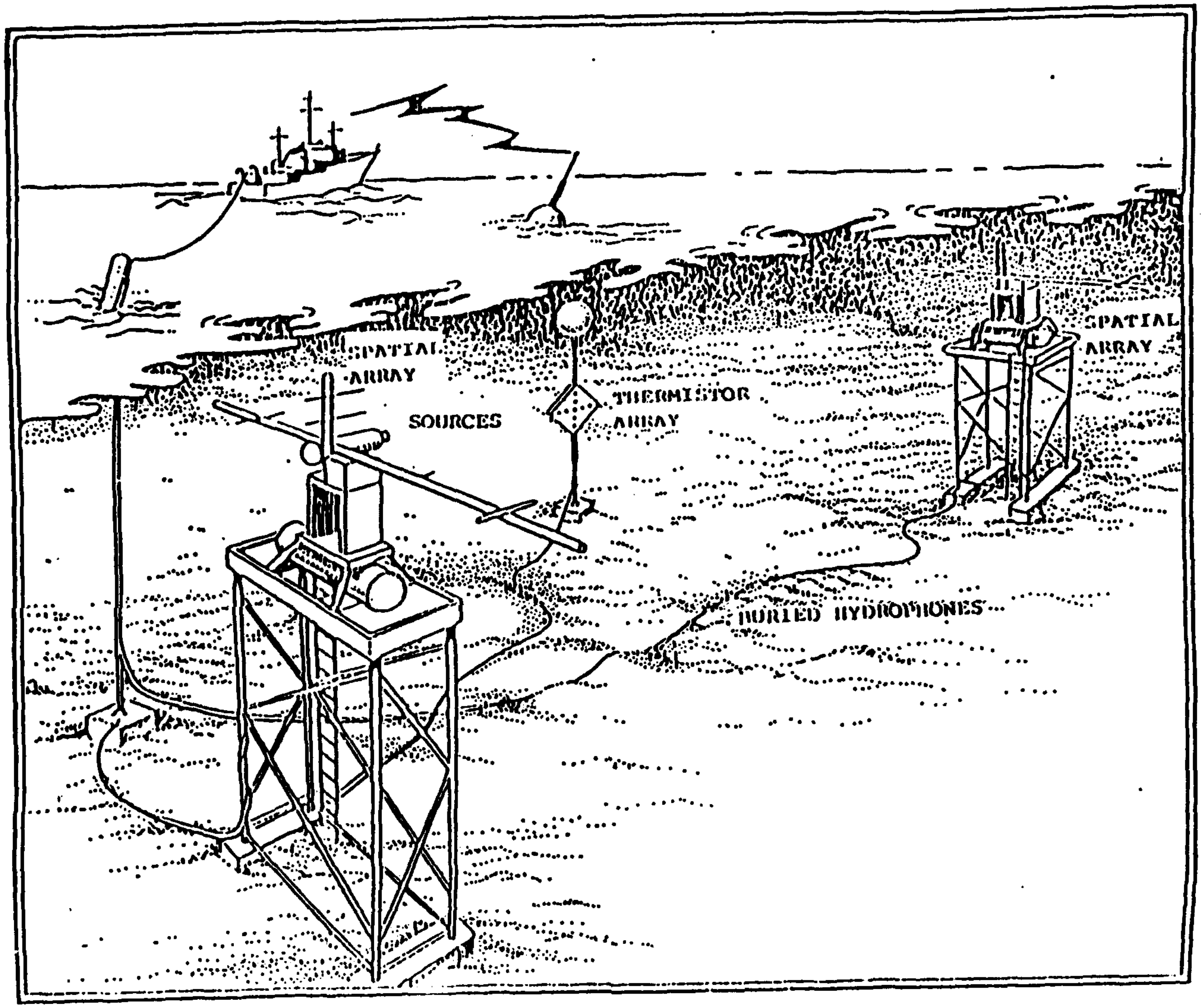

FIGURE 1 EXPERIMENTAL CONFIGURATION

3.20 Experimental and Theoretical Studies of Near-Bottom Sediments to Determine Geoacoustic and Geotechnical Properties (Principal Investigator: R. D. Stoll, Lamont-Doherty)

CBBLSRP FY93 YEAR-END REPORT

Robert D. Stoll
Lamont-Doherty Earth Observatory
Palisades, NY 10964

INTRODUCTION

This report summarizes the participation of the Lamont-Doherty (LDEO) team in the Coastal Benthic Boundary Layer Program (CBBLSRP) during the period of time December 15, 1992 to October 1, 1993. The LDEO team consisted of the following personnel:

Prof. Robert D. Stoll - LDEO
Prof. Roger Flood - SUNY, Stony Brook
Mr. Ivars Bitte - LDEO
Mr. Edgar Bautista - LDEO

Our main objectives during the first year of the program were to improve techniques for measuring shear-wave velocity as a function of depth in the sediments immediately beneath the seafloor and to design, build and test a cone penetrometer that would measure in situ shear strength at the same location as the shear-wave measurements. This allows direct correlation between undrained shear strength at the seafloor, which is very important in mine countermeasures work, and shear-wave velocity, which can be measured remotely using a number of different techniques.

The equipment and techniques that evolved during this first year of work were tested during three separate field experiments:

I. Baltic Sea at Eckernfoerde, Germany in cooperation with Forschungsanstalt der Bundeswehr fur Wasserschall und Geophisik (FWG). (May 11 - 15, 1993)

II. Gulf of La Spezia, near the SACLANT Undersea Research Center, La Spezia, Italy in cooperation with SACLANCEN. (May 24 - 27, 1993)

III. Gulf of Mexico near Panama City, Florida. (August 19 - 23, 1993)

The field work in Germany and Florida was sponsored by the CBBLSRP (Dr. Michael Richardson, Chief Scientist) whereas the work in Italy was sponsored by ONR Code 324OA and the U.S. National Liaison Officer to SACLANCEN (Mr. Edward Estolate).

The experiments carried out by the LDEO team employed several newly developed pieces of equipment which were improved at each stage of the field program outlined above. In one type of experiment, we used a torsional source which generates horizontally polarized shear waves and a cone penetrometer, both mounted on a self-righting sled which is deployed on the seafloor. In a second set of experiments, the torsional source was replaced with an impulsive source which utilizes 22-caliber, blank cartridges to generate p- and sv-waves. The equipment for both types of experiment is shown in Fig. 1.

EQUIPMENT AND TECHNIQUES

Fig. 1 shows two different kinds of seismic source mounted on a self-righting sled which also acts as a platform for a cone penetrometer. In deploying the sled, 12 gimballed geophones attached at regular intervals (5 m) to a multichannel cable, form a linear array spanning a distance of 65 m from the seismic source (see Fig. 2.). After the sled and array are dragged a short distance over the bottom to insure straight alignment of the phones, a pulse is applied to the seafloor by the seismic source. We have employed two different kinds of source in these experiments; one generates strong horizontally polarized shear waves (SH-waves) as a result of torsional motion coupled to the bottom and the other generates vertically polarized shear-waves and compressional waves as a result of a pressure pulse applied vertically to the bottom over a small, circular area. Since virtually all sediments are vertically inhomogeneous with respect to shear wave velocity, the sources described above generate strong, dispersive interface waves (Love waves for the torsional source and Scholte waves for the vertical source) which may be analyzed to obtain the shear-wave velocity as a function of depth in the sediments immediately beneath the seafloor.

The torsional source, shown mounted on the sled in Fig. 1(a), was developed at Lamont (LDEO) under ONR, Code 324OA sponsorship in 1992. The source generates torsional pulses over a small circular area of the seabottom by utilizing energy stored in a rotating flywheel which is driven by a small DC motor. The speed of the flywheel is slowly increased to the test level (typically 200 to 500 rpm) after which two diametrically opposed anvils are impacted by hammers on the outer diameter of the wheel. The sudden torque caused by this impact is transmitted to an external base plate which rests on the seafloor and the torsional motion is coupled into the sediment by vanes or spikes attached to the bottom of the plate. In theory, this type of source should produce a radially symmetric wavefield composed only of horizontally polarized shear waves and the resulting Love modes caused by vertical inhomogeneity, however in reality, some of the energy is converted to p-wave and sv-wave motion for a variety of different reasons.

A schematic of the SH generator and some early test records are shown in Fig. 3. We have deployed the new torsional source at a number of different sites containing both soft and firm sediments and have developed an inversion program to obtain the geoacoustic properties of the sediment based on the dispersion of the Love waves that are generated.

The vertical source, shown mounted on the sled in Fig. 1(b), is a multishot gun which utilizes 22 caliber blanks of the kind used in the construction industry to drive bolts and studs into wood or masonry. In the version shown in the figure there are 11 shells, each confined in a separate chamber by a frangible plastic disk sealed by an "O" ring. When each shell is fired, gas pressure builds until the plastic disk ruptures and the gas is vented downward into a cylindrical, helmet-shaped chamber with no bottom resting on the seafloor. As a result, a sudden pressure pulse normal to the bottom is applied to the sediment. When this source is used the phones in the geophone array are gimballed to respond to vertical motion whereas in the experiments with the torsional source they respond to transverse, horizontal motion (i.e., perpendicular to the cable).

In addition to the two sources mounted on the sled, we utilized a third type of source at some of the experimental sites. This source, shown in Fig. 4, is a three-shot gun utilizing 8-gauge seismic shells to apply a vertical transient pulse to the seafloor. We have successfully used this source for a number of years in conjunction with a longer array. Since a larger amount of energy is applied to the sediment, the center frequency of the transient pulse tends to be somewhat lower while some of the higher frequencies are missing. As a result, the penetration into the seafloor is deeper while the resolution near the water-sediment interface is less.

The newest addition to our equipment is the cone penetrometer shown mounted on the sled in both Figs. 1(a) and 1(b). This device contains a standard 60^{o} cone with a crossectional area of 10 cm^2 which is pushed into the sediment to a depth of 20 to 60 cm at a rate of about 1 cm/sec. The total force necessary to advance the probe is measured by a strain-gage load cell built into the tip. The force and depth of penetration are continuously displayed and recorded by a digital data acquisition system running in conjunction with a PC. Without adding any additional weights to the sled, the maximum force that can be applied to the penetrometer is about 100 lb, however with the addition of lead weights a force of up to 400 lb is possible. Because of the specially designed load cell, the new penetrometer is unique in that it allows us to measure the very low penetration resistance that is often encountered immediately beneath the seafloor.

EXPERIMENTAL RESULTS

I. Eckernfoerde, Germany

The design and construction of the cone penetrometer was begun on Dec. 15, 1992 and the finished sled was delivered to Memphis Tennessee for shipment to Germany on April 1, 1993 (something of a record, I believe).

Experimental work was performed onboard the German ship 'Wilhelm Pulwer' on May 13 and 14, 1993. Since the equipment was designed and built under such a tight schedule, these experiments represent the first sea trials of most of the gear except the torsional source. Experiments were performed at seven different stations which are summarized in Appendix A. The seafloor sediments over the main test area were very soft, fine-grained materials with very little shear strength and very low shear-wave velocity. Typical traveltime curves for Love waves generated by the torsional source are shown in Fig. 5. where it should be noted that it takes over 12 sec for the interface wave to traverse the 65 m length of the receiver array. A multiple filter analysis of the traveltime curve for channel 8 produces the Gabor diagram shown in Fig. 6 and an inversion of the group velocity dispersion curve determined from Fig. 6 results in the model shown in Fig. 7. The surface velocity of 4 or 5 m/s is the slowest we have measured in any of our experiments to date. For a discussion of the various inversion methods used to obtain the model see Stoll et al (1991 and 1993). We were unable to obtain any meaningful data with the penetrometer in the main test area because of the extremely soft nature of the surficial sediments and the fact that there was only time enough to construct one "multipurpose" penetrometer tip before the equipment was shipped. Hence, in order to test the penetrometer, we performed some experiments at stations in the area called "Mittelgrund" where there was reported to be a sand bottom. The results of a penetrometer run in this area are shown in Fig. 8. The penetration resistance in millivolts can be converted to force using the calibration constant 16.4 mv/kgf.

II. La Spezia, Italy

Experimental work was performed on board the NATO ship 'R/V Manning' at several sites in the Ligurian sea just outside of La Spezia. Station locations and other information are given in Appendix B. The "ground truth" at each of the sites is well documented since numerous experiments have been carried out in this area over the past several years (see Richardson et al, 1991). At each site we deployed the sled and made both penetrometer and shear-wave measurements along a line at points about 10m apart. The results of the penetrometer tests at three different sites (Porto Venere, Tellaro and Mariperman Buoy) are shown in Figs. 9, 10 and 11. A set of traveltime curves generated by the vertical source at Porto Venere, the results of a multiple filter analysis and the model obtained from the group velocity dispersion of channel 7 are shown in Figs. 12, 13 and 14. Since one of the main purposes of our experiments is to obtain a correlation between in situ shear-wave velocity (or alternatively maximum dynamic shear modulus), and undrained shear strength, we have tabulated average values of the penetration resistance from the test data of Figs 9 thru 11, the average shear-wave velocity over the first 50 cm below the seafloor, and the range of values of porosity for several different sites in Table 1. The data in this table are rough, first estimates which will be modified as further inversion of the data is completed.

Table -1

Site	Porosity %	Penetration Resist. kg/cm^2	S-Wave Velocity m/s
Porto Venere	62 - 67	3.1 - 6.1	27 - 31
Mariperman Buoy	44 - 59	27.5 - 48.8	44 - 49
Tellaro	3 - 64	4.6 - 30.5	30 - 34
Eckenfoerde	85 - 89	N.A.	4 - 8

In order to obtain the desired correlation, it is necessary to convert the measured penetration resistance to undrained shear strength taking into account such factors as strain-rate dependence, sediment type, percent saturation and a number of other variables. There already exists a considerable literature describing the effects of these factors (e. g. see Strength Testing of Marine Sediments, 1985) however we have deferred our interpretation until new theoretical studies (part of our CBBLSRP work scheduled for 1994) are further advanced and a full review of prior work is completed.

III. Panama City, Florida

In the work at Panama City we performed 66 seismic experiments and 21 penetrometer tests at eight different stations. The locations of the stations are listed in Table C1 and plotted in Fig. C1 of Appendix C. The locations of the stations were chosen so that some of the experiments would be carried out in the area where the surface stratum was known to be "fine Sand" while others would be in the area blanketed by a "coarse, shelly Sand". In addition one station was chosen as close as possible to the border between these to areas. A list of all of the experiments performed including the names of the corresponding data files is given in Table C2 of Appendix C.

Both the torsional source and the 22-caliber source produced excellent traveltime records which may be analyzed in a variety of different ways to obtain geoacoustic models with relatively high resolution (e.g., 25 cm layers) near the seafloor. Examples of traveltime curves for all three sources are shown in Figs. 15, 16, and 17.

We have begun to invert the seismic data by analyzing both group and phase velocity dispersion. Some preliminary models derived from these inversions are shown in Figs. 18, 19 and 20. Detailed analysis will continue through this fall and winter.

Results of some of the penetrometer tests are shown in Figs. 21 and 22. Since the underwater weight of the sled including the seismic source and penetrometer is relatively light, we were only able to produce a vertical thrust on the penetrometer of a little over 100 lbs during the first day of testing (Aug. 20). On the second day, (Aug. 21) the addition of a heavy lead weight allowed the penetrometer thrust to be increased to over 200 lbs. The results shown in Figs. 21 and 22 may be interpreted using a calibration factor of 7.9 millivolts per lb of thrust. As can be seen from these figures, the maximum depth of penetration we were able to attain in these sandy sediments was about 35 cm due to the limitation imposed by the weight of the sled.

SUMMARY

At this point in the CBBLSRP we feel that we have been successful in developing a simple, robust system for in situ measurement of shear wave velocity and penetration resistance. The experiments in Germany, Italy and Panama City, Fla. as well as some additional work in New York Harbor, have allowed us to debug the system and to accumulate a library of data which we will analyze and use in conjunction with our theoretical studies of the relationship between shear strength and shear wave velocity during the second year of the project.

In view of the success of our work to date, we also have made tentative plans to participate in a cooperative program with SACLANCEN aimed at the development of an expendable, rapid deployment system that would immediately provide basic information on the character of the bottom (i. e. penetrable or nonpenetrable, acoustically hard or absorbing, etc.) and could be launched either from a ship or an aircraft. The development of this system will be guided by the results of our current efforts in the CBBLSRP and will clearly be of importance in MCM operations.

REFERENCES

Richardson, M. D., Muzi, E., Miaschi, B. and F. Turgutcan (1991) "Shear wave velocity gradients in near-surface marine sediments," in J. M. Hovem, M. D. Richardson and R. D. Stoll (eds), Shear Waves in Marine Sediments, (Kluwer Academic Publishers, Dordrecht), 295-304.

Stoll, R. D., Bryan, G. M., Mithal, R. and R. Flood (1991) "Field experiments to study seafloor seismo-acoustic response," J. Acoust. Soc. Am., **89**, 2232-2240

Stoll, R. D., Bryan, G. M., and E. Bautista (1993) "Measuring lateral variability of sediment geoacoustic properties," submitted to J. Acoust. Soc. Am.

Strength Testing of Marine Sediments (1985) editors R. Chaney and K. Demars, ASTM Spec. Tech. Pub. No. 883 (Am. Soc. Testing and Materials., Philadelphia)

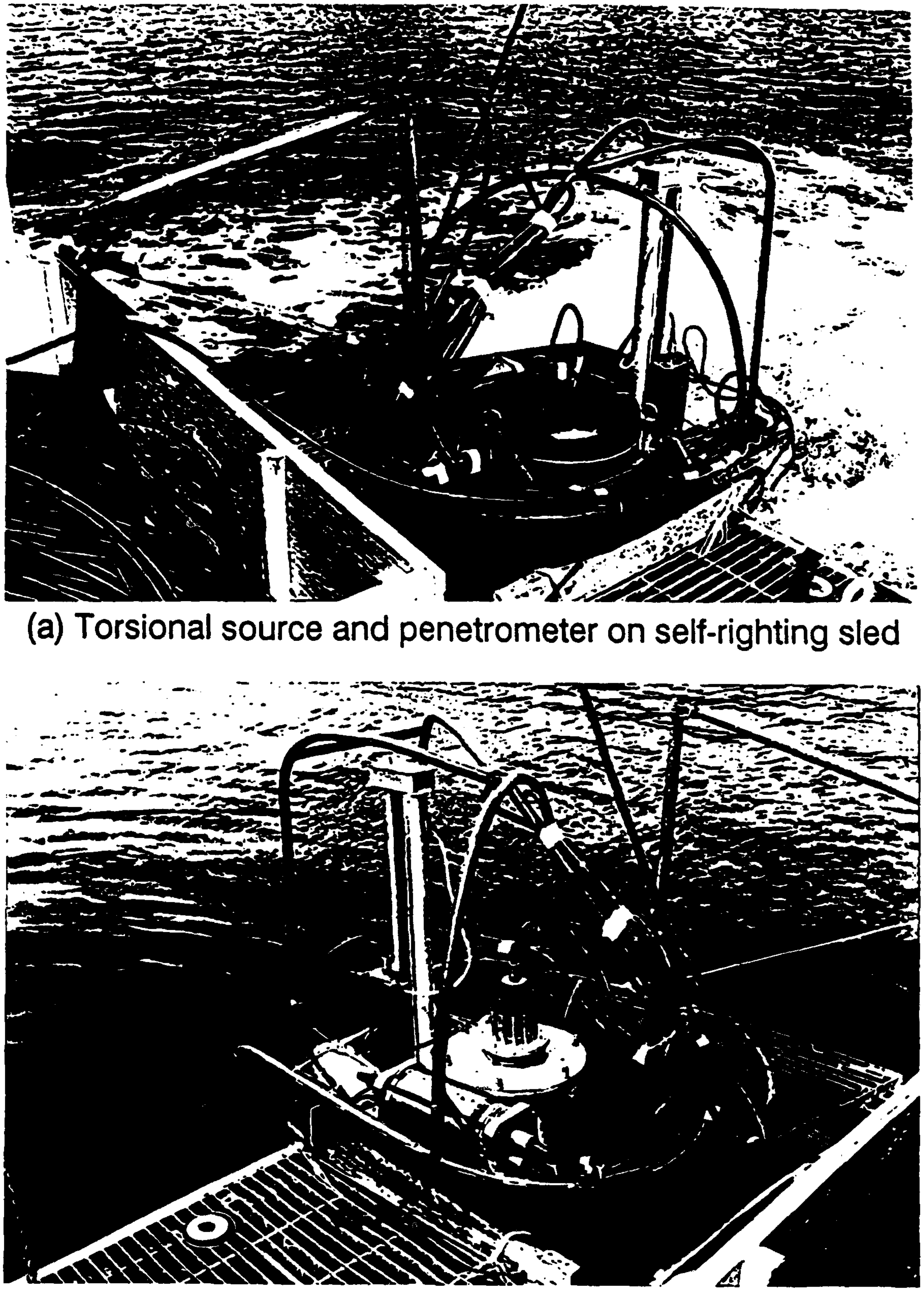

(a) Torsional source and penetrometer on self-righting sled

(b) 22-caliber vertical source and penetrometer

Fig. 1. Self-righting sled with seismic source and penetrometer.

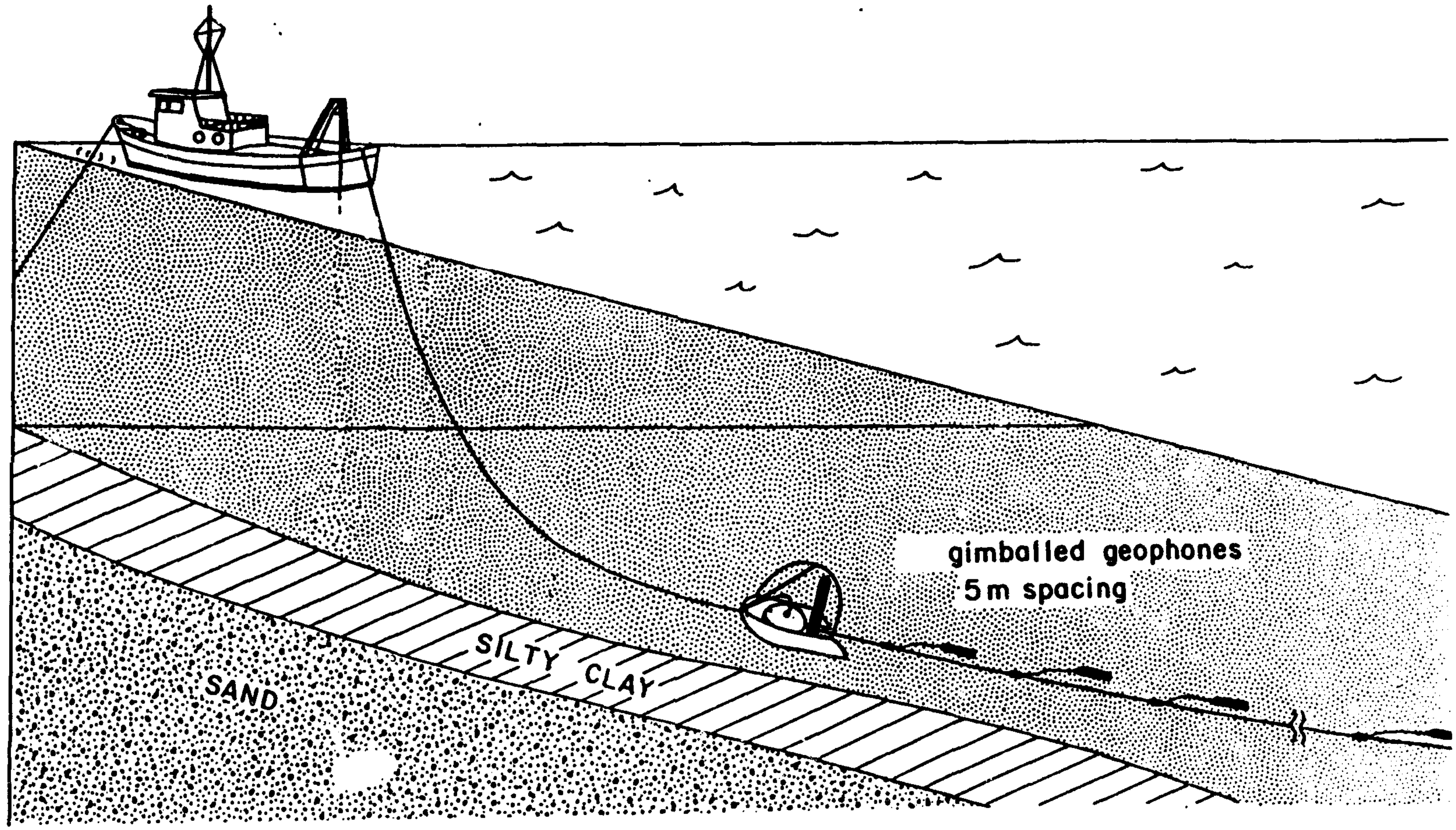

Fig. 2. Experimental configuration.

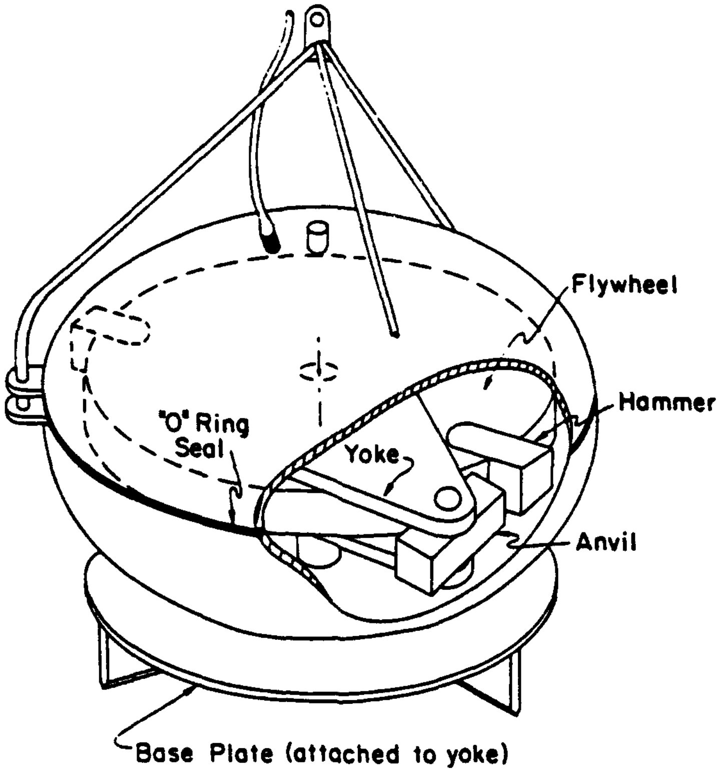

Fig. 3(a). Schematic of SH generator. Movement of anvil into the path of the hammer is syncronized with the rotation of the flywheel. Speed of flywheel is slowly increased to test level (typically 500 rpm).

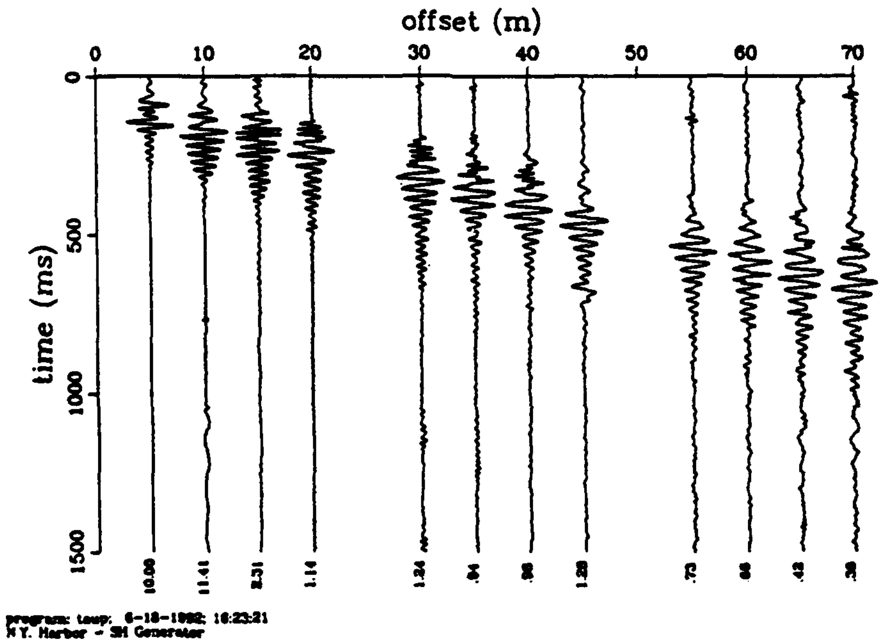

Fig. 3(b). Early test record of SH generator in N.Y. Harbor on sandy sediment.

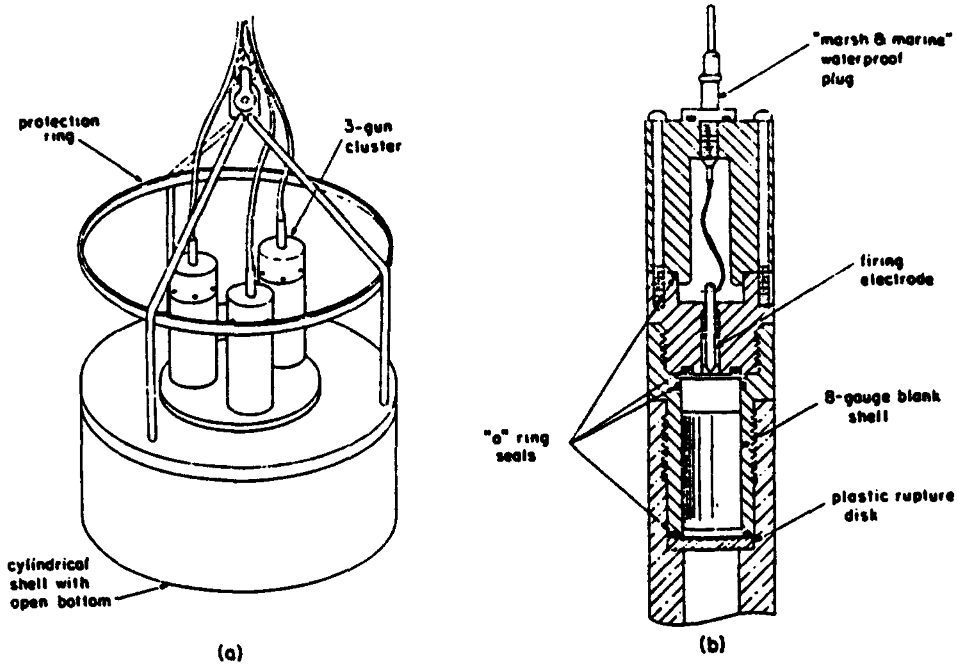

Fig. 4. Impulsive source utilizing 8-gauge, electrically detonated blank shells (Stoll et al, 1991).

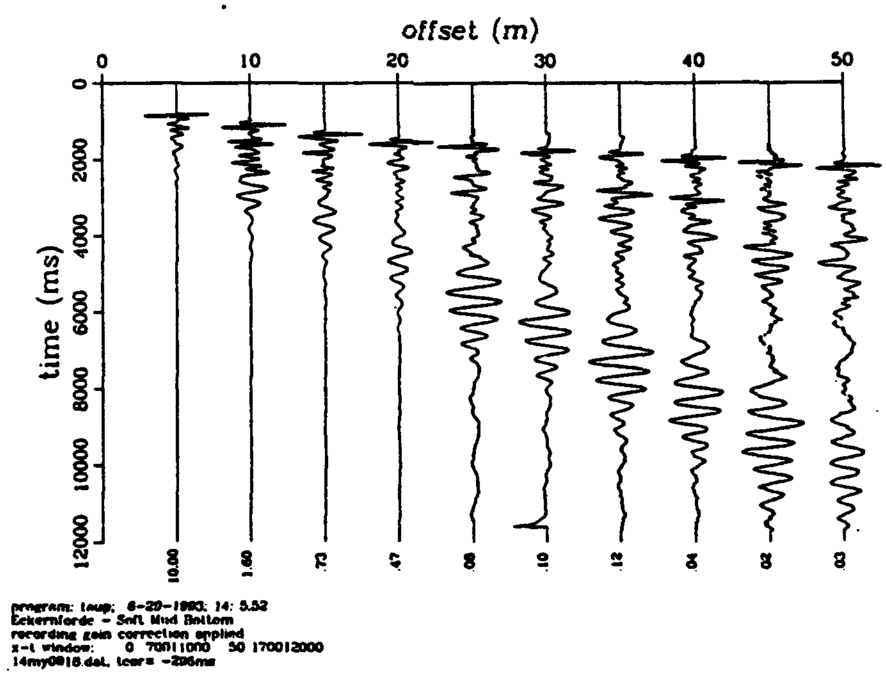

Fig. 5. Traveltime curves generated by the torsional source. Very soft bottom in Eckernforde, Germany.

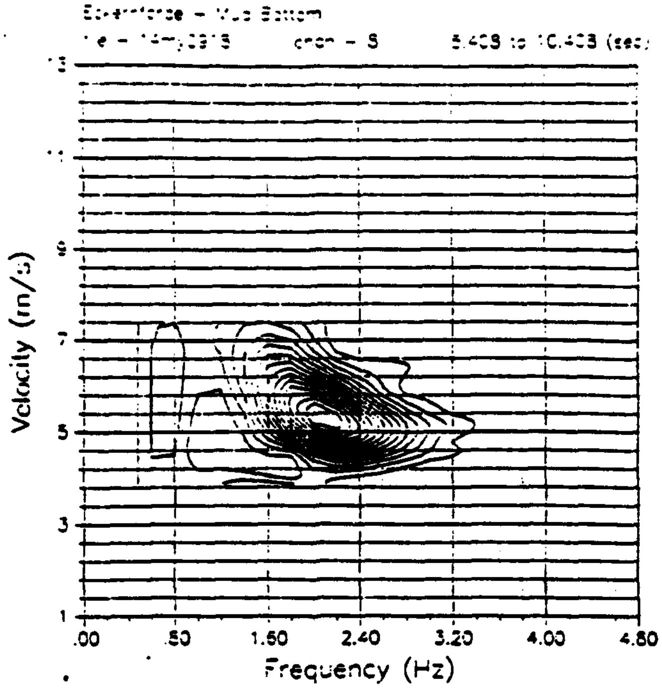

Fig. 6. Results of multiple filter analysis (Gabor diagram) for channel 8 of Fig. 5.

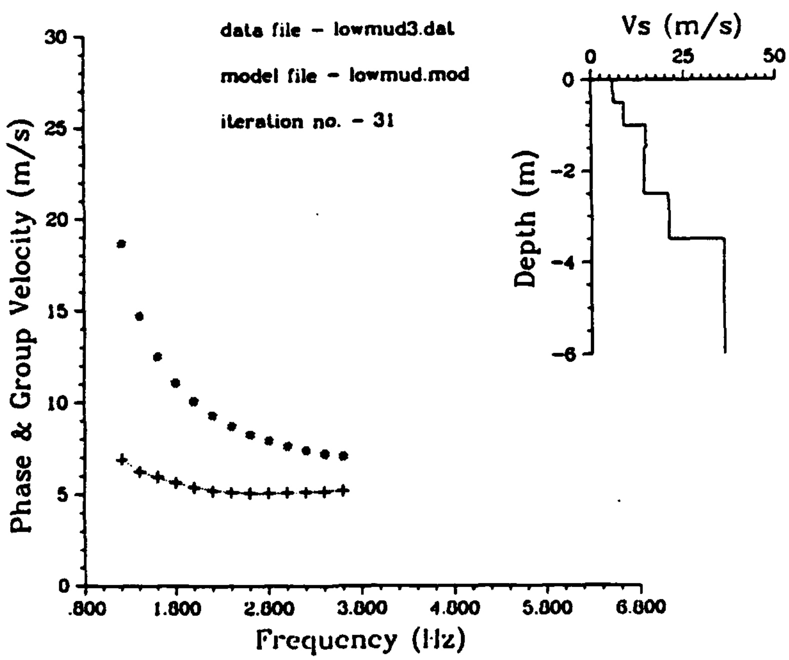

Fig. 7. Inversion of Love wave group velocity dispersion determined from Fig. 6. (+) symbols represent group velocities read from Fig. 6, (*) symbols represent theoretical values of phase velocity and the dashed line is the group velocity dispersion for the model in the righthand panel.

EKENPEN.XLC

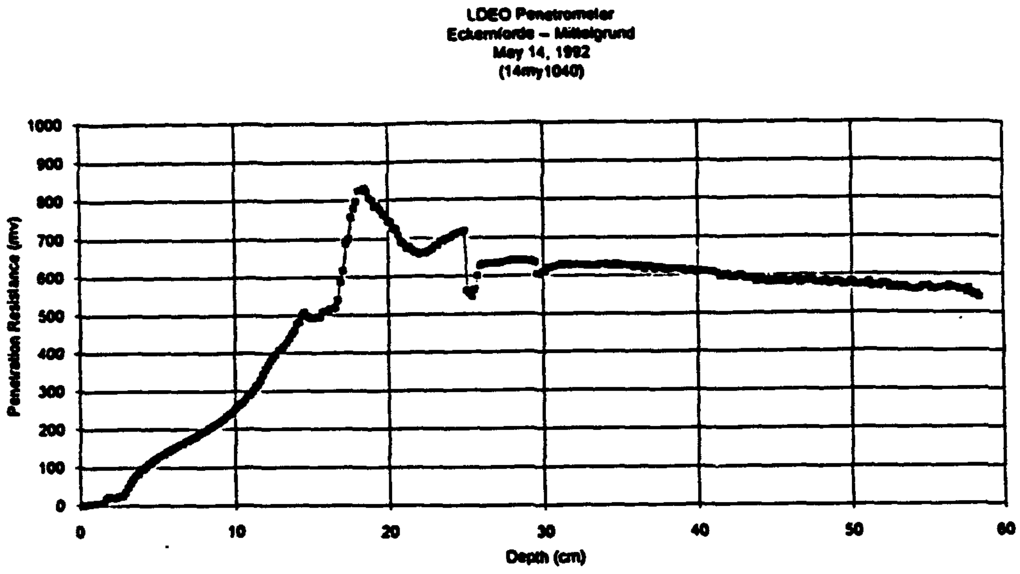

Fig. 8. Penetration resistance versus depth at "Mittelgrund" site, Eckernforde, Germany (calibration factor - 16.4 mv/kgf).

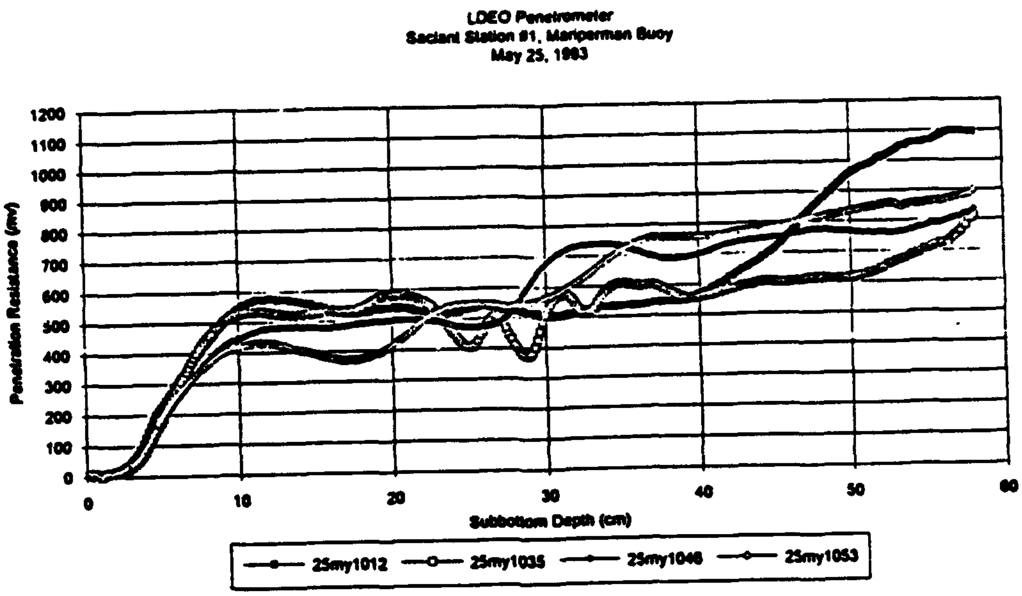

Fig. 10. Penetration resistance versus depth at Mariperman buoy.

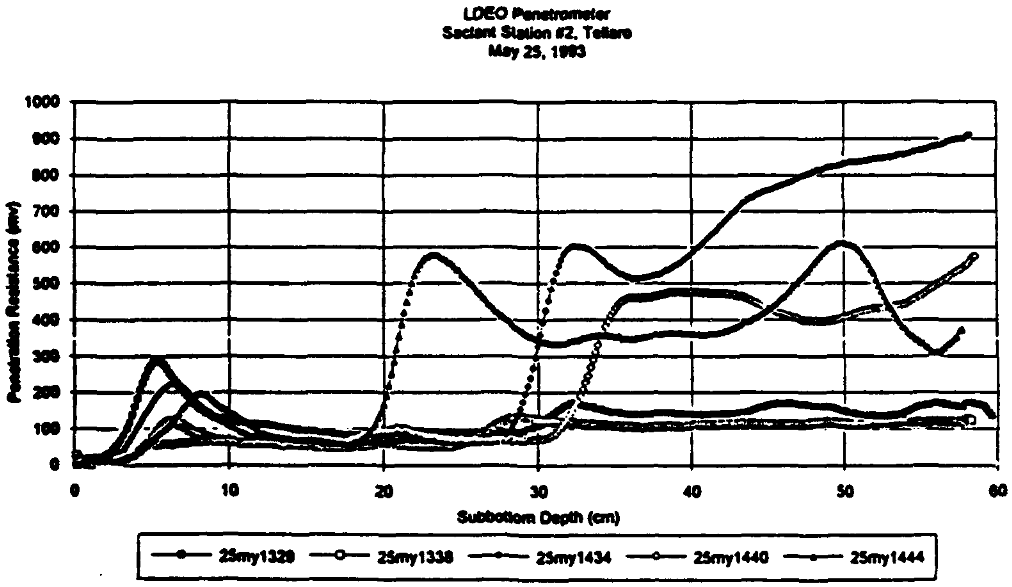

Fig. 11. Penetration resistance versus depth at Tellaro.

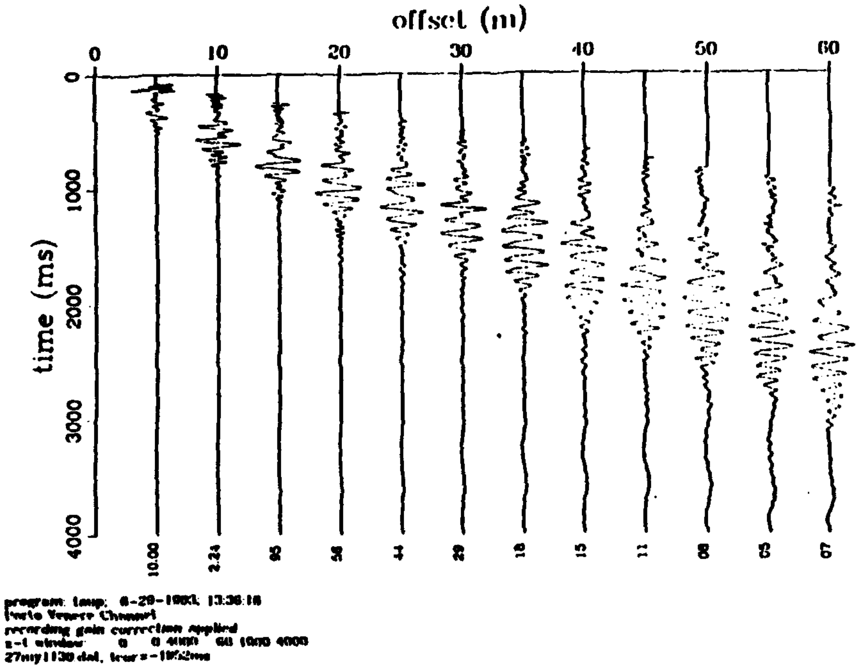

Fig. 12. Traveltime curves at Porto Venere. (22 cal. vertical source).

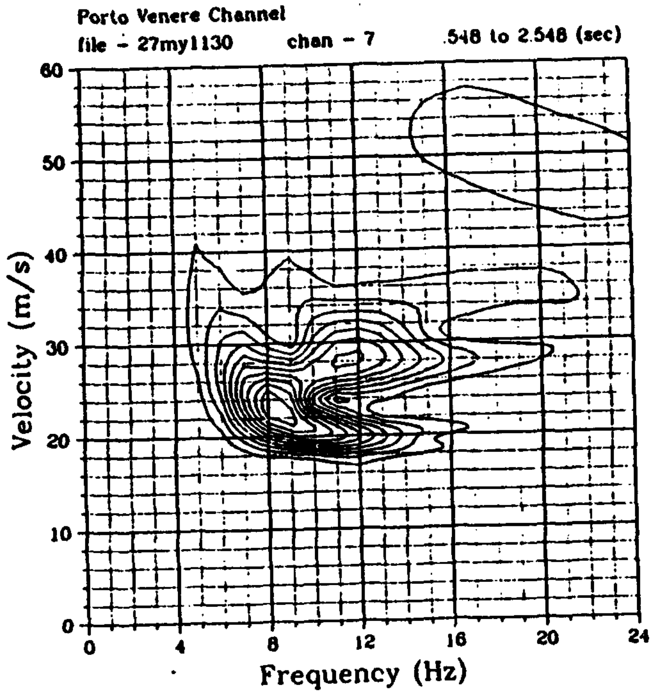

Fig. 13. Results of multiple filter analysis (Gabor diagram) for channel 7 of Porto Venere data shown in Fig. 12.

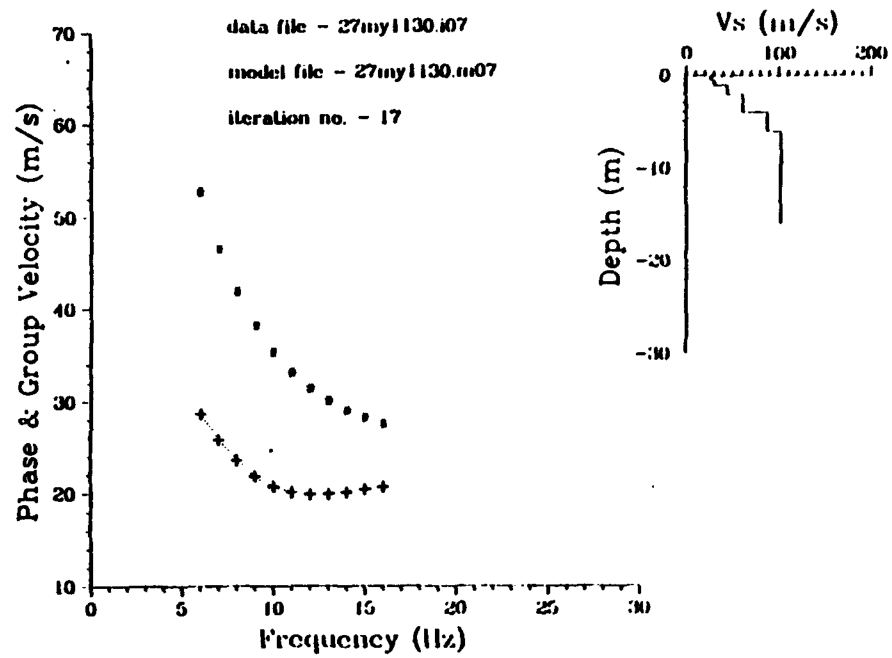

Fig. 14. Inversion of Scholte wave group velocity dispersion determined from Fig. 13. Symbols same as Fig. 6.

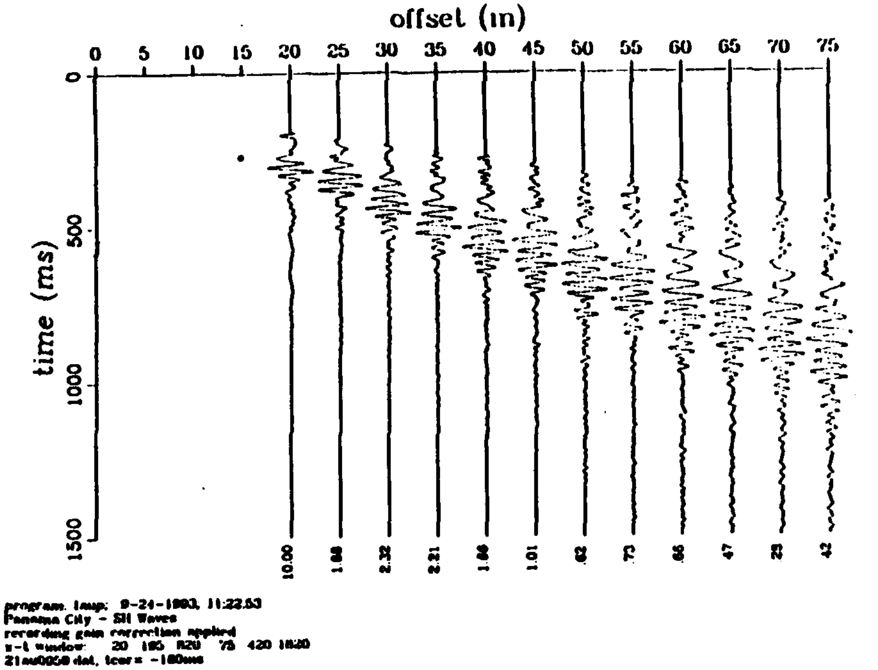

Fig. 15. Traveltime curves from Sta. 4. SH source. Data windowed to exclude first arrivals.

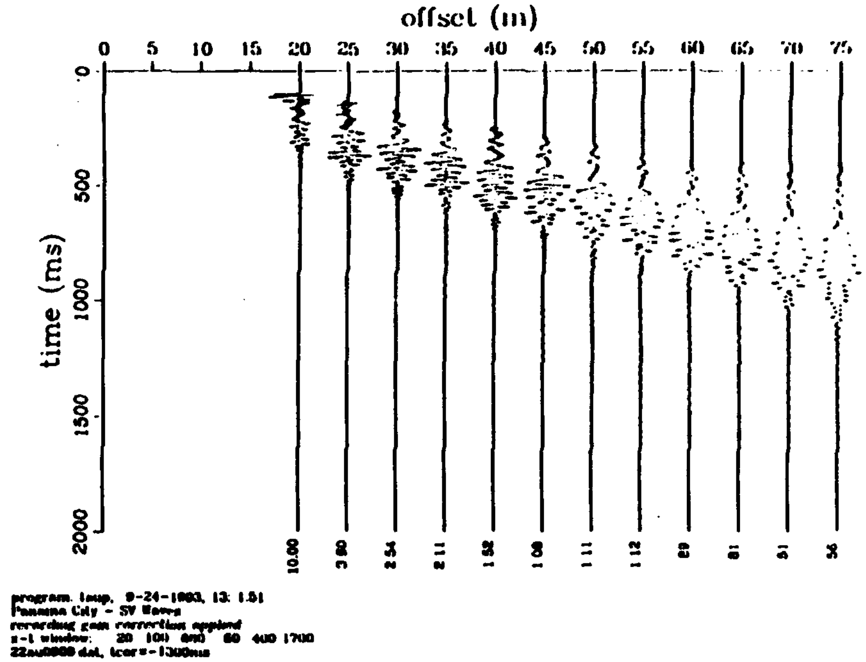

Fig. 16. Traveltime curves from Sta. 7. 22 cal. source. Data windowed.

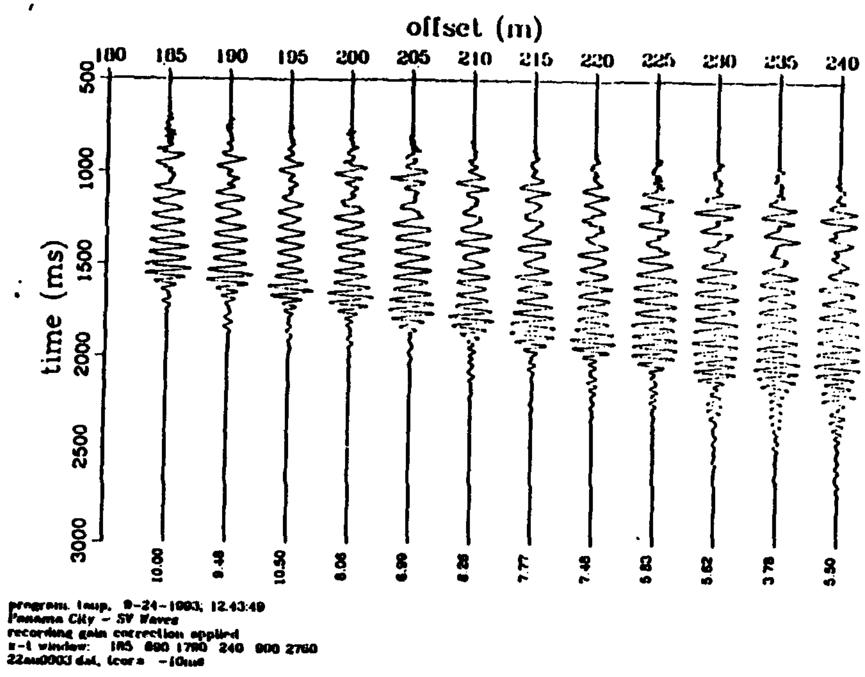

Fig. 17. Traveltime curves from Sta. 7. 8-gauge shotgun source.

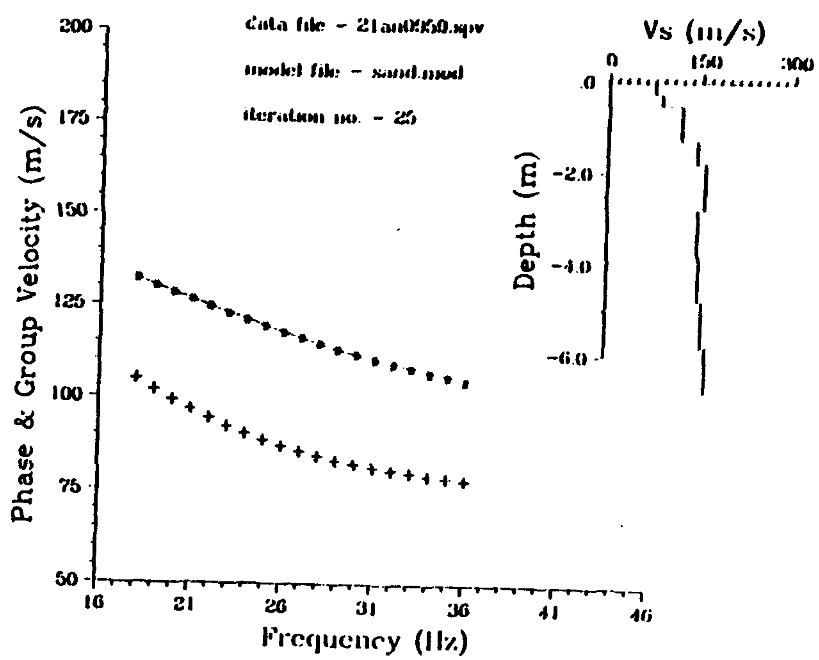

Fig. 18. Inversion of data from Sta. 4. Phase velocity curve is average of 5 channel pairs. SH source. "fine Sand" area.

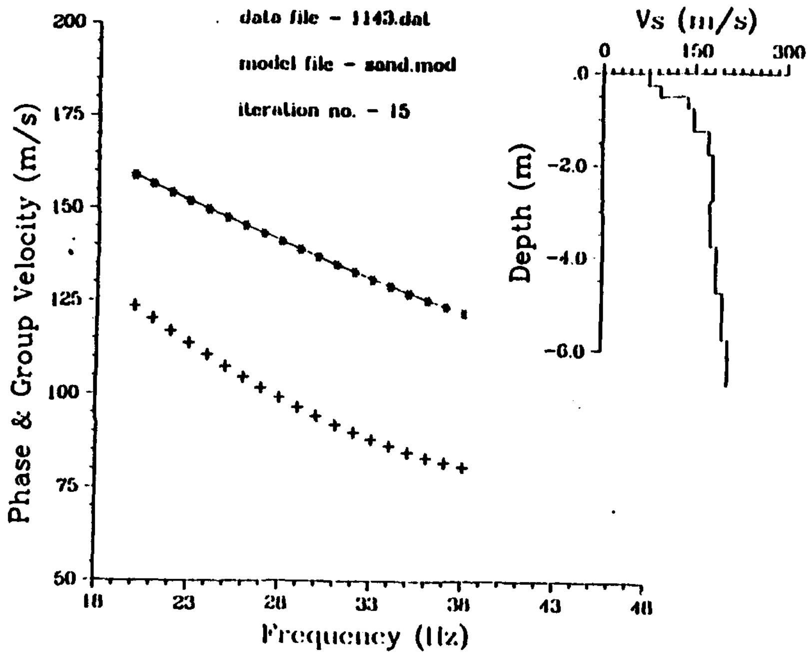

Fig. 19. Inversion of data from Sta. 5. Data from Chan. 16 & 17 smoothed using phase-matched filtering. "coarse Sand" area.

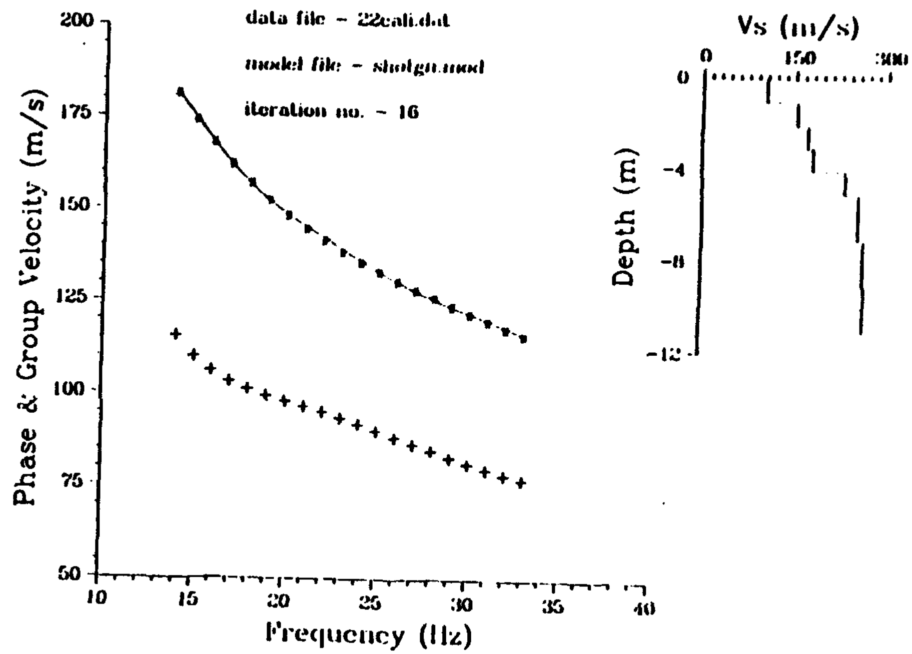

Fig. 20. Inversion of data from Sta. 7. Phase velocity curve is smoothed average of 5 channel pairs. 22 cal. source. "coarse Sand with shells".

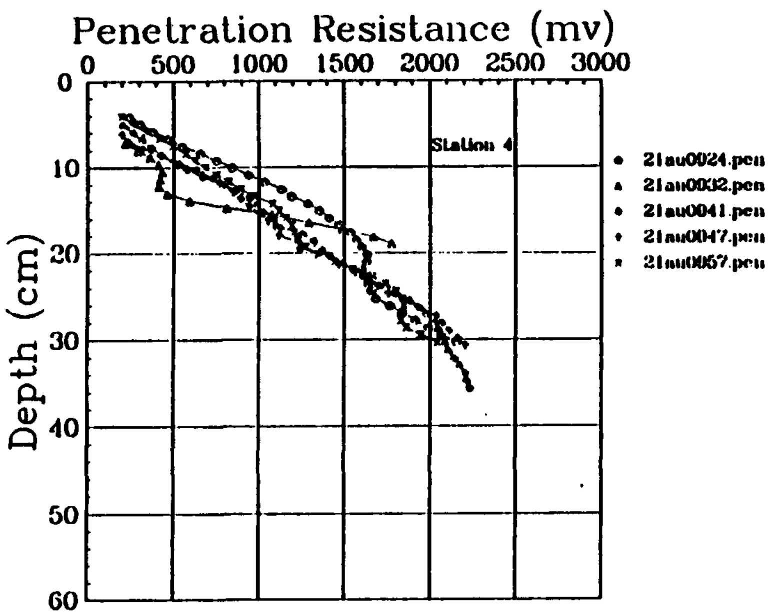

Fig. 21. Penetrometer test data from Sta. 4. "fine Sand" area.

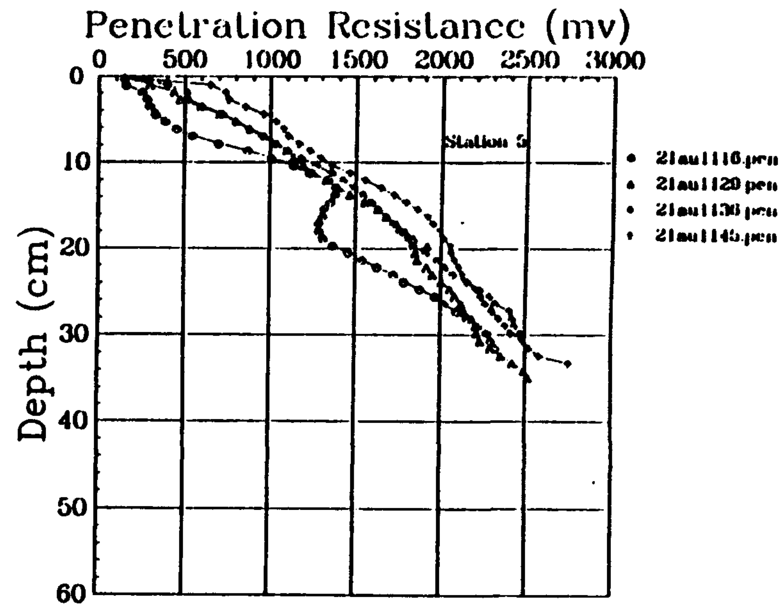

Fig. 22. Penetrometer test data from Sta. 5. "coarse Sand area.

3.21 Characterization of Surfacial Roughness and Sub-Bottom Inhomogeneities from Seismic Data Analysis (Principal Investigators: D. J. Tang, G. V. Frisk and T. Stanton, Woods Hole Oceanographic Institution)

CBBLSRP FY93 YEAR-END REPORT

Dajun Tang, George V. Frisk, and Timothy K. Stanton
Woods Hole Oceanographic Institution
Woods Hole, MA 02543

The first year of the Coastal Benthic Boundary Layer Special Research Program has seen two major experiments successfully completed. The data sets obtained in the experiments will enable us to test the theoretical models that we have been developing, and based on the data, we will have to address problems associated with the specific environments in the two experiment sites.

During the past year, our primary work has been in the areas of developing a theory of high-frequency acoustic scattering from a heterogeneous seabed and communicating with researchers who were directly involved in the experiments in order to facilitate future data processing. Since volumetric inhomogeneities in the sediments for both experiment locations are speculated to be important causes of scattering, we developed a ray-based model to calculate volumetric scattering strength of sediment inhomogeneities using the Born approximation. This model incorporates a sound speed gradient in the top layer of sediment into the scattering process, so that transmission loss is properly accounted for. Simulations show that this is a viable approach and we will test this model on the Baltic Sea backscattering data.

Another challenging area is the evaluation of the interface wave contributions to the scattered field at small grazing angles. Since high frequency acoustic energy suffers strong attenuation in the sediment, interface waves play an important role in the scattering process. However, the behavior of interface waves in the sediments is not well understood, especially when real data comparisons are concerned. We have been working on a theoretical formulation which will predict the interface wave strength in the sediments, and we are planning on testing it using Stanic's buried hydrophone data.

In order to better understand the experiments, D. J. Tang spent a few days at the Panama City site in August, observing the conduct of some of the experiments and exchanging ideas with other scientists.

During the October Acoustical Society of America Meeting in Denver, a data processing plan was developed with Darrell Jackson and Kevin Williams of the Applied Physics Laboratory, University of Washington. The first step will involve processing the backscattered data and finding the influence of gas bubbles in the sediment. Then we will work together on developing a bistatic scattering model and processing their bistatic data. Also we plan to work with Stanic on the interface wave problems.

In general, because of the success of the experiments, we feel confident that important progress can be made in the area of high-frequency acoustics interaction with shallow water sediments, and we are looking forward to starting work on the data. Next year we will present results of our work at the AGU/ASLO and ASA meetings.

3.22 Observations of Bottom Boundary Layer Hydrodynamics and Sediment Dynamics in Eckernfoerde Bucht and in the Gulf of Mexico off Panama City, Florida (Principal Investigator: L. D. Wright, Virginia Institute of Marine Science)

CBBLSRP FY9R YEAR-END REPORT

L.D. Wright
School of Marine Science
Virginia Institute of Marine Science
College of William and Mary
Gloucester Point, VA 23062

Summary

Instrumented bottom boundary layer tetrapods were deployed in Eckernfoerde Bucht at a depth of 26 m for a total period of 40 days in two deployments and in the Gulf of Mexico off Panama City, Florida at a depth of 27 m for a single deployment totaling 20 days. Complete, high quality data sets concerning near-bottom flows, bed stresses, suspended sediment concentrations, and bed micromorphology were recovered from both sites. Soft, fine grained sediment beds prevailed at the Eckernfoerde site whereas the bed off Panama City was composed of coarse material and was rough. However, low physical energy regimes characterized both sites: near-bottom flow velocities were consistently less than 10 cm s^{-1} in Eckernfoerde Bucht and less than 15 cm s^{-1} at the Panama City site. Although local resuspension caused by physical bed stress did not occur at either site, benthic biologic processes were highly active at both sites. Detailed analyses of the field data are currently in progress. Work in FY 1994 will focus on completing the analyses and relating results to numerical and analytical models of benthic processes at both sites.

Study Objectives

The general aims of our study of benthic hydrodynamics are: (1) to evaluate the dominant forcings responsible for bed stress; (2) to characterize the intensities, frequencies and directions of time-varying bed stress; (3) to determine the appropriate drag coefficients associated with both bottom types; (4) to determine the roles that physical transport processes play in resuspending sediment, mixing the sediment column, and molding bed micromorphology (roughness); (5) obtaining supplementary information (via bottom photographs) on the contributions (relative to physical) of benthic biologic processes; and (6) developing and refining models capable of predicting and explaining benthic flows, bed responses, and sediment fluxes in the environments examined.

Field Methodology

The VIMS bottom boundary layer instrumented tetrapod, shown in Figure 1, was used in the two deployments in Eckernfoerde Bucht and in the single deployment off Panama City. Diver observations of sensor height and orientation and of bed conditions were made at times of instrument deployment and retrieval.

The tetrapod was configured with the following instrumentation:

A. A Benthos model 372A Edgerton deep sea camera system with dual strobe flash heads. This was set at 1.65 m above the bed to obtain photographs covering 2 square meters at intervals of 2 hours.

B. An array of four Marsh-McBirney electromagnetic current meters interfaced to a Sea Data model 626 signal processing system and Onset Tattletale data logger. The current meters were set at different elevations within about 1 meter above the bed. This instrumentation was sampled at 1 Hz. The purpose is to obtain velocity profiles from which to measure bed stress.

C. An additional Marsh-McBirney current meter located at 125 cm above the bed and set to sample at 5 Hz for application of the Kolmogorov spectrum technique for estimating bed stress. This sensor was interfaced with a Sea Data model 635 logging system which included a Paroscientific digiquartz pressure sensor.

D. An array of five optical backscatterance (OBS) sensors to obtain suspended sediment concentration profiles. These sensors were situated at different elevations within the lower 1.3 m of the water column above the bed. The array was interfaced to an Onset Tattletale data logger and sampled at 1 Hz.

E. A digital sonar altimeter to measure changes in bed level (relative to tetrapod) or subsidence of the pod.

Field Observations in Eckernfoerde Bucht

During both Eckernfoerde deployments, data loggers were set to sample at four hour intervals for burst durations of 17 minutes giving a total of 2048 samples per burst. The tetrapod was initially deployed from the research vessel *Planet* on 3 April at a depth of 26 m. The location of the initial deployment site was latitude 54° 29' 27.38" N; longitude 9° 59' 08.20" E; the time of deployment was 10:27 GMT (12:27 local). This deployment site was located approximately 200 m from the site at which the APL tower was deployed. The deployment was completely smooth and without incident. Diver observations by VIMS divers (Gammisch, Wright) immediately following the deployment revealed that all instruments were intact and correctly oriented and that the tetrapod "feet" (or pads) experienced negligible sinking into the soft bed.

All loggers were programmed to start the first burst at 1200 Hrs GMT on 3 April 1993. The tetrapod was retrieved, following the initial deployment, using the vessel *Helmsand* at 0615 hrs GMT (0815 local) on 30 April 1993. After downloading the data, servicing the instruments and changing batteries, the tetrapod was redeployed from *Helmsand* on 3 May 1993 at 0815 Hrs GMT. The site of the second deployment was latitude 54°29.644'N, longitude 009°59.242'E. The configuration and sampling program used in the second deployment was the same as in the first. The final retrieval at the end of the second deployment took place aboard the vessel *Hieve* at 1500 Hrs GMT on 15 May 1993.

Both the first and second deployments were successful and yielded good quality data. Diver observations at the end of the first deployment and at the beginning of the second, indicated that the pod experienced only minor sinking into the soft bed and no tilting. During both deployments, excellent photographic information was obtained at two hour intervals for the entirety of the deployment periods. Boundary layer process data were recorded for a maximum of 64 bursts (total duration of 256 hours) during the first deployment and 61 bursts (244 hours) during the second deployment. Table 1 lists, more explicitly, the sampling schemes and successful recording durations of each sensor during each of the two deployments.

Preliminary Results from Eckernfoerde Bucht

Resulting time series of mean current speed and direction at an elevation of 109 cm above the bed during each of the two deployments are shown in Figure 2. Corresponding variations in current u and v velocities at four elevations are shown in Figures 3 and 4. Near-bottom mean current speeds commonly exceeded 5 cm s^{-1} and periodically exceeded 10 cm s^{-1}. The most notable features of both time series are the velocity fluctuations at periods slightly longer than a day. Preliminary spectral analyses of these fluctuations indicate periods in the neighborhood of 30 hours which is relatively close to the 28 hour sieche period reported for the Kieler Bucht region of the Baltic (DeFant, 1961). Pressure records from the second deployment (Fig. 5) indicate corresponding oscillations in surface elevation of about 25 cm. Further analysis and comparison of data with model results must be completed before any final conclusions can be drawn as to the nature of these phenomena.

For most of the time during the first deployment and for all of the time during the second deployment, the OBS and photographic data indicated extremely low turbidities; at no time did local resuspension occur. However, a prolonged event of elevated turbidity occurred during the first deployment centered about hour 120 and was accompanied by a drop in water temperature (Fig. 6). This same event was recorded by the APL acoustic tower. The increase in turbidity was followed by a dramatic increase in southerly flowing current speed. Photo data indicate that the turbidity increase involved the southerly advection of large flocs in association with the southerly surge of cooler water and was not the result of local resuspension.

Although physical resuspension of sediment was not active at either deployment site, camera data reveal that bed micromorphology was extremely active. This activity was biogenic and involved the formation and obliteration of hummocks and depressions as well as the appearance and disappearance of worm tubes. The photographs also suggest active mixing of the upper part of the sediment column by benthic biota.

A paper reporting our Eckernfoerde results to date has been submitted for presentation in the Coastal Benthic Boundary Layer special session at the Ocean Sciences Meeting in San Diego in February of 1994. A copy is appended to this report.

Field Observations at the Panama City Site

During the Panama City observation period, data loggers were set to obtain data bursts at three hour intervals; burst duration was 17 minutes. The details of sensor elevations, burst characteristics and data retrieval are summarized in Table 2. The tetrapod was deployed on 13 August, 1993 from the research vessel *Gyre* at a depth of 27 m in the Gulf of Mexico off Panama City, Florida. The site was located at 29° 41.02'N, 85° 40.90'W and the first burst was recorded at 23:00 GMT on 13 August 1993.

Diver observations at the time of deployment indicated that the tetrapod was completely stable and properly oriented on the hard, coarse-sand bed. The visibility was 5 m to 10 m and no local resuspension was apparent. Observations also revealed no ripples or flow-induced bed forms. However, the bed was roughened significantly by biogenic debris. The median grain diameter of the bed sediment was 0.65 mm.

Preliminary Results from the Panama City Site

Our data from Panama City has been in hand for a shorter period of time than has our Eckernfoerde data and, consequently, we are not as far along in the analyses of these data. However, we have completed the predeployment sensor calibrations and the data prescreening and conversions to units. The records are complete and of high quality and more detailed analyses are now underway.

Figure 6 shows time series of burst-mean current speed and direction at 100 cm above the bed over the 20 day deployment period. For the most part, near-bottom flows were dominated by rotary diurnal tidal currents. Current speeds were below 10 cm s^{-1} for most of the time although maxima of 12 to 13 cm s^{-1} occurred episodically. Preliminary examinations of velocity profiles indicate large hydraulic roughness lengths and, hence, large drag coefficients. However, initial estimates of skin friction shear stresses yield values below the threshold value necessary for sediment to be suspended. Suspended sediment concentrations observed during the first half of the record were near zero. During the second half of the record some sensors recorded high concentrations intermittently whereas others did not. Since concentrations did not correlate with proximity to the bed, we suspect that the apparent high concentrations may have been caused by biofouling of sensors. However, we must complete our analyses before we can confirm this suggestion.

Plan for FY 1994: Analyses and Modeling

At the present time, the data sets from both sites are being used to obtain more accurate estimates of the associated roughness lengths and bottom drag coefficients. In addition to applying the "law of the wall" technique to velocity profiles that meet certain quality control expectations, we are also using different wave-current boundary layer models, including that of Grant and Madsen (1986) to partition the bed stress into form drag and skin friction components and to determine the roles of surface gravity waves. Once the necessary bed stress values have been evaluated we will apply the results to predict the likely rates and frequencies of sediment resuspension and active layer mixing corresponding to different predicted benthic energy conditions. A model is also being developed to explain and predict tidal, wind driven, and seiche-related flows in Eckernfoerde Bucht; the model results will be compared to our field data. A similar model will be applied to the tidal and wind-driven flows off Panama City. Finally, we must relate our results to those obtained by our colleagues at APL and SUNY-Stony Brook before we can complete interpretations of bed roughness, lithostratigraphy, and sediment column dynamics.

We expect an initial publication on Eckernfoerde results to be ready for submission to a journal by spring of 1994. A paper on this subject will be presented at the Ocean Sciences Meeting in San Diego in February 1994.

References

Defant, A., 1961. *Physical Oceanography*, Vol. II, New York, MacMillan, 598 pp. (pages 372-377 deal with tides and sieches in the Baltic).

Grant, W.D., and O.S. Madsen, 1986. The continental shelf bottom boundary layer. *Annual Reviews of Fluid Mechanics* 18:265-305.

TABLE 1

BALTIC 1993A

Sensor		Height above bed	Samples/ burst	Sampling interval	Bursts every	Number of Bursts	Total Duration
635	p	250cm	4096	0.2sec	4hr	0	0hr
635	w	127	4096	0.2	4	0	0
626	u,v 1	19	2048	1.0	4	61	244
	u,v 2	49	2048	1.0	4	61	244
	u,v 3	80	2048	1.0	4	61	244
	u,v 4	111	2048	1.0	4	61	244
OBS	c 1	19	2048	1.0	4	64	256
	c 2	45	2048	1.0	4	64	256
	c 3	81	2048	1.0	4	64	256
	c 4	114	2048	1.0	4	64	256
	c 5	138	2048	1.0	4	64	256
DSA	h		2048	1.0	4	47	188

BALTIC 1993B

Sensor		Height above bed	Samples/ burst	Sampling interval	Bursts every	Number of Bursts	Total Duration
635	p	250cm	4096	0.2sec	4hr	34	136hr
635	w	127	4096	0.2	4	34	136
626	u,v 1	19	1024	1.0	4	61	244
	u,v 2	49	1024	1.0	4	61	244
	u,v 3	80	1024	1.0	4	61	244
	u,v 4	111	1024	1.0	4	61	244
OBS	c 1	19	1024	1.0	4	43	172
	c 2	45	1024	1.0	4	43	172
	c 3	81	1024	1.0	4	43	172
	c 4	114	1024	1.0	4	43	172
	c 5	138	1024	1.0	4	43	172
DSA	h		120	1.0	4	70	280

Instruments and Sensors:

- 635 p = pressure
- 635 w = vertical velocity
- 626 u,v = horizontal velocities at 4 levels
- OBS c = optical backscatter suspended sediments
- DSA h = distance from digital sonar altimeter to bed

TABLE 2

PANAMA CITY, FL 1993

Sensor		Height above bed	Samples/ burst	Sampling interval	Bursts every	Number of Bursts	Total Duration
626	p	238cm	2048	1.0sec	3hr	152	456hr
626	u,v 1	9	2048	1.0	3	152	456
	u,v 2	39	2048	1.0	3	152	456
	u,v 3	70	2048	1.0	3	152	456
	u,v 4	100	2048	1.0	3	152	456
OBS	c 1	7	2048	1.0	3	152	456
	c 2	13	2048	1.0	3	152	456
	c 3	40	2048	1.0	3	152	456
	c 4	70	2048	1.0	3	152	456
	c 5	84	2048	1.0	3	152	456
DSA	h	144	120	1.0	3	111	333

Instruments and Sensors:

626	p = pressure
626	u,v = horizontal velocities at 4 levels
OBS	c = optical backscatter suspended sediments
DSA	h = distance from digital sonar altimeter to bed

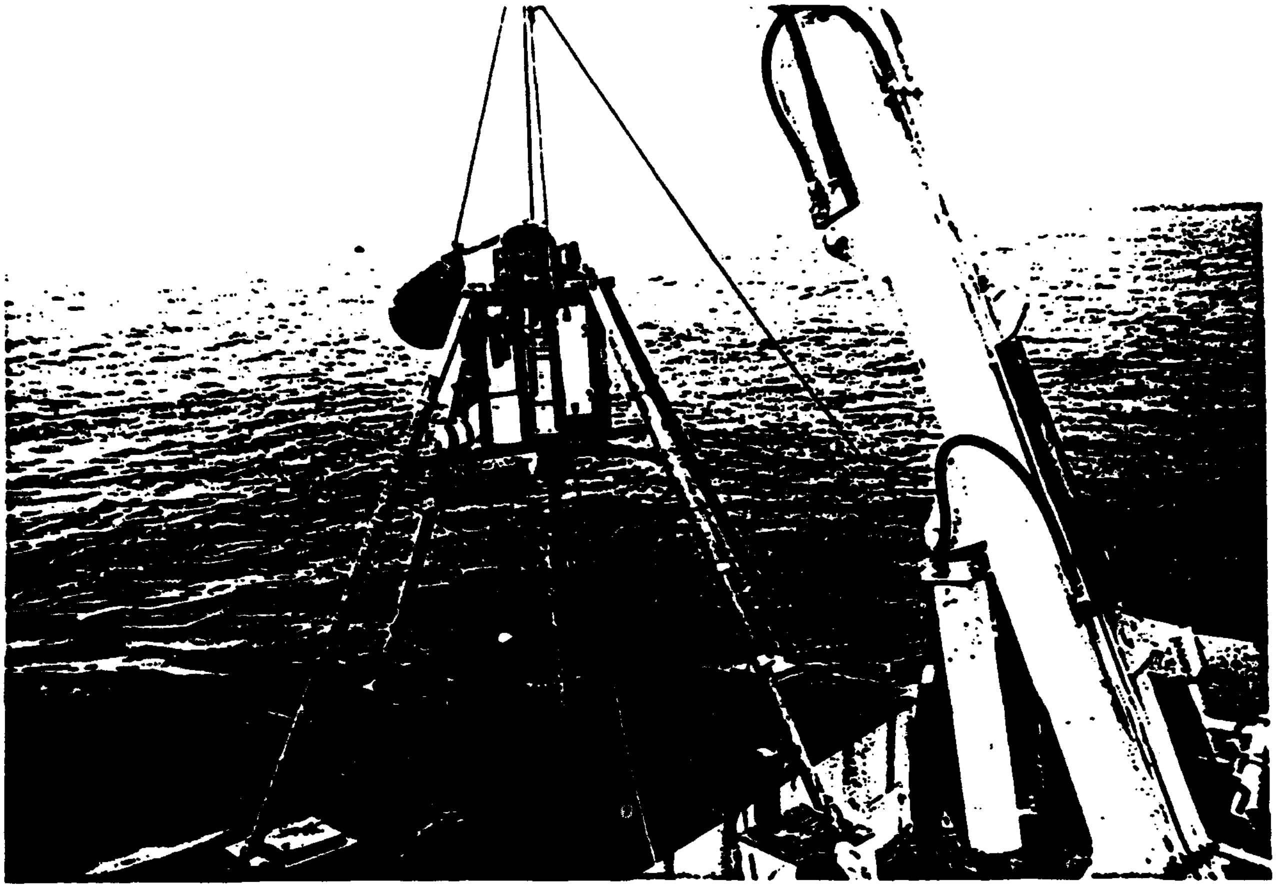

Figure 1. Instrumented tetrapod used in Eckernforde and Panama City deployments.

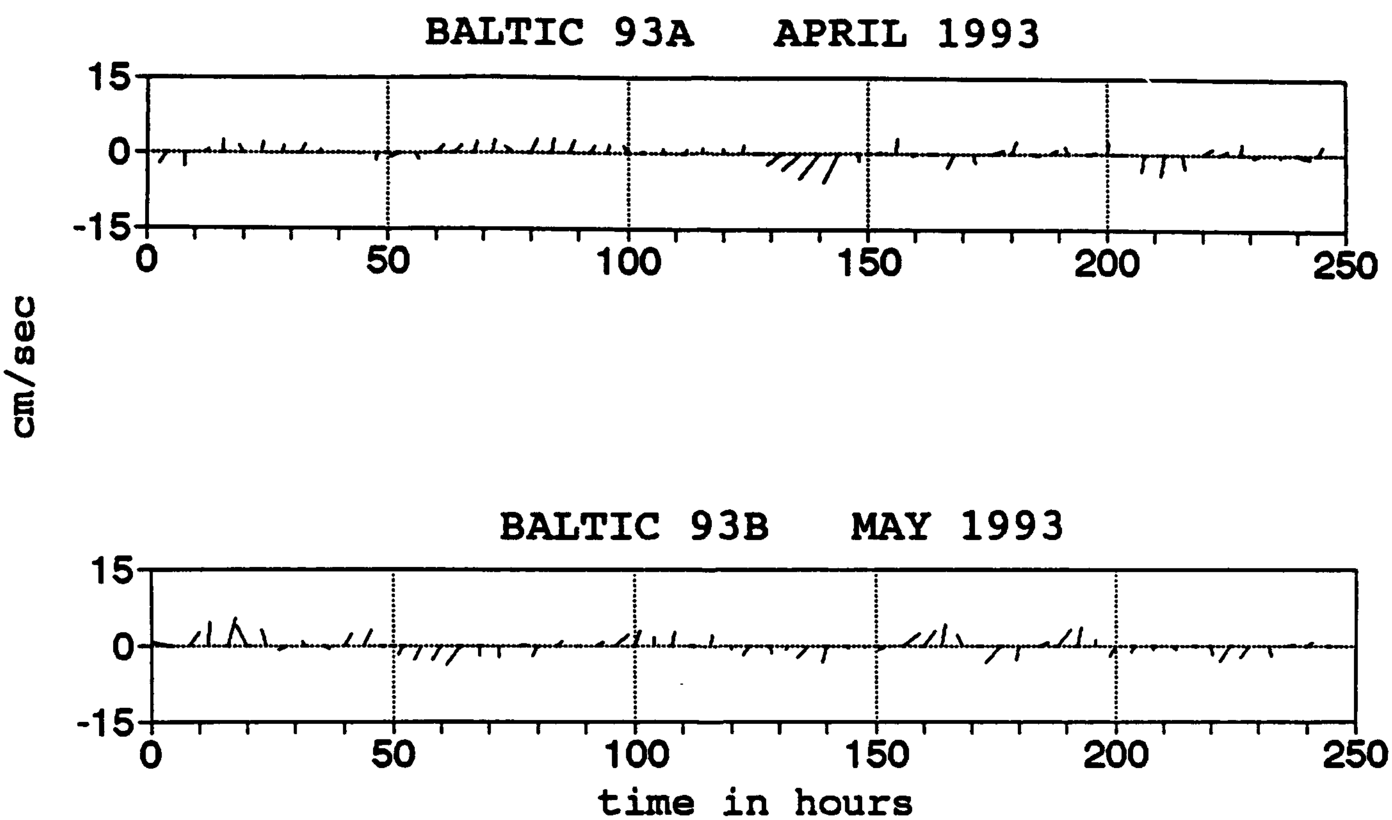

Figure 2. Current stickplots for near-bottom currents observed in Eckernforde Bucht.

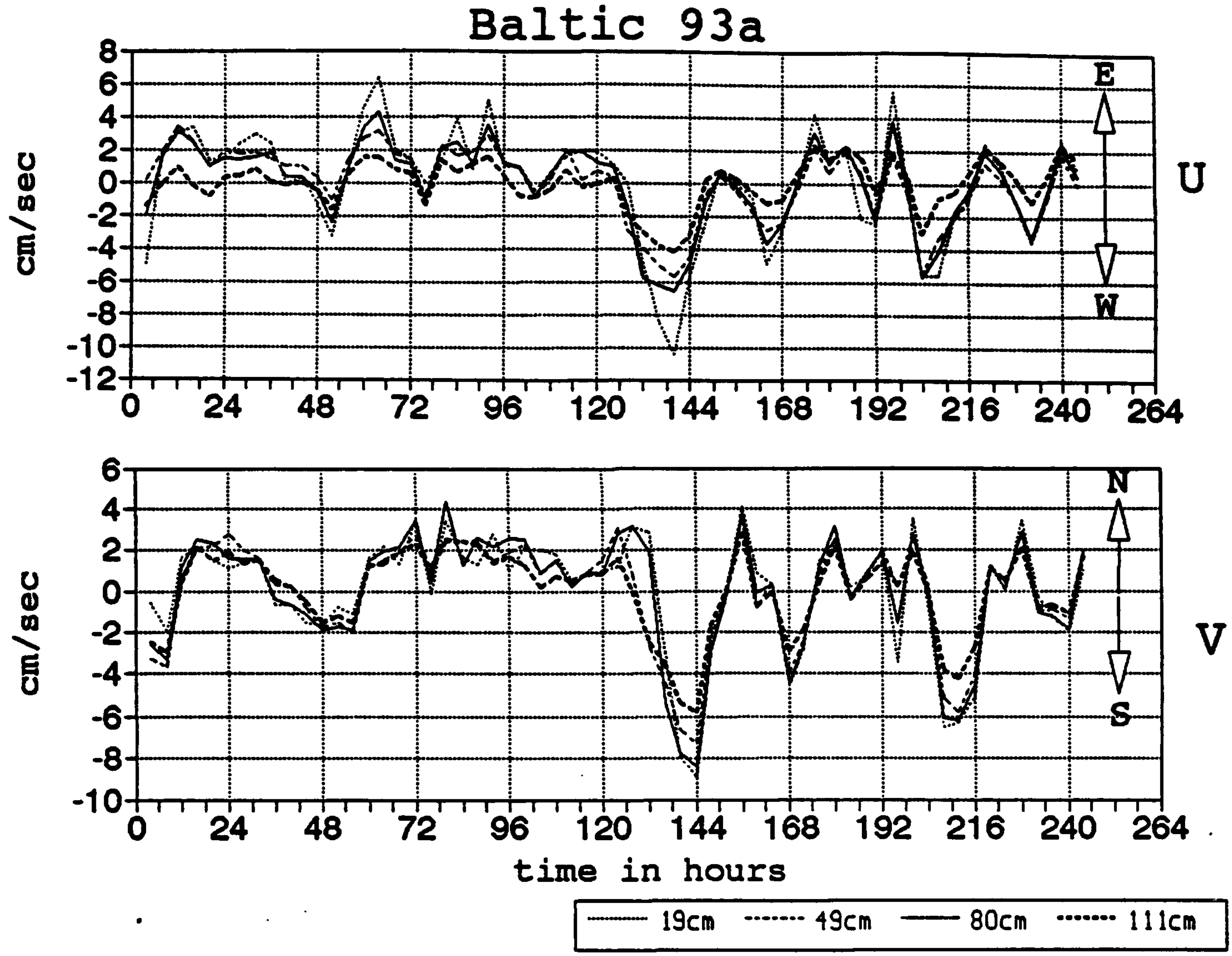

Figure 3. Time series of burst-averaged u(E-W) and v(N-S) components of near bottom flows observed in eckernforde Bucht during the first (April 1993) deployment.

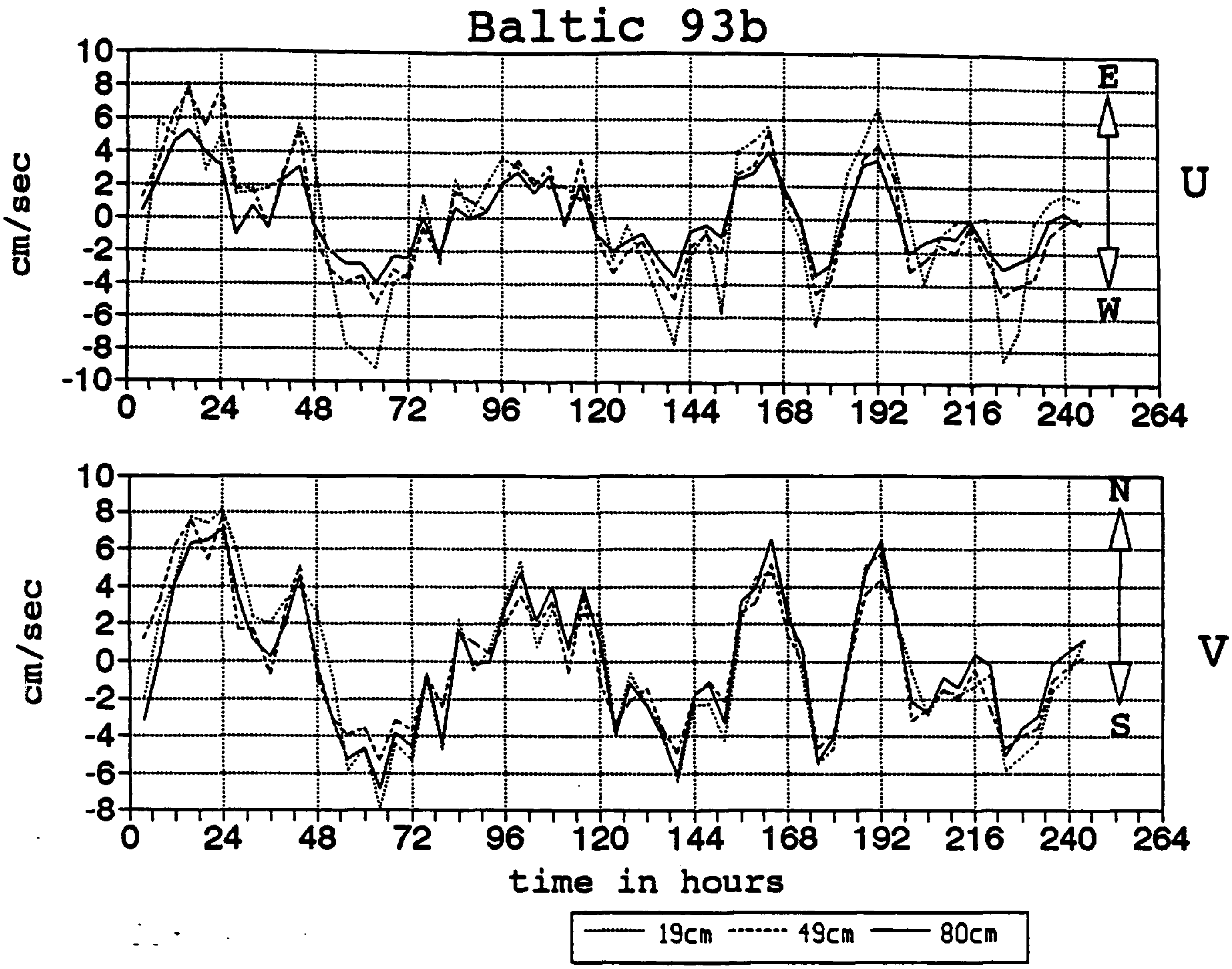

Figure 4. Time series of burst-averaged u(E-W) and v(N-S) components of near bottom flow observed in Eckernforde Bucht during the second (May 1993) deployment.

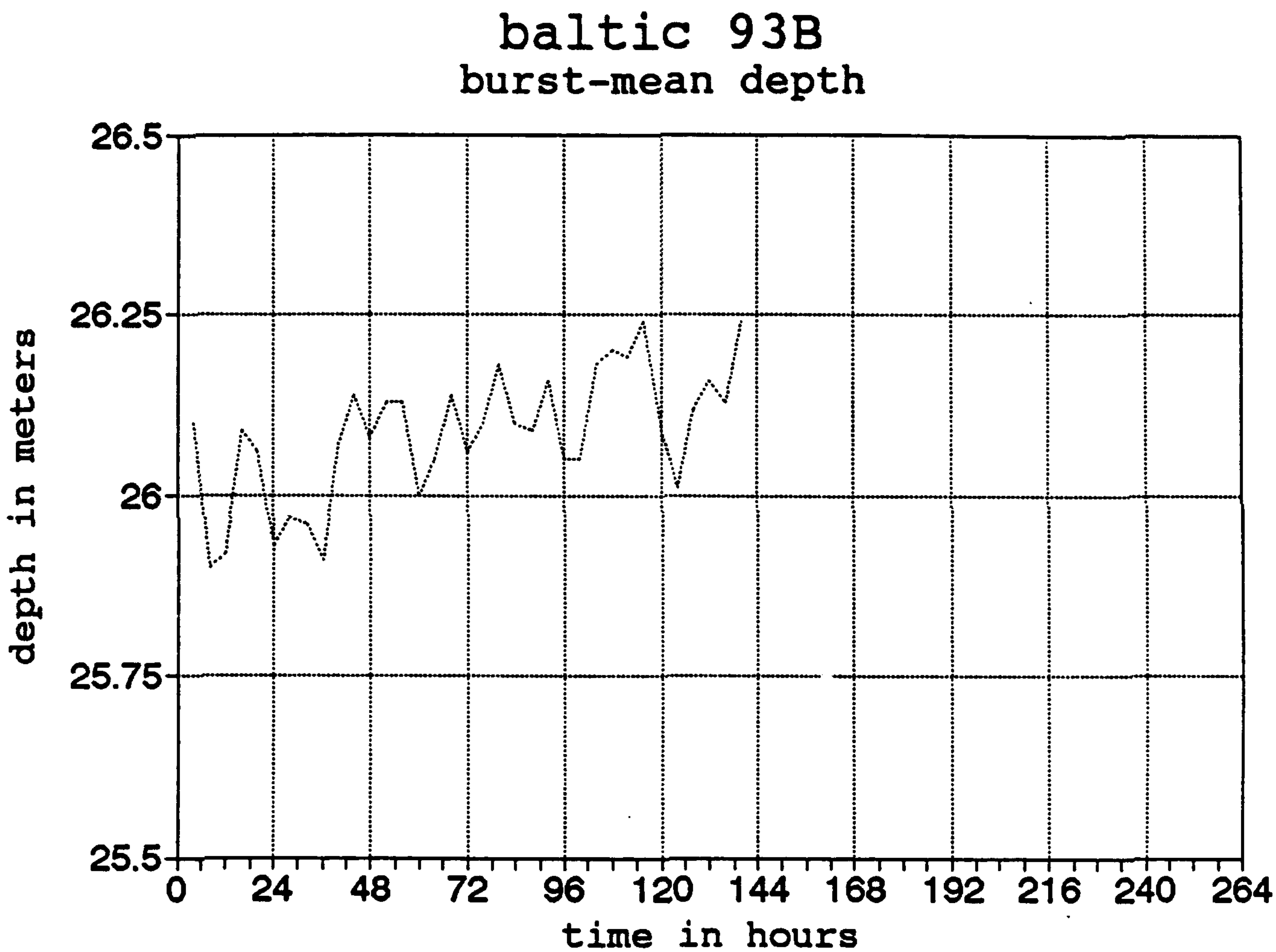

Figure 5. Depth (pressure) sluctuations observed in Eckernforde Bucht during the second deployment.

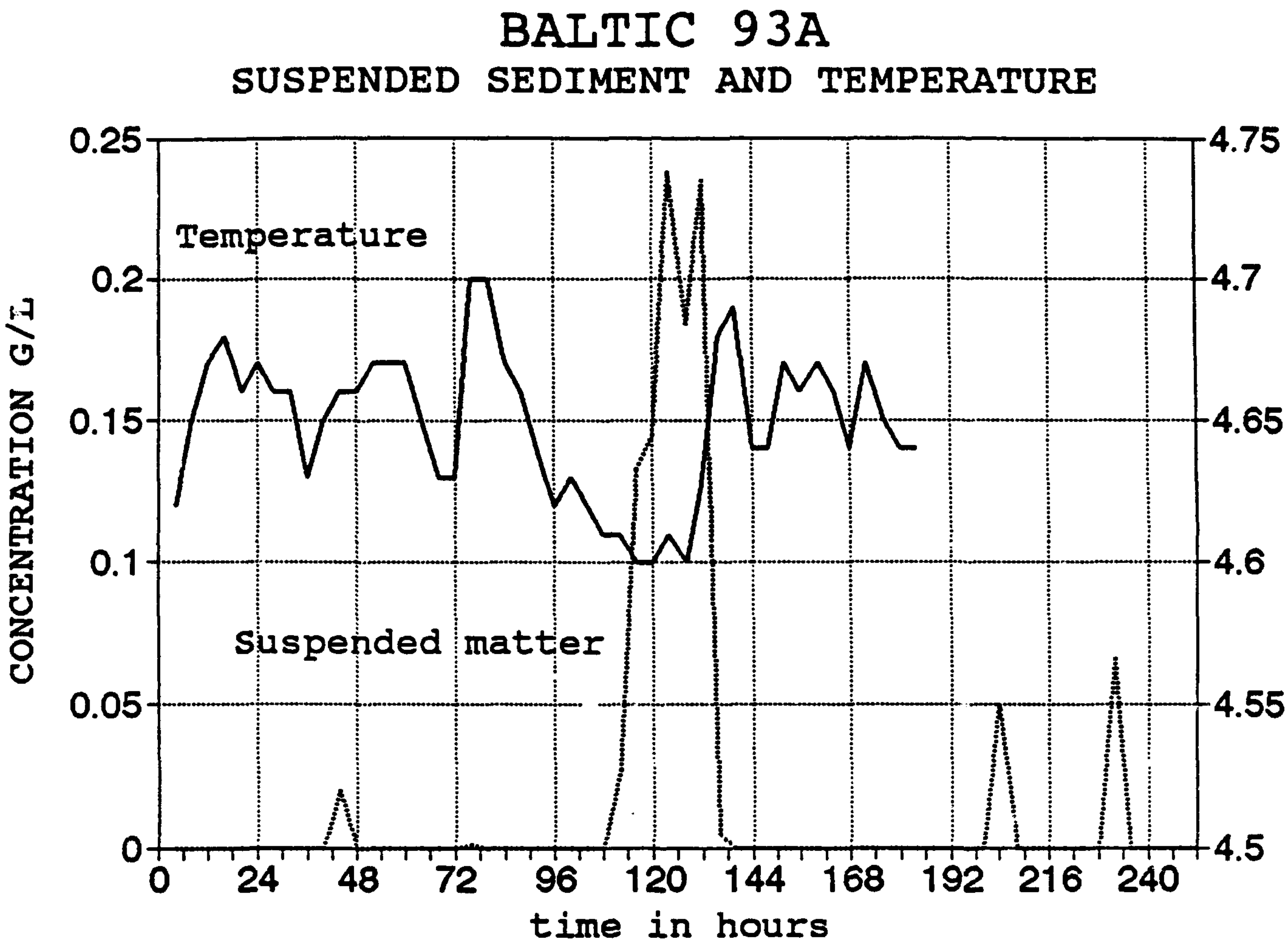

Figure 6. Temperature and suspended sediment concentrations observed near the bed in Eckernforde Bucht during the first deployment.

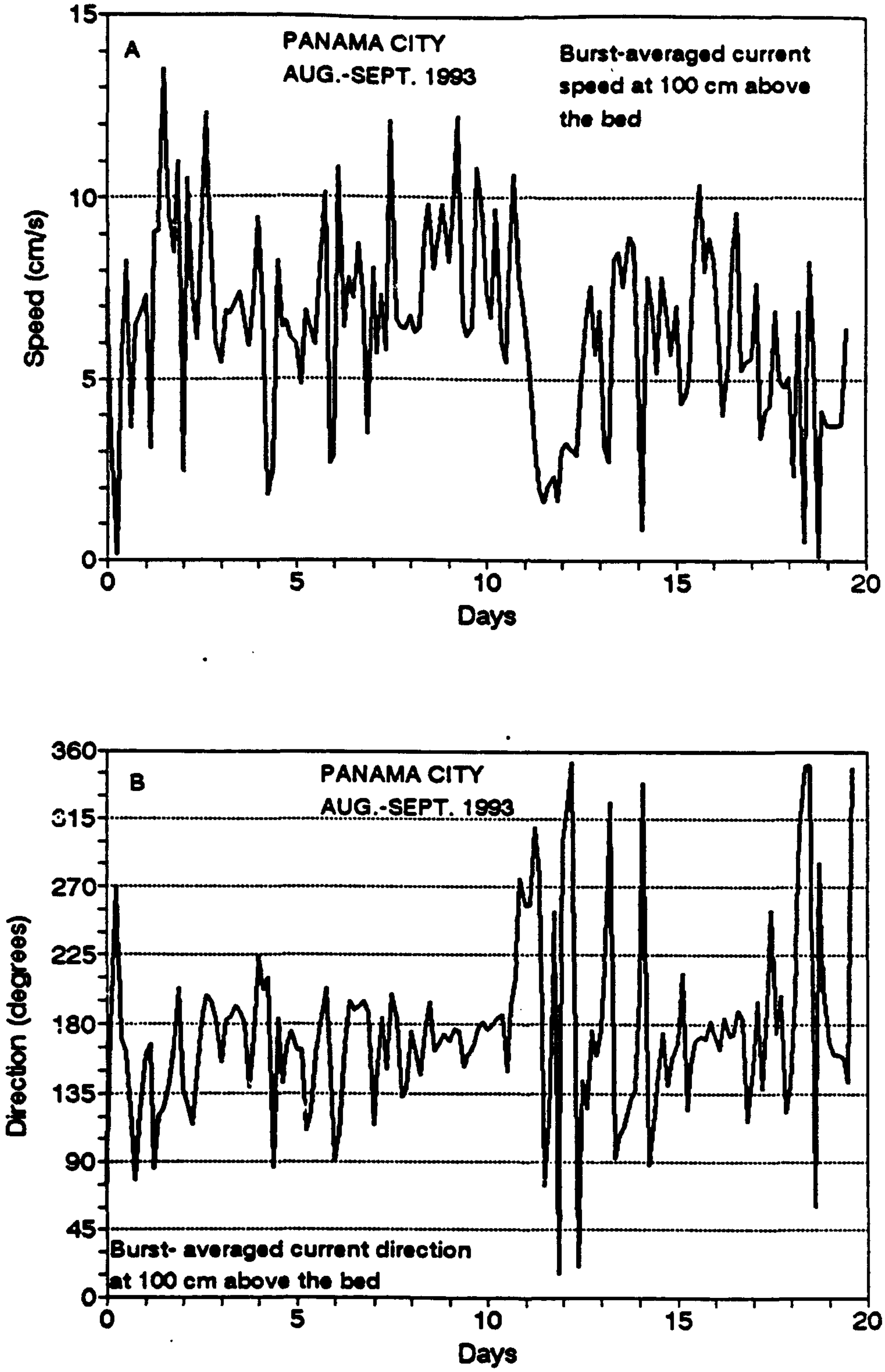

Figure 7. Near bottom current speed and direction observed off Panama City, Florida in August and September 1994.

3.23 Image Analysis of Sediment Texture: A Rapid Predictor of Physical and Acoustic Properties of Unconsolidated Marine Sediments and Processes Affecting Their Relationships (Principal Investigators: D. K. Young and R. J. Holyer, NRL)

CBBLSRP FY93 YEAR-END REPORT

David K. Young, Ronald J. Holyer, Juanita Chase and Richard Ray
Naval Research Laboratory
Stennis Space Center, MS 39529-5004

During FY-93 image enhancement and texture analysis were performed on in situ cross-sectional photography, box core x-radiographs, and electron microscopy images of marine sediments. Images were digitized from original film products.

The most useful enhancement algorithm was found to be the Wallis Filter. This filter is a spatially variant contrast stretch and brightness adjustment. Image contrast and brightness are automatically adjusted at each pixel location based on the image gray-level statistics in a local neighborhood. The algorithm tends to force the local mean gray-level to 128 and the local standard deviation to 63. This has the effect of building contrast in flat areas of the image and reducing contrast in high contrast regions. Dark areas of the image are also brightened and bright areas darkened to pull detail out of regions that are nearly saturated in the original film. One practical outcome from using this algorithm is that differences resulting from varying exposure times of processed images are minimized. Figure 1 is a side-by-side comparison of an original and Wallis Filtered image. Note in the figure that biogenic structure is enhanced and that Lebenspuren can be observed whereas they are not apparent in the original. The Wallis Filter gives an excellent descriptive first look at the imagery.

Quantitative image analysis to date has relied on texture analysis techniques. Second-order gray-level statistics derived from the co-occurrence matrix, and gray-level run length statistics have been applied to the digital images to reveal structure within the image and to quantify the scale and anisotropy of that structure. Figure 2 shows an electron microscope image of marine clay microfabric and the associated co-occurrence matrix texture parameters on the left of the figure. Texture measures have been calculated for numerous scales and orientations within the image. These texture parameters have been displayed in image form for visualization. Texture parameter values at the center of each texture "image" represent small spatial scales while values at the edge represent large spatial scales. Any structure within the original image will be revealed as patterns in the texture measure images. Note that such patterns are observed in Figure 2. The patterns that emerge in the texture parameter visualizations are apparently periodic in two orthogonal directions. The hypothesis is that the periodic nature of the imaged texture information is evidence of the microfabric. The texture images are apparently allowing us to visualize the lattice of the fabric even though it is not readily observable in the original image. From the texture images one can measure lattice spacing and orientation and in other ways parameterize the sediment microfabric.

In images of sediment profiles from Eckernfoerde Bucht, we have observed structure in the electron microscope imagery, but not in x-radiographs. This would imply that for this site, textural structure is dominant at the grain size scale. X-radiographs of sediment profiles from other sites we have analyzed thus far, such as the Arafura Sea and Mississippi Sound, show structure at larger spatial scales. We are, therefore, encouraged that the texture analysis techniques employed will be useful in quantitatively differentiating sediment structure from various regions, and may also correlate with coincident acoustic measurements. At the close of the fiscal year we are in the process of validating a routine to apply to these images to calculate fractal dimension, which we feel may be more descriptive of phenomenology than the statistical texture measures analyzed to date.

During the Eckernfoerde Bucht experiment, project investigators participated in various field operations, including 44 field dives and 2 chamber "dives", in cooperation with other CBBLSRP scientists. Products from this field experiment used in image textural analysis thus far, include x-radiographs taken from ship-deployed box cores and diver-collected cores, and electron microscope images of sediment fabric from pressurized diver-collected cores. Only 6 profile photographs of Eckernfoerde Bucht sediments [out of 66 deployments (bottom-bounce) of the sediment profiling camera system] were obtained because of equipment malfunction. The malfunctioning electrical components of the camera system have been subsequently identified and fixed; unfortunately, the 6 photographs obtained are useful for qualitative purposes only.

We are pursuing opportunities to analyze imagery of sediments, over a wide range of size scales, obtained by other CBBLSRP scientists. The imagery sought covers a wide range of gray scales and is correlatable with other sedimentary and acoustical measurements collected concurrently.

We have achieved a promising gray-level co-occurrence parameterization of isotropy and anisotropy as a measure of and as a function of spatial scale. In collaboration with Kevin Briggs are in the process of comparing results with correlation length analysis of measured bulk sediment properties. Results from these analyses will be presented at the special session of the CBBLSRP at the February '94 AGU meeting ("Sediment Density Structure Inferred by Textural Analysis of Cross-sectional X-radiographs", by Ronald J. Holyer, David K. Young, Juanita Chase and Kevin Briggs).

Figure 1

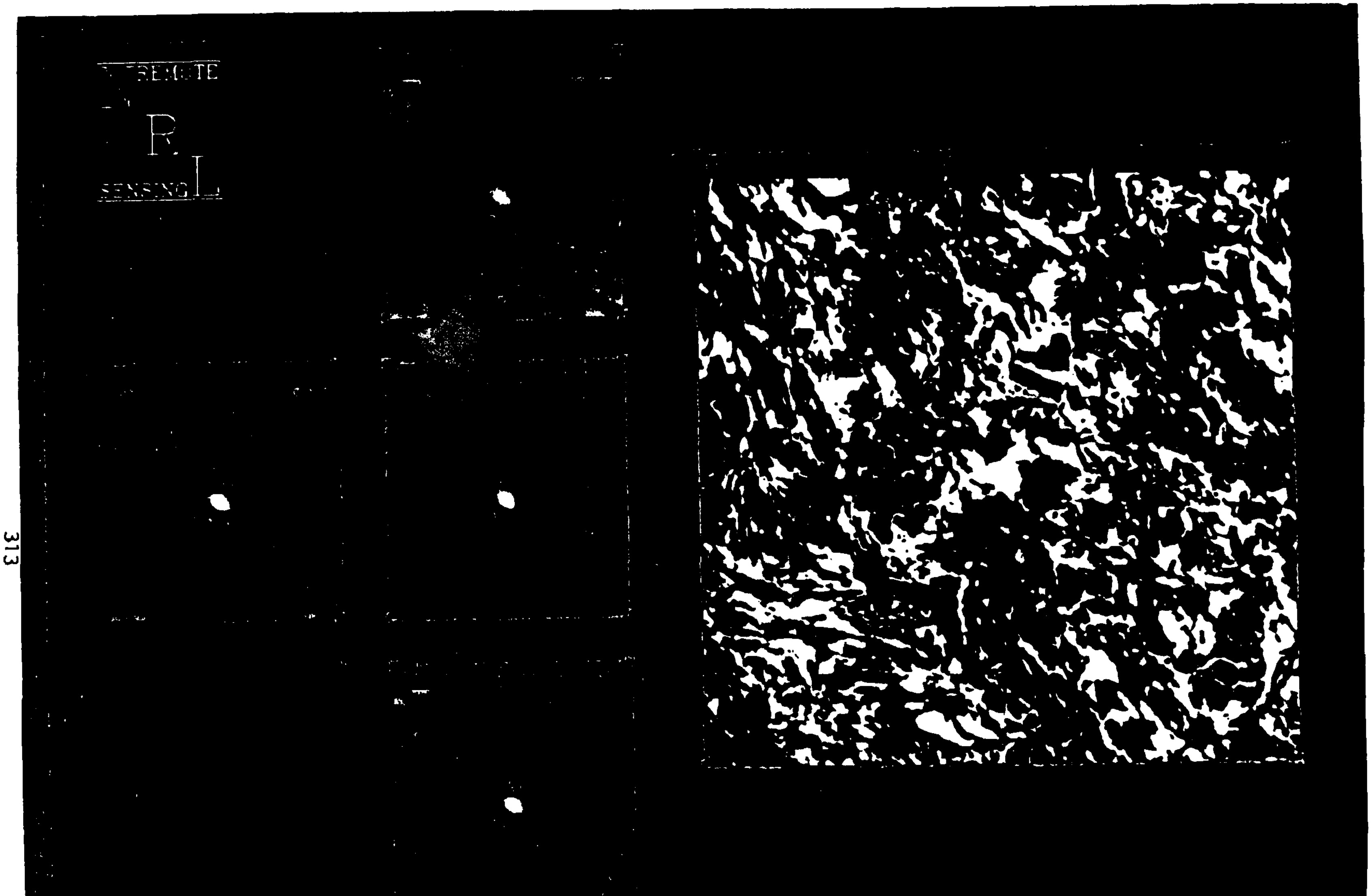

Figure 2

3.24 The Relationship Between High-Frequency Acoustic Scattering and Seafloor Structure (Principal Investigator: Li Zhang, University of Southern Mississippi)

CBBLSRP FY93 YEAR-END REPORT

Li Zhang
Center for Marine Science
University of Southern Mississippi
Stennis Space Center, MS 39529

INTRODUCTION

As a part of CBBLSRP project, our research concentrates on the theoretical development of the acoustic backscattering mechanisms. Based on many previous researches, we have built a method to calculate the backscattering due to the inhomogeneity of the sea floor admittance. The total scattering is expected as the sum of the surface scattering, including the effects of the admittance inhomogeneity and the roughness, and subbottom volume scattering. The combination of these factors will be considered in the future study. After the observations of pulse to pulse fluctuations that were found in Stanic's Panama City experiment, we began to investigate the consequences of the experimental fluctuations caused by the apparent turbulence in the seawater. Numerical simulations confirmed that very small changes in the sound speed in seawater would cause significant phase changes thus result in the pulse to pulse fluctuations. Because of the new observations, before any other development of theoretical model, the next step is to find out how the randomness of the water column can be accounted for in order to distinguish the effects of the water column and those of the sea floor.

SCATTERING FROM SEA FLOOR INHOMOGENEITY

Almost all scattering theories, including Eckart's classic paper[1], are based on Green's theorem[2]. Then Born approximation[3] is applied to the inside of the integral so the sound pressure at any field point can be estimated. Different choices of Green's function will give different results.

In this case, the Green's function includes two terms: incident spherical waves and reflection waves. Usually the reflection term is represented by an image point source also emitting spherical waves with a reflection coefficient indicating its intensity. In Morse and Ingard's book, the reflection coefficient is close to the situation of airborne acoustics[3]. Since the admittance of sea floor differs not too much from that of the seawater, we choose reflection coefficient R_0 as

$$0 = \frac{r_{20}C_{20} \cos q_i - r_1 C_1 \cos q_{t0}}{r_{20}C20 \cos q_i + r_1 C_1 \cos qt0} \qquad (1)$$

where ρ_1 is the density of seawater, C_1 is the sound speed in seawater, ρ_{20} is the average density of sediment, C_{20} is the average sound speed in sediment, θ_i and θ_{t0} are local incident angle and refracting angle, respectively. This is the reflection coefficient corresponding to a incident plane wave reflected by an infinite homogeneous flat plane boundary, used for the Green's function. For sound pressure, the reflection coefficient becomes R which is similar to R_0, except that the local density and sound speed in the sea floor, instead of average values, are used. The local values are no longer constants.

The backscattering sound pressure is then obtained as

$$p_s = \int_S Q \sin(\omega t - \frac{2\omega b}{C_1})\, dS \qquad (2)$$

where ω is the angular frequency of the sound waves, b is the distance between the receiver and a scatter source dS on the sea floor, Q is the amplitude of scattering wave from dS:

$$Q = \frac{-kA}{(4\pi b)^2}(1+R)(1+R_0)\cos\theta_t\,(\beta-\beta_0) \qquad (3)$$

where k is wavenumber, $(A/4\pi)$ is incident sound pressure at unit distance, β_0 is the average bottom acoustic admittance, β is its local value at location dS, and θ_t is the corresponding refracting angle. The integral of equation (2) is over the insonified area S. If the incident sound wave is an impulse signal, at each instant the S is only a part of the whole insonified area.

EFFECTS OF TURBULENCE IN SEAWATER

If the sound speed in seawater C_1 is not a constant but fluctuates around its mean value, due to the turbulence in seawater, the scattering pattern will be affected. Let

$$C_1 = C_{10} + \delta C_1 = C_{10}\left(1 + \frac{\delta C_1}{C_{10}}\right) \quad \delta C_1 \ll C_{10} \qquad (4)$$

where C_{10} is the mean sound speed in seawater and δC_1 is its fluctuation. For δC_1 much smaller than C_{10} it is easy to find out that the amplitude Q keeps almost unchanged while phase term could change significantly. The scattering pressure becomes

$$p_s = \int_S Q \sin(\omega t - \frac{2\omega b}{C_{10}} + \delta\phi)\, dS \qquad (5)$$

where $\delta\phi$ is the phase change due to the turbulence:

$$df = \frac{4\,pf\,b}{C_{10}^2}\,dC_1 \tag{6}$$

where f is the sound frequency.

Numerical Simulation results based on equation (5) for discrete point scatters and random sound speed fluctuations are shown in the attached figures. The scattering waveforms can change dramatically if the random variable δC_1 is big enough. We may define a quantity called critical sound speed fluctuation δC_{1c}, corresponding to that $\delta\phi$ reaches 90°:

$$dC_{1c} = \frac{C_{10}^2}{8fb} \tag{7}$$

If δC_1 is much smaller than δC_{1c}, then the measured scattering waveforms will be roughly in same shape. Otherwise, pulse to pulse fluctuations will be observed. In Stanic's 50 kHz measurement δC_{1c} is about 0.32 m/s, corresponding to a temperature change of 0.07 °C[2]. It seems not to be an unreasonable magnitude. Similar order of sound speed fluctuations near the sea surface was reported in Clay and Medwin's book[2].

FUTURE RESEARCH PLAN

The ultimate objective of this research is to estimate some sea bottom properties through acoustic backscattering measurements. Because of the observations of the pulse to pulse fluctuations, the distinction between the two effects, that of the water column and that of the sea floor, becomes more important. The further research is therefore composed of the following two phases:

1. Estimate Magnitude of Turbulence and Extract Effects of Sea Floor

The fluctuations in backscattering measurements give us a feeling about the turbulence in seawater. But further studies must be conducted in order to better estimate the magnitude of the turbulence. The statistics techniques such as autocorrelation and crosscorrelation calculations are expected to be employed. Meanwhile, direct measurements of sound speed fluctuations are suggested to be made during the future measurements. It can be done by normal incident pulse sound waves towards the sea bottom and measuring the sound speed in seawater, at the same time of recording the backscattering waves. Different sound frequencies should be used since it also affects the phase change. Such measurements, combined with the theoretical calculations, will lead to establish an estimate of the magnitude of the turbulence and a criteria for describing its effects. The next step is to develop a method of extracting the effects of the sea floor itself, also based on the statistics.

2. Combination of Effects of Surface Scattering and Volume Scattering

Still, the scattering theory should include surface scattering as well as volume scattering, after we can extract them from the experimental data. It is best if we can find the solution of the inverse problem: finding some sea floor properties from the measurement data, based on our further understanding of the backscattering mechanisms.

REFERENCES

[1] Eckart, Carl, The Scattering of Sound from the Sea Surface, *J. Acoust. Soc. Am.*, 25(3), 566-570, 1953.

[2] Clay, Clarence S. and Herman Medwin, *Acoustical Oceanography: Principles and Applications*, John Wiley & Sons, New York, 1977.

[3] Morse, P.M. and K. Uno Ingard, *Theoretical Acoustics*, McGraw-Hill, New York, 1968, equation (7.1.17), p 321.

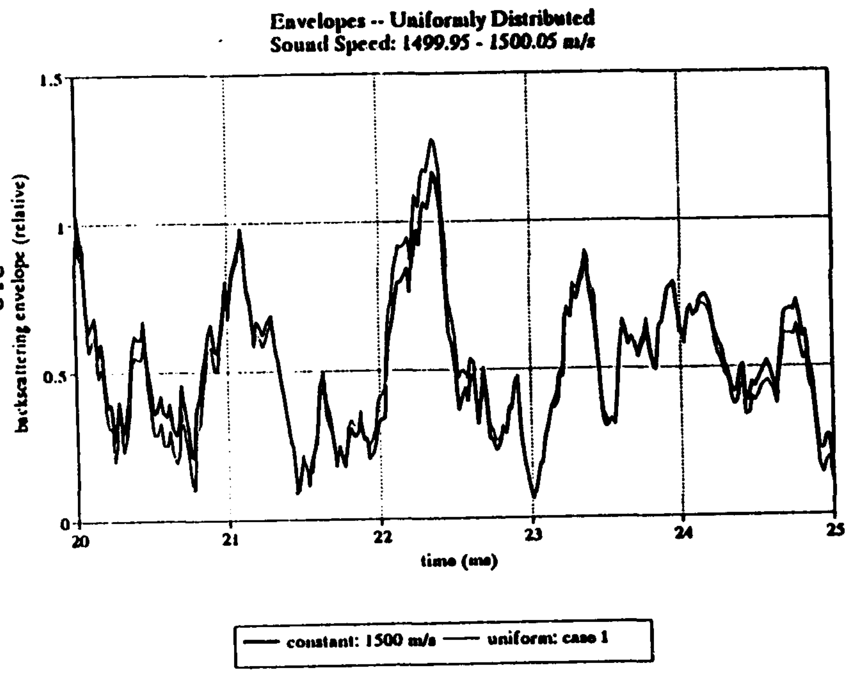
Envelopes -- Uniformly Distributed
Sound Speed: 1499.95 - 1500.05 m/s
backscattering envelope (relative)
0
0.5
1
1.5
20
21
22
23
24
25
time (ms)
constant: 1500 m/s
uniform: case 1

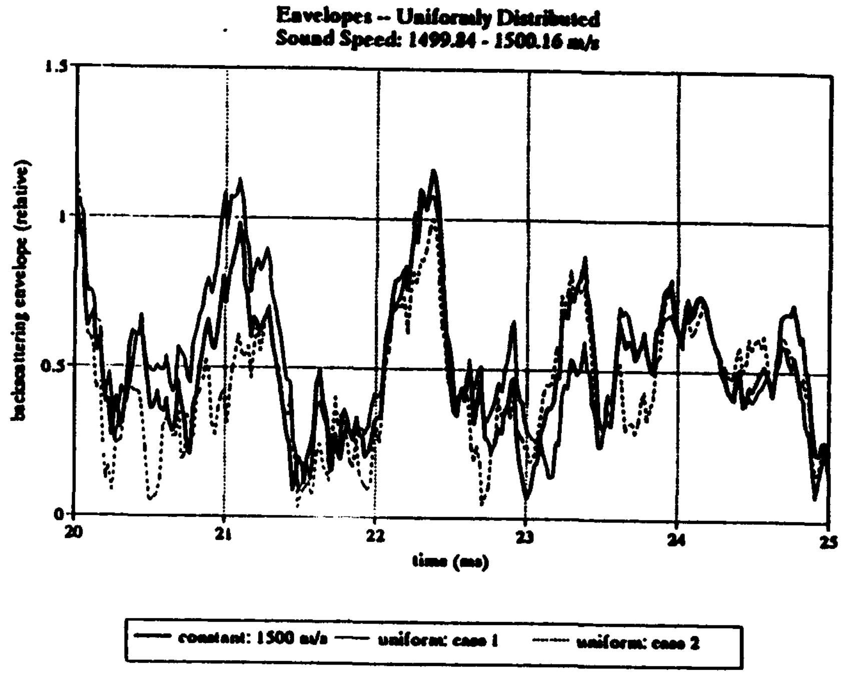
Envelopes -- Uniformly Distributed
Sound Speed: 1499.84 - 1500.16 m/s
backscattering envelope (relative)
0
0.5
1
1.5
20
21
22
23
24
25
time (ms)
constant: 1500 m/s
uniform: case 1
uniform: case 2

Envelopes -- Uniformly Distributed
Sound Speed: 1499.5 - 1500.5 m/s

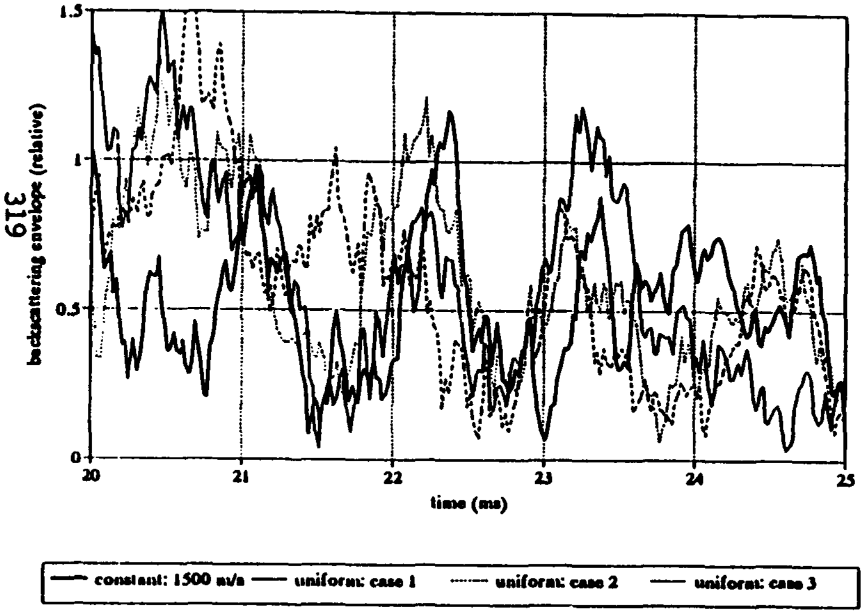

Envelopes -- Uniformly Distributed
Sound Speed: 1499.68 - 1500.32 m/s

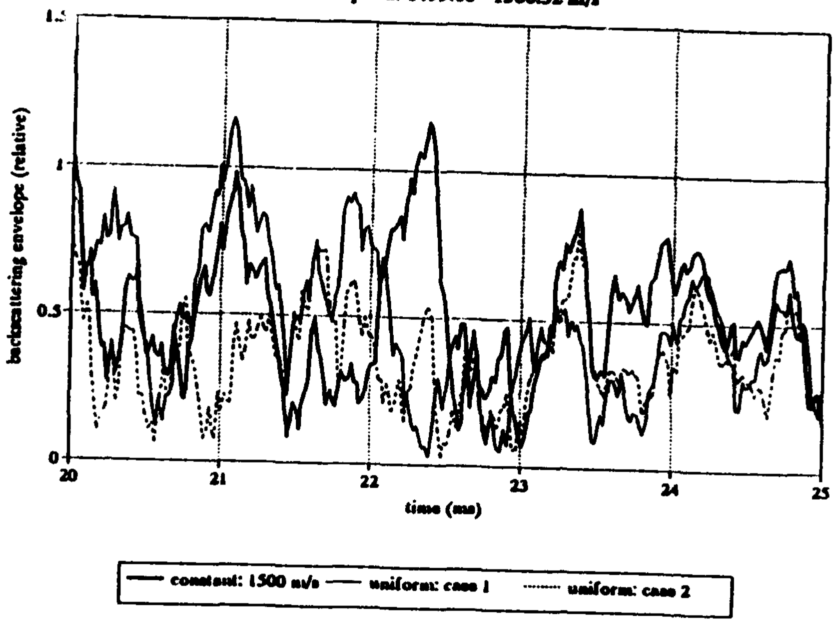

4.0 ACKNOWLEDGMENTS

Operational support was provided by FWG, WTD-71, University of Kiel, and Texas A&M University. The moral support and encouragement of F.E. Saalfeld, T. Coffey, P. Wille, and J. Cornett is gratefully acknowledged, as is the contribution of the SRP review panel, which includes: J.E. Andrews, M.R. Barker, D.L. Bradley, W.K. Ching, H.C. Eppert, J.M. Harding, J.D. Grembi, D. Inman, T. Kinder, J.H. Kravitz, C.M. McKinney, G. Pollitt, C. Stuart, D.G. Todoroff, P.R. Vogt, J.T. Warfield, and B. Winokur. Workshop chairpersons including R.H. Bennett, W.A. Dunlap, H.J. Lee, T.G. Muir, C.S. Clay, D.R. Jackson, P.A. Jumars, and G.D. Gilbert helped with the early development of the SRP program. The CBBLSRP is supported by ONR, Fred Saalfred, Program Manager (Program Element Number 61153N32), with contributing support from NRL and FWG.

Section 3.0 was prepared by the CBBLSRP research team for publication in EOS. The CBBLSRP research team consists of M.D. Richardson (chief scientist), D. Albert, A.L. Anderson, R.J. Baerwald, R.H. Bennett, K.B. Briggs, H.G. Brandes, W.A. Bryant, W. Chiou, N.P. Chotiros, J.C. Cranford, R.W. Faas, P. Fleischer, G.V. Frisk, K.E. Gilbert, J.A. Hawkins, R.J. Hoyler, D.R. Jackson, J.J. Kolle, D.N. Lambert, Dennis Lavoie, Dawn Lavoie, G.R. Lopez, R. Gammish, C.S. Martens, D.F. McCammon, E.C. Mozely, C.A. Nittrouer, H.A. Pittenger, M.H. Sadd, S.G. Schock, A.J. Silva, N.C. Slowey, S. Stanic, T.K. Stanton, R.D. Stoll, D.J. Tang, G.E. Veyera, K.L. Williams, L.D. Wright, D.K. Young, R.K. Young, and L. Zang. Other contributors include I.H. Stender, T. Wever, G. Fechner, and H. Fiedler of FWG, F. Abegg and F. Theilen of the University of Kiel, R.R. Goodman of APL Pennsylvania State, and K.M. Fischer and D.J. Walter of NRL. Their efforts are greatly appreciated. Thanks to Leona Cole for her efforts in collecting and collating the manuscript.